PUBLICATIONS of the EARTH PHYSICS BRANCH

volume 42

DEPARTMENT OF ENERGY, MINES AND RESOURCES

OTTAWA, CANADA 1972

TABLE OF CONTENTS

Volume 42

Page

No. 1 Analysis of Units in Electromagnetism
by F. Primdahl 1

No. 2 Gravity Measurements in Canada – January 1, 1967 to December 31, 1970 25

No. 3 The Ancient Oceanic Lithosphere – Canadian Contributions 1 to 11
to the Geodynamics Project – A Symposium
E. Irving, Editor 47

No. 4 Polar Magnetic Substorms 03 – 06, u.t., December 5, 1968
by E.I. Loomer and G. Jansen van Beek 157

No. 5 An Astatic Magnetometer with Negative Feedback
by J.L. Roy, J. Reynolds and E. Sanders 167

No. 6 The Ottawa PZT Observations – 1956-70, Their Comparison
with BIH Values by Graphical, Spectral and Fourier Analyses
by E.G. Woolsey 183

No. 7 Magnetic Anomaly Maps of British Columbia and the Adjacent Pacific Ocean
by G.V. Haines and W. Hannaford 215

No. 8 Un four électrique pour l'étude des propriétés magnétiques des roches
by J.L. Roy, E. Sanders et J. Reynolds 229

No. 9 Record of Observations at Meanook Magnetic Observatory, 1969
by A.B.Cook and S.J. Sprysak 239

PUBLICATIONS of the EARTH PHYSICS BRANCH

VOLUME 42 - NO. 1

analysis of units in electromagnetism

F. PRIMDAHL

DEPARTMENT OF ENERGY, MINES AND RESOURCES

OTTAWA, CANADA 1971

Cat. No.: M70-42/1

Contents

1 Abstract
1 Introduction
1 Basic units
2 Electrostatics
3 Magnetostatics
3 Electromagnetics
5 Electrodynamics
5 Maxwell's equations in general form
7 Giorgi-pairs
8 Giorgi-transformation of a unit system
9 Maxwell's equations in material bodies
12 Static fields in material bodies
14 Unit systems
16 Logometric formulas
17 MKS-systems
18 Conclusions
19 Acknowledgments
19 References
20 Appendix 1 – Units in the MKSA-subsystems and application of the Haines rule
22 Appendix 2 – Units, dimensions and logometric expressions

analysis of units in electromagnetism

F. PRIMDAHL

Abstract. To define a system of electromagnetic units uniquely, six basic quantities must be chosen. A suitable choice may include one basic unit and five constants, for example, or four basic units and two constants. Maxwell's equations are derived in a general form, independent of any particular choice of the six basic quantities. It is shown that the MKSA-formulation of the field equations involves three different unit systems.

In the relation $\overline{B} = \mu_0 \overline{H}$, the symbols $\overline{B}$ and $\overline{H}$ are called a Giorgi-pair; other Giorgi-pairs are shown to exist in the MKSA-formulation of electromagnetic theory. Although of different dimensions, the members of a Giorgi-pair always describe the same physical phenomenon, and may thus be used arbitrarily, provided the Haines rule is observed. The general form of Maxwell's equations is derived for material bodies. It is shown that the MKSA-formulation uses two conflicting models for polarizable materials, leading to two electric and two magnetic fields, and the introduction of two units for each field in order to remove the constants from Maxwell's equations. Dimensional equations are replaced by more general expressions, called logometric formulas, including all six basic units and constants; they are used to analyze the existing unit systems.

Résumé. Pour donner une définition unique d'un système d'unités électromagnétiques, il faut choisir six quantités de base. On peut choisir, par exemple, une unité de base et cinq constantes ou quatre unités de base et deux constantes. Les équations de Maxwell ont été établies, sous une forme générale, indépendamment de tout choix particulier des six quantités de base. La présente étude démontre que dans le système M.K.S.A. la formulation des équations du champ électromagnétique fait intervenir trois systèmes d'unités différents.

Dans l'équation $\overline{B} = \mu_0 \overline{H}$, les symboles $\overline{B}$ et $\overline{H}$ sont appelés paire de Giorgi; l'auteur démontre qu'il existe d'autres paires de ce genre dans la formulation en M.K.S.A. de la théorie électromagnétique. Bien que de dimensions différentes, les éléments d'une paire de Giorgi décrivent toujours le même phénomène physique et peuvent donc être appliqués de façon arbitraire, à condition d'observer la règle de Haines. La forme générale des équations de Maxwell est établie pour les corps matériels. L'auteur montre que la formulation selon le système M.K.S.A. emploie deux modèles contradictoires pour les matières polarisables, d'où deux champs électriques et deux champs magnétiques et l'introduction de deux unités pour chacun de ces champs afin d'éliminer les constantes des équations de Maxwell. Les équations de dimensions ont été remplacées par des expressions plus générales que l'auteur nomme formules logométriques, qui font intervenir les six unités et constantes de base; ce sont ces formules qui one été utilisées pour analyser les systèmes d'unités existants.

Introduction

For almost 100 years physicists have argued about units and unit systems in electromagnetism and the growing worldwide adoption of the SI†-units has revived this discussion (Rosser, 1969; Stopes-Roe, 1969; Temperly, 1969; Lovering, 1970).

One of the difficulties is, no doubt, that so many different terminologies exist and hence participants in the discussion do not use the same concepts in the same meaning. Much of the disagreement is thus believed to lie in the lack of proper means of communication.

The purpose of this paper is to provide a common denominator in the form of a set of electromagnetic equations written independently of any unit system, and to indicate the characteristic features of some of the existing systems. The equations are only derived as far as necessary to evaluate their general form and the selection is more or less arbitrary. It is, however, hoped that the examples cover a wide enough area to demonstrate the method and to indicate extensions.

The notation is very close to that of O'Rahilly (1965) whose treatment of electromagnetism, units, and dimensions has been the basic source of information. His viewpoint is that the symbols in the physical equations stand for pure numbers representing the ratios between the measured quantities (measure-ratios) and some chosen unit quantities. He replaces the dimensions by so-called logometric formulas giving the number by which a measure-ratio has to be multiplied if the basic units or constants are changed.

†Système international.

Basic units

An earlier paper (Primdahl, 1970) has described, how two constants δ and γ have to be included in Newton's second law and the mass attraction law to generalize them, and similarly how three constants α, β, and a are necessary to generalize the electromagnetic equations.

$$F = \delta M \frac{d^2 r}{dt^2} \quad \text{Newton II} \qquad \ldots.1$$

$$F = \gamma \frac{MM'}{r^2} \quad \text{Newton's law of gravitational attraction} \qquad \ldots.2$$

$$F = \frac{qq'}{\alpha r^2} \quad \text{Coulomb's law for electric charges} \qquad \ldots.3$$

$$F = \frac{mm'}{\beta r^2} \quad \text{for magnetic poles} \qquad \ldots.4$$

Electric current is the time-rate of charge transported through a cross-sectional area of the conductor

$$I = \frac{dq}{dt} \qquad \ldots.5$$

and magnetic field strength or field intensity is introduced as

$$H = \frac{F}{m} \qquad \ldots.6$$

the ratio between the force on a magnetic pole and its pole strength.

The magnetic field strength $\overline{dH}$ from a current element $I\overline{ds}$ at the distance $r = \overline{r} \cdot \hat{r}$ is proportional to

$$\frac{I\overline{ds} \text{ x } \hat{r}}{r^2}$$

so that the field strength at the centre of a circular current loop, radius r, carrying the current I is by integration

$$H = \frac{2 ¶ I}{a \cdot r} \qquad \ldots.7$$

The constants of proportionality $\delta, \gamma, \alpha, \beta$, and a are basic in the same sense as the units for length, mass and time are basic, because they are necessary to uniquely determine the unit system. In mechanics we introduce a unit length, a unit mass, and a unit time. The value of one of the constants δ or γ is then agreed upon internationally, and then the determination of the other is a matter of laboratory measurements. If both the constants δ and γ were fixed by international agreement then only two basic units, e.g. mass and time, would be needed. Similarly, if α and β are chosen in electromagnetism then a and all the electromagnetic units may be determined experimentally, or if a fourth electromagnetic unit is introduced only one of the constants α, β or a has to be chosen.

The seven equations (Equations 1 to 7) contain 13 unknowns so it is necessary to choose six of the 13 unknowns to solve the system. Thus we need, not three or four, but six basic "units" to define uniquely our unit system.

It is emphasized that the letter symbols in the algebraic Equations 1 to 7 represent pure algebraic numbers, e.g. the number M in Equation 1 is thus obtained by comparing the mass in the acceleration experiment to a standard mass. Likewise, if the measure-ratio for one mass can be determined then the measure-ratio for all masses can be determined. Hence for the purpose of counting the number of equations and the number of unknowns all the measure-ratios for mass count for one unknown.

It is interesting to note that as there are only five constants ($\delta, \gamma, \alpha, \beta$, and a) we cannot determine a unit system by fixing the values of the constants only; at least one actual physical sample, for example mass, is needed as a starting point. The six basic quantities cannot be chosen at random from the 13 unknowns; only a combination which does not violate any of the Equations 1 to 7 and 28 given below will be legal. An illegal choice will make the system indeterminate, as can be shown by solving for the remaining unknowns.

The claim † that the MKSA-system is defined uniquely by the choice of the four basic units metre, kilogram, second, and ampere is thus not justified. Equation 1 is always stated with $\delta = 1$ giving a fifth basic "unit" and the definition of the ampere is written in a form tacitly stating $a = 4¶$ which then is our sixth basic "unit".

From Equations 1 to 7 the formula for the force between two current elements is derived to be

$$\overline{d^2F} = \frac{\beta}{a^2} \cdot \frac{I_1 \overline{ds_1} \text{ x } (I_2 \overline{ds_2} \text{ x } \hat{r})}{r^2} \qquad \ldots.8$$

and it is seen that the unit for I may be fixed by specifying the force and the geometry in a standard experiment.

However, in the MKSA-system Equation 8 is normally stated in another form

$$\overline{d^2F} = \frac{\mu_0}{4¶} \frac{I_1 \overline{ds_1} \text{ x } (I_2 \overline{ds_2} \text{ x } \hat{r})}{r^2} \qquad \ldots..8a$$

where $\mu_0 = \beta/a$, as will be shown later. Implicit in the form of Equation 8a is thus the tacit assumption

$$a = 4¶$$

and this is the sixth basic "unit".

Electrostatics

Starting from Equation 3 electric field strength is defined as the force per unit charge

$$\overline{E} = \frac{\overline{F}}{q} = \frac{q'}{\alpha r^2} \hat{r} \qquad \ldots.9$$

If we change the electrostatic constant in Equation 3 from α to α^* then E will change to E^* and q to q^*. Here and in the following F is unchanged as we do not change the mechanical units.

$$F = \frac{q^* q'^*}{\alpha^* r^2} = \frac{q\, q'}{\alpha\, r^2} \qquad \ldots.10$$

and from this

$$\frac{q^*}{q} = \sqrt{\frac{\alpha^*}{\alpha}} \qquad \ldots.11$$

As

$$F = q \cdot E = q^* E^* \qquad \ldots.12$$

† e.g. Stratton, 1941, p. 18.

we have

$$\frac{E^*}{E} = \frac{q}{q^*} = \sqrt{\frac{\alpha}{\alpha^*}} \quad \ldots.13$$

The flux of electric field out through a sphere with radius *r* centred around a charge *q* is, by integration of Equation 9:

$$\Psi = \int_{\text{sphere}} \overline{E} \cdot \overline{da} = \int_{\text{sphere}} \frac{q}{\alpha r^2}\, da = \frac{4\P}{\alpha}\, q \quad \ldots.14$$

This is a special case of the more general Gauss' law:

$$\Psi = \frac{4\P}{\alpha} \int_{\text{Vol}} \rho dv \quad \ldots.15$$

or stated in differential form

$$\nabla \cdot \overline{E} = \frac{4\P}{\alpha}\ \rho \quad \ldots.16$$

where ρ is the measure-ratio for charge density.

Electric current in a conductor is introduced by Equation 5. If A is the cross-sectional area of the conductor then the current density is

$$J = \frac{I}{A} \quad \ldots.17$$

and in general a current density vector is introduced as the current per unit area oriented perpendicularly to the direction of flow of charge.

As the current flowing out of a closed surface is equal to the decrease of charge inside the surface the following continuity equation is valid

$$\nabla \cdot \overline{J} = -\frac{\partial \rho}{\partial t} \quad \ldots.18$$

If we change the electrostatic constant from α to α^* then J becomes J* and we have

$$\frac{J}{J^*} = \frac{\rho}{\rho^*} = \sqrt{\frac{\alpha}{\alpha^*}} \quad \ldots.19$$

The same transformation relation is valid for the current I

$$\frac{I}{I^*} = \sqrt{\frac{\alpha}{\alpha^*}} \quad \ldots.20$$

Magnetostatics

Despite intensive search for magnetic monopoles they have not been found (Fleischer, 1969), and they certainly do not play any role in the magnetostatic effects upon which the theory of electromagnetism is based.

This is often stated as an argument against explicitly writing Equation 4. However, it must be realized that the (mathematical) concept of a magnetic pole is extremely useful in describing forces between magnets, and inevitably every textbook introduces this concept when dealing with magnetized materials. So when the magnetic pole is introduced anyway, why not admit it openly by stating Equation 4 from the beginning taking advantage of its great pedagogic value:

$$F = \frac{mm'}{\beta \cdot r^2} \quad \ldots.\ 4$$

Changing the magnetostatic constant from β to β^* changes m to m* and we have the relation

$$\frac{m}{m^*} = \sqrt{\frac{\beta}{\beta^*}} \quad \ldots.21$$

Magnetic field strength is introduced as

$$H = \frac{F}{m} \quad \ldots.22$$

which gives

$$\frac{H}{H^*} = \sqrt{\frac{\beta^*}{\beta}} \quad \ldots.23$$

for a change of β to β^*.

The flux of the magnetic field out through a sphere is

$$\Phi = \int_{\text{sphere}} \overline{H} \cdot \overline{da} = 0 \quad \ldots.24$$

as magnetic poles always occur in opposite pairs. The differential form of this equation is

$$\nabla \cdot \overline{H} = 0 \quad \ldots.25$$

Electromagnetics

The field at the centre of a circular conductor can be measured by magnetostatic experiments (Gauss' method) and it is found that

$$H = \frac{2\P}{a} \cdot \frac{I}{r} \quad \ldots.26$$

where the factor 2¶ is due to the geometry as stated in the explanation to Equation 7.

This offers a magnetostatic definition of current as opposed to the electrostatic definition in Equation 5:

$$H = 2\P \frac{I_M}{r} \quad \ldots\ldots 26a$$

If $\alpha = 1$ then $I = I_E$ is the measure-ratio in the electrostatic system and if $\beta = 1$ at the same time then I_M is the measure-ratio in the electromagnetic system; now, from a list of conversion factors between E.M.U. and E.S.U. (ASTM Metric Practice Guide; Maxwell, 1954, Art. 787) it can be verified that for the same current

$$\frac{I_E}{I_M} = c \quad \ldots\ldots 27$$

where *c* is equal to the speed of light.

If we want to use I_E in Equation 26a we then have to write

$$H_M = \frac{2\P}{c} \frac{I_E}{r} \quad \ldots\ldots 26b$$

where H_M is the measure-ratio for the magnetic field when $\beta = 1$.

For $\alpha = 1$ and $\beta = 1$ we are thus forced to put $a = c$, and this is the characteristic of the Gaussian system.

Changing α from 1 to α^* and β from 1 to β^* we will have to change a from c to a^* and thus

$$H^* = \frac{2\P}{a^*} \cdot \frac{I^*}{r} \quad \ldots\ldots 26c$$

Using Equations 20 and 23 with $I = I_E$, $\alpha = 1$, and $H = H_M$, $\beta = 1$ we get

$$H^* = \frac{H_M}{\sqrt{\beta^*}} = \frac{2\P}{a^*} \cdot \frac{I^*}{r} = \frac{2\P}{a^*} \cdot \frac{I_E}{r} \sqrt{\alpha^*} \quad \ldots\ldots 26d$$

and from this

$$H_M = \frac{\dfrac{2\P \; I_E/r}{a^*}}{\sqrt{\alpha^* \; \beta^*}} \quad \ldots\ldots 26e$$

By comparison to Equation 26b it is seen that the general limitation on the three constants a, α, and β is

$$\frac{a}{\sqrt{\alpha \; \beta}} = c \quad \ldots\ldots 28$$

It must be remembered that a, α, and β stand for pure algebraic numbers and that c is a number too as it is determined as the ratio between the two measure-ratios I_E and I_M, themselves pure algebraic numbers.

The magnetic field at the centre of a circular conductor of radius r carrying the current I is, by Equation 7 or 26c

$$H = \frac{2\P}{a} \cdot \frac{I}{r} \quad \ldots\ldots 29$$

The force on a magnetic pole, m, would then be

$$F = H \cdot m = \frac{2\P}{a} \cdot \frac{I}{r} \cdot m \quad \ldots\ldots 30$$

and an equal, opposite force would exist on the conductor. This is the classical concept of 'action at a distance' between the magnetic pole and the current-carrying conductor. The force on the conductor may, however, also be considered a direct action from the field around it, in which case

$$F = \frac{2\P}{a} \frac{I}{r} \cdot H' \cdot \beta \cdot r^2 = \frac{\beta}{a} 2\P \, I \cdot H' \cdot r, \quad \ldots\ldots 31$$

where

$$H' = \frac{m}{\beta \; r^2} \quad \ldots\ldots 32$$

is the field at the circular conductor from the magnetic pole placed at its centre. Equation 31 may be derived assuming that the force $\overline{dF}$ on a current element I $\overline{ds}$ in a field $\overline{H}$ is

$$\overline{dF} = \frac{\beta}{a} I \; \overline{ds} \times \overline{H} \quad \ldots\ldots 33$$

At the distance r from a magnetic point-pole m the field is

$$\overline{H} = \frac{m}{\beta \; r^2} \; \hat{r} \quad \ldots\ldots 34$$

If this pole is at the centre of the current loop (current I, radius r) then the field is constant along the conductor and the current element I $\overline{ds}$ is perpendicular to $\overline{H}$; using $ds = rd\theta$ in Equation 33 we get

$$F = \frac{\beta}{a} \cdot I \cdot \frac{m}{\beta \; r^2} \int_0^{2\P} r d\theta = \frac{2\P}{a} \frac{I}{r} \cdot m \quad \ldots\ldots 35$$

which is the same as Equation 30, i.e. Equation 33 is a correct form of the force equation between a current element and a magnetic field.

The field $\overline{H}$ in Equation 33 may be generated by another current element $I_1 \; \overline{ds}_1$ at the distance $\overline{r} = \overline{r} \cdot \hat{r}$ from I $\overline{ds}$; using Equation 7 and the preceding remarks we get

$$d\overline{H}_1 = \frac{I_1}{a} \frac{\overline{ds_1} \times \hat{r}}{r^2} \qquad \ldots .36$$

which inserted into Equation 33 gives

$$d^2\overline{F} = \frac{\beta}{a^2} \frac{I\,\overline{ds} \times (I_1\,\overline{ds_1} \times \hat{r})}{r^2} \qquad \ldots .37$$

This is Equation 8 where $\hat{r}$ is a unit vector along $\overline{r}$.

Electrodynamics

From the experiments of Faraday, Maxwell states the induction law as: (Maxwell, 1954, Art. 541)

"The total electromotive force acting round a circuit at any instant is measured by the rate of decrease of the number of lines of magnetic force which pass through it."

The "total electromotive force" is the line-integral of the electric field strength along the closed circuit and the "number of lines of magnetic force which pass through it" is the flux of the magnetic field vector through a surface bounded by the circuit. Stated in mathematical form this is

$$V = \int_{\substack{\text{closed}\\\text{circuit}}} \overline{E} \cdot \overline{ds} \text{ proportional to } -\frac{d}{dt}\int_{\text{surface}} \overline{H} \cdot \overline{da} \qquad \ldots .38$$

Using Equations 13 and 23 this can be written as

$$\sqrt{\alpha}\int_{\substack{\text{closed}\\\text{circuit}}} \overline{E} \cdot \overline{ds} = -k \cdot \sqrt{\beta}\frac{d}{dt}\int \overline{H} \cdot \overline{da} \qquad \ldots .39$$

where the proportionality-factor k is independent of the unit system used, because $\sqrt{\alpha} \cdot \overline{E}$ and $\sqrt{\beta} \cdot \overline{H}$ are independent of the units. (Throughout this treatment F and the other mechanical units are assumed unchanged.)

The constant k may be determined by experiments. For our purpose we put $\alpha = \beta = 1$ and compare Equation 39 to Faraday's law in the Gaussian system. This gives $k = 1/c$ and from Equation 28 we get

$$\int \overline{E} \cdot \overline{ds} = -\frac{\beta}{a}\frac{d}{dt}\int \overline{H} \cdot \overline{da} \qquad \ldots .40$$

and the differential form is

$$\nabla \times \overline{E} = -\frac{\beta}{a}\frac{\partial \overline{H}}{\partial t} \qquad \ldots .41$$

Equation 40 may also be derived directly from Equation 33 by equating the mechanical and electric work involved in displacing a rigid, closed circuit in a static magnetic field (Slater and Frank, 1947, p. 210 f.).

Maxwell's equations in general form

The field around a linear current I is calculated from Equation 36

$$H = \frac{2}{a} \cdot \frac{I}{r} \qquad \ldots .42$$

The field lines are concentric circles around I.

The line-integral of H along one of the closed circular field lines is

$$\int_{\substack{\text{closed}\\\text{curve}}} \overline{H} \cdot \overline{ds} = \frac{2}{a} I \int_0^{2\P} \frac{r\,d\theta}{r} = \frac{4\P}{a} \cdot I \qquad \ldots .43$$

The general form of Equation 43 is Ampère law

$$\int_{\substack{\text{closed}\\\text{curve}}} \overline{H} \cdot \overline{ds} = \frac{4\P}{a} \Sigma\, I \qquad \ldots .44$$

where Σ I is the total encircled current. The differential form of Equation 44 is

$$\nabla \times \overline{H} = \frac{4\P}{a}\,\overline{J} \qquad \ldots .45$$

The Equations 41, 16, 25, and 45 with an added term are the basic equations for the combined, time-varying magnetic and electric fields:

$$\nabla \times \overline{E} = -\frac{\beta}{a}\frac{\partial \overline{H}}{\partial t} \qquad \ldots .41$$

$$\nabla \cdot \overline{E} = \frac{4\P}{\alpha}\rho \qquad \ldots .16$$

$$\nabla \cdot \overline{H} = 0 \qquad \ldots .25$$

and the incomplete equation

$$\nabla \times \overline{H} = \frac{4¶}{a} J \qquad \ldots 45$$

Of course, the fact that the constant c in Equation 28 is equal to the speed of light within the experimental error, inspired physicists to search for an electromagnetic theory of light. Maxwell saw that the electric and magnetic field vectors had to satisfy wave equations of the following form (Maxwell, 1954, Art. 784).

$$\nabla^2 \overline{E} - \frac{1}{c^2}\frac{\partial^2 \overline{E}}{\partial t^2} = f(x, y, z, t) \qquad \ldots 46$$

$$\nabla^2 \overline{H} - \frac{1}{c^2}\frac{\partial^2 \overline{H}}{\partial t^2} = g(x, y, z, t) \qquad \ldots 47$$

He could derive this from the four equations above if he added the term $\frac{\alpha}{a}\frac{\partial \overline{E}}{\partial t}$ to the right-hand side of Equation 45 giving

$$\nabla \times \overline{H} = \frac{4¶}{a}\overline{J} + \frac{\alpha}{a}\frac{\partial \overline{E}}{\partial t} \qquad \ldots 48$$

Applying ∇x and $\frac{\partial}{\partial t}$ to Equations 41 and 48 successively gives

$$\nabla \times (\nabla \times \overline{E}) + \frac{\beta}{a}\frac{\partial}{\partial t}(\nabla \times \overline{H}) = 0 \qquad \ldots 49$$

$$\frac{\partial}{\partial t}(\nabla \times \overline{E}) + \frac{\beta}{a}\frac{\partial^2 \overline{H}}{\partial t^2} = 0 \qquad \ldots 50$$

$$\nabla \times (\nabla \times \overline{H}) - \frac{\alpha}{a}\frac{\partial}{\partial t}(\nabla \times \overline{E}) = \frac{4¶}{a}(\nabla \times \overline{J}) \qquad \ldots 51$$

$$\frac{\partial}{\partial t}(\nabla \times \overline{H}) - \frac{\alpha}{a}\frac{\partial^2 \overline{E}}{\partial t^2} = \frac{4¶}{a}\frac{\partial \overline{J}}{\partial t} \qquad \ldots 52$$

Substituting Equation 50 into Equations 51 and 52 into Equation 49 and using the vector-operator relation

$$\nabla \times (\nabla \times \overline{A}) = \nabla (\nabla \cdot \overline{A}) - \nabla^2 \overline{A} \qquad \ldots 53$$

together with Equations 16 and 25 gives the wave equations

$$\nabla^2 \overline{H} - \frac{\alpha\beta}{a^2}\frac{\partial^2 \overline{H}}{\partial t^2} = \frac{4¶}{a}(\nabla \times \overline{J}) \qquad \ldots 54$$

$$\nabla^2 \overline{E} - \frac{\alpha\beta}{a^2}\frac{\partial^2 \overline{E}}{\partial t^2} = \frac{4¶}{\alpha}\nabla\rho + \frac{4¶\beta}{a^2}\frac{\partial \overline{J}}{\partial t} \qquad \ldots 55$$

where the constant in front of the time-derivatives of second order equals the reciprocal square of the speed of propagation in agreement with Equation 28.

Maxwell's modification of Equation 45 by adding the term $\frac{\alpha}{a}\frac{\partial \overline{E}}{\partial t}$ is quite understandable as he knew exactly what he was looking for. It is a piece of ingenious mathematical intuition and it led to the prediction and discovery of electromagnetic waves. The modification has no measurable effect on the description of experiments with static and slowly varying electromagnetic fields from which the Equations 41, 16, 25, and 45 were derived. Maxwell tried nevertheless after his successful accomplishment to explain and justify the modification in terms of the static electromagnetic concepts. This of course is impossible as it originates from an entirely different class of experiments. His attempt to explain $\frac{\partial \overline{E}}{\partial t}$ as "displacement current" is well known, and even in recent textbooks this notation is used, although it is clear that no current, i.e. transport of charge, is involved.

Lorenz (1867) suggested, two years after Maxwell, that the charge and current distributions in the Equations 15 and 44 should not be the instantaneous values, but the values r/c earlier where r is the distance from the observed point to the charge or current. His suggestion also leads to a solution of Maxwell's equations.

Lorenz had no difficulties with the interpretation of the modification. In his paper (Lorenz, 1867) he says:

"But as the laws of induced currents, generally admitted and based on experiment, did not lead to the expected result, the question was whether it was not possible so to modify the laws assumed that they would embrace both the experiments on which they rest and the phenomena which belong to the theory of light......... It is at once obvious that the equations, which are deduced in a purely empirical manner, are not necessarily the exact expression of the actual law; and it will always be permissible to add several members or to give the equations another form, always provided these changes acquire no perceptible influence on the results which are established by experiment."

This is the introduction, in 1867, of the correspondence principle, which has proven so successful in the theory of relativity and in quantum mechanics. It states that any new theory must approach the classical theory asymptotically when dealing with classical phenomena. Nobody today maintains that the quantum mechanical equations can be understood entirely in terms of classical mechanics and yet Maxwell's "displacement current" is still defended in textbooks.

Giorgi-pairs

The general form of Maxwell's equations independent of unit systems is

$$\nabla x \overline{E} + \frac{\beta}{a}\frac{\partial \overline{H}}{\partial t} = 0 \qquad \ldots . 56$$

$$\nabla \cdot \overline{H} = 0 \qquad \ldots . 57$$

$$\nabla \cdot \overline{E} = \frac{4\P}{\alpha}\,\rho \qquad \ldots . 58$$

$$\nabla x \overline{H} - \frac{\alpha}{a}\frac{\partial \overline{E}}{\partial t} = \frac{4\P}{a}\overline{J} \qquad \ldots . 59$$

If a new measure-ratio, $\overline{B}$, for magnetic field is defined as

$$\overline{B} = \frac{\beta}{a}\,\overline{H} \qquad \ldots . 60$$

and a new measure-ratio for electric field

$$\overline{D} = \frac{\alpha}{a}\,\overline{E} \qquad \ldots . 61$$

then Equations 56 to 59 become

$$\nabla x \overline{E} + \frac{\partial \overline{B}}{\partial t} = 0, \qquad \nabla \cdot \overline{B} = 0 \qquad \ldots . 62, 63$$

$$\nabla x \overline{H} - \frac{\partial \overline{D}}{\partial t} = \frac{4\P}{a}\overline{J}, \qquad \nabla \cdot \overline{D} = \frac{4\P}{a}\,\rho \quad \ldots . 64, 65$$

This form of Maxwell's equations is independent of the constants α and β, but these are of course reintroduced by the Equations 60 and 61 and instead of the four equations (Equations 56 to 59) we now need the six equations (Equations 60 to 65).

The two relations (Equations 60 and 61) have been referred to as the Giorgi conditions (Stopes-Roe, 1969) and for purpose of the present discussion the two members of a Giorgi condition will be called a Giorgi-pair†. In Equation 60 $\overline{B}$ is the Giorgi-mate of $\overline{H}$ and the process of transforming one to the other is called giorgization.

In discussing the effects of giorgization it is often necessary to distinguish between the two members of a Giorgi-pair; therefore if a Giorgi-pair is given

$$G_2 = \frac{\beta}{a} \cdot G_1 \qquad \ldots . 66$$

then G_1 is called the female member and G_2 the male member of the pair.† The same notation is used if the Giorgi-pair is related by

$$G_2 = \frac{\alpha}{a}\,G_1 \qquad \ldots . 67$$

Giorgization is not limited to the field vectors only. The magnetic moment of a current loop is (Stratton, 1941) introduced as

$$\overline{i_m} = I \cdot A \cdot \overline{n} \qquad \ldots . 68$$

where I is the current, A the area of the loop, and $\overline{n}$ a unit normal vector to A.

Others (Döring, 1948; and Bjerge, 1951) introduce the magnetic moment as

$$\overline{m_m} = \frac{\beta}{a} \cdot I \cdot A \cdot \overline{n} \qquad \ldots . 69$$

Clearly $\overline{i_m}$ and $\overline{m_m}$ are a Giorgi-pair as

$$\overline{m_m} = \frac{\beta}{a}\,\overline{i_m} \qquad \ldots . 70$$

Likewise magnetic poles, electric charges and all other electromagnetic measure-ratios may be giorgized.

An interesting feature of giorgization is that all formulas for force, torque, energy etc. contain both a male and female member of a giorgi-pair, side by side (both in numerator, or both in denominator).††

The torque on a magnetic dipole moment in a magnetic field is

$$\overline{T} = \overline{m_m} \times \overline{H} = \overline{i_m} \times \overline{B} \qquad \ldots . 71$$

The force on an electric charge in an electric field is

$$\overline{F} = q \cdot \overline{E} = q^* \cdot \overline{D} \qquad \ldots . 72$$

where

$$q = \frac{\alpha}{a} \cdot q^* \qquad \ldots . 73$$

The work involved in moving a charge in an electric field is

$$W = \int q \cdot \overline{E} \cdot d\overline{r} = \int q^* \cdot \overline{D} \cdot d\overline{r} \qquad \ldots . 74$$

†In analogy to Maxwell's electrostatic and magnetic pairs, Treatise, Art. 621.

†This notation has been suggested by G.V. Haines, Div. of Geomagnetism, Earth Physics Branch, EMR, Ottawa, Can.

††The Haines male-female rule.

and the energy associated with a current

$$P = V \cdot I = \int_{\text{circuit}} \bar{E} \cdot d\bar{s} \cdot I = \int_{\text{circuit}} \bar{D} \cdot d\bar{s} \cdot I^* \qquad \ldots . 75$$

where

$$I = \frac{\alpha}{a} \cdot I^* \qquad \ldots . 76$$

In view of this the force formula (Coulomb's law) looks like a monstrosity, but replacing one of the charges by its Giorgi-mate overcomes this problem

$$F = \frac{q\, q'}{\alpha\, r^2} = \frac{q^*\, q'}{a \cdot r^2} \qquad \ldots . 77$$

From these considerations it is clear that by giorgizing the proper measure-ratios according to the Haines male-female rule it is possible to completely eliminate the constants α and β from all the electromagnetic formulas.

This elimination is of course only apparent as every quantity now is expressed by two measure-ratios related by one of the Giorgi conditions (Equation 66 or 67).

Giorgi-transformation of a unit system

Starting from one unit system characterized by the constants α, β, and a (the mechanical units are untouched) and consequently giorgizing all the measure-ratios will give two new unit systems characterized by α^*, $\beta^*=\beta$, a^* and $\alpha^{**}=\alpha$, β^{**}, a^{**}.

Coulomb's law for electric charges gives

$$F = \frac{q\, q'}{\alpha\, r^2} = \frac{\frac{\alpha}{a} q^* \cdot \frac{\alpha}{a} q^{*\prime}}{\alpha\, r^2} = \frac{q^*\, q^{*\prime}}{\frac{a^2}{\alpha}\, r^2} \qquad \ldots . 78$$

which means that

$$\alpha^* = \frac{a^2}{\alpha} = c^2 \beta \qquad \ldots . 79$$

using Equation 28. Similarly we get for β^{**}

$$\beta^{**} = c^2 \alpha \qquad \ldots . 80$$

and thus

$$a^* = \frac{a^2}{\alpha} \qquad \ldots . 81$$

and

$$a^{**} = \frac{a^2}{\beta} \qquad \ldots . 82$$

By giorgizing the original system

$$\alpha, \beta, \underline{a} \qquad \ldots . 83$$

we thus express some of the formulas in the System (1)

$$c^2 \beta, \beta, \frac{a^2}{\alpha} \qquad \ldots . 84$$

and other formulas in the System (2)

$$\alpha, c^2 \alpha, \frac{a^2}{\beta} \qquad \ldots . 85$$

All three systems are proper unit systems as

$$\frac{a^2}{\alpha\, \beta} = c^2 \qquad \text{Original system} \qquad \ldots . 83a$$

$$\frac{a^4/\alpha^2}{c^2 \beta \cdot \beta} = c^2 \qquad \text{System (1)} \qquad \ldots . 84a$$

$$\frac{a^4/\beta^2}{\alpha \cdot c^2 \alpha} = c^2 \qquad \text{System (2)} \qquad \ldots . 85a$$

If α, β, and a are the characteristic constants of the unit system of Equations 56 to 59 then α^*, β^*, and a^* given by Equation 84 are the constants of the unit system of Equations 64 and 65, and α^{**}, β^{**}, and a^{**} given by Equation 85 are the constants of the unit system of Equations 62 and 63. As the measure-ratio for current in Equation 64 is unchanged from that of Equation 59 it means that current in System (1) is defined by the magnetostatic units (e.g. Equation 7) rather than by Equation 5 using a and not a^*.

The two new systems of course fulfil the conditions

$$\frac{\alpha^*}{a^*} = \frac{\beta^{**}}{a^{**}} = 1 \qquad \ldots . 85b$$

so Maxwell's equations appear with no constants in front of the time derivatives.

Maxwell's equations in material bodies

The general form of Maxwell's equations is

$$\nabla x \overline{E} + \frac{\beta}{a}\frac{\partial \overline{H}}{\partial t} = 0 \;;\quad \nabla\cdot\overline{H} = 0 \quad \ldots .56, 57$$

$$\nabla x \overline{H} - \frac{\alpha}{a}\frac{\partial \overline{E}}{\partial t} = \frac{4¶}{a}\overline{J}, \quad \nabla\cdot\overline{E} = \frac{4¶}{\alpha}\rho \ldots .59, 58$$

H.A. Lorentz assumed the validity of these equations inside material bodies provided ρ and $\overline{J}$ included charges and currents from the atoms of the material bodies (Casimir, 1969).

ρ is thus taken as

$$\rho = \rho_e + \rho_p \quad \ldots .86$$

and $\overline{J}$ as

$$\overline{J} = \overline{J}_e + \overline{J}_{at} \quad \ldots .87$$

The division in external and material contributions is, as pointed out by Casimir, to a certain extent arbitrary; and ρ_p and $\overline{J}_{at}$ are statistical descriptions of the effect of the presence of matter.

For a small elementary volume, dv_n containing a large number of atoms in order to make average values statistically meaningful, the electric dipole moment per unit volume, $\overline{P_n}$ is introduced as

$$\overline{P_n} = \frac{1}{dv_n} \sum_{dv_n} \overline{m_e}^{\,i} \quad \ldots .88$$

where $\overline{m_e}^i$ is the i'th point-dipole inside dv_n. By a process of continuization (Knudsen, 1955) all the $\overline{P_n}$- values assigned to the individual volume elements, dv_n, are replaced by a continuous vector field $\overline{P}$ having the value $\overline{P} = \overline{P_n}$ at some point inside each volume element dv_n.

This polarization vector field $\overline{P}$ may be visualized as strings of dipoles starting with a negative charge and terminating with a positive. According to the Poisson-Thomson analysis (O'Rahilly, 1938, p. 37 ff) $\overline{P}$ is equivalent to a charge distribution ρ_p where

$$\rho_p = -\nabla\cdot\overline{P} \quad \ldots .89$$

A positive $\nabla\cdot\overline{P}$ means that more strings of dipoles are leaving the elementary volume than entering it, which in turn means that there are some negative ends of dipole strings inside the volume, hence the minus sign.

Equation 89 may be considered an "equation of continuity" following from the fact that the total charge of a collection of dipoles is zero.

The splitting into external and atomic contributions is arranged so that the external charges and currents satisfy the equation of continuity

$$\nabla\cdot\overline{J}_e + \frac{\partial \rho_e}{\partial t} = 0 \quad \ldots .90$$

and the same holds for the atomic charges and currents

$$\nabla\cdot\overline{J}_{at} + \frac{\partial \rho_p}{\partial t} = 0 \quad \ldots .90a$$

or

$$\nabla\cdot\left\{\overline{J}_{at} - \frac{\partial}{\partial t}\overline{P}\right\} = 0 \quad \ldots .91$$

We may then write

$$\overline{J}_{at} = \frac{\partial \overline{P}}{\partial t} + \frac{a}{\beta}\nabla x \overline{M} \quad \ldots .92$$

or

$$\overline{J}_{at} = \overline{J}_p + \overline{J}_{amp} \quad \ldots .93$$

where $\overline{J}_p$ is the current due to changes in polarization and $\overline{J}_{amp}$ are the amperean neutral currents.

$\overline{M}$ is the magnetization vector derived as a mathematical continuization of the magnetic moment per unit volume analogous to $\overline{P}$.

The atoms contain small current loops originating in orbiting and spinning electrons and spinning nuclear particles. The actual description belongs to the quantum mechanics, but for our purpose it is sufficient to postulate an equivalent amperean current loop associated with every atom. The magnetic moment of the i'th current loop in an elementary volume dv_n, large enough to render average values statistically significant, is given by Equation 69

$$\overline{m_m}^{\,i} = \frac{\beta}{a}\cdot I_i \circ A_i \cdot \overline{n}_i \quad \ldots .94$$

where I_i is the current and A_i the area of the current loop.

The magnetic moment per unit volume is

$$\overline{M}_n = \frac{1}{dv_n}\sum_i \overline{m_m}^{\,i} \quad \ldots .95$$

and the continuization of all the $\overline{M}_n$'s is the vector field $\overline{M}$. $\overline{M}$, described by the equivalent current density distribution

$$\overline{J}_{amp} = \frac{a}{\beta} \nabla \times \overline{M} \quad \ldots .96$$

and $\overline{P}$, described by the equivalent charge density distribution

$$\rho_p = - \nabla \cdot \overline{P} \quad \ldots .97$$

are two mathematical models representing the effects of the presence of matter.

Equation 91 follows from

$$\nabla \cdot \overline{J}_{amp} = 0 \quad \ldots .98$$

which means that the amperean currents are neutral.

Maxwell's Equations 56 to 59, using Equations 86, 87, 92, 93, and 89 become

$$\nabla \times \overline{E} + \frac{\beta}{a}\frac{\partial \overline{H}}{\partial t} = 0, \quad \nabla \cdot \overline{H} = 0 \quad \ldots .99, 100$$

$$\nabla \times \overline{H} - \frac{\alpha}{a}\frac{\partial \overline{E}}{\partial t} = \frac{4¶}{a}\overline{J}_e + \frac{4¶}{a}\frac{\partial \overline{P}}{\partial t} + \frac{4¶}{\beta}\nabla \times \overline{M} \quad \ldots .101$$

$$\nabla \cdot \overline{E} = \frac{4¶}{\alpha}\rho_e - \frac{4¶}{\alpha}\nabla \cdot \overline{P} \quad \ldots .102$$

Equations 99 to 102 are Maxwell's equations for magnetic and electric fields inside material bodies. The contributions from the atoms of the present matter are accounted for by the space-average vectors $\overline{P}$ and $\overline{M}$, electric and magnetic dipole moment per unit volume.† J_e and ρ_e are the external current and charge densities.

To solve the equations we must know something about $\overline{P}$ and $\overline{M}$ besides $\overline{J}_e$ and ρ_e.

The solution to the 'external' problem, $\overline{H}_e$ and $\overline{E}_e$, is given by

$$\nabla \times \overline{E}_e + \frac{\beta}{a}\frac{\partial \overline{H}_e}{\partial t} = 0, \quad \nabla \cdot \overline{H}_e = 0 \quad \ldots .103, 104$$

$$\nabla \times \overline{H}_e - \frac{\alpha}{a}\frac{\partial \overline{E}_e}{\partial t} = \frac{4¶}{a}\overline{J}_e, \quad \nabla \cdot \overline{E}_e = \frac{4¶}{\alpha}\rho_e \quad \ldots .105, 106$$

†A consequence of using P and M is that E and H now represent the space-average fields.

$\overline{H}_e$ and $\overline{E}_e$ may be interpreted as the fields we would have if the material bodies were removed. Subtracting Equations 103 to 106 from Equations 99 to 102 and introducing

$$\overline{H}_I = \overline{H} - \overline{H}_e \quad \ldots .107$$

$$\overline{E}_I = \overline{E} - \overline{E}_e \quad \ldots .108$$

gives

$$\nabla \times \overline{E}_I + \frac{\beta}{a}\frac{\partial \overline{H}_I}{\partial t} = 0, \quad \nabla \cdot \overline{H}_I = 0 \quad \ldots .109, 110$$

$$\nabla \times \overline{H}_I - \frac{\alpha}{a}\frac{\partial \overline{E}_I}{\partial t} = \frac{4¶}{a}\frac{\partial \overline{P}}{\partial t} + \frac{4¶}{\beta}\nabla \times \overline{M} \quad \ldots .111$$

$$\nabla \cdot \overline{E}_I = - \frac{4¶}{\alpha}\nabla \cdot \overline{P} \quad \ldots .112$$

where (H_I, E_I) is the solution to the 'internal' problem, i.e. the field contributions from $\overline{P}$ and $\overline{M}$. The total fields $\overline{E}$ and $\overline{H}$ are thus made up of the partial fields $\overline{E}_e + \overline{E}_I$ and $\overline{H}_e + \overline{H}_I$.

$\overline{P}$ and $\overline{M}$ are normally dependent on the field vectors; but whether the 'primary' cause is $(\overline{E}, \overline{H})$, $(\overline{E}_e, \overline{H}_e)$ or $(\overline{E}_I, \overline{H}_I)$ is impossible to say as all three sets of vectors are interdependent. If $\overline{P}$ and $\overline{M}$ have constant parts unaffected by $\overline{E}_e$ and $\overline{H}_e$ it is reasonable to assume $\overline{E}_I$ and $\overline{H}_I$ to be the causes†, but if $\overline{P}$ and $\overline{M}$ have parts dependent also on $\overline{E}_e$ and $\overline{H}_e$ these vectors as well (i.e. the total vectors $\overline{E}$ and $\overline{H}$) must be regarded as the causes.

The torque, $\overline{T}$, on a magnetic dipole, $\overline{m}_m$, in a field, $\overline{H}$, is

$$\overline{T} = \overline{m}_m \times \overline{H} \quad \text{or} \quad T = m_m \cdot H \cdot \sin\theta \quad \ldots .113$$

where θ is the angle between the directions of $\overline{m}_m$ and $\overline{H}$. The work involved in changing θ from θ_1 to θ_2 is

$$W_{mag} = \int_{\theta_1}^{\theta_2} m_m \cdot H \cdot \sin\theta \, d\theta = - m_m H(\cos\theta_2 - \cos\theta_1) \quad \ldots .114$$

†For ferromagnetic materials H_I is not sufficient to explain the very strong spontaneous magnetization existing in the domains. The actual explanation is based on exchange integrals and belongs to quantum mechanics.

If $\theta_1 = 0$ is chosen then

$$W_{mag} = - m_m H(\cos\theta_2 - 1) \cdot \qquad \ldots .115$$

is the potential energy of a magnetic dipole $\overline{m}_m$ in a field $\overline{H}$ where the direction of the dipole has the angle θ_2 to the field. The zero level of the potential energy is arbitrary so we may express

$$W_{mag} = - \overline{m}_m \cdot \overline{H} \qquad \ldots .116$$

From this we have the potential energy of a volume element dv of a magnetized body

$$dW_{mag} = - \overline{M} \cdot \overline{H}\, dv \qquad \ldots .116a$$

Normally there is also some mechanical energy associated with the magnetization so the total energy is

$$dW_{tot} = - \overline{M} \cdot \overline{H}\, dv + dW_{mech} \qquad \ldots .117a$$

If the mechanical potential energy dW_{mech} is independent of the direction of $\overline{M}$ in the volume element then Equation 117a has a minimum when

$$dW_{mag} = - \overline{M} \cdot \overline{H}\, dv \qquad \ldots .117$$

is minimum. The directional independence of dW_{mech} is the characteristic feature of the magnetically isotropic materials, in these materials $\overline{M}$ is thus parallel to $\overline{H}$ everywhere.

Anisotropic materials have dW_{mech} dependent on the orientation of $\overline{M}$ so that the total potential energy dW_{tot} is not necessarily minimum when $\overline{M}$ is parallel to $\overline{H}$, which means that in general $\overline{M}$ and $\overline{H}$ have different directions.

In some materials $\overline{M}$ is a linear function of $\overline{H}$. For isotropic materials

$$\overline{M} = k_m \cdot \overline{H} \qquad \ldots .118$$

where k_m is the scalar proportionality factor between $\overline{H}$ and $\overline{M}$.† In the case of anisotropy we have

$$\overline{M} = \{k\} \cdot \overline{H} \qquad \ldots .118a$$

†Mason & Weaver (1929) uses this notation with $\frac{4¶}{\beta} k_m = (1 - \frac{1}{\mu_r})$.

where (k) is a 3 X 3 matrix.

For the ferromagnetic materials, however, the relation between $\overline{M}$ and $\overline{H}$ is more involved than expressed by Equations 118 and 118a:

$$\overline{M} = \sum_{n=0}^{\infty} \begin{pmatrix} + \\ (-1)^{n-1} \end{pmatrix} m_n \overline{H}^n \qquad \ldots .118b$$

where + is taken if H is decreasing and $(-1)^{n-1}$ if H is increasing. Furthermore the coefficients m_n are dependent on the immediately preceding maximum value of H. This is still the isotropic case where $\overline{M}$ is parallel to $\overline{H}$, so if anisotropy is introduced the relation between $\overline{M}$ and $\overline{H}$ becomes even more complicated.

Traditionally†, still another set of vector quantities is introduced in the treatment of magnetic and dielectric materials.

The basic Equations 101 and 102 are rearranged in the following manner

$$\nabla x \left\{ \overline{H} - \frac{4¶}{\beta} \overline{M} \right\} - \frac{\alpha}{a} \frac{\partial}{\partial t} \left\{ \overline{E} + \frac{4¶}{\alpha} \overline{P} \right\} = \frac{4¶}{a} \overline{J}_e \qquad \ldots .119$$

and

$$\nabla \cdot \left\{ \overline{E} + \frac{4¶}{\alpha} \overline{P} \right\} = \frac{4¶}{\alpha} \rho_e \qquad \ldots .120$$

Two new vectors are then introduced

$$\overline{K} = \overline{H} - \frac{4¶}{\beta} \overline{M} \qquad \ldots .121$$

$$\overline{G} = \overline{E} + \frac{4¶}{\alpha} \overline{P} \qquad \ldots .122$$

and inserted into Equations 99 to 102

$$\nabla x \overline{G} + \frac{\beta}{a} \frac{\partial \overline{K}}{\partial t} = \frac{4¶}{\alpha} \nabla x \overline{P} - \frac{4¶}{a} \frac{\partial \overline{M}}{\partial t} \qquad \ldots .123$$

$$\nabla \cdot \overline{K} = - \frac{4¶}{\beta} \nabla \cdot \overline{M} \qquad \ldots .124$$

$$\nabla x \overline{K} - \frac{\alpha}{a} \frac{\partial \overline{G}}{\partial t} = \frac{4¶}{a} \overline{J}_e \qquad \ldots .125$$

$$\nabla \cdot \overline{G} = \frac{4¶}{\alpha} \rho_e \qquad \ldots .126$$

†Introduced by Maxwell.

There are two mathematical models of polarized media in existence. The Poisson-Thomson model replaces a polarized dielectric by an equivalent charge density distribution

$$\rho_p = -\nabla\cdot\overline{P} \qquad \ldots.97$$

and the amperen model replaces a magnetized medium by an equivalent current density distribution

$$\overline{J}_{amp} = \frac{a}{\beta}\nabla xM \qquad \ldots.96$$

Maxwell's equations for material bodies Equations 99 to 102 contain the terms $\nabla x\overline{M}$, $\nabla\cdot\overline{P}$ and $\frac{\partial\overline{P}}{\partial t}$ because in the derivation we used the amperean model for magnetic materials and the Poisson-Thomson model for dielectrics. In the Equations 123 to 126 we have the reverse situation as the terms $\nabla x\overline{P}$, $\nabla\cdot\overline{M}$ and $\frac{\partial\overline{M}}{\partial t}$ indicate the amperean model for dielectrics and the Poisson-Thomson model for magnetic materials.

The two models give the same field outside the polarized bodies, but in predicting the internal fields they differ. The Poisson-Thomson model is, however, often used to calculate the field around a magnetized body because of its analogy to similar problems already solved in electrostatics, but for calculating the internal magnetic fields this model fails to explain the experimental results and must be rejected. The self-induction of an air-cored coil increases when the coil is filled with magnetic material, indicating an increased internal field according to the amperean model. The $\overline{K}$-field is thus a hypothetical field based on a wrong model for magnetized materials.

Similarly the $\overline{G}$-field is a hypothetical field based on the amperean model for dielectrics. This model fails to explain experiments with the internal fields in dielectrics. The capacity of a condenser increases if the empty space between the plates is filled with a dielectric indicating a decreased field as predicted by the Poisson-Thomson model.

The question of $\overline{K}$-field vs. $\overline{H}$-field and $\overline{G}$-field vs. $\overline{E}$-field is closely related to the question of the existence of a free magnetic pole. In Equation 124 the term $-\nabla\cdot\overline{M}$ is equivalent to a magnetic charge density

$$m = -\nabla\cdot\overline{M} \qquad \ldots.97a$$

and in Equation 123 the terms $\frac{a}{\alpha}\nabla x\overline{P}$ and $\frac{\partial\overline{M}}{\partial t}$ are equivalent to a density of "magnetic current"

$$\overline{J}_m = \frac{\partial\overline{M}}{\partial t} - \frac{a}{\alpha}\nabla\times\overline{P} \qquad \ldots.96a$$

In the section on Giorgi-pairs it is shown that by introducing two units for electric field and two units for magnetic field it is possible to remove the constants in Maxwell's equations. To justify this, the MKSA-formulation simultaneously adopts both models for dielectrics and for magnetic materials, assigning different units to the resulting two electric and two magnetic fields. The $\overline{D}$, $\overline{E}$, $\overline{B}$ and $\overline{H}$-fields in the MKSA-formulation are thus related to the $\overline{G}$, $\overline{E}$, $\overline{H}$ and $\overline{K}$-fields in the notation used here by

$$\overline{D}_{MKSA} = \frac{\alpha}{a}\overline{G}$$

$$\overline{E}_{MKSA} = \overline{E}$$

$$\overline{B}_{MKSA} = \frac{\beta}{a}\overline{H}$$

$$\overline{H}_{MKSA} = \overline{K}$$

Static fields in material bodies

For static and slowly varying fields where the time-derivatives may be neglected the magnetic and electric fields can be separated. This leads to

$$\nabla x\overline{G} = \frac{4¶}{\alpha}\nabla x\overline{P}\ ; \qquad \nabla\cdot\overline{G} = \frac{4¶}{\alpha}\rho_e \qquad \ldots.127, 128$$

$$\nabla x\overline{K} = \frac{4¶}{a}\overline{J}_e\ ; \qquad \nabla\cdot\overline{K} = \frac{4¶}{\beta}\nabla\cdot\overline{M} \ldots 129, 130$$

Considering the magnetostatic part (Equations 129 and 130) we see that if the magnetization vector $\overline{M}$ is divergence-free then $\overline{K}$ is the solution to the external problem. An infinitely long cylinder magnetized uniformly along the axis is a case where $\nabla\overline{M} = 0$ and thus $\overline{K} = \overline{H}_e$. A toroid magnetized uniformly along its circular axis is another example of a body with divergence-less magnetization having $\overline{K} = \overline{H}_e$.

For *isotopic materials* $\overline{M}$ and $\overline{H}$ are collinear and proportional (Equation 118). From the definition (Equation 121) it then follows that $\overline{K}$ is proportional to and collinear with $\overline{H}$ which gives the following interpretation of $\overline{K}$.

A volume element dv, with magnetization $\overline{M}$ and the total field $\overline{H}$ inside a body of arbitrary geometrical shape, has a vector $\overline{K}$ equal to the external field H_e^c that applied axially to an infinite cylinder of the same material would produce the same magnetization $\overline{M}$ and the same total field $\overline{H}$.

For the volume element we have

$$\overline{H} = \overline{H}_e + \overline{H}_I = \overline{K} + \frac{4¶}{\beta}\overline{M} \qquad \ldots.131$$

and for the hypothetical cylinder

$$H = \overline{H}_e^c + \overline{H}_I^c = \overline{K} + \frac{4¶}{\beta}\overline{M} \qquad \ldots.132$$

H_I^c is the field from the distribution of magnetic moment per unit volume in the cylinder which may be calculated from Equations 110 and 111

$$\bar{H}_I^c = \frac{4¶}{\beta}\bar{M} \quad \ldots .133$$

In the body of arbitrary shape the distribution of $\bar{M}$ in general gives a field H_I different from $\frac{4¶}{\beta}\bar{M}$, e.g. for uniformly magnetized sphere we have

$$\bar{H}_I = \frac{2}{3}\cdot\frac{4¶}{\beta}\bar{M} \quad \ldots .134$$

and in the general case

$$\bar{H}_I = \frac{1}{\beta}\int_{Vol} \nabla' x[\bar{M} x \nabla\left(\frac{1}{r}\right)]dv \quad \ldots .135$$

where dv is at (x,y,z), $\bar{H}_I$ at (x',y',z'), $\bar{M}$ at (x,y,z) and $\bar{r} = \{(x'-x),(y'-y),(z'-z)\}$. The operator ∇' works only on (x',y',z'), and ∇ only on (x,y,z).

Equations 132 and 133 give $H_e^c = \bar{K}$ and Equation 131 gives

$$\bar{K} = \bar{H}_e - \left\{\frac{4¶}{\beta}\bar{M} - \bar{H}_I\right\} \quad \ldots .136$$

but as H_I from Equation 135 is dependent on the geometry it is seen that $\bar{K}$ is dependent on the shape of the body.

$$\bar{K}_D = \frac{4¶}{\beta}\bar{M} - \bar{H}_I$$

is normally referred to as the demagnetizing force.

From Equations 118 and 121 we may deduce

$$\bar{H} = \bar{K} + \frac{4¶}{\beta}\bar{M} = \bar{K} + \frac{4¶}{\beta}\cdot k_m \cdot \bar{H} \quad \ldots .137$$

and from this

$$\bar{H} = \frac{1}{1-\frac{4¶}{\beta}k_m}\bar{K} \quad \ldots .138$$

$$\bar{M} = \frac{k_m}{1-\frac{4¶}{\beta}k_m}\bar{K} \quad \ldots .139$$

The factor $\kappa_m = 1/(1-\frac{4¶}{\beta}k_m)$ is normally called the magnetic permeability and $\chi_m = k_m/(1-\frac{4¶}{\beta}k_m)$ the suscepti-ceptibility of the material.

κ_m and χ_m preassumes the introduction of the geometry-dependent, hypothetical vector K; which the paremeter k_m does not, Stratton (1941, p. 12) remarks that k_m would be a more logical way to describe the magnetic materials although he abstains from using this notation due to the traditionally adopted parameters κ_m and χ_m.

Anisotropic materials are normally investigated by cutting long cylinders out in the directions of the anisotropy axes and measuring κ_m or χ_m in these directions. From these measurements the matrix $\{k\}$ in Equation 118a may be constructed and used in further calculations.

The ferromagnetic materials present a special problem. An approximate solution is sometimes possible by assuming $\bar{M}$ to consist of a constant part $\bar{M}_0$ and a part $\bar{M}_H$ proportional to $\bar{H}$.

If Equation 118 and its analog for electric polarization

$$\bar{P} = k_e\cdot\bar{E} \quad \ldots .140$$

are introduced in Maxwell's Equations 99 to 102 we get

$$\nabla x\bar{E} + \frac{\beta}{a}\frac{\partial\bar{H}}{\partial t} = 0\ ; \qquad \nabla\cdot\bar{H} = 0 \quad \ldots .141, 142$$

$$\nabla x\bar{H} - \frac{\alpha}{a}\frac{\partial\bar{E}}{\partial t} = \frac{4¶}{a}\bar{J}_e + \frac{4¶}{a}\frac{\partial}{\partial t}(k_e\cdot\bar{E}) + \frac{4¶}{\beta}\nabla x(k_m\cdot\bar{H}) \quad \ldots .143$$

$$\nabla\cdot\bar{E} = \frac{4¶}{\alpha}\rho_e - \frac{4¶}{\alpha}\nabla\cdot(k_e\cdot\bar{E}) \quad \ldots .144$$

$$\nabla x\bar{E} + \frac{\beta}{a}\frac{\partial\bar{H}}{\partial t} = 0\ ; \qquad \nabla\cdot\bar{H} = 0 \quad \ldots .145, 146$$

$$\nabla x\left\{(1-\frac{4¶}{\beta}k_m)\bar{H}\right\} - \frac{\alpha}{a}\frac{\partial}{\partial t}\left\{(1+\frac{4¶}{\alpha}k_e)\bar{E}\right\} = \frac{4¶}{a}\bar{J}_e \quad \ldots .147$$

$$\nabla\cdot\left\{(1+\frac{4¶}{\alpha}k_e)\bar{E}\right\} = \frac{4¶}{\alpha}\rho_e \quad \ldots .148$$

These equations assume *isotropy* so k_m and k_e are scalars; if we also assume *homogeneous* materials, i.e. k_m and k_e are constants inside the material bodies, we have for interior points

$$\nabla x \overline{E} + \frac{\beta}{a}\frac{\partial \overline{H}}{\partial t} = 0\,, \qquad \nabla \cdot \overline{H} = 0 \qquad \ldots . 149, 150$$

$$\nabla x \overline{H} - \frac{(1 + \frac{4\P}{\alpha} k_e)}{(1 - \frac{4\P}{\beta} k_m)} \cdot \frac{\alpha}{a}\frac{\partial \overline{E}}{\partial t} = \frac{1}{(1 - \frac{4\P}{\beta} k_m)} \cdot \frac{4\P}{a} \overline{J}_e \qquad \ldots . 151$$

$$\nabla \cdot \overline{E} = \frac{1}{(1 + \frac{4\P}{\alpha} k_e)} \frac{4\P}{\alpha} \rho_e \qquad \ldots . 152$$

By introducing three new constants $\alpha' = (1 + \frac{4\P}{\alpha} k_e)\alpha, \beta' = (1 - \frac{4\P}{\beta} k_m)\beta$ and $a' = (1 - \frac{4\P}{\beta} k_m)\, a$ the equations are given the form

$$\nabla x \overline{E} + \frac{\beta'}{a'}\frac{\partial \overline{H}}{\partial t} = 0, \qquad \nabla \cdot \overline{H} = 0 \qquad \ldots . 153, 154$$

$$\nabla x \overline{H} - \frac{\alpha'}{a'}\frac{\partial \overline{E}}{\partial t} = \frac{4\P}{a'} \overline{J}_e \qquad \ldots . 155$$

$$\nabla \cdot \overline{E} = \frac{4\P}{\alpha'} \rho_e \qquad \ldots . 156$$

so that a change of constants formally accounts for the presence of material bodies.

The effective speed of propagation is thus changed from c to c'.

$$c' = \frac{a'}{\sqrt{\alpha' \cdot \beta'}} = c\sqrt{\frac{(1 - \frac{4\P}{\beta} k_m)}{(1 + \frac{4\P}{\alpha} k_e)}} \qquad \ldots . 157$$

as a result of a complicated interaction between the electromagnetic wave and the atoms of the present matter.

Unit systems

On the preceding pages it is shown that a unit system is completely determined by six basic "units" including the constants δ, α, γ, a, and β in this concept. Two sets of mechanical units are in common use, the cm, the sec., the gram, and $\delta = 1$ called the c.g.s.-system, and the metre, the kilogram and the sec. also with $\delta = 1$ called the MKS-system. The reason for including δ in the analysis is that other unit systems having $\delta \neq 1$ exist and so this constant is necessary to make the equations fully general.

Specifying c.g.s. or MKS and tacitly assuming $\delta = 1$ then determines the unit for force in the two systems. If a measure-ratio for force is $F_{c.g.s.}$ in the c.g.s.-system and F_{MKS} in the MKS-system we have

$$F_{MKS} = 1o^{-5} \circ \overline{F}_{c.g.s.} \qquad \ldots . 158$$

and the speed of light in the two systems is

$$c_{MKS} = 1o^{-2} \cdot c_{c.g.s.} \qquad \ldots . 159$$

The electromagnetic units are then specified by choosing two of the three constants α, β, and a. The values of these constants are characteristic for the unit system and once they have been stated no need really exists for any names of the units. This is the reason for the common practice of stating E.M.U. or E.S.U. after measure-ratios when using the equations of the absolute electromagnetic system of the electrostatic system.

Table I gives the values of the constants in the three c.g.s.-systems, in the Practical system, in the MKS-system and in the three versions of the giorgized, rationalized MKSA-system, which is the SI presently being adopted internationally.

The constant c is the measure-ratio for the speed of light using the mechanical units of each particular system.

The absolute electromagnetic system is referred to as E.M.U. and so is the magnetostatic part of the Gaussian system. Maxwell's electrostatic system and the electrostatic part of the Gaussian system are called E.S.U.

The absolute electromagnetic system is in a sense the basic unit system as both the practical system and the MKS-system are derived from it.

The practical system has $\alpha = (\frac{10}{c})^2$ and $a = 10$ which make the unit of current equal to the technical unit, ampere. (1 E.M.U. = 10 amperes). The practical unit for potential difference then becomes 10 times bigger than the E.M.U. for potential (1 E.M.U. = 10^{-1} pra-volts). In the practical system Equation 40 is

$$V = \int \overline{E} \cdot \overline{ds} = -\frac{1}{1o}\frac{d}{dt}\int \overline{H} \cdot \overline{da} \qquad \ldots . 160$$

Table I Characteristic constants of electromagnetic unit systems

Unit System		α	β	a	Mechanical units (δ=1)
Gaussian		1	1	c	c.g.s.
Absolute Electromagnetic		$\frac{1}{c^2}$	1	1	c.g.s.
Maxwell's Electrostatic		1	$\frac{1}{c^2}$	1	c.g.s.
Practical (ampere)		$\frac{100}{c^2}$	1	10	c.g.s.
MKS (volt, ampere)		$\frac{10^7}{c^2}$	10^{-7}	1	MKS
Giorgized, Rationalized MKSA-System (Giorgi-Syst. or SI)	Basic	$\frac{10^7}{c^2}$	$(4¶)^2 \cdot 10^{-7}$	4¶	MKS
	Subsyst. (1)	$(4¶c)^2 \cdot 10^{-7}$	$(4¶)^2 \circ 10^{-7}$	$(4¶c)^2 \cdot 10^{-7}$	
	Subsyst. (2)	$\frac{10^7}{c^2}$	10^7	10^7	

substituting N for $\int \bar{H} \cdot \overline{da}$ and introducing volts by dividing both sides by 10^7 gives (1 volt = 10^8 E.M.U.):

$$V' = \frac{V}{10^7} = -10^{-8}\frac{dN}{dt} \quad \ldots. 161$$

which is the familiar form of Faraday's law in the practical system. As $\beta = 1$ the magnetostatic measure-ratios are in E.M.U., V is in pra-volts and V′ in volts. Because the volt is not the "natural" practical unit for potential difference it became necessary to state explicitly "V′ in volts" and to include the conversion factor 10^7.

This conversion factor of 10^7 between volts and pra-volts was considered impractical so a search for a new unit system based on the volt and the ampere began.

Because of a confusion between conversion factors and constants of nature in the equations the idea came up that by choosing a "proper" unit system any factor in the equations could be eliminated.

In E.M.U. Maxwell's Equations 56 to 59 are

$$\nabla x\bar{E} + \frac{\partial \bar{H}}{\partial t} = 0, \qquad \nabla \cdot \bar{H} = 0 \quad \ldots. 162, 163$$

$$\nabla x\bar{H} - \frac{1}{c^2}\frac{\partial \bar{E}}{\partial t} = 4¶ \cdot \bar{J}, \qquad \nabla \cdot \bar{E} = 4¶c^2 \rho \ldots. 164, 165$$

and in the Gaussian system

$$\nabla x\bar{E} + \frac{1}{c}\frac{\partial \bar{H}}{\partial t} = 0, \qquad \nabla \cdot \bar{H} = 0 \quad \ldots. 166, 167$$

$$\nabla x\bar{H} - \frac{1}{c}\frac{\partial \bar{E}}{\partial t} = \frac{4¶}{c} \cdot \bar{J}, \qquad \nabla \cdot \bar{E} = 4¶ \circ \rho \ldots. 168, 169$$

The $\frac{1}{c}$ and $\frac{1}{c^2}$ constants and especially the 4¶-factors annoyed people. Oliver Heaviside considered the 4¶'s "irrational" and suggested the equations "rationalized" by simply removing the 4¶-factors. Now, the only way to remove the 4¶'s is to choose a = 4¶ and multiply the two other constants α and β by 4¶. Obviously the units then change by factors like $\sqrt{4¶}$ or $1/\sqrt{4¶}$ and the 4¶'s will emerge in other equations, but this did not seem to bother Heaviside. In fact very few people seem to realize what "rationalization" is, and even in recent literature the confusion exists (Avčin, 1961, pp. 5 and 10).

The choice of the values of α, β, and a is, of course, a matter of taste, and it has as such been discussed violently. No real physical arguments can be put forward in favour of one choice over the other; the only thing to be said is that there is no reason for choosing a set of values that will give grossly impractical constants in the equations, or complicated conversion factors to other unit systems.

The statement that, for instance, $\alpha = 1$, $\beta = 1$, and $a = c$ cause 4¶-factors to appear where "they have nothing to do with the geometry" is purely emotional; who can, anyway, say where 4¶-factors really "ought to" be? Maybe Newton's law for mass-attraction really "ought to" be

$$F = \frac{\gamma}{4\P} \frac{MM'}{r^2} \quad \ldots . 170$$

and Newton's second law

$$F = \frac{1}{\sqrt{4\P}} \overline{M} \frac{d^2r}{dt^2} \quad \ldots . 171$$

by rationalizing the mass unit?

However, a new unit system was desired and the conditions it had to satisfy were:

1) 1 Volt = 10^8 E.M.U. should be the unit for potential difference.
2) 1 ampere = 10^{-1} E.M.U. should be the unit for current.
3) No constants in Maxwell's equations.

As will be shown later 3) is contradictory to 1) and 2), but by the technique called giorgization the constants have been removed from Maxwell's equations and put into the Giorgi-conditions. It thus appears as if 3) is fulfilled; but it is not, and the manipulation has caused great confusion in electromagnetic theory.

Logometric formulas

To analyze the problem of changing the E.M.U. to a system having volt and ampere as the units for potential difference and current, we have to investigate the effects of changing also the mechanical units including the constant δ.

In the following the unmarked symbols stand for measure-ratios in the absolute electromagnetic system defined by gram, second, centimetre, $\delta = 1$, $a = 1$, $\beta = 1$, and thus $\alpha = \frac{1}{c^2}$. The symbols marked with a star stand for measure-ratios in some new unit system whose basic units for length, time, and mass and characteristic constants δ^*, α^*, β^*, and a^* we are going to evaluate.

The general form of Newton's second law is

$$F = \delta M \frac{d^2L}{dT^2} \quad \ldots . 172$$

and changing to the starred system we get

$$\frac{F}{F^*} = \frac{\delta}{\delta^*} \circ \frac{M}{M^*} \cdot \frac{L}{L^*} \cdot \frac{T^{*2}}{T^2} \quad \ldots . 172a$$

Coulomb's law for electric charges

$$F = \frac{Q \quad Q'}{\alpha \cdot L^2} \quad \ldots . 173$$

and

$$\frac{F}{F^*} = \left(\frac{Q}{Q^*}\right)^2 \cdot \frac{\alpha^*}{\alpha} \cdot \left(\frac{L^*}{L}\right)^2 . \quad \ldots . 173a$$

Electric potential is

$$V = \frac{Q}{\alpha L} \quad \ldots . 174$$

and

$$\frac{V}{V^*} = \frac{Q}{Q^*} \cdot \frac{\alpha^*}{\alpha} \cdot \frac{L^*}{L} \quad \ldots . 174a$$

Electric current

$$I = \frac{dQ}{dT} \quad \ldots . 175$$

and

$$\frac{I}{I^*} = \frac{Q}{Q^*} \cdot \frac{T^*}{T} \quad \ldots . 175a$$

The formulas (Equations 172a to 175a) are the so-called logometric formulas introduced by O'Rahilly, except for a small change in notation†. These logometric formulas, of course, perform much the same function as dimensional equations, and except for the inclusion of the constants δ and α etc. the logometric expressions are identical to the dimensions.

The reason for including δ, α, and other characteristic constants is that we are completely free to choose and change these independently of the basic units for length, mass, and time. The logometric formulas are thus more general than the dimensional equations.

The four equations (172a to 175a) contain the following nine unknown transformation-ratios

$$\frac{M}{M^*} ; \frac{L}{L^*} ; \frac{T}{T^*} ; \frac{\delta}{\delta^*} ; \frac{F}{F^*} ; \frac{\alpha}{\alpha^*} ; \frac{Q}{Q^*} ; \frac{V}{V^*} \text{ and } \frac{I}{I^*} \quad \ldots . 176$$

†O'Rahilly uses $[L] = \frac{L}{L^*}$, $[\alpha] = \frac{\alpha}{\alpha^*}$ etc. to symbolize the transformation-ratios between the equivalent measure-ratios in the unstarred and the starred systems. To avoid introducing new symbols, the transformation ratios are used directly here.

which means that we are free to choose five of the transformation-ratios.

The aim of this investigation is to find out how the volt and the ampere can be incorporated in a unit system, so the first two choices are

$$\frac{I}{I^*} = 10^{-1} \quad \ldots. 177$$

and

$$\frac{V}{V^*} = 10^{8} \quad \ldots. 178$$

Then we choose

$$\frac{\delta}{\delta^*} = 1 \quad \ldots. 179$$

to keep Newton's second law free from constants and

$$\frac{T}{T^*} = 1 \quad \ldots. 180$$

so that the time-unit is unchanged.

If we, as the last choice, put $M/M^* = 1$ then by solving the Equations 172a to 175a we get $L/L^* = 10^7$ which is a rather crastic change. More acceptable is

$$\frac{L}{L^*} = 10^{2} \quad \ldots. 181$$

which means that the unit for length is changed from cm to metre. By solving the equations we get

$$\frac{M}{M^*} = 10^{3} \quad \ldots. 182$$

so that the unit for mass in system (*) is the kilogram instead of the gram: a very acceptable change.

The transformation-ratio for α is then

$$\frac{\alpha}{\alpha^*} = 10^{-11} \quad \ldots. 183$$

or

$$\alpha^* = 10^{11}\,\alpha = \frac{10^{11}}{c^2} \quad \ldots. 184$$

The definition of a speed is

$$v = \frac{dL}{dT} \quad \ldots. 185$$

so

$$\frac{v}{v^*} = \frac{L}{L^*} \cdot \frac{T^*}{T} \quad \ldots. 186$$

and

$$\frac{c}{c^*} = \frac{L}{L^*} = 10^{2} \quad \ldots. 187$$

so we get

$$\alpha^* = \frac{10^{11}}{10^4 c^{*2}} = \frac{10^7}{c^{*2}} \quad \ldots. 188$$

which is the value of the constant α in the MKS-system and in the basic Giorgi-system.

MKS-systems

In the preceding section it has been shown that using kg, metre, second, and $\delta = 1$ as the mechanical units it is possible to construct a unit system with the volt and the ampere as units for potential difference and for current if we at the same time take

$$\alpha = \frac{10^7}{c^2} \quad \ldots. 189$$

We are still free to choose one of the constants a or β, and it would have been tempting to take $\beta = 10^{-1}$ so the magnetostatic unit for field strength would have been equal to the E.M.U. for magnetic field. The constant a would then have been $a = 10^3$ using Equation 28.

However, the historical fact is that a was chosen as

$$a = 1 \quad \ldots. 190$$

and thus

$$\beta = 10^{-7} \quad \ldots. 191$$

These values characterize the unrationalized MKS-system, and Maxwell's equations in this system are

$$\nabla \mathrm{x} \overline{E} + 10^{-7}\frac{\partial \overline{H}}{\partial t} = 0, \qquad \nabla \cdot \overline{H} = 0 \quad \ldots. 192, 193$$

$$\nabla x\overline{H} - \frac{10^7}{c^2}\frac{\partial \overline{E}}{\partial t} = 4\P\cdot\overline{J}, \quad \nabla\cdot\overline{E} = \frac{4\P\cdot c^2}{10^7}\cdot\rho \qquad \ldots.194, 195$$

By giorgization, as shown earlier, it is possible to get rid of the constants in front of the two time derivatives. But to cancel the 4¶'s we have to choose $a = 4\P$ additionally. This means that $\beta = (4\P)^2 \cdot 10^{-7}$ as we can not change α if we still want the volt and the ampere.

The magnetostatic units then become badly "rationalized" so the conversion factors to E.M.U.'s include 4¶-factors.

The rationalized MKS-system thus has the following characteristic constants

$$\alpha = \frac{10^7}{c^2}, \ a = 4\P, \text{ and } \beta = (4\P)^2 \cdot 10^{-7} \qquad \ldots.196$$

and Maxwell's equations are

$$\nabla x\overline{E} + 4\P\cdot 10^{-7}\cdot\frac{\partial \overline{H}}{\partial t} = 0\,; \quad \nabla\cdot H = 0 \qquad \ldots.197, 198$$

$$\nabla x\overline{H} - \frac{10^7}{4\P\cdot c^2}\cdot\frac{\partial \overline{E}}{\partial t} = \overline{J}\,; \quad \nabla\cdot\overline{E} = \frac{4\P\cdot c^2}{10^7}\rho \qquad \ldots.199, 200$$

In the giorgized, rationalized MKS-system the equations are

$$\nabla x\overline{E} + \frac{\partial B}{\partial t} = 0\,; \qquad \nabla\cdot\overline{B} = 0 \qquad \ldots.201, 202$$

$$\nabla x\overline{H} - \frac{\partial D}{\partial t} = \overline{J}\,; \qquad \nabla\cdot\overline{D} = \rho \qquad \ldots.203, 204$$

together with the Giorgi-conditions

$$\overline{B} = 4\P \cdot 10^{-7} \cdot H \qquad \ldots.205$$

$$\overline{D} = \frac{10^7}{4\P\cdot c^2}\cdot\overline{E} \qquad \ldots.206$$

As shown in the section on Giorgi-transformation of a unit system, the giorgization means that we use two different unit systems in Equations 201, 202 and 203, 204, and that 205 and 206 are the necessary transformation rules between these systems.

Referring to Table I, Equations 201, 202 are in Giorgi-subsystem (2) and Equations 203, 204 are in subsystem (1). The basic system is used when potential difference and current simultaneously enter the equations, e.g. in Kirchhoff's equations involving resistance, self-induction and capacitance in AC-circuits.

The two transformation rules Equations 205 and 206 are, by a misinterpreted analogy to the Equation 138 and the corresponding equation for dielectrics, stated to be the relations between 'magnetic induction' and 'magnetizing force', 'electric induction', and 'polarizing force', respectively, in free space, the two constants are concealed behind the symbols

$$\mu_0 = 4\P \cdot 10^{-7} \qquad \ldots.207$$

and

$$\epsilon_0 = \frac{10^7}{4\P\cdot c^2} \qquad \ldots.208$$

where μ_0 is called the "permeability of free space" and ϵ_0 the "permittivity of free space".

The original aim of all these manipulations was to include the volt and the ampere in an absolute unit system; but this has long been lost in the discussions about "rationalization" and a "fourth unit".

Heaviside's suggestion of rationalization has truly been disastrous; we are now stuck with μ_0 and ϵ_0, two sets of electromagnetic units belonging to three unit systems, and a stubborn confusion about magnetic and dielectric materials.

Life was simpler when the only conversion factors to remember were

$$1 \text{ volt} = 10^8 \text{ E.M.U.}$$

$$1 \text{ ampere} = 10^{-1} \text{ E.M.U.}$$

and only one magnetic and one electric field existed.

Conclusions

It is possible to develop an electromagnetic theory independent of any unit system, and this formulation is extremely useful in distinguishing the features inherent in the theory from the features imposed by the different existing unit systems.

Inherent in the theory is thus the necessity of constants in the equations including the occasional occurrence of 4¶-factors. One system in particular, the MKSA-system or the SI, contains a duality of dimensionally different units for the physical phenomena.

The problems in the MKSA-system can be traced back to Maxwell's "displacement current" which caused him unnecessarily to introduce two different electric field concepts, to

Heaviside's "removal" of 4¶-factors from Maxwell's equations, and to the simultaneous adoption of two conflicting models in the theory of polarizable media. The "brute force" removal of constants from Maxwell's equations by giorgization has resulted in two sets of units with the conversion factors μ_0 and ϵ_0, which, of course, have nothing to do with permeability or permittivity.

Once this is realized all the ambiguity about B- or H-units, about I·A or μ_0·I·A being the "real" magnetic moment, etc. disappears, and we are free to use which one we please, as long as the formulas are consistent.

The magnetostatic E.M.U.'s can then be converted to SI-units using the following power-of-ten conversion factors.

Magnetic field strength:

$$1 \text{ oersted} = 10^{-4} \text{ tesla}$$

Magnetization intensity:

$$1 \frac{\text{E.M.U. of mag. moment}}{\text{cm}^3} = 10^3 \frac{\text{amp}}{\text{m}}$$

In this way we are, of course, avoiding the "rationalized" SI-units and leaving it to the user in SI to rationalize or to work his problem out in a consistent set of unrationalized SI-equations.

Acknowledgments

This work was carried out at the Division of Geomagnetism, Earth Physics Branch, Department of Energy, Mines and Resources, Ottawa, Ont., Canada under a postdoctorate fellowship granted by the National Research Council of Canada.

The author is greatly indebted to Prof. Alfred O'Rahilly who, in his book, among other things pointed out the need for a third constant in electromagnetism, the existence of two units for magnetic field in the MKSA-formulation, and who reintroduced reality into dimensions by stating them as ratios between measures of the same quantity in different unit systems.

Special thanks are given to G.V. Haines for his contributions to the analysis of Giorgi-pairs, to E.I. Loomer and to P.H. Serson for many clarifying discussions and for encouragement during the work; also E. Irving is thanked for discussions on the units in paleomagnetism.

References

ASTM Metric Practice Guide. *National Bureau of Standards, Handbook* 102, United States Department of Commerce, Avail: Superintendent of Documents, U.S. Gov. Printing Office, Washington, D.C., 204 02.

Avčin, F. 1961. Some difficulties around the quantities describing the magnetic field. *Academia Scientarium et Artium Slovenica,* Class III, Ser. A, IX/1, Ljubljana. (In English.)

Bjerge, T. 1951. Elektricitet og magnetisme, 3rd edition. *Munksgaard,* Copenhagen. (In Danish.)

Campbell, N.C., and I. Hartshorn. 1949. The experimental basis of electromagnetism. *Proc. Phys. Soc. London,* Sec. A, Vol. 62, pp. 422-445.

Casimir, H.B.G. 1969. Remarks on the formulation of magnetic theory. *IEEE Trans. Mag., Mag.-5,* pp. 159-161.

Collinson, D.W. *et al.* (editors) 1967. Developments in solid earth geophysics, 3, Methods in Paleomagnetism (Book), Elsevier, London.

Döring, W. 1949. Zur definition des magnetischen momentes. *Ann. Phys.,* Ser. 6, Vol. 6, pp. 69-88. (In German.)

Duckworth, H. E. 1960. Electricity and magnetism. *MacMillan Co., Toronto.*

Fleischer, R.L., *et al.,* 1969. Search for magnetic monopoles in deep ocean deposits. *Phys. Rev.,* Vol. 184, pp. 1393-1398.

Fleischer, R.L., *et al.,* 1969. Search of tracks of massive multiply charged magnetic poles. *Phys. Rev.,* Vol. 184, pp. 1398-1402.

Ham, J.M., and G.R. Slemon. Scientific basis of electrical engineering. *Wiley & Sons.*

Kenelly, A.E., July 1932. Meeting of the committee on symbols, units and nomenclature, *Terr. Magn.,* 37, pp. 447-454

Knudsen, H.L. 1955. Elektromagnetisk feltteory. *Polyteknisk Forening,* Copenhagen. (In Danish.)

Lorenz, L.V. 1867. On the identity of the vibrations of light with electrical currents. *Phil. Mag.,* Vol. 34, pp. 287-301.

Lovering, W.F. 1970. Magnets in electromagnetic theory. *Nature,* 225, p. 1127.

Mason and Weaver. 1929. The electromagnetic field. *Dover S185,* first published by U. of Chicago.

Maxwell, J.C. 1954. A treatise on electricity and magnetism, *Vols. I and II. Dover S636 and S637,* New York, 1954. (First edition published in 1873, the Dover issue is a reproduction of the third edition from 1891.)

O'Rahilly, A. 1965. Electromagnetic theory, Vols. I and II. *Dover S126,* New York. (First published in 1938, Cork University Press.)

Primdahl, F. 1970. Short note on units in magnetostatics. *Geomagnetic report No. 70-4* Division of Geomagnetism, Earth Physics Branch, Department of Energy, Mines and Resources, Ottawa, Ont., Canada.

Rosser, W.G.V. 1969. Four macroscopic vectors of electromagnetism. *Nature,* 224, pp. 577-579.

Sarbacher, R.I., and W.A. Edson. 1946. Hyper and ultrahigh frequency engineering. *Wiley & Sons.*

Silsbee, F.B. 1962. Systems of electrical units. *J. Res. NBC,* 66 c, pp. 137-178.

Slater, J.C., and N.H. Frank. 1947. Electromagnetism. *McGraw-Hill.*

Stopes-Roe, H.V. 1969. Essential failure of the Giorgi-system. *Nature,* 224, pp. 579-581.

Stratton, J.A. 1941. Electromagnetic theory. *McGraw-Hill.*

Temperly, H.N.V. 1969. SI-Units, *Nature,* 222, P. 806.

Appendix I – Units in the MKSA-subsystems and application of the Haines rule

Because of the existence of two sets of units in the MKSA-system it is necessary to state the names of the units together with the measure-ratios in order to avoid inconsistency. However, once this is done it is always possible to go back and forth between the subsystems by giorgization of the measure-ratios observing the Haines male-female rule.

The MKSA-notation is used

$$\epsilon_0 = \frac{\alpha}{a} \quad \text{.... A1.1}$$

$$\mu_0 = \frac{\beta}{a} \quad \text{.... A1.2}$$

where α, β, and a belong to the basic MKSA-system (see Table I). The symbols used in the following two tables are not completely consistent with international practice nor with the earlier notation but no misunderstandings should arise from this.

The force on an electric charge Q in the field E is:

$$\overline{F} = \overset{♂}{Q} \cdot \overset{♀}{\overline{E}} = \overset{♀}{Q^*} \cdot \overset{♂}{\overline{D}} \quad \text{.... A1.3}$$

Power is:

$$P = \overset{♀}{V} \cdot \overset{♂}{I} = \overset{♂}{V^*} \cdot \overset{♀}{I^*} \quad \text{.... A1.4}$$

Work:

$$W = \overset{♀}{V} \cdot \overset{♂}{Q} = \overset{♂}{V^*} \cdot \overset{♀}{Q^*} \quad \text{.... A1.5}$$

Torque on an electric dipole in the field E

$$\overline{T} = \overset{♂}{\overline{m}_e} \times \overset{♀}{\overline{E}} = \overset{♀}{\overline{m}_e^*} \times \overset{♂}{\overline{D}} \quad \text{.... A1.6}$$

Force between two electric charges (Coulomb's law):

$$F = \frac{\overset{♂}{Q} \cdot \overset{♂}{Q'}}{a \cdot \epsilon_0 \cdot r^2} = \frac{\epsilon_0 \cdot \overset{♀}{Q^*} \cdot \overset{♀}{Q^{*\prime}}}{a \cdot r^2} = \frac{\overset{♂}{Q} \cdot \overset{♀}{Q^{*\prime}}}{a \cdot r^2} \quad \text{.... A1.7}$$

Table II. Electrostatic part of the MKSA-system

Name	Symbol, Name of unit, gender	Symbol, Name of unit, gender	Giorgization rule $\epsilon_0 \left[\frac{\text{Coulomb}}{\text{volt·m}}\right]$
	Basic system	Sub-system (1)	
Charge	Q Coulomb, ♂	Q* volt·m, ♀	$Q = \epsilon_0 \cdot Q^*$
Electric field intensity	E volt/m, ♀	D Coulomb/m^2, ♂	$D = \epsilon_0 \cdot E$
Electric flux	Ψ* volt·m, ♀	Ψ Coulomb, ♂	$\Psi = \epsilon_0 \cdot \Psi^*$
Potential difference	V volt, ♀	V* Coulomb/m, ♂	$V^* = \epsilon_0 \cdot V$
Polarization	P Coulomb/m^2, ♂	p* volt/m, ♀	$P = \epsilon_0 \cdot P^*$
Electric dipole-moment	$\overline{m}_e$ Coulomb·m, ♂	$\overline{m}_e^*$ volt·m^2 ♀	$\overline{m}_e = \epsilon_0 \cdot \overline{m}_e^*$
Current	I ampere $= \frac{\text{Coulomb}}{\text{sec}}$, ♂	I* $\frac{\text{volt·m}}{\text{sec}}$, ♀	$I = \epsilon_0 \cdot I^*$
Time-derivative of flux	$\frac{d\Psi^*}{dt}$ $\frac{\text{volt·m}}{\text{sec}}$, ♀	$\frac{d\Psi}{dt}$ $\frac{\text{Coulomb}}{\text{sec}}$ = amp, ♂	$\frac{d\Psi}{dt} = \epsilon_0 \cdot \frac{d\Psi^*}{dt}$

Table III. Magnetostatic part of the MKSA-system

	Symbol, Name of unit, gender	Symbol, Name of unit, gender	Giorgization rule $\mu_0\left[\frac{\text{Webers}}{\text{amp}\cdot\text{m}}\right]$
	Basic system	Sub. system	
Magnetic pole strength	m Webers, ♂	m* † amp•m, ♀	$m = \mu_0 \cdot m^*$
Magnetic field strength	$\overline{H}$ amp/m, ♀	$\overline{B}$ Webers/m², ♂ = tesla	$\overline{B} = \mu_0 \cdot \overline{H}$
Magnetic flux	Φ* amp•m, ♀	Φ Webers, ♂	$\Phi = \mu_0 \cdot \Phi^*$
Magnetization	$\overline{M}$ Webers/m², ♂	$\overline{J}$ †† amp/m, ♀	$\overline{M} = \mu_0 \cdot \overline{J}$
Magnetic dipole-moment	$\overline{m}_m$ Webers•m, ♂	$\overline{m}^*_m$ amp•m², ♀	$\overline{m}_m = \mu_0 \cdot \overline{m}^*_m$
Time-derivative of flux	$\frac{d\Phi^*}{dt}$ amp•m/sec, ♀	$\frac{d\Phi}{dt}$ † $\frac{\text{Webers}}{\text{sec}}$ = volt, ♂	$\frac{d\Phi}{dt} = \mu_0 \cdot \frac{d\Phi^*}{dt}$

† Volt and ampere change gender according to whether they are members of a magnetic or an electric Giorgi-pair.

†† Not to be confused with the symbol for current density.

If we want to avoid the constant ϵ_0 in the formula, Haines rule has to be observed.

The force on a magnetic pole in a magnetic field

$$\overline{F} = \overset{♂}{m} \cdot \overset{♀}{\overline{H}} = \overset{♀}{m^*} \cdot \overset{♂}{\overline{B}} \qquad \text{....A1.8}$$

Torque on a magnetic dipole:

$$\overline{T} = \overset{♂}{\overline{m}_m} \times \overset{♀}{\overline{H}} = \overset{♀}{\overline{m}^*_m} \times \overset{♂}{\overline{B}} \qquad \text{....A1.9}$$

Force between poles:

$$F = \frac{\overset{♂\,♂}{mm'}}{a \cdot \mu_0 \cdot r^2} = \frac{\mu_0}{a} \cdot \frac{\overset{♀\,♀}{m^* m^{*\prime}}}{r^2} = \frac{\overset{♂\,♀}{m\, m^{*\prime}}}{a \cdot r^2} \qquad \text{....A1.10}$$

Again the constant μ_0 disappears if the Haines rule is followed.

In magnetic materials the following general formula is given (Equation 121):

$$\overline{H} = \overline{K} + \frac{4¶}{\beta}\overline{M} \qquad \text{....A1.11}$$

if all the terms are giorgized we get

$$\overline{B} = \mu_0 \overline{K} + \overline{M} \qquad \text{....A1.12}$$

as

$$\mu_0 = \frac{\beta}{a} \text{ and } a = 4¶$$

By giorgizing $\overline{M}$ according to Table III then Equation A1.12 becomes

$$\overline{B} = \mu_0 (\overline{K} + \overline{J}) \qquad \text{....A1.13}$$

In Equation A1.11 the three measure-ratios $\overline{H}$, $\overline{K}$, and $\overline{M}$ all belong to the basic system of Table III. Equation A1.12 thus contains measure-ratios belonging to two different unit systems as $\overline{B}$ is the magnetic field strength in the subsystem. The same is the case in Equation A1.13, $\overline{B}$ and $\overline{J}$ belong to the subsystem in Table III and $\overline{K}$ to the basic system. The factor $\frac{4¶}{\beta}$ is thus eliminated in the two MKSA-versions of Equation A1.11 by mixing the units; but this elimination is, of course, only apparent as it must have been included earlier in the definition of $\overline{M}$ or of $\overline{B}$.

Maxwell's equations in the giorgized, rationalized MKSA-system are (Equations 201 to 204)

$$\nabla x\overline{E} + \frac{\partial \overline{B}}{\partial t} = 0 \; ; \qquad \nabla \cdot \overline{B} = 0 \qquad \ldots . 201, 202$$

$$\nabla x\overline{H} - \frac{\partial \overline{D}}{\partial t} = \overline{J} \; ; \qquad \nabla \cdot \overline{D} = \rho \qquad \ldots . 203, 204$$

The unit for $\nabla x\overline{E}$ is [volt/m^2] so $\overline{E}$ belongs to the basic system of Table II. $\frac{\partial \overline{B}}{\partial t}$ is in $[\frac{\text{Webers}}{\text{m}^2 \cdot \text{sec}}]$ or [tesla/sec] so this term belongs to subsystem (2) of Table III.

$\nabla x\overline{H}$ is in [ampere/m^2] belonging to the basic system and $\frac{\partial \overline{D}}{\partial t}$ is in $[\frac{\text{Coulomb}}{\text{m}^2 \cdot \text{sec}}]$ belonging to subsystem (1).

Now, subsystem (1) and the magnetic part of the basic system form a consistent unit system, and subsystem (2) together with the electric part of the basic system also constitute a unit system. These are the two systems referred to as (1) and (2) in Table I, and they are both different from the basic MKSA-system. Maxwell's Equations 201 to 204 are thus given in two different unit systems and the conversion factors from these systems to the basic MKSA-system are

$$\overline{B} = \mu_0 \cdot \overline{H}$$

and

$$\overline{D} = \epsilon_0 \cdot \overline{E}$$

Appendix 2 – Units, dimensions and logometric expressions

A unit is a name attached to a measure-ratio to state which unit system it belongs to. Units like volt, ampere, coulomb, etc. and compounded units such as volt•sec, ampere•m, etc. are used to ensure that the formulas we use are correct or that the measure-ratios are in the same unit system.

The equation

$$\nabla x\overline{E} + \frac{\partial \overline{B}}{\partial t} = 0 \qquad \ldots . A2.1$$

is stated in a unit system having volt/m as the unit for electric field strength $\overline{E}$ and tesla as the unit for magnetic field strength. If the measure ratio for magnetic field strength has been given in ampere/m we would immediately recognize either the formula in Equation A2.1 as wrong or the measure-ratio as belonging to another unit system. We may then use the corresponding formula in the other system

$$\nabla x\overline{E} + 4¶ \cdot 10^{-7} \frac{\partial \overline{H}}{\partial t} = 0 \qquad \ldots . A2.2$$

or, which amounts to the same thing, convert the measure-ratio for magnetic field from ampere/m to tesla by using the conversion factor μ_0

$$\overline{B} = \mu_0 \, \overline{H} \qquad \ldots . A2.3$$

where

$$\mu_0 = 4¶ \cdot 10^{-7} \left[\frac{\text{Webers}}{\text{amp}\cdot\text{m}}\right] \qquad \ldots . A2.4$$

The unit attached to μ_0 is of the same kind as the unit metres/inch attached to the conversion factor between inches and metres

$$L \left[\text{metres}\right] = 0.0254 \left[\frac{\text{metres}}{\text{inch}}\right] \cdot L^* \left[\text{inches}\right] , \qquad \ldots . A2.5$$

i.e. it is a mnemotechnical help to remember whether it is the measure-ratio in inches or in metres we have to multiply by the conversion factor.

Also, if we change the unit of a measure-ratio to a subunit, i.e. from volts to millivolts, microvolts, kilovolts etc., then the units are useful to derive the conversion factors. If $\overline{E}$ is the measure-ratio for electric field in volts/m and $\overline{E}^*$ is the measure-ratio for the same field in microvolts/cm we have

$$\overline{E} \left[\frac{\text{volts}}{\text{m}}\right] = \overline{E}^* \left[\frac{\text{microvolts}}{\text{cm}}\right] \cdot k \left[\frac{\text{cm}}{\text{m}} \cdot \frac{\text{volts}}{\text{microvolts}}\right] \ldots . A2.6$$

where k is the conversion factor. It is easily derived that

$$k = 10^2 \cdot 10^{-6} = 10^{-4} \qquad \ldots . A2.7$$

and thus

$$\overline{E}^* = 10^4 \cdot \overline{E} \qquad \ldots . A2.8$$

Dimensions are the units stated in terms of the chosen basic units, but ignoring the basic constants. In the c.g.s. systems the basic units are cm, gram, and second normally represented by L, M, and T and the basic constants are $\delta = 1$, $\beta = 1$ or $\frac{1}{c^2}$, and $\alpha = \frac{1}{c^2}$ or 1.

The dimension of force is

$$[F] = \left[\frac{ML}{T^2}\right] \qquad \ldots\ldots A2.9$$

which states how the measure-ratios for force change if we change the units, and thus the measure-ratios, for mass, length, and time. Comparing to Equation 172a we see that tacitly we have limited ourselves to $\delta = 1$, unchanged, as this constant is not included in Equation A2.9. It is well known that the three-unit dimensions lead to contradictions in the electromagnetic part of the C.G.S.-systems.

The MKSA-systems have four basic units - metre, kilogram, second, and ampere, symbolized by L, M, T, and I, and the two constants $\delta = 1$ and $a = 4¶$. The use of four units in the dimensions removes the double-dimensions in electromagnetism, but as δ and a are not included we are restricted to unit systems having $\delta = 1$ and $a = 4¶$. The change from the unrationalized MKS-system to the rationalized MKSA-system cannot be analyzed by dimensions as the rationalization is equivalent to a change from $a = 1$ to $a = 4¶$. Neither can the change from the absolute electromagnetic system to the unrationalized MKS-system be analyzed by dimensions as it involves a change of the constant α from $\alpha = \frac{1}{c^2}$ to $\alpha = \frac{10^7}{c^2}$ and of β from $\beta = 1$ to $\beta = 10^{-7}$.

Logometric formulas are the fully general expressions including all six basic units and constants. The logometric expression for force is (Equation 172a)

$$\frac{F}{F^*} = \frac{\delta}{\delta^*} \cdot \frac{M}{M^*} \cdot \frac{L}{L^*} \cdot \left(\frac{T^*}{T}\right)^2 \qquad \ldots\ldots A2.10$$

where F, δ, M, etc. are measure-ratios and constants in system (1) and F*, δ^*, M*, etc. belong to system (2). Using O'Rahilly's notation $[F] = F/F^*$, $[\delta] = \delta/\delta^*$, etc., we have

$$[F] = \left[\frac{\delta ML}{T^2}\right] \qquad \ldots\ldots A2.11$$

and it is seen that the logometric formula reduces to the dimension of force if $[\delta] = \delta/\delta^* = 1$.

The expression "logometric" is also O'Rahilly's. According to him it is derived from Greek "logos" = ratio and "metron" = measure and means "ratio between measures".

As an example of the use of logometric formulas we will derive the logometric expressions for the constants α and β in the MKSA-system.

The MKSA-system is defined by metre, kilogram, second, $\delta = 1$, ampere, and $a = 4¶$. The logometric expression for force is Equation A2.11

$$[F] = \left[\frac{\delta ML}{T^2}\right] \qquad \ldots\ldots A2.11$$

The definition of the ampere is based on Equation 8

$$d^2F = \frac{\beta}{a^2} \frac{I_1\, ds_1 \times (I_2 ds_2 \times r)}{r^2} \qquad \ldots\ldots 8$$

which gives the following logometric formula

$$[F] = \left[\frac{\beta}{a^2} \cdot I^2\right] \qquad \ldots\ldots A2.12$$

From Coulomb's law for two electric charges we get

$$[F] = \left[\frac{Q^2}{\alpha L^2}\right] \qquad \ldots\ldots A2.13$$

and from Equation 5

$$[I] = \left[\frac{Q}{T}\right] \qquad \ldots\ldots A2.14$$

Combining Equations A2.13 and A2.14 and equating [F] to [F] in Equations A2.11 and A2.12 we have

$$[F] = \left[\frac{\delta ML}{T^2}\right] = \left[\frac{\beta}{a^2} \cdot I^2\right] = \left[\frac{I^2T^2}{\alpha\, L^2}\right] \qquad \ldots\ldots A2.15$$

From this we may derive

$$\left[\frac{a^2}{\alpha\, \beta}\right] = \left[\frac{L}{T}\right]^2 \qquad \ldots\ldots A2.16$$

which is the logometric expression corresponding to Equation 28. Further we have

$$[\alpha] = \left[\frac{I^2 \cdot T^4}{\delta \cdot M \cdot L^3}\right] \qquad \ldots\ldots A2.17$$

and

$$[\beta] = \left[\frac{\delta \cdot a^2 M \cdot L}{I^2 \cdot T^2}\right] \quad \ldots\ldots A2.18$$

From the section on Giorgi-pairs we have

$$\epsilon_0 = \frac{\alpha}{a} \quad \ldots\ldots A2.19$$

and

$$\mu_0 = \frac{\beta}{a} \quad \ldots\ldots A2.20$$

The logometric expressions are then

$$\epsilon_0 \left[\frac{I^2 \cdot T^4}{\delta \cdot a \cdot M \cdot L^3}\right] \quad \ldots\ldots A2.21$$

and

$$\mu_0 \left[\frac{\delta \cdot a \cdot M \cdot L}{I^2 \cdot T^2}\right] \quad \ldots\ldots A2.22$$

If we choose $\delta = \delta/\delta^* = 1$ and $a = a/a^* = 1$ we get the four-unit dimensions

$$\epsilon_0 \left[\frac{I^2\ T^4}{M \cdot L^3}\right] \quad \ldots\ldots A2.23$$

and

$$\mu_0 \left[\frac{M \cdot L}{I^2 \cdot T^2}\right] \quad \ldots\ldots A2.24$$

If we replace M by kg, L by metre, T by second, and I by ampere and use the relations

$$\frac{\text{kg} \cdot \text{metre}}{\text{sec}^2} = \text{newton}$$

$$\frac{\text{Newton} \cdot \text{metre}}{\text{Coulomb}} = \text{volt} \quad \ldots\ldots A2.25$$

$$\text{Volt} \cdot \text{sec} = \text{weber}$$

$$\text{ampere} \cdot \text{sec} = \text{coulomb}$$

we get the units for μ_0 and ϵ_0

$$\mu_0 \left[\frac{\text{Webers}}{\text{amp} \cdot \text{m}}\right] \quad \ldots\ldots A2.26$$

$$\epsilon_0 \left[\frac{\text{Coulomb}}{\text{volt} \cdot \text{m}}\right] \quad \ldots\ldots A2.27$$

PUBLICATIONS of the EARTH PHYSICS BRANCH

VOLUME 42 - NO. 2

gravity measurements in canada january 1, 1967 to december 31, 1970

J. G. TANNER and R. A. GIBB

DEPARTMENT OF ENERGY, MINES AND RESOURCES

OTTAWA, CANADA 1971

Cat. No.: M70-42/2

Contents

25 Introduction
25 Earth Physics Branch
25 Gravity standards
25 National primary net
26 World Gravity net
26 Gravimeter tilt calibrator
27 Gravity Storage and retrieval system
27 Network processing and adjustment system
28 Regional gravity surveys
28 Regional gravity interpretation
28 Gulf of St. Lawrence.
31 Scotian Shelf
31 Canadian Shield
32 Interior Plains
32 Canadian Cordillera
32 Hudson Bay
33 Arctic Canada
33 Detailed gravity investigations
33 Alexandria area, Ontario
33 Bancroft area, Ontario
33 Timmins-Senneterre area, Ontario-Quebec
34 Piercement structures in the Arctic Islands
34 Darnley Bay, Northwest Territories
34 Crater investigations
34 Earth tides and crustal loading
35 Flexural rigidity, thickness and viscosity of the lithosphere
35 Gravity interpretation methods
35 Physical geodesy
36 Polar studies
37 Bedford Institute (Atlantic Oceanographic Laboratory)
37 Detailed gravity surveys
37 Hydrographic-geophysical survey of the eastern Canada Continental Shelf
37 Grand Banks
38 Gulf of St. Lawrence
38 Western Arctic
38 Regional geophysical surveys
38 Mid-Atlantic Ridge
39 Bay of Fundy
39 Hudson Strait
39 North American Basin
39 Hudson '70
39 Environmental tests
39 Satellite navigation cruise (*CSS Baffin* 022-69)
40 Laboratory tests
40 Memorial University of Newfoundland
40 Nova Scotia Research Foundation
41 University of New Brunswick
41 McGill University
41 University of Manitoba
42 University of Alberta
42 University of Calgary
42 University of Saskatchewan
42 University of British Columbia
42 Petroleum Industry
43 Bibliography

gravity measurements in canada january 1, 1967 to december 31, 1970

J. G. TANNER and R. A. GIBB

Introduction

This report has been compiled at the request of the International Union of Geodesy and Geophysics (IUGG) for presentation at the Fifteenth General Assembly on behalf of the Associate Committee of Geodesy and Geophysics (ACGG), the National Committee representing Canada in the international union. Annual reports published by the subcommittee on Gravity of the ACGG in the Canadian Geophysical Bulletin (C.M. Carmichael, Editor) form the basis for this compilation. The gravity subcommittee includes representatives from universities, from government institutions and from the mineral industry. The present membership is:

A.E. Beck	University of Western Ontario
D.E.T. Bidgood	Nova Scotia Research Foundation
W.C. Brisbin	University of Manitoba
E.R. Deutsch	Memorial University of Newfoundland
R.M. Ellis	University of British Columbia
R.A. Gibb	Earth Physics Branch, Secretary
R.T. Haworth	Atlantic Oceanographic Laboratory, Bedford Institute
E. Krakiwsky	University of New Brunswick
T.H. Pezarro	Voyager Petroleums Ltd.
J.G. Tanner	Earth Physics Branch, Chairman
H.D. Valliant	Earth Physics Branch

The largest contributor to this report is the Earth Physics Branch (formerly the Dominion Observatory) of the Department of Energy, Mines and Resources, the federal agency responsible for mapping the gravity field in Canada and its coastal waters. Allied responsibilities include maintenance of gravity standards for Canada, operation of a gravity data bank, instrumental development and the application of gravity to geologic and geodetic problems in Canada.

A major contribution comes from the Atlantic Oceanographic Laboratory, Bedford Institute of the Marine Sciences Branch, Department of Energy, Mines and Resources. This institute is involved with surface gravity measurements at sea.

Several provincial agencies and several Canadian Universities are increasingly active in a diversity of gravity investigations as reported here.

Earth Physics Branch

Gravity standards

National primary net. An extensive series of pendulum and gravimeter measurements were carried out on the national primary net between 1967 and 1970. This network (Figure 1) consists of 64 stations interconnected by 1,500 LaCoste and Romberg gravimeter ties and six pendulum intervals.

The first full scale field evaluation of the rebuilt Canadian bronze pendulum apparatus was carried out over the North American calibration line between Mexico City and Fairbanks in 1967. The results of these measurements (Valliant, 1969) when compared with earlier Gulf and Cambridge pendulum measurements and with gravity values derived from combined adjustments of all existing gravimeter and pendulum measurements on the NACL, showed that an accuracy better than ±0.2 mgal could be achieved with two sets of measurements in opposite directions on any interval. In 1969, pendulum measurements were carried out at Ottawa, Winnipeg, Vancouver, Edmonton, Yellowknife, Fairbanks and Resolute. Environmental problems at Resolute and logistic difficulties in the initial Fairbanks - Resolute and Resolute - Ottawa ties caused large discrepancies between the incoming and outgoing legs. Satisfactory results were obtained on the repeated Ottawa - Resolute measurements but transportation difficulties have prevented a remeasurement of the Resolute - Fairbanks interval. An analysis of these measurements (Valliant, 1970, in press) indicates that an accuracy better than 0.2 mgal has been achieved. Comparisons with absolute measurements at Fairbanks, Denver and Boston carried out by Air Force Cambridge Research Laboratories, Bedford, Mass., using Faller's apparatus show that the Canadian pendulums agree with the absolute measurements to about 1 part in 20,000.

In order to minimize errors due to excentre corrections at points in the primary network nearly all excentre networks were reobserved or strengthened with new measurements. A large proportion of the 270 excentre stations in the network were reobserved during 1968 to 1970 and each excentre network readjusted. The standard errors of the adjusted excentre stations are generally less than 0.02 mgals.

During the period under review about 700 long range measurements with LaCoste and Romberg gravimeters were added to the 800 older LaCoste and Romberg measurements, the Canadian pendulum measurements, and the absolute measurements at Fairbanks and Boston to form the basis for adjusting the Canada net. During the adjustment, a larger dispersion in the gravimeter measurements carried out before the installation of vibration insulators in 1966, led to the development of a weighting system based on the elapsed time between successive readings of the gravimeters. Pendulum and absolute measurements were weighted according to their respective estimated variances.

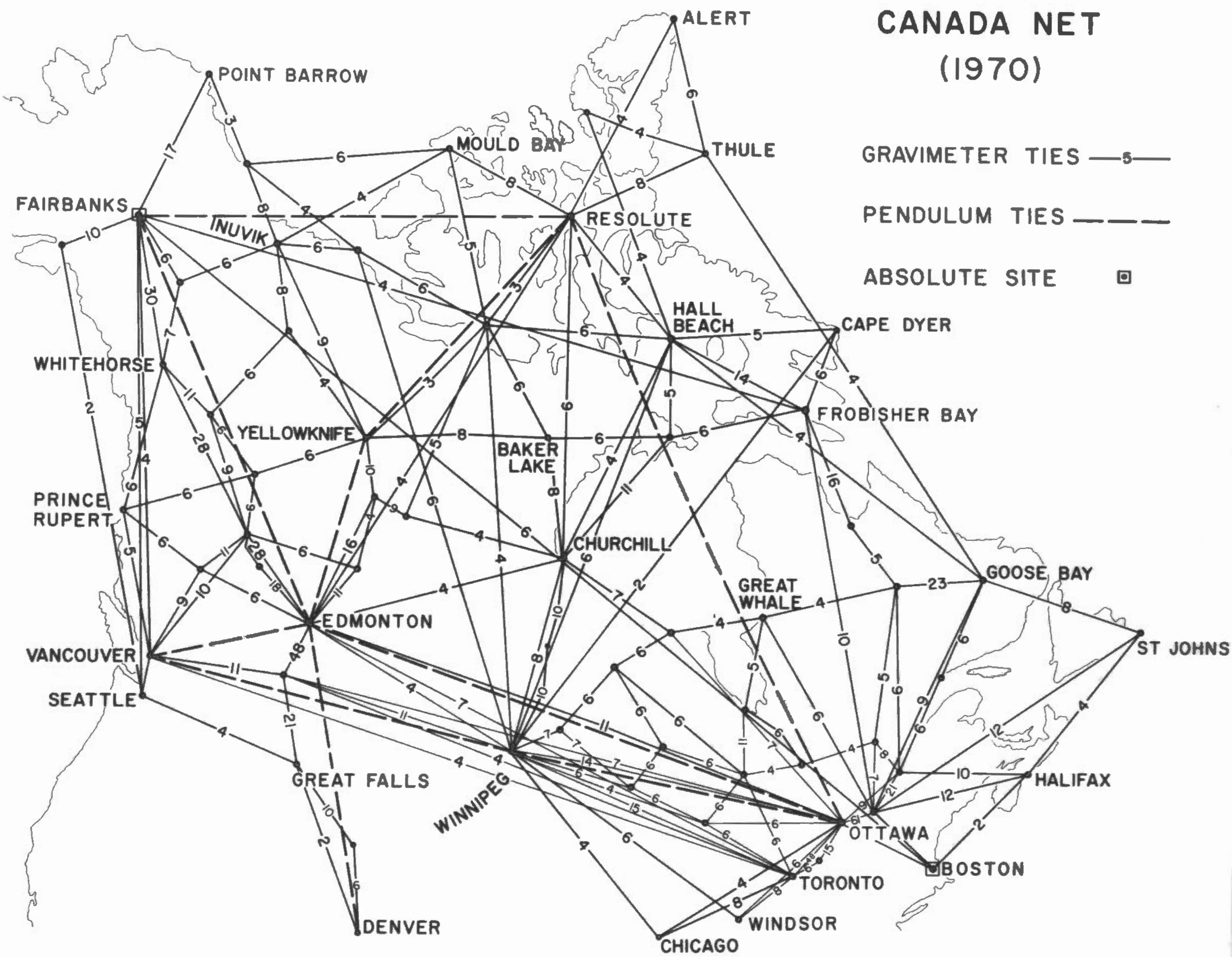

Figure 1. The Canadian primary net (1970).

The analysis of the primary network adjustment (R.K. McConnell, Earth Physics Branch, personal communication) indicates that gravity values in the primary net are accurate to ±0.05 mgals relative to the datum defined by the absolute measurements.

Adjustment of the secondary networks comprising some 17,000 ties between 3,000 control stations has been underway for some time. In order to reduce, adjust, and analyze this rapidly expanding file of data quickly and efficiently, considerable emphasis has been placed upon computer filing, retrieval and data reduction systems. These are described briefly in a subsequent paragraph.

World gravity net. The Earth Physics Branch has continued its participation in the work of Special Study Group 5 of the International Association of Geodesy. In 1967, C.T. Whalen of the 1381st Geodetic Survey Squadron, Cheyenne, Wyoming visited Ottawa to carry out preliminary adjustments of the world net using all available gravimeter and pendulum data. In 1968, R.K. McConnell of the Earth Physics Branch collaborated again with Mr. Whalen using the computing facilities of Aerospace Corporation in San Bernardino, California. In September of 1970 J.G. Tanner and R.K. McConnell presented the results of an adjustment of a world gravity net consisting of 270 stations to the Special Study Group 5 meeting held in Paris and participated in the development of plans for the final adjustment to be accomplished in 1971.

A few additional measurements on the world net were made by Earth Physics Branch personnel in 1969. Direct ties between absolute sites at Fairbanks, Boston and Bogota were carried out using three LaCoste and Romberg meters. Additional ties were made between South America and South Africa in co-operation with Professor Baglietto of the Institute of Geodesy, University of Buenos Aires.

Gravimeter tilt calibrator. A gravimeter tilt calibrator built at the Earth Physics Branch from plans supplied by Texas

Instruments Ltd., was used extensively by A.C. Hamilton to investigate dial non-linearaties in Worden type gravimeters. Discrepancies between calibrations of the same meter on the Earth Physics Branch tilt table and one at Texas Instruments led to an investigation of the table design. Precise angle measurement carried out by E. Greene of the National Research Council of Canada, Ottawa showed that the knife edge surface and the surface on which the Johannsen blocks rest were not sufficiently coplanar to eliminate erratic tilt angles due to slight horizontal movements of the table. As a result R.K. McConnell and J. Geuer designed a new tilt calibrator using a cast iron table tilted on precision steel balls. Automated lifting and tilting features were incorporated into the new design. Construction of the new table was completed late in 1970 and an extensive series of evaluation tests will be carried out in 1971. If the new design proves satisfactory, it will provide an efficient means of calibrating quartz type gravimeters before and after each field survey.

Gravity storage and retrieval system

In 1965, it became apparent that the existing punch card storage and retrieval system would soon be inadequate to handle the increasing number of new observations and the increasing requirement for plotting and other computer processing of the output file. Consequently, in that year, a study was made of the feasibility of a new storage and retrieval system using data files on magnetic tape and disk. This study included the preparation and documentation of the computer hardware requirements, system flow charts, program specifications, and program flow charts. Although some preliminary experimental programming was done, the project had to be postponed for two years because there was no access to a large computer suitable for use with such a system.

In 1967, with the installation of an IBM 360 Model 65 computer at the Computer Bureau in Ottawa and with the acquisition by the Division of a new X-Y data plotter which used magnetic tape as input, the development of the planned storage and retrieval system was begun. By the spring of 1969, the new system was operational. The present version of the system operates on an IBM 360 Model 85 computer at Systems Dimensions Limited in Ottawa. Its main components are a principal facts file of approximately 120,000 gravity observations stored on an IBM 2316 disk pack, and a suite of programs to store, update, and retrieve data from this file. Provision is made for output on the data plotter, the computer printer, punched cards, and magnetic tape.

Six major programs are used in this system. The **gravity traverse reduction program** is used to process the new observations, to detect errors in these observations, and to produce output records suitable for inclusion in the disk file. The **general program** produces maps at any scale on one of four different map projections showing the positions and values of selected gravity observations within a specified geographic area. Input in any combination from punched cards, card-image magnetic tape, and the disk file is possible. The plotting program can also select and display data within a specified range of any of the 14 data fields. Complete listings of the observations plotted on each map are provided automatically. The **general utility program** uses the disk file as input and produces punched cards, a card-image magnetic tape file, or a printer listing of selected observations within a specified geographical area. Given the latitude and longitude of the end points of a profile, the **profile plotting program** will select observations within a band of specified width along this line, interpolate them to the line, and plot a profile to the specified scale. The **file updating program** and the **file reorganization program** are used to update the disk file by the correction, deletion, or addition of data records. The former is used to process a small number of update records, while the latter is run whenever a large number of observations must be added to the file.

Using this system, the Division has been able to satisfy the needs of not only its own field officers and scientists but also those of universities, research institutions and the exploration industry. During the past year, the Division has processed approximately 100 requests for data from external agencies, involving the production of approximately 1,000 special maps and associated printer listings.

During the past year, work has progressed on the adjustment of the world gravity network and the Canadian gravity network and new values of gravity for the control stations in these networks will probably be adopted in the near future. In this same period, certain agencies in Canada such as the Bedford Institute and the Nova Scotia Research Foundation have offered their data for the file. Also, the subcommittee on gravity has recommended that this file will become a national repository for gravity data. These developments will require the recomputation of the input data during the coming year and some redesign of the system. The result of this redesign and recomputation will be a more complete and compact data record, a new file indexing system which will allow the addition of data from any part of the world, and a suite of more modular and more flexible programs. It is expected that this new system will be operational sometime in 1972.

Network processing and adjustment system

Concurrent with the development of the gravity storage and retrieval system, a compatible system for the processing, editing, and adjustment of observations taken at control stations in the Canadian gravity network has been developed. This system consists of four data files and eight major computer programs.

The **control station file**, which is the primary source for all control station information required by the system, consists of approximately 3,200 data records stored on a direct access file on an IBM 2316 disk pack, and a backup file on punched cards which provides the records necessary for the updating of this file. The **gravimeter file** consists of the conversion tables, calibration constants, and other parameters for approximately 50 instruments, and is stored as a direct access file on the same disk pack. The **network observation file** contains approximately 15,000 observations which have been taken at control stations in Canada and throughout the world, and is stored on punched cards. The **network tie file** is an intermediate file which is computed from the network observation file and is stored on magnetic tape with a backup file on punched cards.

The **control station file updating program** is used to modify the control station file by correction, deletion, or addition of data records. The **control station utility program** can select data records based on a number of different parameters and conditions, sort the output in various ways, and produce punched cards, a card-image tape file, or a printer listing of the selected and sorted control station records. All requests for control station descriptions are accompanied by a current printer listing from this program. The **tie processing program** uses the control station and gravimeter files to process the new network observations to produce network tie records on punched cards and a listing of these new ties. The **tie file updating program** uses punched card input to update the network tie file on magnetic tape by correction, deletion, and addition of these records. Using a file of control stations such as is produced by the control station utility program, the **network selection program** will select the gravimeters and network ties required for the adjustment of a particular network. This selected network can be plotted using the **network plotting program** to show the positions of the control stations, their names or identification numbers, and the gravity ties observed. The colour and type of line indicate the type of instrument used for a particular gravity tie. The gravity difference and the number of ties observed are also given. These network diagrams are very useful for editing a network and determining its structure. The **network editing program** is then used to edit and check the selected observations, set up the observation and fixing equations, apply various weighting functions, and produce an output file of the results. The **network adjustment program** uses this output file to form and solve the normal equations, list the adjusted observations, punch new control station cards, and perform statistical analysis on the results. The solution of the normal equations may be carried out either by matrix inversion for systems of less than 550 unknowns or by the Seidel iteration method for systems up to 3,500 unknowns.

Future development of this system will include the creation of a new network observation file on magnetic tape or disk, eliminating the intermediate network tie file, and the modification of the tie processing and network selection programs so that all computations and selections will be performed on a single file.

Regional gravity surveys

During the period under review emphasis continued to be given to the completion of the regional gravity mapping of Canada (gravity stations spaced at intervals of 10-15 km). Approximately 85 per cent of the regional measurements during the past four years were made by large helicopter supported field parties. Table I summarizes the observations by region and Figures 2 and 3 show the geographical coverage of the measurements.

Within the Canadian Shield and south of the Arctic Circle (latitude 66° 30'N) regional gravity observations are now complete. The first of the large systematic, helicopter supported regional mapping surveys was commenced in the southern Cordillera of British Columbia in 1968 using locations especially surveyed by the Surveys and Mapping Branch of the Department of Energy, Mines and Resources and by the Mapping and Charting Establishment, Department of National Defence. Gravity observations were made at elevations of up to 3,000 metres above sea level during this survey. In 1970 an Armed Forces survey party from the Mapping and Charting Establishment carried out gravity observations in conjunction with establishing horizontal and vertical control for topographical mapping.

During 1969 the Polar Continental Shelf Project moved from Mould Bay on Prince Patrick Island to its present site on the Mackenzie River Delta. The gravity coverage in the Beaufort Sea is shown in Figures 2 and 3.

Detailed surveys have been made over various geological features, of which the Morin Anorthosite is an example. Detailed studies of this type have shown the need for a more rapid and accurate means of obtaining vertical control. An elevation meter acquired in 1969 will provide a means of increasing both accuracy and density of elevation control in those areas with an adequate road network.

Regional gravity interpretation

Gulf of St. Lawrence. The underwater gravity survey of the Gulf of St. Lawrence was completed in 1967. Three important conclusions emerged from the study of these data (Goodacre, Brule and Cooper, 1969). The Bouguer anomaly field over the northern portion of the Gulf is similar to that of the adjacent Precambrian Shield, but a distinct change in anomaly level from negative in the north to more positive in the south occurs in the Gulf and is believed to mark the boundary between the Grenville and Appalachian geological provinces. Basic intrusive rocks characteristic of this boundary are out-

Table I. Regional Gravity Mapping by the Earth Physics Branch

Region	Area (sq. mi.)	No. of observations
1. Quebec and Newfoundland	210,000	3,041
2. Maritimes	80,000	1,833
3. Ontario	75,000	5,104
4. Prairie Provinces	35,000	3,572
5. Northwest Territories and Yukon	560,000	7,955
6. British Columbia	60,000	1,555
7. Polar Shelf	210,000	4,716
		27,776

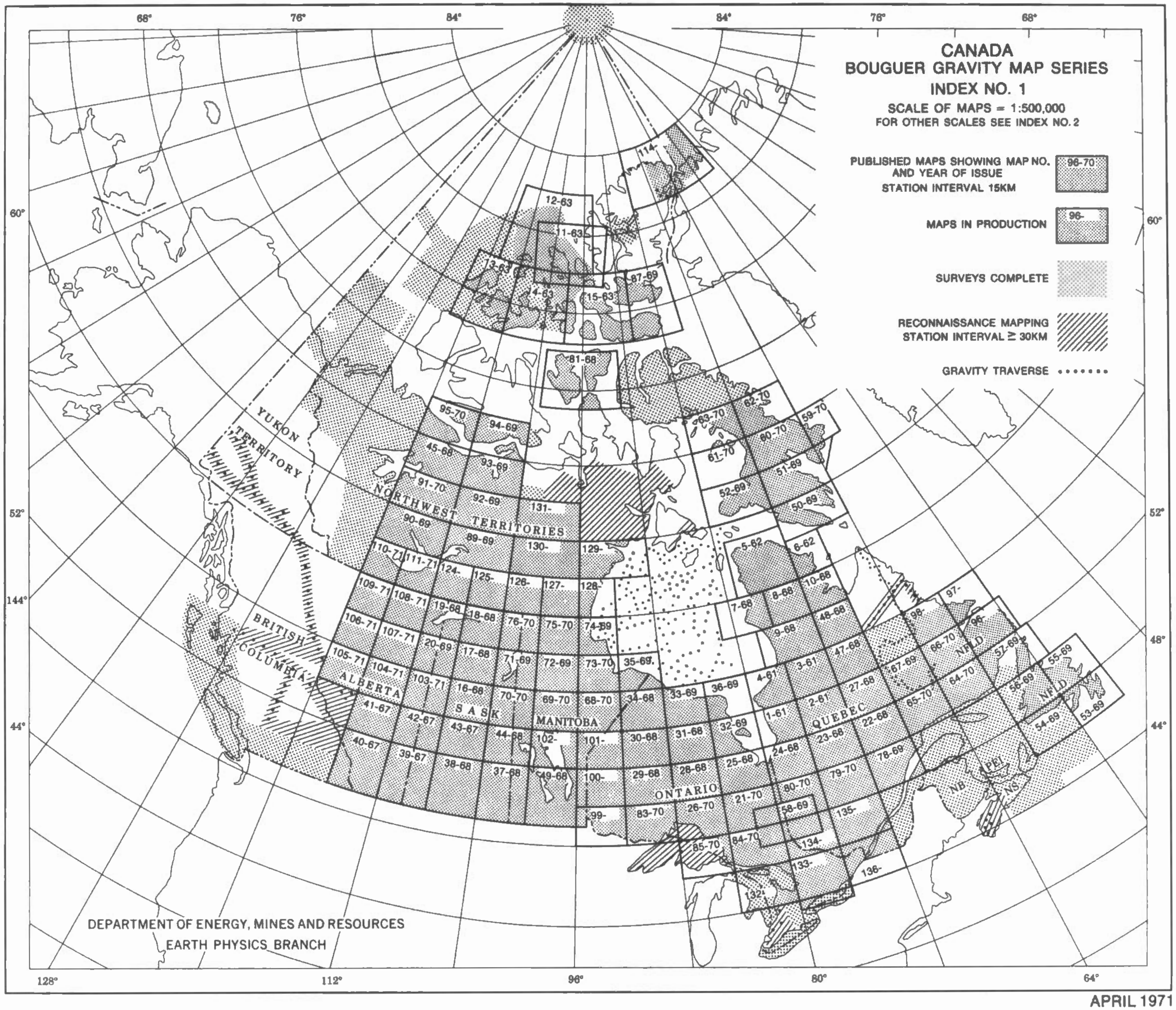

Figure 2. Distribution of gravity observations by the Earth Physics Branch to April, 1971.

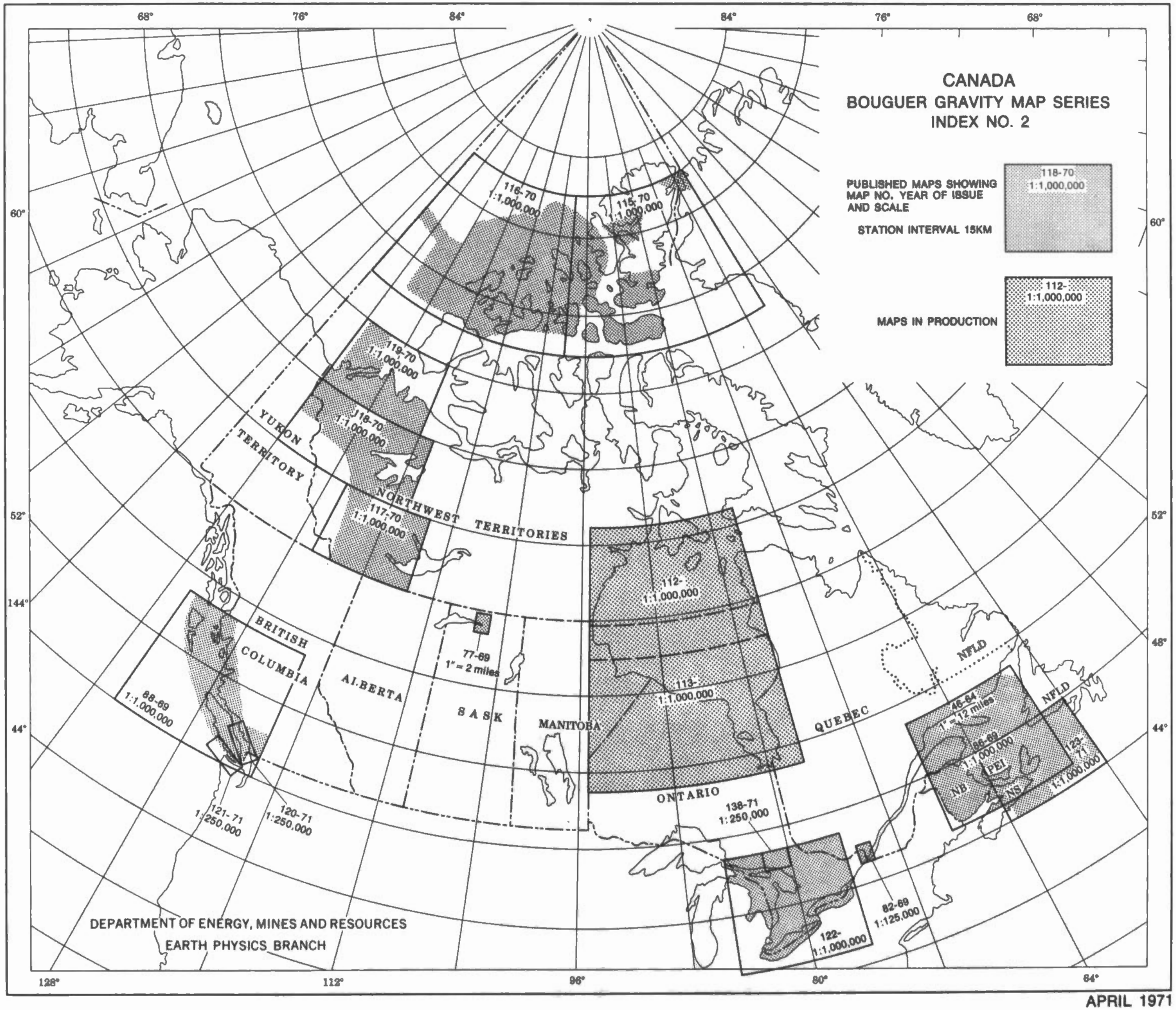

Figure 3. Additional maps published by the Earth Physics Branch to April, 1971.

lined by a series of gravity highs extending from Gaspe Peninsula to Port au Port Peninsula, Newfoundland. A gravity low of −60 mgal near the Magdalen Islands is attributed to Carboniferous sediments of low density or to Devonian granite or alternatively their combined effect.

Scotian Shelf. In 1970 the east coast underwater gravity survey was extended to cover Cabot Strait, the Laurentian Channel, and parts of St. Pierre Bank and Scotian Shelf (Stephens, Goodacre and Cooper, 1971). The gravity anomalies between southwestern Newfoundland and Cape Breton Island suggest a structural continuity between these regions. On the shelf the dominant feature of the gravity field is the Orpheus anomaly, a linear gravity low, first described by Loncarevic and Ewing (1967). Loncarevic and Ewing attribute the low to a trough filled with Carboniferous deposits including evaporites and younger sediments of low density. A broad gravity low south of the Orpheus anomaly resembles anomalies underlain by granite batholiths in Nova Scotia and may have a similar source. Positive anomalies on the Shelf are believed to be related to dense pre-Carboniferous metamorphic rocks (Stephens *et al.*, 1971).

Canadian Shield

Quebec. The major gravity anomalies of Quebec were described by Tanner (1969). Three major anomalies, the Cape Smith high, the Labrador Trough low and the Grenville Front low, are associated with the boundaries between the Superior Province and younger structural provinces of the Shield. The Cape Smith high is believed to be caused by a fold belt of dense Proterozoic volcanic, sedimentary and basic intrusive rocks. Flanking gravity lows probably result from local crustal thickening which compensates the crustal load of the fold belt. The negative anomalies associated with the Labrador Trough and the Grenville Front are interpreted as edge effects between continental blocks of differing density and thickness which are in relative isostatic equilibrium. In both cases the crust of the younger provinces are denser and thicker than the Superior nucleus.

Another set of major anomalies described by Tanner occurs over the anorthosite masses of the eastern Grenville Province. Interpretation of these anomalies suggests that the anorthosites extend to considerable depth in the crust. Tanner and McConnell (1970) noted a correlation between gravity highs and occurrences of granulites in northern Quebec. They suggest the possibility of a 'granulite layer' throughout the Superior Province of northern Quebec.

Northern Ontario. Innes, Goodacre, Weber and McConnell (1967) presented evidence which strengthens the hypothesis previously proposed by Innes that the Kapuskasing gravity high marks an ancient zone of crustal rifting. The Kapuskasing anomaly, a major feature of the gravity field of northern Ontario, cuts across the characteristic east-west trends of the Superior Province. Several carbonatite complexes, some as old as 1.7 m.y., are aligned along the Kapuskasing structure and may place an upper limit on the age of the rift.

Studies of the geology and geophysical results in northern Ontario have also led to formulation of two new hypotheses concerning the early structural history of the Canadian Shield. These hypotheses assume that plate tectonics operated in Precambrian time. Gibb (1971) suggests that the Slave and Superior cratons were once contiguous forming a single Archean craton. Rupture and sea-floor spreading caused them to separate with formation of an early Proterozoic ocean. This hypothesis is based on the remarkable morphological fit of the Slave Province and eastern Hudson Bay obtained by rotating the Slave Province about a pole at 75° 45′N (±15′), 51°W (±1°). Gibb and Walcott (1971) further suggest that closure of this ocean was responsible for formation of the now intervening Churchill Province mainly by accretion and coalescence of crustal fragments during the Hudsonian period of orogeny. Remnants of ancient oceanic deposits and oceanic crust juxtaposed with ancient continental margin deposits may still be preserved in suture zones within the Churchill Province. The most readily recognized probable suture is the circum-Superior belt which includes the Setting-Moak Lakes structure, the Fox River structure, and Cape Smith Belt, and Labrador Trough.

Northern Manitoba. Gibb (1968a and b) completed a study of the gravity anomalies adjacent to the Churchill-Superior boundary in northern Manitoba. Density determinations of some 2,000 Precambrian rock samples provided a basis for interpretation of the Bouguer anomalies in terms of relatively near-surface mass distributions in the upper crust. In some parts of the area there is excellent correlation between the surface rocks, their densities, and the Bouguer anomalies. The Nelson River gravity high outlines a belt of dense granulites. To the northwest three gravity lows are interpreted as the gravity effects of three granitic intrusions of which one is largely exposed at Split Lake and the others are largely buried although their presence is supported by the occurrence of numerous stocks of intrusive granite within the gravity lows. The Nelson River high is separated from these lows by a steep gravity gradient which marks a boundary between rocks of predominantly different ages (Hudsonian and Kenoran) between latitudes 54° and 56°N.

Northern Saskatchewan. A study of the gravity anomaly field of northern Saskatchewan and part of northeastern Alberta was completed by Walcott (1968). The principal feature of the Bouguer anomaly field is a belt of intense anomalies parallel to the northeast structural trend of the crystalline basement of the region, bounded on the northwest and southeast by regions of comparatively low gravity relief. This belt comprises the Fond du Lac low, a linear anomaly at least 500 km long, about 70 km broad and with an amplitude of about −30 mgal, and the smaller Lisgar Lake and Stony Rapids highs with amplitudes of about +20 mgal. The Fond du Lac low defines a belt of low density rocks which geological mapping of one area suggests are granites. If the change in load due to the crustal density changes is compensated, as implied by studies of earth deformation due to unloading of

Pleistocene lakes, then the crust is about 5 km thinner beneath the low than in adjacent areas. A three dimensional model based on postulates of complete compensation and lateral changes in crustal density can explain the major features of the anomaly field.

Northwest Territories. A gravity map of the Coppermine region, Northwest Territories has been published by Hornal (1968). A large gravity high is related to the Coppermine basalt flows, the Muskox ultrabasic intrusion and the diabase dyke swarms in the area. Secondary features include (i) gravity highs along the north shore of Great Bear Lake and south of the Muskox intrusion, and (ii) gravity lows attributed to granites, in the vicinity of the Dismal Lakes and Coronation Gulf. A detailed gravity survey over the Muskox intrusion showed a smoother gravity field than expected, probably because a considerable portion of the dense olivine layers of the intrusion have been altered to less dense serpentine.

Interior Plains. In northern Alberta the gravity field is dominated by the gradual decrease in Bouguer anomaly towards the Rocky Mountains; this decrease reflects the isostatic compensation for the increasing topographic load (Walcott and Boyd, 1970). Other major anomalies indicate changes in lithology within the upper part of the Precambrian basement. The MacDonald fault is well defined gravitationally in the area of its exposure as far southwestward as Pine Point. The Peace River Uplift of northern Alberta may be isostatic in origin. Walcott (1970b) has discussed this interpretation in terms of differential loading by sediments on originally compensated basement topography. If the wavelength of topography is large, differential vertical movements can occur causing amplification of the original topography and growth of an arch with sediments thicker and the load greater on either side of the arch.

Prior to interpreting the major gravity anomalies of the sedimentary basin in the southern Interior Plains, Dr. J. Maxant, a postdoctorate fellow, has undertaken an intensive study of the densities of the sedimentary rocks. Gamma-gamma logs from about 450 wells distributed throughout the basin are the main source of density information. Densities, formation tops and lithological descriptions, made available through the co-operation of numerous oil companies in Canada, are now stored on cards and preliminary analysis of these data has commenced.

Canadian Cordillera. A Bouguer anomaly map (scale 1:1,000,000) covering the continental shelf, Vancouver Island, the Queen Charlotte Islands and the fiords of the west coast of British Columbia has been published by Stacey, Stephens, Cooper and Brule (1969). More detailed gravity, magnetic and bathymetric maps are available for the Strait of Georgia and the Strait of Juan de Fuca (Stacey and Steele, 1970). The major features of the gravity field are: (1) a positive Bouguer anomaly along the western edge of the area, which is associated with the change from continental to oceanic crust, and (2) a negative anomaly along the Coast Mountains, which is attributed to the thickening of the continental crust below these mountains. On the eastern side of the Queen Charlotte Islands, Hecate Strait, Queen Charlotte Sound, and Vancouver Island, the average Bouguer anomaly is approximately zero, with local anomalies superimposed on a fairly flat gravity field. Several of these local anomalies are related to density variations in the surface rocks. A crustal model for the southern part of the Canadian Cordillera has been developed on the assumption that isostatic compensation is complete and local. The area included in the model lies between 49° and 51°N and extends from the Plains of southern Alberta to the vicinity of the Juan de Fuca Ridge. In the model, the thickness of the crust below the Plains, below the mountains of British Columbia and below the ocean west of Vancouver Island appears to be in good agreement with the depth of the M-discontinuity derived from seismic data. The results are ambiguous over Vancouver Island due to the very strong gravity anomaly related to the thinning of the crust west of the Island towards the ocean. However, the results suggest that the crust below the Island may be 70 km thick, which would be in reasonable agreement with seismic and magnetotelluric results, and with the requirements of plate tectonics (Berry, Jacoby, Niblett and Stacey, in press).

Hudson Bay. Weber and Goodacre (1968) have completed an analysis of the crust-mantle boundary in Hudson Bay from gravity and seismic observations. A study of the results of the gravity and seismic surveys in Hudson Bay in 1965 showed that the gravitational effect of a two-layer crustal model based on the seismically determined depths has no correlation with the observed gravity anomalies (Innes *et al.*, 1968). On the profile from Churchill to Povungnituk the gravity and seismic observations could be reconciled by postulating lateral variations of the acoustic compressional wave velocity within the crust. A crustal model was calculated, consistent with the seismic and gravity observations for which the crustal velocity varies from 6.15 to 6.56 km/sec and the postulated depths were almost entirely within the confidence limits of the original model.

The postulated velocity variations were compared with the lower refractor velocities of the shallow seismic survey on the hypotheses that the crustal velocities are systematically higher than the crystalline surface velocities and that there is a correlation between variations in crustal and surface velocities. The test was inconclusive because bottom refractor velocities were higher than crustal velocities in two areas where volcanic flows and high-velocity sediments might be present.

The case of linearly related velocity (V) and density (ρ) variations was analyzed and it was shown that the gravitational effect of the crust-mantle boundary undulations might be completely masked or even over-balanced by density changes in the crust if $\frac{d\rho}{dV} \geq 0.11 \, g \, cm^{-4} sec$. The crust could be characterized by having dominant velocity variations (in which case the gravity anomaly reflects the undulations of the crust-mantle boundary) or dominant density variations (in which case the gravity anomaly inversely reflects the crust-mantle boundary undulations) depending on the relationship between average crustal density and average crustal velocity.

Arctic Canada. Two Bouguer anomaly maps at a scale of 1:1,000,000 covering the area bounded by latitudes 74°N and 82°N and longitudes 60°W and 141°W have been compiled from about 8,800 gravity observations made in the period 1960-68 (Sobczak and Weber, 1970). On land, relationships between gravity anomalies and sedimentary facies changes and thickness of sediments have been established. Models of crustal structure have been derived from gravity, density, magnetic and seismic measurements. The regional free air anomaly map shows a series of positive elliptically-shaped anomalies aligned along the Polar Continental Margin. These anomalies, with amplitudes in excess of 100 mgal and with horizontal gradients of up to 2.5 mgal/km, are explained by the combined effect of sedimentary thickening (to 10 km) and crustal thinning (to 20 km) at the margin (Sobczak and Weber, in press).

A paper on the densities of crystalline, carbonate and clastic rocks from the Queen Elizabeth Islands has also been published (Sobczak, Weber and Roots, 1970).

A study of the gravity field over Somerset, Prince of Wales, and northern Baffin Islands has been presented by Berkhout (1970). Major negative anomlies occur on Borden and Brodeur peninsulas, in the area east of Agu Bay, on northeastern Somerset Island, and on northwestern Prince of Wales Island. These lows are explained by the presence of Upper Proterozoic metasedimentary rocks. An important conclusion is that during Upper Proterozoic time vast basins existed which were the sites of accumulation of clastic sediments. The observed gravity field outlines these basins and suggests that they may be interconnected.

A northerly trending gravity high is associated with the Boothia Uplift and two parallel highs occur to the west of it, all three being separated by gravity lows. The density contrast between crystalline rocks of the uplift and the adjacent Paleozoic rocks is not sufficient to explain the change of gravity over the Boothia Uplift. It is suggested that three northerly trending basement uplifts exist, separated by graben in which Upper Proterozoic quartzitic rocks occur. The Boothia Uplift became active again in Paleozoic time and overthrusts the quartzitic rocks in the west; this is reflected by observed negative anomalies along its western flank.

The gravity high over Prince Regent Inlet may reflect a basemant fault block beneath the Paleozoic rocks, whereas adjacent gravity lows represent the depressed areas occupied by thick deposits of Upper Proterozoic quartzitic rocks. The northerly and northeasterly trends of the two systems of basement fault blocks cut across the generally easterly (Archean) trend of basement structures, as on Baffin Island. Similar observations have been made in the Canadian Shield. Berkhout concludes that these unusual trends may possibly originate along ancient orogenic zones with northerly and northeasterly trends.

Three Bouguer anomaly maps at a scale of 1:1,000,000 and contoured at 5 mgal intervals have been prepared from 6,100 gravity observations made in the northern Interior Plains and on the Beaufort Sea from latitude 60°N to 72°N (Hornal, Sobczak, Burke and Stephens, 1970). The major features of the gravity field are: a gravity low over the Mackenzie Mountains which is attributed to a thickened sedimentary sequence and a deeper crust-mantle boundary; a relatively positive anomaly of 50 mgal striking north from Trout Lake to Great Bear Lake which reflects a ridge of mafic rock within the Precambrian basement; a negative anomaly over the Mackenzie River Delta of 55 mgal which results from the deposition of more than 21,000 feet of Cretaceous and Tertiary sediments; and a circular positive anomaly of 130 mgal situated south of Darnley Bay which is explained by a cone-shaped basic intrusion. Smaller variations in the gravity field in the Interior Plains may be attributed to changes in the depth to the Precambrian basement and density variations within the sedimentary column.

Detailed gravity investigations

Alexandria area, Ontario. Sobczak (1969) has completed a study of the gravity field in the Alexandria area of eastern Ontario. Negative Bouguer anomalies are correlated with the Chatham-Grenville syenite stock and a similar intrusion at Mount Rigaud on the southern border of the Grenville-A subprovince. It is postulated that the negative anomaly near Plaisance indicates the presence of a similar intrusion below the Paleozoic cover. The Alexandria high, a positive residual Bouguer anomaly which extends from Lunenburg to Pointe aux Chênes, may be explained by the presence of a basic lenticular body of thickness varying from 6,000 to 9,000 feet and width of 50,000 feet at a depth varying from 3,000 to 5,000 feet. The approximate thickness of the Grenville Series is 11,000 to 12,000 feet along the crest of the Alexandria high. The regional gravity gradient which increases from −30 milligals in the northwest to +10 milligals in the southeast of the area is correlated with a rise of over 3 kilometres (10,000 feet) of the Mohorovicic discontinuity.

Bancroft area, Ontario. W.R. Jacoby has completed a detailed gravity study of the Bancroft area, Ontario. The correlation between surface geology and gravity is excellent and there is enough density information to calculate the sub-surface mass distribution with considerable confidence. The low density granite gneiss, outcropping in large domes, batholiths and smaller plutons, seems to be extensive under a rather shallow metasedimentary cover 1-4 km thick. This indicates that the granite may represent partly pre-Grenville basement, remobilized or anatectically melted, and partly Grenville deposits, intensely metamorphosed and granitized. The granites and the gravity field show a distinct waveform over several wavelengths (20 to 30 km and 5 to 6 km). This wavelength is used to study the mechanics of granite emplacement. No vertical variation of the base of the granitic layer was indicated for the region.

Preparation of a comprehensive paper on this study was nearing completion at the end of 1970.

Timmins – Senneterre area, Ontario-Quebec. A study of the gravity field in the Timmins Senneterre mining belt was completed by Gibb, van Boeckel and Hornal (1969). The area is studded with many granite batholiths of variable composition which are outlined by intense negative gravity anomalies. The whole region was regarded as one great roof pendant and on this assumption model studies show that the volcanic belts extend to depths ranging from 3 to 5 km. Variations in anomaly level within the batholiths were correlated with compositional and density differences in the granites which have a compositional range which includes granodiorite and diorite. One of these batholiths, the Round Lake batholith, was the subject of a separate study (Gibb and van Boeckel, 1970). Two possible three-dimensional models of the batholith were presented which depend on different assumptions. The first model involves normal faulting of the batholith to explain the variations in anomaly level within the batholith. In this model the granite is assumed to be homogeneous in density and extends to a maximum depth of 10 km. Alternatively density variations corresponding to a facies change within the pluton may be the major cause of the local internal anomaly variations. In this interpretation the true thickness of the granite connot be evaluated as the whole region is assumed to be underlain by granite, but the maximum thickness of the surrounding basic volcanic rocks is 5 km.

Piercement structures in the Arctic Islands. Reconnaissance gravity surveys over three evaporite piercement domes in the Canadian Arctic Islands have been interpreted by Spector and Hornal (1970). Each dome was considered as a right-vertical cylinder divided into two homogeneous regions, a high density anhydrite zone (2.9 g/cm^3) overlying a low density gypsum and/or rock salt zone (2.3 g/cm^3). The cylinder is surrounded by a sedimentary sequence which has a uniform density of 2.4 g/cm^3. A least-squares approach was used to estimate the thickness of the anhydrite and gypsum-rock salt zones. The three sets of estimates gave a range of 200 to 550 m for the anhydrite thickness and a range of 700 to 5,500 m for the vertical extent of domes. In each case the depths were less than expected on the basis of estimates from seismic and geological data. Possible explanations for this are: (a) the cross-sectional area of each dome decreases with depth; (b) the existence of a transition zone where a gradation occurs between the high and low density zones; and (c) the effective density contrast of the low density zone is less than 0.1 g/cm^3.

Darnley Bay, Northwest Territories. The largest isolated gravity anomaly (130 mgal) discovered in Canada so far occurs at Darnley Bay, N.W.T. This anomaly was described by Hornal *et al.*, (1970) who suggested that it is caused by a basic intrusion with the shape of an inverted cone and a thickness of crustal dimensions (~40 km). Stacey (in press) has completed a further study of this anomaly and concludes that a cone-shaped basic intrusion with or without an ultrabasic core can explain the anomaly equally well. He compares his models with lopoliths having similar gravity anomalies, with Tertiary igneous centres in Scotland, and with present day sea-mounts.

Crater investigations. The investigation of Canadian structural and topographic features for evidence of origin by hyper-velocity impact of cosmic bodies began in 1950. By 1966 twelve Canadian sites had been shown to have the approximately circular outline, strong fracturing and brecciation and megascopic and microscopic evidence for shock metamorphism which are the main characteristics of eroded but otherwise undisturbed impact structures. Most of the sites had been investigated by gravity, magnetic and, in some cases, seismic methods. These studies showed the structures to have moderate to weak gravity anomalies consistent with their being underlain by rocks of low density, generally weak magnetic susceptibility and low seismic velocity to depths no greater than their radius at the surface.

Since 1966, a further six sites have been shown to contain shock metamorphosed rocks. Two of these, Steen River, Alberta and Lake St. Martin, Manitoba have weak surface expression, being buried by later sediments to a large extent. Two others, Mistastin Lake, Labrador, and Lake Wanapitei, Ontario closely resemble craters such as those at Clearwater Lake and Deep Bay. The remaining two, Charlevoix, Quebec and Sudbury, Ontario have been eroded and also deformed to some extent by tectonic events subsequent to their formation.

Geophysical data acquired to 1966 included gravity and magnetic surveys of eight craters and seismic surveys of five. Magnetic data mainly airborne are now available for an additional five sites and gravity for eight. A gravity Bouguer anomaly map has been published for Nicholson Lake crater (Dence *et al.*, 1968) while detailed maps by Dr. J. Popelar for Sudbury and Lake Wanapitei are in an advanced stage of preparation. Detailed gravity data are also available for Manicouagan and have been included in the regional gravity map series. Altogether of the eight, only Nicholson Lake and Lake Wanapitei have clearly expressed negative gravity anomaly fields. The rest all show indications of gravity lows, but lie within complex regional fields which appear to obscure or distort the crater anomalies. More detailed data are required to define clearly the anomalies associated with these structures.

Earth tides and crustal loading

Both the Earth Physics Branch and Dalhousie University have been concerned with this subject. Theoretical and experimental work has been directed mainly to the problem of correcting for the perturbing effect of the ocean tide on measurements of the earth tide. Until this correction can be made with high accuracy the original purpose of earth-tide measurements, the determination of the Love numbers, cannot be realized. A technique for estimating the correction has been developed by the Earth Physics Branch on the assumption of a given global distribution of ocean tides loading a Gutenberg-model earth. However, the Love numbers are presently better known than is the global distribution of ocean tides or the response of the lithosphere to surface loading. Consequently, this technique has been used only to explain the general features of the global variation in earth-tide measurements and, in a reverse sense, to identify definite regional anomalies due either to incorrect ocean tide data or to anomalous response of the lithosphere to surface loading. One such anomaly has been revealed by the disagreement between theoretical results obtained by the Earth Physics Branch with earth-tide measurements made at several locations across the United States by Columbia University. Measurements in the western half of the United States show a loading effect due to the tides in the eastern Pacific Ocean which is smaller than that expected on the basis of published ocean-tide data. The Earth Physics Branch intends during the next two years to make a series of earth-tide gravity measurements throughout Canada to identify and investigate other anomalies. These will be fairly short observations beginning in the north at Alert (lat. 83°N) and proceeding south along a mid-continental line to link with similar measurements in the United States.

On a regional scale the ocean tide is sometimes accurately known and the feasibility of using it to probe the upper layers of the earth has been investigated by Bower (1969) with measurements in England and by Lambert (1970) and Beaumont and Lambert with measurements in the Bay of Fundy area. This type of investigation, which relies principally on precise tilt measurements, will continue with a view to improving both the experimental and the analysis techniques available. At the Earth Physics Branch D. Bower is developing a long watertube tiltmeter which can be precisely calibrated and which is expected to be zero stable. Also at the Earth Physics Branch data analysis techniques such as the "response method" are being applied by A. Lambert in order to isolate the tidal component of tilt from coherent "noise" effects. C. Beaumont at Dalhousie University is constructing a finite-element crustal model of the Bay of Fundy area which will permit a generalized theoretical approach allowing for multilayers, lateral homogeneities and discontinuities.

The underground recording station near Ottawa was closed early in 1970 after approximately four years of recording both gravity and tilt earth-tide measurements. A new site in the same area is being prepared as a permanent station and will be equipped with both pendulum and hydrostatic type tiltmeters.

Flexural rigidity, thickness and viscosity of the lithosphere

In a series of recent studies Walcott (1970b) has modelled the earth's lithosphere and asthenosphere as a thin sheet and a fluid substratum respectively. The flexural rigidity of the lithosphere was deduced from observations of the wavelength and amplitude of bending in the vicinity of supercrustal loads. Data from Lake Bonneville given by M.D. Crittenden, Jr. were reinterpreted to give a value for the flexural rigidity of the lithosphere in the Basin and Range province of the western United States of 5×10^{22} Newton meters. Observations of loading in Canada give values for the flexural rigidity greater than 3×10^{23} N m for the Caribou Mountains in Northern Alberta (Walcott, 1970a); about 4×10^{23}N m for the topography over the Interior Plains (Walcott, 1970a); about 10^{23}N m for the Boothia uplift in arctic Canada (Walcott, 1970b); and about 10^{25}N m for the bending of the beaches of Pleistocene Lakes Agassiz and Algonquin. The flexure of the lithosphere at Hawaii and the bending of the oceanic lithosphere near island arcs give values of about 2×10^{23}N m (Walcott, 1970c). For short-term loads (10^3-10^4 years) the flexural rigidity of the continental lithosphere is almost two orders of magnitude larger than for long-term loads, indicating nonelastic behaviour of the lithosphere with a viscous (about 10^{23}N sec m^{-2}) as well as an elastic response to stress. From the values of the flexural rigidity the thickness of the continental lithosphere is inferred to be about 110 km and that of the oceanic lithosphere about 75 km or more. The anomalously low flexural rigidity of the lithosphere of the Basin and Range province may be due to a very thin lithosphere, only about 20 km thick, with hot, lower crustal material acting as an asthenosphere.

Gravity interpretation methods

Jacoby (1970) has published sets of diagrams of the normalized peak gravity effect of exposed rock bodies which can be used to determine the depth to which the bodies extend. The method is straightforward and is applicable to rock bodies of any shape.

An accurate method of computing the first vertical derivatives at different elevations from two-dimensional gravity profiles has been published by Paul (1970). He has shown that the accuracy of the computed first vertical derivative values depends significantly on a remainder term due to the finite length of the anomaly profile. Paul has also completed the development of a quantitative method to interpret gravity anomalies with circular symmetry. In this method the radial profile is first transformed to a vertical profile using the upward continuation principle, direct interpretation of the physical and geometrical parameters of the local causative body is then possible.

A weighted summation method for upward continuation of gravity data from a plane has been developed by Paul and Nagy (in press) under the assumption that the observations are available at regular intervals. The upward continued value has been expressed as the sum of individual gravity values and the corresponding theoretical coefficients. Besides the usual parameters involving horizontal and vertical distances, these theoretical coefficients have been generalized to be dependent also upon (i) the order of a low order polynomial assumed to represent the gravity variation around a grid point and (ii) the weights assigned to the gravity values at the nearest four points used for least square determination of the polynomial. The method has been tested with theoretical models and field gravity data and a paper has been submitted for publication.

Physical geodesy

Graphic representation. For the purpose of correlating various types of data (gravimetric, geodetic) and selecting areas to test various hypotheses, graphic representation of data is essential. The following developments are mentioned:

1. Compilation of an average free air gravity anomaly map of Canada. Using piecewise surface fitting technique, representative values over surface elements are obtained. The selection of a grid separation of about 55 km resulted in 2,923 surface elements on

which basis the free air map has been compiled. A paper describing the details is forthcoming.

2. Development of a special plotting package by which deflections of the vertical (input data represented as vector), geoidal height changes calculated from these reflection values can be plotted in the desired map projections and scales.

Computation of changes in the deflections of the vertical from gravity data. Programming of a method using local plane co-ordinate system and integrating out to a few hundred km around the computation point has been compiled. For checking the procedure see paragraph on model studies.

Model studies. The basic element for model studies is a right rectangular parallelopiped for which the gravity, the deflection of the vertical, the potential, and other quantities can be calculated with high precision. By combinations of elements, various potential fields can be computed to simulate practical situations satisfactorily. The model gravity field can then be used as a basis for upward continuation, computation of the deflections of the vertical, and other operations. Comparison of computations using the model field with those values obtained directly from the mass model serve not only to check the computations but also to provide a basis to specify requirements in the practical situation.

Upward continuation of gravity data from a plane. A method of upward continuation of potential fields has been developed assuming that the input data is regularly distributed over a plane. The computational procedure has been verified on a model for various elevations. A paper on this study by M. Paul and D. Nagy has been submitted for publication.

Upward continuation from an irregular surface. This is an extension of the above work and is being carried out by M. Paul. This method recognizes that the observations are made on actual topographic surface. The computational procedure is an iterative one which involves the integral for downward continuation from a plane.

Data representation. Y. Hagiwara, postdoctorate fellow, has investigated various methods of obtaining representative values from point distribution and techniques for predicting values in unsurveyed areas. Spherical harmonics expansion requires too many terms for adequate short wavelength representation to render its use feasible at present. The method accepted is that based on double Fourier series expansion.

Computation of geoid and the deflection of the vertical. Y. Hagiwara has also investigated techniques of using surface gravity data to provide the detail lacking in satellite measurements. The large wavelength structures for both the geoid and the deflection of the vertical have been computed from the spherical harmonics representation of the potential and gravity as determined by the Smithsonian Astrophysical Observatory 1967. More detailed computations of the geoid and the deflection values have been made using representative values from surface gravity data in surveyed regions and extrapolated values for unsurveyed regions within Canada. Co-ordinate transformation of the surface gravity data was also made for compatibility with satellite data. A publication giving the details of the various methods used and results obtained is under preparation.

Singularity. The singularities of the Stokes' and Vening-Meinesz's functions at the origin and their treatments are well known. In other cases when Fourier techniques or the methods of Molodenskii and Bjerhammer are used for the calculation of geoidal heights or the deflections of the vertical, the treatments of the singularities are more involved. M. Paul has examined this problem from the standpoint of practical computations.

Polar studies

In May 1967 and in April 1969 the Earth Physics Branch in co-operation with the Polar Continental Shelf Project carried out multidisciplinary geophysical studies in the vicinity of the North Pole. The expeditions under the leadership of J.R. Weber included participants from private industry and universities. The original objective was to establish a gravity traverse from Ellesmere Island to the North Pole. The biggest problem facing the project was precise navigation. Drift of the pack ice and atmospheric refraction results in accuracy of position fixes in the polar region obtained from conventional sun observations that is no better than a few kilometres. The problem was solved by R.L. Lillestrand from the Research Division of Control Data Corporation in Minneapolis who developed techniques involving sighting on various celestial targets during daytime and improved methods to solve for ice drift by computer. The computer was programmed to convert time of observations and zenith angles of the celestial target into position and drift velocity. A communication link for data transmission between the expedition and the computer in Minneapolis was established with the help of radio amateurs in Alert and Ottawa (Lillestrand, Grosch and Vanelli, 1967).

For logistical reasons it was not possible in 1967 to obtain aircraft suitable for making spot landings between Ellesmere Island and the Pole. Instead the expedition was airlifted to the Pole with a Bristol Freighter aircraft. The scientists drifted with the pack ice a distance of 30 km over a seven-day period during which time gravity observations were taken and the experimental navigational techniques were tested. These tests included ranging to an acoustic transponder dropped to the ocean floor.

Tilt measurements carried out on Fletcher's Ice Island (T-3) by Browne and Crary (1959)* more than a decade earlier, prompted an attempt to measure the tilt of the fluid surface of the ocean. Three holes were drilled through the ice and by levelling from water surface to water surface a tilt of eight seconds of arc was observed. It was realized that if such tilts persist over long distances along atmospheric pressure gradients (as Browne and Crary's observations indicated) it would imply sea level changes of a magnitude which would significantly affect the gravity measurements. Accordingly J.R. Weber developed a hydrostatic levelling

*Browne, I.M. and A.P. Crary. The movement of ice in the Arctic Ocean. In Arctic Sea Ice (ed. W.R. Thurston), N.R.C. Publ. 598, 191-209, *Nat. Acad. Sci.*, Washington, D.C.

system capable of measuring the tilt of the fluid ocean surface to an accuracy of about ±0.01 second of arc. Spot observations with this instrument in the vicinity of the North Pole in 1969 and in the Gulf of St. Lawrence in 1970 indicated tilts of up to about one second of arc (Weber and Lillestrand, 1971). Instrumentation is presently being developed with the aim of setting up an array of automatic tilt recording meters during the Arctic Ice Deformation Joint Experiment (AIDJEX) in the Arctic Ocean in 1973 in order to determine the deformation of the ocean surface with time.

During the 1969 expedition some 40 gravity stations were established between the Lincoln Sea and the North Pole, across the Lomonosov Ridge and in the vicinity of the North Pole using navigational techniques developed during the earlier expedition. The expedition established a base camp 50 km from the North Pole and over a period of 26 days drifted a distance of 80 km with the transpolar current. Advanced navigational techniques involving some 400 star observations, the use of satellite transit observations, and sonar trilateration from a number of acoustic transponders on the ocean floor were used to determine the path of the ice floe. An Omega VLF receiver was also used as a navigational aid, but because of unusually poor radio propagation conditions the system was inoperative most of the time. The relative agreement between the sonar drift path and the positions determined from the celestial observations is excellent, being of the order of 70 m. Evaluation of the satellite data has been delayed because the unique geometric configuration of satellite observations in the polar areas requires a different method for the reduction of the data than in more southerly latitudes. It is hoped to apply the results of the satellite data, the astronomic observations and the sonar trilateration to determine the absolute deflection of the plumbline. In addition to these geodetic observations continuous current measurements 2 m and 100 m below sea level and wind measurements 3 m above the ice surface as well as a number of hydro-casts were made.

Bedford Institute (Atlantic Oceanographic Laboratory)

Detailed gravity surveys

Hydrographic-geophysical survey of the eastern Canada Continental Shelf. Since 1966, the Atlantic Oceanographic Laboratory at the Bedford Institute has greatly increased its geophysical coverage of the eastern continental margin of Canada. This has been largely due to the collaboration existing between the Marine Geophysics Section and the Hydrographic Section of the Institute. The prime responsibility of the A.O.L. Hydrographic Section is charting all navigable waters within the Atlantic Region, as applicable to navigation requirements. The Region is defined as Canada's Atlantic Seaboard, the Gulf of St. Lawrence east of Pointe-des-Monts, Hudson Bay and the eastern Arctic. The surveys conducted by the Section satisfy requirements in navigation, fisheries and mineral exploration. All positioning of the ship is done by Lambda (low ambiguity decca) in the range/range mode, thus providing the most accurate navigation available in the areas surveyed so far. After a mutual study of each group's surveying techniques, it was decided that the two disciplines could be combined to produce a highly effective multi-disciplinary survey operation covering the Canadian east coast continental margin with measurements of bathymetry, gravity and magnetics.

The method of operation now existing is that the hydrographers carry out an initial survey of their proposed survey area at a line spacing of 2 or 4 miles, depending upon the density of measurements required to give good geophysical control. With the completion of this multidisciplinary portion of the survey, the hydrographers continue surveying the same area at a reduced line spacing, this being $^1/_2$ or 1 mile line spacing at water depths less than 50 fathoms. During this latter portion of the cruise geophysical studies are carried out as opportunity and manpower permits.

The data collection and reduction operation has now passed into the hands of the Hydrographic Section and a series of natural resources charts* are to be produced by them, with editions covering bathymetry, gravity (free air anomaly) and magnetics (total field). At present only the three editions of sheet 14956 are available (covering Marsden Squares 14956 and 14957: latitude 45° – 46°N, longitude 46° – 48°W). Four sheets covering the Tail of the Bank area (latitude 42° – 44°N, longitude 48° –52°W) are expected to be published before spring 1971. Geophysical data from the Grand Bank of Newfoundland and the Gulf of St. Lawrence is undergoing final processing at the Institute, and will be turned over to the cartographers at about the same time. The feasibility of extending natural resources charts to cover all Canadian offshore is presently being investigated by the Canadian Hydrographic Service.

While the routine data collection, reduction and chart production are in the hands of the Hydrographic Section, responsibilities for the initial planning of the geophysical aspects of the multidisciplinary cruises and their data interpretation still lie with the Marine Geophysics Section. This development is still in its infancy to the extent that the Hydrographic Section is still learning the techniques of geophysical surveying and data reduction. Meanwhile, Marine Geophysics is still attempting to exploit the positioning facilities provided by the surveys, in increasing the accuracy of sea surface gravity measurements as limited by the calculation of the Eotvos correction. The seismic group is also investigating the possibility of adding seismic reflection profiling to the functions of the survey.

Grand Banks. The area surveyed in 1966 and 1967 lies approximately between longitude 53°W and 44°W and latitude 45°N and 48°N. The most interesting features of the gravity charts reveal:

1. Steep horizontal gradients (up to 12 mgals per km).
2. A large "low" near the central portion of the survey area (minimum of −35 mgals with general low area extending over approximately 1° x 1°).

*Requests for these charts (price $1.00 each) may be made to: Hydrographic Chart Distribution Office, Canadian Hydrographic Service, 615 Booth Street, Ottawa, Canada.

3. An extensive "high" in the north central portion of the survey area (maximum of +136 mgals with general high area extending over approximately 1° x 1°).
4. A positive zone of +60 to +80 mgals associated with the Flemish Cap.
5. A belt of circular positive features with amplitudes from 20 to 100 mgals lying within and parallel to the 100 and 1,000 fathoms contour lines.

The top of the Grand Banks, especially within the 50 fathom contour is remarkably flat; therefore the steep gradients of the gravity field are due to major variations in the density distribution and/or structure of the subsurface rocks. This, coupled with the fact that the magnetic field in the same area is very smooth, indicates that the density variations are due to changes in structure within the sedimentary rock section. The gravity "lows" that are relatively small in areal extent are believed to be due to salt structures, while the large low in the central portion of the survey area is believed to be a basinal type feature with a total sedimentary rock thickness probably in excess of 6 km. In the area of survey, two 30-mile and one 150-mile refraction seismic lines were shot. Six distinct refraction layers were mapped with the following velocities: 1.67, 1.84, 2.69, 4.59, 5.40 and 6.03 km/sec. The highest velocity probably identifies cristalline basement rock in this area. As expected from previous investigations, a thickness of sedimentary rock in excess of 3 km was found in the vicinity of the long profile near 45°N and 49°W.

Gulf of St. Lawrence. In 1968 and 1969 a multidisciplinary survey was carried out in the Gulf of St. Lawrence. In surveying the Gulf east of 62°W and north of 47°N approximately 55,000 km of bathymetry, magnetics and gravity data were obtained. In the northeastern areas, surveyed in 1968, the gravity map covering part of the western flank of the Canadian Appalachians is featureless when compared with the gravity map of the Grand Banks which comprise part of the eastern flank. In the southeast Gulf, the gravity field is more complex and is dominated by a large negative free-air anomaly of −100 mgals (Bouguer anomaly of −60 mgals) to the northeast of Magdalen Islands. The analysis of this gravity information has only recently been started.

The surveyed area of the Gulf has been covered previously with sea-bottom gravity measurements made by the Gravity Division of Earth Physics Branch. The data in the eastern Gulf of St. Lawrence covering the areas of both the 1968 and 1969 A.O.L. surveys are being analyzed with the intention of determining whether this type of survey with greater concentration of survey lines (1- or 2-mile intervals), speed of data collection, and higher resolution of gravity anomalies is a better investment of money and manpower than the 8-mile grid bottom gravimeter survey providing more accurate gravity values. Initial comparison of the data yields a mean difference of 2.1 mgals between A.O.L. and E.P.B. over the 1969 survey area with the E.P.B. measurements being higher. Separating the E.P.B. measurements into different years of operation, there also appears to be a temporal variation in the underwater measurements. This is suspected to be the result of using different depth transducers in each of those years' operations. These and further results derived from the analysis will provide a basis for planning future complementary surveys by the two agencies.

Western Arctic. In response to the requirement for better navigation charts in the north the locale of the mapping program was shifted to the western Arctic for the 1970 field season. In the Beaufort Sea, bathymetry, gravity, and total magnetic field were measured at $^1/_4$ mile line spacing over 1,500 square miles. The area surveyed was centred on the Admiral's Finger, a shoal located approximately 50 miles north of Atkinson Point, and discovered in 1969 by *S.S. Manhattan* during her passage to Prudhoe Bay, Alaska.

During the course of the survey, about 80 additional shoals were discovered, some rising to within 17 metres of the surface. Observed gravity in the area was dominated by the shelf anomaly, exceeding 80 mgal at its maximum value, and paralleling the 100-metre contour. Except for the northeast corner of the survey area, there was no indication of shallow disturbances to the earth's magnetic field.

In conjunction with the western Arctic program, ships' passages from Victoria to the Beaufort Sea and then to Halifax provided additional opportunities for the collection of geophysical data, especially in Baffin Bay. Eight thousand km of gravity data were obtained by *CSS Hudson* and *CSS Baffin* between Resolute and Funk Island, Newfoundland. About one half of the data were collected during a survey of Baffin Bay in an attempt to ascertain its crustal structure.

Future plans. The proposed hydrographic-geophysical survey for 1971 will complete the surveying of Flemish Cap and then proceed northward along the continental shelves of Newfoundland and Labrador. At the present rate of coverage, and if priorities do not change, it is hoped to complete the survey up to Cape Chidley within the next five years.

Regional geophysical surveys

Mid - Atlantic Ridge. In 1968, the third Institute expedition to the Mid-Atlantic Ridge continued the comprehensive geophysical survey of the area between 45° and 46° which began with the voyage of *R.R.S. Discovery II* in 1960. Two ships were used in this survey to provide a shooting and receiving ship for a seismic experiment carried out on the eastern flanks of the ridge. Satellite navigation provided absolute positioning for the survey and radar transponder buoys were moored to provide accurate navigation within the survey area. Nine thousand km of bathymetric, magnetic and gravity measurements were made at a spacing of less than two miles to complete the detailed survey of the western flank of the ridge. In addition some 4,000 km of surveying were completed on the eastern flank. The total coverage is now approximately between 45°N and 46°N from 26°30'W to 30°W. All the gravity data obtained during the three expeditions have now been compiled and the data adjusted. Free air and Bouguer anomalies have been calculated for the entire region and interpretation is proceeding. The associated seismic refraction data will be used in model studies to be made on the crustal structure of the 3° by 1° area. Preliminary gravity results from the combined surveys were included in a paper presented at the 50th Annual General Meeting of the American Geophysical Union (A.G.U.).

Bay of Fundy. Three thousand seven hundred kilometres of gravity, magnetic and bathymetric data acquired in the Bay of Fundy (between 66°W and 67°10′W from 44°10′N to 45°10′N) have been processed and reduced to free air and Bouguer gravity anomalies and total magnetic field. An interpretation of the data has been made and a paper is being prepared for publication.

Hudson Strait. Gravity data on two tracks to and from Hudson Bay have been reduced and are being used in an interpretation of the structure of Ungava Bay and Hudson Strait based on all geophysical observations in this area. This work has been published by Grant and Manchester (1970).

North American Basin. A series of N-S traverses on which geophysical data are collected is in progress in the western North Atlantic. For this program, *CSS Baffin* and *CSS Hudson* were used on an opportunity basis as they travelled to and from the Caribbean on hydrographic training and geological research cruises. Magnetic and gravity coverage now extends between 45°N and 20°N along meridians at 2 $^1/_2$° intervals between 55°W and 70°W. Gravity data have also been collected along meridians 55°W, 57 $^1/_2$°W, 64°W and 70°W. A graduate student at Queen's University is examining the combined data.

Hudson '70. As a Canadian contribution to the Oceanographic Decade, *CSS Hudson* undertook a one-year oceanographic expedition named Hudson '70 comprising a circumnavigation of North and South America. An extensive marine geophysical program has been carried out as part of the expedition. Upon the departure of *CSS Hudson* for the Arctic from Victoria, British Columbia, 35,000 km of bathymetry, gravity and magnetic field data had been collected. This had been supplemented with 1,670 km of continuous seismic profiling, a major seismic refraction experiment, 13 heat flow measurements, 14 dredge hauls and the collection of two cores during detailed surveys in selected areas.

In the Atlantic, the track of *CSS Hudson* from Halifax to Rio de Janeiro provided gravity, magnetic and bathymetry data to add to that collected by *CSS Hudson* and *CSS Baffin* on long traverses from Nova Scotia to Europe, the Caribbean and the Arctic. These regional data will assist in our investigation of the northwest Atlantic-North America plate.

In the Pacific the geophysical investigation, while providing similar regional data to that obtained in the Atlantic, included the survey of an area adjacent to the contact between the Juan de Fuca, North America and Pacific plates. Seven thousand kilometres of gravity and magnetic data and 9,500 km of bathymetry data extended the previously surveyed section of the Juan de Fuca Ridge (the western boundary of the Juan de Fuca plate) towards the Queen Charlotte Island fault. Detailed station work was also carried out in the Explorer Trench which may be the last expression of the East Pacific Rise before its termination at the Queen Charlotte Island fault.

Regional studies of the Gulf of Alaska are also planned as a result of bathymetry, gravity and magnetic field data collected on five adjacent tracks of *CSS Hudson, CSS Baffin* and *CSS Parizeau* in the area while en route to and from the Arctic.

In the southeast Pacific, a geophysical profile was made over a feature which may be associated with the southern portion of the East Pacific Rise. A deep trench and adjacent peak (with a vertical separation of 3 km) were found in an area previously thought to exhibit few tectonic features. It appears that the feature may be part of a long fracture of the East Pacific Rise and it is hoped to name it the Hudson Fracture Zone.

The gravity data collected along latitude 150°W from the Antarctic ice field to the Alaska Shelf are being used in a geodetic program in ultimate support of a proposed oceanographic satellite. Determination of the difference in height between the isobaric sea surface and the geoid gives the change in potential of an isobaric surface. From this can be calculated the potential of all other isobaric surfaces, wherein lies the key to ocean current transport. Orbital perturbation analysis of satellite track observations provides the low order harmonics of the geoid. At present the higher order harmonics may only be obtained at the sea surface. In order to determine the high harmonics of the geoid along the path of a polar orbiting satellite, a gravimetric determination of the geoid was made along 150°W between 63°S and 57°N on the assumption that variations in the gravity are independent of longitude. Future satellite altimeter profiling of the sea surface with reference to this geoidal section will enable an absolute dynamic section to be made.

En route home to Dartmouth, *CSS Hudson* and *CSS Baffin* carried out a geophysical program in Baffin Bay. Previous work in the Labrador Sea has indicated the presence of a ridge structure buried beneath the sea floor. This ridge may have been the focus for the ancient separation of Greenland from Canada. Whether this proposed ridge extends into Baffin Bay is not known. The few days spent by the two ships in Baffin Bay were intended to provide the answer to one fundamental question: is the crust of Baffin Bay oceanic or continental? The main evidence for concluding that the crust was oceanic came from a seismic refraction experiment conducted along the axis of the Bay. In support of this, seismic reflection profiling together with bathymetry, gravity and magnetic surveying was carried out. The results of this activity will be used for planning subsequent cruises to areas of Baffin Bay requiring detailed investigation.

Environmental tests

Satellite navigation cruise (CSS Baffin 022-69). Extensive trials and comparisons between the ITT and Magnavox satellite navigation receivers were carried out on this cruise. Because of the excellent navigation facilities available (incorporating positioning by automatically recorded D.R., satellite fixes, Decca, Hi-fix, Omega and VLF) it was hoped to isolate some of the errors involved in the measurement of gravity at sea. Our two Askania sea gravimeters were operated on the same Anschutz gyrostabilized platform, each gravimeter being connected to a separate cross-coupling analog computer. Unfortunately the weather was so good and the ship motion so limited that the errors encountered were very small.

Laboratory tests. The extension of the laboratory wing of Bedford Institute in 1969 has included the provision of two laboratories dedicated solely to gravity studies. One is used as a "quiet laboratory" with a floor level platform isolated from the building. Another platform, provided for seismic studies, is coupled directly to bedrock and is also isolated from the building. No vibration testing has yet been performed on either of these platforms to determine the extent of their isolation. When this has been done, consideration will be given to setting up a gravity reference station on each of these platforms.

While the two Askania sea gravimeters have been land based, work has been carried out to determine some of the torsional parameters of the measuring system, and in particular linearity. This work was necessary on two counts. A proposal has been made to produce a completely digital processing system for the sea gravimeter. To do this, the digital filter employed must be tailored precisely to the linearity of the gravimeter measuring system. Secondly, the investigation of cross-coupling errors in gravity measurements at sea suggested that there might be an asymmetry in these errors and that this might be attributed to the non-linearity of the meter. The investigation demonstrated a non-linearity in the system which will have to be compensated for in the proposed digital processing system.

The cross-coupling computer originally built in 1965 has been modified, redesigned and completely rebuilt. It underwent extensive sea trials in its revised form early in 1969 and has been employed in correction of gravity data in the field ever since. With the continuous computation and logging of cross-coupling error data, on line correction for these errors is now feasible.

Memorial University of Newfoundland

Trans-Newfoundland gravity profile

An 800-km gravity profile, with 0.8 km station spacing, has been established along the Trans-Canada Highway between Port-aux-Basques and Come-by-Chance, Newfoundland. About one-third of the elevations were obtained from precise levelling, the remainder from an improved "one-base" barometric method which yielded a standard deviation less than half as large as that associated with the traditional "one-base" method. A total of 144 rock samples was collected along or near the profile to aid in the interpretation.

A qualitative profile interpretation has suggested the presence of unmapped gypsum deposits in southwestern Newfoundland, and intrusive bodies at several locations along the route. A detailed model study between Notre Dame Junction and Traytown shows the Ackley batholith to be a funnel shaped lopolith; it also shows this region to be underlain by an intermediate to basic layer, which may be a continuation of the layer inferred at 5-10 km depth from a gravity survey in eastern Notre Dame Bay (Miller, 1970).

Notre Dame Bay gravity investigation

A gravity survey covering 2,500 km^2 at 2.5 km spacing was conducted on islands and the coast of Notre Dame Bay near the eastern boundary of the Paleozoic Mobile Belt of Newfoundland. The Bouguer anomaly field shows good correlation with dominant features of the surface geology: (1) a strong northeasterly structural trend; (2) the Luke's Arm fault; (3) several extensive granitic bodies; however, no significant anomalies were observed over sedimentary areas. Preliminary qualitative interpretation of the published total-intensity aeromagnetic maps indicates some overall correlation with gravity and surface geology.

A satisfactory fit to the Bouguer field was obtained from three-dimensional model studies, dividing the area by geological criteria into 13 blocks, each with a mean density derived from rock samples. From the model results, two new features may be proposed:

1. A structural discontinuity near Change Islands, suggested also on the aeromagnetic maps, separating the eastern (Fogo-Change Islands) and western parts of the survey area.
2. A basic to ultrabasic layer at 5-10 km depth to explain the overall positive character of the Bouguer anomalies. This layer appears to be a landward continuation of the intermediate layer of Sheridan and Drake (1968).*

Nova Scotia Research Foundation

During the past four years some 15,000 gravity stations have been observed by the Nova Scotia Research Foundation in Nova Scotia and adjacent regions. A program of regional gravity surveying in Nova Scotia is underway. Particular emphasis is given to areas underlain by Lower Mississippian rocks which may contain diapiric salt structures. Many detailed surveys have been made to investigate possible deposits of barite, celestite, manganese and fluorite. Future plans include the extension of the regional gravity surveys in northern and eastern Cape Breton, the production of a new series of gravity maps for Nova Scotia including both Bouguer and residual anomaly maps, and a detailed study of the Chedabucto fault which runs east-west across the province and may continue seaward into the Atlantic.

During the last few years a computer oriented data handling system has been developed and is now in routine use. Data reduction, sort, merge, update, search and retrieval programs are in use. Plotting and interpretation programs are also available and a contouring package is presently being tested. All existing gravity data in Nova Scotia are gradually being incorporated in the data file.

Precise levelling methods used at present will be supplemented in 1971 by a hydrostatic levelling device currently

*Sheridan, R.E., and C.L. Drake. 1968. Seaward extensions of the Canadian Appalachians. *Can. J. Earth Sci.*, 5, 337-373.

under development. This device should find practical application in surveys involving loops or closures of distances up to a few miles.

University of New Brunswick

The Department of Surveying Engineering at the University of New Brunswick has completed a regional gravity survey of the province of New Brunswick and published eight Bouguer anomaly maps with 5 mgal contours at a scale of 1:250,000. Listings of 4,000 stations are also available. Professor K.B.S. Burke has commenced a geological interpretation of these results. Additional gravity observations have since been made as part of a program of the New Brunswick Department of Mines to map gravity lows associated with evaporite deposits in the Plumweseep-Penobsquis area.

Free-air anomaly maps have also been compiled and were used to calculate gravimetric deflections of the vertical at four triangulation stations in the province. These deflections were compared with astro-deflections. E.J. Krakiwsky has analyzed existing astrogeodetic deflection data in Canada. The objective of this analysis is to compute geoidal profiles using gravity data to interpolate deflection values between astrogeodetic stations.

Krakiwsky also reports that the satellite geodesy team at the University has made significant progress in defining the geodetic positioning of Canada's vast and remote land and sea areas. A satellite observing experiment was organized in November, 1970 in eastern Canada where seven satellite receivers (five on land, two at sea) simultaneously observed the doppler shift to five satellites in polar orbit. Simultaneous data was achieved for approximately 30 passes in a few days. The amount and type of data collected may be second only to that obtained in the U.S.A. The project was a joint program with Shell Canada Ltd. and Bedford Institute. The 60,000 feet of punched paper tape containing the data is now at the University for analysis. A mathematical model for the solutions of the positioning problem has been developed and programmed on an IBM 360/50 computer. Datum shift components between the geometric centre of the N.A.D. 1927 ellipsoid and the centre of gravity of the Earth will be determined from the data obtained in the experiment.

McGill University

At the Department of Mining, Engineering and Applied Geophysics, McGill University, four theses on different aspects of gravity have been completed in the four-year period 1967-1970. Theoretical formulae for the gravity effect of multiple horizontal semi-infinite blocks, truncated by a dipping plane, have been developed (B. Sharma, unpublished thesis, 1968; Sharma and Geldart, 1968) and the results checked over several two-dimensional faults in the St. Lawrence lowlands.

M. Vyas (unpublished thesis, 1969) has studied gravity anomalies over semi-infinite tilted slabs. The effect of tilt angle on semi-infinite blocks was calculated. It was necessary to terminate the block at finite depth. Extension of the results to calculate the effect of two-dimensional anticlinal and synclinal features was carried out by dividing the cross-section into several horizontal and tilted slabs.

H.P. Parsneau (unpublished thesis, 1970) studied two dimensional digital operations for filtering potential field data. The collection and manipulation of gravity and magnetic data in applied geophysics can be described in terms of sampling and filtering of continuous two-dimensional waveforms. Use of filter theory and modern processing techniques allows a more accurate approximation of potential field operations. The inverse Hankel transform and a wavelength filter were used for derivation of zero phase two-dimensional field operations.

A new approach for making terrain corrections using terrain profiles was described by W.B. Chang (unpublished thesis, 1970). The method is based on a simple formula for a three-dimensional shell in cylindrical co-ordinates. The terrain effect is calculated by superimposing a special graticule upon the terrain profiles and counting graticule elements. Results obtained were compared with results obtained by conventional methods and agreed within 0.1 mgal. The new approach is faster than previous methods employing graticules.

University of Manitoba

Gravity studies at the University of Manitoba have been concentrated mainly in the Rice Lake area of Manitoba. These investigations cover an area of some 2,000 km^2 and form part of Project Pioneer a joint geophysical-geological study by the Manitoba Mines Branch and the University.

The southern part of this area is underlain by granitic gneisses of the English River gneissic belt which appear to be in fault contact with rocks of the Rice Lake greenstone belt lying to the north. The Rice Lake volcanic-sedimentary belt has been intruded by several igneous bodies, only one of which, southeast of Gold Lake, is completely surrounded by greenstone. The rocks of the gneissic belt exhibit a completely different metamorphic history to those of the greenstone belt and also have entirely different structural characteristics. The juxtaposition of the two-rock types undoubtedly indicates some major dislocation.

A total of 1,260 gravity stations has now been established in the Rice Lake area. The gravity station distribution is not uniform and depends on a combination of accessibility and identification of critical areas. All of the gravity data observed to date have been reduced to Bouguer anomalies using a density of 2.67 g/cm^3.

Determination of densities of surface rocks forms an important phase of the work. Two methods are being used; determination from surface samples, and short detailed gravity traverses across outcrops with good relief to determine the average density of major rock units.

Interpretation of anomalies and preparation of final Bouguer anomaly maps is now underway. Some of the results have been published by Brown (1968) and by Hall and Hajnal (1969).

All available gravity data in Manitoba have been compiled at the University and a preliminary draft of a new gravity map of the province is in the editorial stage.

University of Alberta

The University of Alberta completed a gravity survey of an area of about 40,000 km^2 centred near Brooks in southern Alberta. Seismic reflection-refraction studies have led to the discovery of a rift valley, bounded by faults, at depths between 30 and 50 km in the lower crust (Kanasewich, 1966, 1968). This feature strikes nearly east-west. Gravity and magnetic surveys were used to follow the structure beyond the area of the detailed seismic study. Recently mapped magnetic anomalies show that it continues under the Rocky Mountains into British Columbia. The gravity anomalies have been shown to support the seismically-discovered rift structure, on a two-dimensional calculation.

A gravity survey made by the Dominion Observatory in the Stoney Rapids area of northern Saskatchewan is described by Agarwal and Kanasewich (1968). A major positive anomaly is underlain by a norite intrusion with an estimated anomalous mass of 10^{16} kg. A simple three-dimensional model was constructed for this mass distribution. In this model the norite outcrop in the northwest is gently dipping under the sandstone, and the main norite body is about 7 km thick in the centre with a sandstone layer almost 1 km thick on top of it. Considering the occurrence of economic minerals in the exposed part of the noritic rocks, it is suggested that several drill-holes in the sandstone area would enhance the geophysical interpretation of the main norite body and its economic importance for future development.

A method for automatic computer determination of geological or geophysical trends has been developed at the university using cross-correlation techniques. The trend direction is obtained by scanning cross-correlation coefficients and fitting a third degree polynomial equation to the selected contiguous maxima. The degree of correlation and the direction is obtained in a computer program that makes extensive use of logic statements and involves an interesting example of the possibility for programmed decision making. This study is described by Agarwal (1968).

Potential field data have been analyzed in a two-dimensional wave number domain to obtain the ratio of intensity of magnetization to the density (J/ρ) (Kanasewich and Agarwal, 1970). A two-dimensional fast Fourier transform was used to obtain auto-correlations, cross-correlations, convolution, upward continuation, vertical and horizontal derivatives and reduction of the total field to the pole. A coherency test was used on the two sets of data to evaluate the validity of the calculated J/ρ ratio for each wavelength. A high coherency value was assumed to arise if the gravity and magnetic anomalies are caused by the same body. A theoretical prismatic model and a field example from northern Saskatchewan were used to illustrate the techniques.

University of Calgary

At the University of Calgary F. Syber and P.E. Gretener are investigating the postulate that gravity anomalies are associated with deep seated reed structures. This project should be completed in 1971.

University of Saskatchewan

Gendzwill (1968, 1969a and b) completed a detailed survey and interpretation of gravity and density data in the Amisk Lake-Flin Flon region which covers an area of about 750 km^2 in east-central Saskatchewan. The main results include a Bouguer anomaly map, a density map and several new interpretation techniques (see also Gendzwill, 1970). The Bouguer anomalies correlate well with the densities of the Precambrian surface rocks and interpretation suggests that the surface density distribution must extend to depths of between 3 and 5 km to explain the gravity anomalies.

University of British Columbia

The University of British Columbia has published the results of a gravity survey of southwestern British Columbia covering an area of some 50,000 km^2 (Walcott, 1967). The Bouguer anomalies were divided into first- and second-order anomalies. Despite the obscuring effect of second-order anomalies the first order anomalies could be isolated to allow quantitative analysis. A positive anomaly over Vancouver Island and a negative anomaly over the Olympic Peninsula together define a linear anomaly pattern which was named the Coastal Anomaly. Using geological, seismic and gravity information, and the assumption of hydrostatic equilibrium, this feature was interpreted as the edge effect between two crustal blocks of different thickness and density. The model demonstrates that isostatic anomalies may arise through lateral variations in crustal density and thickness and need not indicate departures from equilibrium.

At the University of British Columbia the design and analysis of linear filters for the enhancement of potential field data have also been studied. Standard techniques such as regional/residual separation, second derivative computation and upward and downward continuation have been considered from the linear filter viewpoint. The effects of improved filters were examined (Clarke, 1969a and b, 1971; Ulrych, 1968, 1969).

Petroleum industry

The use of gravity surveying as a reconnaissance tool for petroleum exploration in Canada has recently increased significantly. During the last four years the average number of crew months has been 128 per year. This increased activity can be directly correlated with the shift in exploration to new frontier areas which include the Northwest Territories, the Arctic and the continental shelves. Large land holdings and difficult working conditions have stimulated the need for effective reconnaissance survey methods. Considerable effort is being made to solve logistical and operational problems in these remote areas.

Significant progress has been made in the use of computer-oriented data handling systems. Computers are now in routine use to reduce and interpret gravity data. More surveys completed by industry are being tied to the national gravity net established by Earth Physics Branch of the Department of Energy, Mines and Resources. Widespread use of gravity standards established by the Earth

Physics Branch ensures the long term value of oil company data.

Acknowledgments

Thanks are due to the following Canadian scientists who submitted contributions for this four-year report, thereby facilitating the compilation: D.R. Bower, J.B. Boyd, R.J. Buck, M.R. Dence, A. Lambert, R.K. McConnell, D. Nagy, J.R. Weber all of Earth Physics Branch; R.T. Haworth of the Bedford Institute; E.R. Deutsch of Memorial University of Newfoundland; D.E.T. Bidgood of the Nova Scotia Research Foundation; W.M. Telford of McGill University; D.J. Gendzwill of the University of Saskatchewan; R.M. Ellis of the University of British Columbia; and T.A. Pezarro of Voyager Petroleums Ltd., Calgary.

Bibliography, 1967-1970

Agarwal, R.G. 1968. Two-dimensional harmonic analysis of potential fields. Unpublished Thesis, University of Alberta, Edmonton.

Agarwal, R.G., and E.R. Kanasewich. 1968. A gravity investigation of the Stoney Rapids area, northern Saskatchewan. *Sask. Dept. Min. Res.* Rpt. 124.

Anderson, C.D., and H.G. Sherwood. 1970. Ore-densities of thirty-seven Canadian base metal sulfide deposits. *Can. J. Earth Sci.*, 7(3).

Beals, C.S., M.R. Dence, and A.J. Cohen. 1966. Evidence for the impact origin of Lac Couture. *Pub. Dom. Obs.*, 31(10).

Berkhout, A.W.J. 1968. Gravity in the Prince of Wales, Somerset and northern Baffin Islands region, District of Franklin, Northwest Territories. Unpublished Thesis, Queen's University, Kingston.

Berkhout, A.W.J. 1970. The gravity anomaly field of Prince of Wales, Somerset and northern Baffin Islands, District of Franklin, N.W.T. *Pub. Dom. Obs.*, 39(7).

Berkhout, A.W.J., and L.W. Sobczak. 1967. A preliminary investigation of gravity observations in the Somerset and Prince of Wales Islands, Arctic Canada. *Gravity Map Series Dom. Obs.* No. 81.

Berry, M.J., W.R. Jacoby, E.R. Niblett, and R.A. Stacey. A review of geophysical studies in the Canadian Cordillera. *Can. J. Earth Sci.* (in press).

Bidgood, D.E.T. 1970. The distribution and diapiric nature of some Nova Scotia evaporites. A geophysical evaluation. *Contr. to Third Symp. on Salt,* Northern Ohio Geol. Soc. Inc.

Bidgood, D.E.T., and J.E. Blanchard. 1970. Geophysical investigations of evaporites in Nova Scotia. Mining and Groundwater Geophysics /67 ed. L.W. Morley. *Geol. Surv. Can. Econ. Geol.* Rpt. 26.

Bower, D.R. 1969. Some numerical results in the determination of the indirect effect. *Symp. Vol. 6th Int. Symp. Earth Tides,* Strasbourg.

Bower, D.R., and B.D. Loncarevic. 1967. Sea gravimeter trails on the Halifax test range aboard *CSS Baffin,* 1963. *Pub. Dom. Obs.*, 36(1).

Brown, R.J. 1968. Isostasy and crustal structure in the English River gneissic belt. Unpublished Thesis, University of Manitoba, Winnipeg.

Buck, R.J. 1967. The gravity anomaly field in western Canada with maps: Part I. *Gravity Map Series Dom. Obs.* Map Nos. 39-43.

Buck, R.J. 1968. The gravity anomaly field in western Canada with maps: Part II. *Gravity Map Series Dom. Obs.* Nos. 37, 38, 44 and 49.

Bunch, T.E., A.J. Cohen, and M.R. Dence. 1968. Shock induced structural disorder in plagioclase and quartz. Shock metamorphism of natural materials, ed. B.M. French and N.M. Short. Mono Book Corp., Baltimore.

Burwash, R.A., and J. Krupicka. 1970. Cratonic reactivation in the Precambrian basement of western Canada: Part II. Metasomatism and isostasy. *Can. J. Earth Sci.*, 7(5).

Caputo, M. 1967. The gravity field of the Earth from classical and modern methods. *Int. Geophys. Series,* Vol. 10, ed. T. Van Mieghem.

Clarke, G.K.C. 1969a. Optimum second-derivative and downward-continuation filters. *Geophysics,* 34.

Clarke, G.K.C. 1969b. Applications of optimum filters in mining geophysics in Proc. Symp. Decision making in mineral exploration, Part II, ed. A.M. Kelly and A.J. Sinclair, Univ. British Columbia.

Dence, M.R. 1968. Shock zoning at Canadian craters: petrography and structural implications. Shock metamorphism of natural materials, ed. B.M. French and N.M. Short. Mono Book Corp., Baltimore.

Dence, M.R. 1970. Meteorite crater investigations. In Background papers on the Earth sciences in Canada (ed. C.H. Smith). *Geol. Surv. Can.* Papers 69-56, 79-83.

Dence, M.R., M.J.S. Innes, and P.B. Robertson. 1968. Recent geological and geophysical studies of Canadian craters. Shock metamorphism of natural materials, ed. B.M. French and N.M. Short. Mono Book Corp., Baltimore.

Gendzwill, D.J. 1967. Subsurface and surface gravity measurements, Yarbo area. *Saskatchewan Research Council Report,* Physics Division, P-67-1.

Gendzwill, D.J. 1968. A gravity study in the Amisk Lake area of Saskatchewan. Unpublished Thesis, University of Saskatchewan, Saskatoon.

Gendzwill, D.J. 1969a. A gravity survey in the Amisk Lake area, Saskatchewan. In Symposium on the geology of the Coronation Mine, Saskatchewan. *Geol. Surv. Can.* Paper 68-5.

Gendzwill, D.J. 1969b. Densities of Precambrian rocks of the Amisk Lake – Flin Flon area. A detailed study. *Can. J. Earth Sci.*, 6(5).

Gendzwill, D.J. 1970. A gradational density contrast as a gravity interpretation model. *Geophysics,* 35(2).

Grendzwill, D.J., and J. Maybank. 1969. Gravity variations and precipitation onset. *Can. J. Earth Sci.*, 6(5).

Gibb, R.A. 1968a. The densities of Precambrian rocks from northern Manitoba. *Can. J. Earth Sci.*, 5(3).

Gibb, R.A. 1968b. A geological interpretation of the Bouguer anomalies adjacent to the Churchill – Superior boundary in northern Manitoba. *Can. J. Earth Sci.*, 5(3).

Gibb, R.A. 1971. Origin of the great arc of eastern Hudson Bay. A Precambrian continental drift reconstruction. *Earth Planet. Sci. Lett.*, 10(3).

Gibb, R.A., and R.K. McConnell. 1969. The gravity anomaly field in northern Manitoba and northeastern Saskatchewan. *Gravity Map Series Dom. Obs.* Map Nos. 68-76.

Gibb, R.A., and R.K. McConnell. 1970. Gravity measurements in northern Ontario. *Gravity Map Series Earth Phys. Br.* Nos. 25, 28-36.

Gibb, R.A., and J. van Boeckel, 1970. Three-dimensional gravity interpretations of the Round Lake batholith, northeastern Ontario. *Can. J. Earth Sci.*, 7(1).

Gibb, R.A., R.I. Walcott. 1971. A Precambrian suture in the Canadian Shield. *Earth Planet. Sci. Lett.*, 10(4).

Gibb, R.A., J.J.G.M. van Boeckel, and R.W. Hornal. 1969. A preliminary analysis of the gravity anomaly field in the Timmins-Senneterre mining areas with map. *Gravity Map Series Dom. Obs.* No. 58.

Goodacre, A.K. 1968. Systematic errors in the Decca navigation system used in Hudson Bay for the 1965 oceanographic project. Proc. Earth Science Symp. on Hudson Bay. *Geol. Surv. Can.* Paper 68-53.

Goodacre, A.K., B.G. Brule, R.V. Cooper 1969. Results of regional underwater gravity surveys in the Gulf of St. Lawrence with map. *Gravity Map Series Dom. Obs.* No. 86.

Grant, F.S. 1968. Two gravity profiles in the Manicouagan – Wabash area of west-central Quebec. *Can. J. Earth Sci.*, 5(4).

Grant, A.C., and K.S. Manchester. 1970. Geophysical investigations in the Ungava Bay – Hudson Strait region of northern Canada. *Can. J. Earth Sci.*, 7(4).

Hall, D.H. 1968. A seismic-isostatic analysis of crustal data from Hudson Bay. *Geol. Surv. Can.* Paper 68-53, 337-364.

Hall, D.H., and Z. Hajnal. 1969. Crustal structure of northwestern Ontario: Refraction seismology. *Can. J. Earth Sci.*, 6(1).

Hamilton, A.C., and B.G. Brule, 1967. Vibration-induced drift in LaCoste and Romberg geodetic gravimeters. *J. Geophys. Res.*, 72(8).

Haworth, R.T. 1969. Cross-coupling errors as a function of gravimeter orientation. *Trans. Am. Geophys. Union*, 50(4).

Hornal, R.W. 1968. The gravity anomaly field in the Coppermine area of the Northwest Territories with map. *Gravity Map Series Dom. Obs.* No. 45.

Hornal, R.W., L.W. Sobczak, W.E.F. Burke, and L.E. Stephens. 1970. Preliminary results of gravity surveys over the Mackenzie Basin and Beaufort Sea. *Gravity Map Series Earth Phys. Br.* Nos. 117-119.

Innes, M.J.S., and A. Argun-Weston. 1967. Gravity measurements in Appalachia and their structural implications. *Roy. Soc. Can.*, Spec. Publ. No. 10.

Innes, M.J.S., and R.A. Gibb. 1970. A new gravity anomaly map of Canada: an aid to mineral exploration. Mining and groundwater geophysics /67, ed. L.W. Morley. *Geol. Surv. Can. Econ. Geol.* Rpt. 26.

Innes, M.J.S., J.R. Goodacre, J.R. Weber, and R.K. McConnell. 1967. Structural implications of the gravity field in Hudson Bay and vicinity. *Can. J. Earth Sci.*, 4(5).

Innes, M.J.S., A.K. Goodacre, A. Argun-Weston, and J.R. Weber. 1968. Gravity and isostasy in the Hudson Bay region. *Science, History and Hudson Bay*, ed. C.S. Beals and D.A. Shenstone, Dept. Energy, Mines and Resources, Canada.

Jacoby, W.R. 1969. Gravity variations and precipitation: Discussion. *Can. J. Earth Sci.*, 6(4 Pt. 1).

Jacoby, W.R. 1970. Instability in the upper mantle and global plate movements. *J. Geophysics*, 35(3).

Jacoby, W.R. 1970. Gravity diagrams for thickness determination of exposed rock bodies. *Geophysics*, 35(3).

Kanasewich, E.R. 1966. Deep crustal structure under the Plains and Rocky Mountains. *Can. J. Earth Sci.*, 3(7).

Kanasewich, E.R. 1968. Precambrian rift: genesis of strata-bound ore deposits. *Science*, 161.

Kanasewich, E.R., and R.G. Agarwal. 1970. Analysis of combined gravity and magnetic fields in wave number domain. *J. Geophys. Res.*, 75(29).

Krakiwsky, E.J., and J. Kouba. 1970. An exploratory investigation into satellite positioning techniques to be employed in Canadian Continental Shelf and Arctic areas. Department of Surveying Engineering Technical Report No. 4, University of New Brunswick, Fredericton, N.B.

Kumarapeli, R.S., M.E. Coates, and N.H. Gray. 1968. The Grand Bois anomaly: the magnetic expression of another Monteregion pluton. *Can. J. Earth Sci.*, 5(3).

Kumarapeli, R.S., and B. Sharma, 1969. A gravity profile across the Shield margin in the vicinity of St. Jerome, Quebec. *Can. J. Earth Sci.*, 6(5).

Lambert, A. 1970. The response of the Earth to loading by the earth tide around Nova Scotia. *Geophys. J. Roy. Astr. Soc.*, 19.

Lillestrand, R.L., A. Grosch, and P. Vanelli. 1967. Interim technical report on astronavigation during Dominion Observatory polar research project. Res. Rpt. RD 1023, Aerospace Res. Dept. Control Data Computation, Minneapolis.

Loncarevic, B.D. 1967. Techniques of gravity measurements at sea. *International Dictionary of Geophysics*, pp. 694-700. Pergamon Press, London.

Loncarevic, B.D., and G.N. Ewing. 1967. Geophysical study of the Orpheus gravity anomaly. *Proc. 7th World Petroleum Cong.*,

Loncarevic, B.D., D.I. Ross, K.S. Manchester, J. Woodside, and F. Aumento. 1969. The Mid-Atlantic Ridge near 45°N. *Trans. Am. Geophys. Union*, 50(4).

Manchester, K.S. 1969. Anschutz gyro table repair and overhaul manual. *Bedford Inst. Internal Note*, 1969-13-1.

Miller, H.C. 1970. A gravity survey of eastern Notre Dame Bay, Newfoundland. Unpublished M.Sc. Thesis, Memorial University of Newfoundland.

Morley, L.W. 1970. Exploration geophysics. In Background papers on the Earth sciences in Canada (ed. C.H.

Smith). *Geol. Surv. Can.* Paper 69-56, 158-169.

Paul, M.K. 1970. Computation of the vertical gradient of gravity for two-dimensional bodies. *Pur Appl. Geophys.*, 19.

Paul, M.K., and D. Nagy. A study on the upward continuation of gravity data from a plane surface. *Studia Geoph. et Geod.* (in press).

Picklyk, D. 1969. A regional gravity survey of Devon and southern Ellesmere Islands, Canadian Arctic Archipelago with map. *Gravity Map Series Dom. Obs.* No. 87.

Robertson, P.B. 1968. La Malbaie Structure, Quebec – a Palaeozoic meteorite impact site *Meteoritics*, 4(2).

Robertson, P.B., M.R. Dence, and M.A. Vos. 1968. Deformation in rock-forming minerals from Canadian craters. Shock metamorphism of natural materials, ed. B.M. French and N.M. Short. Mono Book Corp., Baltimore.

Rondot, J. 1968. Nouvel impact météoritique fossile? La structure semi-circulaire de Charlevoix. *Can. J. Earth Sci.*, 5(5).

Ross, D.I. 1970. Marine geophysics. In Background papers on the Earth sciences in Canada (ed. C.H. Smith). *Geol. Surv. Can.* Paper 69-56, 180-186.

Sharma, B. and L.P. Geldart. 1968. Analysis of gravity anomalies of two-dimensional faults using Fourier transforms. *Geophys. Prosp.*, 16(1).

Sobczak, L.W. 1969. Gravity surveys in the Alexandria area, eastern Ontario. *Publ. Dom. Obs.*, 39(6).

Sobczak, L.W., and W.R. Jacoby. A gravity survey of the Kinmount geophysical test range, Ontario. Geophysical Test Range, Cavendish Township, Ontario. *Geol. Surv. Can.* Paper (in press).

Sobczak, L.W., and G.J. Taylor. 1970. Results of a differential Omega test in the Mackenzie River Delta. *Geophysics*, 35(3).

Sobczak, L.W., and J.R. Weber. 1970. Gravity measurements over the Queen Elizabeth Islands and Polar Continental Margin. *Gravity Map Ser. Earth Phys. Br.*, Nos. 115-116.

Sobczak, L.W., and J.R. Weber. Crustal structure of the Queen Elizabeth Islands and the Polar Continental Margin. *Proc. 2nd Int. Symp. Arctic Geol.*, San Francisco (in press).

Sobczak, L.W., J.R. Weber, and E.F. Roots. 1970. Rock densities in the Queen Elizabeth Islands, Northwest Territories. *Proc. Geol. Ass. Can.*, 21.

Spector, A., and R.W. Hornal. 1970. Gravity studies over three evaporite piercement domes in the Canadian Arctic. *Geophysics*, 35(1).

Stacey, R.A. Interpretation of the gravity anomaly at Darnley Bay, N.W.T. *Can. J. Earth Sci.* (in press).

Stacey, R.A., and J.P. Steele. 1970. Geophysical measurements in British Columbia. *Gravity Map. Ser. Earth Physics Br.*, Nos. 120, 121.

Stacey, R.A., and L.E. Stephens, 1969. An interpretation of gravity measurements on the west coast of Canada. *Can. J. Earth Sci.*, 6(3).

Stacey, R.A., and L.E. Stephens. 1970. Procedures for calculating terrain corrections for gravity measurements. *Publ. Dom. Obs.*, 39(10).

Stacey, R.A., L.E. Stephens, R.V. Cooper, and B.G. Brule. 1969. Gravity measurements in British Columbia with map. *Gravity Map Ser. Dom. Obs.* No. 88.

Stephens, L.E., A.K. Goodacre, and R.V. Cooper. 1971. Results of underwater gravity surveys over the Nova Scotia continental shelf. *Gravity Map Series Earth Physics Br.*, No. 123.

Strange, W.E. 1970. The use of gravimeter measurements in mining and groundwater exploration. Mining and groundwater geophysics /67, ed. L.W. Morley. *Geol. Surv. Can. Econ. Geol.* Rpt. 26.

Tanner, J.G. 1967. An automated method of gravity interpretation. *Geophys. J. Roy. Astro. Soc.*, 13.

Tanner, J.G. 1967. Gravity measurements in Canada, January 1, 1963 to December 31, 1966. *Pub. Dom. Obs.*, 36(2).

Tanner, J.G. 1969. A geophysical study of structural boundaries in the eastern Canadian Shield. Unpublished Thesis, University of Durham, England.

Tanner, J.G., and R.A. Gibb. 1970. Gravity. In Background papers on the Earth sciences in Canada (ed. C.H. Smith). *Geol. Surv. Can.* Paper 69-56, 218-230.

Tanner, J.G., and R.K. McConnell. 1970. The gravity field in the Richmond Gulf – Fort Chimo area, Quebec. *Gravity Map Ser. Earth Phys. Br.*, Nos. 7-10, 48.

Taylor, F.C., and M.R. Dence. 1969. A probable meteorite origin for Mistastin Lake, Labrador. *Can. J. Earth Sci.*, 6(1).

Ulrych, T.J. 1968. Effect of wavelength filtering on the shape of the residual anomaly. *Geophysics*, 33.

Ulrych, T.J. 1969. Wavenumber domain analysis and design of potential field filters. In *Proc. Symp. Decision making in mineral exploration*, Part II, ed. A.M. Kelly and A.J. Sinclair, Univ. British Columbia.

Valliant, H.D. 1967. An electronic system for measuring pendulum periods. *I.E.E.E. Trans. on Geoscience Electronics*, GE5(3).

Valliant, H.D. 1967. The role of the invariable pendulum in gravity measurements. *Physics in Canada*, 23(2).

Valliant, H.D. 1968. SCR switching circuit. Contribution to source book of electronic circuits. *McGraw-Hill.*

Valliant, H.D. 1969. The effect of humidity on the length of invariable pendulums. *Geophys. J. Roy. Astr. Soc.*, 17.

Valliant, H.D. 1969. Gravity measurements on the North American calibration line with the Canadian pendulum apparatus. *Geophys. J. Roy. Astr. Soc.*, 17.

Valliant, H.D. 1970. The Canadian pendulum apparatus design and operation. *Pub. Earth Phys. Br.*, 41(4).

Valliant, H.D. A canadian network of gravity measurements with pendulums. *Geophys. J. Roy. Astr. Soc.* (in press).

Valliant, H.D., I.R. Grant, and J.W. Geuer. 1967. A temperature control system for pendulum measurements. *I.E.E.E. Trans. on Geoscience Electronics*, GE 5(3).

Vine, F.J., and R.F. Macnab. 1968. Upward continuation of magnetic and gravity anomalies: The two-dimensional case. *BIO* Computer Note 67-6-C.

Walcott, R.I. 1967. The Bouguer anomaly map of southwestern British Columbia. *Univ. B.C. Inst. Earth Sci.*, Scientific Report No. 15.

Walcott, R.I. 1968. The gravity field of northern Saskatchewan and north-eastern Alberta. *Gravity Map Series Dom. Obs.* Map Nos. 16-20.

Walcott, R.I. 1970a. Isostatic response to loading of the crust in Canada. *Can. J. Earth Sci.*, 7(2).

Walcott, R.I. 1970b. An isostatic origin for basement uplifts. *Can. J. Earth Sci.*, 7(3).

Walcott, R.I. 1970a. Flexure of the lithosphere at Hawaii. *Tectònophysics*, 9.

Walcott, R.I. 1970d. Flexural rigidity thickness and viscosity of the lithosphere. *J. Geophys. Res.*, 75(20).

Walcott, R.I., and J.B. Boyd. 1970. The gravity field of northern Alberta and parts of Northwest Territories and Saskatchewan. *Gravity Map Series Earth Phys. Br.*, Nos. 103-111.

Wallis, R.H. 1970. A geological interpretation of gravity and magnetic data, northwest Saskatchewan. *Can. J. Earth Sci.*, 7(3).

Weaver, D.F. 1967. A geological interpretation of the Bouguer anomaly field of Newfoundland. *Pub. Dom. Obs.*, 35(5).

Weaver, D.F. 1968. Preliminary results of the gravity survey of the Island of Newfoundland. *Gravity Map Series Dom. Obs.* Map Nos. 53-57.

Weber, J.R. 1970. In Cruise report from the ice drift study in the Gulf of St. Lawrence, p. 38, Marine Sciences Centre Manuscript Report No. 15, McGill University.

Weber, J.R., and P. Andrieux, 1970. Radar soundings on the Penny Ice Cap, Baffin Island. *J. Glaciology*, 9(55).

Weber, J.R., and A.K. Goodacre. 1967. A reconnaissance underwater gravity survey of Lake Superior. The earth beneath the continents. Geophys. Monograph No. 10, *A.G.U.*

Weber, J.R., and A.K. Goodacre. 1968. An analysis of the crust-mantle boundary in Hudson Bay from gravity and seismic observations. *Can. J. Earth Sci.*, 5(5).

Weber, J.R., and R.L. Lillestrand. 1971. Measurement of tilt of a frozen sea. *Nature* 229, 550-551.

Weir, H.C. 1970. A gravity profile across Newfoundland. Unpublished M.Sc Thesis, Memorial University of Newfoundland.

Wells, D.E. (editor) 1969. Satellite navigation cruise report. *Bedford Institute Cruise* Rpt. No. 69-022, CSS *Baffin*. April 28 – May 7.

PUBLICATIONS of the EARTH PHYSICS BRANCH

VOLUME 42—NO. 3

the ancient oceanic lithosphere

papers presented at a short symposium held at carleton university, ottawa, october 1970 as canadian contributions nos 1 to 11 to the geodynamics project

E. IRVING
Earth Physics Branch
Chairman, Geodynamics Subcommittee

DEPARTMENT OF ENERGY, MINES AND RESOURCES

OTTAWA, CANADA 1972

Cat. No.: M70-42/3

Contents

Frontispiece

Contribution
No.

1 THE ANCIENT OCEANIC LITHOSPHERE – Identification within the present continents – STATEMENT OF THE PROBLEM – E. Irving 47

2 THE OCEANIC CRUST OF THE MID-ATLANTIC RIDGE AT 45°N – F. Aumento 49

3 MESOZOIC AND TERTIARY VOLCANISM OF THE WESTERN CANADIAN CORDILLERA – J.G. Souther 55

4 OCEANIC CRUST IN THE CANADIAN CORDILLERA – J.W.H. Monger 59

5 OPHIOLITES OF SOUTHERN QUEBEC – R.Y. Lamarche 65

6 OPHIOLITE: ITS DEFINITION, ORIGIN AS OCEANIC CRUST, AND MODE OF EMPLACEMENT IN OROGENIC BELTS, WITH SPECIAL REFERENCE TO THE APPALACHIANS – W.R. Church 71

7 PALEOMAGNETISM AND THE KINEMATIC HISTORY OF MAFIC AND ULTRAMAFIC ROCKS IN FOLD MOUNTAIN BELTS – E. Irving and R.W. Yole 87

8 ALPINE-TYPE PERIDOTITE WITH PARTICULAR REFERENCE TO THE BAY OF ISLANDS IGNEOUS COMPLEX – T.N. Irvine and T.C. Findlay 97

9 SOME PHYSICAL AND CHEMICAL ASPECTS OF PRECAMBRIAN VOLCANIC BELTS OF THE CANADIAN SHIELDS – W.R.A. Baragar 129

10 ARCHEAN ULTRAMAFIC ROCKS – A.J. Naldrett 141

11 OCEANIC CRUST AND THE IDENTIFICATION OF ANCIENT OCEANIC CRUST ON THE CONTINENTS: A SUMMARY – R.F. Emslie 153

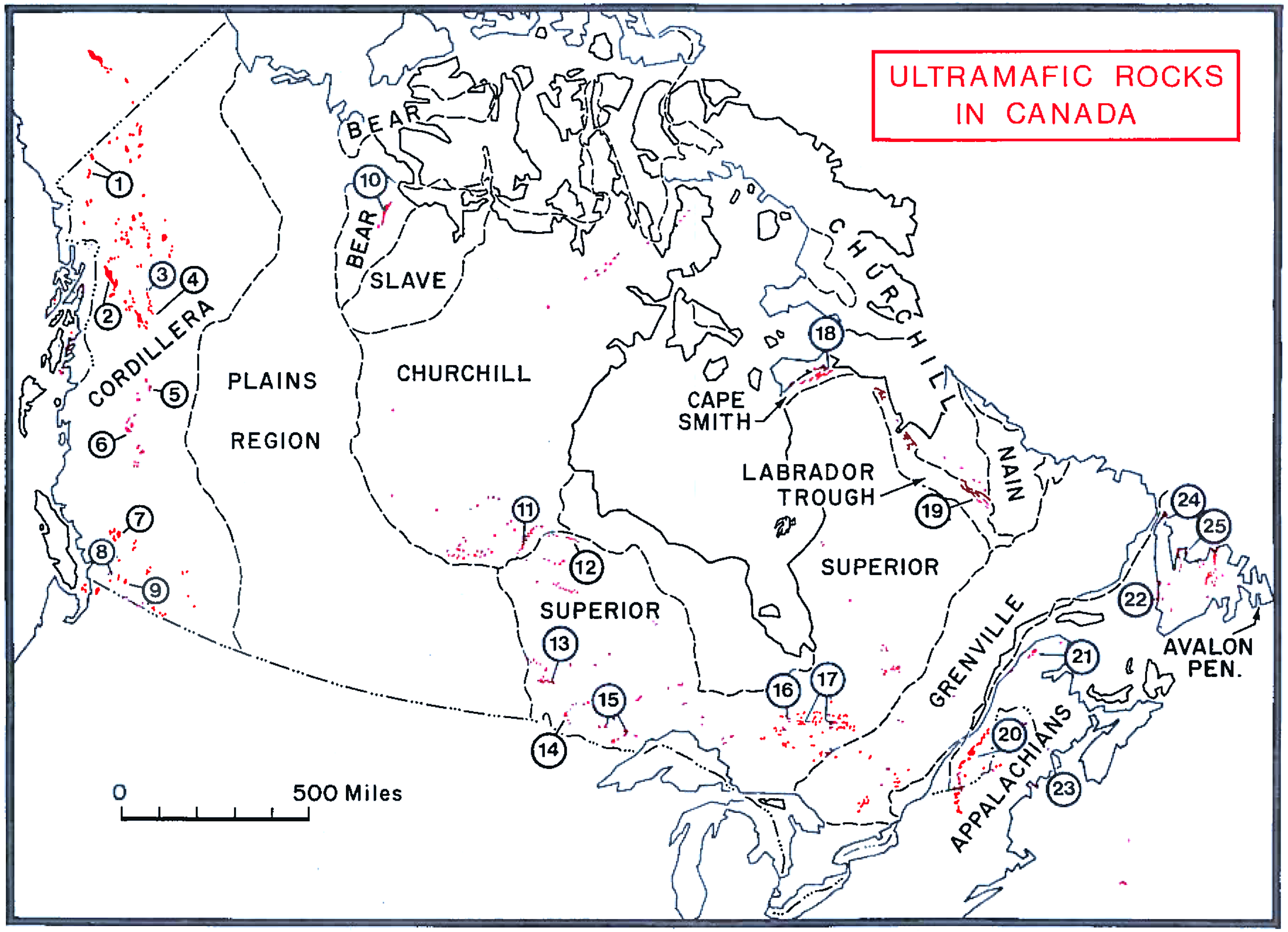

General distribution of ultramafic rocks in Canada (compiled by T.N. Irvine from Smith (1962), Scoates (1970) and other sources. Generalized structural boundaries are given as dotted lines. The sizes of individual bodies are necessarily exaggerated. Better known localities and areas numbered as follows: (1) Kluane Range intrusions; (2) Nahlin complex; (3) Blue River intrusion; (4) Cassiar asbestor body; (5) Polaris complex; (6) Middle River bodies; (7) Shylaps complex; (8) Tulameen complex; (9) Giant Mascot complex; (10) Muskox intrusion; (11) Manitoba Nickel Belt; (12) Fox River Sill; (13) Bird River Sill; (14) Kakagi Lake Sill; (15) Quetico-Sherbandowan intrusions; (16) Dundonald Sill and associated lenses; (17) Abitibi Sills; (18) Cape Smith-Wakeham Bay Sills; (19) Labrador Trough Sills; (20) Eastern Townships complexes; (21) Mount Albert intrusion; (22) Bay of Island complex; (23) Hare Bay complex; (24) Burlington Penninsula complexes and (25) St. Stephen complex.

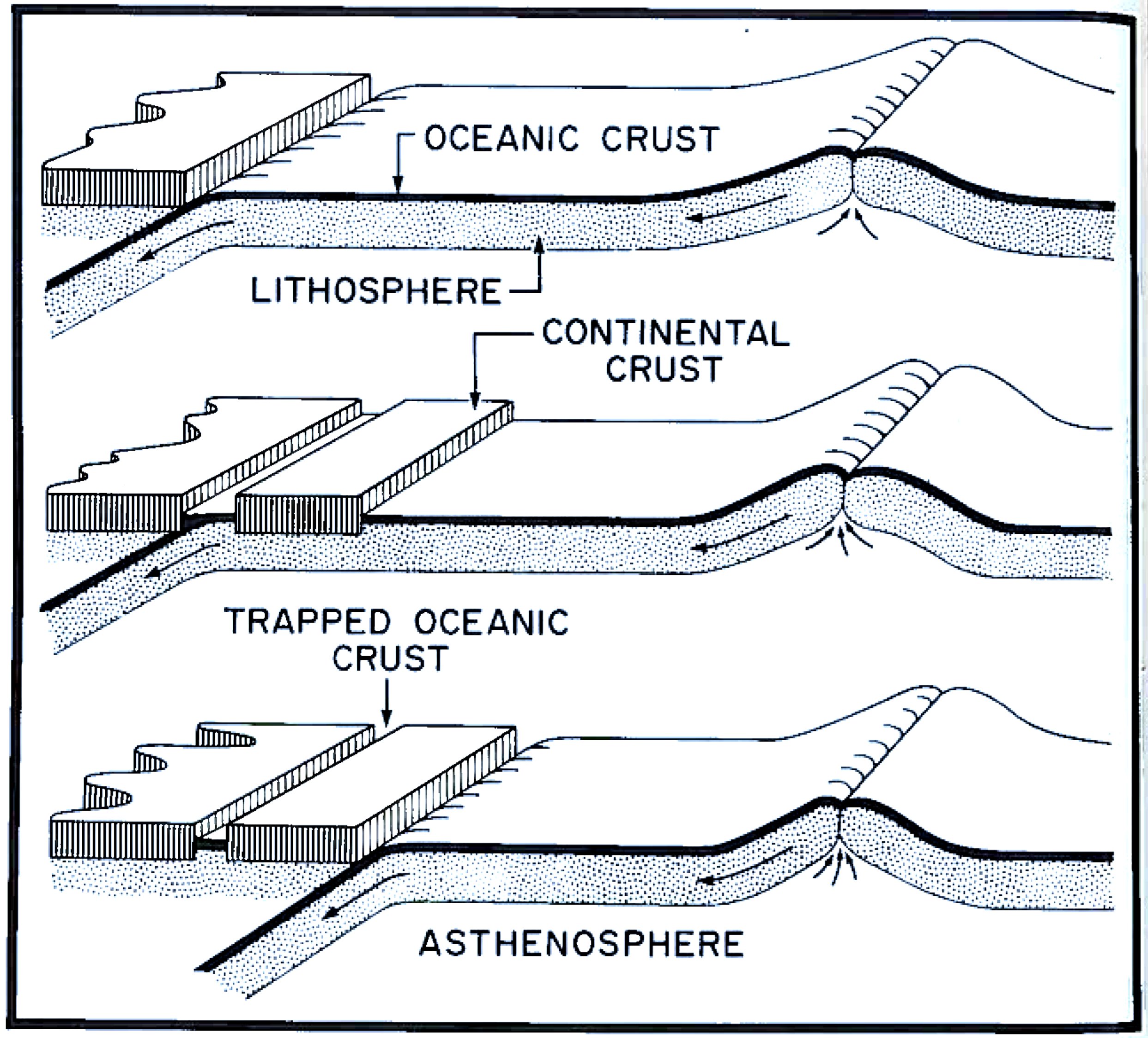

This illustration intends to show, in a wide diagrammatic fashion, one of the ways in which oceanic lithosphere may become trapped within the continental crust. Above, the single plate tectonic model is shown. In the centre, a fragment of continental crust is imagined to be situated in the downgoing slab of lithosphere. When the two continents collide, a sliver of oceanic lithosphere may become trapped between them.

No. 1

the ancient oceanic lithosphere— identification within the present continents

statement of the problem

E. IRVING
Earth Physics Branch
Chairman, Geodynamics Subcommittee

The theory of plate tectonics has been very successful in explaining the observations relating to the later Mesozoic and Cenozoic history of the earth. Its applicability to earlier times is uncertain. According to this theory oceanic lithosphere is produced at the axis of a mid-ocean ridge by accretion from the mantle. It then spreads laterally (acting approximately as a rigid spherical shell or plate) passing finally beneath one of the deep ocean trenches. During its passage beneath the trench, fragments of the ridge-generated oceanic lithosphere may become trapped, and eventually incorporated into the continental crust (a greatly oversimplified scheme is given in the Frontispiece) so that one of the interesting consequences of plate tectonics is that fragments of old oceanic crust should occur, not invariably perhaps, but at least occasionally, at the sites of old trenches. Should such occurrences never be found, then the theory is perhaps not applicable to Paleozoic and earlier times. If, on the other hand, definite identification of ridge-generated oceanic fragments within present day continents can be made, it would strengthen the case for extending concepts of plate tectonics back into the more remote history of the earth. In fact such identifications would constitute one of the most powerful means of testing whether or not it is reasonable to extend this dynamic view of the earth into more remote times. This is why the subject of this symposium is so relevant to the Geodynamics Project.

There are two parts to this task of identification. Firstly, there is the "rock problem" which requires comparisons to be made of the geological, chemical, and physical properties of the rocks of present-day ridges with their possible older equivalents now within the continents. Secondly, there is the "kinematic problem" which requires that the present sites of possible old oceanic lithosphere must be shown to have been zones of lithosphere convergence. There will be no satisfactory discussion until the kinematic framework of at least some of the older fold belts has been established quantitatively, through the application of a whole range of geological, geochemical, and geophysical techniques.

The relevance of these ideas to the origin of mineral deposits should not be overlooked. Rich deposits are being formed today in the hot brine pools of the deep axial parts of the Red Sea which is a constricted juvenile rift. In the open ocean ridge systems disseminated metallic sulphides occur ubiquitously in pillow basalts. Asbestos is produced by the alteration of ultrabasic rock which may, on these ideas, originally have had an oceanic source. Thus, the very important mineralization of many such ultrabasic and basic rocks, at least insofar as the original source of metals is concerned, may become explicable in terms of volcanic and tectonic processes currently active.

The purpose of this short symposium was not to even attempt to cover the entire field, or even to answer specific questions, but rather to draw attention to an important general problem of particular significance to the earth sciences in Canada where there are such splendid displays of mafic and ultramafic rocks of all ages (*see* Frontispiece).

The subcommittee wishes to express its thanks to Carleton University for the use of a meeting room, Professor W. Tupper of Carleton University who made the accommodation arrangements, and to Professor A. Goodwin of the University of Toronto who very kindly chaired the meeting with grace and good humour. Finally, we would like to acknowledge the very great help given by Dr. G. Skippen of Carleton University in reviewing these papers prior to their publication.

ations
and
probably
According to
there is produced
ocean ridge
. It then
ximately as a
pressing flush
ocean trenches
h the trench
generated
e trapped
d into the
y overlapping
Frontispiece
among conce
is that they

No. 2

the oceanic crust of the mid-atlantic ridge at 45°N

F. AUMENTO
Department of Geology
Dalhousie University
Nova Scotia

Abstract. Detailed geological and geophysical investigations on the crest and High Fractured Plateaus of the Mid-Atlantic Ridge at 45°N have permitted the synthesis of a clear picture of the structure, petrography, geochemistry and geochronology of a section through a modern, slowly spreading oceanic ridge. This paper does not dwell on the methods of data acquisition and processing which were essential to the synthesis, nor does it enter into many of the controversies which have arisen from the data; these have been described by Aumento 1967, 1968, 1969. It is emphasized that the active, slowly spreading ridge described may show significant differences from a rapidly spreading ridge (e.g. the East Pacific Rise) and may, by nature of its youth, bear little obvious resemblance (especially geochemically) to old, deformed, altered and metamorphosed oceanic remnants found on the continents.

Structure

The oceanic crust near the crest of the Mid-Atlantic Ridge consists of discontinuously layered sequences of igneous and metamorphic rocks 5 km thick, overlain by a veneer of sedimentary material (Figure 1) (Keen and Tramontini, 1970; Barrett and Aumento, 1970). The layering is disrupted by steep normal faults roughly parallel to the axis of the ridge; their 45° scarp slopes generally face the axis, and have vertical throws of up to 2 km (Keen and Manchester, 1970; Barrett and Aumento, 1970). These faults are responsible for much of the topographic relief found on the ridge. This rugged relief has been subsequently moderated by rapid sedimentation (Keen and Manchester, 1970). Sedimentary thicknesses increase with distance from the axis, such that at distances of 100 km from the axis intermontane valleys are buried under many hundreds of metres of sediments, resulting in an apparent smoothing out of the bottom topography. This observation is consistent with the hypothesis of an actively spreading ocean floor (Keen and Manchester, 1970).

The mean crustal thickness is approximately 5 km, but shows local variations of up to 3 km (Keen and Tramontini, 1970). These variations are presumably the result of block faulting and the variable nature of the Mohorovicic discontinuity beneath the oceanic crust. The oceanic crust can be subdivided into three main layers, with a fourth beneath representing the top of the upper mantle.

Layers 1, 2, 3 and 4 have been correlated with specific rock types as shown in tabular form below: (Barrett and Aumento, 1970)

Layer 1, varying in thickness from 0 km at the axis, to many thousands of metres in the abyssal plains, is a low-velocity sedimentary layer. Layer 2, with a mean thickness of 1.6 km, thickens to 2 km near the axis, and layer 3, with a mean thickness of 3.4 km, thins to 1.3 km near the axis. Layer 2 can be subdivided further into two discontinuous layers with velocities of 3.8 and 4.7 km s^{-1} for the upper and lower layers respectively. Layer 4, the uppermost upper mantle beneath the Mohorovicic discontinuity, consists of a thick sequence of high-velocity rocks (8.1 km s^{-1}) exhibiting a velocity anisotropy of some 0.25 km s^{-1} (Keen and Tramontini, 1970).

The serpentinites which appear in the table do not belong to any one layer, but rather occur as diapiric intrusions cutting through the igneous/metamorphic layering of the mafic rocks. Ultramafic diapiric intrusives are characteristic of slowly spreading ridges, but may be absent on rapidly spreading ridges (Aumento and Loubat, 1971).

Layers 2, 3 and 4 apparently originate beneath the axis of the ridge in the following way: large, discontinuous, totally liquid lopoliths of mafic magma are emplaced beneath the axis of the ridge following a phase of major lateral fracturing due to the forces responsible for ocean-floor spreading. The floors of these lopoliths lie at depths of less than

Oceanic Layer	Thickness km	Velocity km s^{-1}	
1	0	2.2	Foraminiferal sand and ooze
	to		
	1.0	2.8	Highly weathered material and compacted sediment
2	1.6	3.8	Weathered pillow basalt and weathered serpentinite
	to		
	2.0	4.7	Massive basalt, diabase and fresh serpentinite
3	1.3 - 3.4	5.8 - 6.8	Meta-basalt, gabbro and meta-gabbro
	Mohorovicic	discontinuity	
4	uncertain	8.1	Ultramafics (layered peridotites and dunites)

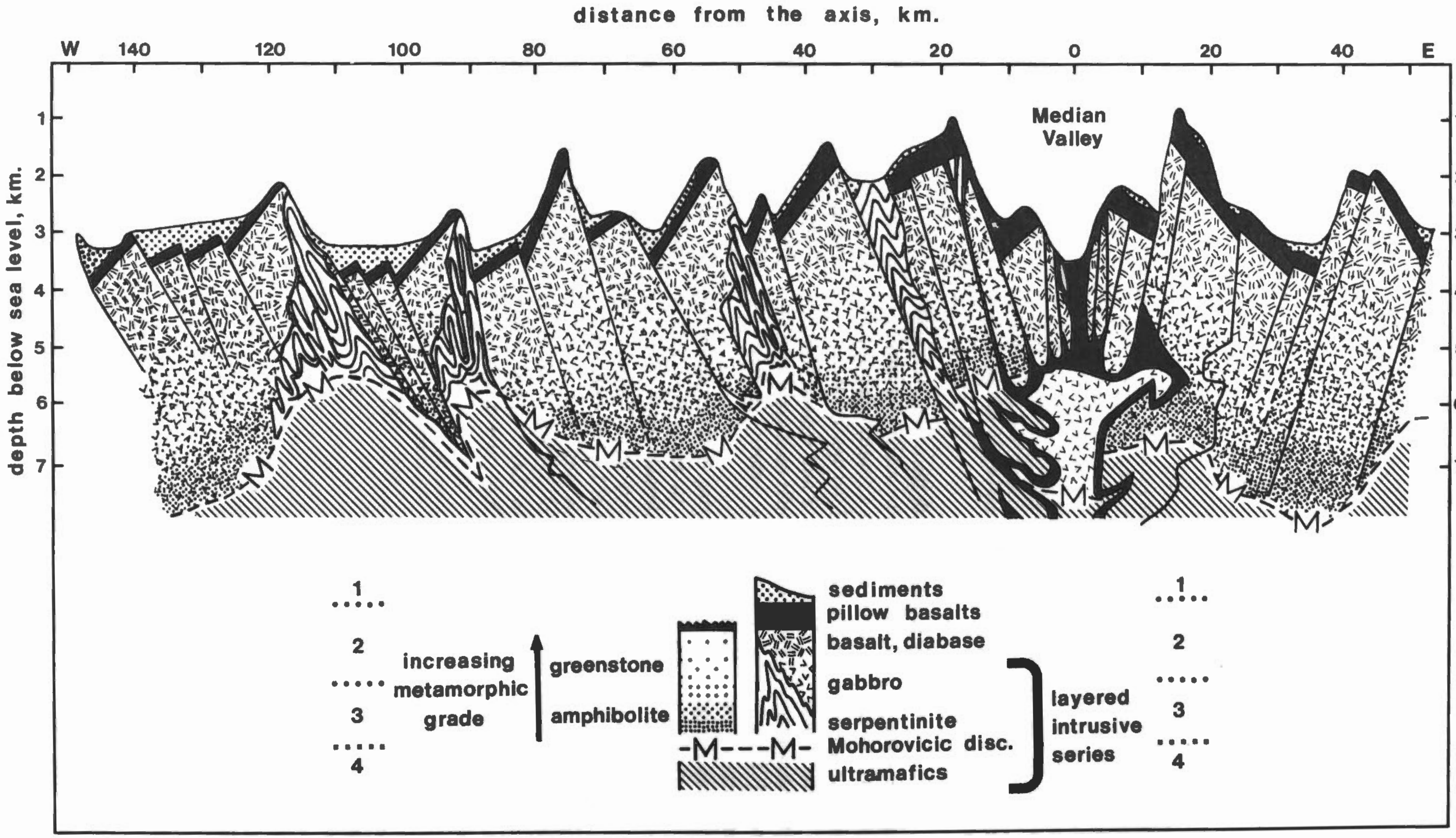

Figure 1. Schematic cross-section through the oceanic crust beneath the Mid-Atlantic Ridge at 45°N.

24 km below sea level, while their roofs may be within 1 - 2 km of the ocean floor hence these bodies encroach upon the uppermost levels of the upper mantle and the base of the crust (Aumento and Loubat, 1971). Magmatic differentiation by gravity crystal settling takes place after emplacement under quiescent conditions, producing igneous layering with an upward dunite-peridotite-gabbro-extrusives stratigraphy. The gabbros and extrusives accrete to the base of the crust, whereas the ultramafics beneath them accrete to the top of the upper mantle. The gabbro-peridotite interface so formed represents the local Mohorovicic discontinuity between layers 3 and 4, which, by nature of its origin, exhibits considerable variations in depth from lopolith to lopolith.

Metamorphism (Aumento and Loncarevic, 1968) due to burial, subsequent intrusions and extrusions and generally high heat flow affects these rocks in a manner approaching that of continental regional metamorphism, transforming gabbros and diabases into greenstones and amphibolites. This upwardly encroaching metamorphic horizon is thought to represent the junction between layers 2 and 3, layer 2 consisting of the unmetamorphosed mafic rocks, and layer 3 their metamorphosed equivalents (Barrett and Aumento, 1970).

The final complete crystallization and solidification of these lopoliths restricts further plastic stress release, and contributes to a new cycle of tensional stress build up, resulting in renewed fracturing beneath the axis. A new generation of totally liquid bodies is then intruded into the voids formed, while the solid rocks formed during the previous cycle are deformed cataclastically as they are moved apart; however, these rocks may often succeed in repairing the tectonic damage by renewed, solid-state recrystallization under a hot, high stress environment. Cataclasism is followed by amphibolitization through the action of juvenile water hydration. Rodingitizing metasomatism appears contemporaneous with the last stages of amphibolitization, and heralds incipient serpentinization. The bulk of the serpentinization results from later, more extreme, periods of hydration. Diverse physical conditions are evident here: initially the result of very hot juvenile waters, the final phases are produced under tensional stress, by the hydrating effects of cooler meteoric waters possibly contemporaneous with diapiric emplacement through the oceanic crust.

Magnetics

The magnetic anomaly pattern of the oceanic crust at 45°N, as elsewhere on the axes of ridge systems, is dominated by a strong positive lineation (over 800γ) coincident in position with the Median Valley (Loncarevic *et al.*, 1966). On either side of this central anomaly the detailed pattern is confused, but is characterized nevertheless by numerous elongate anomalies of short continuity parallel to the central anomaly. Some 120 km west of the axis there appears a continuous anomaly of +350γ maximum amplitude, corresponding to an anomaly which is readily identifiable over other axial regions, and which has been designated as oceanic anomaly 5. The relative position of anomaly 5 with respect to the axis (anomaly 1) indicates that the ocean floor has probably been spreading at an overall average rate of 1.28 cm/y over the last 10 m.y. (Aumento, 1969 and Aumento *et al.*, 1970).

Paleomagnetic tests on the rocks from the area have shown that only the eruptives belonging to the uppermost part of oceanic layer 2 are likely contributors to the regular magnetic anomaly pattern over the ridge (Irving, Robertson and Aumento, 1970; Irving, Haggerty, Aumento and Loncarevic, 1970). These eruptives have an average n.r.m. (natural remanent magnetization) of 78×10^4 cm^{-3} cgs over the Crest Mountains, decreasing to 50×10^4 over the High Fractured Plateaus, whereas the gabbros and diabases beneath have an average of only 1.2×10^4, and their metamorphic equivalents 0.3×10^4 cm^{-3} cgs. In contrast, serpentinites average 40×10^4 cm^{-3} cgs; such high intensities of n.r.m. for the serpentinites produce substantial disruptions of the magnetic anomaly lineations in the surface anomaly patterns coincident with diapiric intrusions of serpentinized ultramafics. These high n.r.m. intensities also suggest that the oceanic layer 3 is not composed primarily of serpentinites (Aumento *et al.*, 1970; Irving, Robertson and Aumento, 1970).

Geochronology

Radiometric ages (potassium-argon and fission track) show that the spreading rate of the ocean floor may have changed from 1 cm/yr. over the High Fractured Plateau for the period 3 - 16 m.y. to 4 cm/yr. over the Crest Mountains for the period 3 m.y. to the present (Fleischer *et al.*, 1968; Aumento, Wanless and Stevens, 1968; Aumento, 1969). The change in rate cannot be detected in the magnetic anomaly patterns due to their confused nature (they give the average rate of 1.28 cm/yr. only), but shows a remarkable coincidence with the physiographic boundary between the Crest Mountains and the High Fractured Plateaus and possibly also with increased sedimentary thicknesses and in the thickness of ferromanganese encrustations on rocks at that boundary. Similar changes in spreading rate have been suggested for other ocean-ridge systems.

A number of geochemical and geophysical parameters vary with distance from the axis of the ridge, and hence with time: among these are the intensities of remanent magnetization (Irving, Robertson and Aumento, 1970), Fe_2O_3/FeO ratios, H_2O and U contents, and $\delta O^{18}/O^{16}$ and Sr^{87}/Sr^{86} ratios of basalts (Aumento, 1971). An understanding of these variations with time is important if we are to anticipate the characteristics of rocks from ancient oceanic crusts outcropping on the continents relative to those we know are characteristic of fresh rocks collected over modern ridge systems.

Igneous and metamorphic rocks

Mafic rocks: these vary in texture from glassy, sometimes spherulitic pillow basalts, to more massive, diabasic and gabbroic rocks. Pillow lavas are often vesicular, the vesicles showing no correlation with the depth of water under which the extrusion occurred. Resorbed calcic plagioclase xenocrysts, indicative of gravity crystal differentiation in lopoliths beneath the axis, are characteristic of many of the pillow basalts (Muir and Tilley, 1964; Aumento, 1968; Aumento and Loncarevic, 1968).

Mafic rocks vary in composition from quartz-normative tholeiites to nepheline-normative alkali basalts. Many of these rocks fall into the low olivene-normative field, with a smaller concentration occupying the field of incipient normative nepheline (Muir and Tilley, 1964; Aumento, 1968; Aumento and Loncarevic, 1968). Table I lists the average compositions of the main types of rocks at 45°N.

Meta-basites: zeolite facies metamorphism of basalts and diabases takes place under very shallow burial conditions, possibly of the order of a few tens of metres. Plagioclase phenocrysts are altered to analcite, and the groundmass to other zeolites. In the greenschist facies the mafic rocks still retain their igneous textures; here calcic plagioclase alters to albite, augite to actinolite, olivine and glass to chlorite. In the higher grades epidote, tremolite, quartz, calcite, talc, titanomaghemite and green hornblende also occur (Aumento *et al.*, 1970).

Amphibolite facies meta-basites occur at greater crustal depths (well into layer 3). These rocks have lost all igneous textures and most relict minerals, and exhibit strong fabric lineations. Minerals include (a) lower grade assemblages of quartz, plagioclase (oligoclase-andesine), biotite, hornblende, epidote, sericitized orthoclase, magnetite and sphene; (b) a higher grade assemblage of hornblende, diallagic diopside, plagioclase (oligoclase-andesine), sericitized orthoclase and minor biotite (Aumento *et al.*, 1970).

Serpentinized ultramafics: these rocks include dunites, harzburgites, lherzolites, peridotites, amphibole peridotites, wehrlites and troctolitic gabbros (Aumento *et al.*, 1970; Aumento and Loubat, 1971). Many show evidence of gravity crystal cumulate layering, of subsequent mylonitization, and other mechanical deformations, as well as metasomatic changes such as amphibolitization and rodingitization, and ubiquitous, almost total serpentinization. In these features, as well as textures, they are comparable to the classical stratiform massifs of the continents, the mediterranean ultramafic massifs and the alpine-type ophiolites. However, these affinities are never clear cut: important discrepancies always appear. Oceanic ultramafics may represent an intermediate stage between the large layered massifs and the smaller, highly deformed alpine bodies. Indeed, oceanic ultramafics may offer unique opportunities to solve problems encountered in the more disturbed continental environments.

Sialic intrusives: hornblende-rich quartz-diorites grading into trondhjemites or albite granites occur as small pockets in intimate association with the ultramafic rocks. They contain xenoliths of basalt, serpentinites and metabasites. These rocks are reminiscent of the albitized diorites characteristic of the late stages of alpine intrusive complexes (Aumento, 1969).

Conclusions

A modern oceanic crust consists of a layered sedimentary sequence of variable thickness underlain by 5 km of systematically layered igneous and metamorphic rocks. The latter consist of a thin upper "layer" of pillow lava underlain by massive basalts, diabases and gabbros. These rocks show increasing metamorphism with depth, and reach the equivalent of the amphibolite facies near the base of the crust. Layered ultramafic bodies make up the top of the upper mantle beneath the amphibolites. On the slowly spreading ridges the hydrated equivalents of these ultramafics (the serpentinites) pierce through the crustal layering; however, under rapidly spreading ridges they may be unable to do so, since vertical tectonic movements are less characteristic of rapid spreading.

At present only the gross features described above may be used in the preliminary identification of ancient oceanic crusts on the continents. The geochemical parameters which are characteristic of modern ridges (Table I) appear to be too dependent on time variations to permit direct comparisons to be made. It is possible, however, that in the near future we may find parameters that are independent of geological time for use in the unequivocal identification of ancient oceanic crusts.

Bibliography

Aumento, F. 1967. Magmatic evolution on the Mid-Atlantic Ridge. *Earth Planetary Sci., Letters*, 2, 225-230.

——— 1968. The Mid-Atlantic Ridge near 45°N: II. Basalts from the area of Confederation Peak. *Can. J. Earth Sci.*, 5, 1-21.

——— 1969. Diorites from the Mid-Atlantic Ridge at 45°N. *Science*, 165, 1112-1113.

——— 1969. The Mid-Atlantic Ridge near 45°N: V. Fission track and ferro-manganese chronology. *Can. J. Earth Sci.*, 6, 1431-1440.

——— 1971. Uranium content of mid-oceanic basalts. Submitted to *E.P.S.L.*, Dec. 1970.

———B.D. Loncarevic. 1968. The Mid-Atlantic Ridge near 45°N: III. Bald Mountain. *Can. J. Earth Sci.*, 6, 11-23.

———B.D. Loncarevic, and D.I. Ross. 1970. Hudson geotraverse, geology of the Mid-Atlantic Ridge at 45°N. Royal Society meeting on the petrology of igneous and metamorphic rocks from the ocean floor. *Phil. Trans. Roy. Soc. Lond.*, 243-270.

———H. Loubat. 1971. The Mid-Atlantic Ridge near 45°N: XV. Serpentinized ultramafic intrusions. Submitted to *Can. J. Earth Sci.*, Oct. 1970.

———R.K. Wanless, and R.D. Stevens. 1968. Potassium-argon ages and spreading rates on the Mid-Atlantic Ridge at 45°N. *Science*, 161, 1338-1339.

Barrett, D. and F. Aumento, 1970. The Mid-Atlantic Ridge near 45°N: XII. Seismic velocities and crustal layering. *Can. J. Earth Sci.*, Vol. 7, 1117-1124.

Carmichael, C. 1970. The Mid-Atlantic Ridge near 45°N: VI. Magnetic properties and opaque mineralogy of dredged samples. *Can. J. Earth Sci.*, Vol. 7, 239-256.

Fleischer, R.L., H.R. Hart, I.S. Jacobs, P.B. Price, W.M. Schwarz, and F. Aumento. 1969. Search for magnetic monopoles in deep-ocean deposits. *Phys. Rev.*, Vol. 184, 1393-1397.

———J.R.M. Viertl, P.B. Price, and F. Aumento, 1968. Mid-Atlantic Ridge, age and spreading rates. *Science*, 161, 1339-1342.

Garner, D.M., and W.L. Ford. 1969. The Mid-Atlantic Ridge near 45°N: IV. Water properties in the median valley. *Can. J. Earth Sci.*, 6, 1359-1363.

Haggerty, S.E. 1970. The Mid-Atlantic Ridge near 45°N: XIII. A reflection microscopic study of magnetic minerals. *Can. J. Earth Sci.* (In press.)

Irving, E., S.E. Haggerty, F. Aumento, and B.D. Loncarevic. 1970. Magnetism and opaque mineralogy of basalts from the Mid-Atlantic Ridge at 45°N. *Nature*, 228, 974-976.

———W.A. Robertson, and F. Aumento. 1970. The Mid-Atlantic Ridge near 45°N: VII. Remanent intensity, susceptibility and iron content of dredged samples. *Can. J. Earth Sci.*, Vol. 7, 226-238.

Keen, C.E., and C. Tramontini. 1970. A seismic refraction study on the Mid-Atlantic Ridge. *Geophys. J. Roy. Astron. Soc.*, Vol. 20, 473-491.

Keen, M.J., and K.S. Manchester. 1970. The Mid-Atlantic Ridge near 45°N. X. Sediment distribution from seismic profiling. *Can. J. Earth Sci.*, Vol. 7, 735-747.

Loncarevic, B.D., C.S. Mason, and D.H. Matthews. 1966. The Mid-Atlantic Ridge near 45°N: I. The Median Valley. *Can. J. Earth Sci.*, 3, 327-349.

Matthews, D.H., and J. Bath. 1967. Formation of magnetic anomaly patterns of Mid-Atlantic Ridge. *Geophys. J. Roy. Astron. Soc.*, 13, 349-357.

Muir, I.D., and C.E. Tilley. 1964. Basalts from the northern part of the rift zone of the Mid-Atlantic Ridge. *J. Petrol.*, 5, 409-434.

Paterson, I.S. 1970. The Mid-Atlantic Ridge near 45°N: XI. Continental Rocks. Submitted to *Can. J. Earth Sci.*

Legend for Table I

Column 1. Average of 15 analyses of almost totally serpentinized ultramafic rocks (pre-serpentinization rock types include peridotites, lherzolites, harzburgites and dunites).

Column 2. Average of two analyses of gabbros, both showing incipient greenstone metamorphism.

Column 3. Average of 10 analyses of extremely fresh tholeiitic basalts from the Median Rift Valley floor.

Column 4. Average of 10 analyses of fresh tholeiitic basalts from the Median Valley scrap showing incipient weathering (note higher Fe_2O_3/FeO ratio and H_2O content relative to analysis in column 3).

Column 5. Average of 10 analyses of basalts showing alkaline affinitives. These basalts characteristically show more advanced weathering than do the associated tholeiites. This may be due to the particular susceptibility of alkali basalts to weathering, to their initially higher oxydation state, or both.

Column 6. Average of 10 analyses of basalts and diabases showing incipient or complete greenstone metamorphism.

Column 7. Average of five analyses of quartz-diorites and trondhjemites.

Table I. Average major, minor and trace element compositions of rocks from the Crest Mountains of the Mid-Atlantic Ridge at 45° N.

	1	2	3	4	5	6	7
	SERPE	GABBR	THOLE	THOLE	ALKAL	GREEN	DIORI
SiO_2	37.65	47.55	50.24	50.19	48.09	49.33	65.76
Al_2O_3	2.45	16.02	15.77	16.77	16.19	15.23	14.95
Fe_2O_3	7.71	1.47	1.24	2.66	4.55	3.08	2.97
FeO	0.56	5.02	8.12	6.50	4.75	7.07	3.18
CaO	0.20	12.64	11.45	11.65	9.80	9.15	2.86
MgO	36.94	11.16	8.18	6.55	7.61	7.18	1.85
Na_2O	0.18	1.70	2.55	2.75	3.68	3.22	5.35
K_2O	0.02	0.04	0.23	0.44	0.88	0.14	0.76
TiO_2	0.06	0.64	1.34	1.40	1.72	1.42	0.77
PiO_5	0.02	0.04	0.11	0.14	0.26	0.17	0.21
H_2O	12.67	2.66	0.48	0.77	2.23	3.03	1.00
MnO	0.12	0.15	0.14	0.14	0.18	0.39	0.10
S	0.0	0.0	0.0	0.0	0.0	0.0	0.0
NiO	0.13	0.02	0.01	0.0	0.01	0.01	0.0
$CrIO_3$	0.24	0.01	0.02	0.01	0.03	0.01	0.0
CO_2	0.18	$<$0.10	$<$0.10	0.15	0.15	0.37	$<$0.05
TOTAL	99.13	99.24	99.98	100.12	99.98	100.80	99.86
Q	0.0	0.0	0.0	0.24	0.0	0.54	22.80
Or	0.14	0.24	1.37	2.62	5.32	0.86	4.55
Ab	1.76	14.89	21.68	23.42	30.66	28.15	45.81
An	0.0	37.25	31.06	32.33	25.60	27.58	12.65
Ne	0.0	0.0	0.0	0.0	0.62	0.0	0.0
Ag	0.0	21.34	20.07	19.38	16.84	12.75	0.0
Hy	34.81	13.22	16.25	14.78	0.0	21.42	6.99
Ol	50.21	9.23	4.69	0.0	9.88	0.0	0.0
Mt	2.38	2.21	1.81	3.88	6.74	4.61	4.36
Il	0.13	1.26	2.56	2.68	3.34	2.79	1.48
Hm	7.28	0.0	0.0	0.0	0.0	0.0	0.0
Ap	0.05	0.10	0.26	0.33	0.62	0.41	0.49
C	2.47	0.0	0.0	0.0	0.0	0.0	0.76
Cr	0.41	0.01	0.03	0.01	0.04	0.01	0.0
La	0.0	0.0	0.0	0.0	0.0	0.0	0.0
Cc	0.36	0.24	0.23	0.34	0.35	0.87	0.11
TOTAL	100.00	100.00	100.00	100.00	100.00	100.00	100.00
Sr	20	75	97	120	274	195	120
Ba	25	14	61	94	142	24	226
Cr	2450	160	200	125	328	84	$<$20
Zr	$<$30	116	120	342	208	116	468
V	57	140	392	360	351	348	37
Ni	1300	163	131	56	104	95	35
Cu	120	19	91	73	124	150	25
Co	136	31	41	42	39	33	$<$20
Sc	$<$10	33	47	42	38	30	$<$10
Zn	nd	87	91	99	81	102	25
Pb	nd	1.4	1.6	2.3	3.0	3.4	2.1
Ga	nd	20	35	27	12	19	30
B	nd	$<$5	$<$5	5.5	2.4	$<$1	1.8
Rb	nd	$<$5	$<$5	5	$<$30	$<$5	$<$5
U	0.45	0.17	0.25	0.42	0.85	0.41	0.66
La	nd	ndd	5.29	7.52	nd	nd	nd
Sm	nd	nd	3.13	3.55	nd	nd	nd
Eu	nd	nd	0.98	1.09	nd	nd	nd
Tb	nd	nd	0.53	0.60	nd	nd	nd
Lu	nd	nd	0.42	0.39	nd	nd	nd
Hf	nd	nd	1.85	2.12	nd	nd	nd
Yb	nd	nd	2.25	2.29	nd	nd	nd

No. 3

mesozoic and tertiary volcanism of the western canadian cordillera

J.G. SOUTHER
Geological Survey of Canada
Vancouver, B.C.

Abstract. No Mesozoic or Tertiary rocks with the characteristics of oceanic crust are known in the Canadian Cordillera. The early Mesozoic was dominated by the successive formation and erosion of island arcs situated near the continent, whereas volcanism during the late Mesozoic and Tertiary was entirely continental. Spatial and temporal changes in the style of volcanism and the composition of lavas is believed to reflect changes in the interaction between Pacific crust and the continental margin.

Introduction

The record of Mesozoic and Tertiary volcanism in the Cordillera is a record of continental and island arc volcanism, for nowhere in western Canada do rocks of this age exhibit the characteristics of oceanic crust. Nevertheless, the changing styles of Cordilleran volcanism must reflect changes in the interaction between Pacific crust and the continental margin. In our present state of knowledge any attempt to interpret this record requires that certain assumptions be made. Foremost of these concerns is the amount and timing of transcurrent movement between the various tectonic belts of the western Cordillera for clearly, variations in magma type are significant only if their original spatial relationships are known. Pre-Tertiary right lateral movement has been suggested for several northwesterly trending lineaments, particularly the Yalakom and Tintina trenches, and parts of the Rocky Mountain Trench. Moreover, Permian and Triassic faunas in central British Columbia are similar to faunas in the southwestern United States, suggesting that large-scale translation may have continued into late Triassic or early Jurassic time. Conversely, the stratigraphic record in many parts of British Columbia suggests that Upper Triassic and younger clastic sediments were derived from immediately adjacent source areas, and that structures related to Mesozoic tectonic events may be traced across, as well as along, the Cordilleran structural trend. The latter evidence is sufficiently strong, in the writer's opinion, to justify the view that the Insular Belt, the Coast Crystalline Belt, and the western part of the Intermontane Belt have been in their present positions relative to one another since late Triassic time. The possibility remains that this entire segment of the Cordillera may be allochthonous with respect to Triassic rocks farther east. The present paper is restricted to a discussion of this most westerly segment of the Cordillera and adjacent parts of the Pacific Basin. The larger problem of relating this region to global plate motion, and to the southern Cordillera, is dealt with in a more comprehensive paper now in preparation.

Distribution of volcanic rocks

Both the Insular Belt of western British Columbia and the Intermontane Belt of central British Columbia contain great thicknesses of Mesozoic and Tertiary volcanic rocks. These two belts are separated by the tectonically high Coast Mountains, consisting mainly of crystalline rocks that were emplaced in a series of pulses, approximately synchronous with the major volcanic episodes.

The two distinct belts of Triassic and early-to-middle Jurassic outcrops in the Intermontane Belt (Figure 1) may be more apparent than real since the interior of this belt is largely covered by younger sediments and Tertiary plateau lavas. Conversely, the outcrop distribution of Early Tertiary volcanics (Figure 2) is misleadingly small since most of this material is poorly indurated subaereal ash-flows that were rapidly eroded. Very thick sections preserved in small downfaulted blocks within and adjacent to the Coast Mountains indicate that the early Tertiary volcanism was a more important and more widespread event than the present outcrop distribution suggests. Similarly, the presence of Miocene basaltic dyke swarms thoughout the Coast Mountains suggest that the plateau lavas may originally have extended much farther west. Only the Pleistocene and younger volcanoes are sufficiently well preserved to permit recognition of individual vents. With few exceptions these are aligned in north-south and east-west trending linear belts.

Sequence of volcanic events

During Late Triassic (Karnian) time volcanism in the Intermontane Belt was dominated by the eruption of clastic, augite andesite lava from both submarine and subaerial vents. These are interbedded with rapidly deposited eugeosynclinal sediments that exhibit abrupt facies changes and numerous local unconformities. Contemporaneous volcanism farther west, in the Insular Belt, produced thick piles of tholeiitic pillow lavas, aquagene tuffs and breccias. Despite their submarine origin these Triassic lavas, unlike those of Permo-Carboniferous age, are not associated with ultramafic rocks or chert and are therefore not typical of deep oceanic basalts of the ophiolite suite.

The quiet effusion of tholeiite in the Insular Belt ended in earliest Jurassic time and was followed by sporadic eruption of clastic andesite from subaerial as well as submarine vents. Similar early Jurassic, andesitic volcanism continued in the southern part of the Intermontane Belt but diminished northward, and, north of Stikine River, the entire Lower and Middle Jurassic succession is represented by clastic sedimentary rocks locally containing piles of pillow basalt and

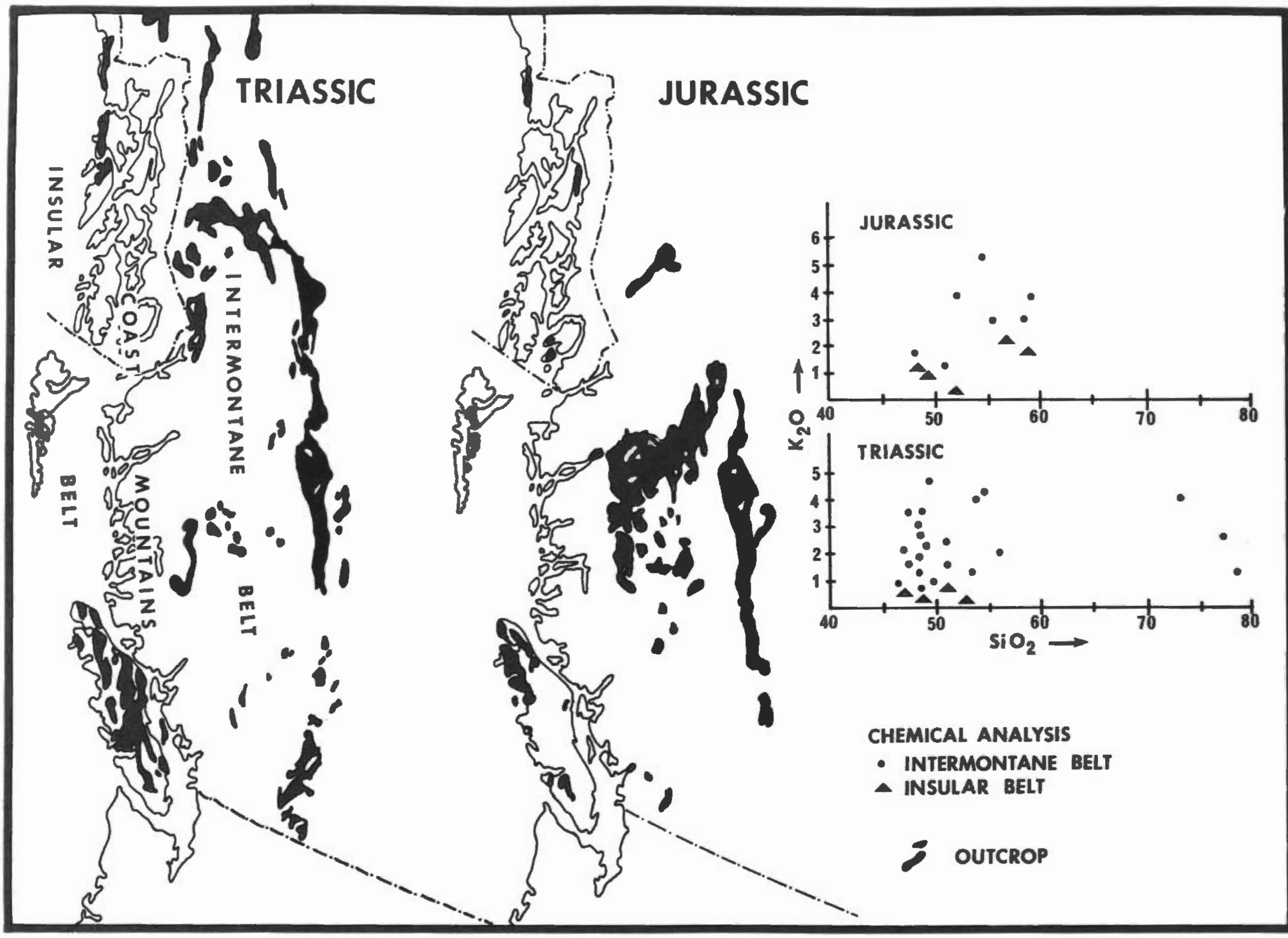

Figure 1. Distribution and chemistry of Mesozoic volcanic rocks.

peperites that formed isolated seamounts within the sedimentary basin.

By late Jurassic time large segments of the Cordillera had become emergent and thick sections of clastic sediments were deposited in successor basins within the central part of the Intermontane Belt. Regional uplift, particularly of the Coast Geanticline, was accompanied by plutonism, but volcanic activity did not resume until the late Cretaceous. By that time the Cordillera was almost completely emergent, and profound uplift of the Coast Geanticline during the late Createaceous and early Tertiary was accompanied by extensive high-level plutonism, block faulting, and explosive, subaerial eruption of enormous volumes of rhyolite, rhyodacite, and dacite ash-flows and ignimbrites. Their close spatial relationships and similar chemistry suggest that these lavas are genetically related to plutons and to north-south trending dyke swarms of the same age. Acid volcanism reached its climax in the Eocene, declined rapidly, and was followed in the Oligocene by a period of quiescence that lasted until the Miocene. At that time a flood of alkali-olivine basalt issued from a multitude of vents and fissures to form the plateau lavas of central British Columbia. This activity culminated in the late Miocene but intermittent eruption of similar lava continued from belts of central vents thoughout Pleistocene and into Recent time.

Chemistry

Very few chemical analyses are available of early Mesozoic or early Tertiary volcanic rocks and, although a large number of Miocene and younger lavas have been analyzed, they are mostly from small, intensively studied areas and are not a regional sample. However, even these few analyses indicate several important trends. Both Triassic and Jurassic volcanics exhibit a distinct east-west polarity with respect to potash, those in the Intermontane Belt having an appreciable higher K_2O content than equivalent rocks in the Insular Belt (Figure 1).

The early Tertiary volcanics, as one would expect from their explosive origin, are relatively high in silica. The random scatter of both silica and alkali values is also significant, and contrasts markedly with the narrow range of compositions exhibited by the Miocene alkali-olivine basalt of the plateau lavas (Figure 2).

Most Pleistocene and Recent volcanoes consist of similar alkali-olivine basalt however a few of the larger centres such as Edziza and Garibaldi have produced highly differentiated lava series. In most cases these show a direct line of descent from primary alkali-olivine magma similar to that of the plateau lavas (Figure 2).

Discussion

If the initial assumption of this paper is accepted, namely that the three most westerly tectonic subdivisions of the Cordillera have maintained their present relative positions since late Triassic time, then the changing pattern of volcanism through time and space becomes meaningful within the framework of plate tectonic theory. According to this concept (Hamilton, 1969) the underflow of spreading oceanic crust into a trench and down an inclined subduction zone beneath the continental margin is the driving mechanism of tectonic processes including volcanicity. Empirically,

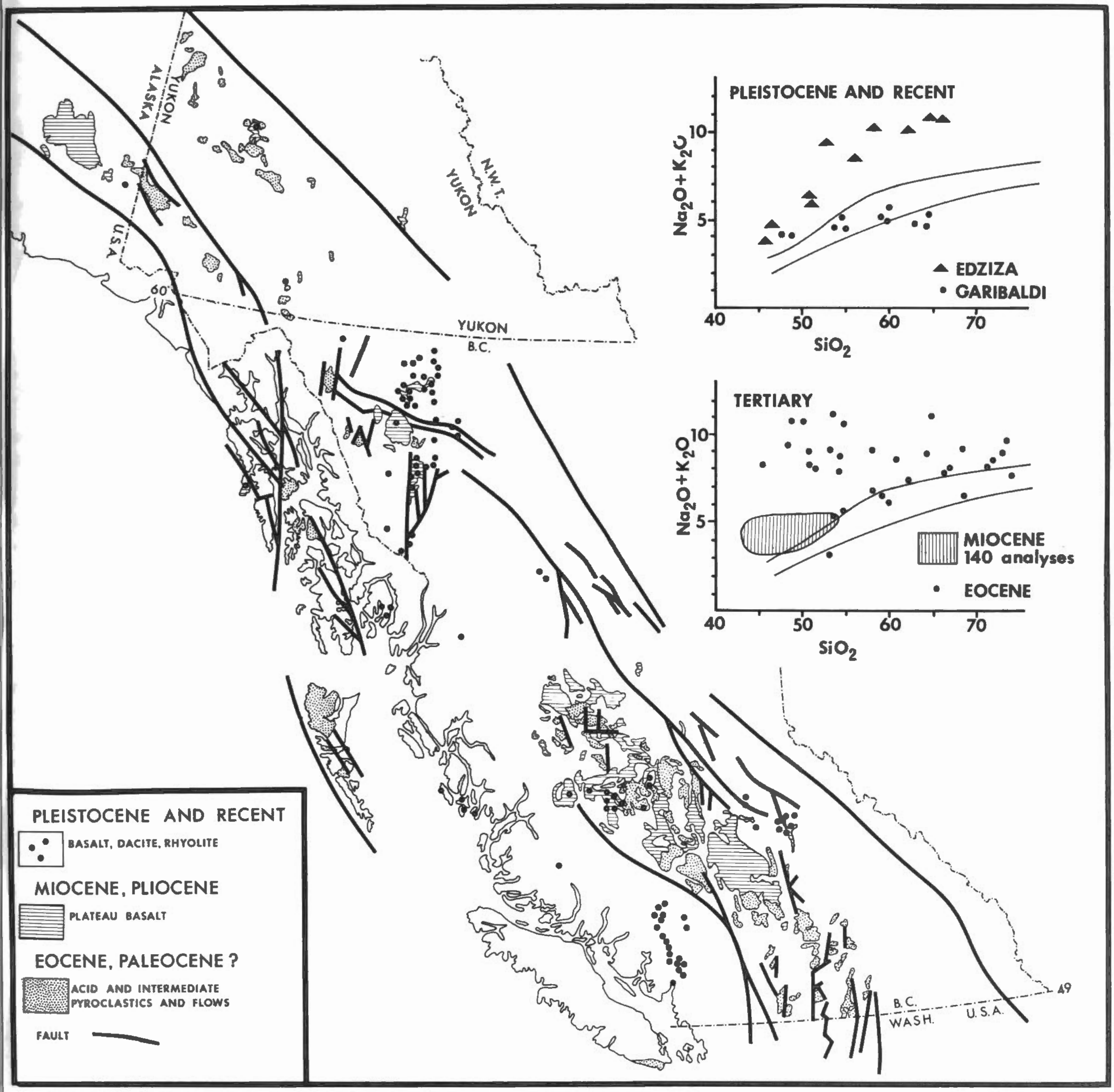

Figure 2. Distribution and chemistry of Tertiary and Quaternary volcanic rocks.

andesitic volcanism of the island arc type is confined to belts above such subduction zones and lavas erupted farthest from the trench are more alkaline, particularly more potassic, than those closer to it (Dickinson, 1968). Similarly, the basaltic rocks derived deep within the mantle have an alkaline affinity while those of shallower origin tend toward tholeiite (Kuno, 1966).

Applying this model to the western Cordillera, the late Triassic volcanics of the Intermontane Belt are considered to represent a series of volcanic arcs that formed above a gently inclined subduction zone. Contemporaneous submarine volcanism in or near the trench produced the great elongate piles of less potassic lavas found in the Insular Belt. Westward migration of andesitic arcs in the early Jurassic may reflect steepening of the subduction zone in response to the development of a deep root of granitic rocks beneath the arcs.

The termination of andesitic, arc-type volcanism in the late Jurassic may reflect a change in the direction of relative motion between the Pacific and North American crustal plates, resulting in cessation of underflow. The profound late Jurassic regional uplift is thus explained by rebound of the gravitationally unstable granitic root zone that lay beneath the arcs and which is now exposed in the Coast Mountains.

This block, formed by partial or complete melting of heterogeneous plutons, neared the surface, and block foundering and cauldron subsidence accompanied the explosive volcanics of central British Columbia (Souther, 1967). This activity persisted until mid-Tertiary when isostatic equilibrium was restored. Uplift of the Coast Mountain belt declined, and the present stable, aseismic continental margin emerged. Late Miocene and younger activity, dominated by effusion of mantle-derived alkali-olivine basalt, is characteristic of interplate continental volcanism, unrelated to crustal underflow (Souther, 1970). The east-west, north-south alignment of Pleistocene and younger volcanic centres suggests that the magma rose along gash fractures related to right lateral shear between the Pacific plate and the continent along the northwesterly trending Queen Charlotte-Fairweather Fault system.

Until further data are available, this, or any other comprehensive model of Cordilleran tectonism must be at best highly speculative. However, it provides the nucleus of a mechanistic theory of tectonism that relates the continental margin to the adjacent ocean basin and provides a basic framework within which the cause and effect of many different tectonic processes may be tested. Viewed in this light, it can serve a useful function in giving direction to further research, both in the field and in the laboratory.

Future research

A better understanding of the relative positions of the various tectonic segments of the Cordillera during Mesozoic and Tertiary time is essential. Until this has been established no confident interpretations can be drawn from any body of data pertaining to the regional distribution of rock properties. Particular emphasis should therefore be placed on the following:

1. stratigraphic studies designed to identify the source of clastic sediments in Mesozoic and Tertiary basins to establish stratigraphic ties between those parts of the Cordillera that have not undergone large scale relative displacement,
2. paleomagnetic study of Mesozoic and Tertiary volcanic rocks in several different tectonic domains and comparison of their pole positions, and
3. regional geochemistry of volcanic rocks to identify individual volcanic eras and establish their chemical polarity.

References

Dickinson, W.R. 1968. Circum-Pacific andesite types. *J. Geophys. Res.*, Vol. 73, No. 6, 2261-2269.

Hamilton, W. 1969. Mesozoic California and the underflow of Pacific mantle. *Geol. Soc. Amer. Bull.*, Vol. 80, 2409-2430.

Kuno, H. 1966. Lateral variation of basalt magma type across continental margins and island arcs. *Bull. Volcanologique*, XXXIX, 195-222.

Souther, J.G. 1967. Acid volcanism and its relationship to the tectonic history of the Cordillera of British Columbia. *Bull. Volcanologique*, XXX, 161-176.

——1970. Volcanism and its relationship to recent crustal movements in the Canadian Cordillera. *Can. J. Earth Sci.*, Vol. 7, No. 2, 553-568.

No. 4

oceanic crust in the canadian cordillera

J.W.H. MONGER
Geological Survey of Canada
Vancouver, B.C.

Abstract. Analysis of available information on the distribution of lithologies of the upper Paleozoic in the western Canadian Cordillera leads to the conclusion that, by analogy with modern examples, elements of both ancient oceanic basins and island arcs are represented. A westernmost upper Paleozoic arc along the present site of the Coast Mountains is succeeded eastward by upper Paleozoic oceanic rocks in the modern Intermontane Belt, a Permian (?) arc in the modern Cassiar-Omineca-Columbia Mountains and, eastern most, Mississippian oceanic rocks on the east flank of these mountains.

Introduction

Possible representations of extensive ancient oceanic rocks in the Canadian Cordillera are some of the upper Paleozoic (Mississippian, Pennsylvanian and Permian) volcanic and sedimentary assemblages. In places these assemblages contain the association of basalt, ultramafic rock and chert, that is commonly regarded as being characteristic of rocks formed in deep ocean basins. The only other assemblage of a similar nature in the Canadian Cordillera is represented by the small area of Tertiary basalt on southernmost Vancouver Island that is the northerly extension of the "oceanic" Olympic Mountains province. This paper is a preliminary attempt to identify the location of possible ancient oceanic rocks within the Canadian Cordillera by briefly reviewing the distribution of lithologies and the stratigraphic character of these upper Paleozoic rocks.

The following review is largely compiled from reconnaissance data in regional mapping reports of the Geological Survey of Canada, and a few local detailed studies. These data are summarized with references in a recent paper by Monger and Ross (in press, Table II). The writer is personally familiar from detailed mapping only with upper Paleozoic rocks in southwestern British Columbia (Localities 1 and 2, Figure 1) and northwestern British Columbia (Localities 4 and 9, Figure 1), and the conclusions drawn here are therefore influenced strongly by the writer's work in these areas.

Distribution of upper Paleozoic rocks in the western Cordillera

The distribution of upper Paleozoic rocks in the western Cordillera is shown on the Index Map (Figure 1) in relation to (1) present physical features, (2) older stratigraphic units and (3) time-equivalent, non-volcanic shelf rocks to the east. Noteworthy is the absence of any known pre-upper Paleozoic rock in the central Intermontane Belt and Coast Mountains. Oldest known rocks are Lower to mid-Mississippian strata from Locality 9 (Figure 1), although the possibility exists that some rocks from Locality 2 may be as old as Devonian (H.W. Tipper, pers. comm.). Some of the outcrop areas in the Intermontane Belt (e.g. Locality 9, Figure 1) are extensive and contain strata that commonly dip steeply (thus exposing great thicknesses) and this absence of older rocks may therefore not be fortuitous.

Distribution of upper Paleozoic magmatic rocks

The distribution of the upper Paleozoic volcanic assemblages shown in Figure 2A is provisional owing to the scarcity of information on composition from most localities. This scarcity is partly because of the reconnaissance nature of many reports but also is because the primary nature of these rocks is obscured by low-grade metamorphism, mainly of the sub-greenschist, pumpellyite-chlorite or pumpellyite-actinolite facies of Seki (1969). Chemical analyses of these rocks come from only four areas (Locality 9, Aitken, 1959; Monger, 1969; Locality 10, Sutherland Brown, 1957; K.V. Campbell, pers. comm.; Locality 13, Gabrielse, 1963; Locality 14, Tempelman-Kluit, in press) and all are of basalts and thus not a representative sample of all upper Paleozoic volcanic rocks. In addition, stratigraphic information is insufficient to show distribution of the volcanic rocks by geological systems, and lumping all together under the heading of upper Paleozoic probably blurs some distinctions that could otherwise be made. Nevertheless, sufficient data are available to divide the volcanic rocks into two groups: (a) basalts with relatively little associated pyroclastic material and (b) mixed volcanic rocks, comprising basalts, andesites, and acid lavas, with abundant pyroclastic rocks.

Four belts of volcanic rocks can be recognized (Figure 2A). Westernmost are mainly andesite and pyroclastic rocks with some basalt. Acid volcanic rock has been reported from Localities 1, 3 and 5 (Monger, 1970a, J.K. Rigby, pers. comm., Buddington and Chapin, 1929) and latite from Locality 6 (Muller, 1967). These rocks are apparently of Mississippian and Permian age. In the Intermontane Belt basalts are of Mississippian, Pennsylvanian and Permian age. Texturally these rocks are typical tholeiites, although it is not possible to characterize the type of basalt from the chemical data available, as the potassium content is widely variable, possibly as the result of later metasomatism. To the east of this is Permian and Pennsylvanian (?) pyroclastic rock and acid volcanic rock (Localities 11, 12, Lord, 1948; H. Gabrielse, pers. comm.). Finally, the easternmost belt consists mainly of basalts of Mississippian age in

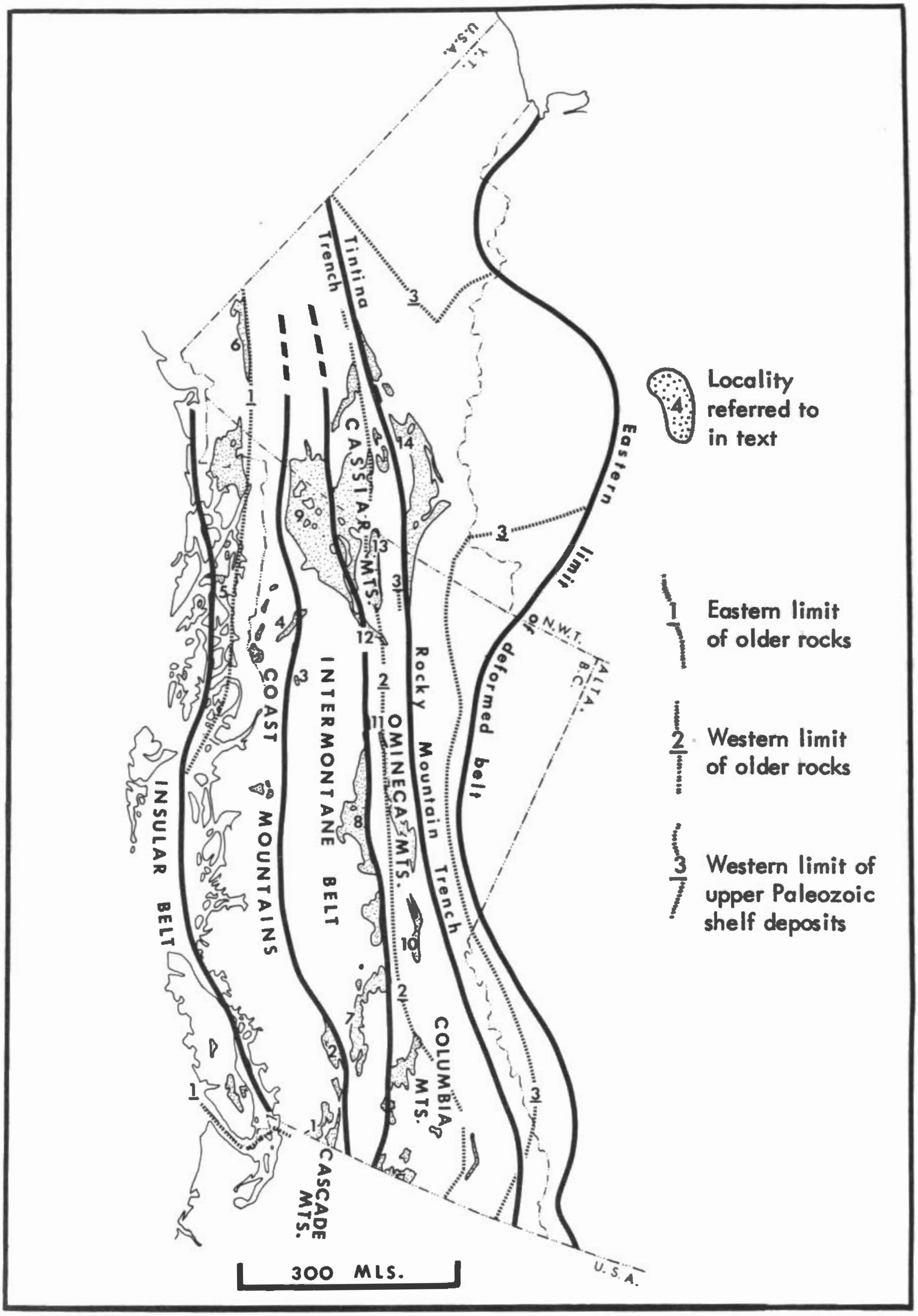

Figure 1. Index map of upper Paleozoic rocks in the western Cordillera.

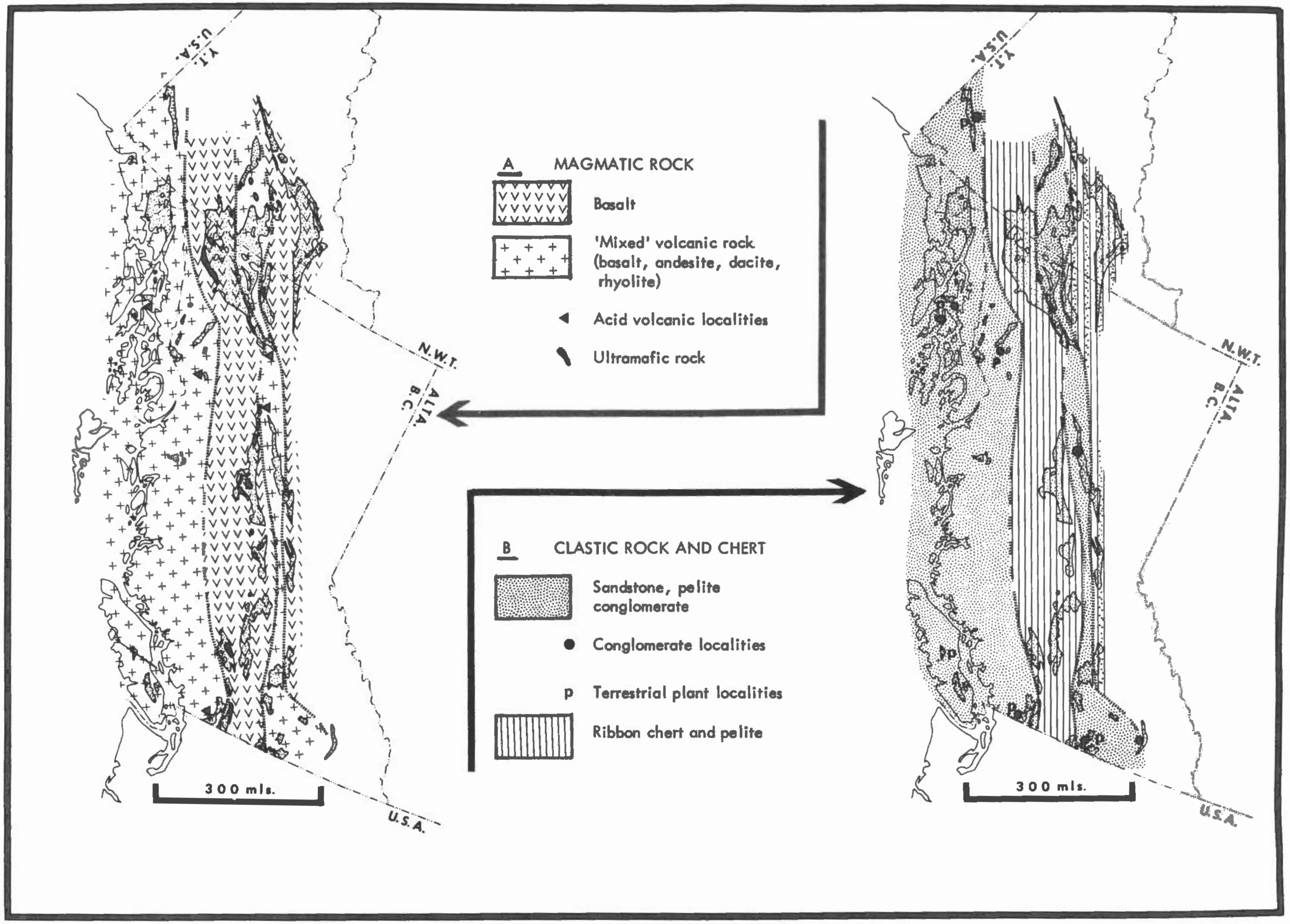

Figure 2. Distribution of upper Paleozoic lithologies.

the south, Mississippian and younger in the north.

Most ultramafic rocks of Alpine-type in the western Cordillera are spatially associated with upper Paleozoic rocks in the central belt, although some are in the easternmost belt. They vary in size from small dyke-like masses to the enormous Nahlin body of northwestern British Columbia (Locality 9) that is more than 60 miles long and 4 miles wide. In composition they range from serpentinite to variably serpentinized peridotite, with minor dunite and pyroxenite (e.g. Leech, 1953). In many places they are associated with gabbros, diabases and altered basalts, although nowhere has the stratified association characteristic of the ophiolite suite (e.g. Aubouin, 1965, p. 153) been reported.

The ultramafic bodies are extremely difficult to date. This problem is exemplified by the Shulaps body (Locality 2, Figure 1) that is enclosed partly by upper Paleozoic and partly by Triassic rocks (Leech, 1953). The serpentine phase of this body clearly intrudes Upper Triassic rocks but with no contact metamorphism. Chromite, probably derived from the body is found in late Lower Jurassic clastic rocks in the area and these in turn are intruded by ultramafic rocks. It is evident therefore that at least two phases of intrusion are represented but typically there is no information about time of cooling and crystallization of the body. In general, the lithological and common spatial association of the ultramafic rocks indicate a late Paleozoic age but, locally, they have been remobilized during Mesozoic deformation and have intruded post-Paleozoic rocks.

Distribution of upper Paleozoic clastic rocks

The distribution of upper Paleozoic clastic rocks in the Cordillera follows the same pattern as the volcanic rocks. Abundant sandstones and pelites and some conglomerates occur in the westernmost belt and along the western side of the Cassiar-Omineca-Columbia Mountains (Figure 2B). Ribbon-chert with radiolaria, indicative of a very slow influx of fine-grained clastic material, characterizes assemblages in the Intermontane Belt where it occurs with pelitic rocks. The easternmost belt consists of a lower clastic sequence overlain by abundant ribbon cherts (and therefore is shown as a 'mixed' pattern on Figure 2B).

The clastic sedimentation can be linked closely with the nature of the upper Paleozoic volcanism but also probably reflects differences in the tectonic behaviour of the belts. Detritus in the western and eastern belts has a two-fold source. Some was contributed directly to the basin by explosive pyroclastic activity reflecting the intermediate and acidic nature of the volcanism. In contrast, basaltic volcanism in the central belt produced relatively little clastic material. Secondly, other clastic material results from erosion of previously consolidated rocks, mainly volcanic rocks and carbonates. Evidence that landmasses were available for erosion in the eastern and western belts is provided by terrestrial plant fossils and conglomerates containing well-rounded cobbles at several localities (Figure 2B). These landmasses presumably resulted from the building-up of volcanic piles above sea level or from local tectonic uplift.

Distribution of the upper Paleozoic carbonates in the western Cordillera

Marked differences between the nature of the carbonates in the central belt and those in the eastern and western belts cannot be related solely to the greater amount of clastic material in the eastern and western belts. Carbonate in the central belt (Localities 7, 8, 9, Figure 1) is pure and forms enormous linear masses up to 6,000 feet thick that appear to have been deposited in shallow water as banks, reefs and tidal flats over a considerable length of time (the body at Locality 9 contains Upper Mississippian, Pennsylvanian and Permian fossils). Carbonate in the eastern and western belts is impure in many places, is nowhere as extensive as that in the central belt although locally it may be up to 2,000 feet thick, and it is generally restricted in time to a single system or part of a system. Much appears to have been deposited in a lower energy environment than carbonate in the central belt.

Tectonic behaviour of upper Paleozoic depositional sites

Preliminary stratigraphic evidence suggests that the tectonic behaviour of the central belt differed from that of the eastern and western belts. The central belt appears to have undergone more or less continuous subsidence in upper Paleozoic time as shown by the Upper Mississippian to Upper Permian shallow water carbonate. Some stages, such as the Virgilian and Missourian (Upper Pennslyvanian) are missing from this carbonate (Link, 1965; Monger and Ross, 1971, Table I), but no physical break has been recognized apart from a post-Upper Permian unconformity. In addition, the scarcity of coarse clastic rocks in the central belt indicates that there was no local erosion and redeposition in this belt. By contrast, stratigraphic breaks that at least in places record uplift are known from the western and possibly the eastern belt. At Locality 4, Permian strata sit with angular unconformity on Mississipian beds (Monger, 1970b). The only Pennsylvanian strata known from the eastern belt belong to the very top of that system (Monger and Ross, 1971). Many of the clastic rocks in the eastern and western belts that were derived from previously consolidated rock could well result from uplift and erosion, although all detritus known is derived from essentially surficial rock, indicating that if uplift took place it was relatively minor. These scarce data suggest that in the upper Paleozoic there was more or less continuous subsidence in the central, Intermontane Belt, whereas deposition was broken by uplift in the eastern and western belts.

Conclusions

The above distribution of upper Paleozoic rocks can be explained in terms of oceanic basins and island arcs if criteria such as those outlined by Hamilton (1969, pp. 2410-2412) from modern examples are used.

(1) The western belt of volcanic rocks of variable composition, clastics and carbonates on the site of the modern Insular Belt and Coast Mountains was an active arc in at least Mississippian

and Permian time. It may have developed, at least partly, on old continental crust formed during the time of the lower and mid-Paleozoic orogenic activity, which has been reported from southeastern Alaska by Brew *et al.* (1966).

(2) The central belt of basalts, cherts, ultramafic rocks (?) and carbonates of Mississippian, Pennsylvanian, and Permian age in the modern Intermontane Belt was an oceanic basin during the upper Paleozoic. This inference is supported by the lack (in contrast with adjacent belts) of a recognizable base to the succession, and the apparently continuous subsidence of this belt through late Paleozoic time. The presence of shallow-water carbonate seems incompatible with the requirements of isostacy if this is old oceanic crust, but it should be noted that very similar carbonate accumulations occur elsewhere in the world in close proximity to rocks of oceanic type. For example, carbonate of the Bahama Banks, believed by Dietz *et al.* (1970) to be underlain by oceanic crust, is of similar lithology and areal extent, and has formed in shallow water on a surface that has subsided for about 135 million years at an average rate of about 28 m/m yr. (Lynts, 1970). Also, Upper Triassic to Eocene shallow-water carbonate in the Alpine mountain chains of Greece, is associated with radiolarites and ophiolites, and subsided for a similar length of time at a rate of approximately 28 m/m yr. (calculated from Aubouin, 1965; Temple, 1968, Figure 5). Comparable figures for the carbonate accumulations at Locality 9 (Figure 1) are 90 million years at 22 m/m yr. Reinhardt (1969) has reported Upper Permian to Lower Jurassic shallow-water carbonates in association with ophiolites in the Oman, and suggested that these formed on an ocean ridge. Perhaps, due to some as yet unexplained cause, this type of thick relatively localized carbonate accumulation characterizes oceanic crust.

(3) The eastern belt along the Cassiar-Omineca-Columbia Mountains, is poorly known, but contains at least Permian and probably Pennsylvanian mixed volcanics, suggesting that an arc existed there at least in younger late Paleozoic time.

(4) The easternmost belt, on the east flank of the Cassian-Omineca-Columbia Mountains consists of basalt, chert and some ultramafics. These are Mississippian in the south and Mississippian and younger in the north. They overlie a thick clastic sequence, that in turn lies on older shelf deposits. J. Dercourt (pers. comm.) has suggested that these rocks may be allochthonous and have overridden an eastward continental plate, in a situation somewhat analogous to that in Papua described by Davies (1968).

These data can be used to construct various plate tectonic models (e.g. Monger and Ross, in press) that will not be discussed here except to say that if the rules are followed the conclusion seems inescapable that the Coast Range, Insular, and Intermontane Belts are allochthonous with respect to the continent. The available information has been exploited to a maximum in the present paper, and before these models can be more than speculative, far more basic data is needed, along the following lines:

(a) Detailed stratigraphic studies of all upper Paleozoic localities are fundamental for any future work.
(b) Arising from the above, a knowledge of the composition of dated volcanic rocks is basic to any understanding of plate tectonics and can be used to interpret the polarity of the arcs (*see* Dickinson and Hatherton, 1967) and thus restrict the number of possible models.
(c) Detailed work on ultramafic bodies and their surrounding rocks to see if any "classical ophiolite" complexes are, in fact, present in the Cordillera.
(d) Detailed paleontological studies may be able to suggest, but will probably not confirm, some upper Paleozoic paleogeographic patterns.
(e) Finally, upper Paleozoic rocks should be tested for their suitability for paleomagnetic studies. Most of these rocks appear too metamorphosed and complexly deformed for this to be of much value, but so far no systematic testing has been carried out.

References

Aitken, J.D. 1959. Atlin map-area, British Columbia. *Geol. Surv. Can.* Mem. 307.

Aubouin, J. 1965. Geosynclines. Elsevier Pub. Co., Amsterdam-London-New York.

Brew, D.A., R.A. Loney, and L.J.P. Muffler. 1966. Tectonic history of southeastern Alaska. In *Can. Inst. Min. Met.*, Spec. Vol. 8, 149-170.

Buddington, A.F. and T. Chapin. 1929. Geology and mineral deposits of southeastern Alaska. *U.S. Geol. Surv.* Bull. 800.

Davies, H.L. 1968. Papuan ultramafic belt. Rept. *23rd Int. Geol. Congress*, Sect. 1, 209-220.

Dickinson, W.R. and T. Hatherton. 1967. Andesitic volcanism and seismicity around the Pacific. *Science*, Vol. 157, 801-803.

Dietz, R.S., J.C. Holden, and W.C. Sproll. 1970. Geotectonic evolution and subsidence of Bahama Platform. *Geol. Soc. Amer. Bull.*, Vol. 81, 1915-1928.

Gabrielse, H. 1963. McDame map-area, Cassiar District, British Columbia. *Geol. Surv. Can.* Mem. 319.

Hamilton, W. 1969. Mesozoic California and the underflow of Pacific mantle. *Geol. Soc. Amer. Bull.*, Vol. 80, 2409-2430.

Leech, G.B. 1953. Geology and mineral deposits of the Shulaps Range. *B.C. Dept. Mines and Petrol. Res.* Bull. 32.

Link, P.K. 1965. Stratigraphy of the Mount White - eastern Atlin Lake area, Yukon Territory. Unpub. Ph. D. thesis, Univ. Wisconsin.

Lord, C.S. 1948. McConnell Creek map-area, Cassiar District, British Columbia. *Geol. Surv. Can.* Mem. 251.

Lynts, G.W. 1970. Conceptual model of the Bahamian Platform for the last 135 million years. *Nature*, Vol. 225, 1226-1228.

Monger, J.W.H. 1969. Stratigraphy and structure of upper Paleozoic rocks, northeast Dease Lake map-area, British Columbia (104J). *Geol. Surv. Can.* Paper 68-48.

——— 1970a. Hope map-area, west half, British Columbia. *Geol. Surv. Can.* Paper 69-47.

——— 1970b. Upper Paleozoic rocks of Stikine Arch, British Columbia. In Report of Activities, *Geol. Surv. Can.* Paper 70-1, 41-43.

Monger, J.W.H. and C.A. Ross. Distribution of fusulinaceans in the western Canadian Cordillera. *Can. J. Earth Sci.* (in press).

Muller, J.E. 1967. Kluane Lake map-area, Yukon Territory. *Geol. Surv. Can.* Mem. 340.

Reinhardt, B.M., 1969. On the genesis and emplacement of ophiolites in the Oman Mountains geosyncline, *Schweiz. Min. Pet. Mitt.* Vol. 49, 1-30.

Seki, Y. 1969. Facies series in low-grade metamorphism. *J. Geol. Soc. Japan,* Vol. 75, 255-266.

Sutherland Brown, A. 1957. Geology of the Antler Creek area, Cariboo District, British Columbia. *B.C. Dept. Mines and Petrol. Res.* Bull. 38.

Temple, P.G. 1968. Mechanics of large-scale gravity sliding in the Greek Peloponnesos. *Geol. Soc. Amer. Bull.,* Vol. 79, 687-700.

No. 5

ophiolites of southern quebec*

R.Y. LAMARCHE
Department of Natural Resources
Quebec City, Quebec

Abstract. The Eastern Townships ultramafics of southern Quebec are of great economic importance, for they host numerous chromite occurrences and all of the asbestos deposits exploited in the Asbestos and the Thetford-Black Lake areas.

Preliminary results from a systematic field study recently conducted by the writer in the Thetford-Black Lake area suggest close spatial, temporal, and genetic associations of the ultramafics (mainly peridotite, pyroxenite, and dunite) with one another and with other coarse-grained igneous rocks of gabbroic, dioritic, syenitic, and granitic compositions, as well as with mafic to intermediate massive, pillowed, and fragmental volcanics. Hence, all these igneous rocks are interpreted as being part of so-called alpine-type ultramafic complexes, herein referred to as ophiolitic complexes or simply as ophiolites.

The ophiolites of southern Quebec are interpreted as being Lower Ordovician in age, for they occupy a constant stratigraphic position between the Caldwell group of Lower Ordovician or older age, on which they rest unconformably, and the St. Daniel wildflysch-type sediments of pre-Normanskill age.

Field evidence suggests that these ophiolitic complexes were extruded on a eugeosynclinal ocean floor, through a major zone of distensional fractures running along the northwestern margin of the complexes, as testified locally by a wide zone of amphibolitized Caldwell metagreywackes.

Natural features strongly suggest that liquid immiscibility is the sole process responsible for the magmatic differentiation that took place under a self formed roof of mafic volcanics in the submarine ophiolites of southern Quebec. Podiform chromites are hence interpreted as primary features resulting from the coalescent growth of chromite-rich immiscible liquid droplets in an ultramafic melt.

Introduction

Most previous workers interpreted the phanerites (coarse-grained igneous rocks) of the ophiolites of southern Quebec (Figure 1) as intrusive into the mafic to intermediate volcanics**, near the contact between what are herein considered the Caldwell metasediments and the St. Daniel wildflysch-type sediments (Adams, 1880-81-82; Ells, 1887; Dresser, 1913; Harvie, in Knox, 1916; Cooke, 1937; Riordon, 1954; and St. Julien, 1965). Of these, Dresser was the first to venture farther into the genesis of these phanerites by suggesting that the pyroxenites, gabbros, and granites of the Thetford-Black Lake district were derived, through gravitative differentiation after intrusion, from the same magma as that which gave rise to the serpentinized ultramafics. Likewise, most writers succeeding Dresser have considered at least some of the coarse-grained igneous rocks of the district, and especially those of mafic and ultramafic compositions, as being comagmatic intrusives.

The interpretation proposed by the writer differs from those offered previously in that all of the spatially and temporally related ultramafic to felsic phanerites and the mafic to intermediate aphanerites (fine-grained igneous rocks) of southern Quebec are interpreted as comagmatic differentiates within ophiolitic complexes. These complexes are believed to have been extruded on a eugeosynclinal ocean floor during the Lower Ordovician epoch; thereby reviving, but in a modified form (Figure 2), Brunn's (1956, 1960) and Aubouin's (1959, 1965) classic hypothesis of ophiolite genesis, which has been rather unpopular in recent years.

Distribution

All of the ophiolitic complexes of southern Quebec lie within the Serpentine tectonic belt, east of the axis of the Green Mountain-Sutton Mountain anticlinorium (also known as the Sutton-Bennett belt in Quebec) and west of the Stoke Mountain anticlinal track (Cady, 1969). From the St. Magloire area (Béland, 1957), some 50 miles east-southeast of Quebec City, they extend southwestward for 175 miles, through the Thetford-Black Lake, Asbestos, and Orford areas, entering Vermont just west of Lake Memphremagog (Figure 1).

Several small, sill-like, masses of serpentinized (and locally carbonatized) peridotite, apparently intrusive in nature, are also found at various levels within the highly schistose rocks of the Sutton-Bennett belt. The most prominent of these is the Pennington sill, just north of Thetford Mines (not shown on Figure 1). The relationship between these ultramafic masses emplaced in the Sutton-Bennett schists and the main ophiolitic complexes is still unclear.

General lithology and contact relations

The various lithological units present in the ophiolites of southern Quebec are: spilitized mafic to intermediate volcanics (fragmental, pillowed, and massive), serpentinized dunite and peridotite (mainly harzburgite) with local chromitite concentrations, pyroxenite, doleritic and gabbroic rocks, diorite, syenite, and granitic rocks. Some pyroxenites, gabbros, and diorites have locally suffered various degrees of rodingitization (Marshall, 1911; Grange, 1927).

The lower volcanic member of the ophiolites rests unconformably on schistose and folded eugeosynclinal metasedimentary rocks of the Caldwell group and are locally separated from them by interformational pelitic or cherty sedimentary rocks which are also typical of a eugeosynclinal environment (Figure 2).

The peripheral volcanics (including the lower volcanic member) of these ophiolites grade inward from a pillowed

---

*Published with the permission of the Deputy Minister, Department of Natural Resources, Quebec.

**Considered by Cooke (1937) and Riordon (1954) as part of the Caldwell group or series and by St. Julien (1965) as part of the Caldwell group and part of the St. Daniel formation.

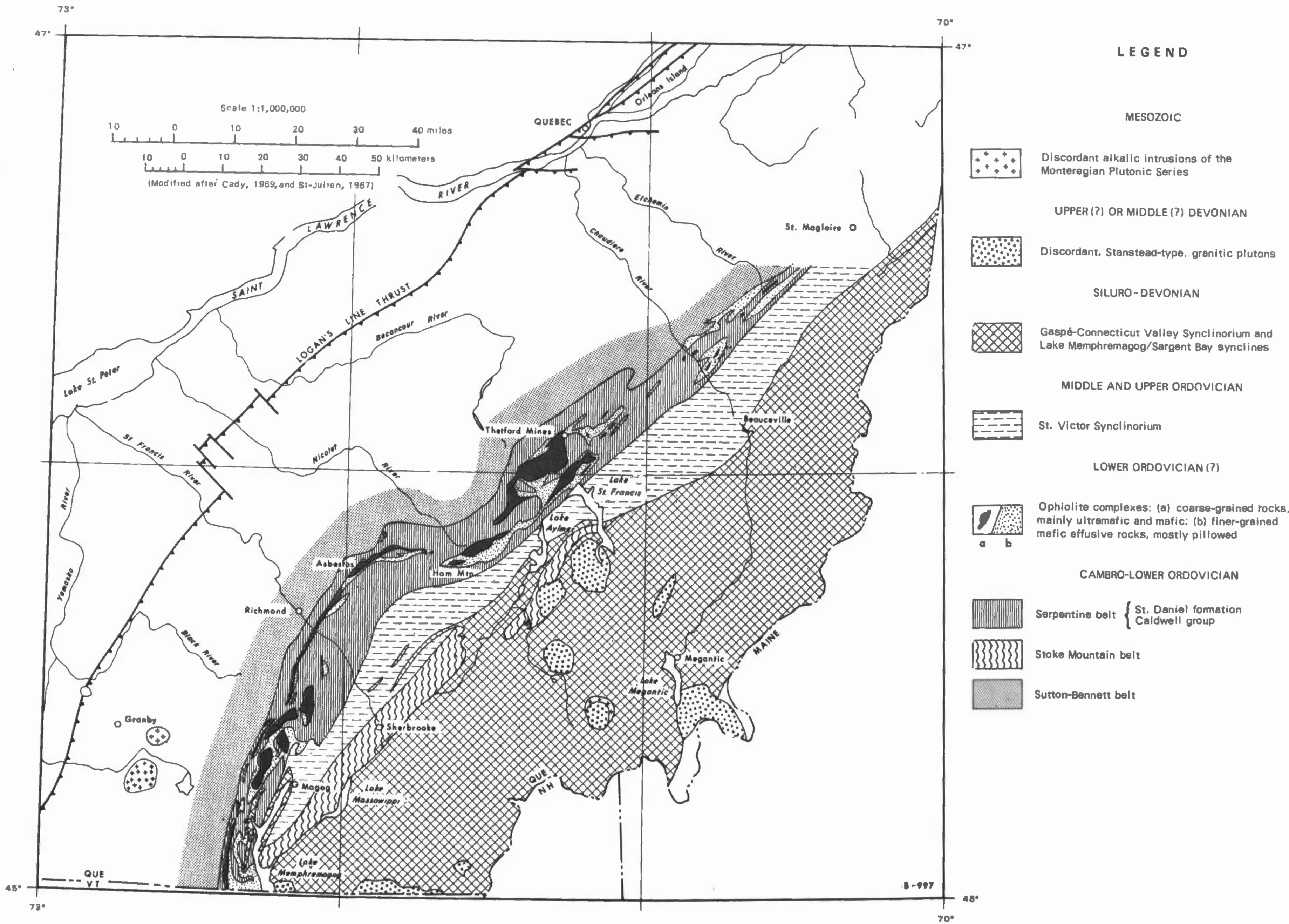

Figure 1. Tectonic map of the Appalachian region of southern Quebec, showing alpine-type ophiolite complexes.

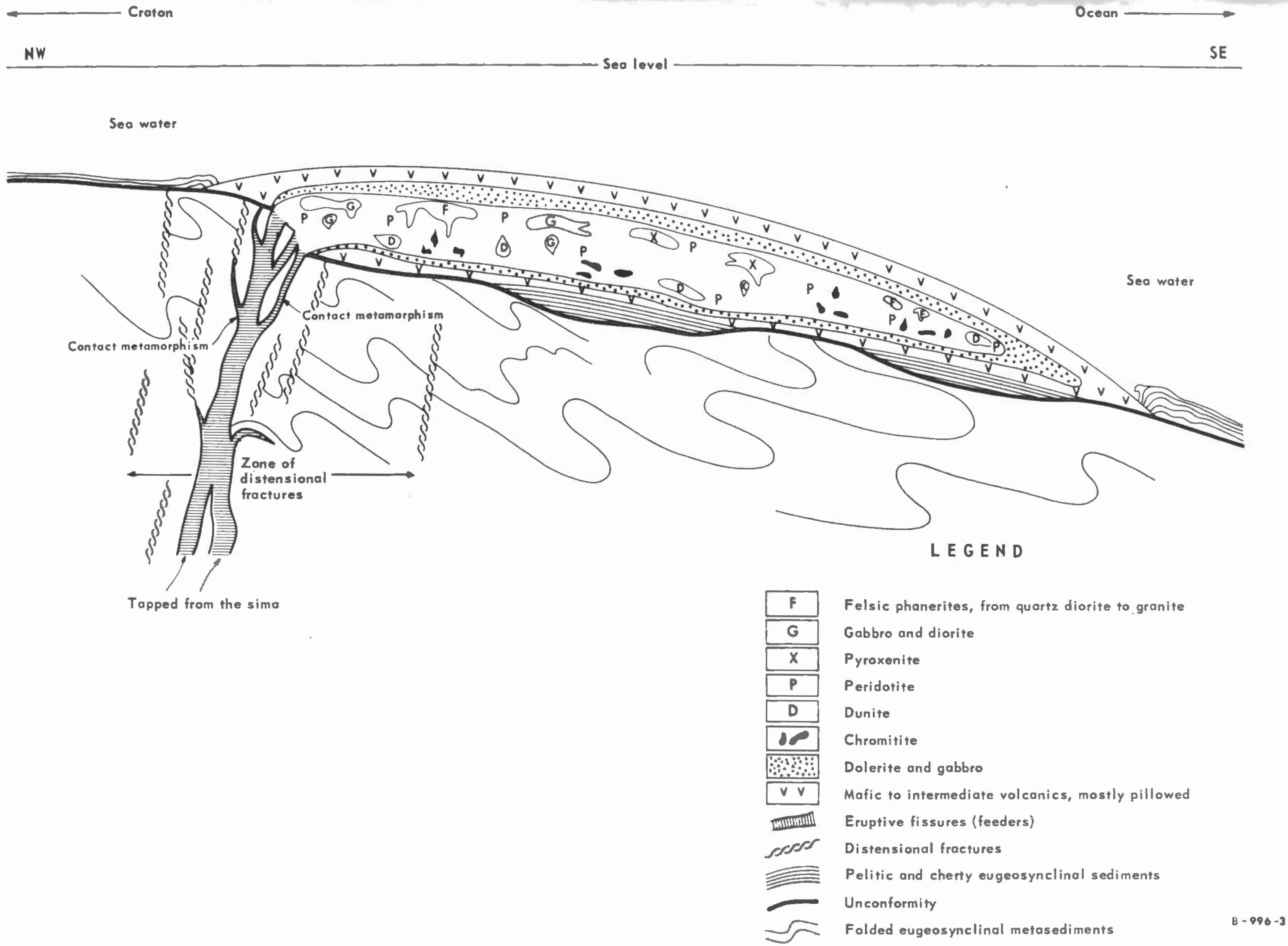

Figure 2. Synoptic cross-section of the Thetford-Ham submarine ophiolite flow, showing irregular globules of the various rock types, differentiated through liquid immiscibility (modified after Aubouin, 1959, fig. 17). The size of most globules has been exaggerated, due to the scale of the section. Original NW-SE width of this flow may have exceeded 20 km.

or agglomeratic facies to more massive and somewhat coarser-grained doleritic and gabbroic rocks. Locally, phanerites from within the complexes were brought in direct and cold contact with the adjacent metasedimentary rocks through overthrust or underthrust faulting, especially along the well lubricated serpentinized ultramafics, close to the northwestern margin of the complexes.

Intrusive contacts showing remarkable metamorphic effects grading from the greenschist to the garnet-amphibolite facies were observed locally, but only where ultramafic feeders or apophyses from the main feeders are in contact with rocks of the underlying Caldwell. This contact metamorphism is nowhere found in any of the surrounding volcanics, however.

The ultramafic to felsic phanerites are texturally either massive or layered and show local brecciation. As is generally the case in ophiolitic complexes the world over (Thayer, 1967), phanerites of various compositions are disposed in a rather chaotic way, without showing the cumulate sequence usually found in classic examples of layered intrusions such as the Skaergaard, the Stillwater, and the Bushveld (Wager and Brown, 1968).

Furthermore, even though most contacts between any two phanerites are sharp, they are far from being geometrically simple. Indeed they show complicated contact relations, with numerous examples of contradicting "intertonguing" and so-called "inclusions" (e.g. "tongues" or "inclusions" of pyroxenite in peridotite and vice versa), without chilled margins or contact metamorphic effects.

Stratigraphy and age

In the Serpentine belt, the ophiolite complexes of southern Quebec occupy a constant stratigraphic position between the Lower Ordovician or older Caldwell metasediments, (on which they rest (Lamarche, 1969, in press)), and the pre-Normanskill St. Daniel wildflysch-type sediments (St. Julien, 1968). The St. Daniel is unconformably overlain by the basal beds of the Beauceville formation of the Magog group. These beds are well dated as Normanskill from their abundant graptolite fauna, particularly from the Castle Brook locality on the west side of Lake Memphremagog (Berry, 1962). The Caldwell metasediments are usually to the northwest of these ophiolites, whereas the wildflysch-type sediments lie to the southeast.

The basal part of the volcanic member of the ophiolites rests either directly over the Caldwell metasedimentary rocks, with a marked angular unconformity, or conformably on pelitic eugeosynclinal rocks* which, themselves, overlie the Caldwell unconformably (Figure 2).

Several sills, dykes, and lenticular masses of peridotite cutting through the underlying Caldwell metasedimentary rocks are believed to be subsidiary feeders or aphophyses from the main feeders to the ophiolitic complexes, for they show some evidence of contact metamorphism from a few feet to a few tens of feet and grade from the greenschist to the garnet-amphibolite facies. The contact metamorphic effects bordering the main zone of feeders along the northwestern margin of the Thetford-Ham complex, on the other hand, are visible over widths exceeding 3,000 feet and also grades inward from the greenschist to the garnet-amphibolite facies (Figure 2).

Hence, on a purely stratigraphic basis, all rocks of the ophiolitic complexes of southern Quebec are considered post Caldwell and pre-Normanskill, or, in all probability, of Lower Ordovician age. Moreover, the ± 480 m.y. K-Ar dates (Poole *et al.*, 1963) obtained on granitic rocks that are here considered as comagmatic differentiates within the Thetford-Ham ophiolitic complex are interpreted as a minimum radiometric age for the whole complex and, by correlation, for the other ophiolites of southern Quebec. This determination also points to a Lower Ordovician age, according to Kulp's (1961) and Holme's (1959) time scales.

*Mapped by Cooke (1937) as part of the Caldwell series and by Riordon (1954) as part of the Middle Ordovician Beauceville group (formation).

Origin

As reviewed by Moores (1969), four possible origins of ophiolitic complexes are worthy of consideration.

1. Giant submarine extrusions, differentiated under a self formed roof of mafic volcanics, as proposed by Brunn (1956, 1960) and Aubouin (1959, 1965), and herein modified by the writer.
2. Allochthonous sheets of oceanic crust and mantle, formed at mantle upwellings or ridges and subsequently thrust onto the continental margin (de Roever, 1956; Gass and Masson-Smith, 1963; Irwin, 1964; Hess, 1965; Davies, 1968; Church, 1969).
3. Stratified peridotite-gabbro complexes, differentiated in the mantle (Thayer, 1969) or in basic magma chambers high in the crust (McTaggart, 1971), by crystal settling from fluid magma, broken up and modified during re-emplacement as crystal mushes.
4. A partial combination of all three – an origin by partial fusion of mantle material and for its emplacement as a deforming and differentiating solid-liquid mass on the ocean floor (Hess, 1962; Ringwood, 1966; Moores, 1969).

In the light of field observations made on the ophiolitic complexes of southern Quebec and in view of the fact that the lower volcanic member of these complexes rests unconformably (Lamarche, 1969) on schistose and folded eugeosynclinal metasedimentary rocks, locally separated from them by interformational pelitic or cherty metasediments which are also typical of a eugeosynclinal environment, the writer favours the first of the four origins and therefore interprets all of the spatially and temporally related ultramafic to felsic phanerites and the mafic to intermediate volcanic aphanerites of the Serpentine belt of southern Quebec, as being comagmatic within ophiolitic complexes, believed to have been extruded as a simatic (ultramafic) fluid magma on a sialic eugeosynclinal ocean floor during the Lower Ordovician epoch (Figure 2).

Liquid immiscibility is believed to be the sole process responsible for the magmatic differentiation of the ophiolitic complexes of southern Quebec (Figure 2) for many reasons, some of which are:

1. Contacts between the various phanerites are sharp rather than gradational.
2. Lack of chilling and lack of contact metamorphism between the various phanerites.
3. Contradictory "intertonguing" and "inclusions", herein considered as embayments and globules of one liquid in another (e.g. pyroxenite in peridotite and vice versa).
4. Globules of the lighter liquid often have a tail pointing one way whereas the tails of the heavier globules point the opposite way.
5. The smaller the globules, the better the sphericity.
6. Coalescent features arrested at various stages between globules that have come in contact.

Hence, podiform, nodular, and orbicular features in chromite deposits, universally associated with ophiolitic complexes, are interpreted as primary features resulting from the coalescent growth of chromite-rich immiscible liquid droplets in an ultra-mafic melt.

Because of their great number and similarity to the ophiolites of southern Quebec, other well known ophiolitic complexes such as those of western Newfoundland, Canyon Mountain of Oregon, New Caledonia, Oman, Sesia Lanzo zone of the western Alps, Troodos of Cyprus, and Vourinos of northern Greece (regardless of their respective ages and sizes) are also believed to have been extruded as huge submarine ophiolite flows on ocean floors and to have undergone differentiation through liquid immiscibility in this relatively fast cooling submarine environment.

References

Adams, F.D. 1880-81-82. Notes on the microscopic structure of some rocks of the Quebec Group: *Geol. Surv. Can.*, Rept of Prog. 1880-81-82, Part A, 8-23.

Aubouin, J., 1959. Contribution à l'étude géologique de la Grèce septentrionale: les confins de l'Epire et de la Thessalie (1e thèse, Paris, 1958): *Ann. Géol. Pays Helléniques*, 10, 1-483.

———1965. Developments in Geosynclines: Elsevier Publishing Company, New York, 335 p.

Béland, J. 1957. St. Magloire and Rosaire-St. Pamphile areas: *Quebec Dept. Mines*, Geol. Rept. No. 76, 49 p.

Berry, W.B.N. 1962. On the Magog, Quebec, graptolites: *Amer. J. Sci*, Vol. 260, No. 2, 142-148.

Brunn, J.H. 1956. Contribution à l'étude géologique du Pinde septentrional et d'une partie de la Macédoine occidentale. *Ann. Géol. Pays Helléniques*, 7: 1-358.

———1960. Mise en place et différenciation de l'association pluto-vol-canique du cortège ophiolitique: *Rev. Géograph. Phys. Géol. Dyn*, 3 (3), 115-132.

Cady, W.M. 1969. Regional tectonic synthesis of northwestern New England and adjacent Quebec: *Geol. Soc. Amer.* Mem. 120, 181 p.

Church, W.R. 1969. Metamorphic rocks of Burlington peninsula and adjoining areas of Newfoundland, and their bearing on continental drift in North Atlantic. North Atlantic Geology and continental drift (Marshall Kay *et al.*), 212-233.

Cooke, H.C. 1937. Thetford, Disraeli and eastern half of Warwick map-areas, Quebec: *Geol. Surv. Can.* Mem. 211.

Davies, H.L. 1968. Papuan ultramafic belt: International Geological Congress, report of the twenty-third session Czechoslovakia, 1968, 209-220.

de Roever, W.P. 1956. Sind die alpinotypen Peridotit-massen vielleicht tektonisch verfrachtete Bruchstücke der Peridotitshale? : *Geol. Rundschau*, 46, 137-146.

Dresser, J.A. 1913. Preliminary report on the serpentine and associated rocks of southern Quebec: *Geol. Surv. Can.* Mem. 22.

Ells, R.W. 1887. Report on the geology of a portion of the Eastern Townships of Quebec, Counties of Compton, Stanstead, Beauce, Richmond, and Wolfe: *Geol. Surv. Can.* Ann. Rept. 170.

Gass, I.G. and Masson-Smith, D. 1963. The geology and gravity anomalies of the Troodos Massif, Cyprus: Philosoph. *Trans. Roy. Soc. London.*, Vol. 255, Ser. A, 417-467.

Grange, L.I. 1927. On the "Rodingite" of Nelson: *New Zealand Inst. Trans. and Proc.*, Vol. 58, 160-166.

Hess, H.H. 1962. History of ocean basins: *Geol. Soc. Amer.* Buddington Vol., 599-620.

———1965. Mid-oceanic ridges and tectonics of the sea floor; submarine geology and geophysics: *Proc. Seventeenth Symp. Colston Res. Soc.*, Butterworths, London, 317-334.

Holmes, A. 1959. A revised geological time scale: *Edinburgh Geol. Soc. Trans.*, Vol. 17, Part 3, 183-216.

Irwin, W.P. 1964. Late Mesozoic orogenies in the ultramafic belts of northwestern California and southwestern Oregon: *U.S. Geol. Survey*, Prof. Paper, 501-C, C1-C9.

Knox, J.K. 1916. Southwestern part of Thetford-Black Lake mining district: *Geol. Surv. Can.*, Sum. Rept., 229-245.

Kulp, J.L. 1961. Geological time scale: *Science*, Vol. 133, No. 3459, 1105-1114.

Lamarche, R.Y. 1969. Evidence of a Cambrian orogeny in the Disraeli area, Eastern Townships, Quebec [abs.]: *Geol. Assoc. Can.* Ann. Meeting, 1969, Montreal, p. 26.

Marshall, P. in Bell, J.M., Clarke, E. de C., and Marshall, P., 1911. The geology of the Dun Mountain subdivision, Nelson. *New Zealand Geol. Surv.* Bull. 12, 29-40.

McTaggart, K.C. 1971. On the origin of ultramafic rocks: *Geol. Soc. Amer.* Bull., Vol. 82, 23-42.

Moores, E.M. 1969. Petrology and structure of the Vourinos ophiolitic complex of Northern Greece: *Geol. Soc. Amer.* Spec. Paper No. 118, 74 p.

Poole, W.H., J.R. Béland, and R.K. Wanless 1963. Minimum age of Middle Ordovician rocks in southern Quebec: *Geol. Soc. Amer.* Bull., Vol. 74, No. 8, 1063-1065.

Ringwood, A.E. 1966. Mineralogy of the mantle: in Hurley, P.M., ed., Advances in Earth Science, 357-399. The M.I.T. Press, Cambridge, Mass.

Riordon, P.H. 1954. Premilinary report on Thetford Mines-Black Lake area, Frontenac, Megantic, and Wolfe Counties [Quebec]: *Quebec Dept. Mines*, Prelim. Rept. 295.

St. Julien, P. 1965. Régions de St-Victor et de Thetford Mines (Moitié est), comtés de Beauce, Frontenac et Mégantic: Unpublished Geol. Rept., *Quebec Dept. Nat. Resources*.

———1967. Tectonics of part of the Appalachian region of southeastern Quebec (southwest of the Chaudière River): *Royal Soc. Can.*, Spec. Pub. 10, 41-47.

———1968. Les "argiles-à-blocs" du sud-ouest des Applaches du Québec: *Naturaliste can*, Vol. 95, No. 6, 1345-1356.

Thayer, T.P. 1967. Chemical and structural relations of ultramafic and feldspathic rocks in Alpine intrusive complexes: In Ultramafic and related rocks, P.J. Wyllie (editor), Wiley and Sons Inc., New York, 222-239.

———1969. Alpine-type sensu strictu (ophiolitic) peridotites: Refractory residues from partial melting or igneous sediments? A contribution to the discussion of the paper: "The origin of ultramafic and ultrabasic rocks" by P.J. Wyllie: Tectonophysics – Elsevier Publishing Co., Amsterdam, 7(5-6), 511-516.

Wager, L.R. and Brown, G.N. 1968. Layered igneous rocks: Oliver and Boyd, Edinburgh and London, 588 p.

ophiolite: its definition, origin as oceanic crust, and mode of emplacement in orogenic belts, with special reference to the appalachians

No. 6

W.R. CHURCH
Department of Geology
University of Western Ontario
London, Ontario

Abstract. Alpine-type ophiolites are allochthonous stratiform complexes composed of complete or partial sequences of peridotite, pyroxenite-troctolite-gabbro, 'sheeted diabase', and pillow lava. Such sequences are probably generated at 'oceanic' ridges. The peridotite component of ophiolite is a cumulate derived from an ultramafic liquid which crystallized at some depth within the mantle, whereas the gabbros and associated pyroxenites and troctolites are cumulates formed at a relatively high level in fissures below ridges. The peridotites were deformed during their emplacement as solid material and have nonconformable contacts with the overlying gabbro cumulates.

Alpine ophiolites are also characterized by the presence, when preserved, of basal contact aureoles of pyroxene-garnet-amphibole-plagioclase granofels and amphibolite. In contrast ophiolites of the Circum-Pacific region are underlain by blueschist metamorphic rocks. The time span between the origin of ophiolite at an oceanic ridge and its emplacement as an allochthonous sheet may be quite short, and some ophiolites may have been directly emplaced over their adjacent continental margins as thick sheets of 'hot', yet crystalline, oceanic lithosphere.

The Appalachian geosyncline was initiated on a Precambrian sialic crust. Oceanic crust of the northern Appalachians may not have appeared as a significant component of the geosyncline until early Ordovician time. There is no evidence to suggest that the ocean basin ever achieved the dimensions of the present Atlantic or Pacific. In the southern Appalachians, where alpine-type ophiolites appear to be absent, crustal distension during the early Phanerozic may have been too limited to allow the development of recognizable oceanic crust. The appearance in the northern Appalachians of ophiolites during the early Ordovician may reflect a stage in the evolutionary change from Precambrian-type tectonism to that associated with the large-scale plate motions characterizing the late Phanerozoic.

It is the purpose of this paper to outline the origin and subsequent use of the term "ophiolite", and the several theories pertaining to the origin of rocks denoted by this term; secondly, to show that the ultramafic-mafic associations of the Newfoundland Appalachians and possibly also those of Quebec and Maine are comparable to ophiolites of the Alpine fold belt, and that the Appalachian system is therefore an alpine-type rather than cordilleran-type mountain chain; thirdly, to point out that, of the various ultramafic-mafic complexes referred to as alpine-type, those resembling true Alpine ophiolites are most likely to represent complete sections of oceanic lithosphere; and fourthly, to suggest that some ophiolite complexes may have been emplaced during periods of ocean formation rather than ocean closure.

Definition and origin of the term "ophiolite"

Steinmann (1905, 1927) in describing the ophiolite zone of the Mediterranean Mountain Chain states (1927, p. 637) that "as ophiolite one should designate only the consanguineous association of chiefly ultrabasic rocks, the most important component of which consists of peridotite (serpentinite) the more subordinate of gabbro, diabase, spilite or norite and related rocks". Steinmann pointed out that the peridotite (serpentinite) gabbro, diabase-spilite members of the ophiolites were ordered in stratigraphic sequences in which the peridotite was always the lowermost member.

Benson (1926, pp. 6, 68) referred to the ophiolites as "Green Rocks of the Alpine Type" noting that their special character lay in the intimate association of coarse-grained peridotite and gabbro, clearly *plutonic* in nature, with finer-grained diabase, spilite, and pillow lava. On this basis they were to be distinguished from another group of more or less stratiform or sill-like masses of peridotite and gabrro which he referred to as 'sill-and-batholith' or 'cordilleran type' complexes. These rocks were considered by Benson to represent parts of differentiated mafic intrusives that had been separated during periods of 'great lateral pressure' (cf. Bowen, 1920, 1927; McTaggart, 1971), and which were invaded subsequently by less regular batholiths of diorite and granite. Cordilleran-type complexes include ultramafic and mafic rocks of the Ivrea zone the Harz Mountains, the Highlands of Scotland, and, apparently (Benson, 1926, p. 76) the Great Serpentine Belt of New South Wales. Such complexes have also been referred to as orogenic or orogenotype (cf. Green, 1964, p. 185; Den Tex, 1965, 1969; Rost, 1968; Forestier, 1968).

It is suggested that use of the term "ophiolite" should be restricted to those ultramafic-mafic sequences which are comparable in petrography and structure to the Mesozoic layered plutonic-effusive rock associations of the Mediterranean Alpine system (cf. Vuagnat, 1968). The term should not be used for such patently intrusive ultramafic sheets or diapirs as those of the Lizard (Green, 1964) Beni Bouchera (Kornprobst, 1969) Lherz (Ravier, 1959) La Ronda (Hernadez-Pacheco, 1967) Tinaquillo (MacKenzie, 1960) the Caribbean (Bowin, 1966; Kozary, 1968) Japan (Igi, 1953; Yoshino, 1961, 1964; Myashiro, 1966) Dun Mountain-Red Hills (Challis, 1965, 1969; Challis and Lauder, 1966) Darvel Bay (Hutchison and Dhonau, 1969) Blue River (Wolfe, 1965) and California (Ragan, 1963; Raleigh, 1965; Irwin, 1964).

Theories of the origin of ophiolite

Early theories

Most theories are based on either an affirmation or denial of the consanguinity of the plutonic and effusive components of ophiolite. The simplest explanation for their origin was advanced by Steinmann (1927) who considered all the components of ophiolite, including pillow lava, to have crystallized from ophiolite magma intruded into a thick section of Mesozoic deep-sea sediments. He proposed that ophiolites represent abyssal-type mafic magmatism as opposed to hyperbyssal magmatism represented by spilitic rocks (also considered by Steinmann to be intrusive) and neritic-type magmatism represented by effusive rocks such as the volcanic rocks of the Andes (cf. Rocci and Juteau, 1968) . In opposition to Steinmann, Suess (1909) considered the ophiolites to have been intruded during Tertiary main-phase orogenic movements. Benson (1926) supported the views of Suess. He attempted to reconcile the association of plutonic and effusive rocks in ophiolites, and also explain their location within fold belts, by suggesting that "basic magma rising along a plane of shearing (is) pressed out at the surface in front of an advancing overthrust anticline or crust flake, and may consolidate in the form of volcanic rocks, ... (which) may be overridden by the advancing sheet; the magma passing along the thrust plane may now be injected into the previously formed volcanic rocks, thus (forming) a plutonic series of intrusions". It has now been established however (Gannser, 1959; Trumpy, 1960; Karamata, 1970; Abbate *et al.*, 1970) that the ophiolites of the Mediterranean Alpine system were emplaced relatively early in the Alpine tectonic cycle; much earlier than the main orogenic movements of Tertiary age. Consequently the association of plutonic and effusive rocks in ophiolites has remained an enigmatic and unsolved problem (Anonymous, 1968, 1969; Wyllie, 1967).

Current theories

The main hypotheses for the origin of ophiolite are those of:

(1) Routhier (1946, 1953) Bailey and McCallien (1953) Brunn (1954, 1960) Dubertret (1955) Borchert (1961) (Aubouin, 1964) and Lamarche (1971) who consider ophiolites to be products of gravitational differentiation within a large submarine mafic lava flow.

(2) Maxwell (1969) who states that Alpine ophiolites perhaps resulted from diapiric up-welling and partial melting of mantle material during an early, possibly tensile, stage in the Alpine orogenic cycle; lavas were extruded into deep troughs and residual ultramafic rocks, perhaps lubricated by intragranular melt, moved plastically beneath the volcanic carapace. The resulting ophiolite complex is thus a composite subsea laccolith.

(3) Moores (1969) who suggested that ophiolite complexes may represent the closest existing approach to ultramafic extrusives, and may originate by partial fusion of mantle material and its emplacement as a deforming and differentiating solid-liquid mass on the ocean floor.

(4) Peters (1969) Decandia and Elter (1969) Abbate *et al.* (1970) Bortolami and Dal Piaz (1970) and Bezzi and Piccardo (1971) who consider ophiolites of the Alpine region to be allochthonous fragments of an "ophiolitic window" formed during attenuation and disruption of continental crust. The ophiolites are therefore composed of mantle and lower crust and were emplaced during reconvergence of the separated crustal blocks. Avariation of this view is given by Hsu (1970) for the Jurassic ophiolites of the Franciscan of California.

(5) Dietz (1963) Hess (1964) Gass (1968) Laubscher (1969) Reinhardt (1969) who have suggested that Alpine ophiolites may represent allochthonous fragments of oceanic floor emplaced, according to Hess and Reinhardt, by gravity sliding from a mid-ocean ridge. As a variant of this hypothesis, and of hypothesis (4) Church and Stevens (1970(a) and (b), 1971) put forward the possibility that some ophiolites of the Appalachians, although formed at a 'mid-ocean' ridge in the manner suggested by Reinhardt, may have been emplaced as 'hot' layered complexes directly over sialic crust at the time of inception of an oceanic ridge within a continental plate during the development of an intrasialic small ocean basin (cf. Church, 1971).

(6) Davies (1968) Dewey and Bird (1970) Hamilton (1969) Moores (1970) Stevens (1970) Coleman (1971) Dickinson (1971) propose that ophiolites are overthrust segments of 'cold' oceanic lithosphere emplaced as a result of continent-ocean collision.

Hypotheses (4), (5) and (6) are in agreement in interpreting ophiolite as oceanic lithosphere, but differ with respect to the relative age and manner of ophiolite emplacement within eugeosynclinal sequences. Opinions also vary concerning the mechanism by which the gross compositional layering of ophiolites is produced. Gass (1968) postulates that the Troodos ophiolite complex of Cyprus represents oceanic lithosphere formed at a mid-ocean ridge by fusion of the upper mantle. Melting of the upper mantle was sufficient to allow gravity fractionation at depth, thus producing the gross compositional layering of the oceanic crust, and provision of a liquid phase to be injected as dykes and poured out as lava flows. Reinhardt (1969) however considers ophiolite to be a polygenetic assemblage, the peridotitic component of which may have formed in an independent, highly contrasted environment to that of the gabbro, diabase and spilite. The peridotite component of ophiolite was, according to Reinhardt (1969, p. 26), formed deep within the mantle and brought to near surface by mantle convection cells, whereas the gabbro, diabase and spilite components of ophiolite crystallized from basaltic magma at different levels in the fissures below oceanic ridges. Maxwell's hypothesis, although an attractive one, does not explain the formation of 'sheeted diabase' units (cf. Reinhardt, 1969), such as those of the Oman, Troodos, and Appalachian ophiolites, as well as does the 'oceanic lithosphere' hypothesis as illustrated by Reinhardt (1969, fig. 17). On the other hand the presence of a basal high-temperature contact aureole in some ophiolite complexes (Karamata, 1968; Bilgrami, 1963; Ricou, 1971; Church and Stevens, 1971) is a feature which is not in accord with their interpretation as 'cold' sheets of oceanic lithosphere.

Ultramafic-mafic associations of the Appalachians

Distribution

The first comprehensive description of the belt of ultramafic intrusions extending the length of the Appalachians was given by Pratt and Lewis (1905) who considered that "the principal period of intrusion was closely associated with the great orogenic movements of the revolution at the close of the Ordovician period .... The late Appalachian disturbance at the close of the Carboniferous would account for the widespread lamination developed in the peridotites," (quoted by Benson, 1926, p. 56). This view of the ultramafic rocks as synorogenic intrusives was echoed by Hess who showed the Appalachian ultramafic rocks distributed in two belts which he considered to define the axis of the Appalachian system. It is now known however that in the Newfoundland Appalachians there are four belts of ultramafic rocks (Figure 1): the Bay of Islands-Hare Bay belt; the Baie Verte belt; the Betts Cove belt; and the Gander Lake belt. The first three ultramafic occurrences are formed of layered ultramafic-gabbro-diabase-spilite sequences which are structurally and petrographically identical to Mesozoic Alpine ophiolite complexes (Church and Stevens, 1970, 1971).

The Gander Lake belt, along with other minor occurrences of ultramafic rock in the Central Mobile belt of the Newfoundland Appalachians, represent cordilleran-type ultramafic-mafic rocks related to Acadian (mid-Devonian) igneous and tectonic activity (cf. Chapman, 1968).

Extrapolation of major tectonic structures of the Newfoundland Appalachians to the southwest (Figure 1) suggests that the Baie Verte and Betts Cove ophiolite belts of Newfoundland may be lateral equivalents of the ultramafic-mafic complexes of the Eastern Townships of Quebec and the Chain Lakes region of southwestern Maine, respectively (Boudette, 1970). In each case the ophiolite sequence overlies deformed and metamorphosed rocks of Late Proterozoic to Cambrian age—the Fleur de Lys of Newfoundland, the Sutton-Bennet-Caldwell Schists of Quebec, and metamorphic rocks of the Chain Lakes Massif of southwest Maine (Figure 1). In the British Caledonides, the equivalents of the Baie Verte and Betts Cove ophiolite belts would be those of the Highland Boundary fault zone and the Ballantrae complex of the Girvan region of Scotland, respectively (Church, 1969, fig. 12; Church and Stevens, 1970(b)). The above correlations are supported by the existence of a belt of pre-ophiolite basalt-rhyolite-porphyry volcanic rocks (Paquet Harbour-Grand Cove-Cape St. John volcanic groups of Newfoundland, and the Stoke Mountain belt of Quebec) between both the Baie Verte-Betts Cove ophiolites and the Eastern Townships-Chain Lakes ophiolites. In both regions the volcanic rocks are the loci of Cu-Zn mineralization typified by deposits of the Eustis Mine of the Eastern Townships and the Rambler Mine of the Burlington Peninsula, Newfoundland. As a point of metallogenic interest it may therefore be noted that in the Appalachians ophiolites do not represent the earliest phase of volcanic activity associated with base metal mineralization (cf. Hutchinson *et al.*, 1971).

Pre-ophiolite ultramafic rocks of the Appalachians

Ultramafic bodies occurring within the Cambro-Ordovician (?) rocks of Vermont (Chidester, 1968) and areas to the south (Piedmont ultramafics) may represent parts of ophiolites dismembered and reintruded during the Acadian orogeny, or, alternatively and more likely, cordilleran-type ultramafic rocks introduced directly as solids or crystal mushes from a deep crustal or mantle source. Such an origin seems most plausible for the clearly sheet-like ultramafic rocks intrusive into the Caldwell formation west of the Thetford Mines area. Such rocks also form part of the pre-ophiolite Fleur de Lys metamorphic complex of the Burlington Peninsula, Newfoundland (Church, 1969) and of the mid-Cambrian metamorphic rocks of the northern part of the Piedmont zone of the southern Appalachians (Southwick, 1970). The complexity of the ultramafic associations of the Eastern Townships region may therefore be the result of the presence of both ophiolitic and cordilleran-type ultramafic-mafic complexes (cf. Lamarche, this volume) as in New Caledonia (Routhier, 1953; Avias, 1967; Guillon, 1969).

Post-ophiolite flysch and calc-alkaline volcanism

The ophiolite sequence of the Eastern Townships of Quebec is overlain by a flysch sequence which includes olistostrome units (St. Daniel 'argilles à blocs', St. Julien, 1968). Analogous rocks to the diatostromes may be represented in the Baie Verte ophiolite belt of Newfoundland by a black-slate conglomerate (containing granodiorite and peridotite debris) which overlies pillow lavas of the Baie Verte ophiolite. The ophiolites of the Betts Cove-Chain Lakes belt are overlain by greywackes (containing chromite), slates, and volcanic rocks (pyroxene and amphibole andesites; keratophyres) indicative of post-ophiolite calc-alkaline volcanic activity (Snooks Arm Group and parts of the Lushs Bight Group of the Notre Dame Bay region of Newfoundland; unnamed formations and Ammonoosac volcanic rocks of Maine and New Hampshire, Boudette, 1970).

Ophiolites of the Newfoundland Appalachians

A composite section of the Newfoundland ophiolites of the Bay of Islands, Baie Verte, and Betts Cove regions is shown in Figure 2. The ophiolites are characterized by the following features:

(1) they are thick (c. 7-10 km), (Smith, 1958, p. 78) stratiform bodies composed of a lower unit of ultramafic tectonites overlain by pyroxenite-gabbro or dunite-troctolite-gabbro cumulate sequences, 'sheeted diabase' units, and pillow lavas. On a gross scale the sequences are comparable to ophiolite complexes of the Alpine system (cf. Reinhardt, 1969; Bezzi and Piccardo, 1971).

(2) the presence of ultramafic debris in dated underlying and overlying flysch sediments shows that the ophiolites were emplaced prior to mid-Arenigian (early Ordovician) time, but after the late Cambrian (?) metamorphism of the underlying Fleur de Lys metasediments (Church, 1969; Stevens *et al.*, 1969; Stevens, 1970; Church and Stevens, 1971). The ophiolites were therefore not intruded during the mid-late Ordovician Taconic orogeny, and in common with the Mesozoic Alpine ophiolites their emplacement is demonstrably not 'syntectonic'.

(3) where the lower contact of the ophiolites are exposed a high-temperature contact aureole may be observed (Smith, 1958). At Trout River in the Bay of Islands the contact aureole immediately adjacent to the peridotite is composed of a pyroxene-garnet-amphibole-plagioclase-ilmenite granofels. The contact aureole is superposed on mafic schists with a pre-existing regional metamorphic fabric. The thickness (less than one metre) and distribution of the garnet-pyrabole relative to the base of the ophiolite makes it clear that the aureole was formed by contact metamorphism induced by emplacement of a high-temperature solid. In the Hare Bay region garnets in the contact aureole are helicitic and contain relicts of the earlier regional polymetamorphic fabric.

(4) high-pressure mineral assemblages have been recorded in the basal part of the lherzolitic member (Figure 2, zone B) of the peridotite at Trout River (Church and Stevens, 1971, fig. 2) indicating that at least part of the peridotite crystallized at depth within the mantle.

Mineral assemblages include:

(a) olivine-orthopyroxene-clinopyroxene-spinel.
(lherzolite spec. Tr6932) Al_2O_3 in spinel c. 45 weight per cent; Al_2O_3 in clinopyroxene c. 5 weight per cent.

(b) clinopyroxene-orthopyroxene-spinel.
(normal ariegite spec. Tr6932)

(c) olivine (Fa_{25})-kaersutite-orthopyroxene-clinopyroxene-ceylonite.
(kaersutite-lherzolite spec. Tr6813)

(d) kaersutite-clinopyroxene (c. 8 weight per cent Al_2O_3) – garnet (FeO/MgO mole ratio – 1.0; CaO weight per cent – 5.5) – ceylonite.
(garnetiferous amphibole ariegite spec. Tr6813)

(e) kaersutite – Ti-phlogopite (TiO_2 weight per cent – c. 5)
(lherzolite spec. Tr6920)

Mineralogically and chemically the ariegites at Trout River are comparable to the kaersutite-bearing ariegites occurring as dykes and veins in the lherzolite of the type locality at Lherz in the French Pyrénées (Ravier, 1959, 1964; Church, 1966, 1968; Avé Lallemant, 1967; Conquéré, 1971). Of particular interest is the occurrence in the Trout River ariegites of grass-green spinel (ceylonite) with rims of garnet, a texture which is particularly characteristic of the ariegites at Lherz (Church, 1966, 1968, p. 784) and also of some garnet-ariegites occurring as inclusions in basalts of Hawaii (Jackson and Wright, 1970, p. 417). Garnet-ariegites also occur in association with ultramafic rocks of the Ballantrae ophiolite at Girvan, Scotland. The latter occupies a structural position analogous to the Betts Cove complex of Newfoundland. The ariegites are NOT eclogites and are in no way related to the post-ophiolite blueschist metamorphism of the Cirvan area (Bloxam and Allen, 1959).

(5) podiform chromite associated with clinopyroxenite occurs towards the top of the peridotite of the Bay of Islands ophiolite. At Blow Me Down Mountain chromite is relatively rich in alumina (Al_2O_3/Cr_2O_3 weight ratio – 1.0; Smith, 1958, p. 103).

(6) cumulate and tectonite fabrics may be found in both the peridotite and pyroxenite-troctolite-gabbro components of the ophiolites. Graded beds of pyroxenite have been observed within the peridotite tectonite at Betts Cove, as have also websterite layers with a laminated cumulate fabric and euhedral clinopyroxenes. Anhedral pyroxenes and olivines in adjacent bands of wehrlite may however show a strong preferred crystallographic orientation. The associated grey pyroxenite and gabbro cumulates (Figure 2, zone D) which intrude the above rocks are not deformed. However in the Bay of Islands at Trout River (Church and Stevens, 1971, fig. 2) both the peridotite and gabbro have strong deformation fabrics. Gabbros contain irregularly shaped plagioclases with a strong preferred crystallographic orientation, and pyroxenes are concentrated in parallel but discontinuous layers. The gabbros show no signs of diaphthoresis other than the development of rims of brown amphibole about some pyroxenes. The preferred orientation of the plagioclase is probably a piezocrystalline deformation fabric formed at elevated temperatures (Den Tex, 1965, 1969).

(7) the contact relations of the peridotite and pyroxenite-gabbro units (Figure 2, Zones C and D) are well displayed at Betts Cove where grey clinopyroxenite, representing the basal unit of the gabbro, and also the gabbro, cut in the form of dykes, sheets, and veins the underlying peridotite, websterite and wehrlite. Ultramafic xenoliths are also common in the pyroxenite and gabbro. At Trout River, although ultramafic xenoliths may also be observed in the gabbro, the transition zone is marked by the presence of feldspathic dunites, troctolites and anorthosite. Where deformation has been strong the contact relations between these transition-zone rocks and the underlying peridotite are not clear. However, in association with the troctolite zone of the Lewis Hills region of the Bay of Islands, Cooper (1936, p. 31) recorded the presence of selvages of picotite up to four inches thick separating layers of anorthosite and feldspathic dunite. This rela-

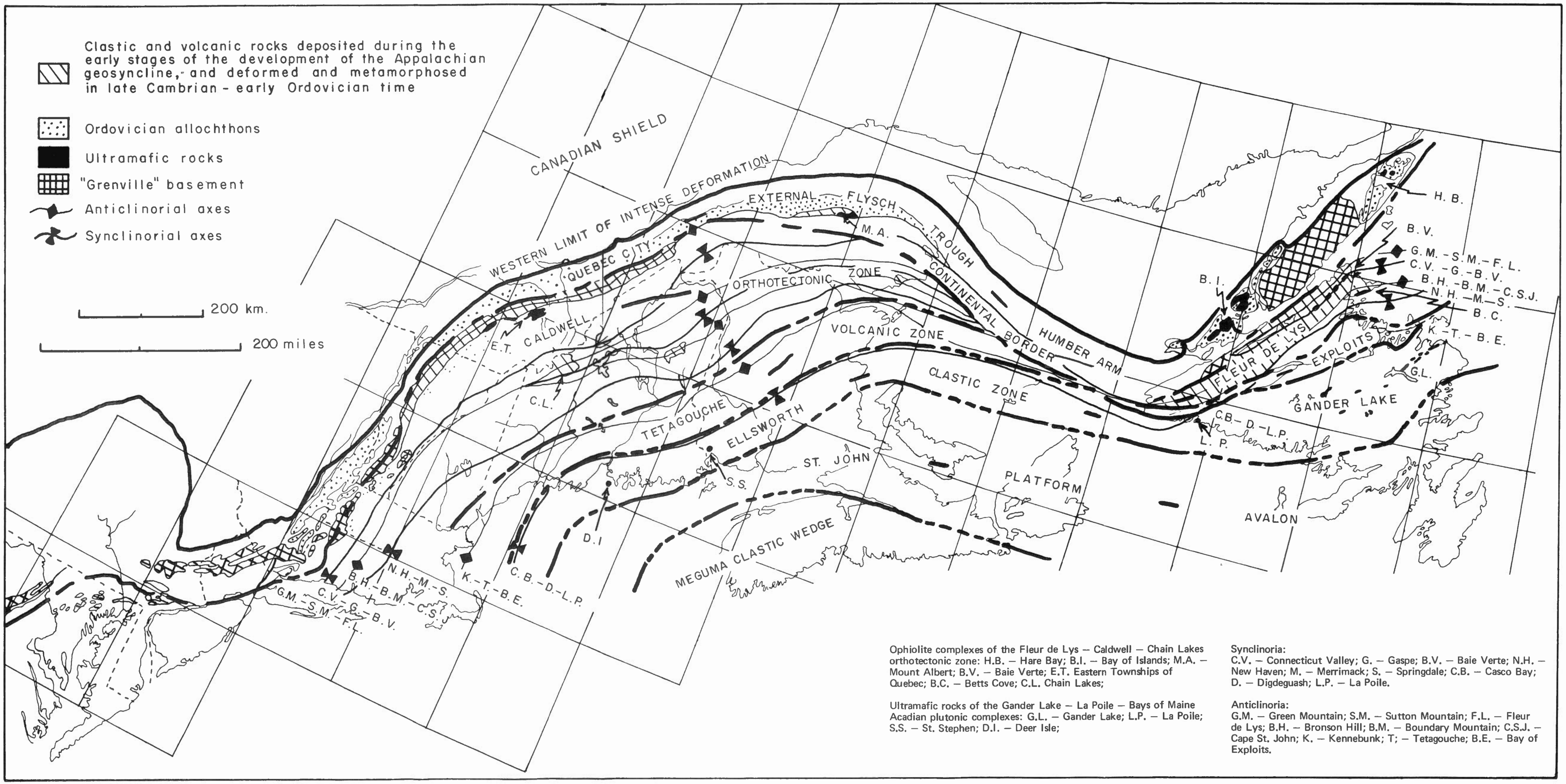

Figure 1. Tectonic zonation, trends of anticlinorial and synclinorial fold axial traces, and distribution of Ordovician ophiolites and Acadian ultramafic-mafic layered intrusives in the northern Appalachians.

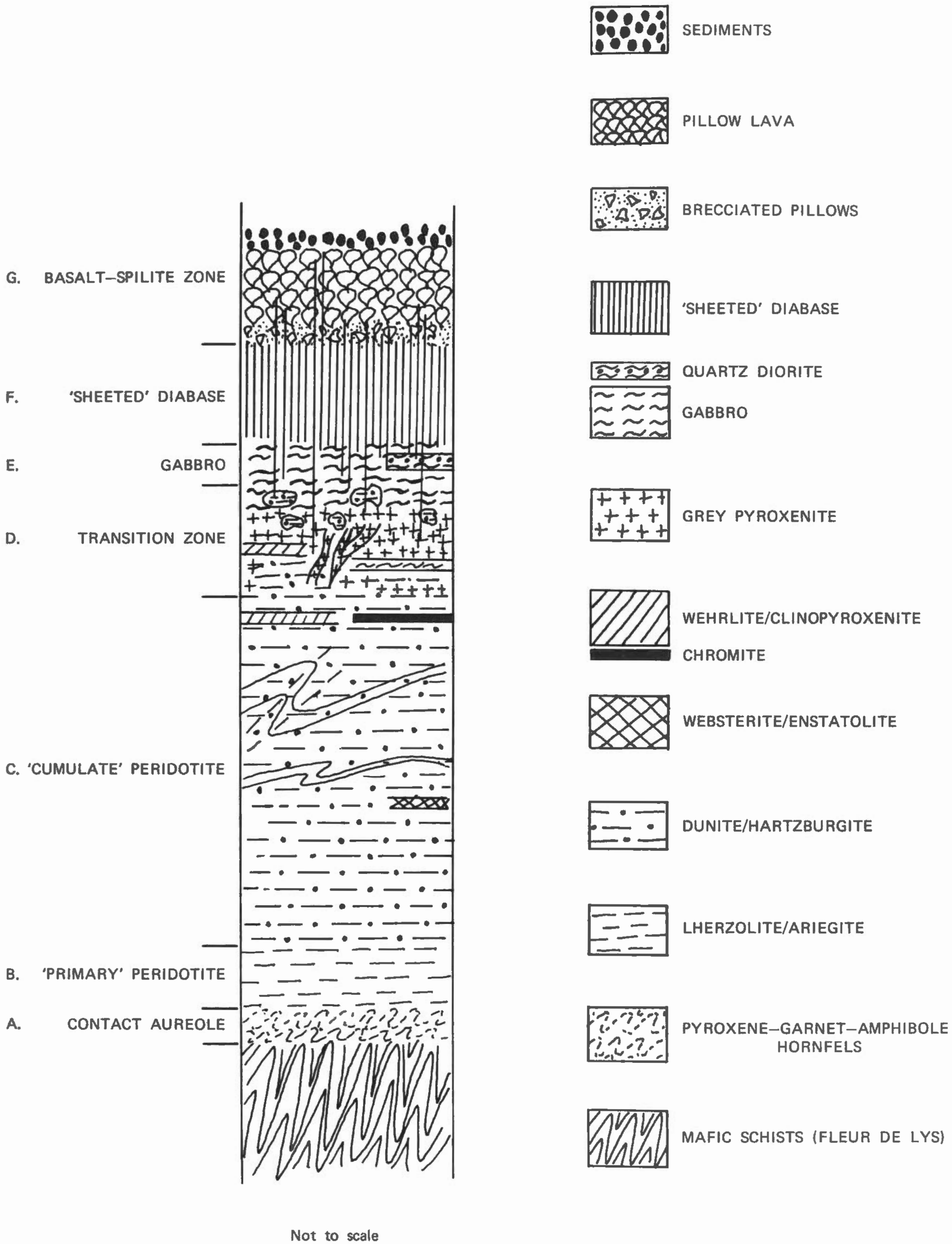

Figure 2. Idealized composite section of an early Ordovician ophiolite based on the Trout River and Betts Cove ophiolites of western Newfoundland and the Burlington Peninsula, respectively (Church and Stevens, 1971, fig. 2). Thickness of the section is about 10 km.

tionship has also been observed by Bezzi and Piccardo (1971, figures 13 and 14) where gabbroic and peridotitic rocks are interbanded in the ophiolites of eastern Liguria. Such rocks are considered by Bezzi and Piccardo (1971) to be cumulates related to the gabbro.

(8) 'sheeted diabase' units separate the gabbro and spilite components of the ophiolites at Betts Cove (Church and Stevens, 1970, 1971) Flatwater Pond in the Baie Verte belt, and Blow Me Down Mountain in the Bay of Islands (F. Graham, personal communications). At Trout River, the gabbro, according to Smith (1958) metamorphoses the overlying pillow lavas. However as Smith notes (p. 20-21) the contact relations between gabbro and volcanic rocks are difficult to define and their true relationship is at present not known.

(9) satellitic bodies of quartz diorite and trondjemite are associated with the ophiolites (Smith, 1958).

(10) volcanic rocks associated with the ophiolite at Betts Cove are low K tholeiites.

The presence of an "ophiolite stratigraphy", the nonconformable relationship between peridotite and gabbro, the upper mantle origin of some of the peridotite, the presence of sheeted diabase, their pretectonic emplacement, their age relative to the development of the Appalachian flysch basins of Ordovician age, all combine to suggest that the Newfoundland ultramafic-mafic complexes are true alpine-type ophiolites, and that the northern Appalachians at least in part developed in a similar manner to the Alpine orogen of the Mediterranean region.

Ophiolite as oceanic lithosphere

The main difficulty in comparing ophiolite complexes with oceanic lithosphere is the absence of detailed petrographic and structural descriptions of actual sections of oceanic crust. Any comparison between oceanic lithosphere and ophiolite must of necessity be circumstantial.

Layered nature of ophiolites and oceanic lithosphere

Seismic evidence and deep-sea dredging show that the ocean crust is formed of three layers, the uppermost two of which are composed of sediments and basaltic submarine volcanic rocks, respectively, pierced by serpentine intrusions (Cann and Funnell, 1967; Barret and Aumento, 1970). There is less agreement as to the constitution of the third oceanic layer, and it is usual to consider it as formed of either gabbro, serpentine, or amphibolite. Comparison with ophiolites suggests that it is made up of gabbro and 'sheeted diabase', both of which rock types have seismic velocities comparable to those of the third layer. Lesser amounts of brown hornblende-bearing gabbro and amphibolite may also be present since these have been recorded by Reinhardt (1969, p. 6) in the Oman ophiolite, Smith (1958, p. 47) in the Bay of Islands, and T. Schroeter and L. Riccio (personal communication) in gabbros and diabases of the Betts Cove ophiolite. Myashiro *et al.* (1970) point out that brown hornblende occurs in many gabbros from the Mid-Atlantic Ridge, but is not common in tholeiitic gabbros on the continents and in island arcs. Brown amphibole in ophiolites occurs as an alteration, and sometimes total recrystallization product of pyroxene, its formation representing the relatively high-temperature hydrous metamorphic conditions attained in the regions below ocean ridges. The occurrence of clinopyroxene rimmed by clear tremolite-actinolite and orthopyroxene pseudomorphed by talc, in ultramafic rocks of the Betts Cove ophiolite of Newfoundland (L. Riccio, personal communication) and in samples dredged from the Mid-Alantic Ridge (Aumento and Loubat, 1971, p. 637, 644) further emphasizes the identity of the alteration processes which have affected both ophiolites, and mafic rocks formed at ocean ridges.

'Sheeted' diabases

One of the more potent reasons for considering ophiolites as oceanic lithosphere is that the mechanism for their formation at an ocean ridge as outlined by Reinhardt (1969) explains in a very satisfactory manner the structural and stratigraphic relationships of the various cumulate units, and also of the gabbros and 'sheeted diabases'. The latter have now been recorded in ophiolites in Cyprus (Gass, 1968) the Oman (Reinhardt, 1969) Kizil Dagh, Turkey (Vuagnat and Cogulu, 1968) Newfoundland (Church and Stevens, 1970, 1971) and the Vardar zone of Yugoslavia (S. Karamata, personal communication, 1970). At Betts Cove in Newfoundland the 'sheeted diabases' form a discrete unit between the gabbro and the overlying pillow lava sequence. In places the unit is composed entirely of diabase dykes intrusive into one another, and inclined at a high angle to the gross layering of the ophiolite (Figure 2). The presence of 'sheeted diabase' units within any ophiolite sequence may be one of the best criteria for considering it as oceanic lithosphere. However the actual sequence present in any section of oceanic lithosphere will depend on the spreading rate and the availability of basaltic magma. Thick sections of gabbro may imply periods of slow or no spreading.

Peridotite-gabbro boundary and the Mohorovicic discontinuity

The boundary between peridotite and gabbro in ophiolites represents the Mohorovicic discontinuity. The boundary is a nonconformity as is indicated by the kind of intrusive and migmatitic contacts observed between gabbro and peridotite in many ophiolites (e.g. Oman, Reinhardt, 1969, p. 7; Kizil Dagh, Vuagnat and Cogulu, 1968; Newfoundland, Church and Stevens, 1970; northern Appenines, Elter in Bezzi and Piccardo, 1971, p. 59). The independence of the peridotite and gabbro may also be marked by the presence of a deformation fabric in the former and a lack of such in the overlying gabbro, diabase and spilite. Aumento and Loubat (1971, p. 655) state in their description of the ultramafic rocks collected from the Mid-Atlantic Ridge near 45°N that "whereas all the dredged ultramafics have been deformed and altered there is an absence of volcanic and diabasic dredged specimens which have undergone similar mechanical and chemical action".

Dunite-harzburgite and lherzolite components of ophiolite as mantle-derived material

Bonatti, Honnorez, and Ferrara (1970) suggest on the basis of strontium isotopic studies of peridotite, and the analogy of ophiolite with oceanic lithosphere, that a boundary should exist within the upper part of the mantle separating depleted 'residual' mantle with high Sr87/Sr86 from primary mantle typified by the lherzolite inclusions commonly found in basalts. Since the kaersutite-bearing high-pressure mineral assemblages occurring as layers in the basal lherzolite (Figure 2, Zone B) of the ophiolite section at Trout River closely resemble mineralogically and chemically the kaersutite-bearing ariegites associated with mantle lherzolites of the type locality at Lherz in the French Pyrénées, and also the ariégites occurring as inclusions in basalt (Ravier, 1964; Church, 1968, p. 783; Jackson and Wright, 1970, p. 417; Beeson and Jackson, 1969) it is conceivable that the lherzolite/harzburgite boundary within the peridotite at Trout River represents the primary peridotite-residual peridotite boundary judged to exist within the upper mantle of oceanic regions by Bonatti *et al.* However, petrographic studies, in particular the identification of cumulate textures, indicate that the harzburgitic and dunitic rocks of the peridotite component of the ophiolites of Newfoundland are deformed cumulate igneous rocks rather than residual primary mantle material. The deformation fabric of the peridotites, and also the sometimes complex distribution of rock types within it, were presumably induced during vertical flowage of the peridotite below the mid-ocean ridge (cf. de Roever, 1957) and lateral flowage during sea-floor spreading. At higher levels in the oceanic crust the peridotite may have formed the walls and floors of the magma chamber in which crystallized the gabbro component of the ophiolites. In turn, the basal 'high-pressure' lherzolite at Trout River may have formed part of a wall or floor of a magma chamber in which the harzburgite and dunite crystallized.

'High-pressure' lherzolite and ariégites occur as inclusions in basalts, as intrusive sheets or diapirs in metamorphic complexes (Green, 1964; Kornprobst, 1969) as allochthonous blocks in explosion breccias (Ravier, 1959) and as basal units of some Alpine ophiolites (Nicolas, 1967, 1969; Bezzi and Piccardo, 1971). Although tectonism has largely obscured their primary textures, chemical data and the rare preservation of what can be interpreted as relict cumulate textures suggest that these rocks may also have originated as differentiates of a silicate melt.

The layered lherzolite bodies at the type locality of Lherz (and also Beni Bouchera, Kornprobst, 1969) are not homogeneous but vary in composition from layer to layer due to changes in the proportions of olivine, pyroxenes, and spinel, and also changes in the chemical composition of the pyroxenes and spinels. Al_2O_3 in clinopyroxenes varies from 3 to 6 weight per cent, and Cr_2O_3 in spinels from 2 to 15 weight per cent (Collée, 1962; Conquéré, 1971; Church, and O'Hara and Mercy, unpublished data). Concentration of the pyroxenes and spinels in layers produces pyroxenites ranging from bright-green diopsidic pyroxenite to the typical ariégite (2-pyroxene spinel rock) which most clearly identifies the lherzolite assemblage as having formed at high pressures (cf. Green, 1964; Church, 1968, p. 781).

The pyroxene compositions, bulk alumina content of lherzolite, and the composition of olivine (Fa_{7-10}, Collée, 1962; Conquéré, 1971) imply, following the arguments of Carter (1970) whereby it is assumed that primary mantle material has an alumina content of 6 to 8 weight per cent, that lherzolites are either the refractory residuum following partial melting of aluminous-peridotite (e.g. garnet-'lherzolite' spec. 66SAL-1, Jackson and Wright, 1970, p. 417) or early cumulates from an aluminous peridotitic liquid. Although the lherzolites from Lherz have been strongly tectonized (Avé Lallemant, 1967) euhedral to subhedral inclusions of spinel in olivine, of spinel and olivine in orthopyroxene (Conquéré, 1971, p. 297) and subhedral grains of clinopyroxene in contact with spinel are sometimes still preserved in the pyroxenites. Such textures as well as the rhythmic and chemical layering of the lherzolite suggest that it was originally formed as an igneous cumulate. The occurrence of garnetiferous ariégites and lherzolites as dykes and veins (Avé Lallemant, 1967) and the presence of garnet reaction coronas about spinel (Church, 1966) indicate that these rocks are also the products of crystal fractionation of a silicate melt at high pressure.

Clinopyroxenes of ariégites are much richer in alumina compared with clinopyroxenes from websterites associated with dunite-harzburgite suites such as those of New Zealand (1.0-1.7 weight per cent, Challis, 1965) and Betts Cove (1.7 weight per cent, L. Riccio, personal communication) and correspondingly lower in iron and magnesium. It is the higher alumina content of pyroxenes in lherzolites and ariégites (Figure 2, zone B) compared with that of pyroxenes from harzburgites and websterites (Figure 2, zone C) which forms the basis for the separation of these suites of rocks into 'high-pressure' and 'low-pressure' associations; and also for the assumption that the lherzolite-ariégite and harzburgite-dunite-websterite components of ophiolite peridotite must have formed in very different environments, and are therefore not comagmatic. The different compositions of pyroxenes in lherzolite and harzburgite could be reconciled with their origin from a common body of magma, however, if it is assumed that the magma chamber in which they crystallized migrated upwards during differentiation of the magma beneath an active oceanic ridge. The pyroxenes may also have crystallized from the same melt under the same high-pressure conditions, the difference in pyroxene compositions merely reflecting the change in composition of the magma, in particular its depletion in alumina, during its progressive differentiation.

Which explanation, if any, is correct has yet to be resolved.

Emplacement of ophiolite

Primary and secondary emplacement

Alpine-type ophiolites are allochthonous sheets which have been emplaced by subhorizontal thrust movements. Their movement history can be divided into two phases:

(1) primary emplacement as large stratiform sheets overthrust onto, or underthrust by, sialic continental rocks (as a result of sea-floor spreading);

(2) secondary emplacement in association with the formation of olistostromes (argille scagliose) due to vertical uplift and gravity sliding of segments of the ophiolite sheets into a migrating flysch basin or basins.

In the Dinaric-Hellenic mobile belt of the Eastern European Alpine system, the ophiolite-bearing sub-Pelagonian and Vardar zones appear to be independent eugeosynclinal systems separated during their development by a shelf area of crystalline rocks (the Pelagonian Massif) which in places is also overlain by ophiolite (Vourinos, Moores, 1969). The ophiolites of the Vardar zone (Milovanovic and Ciric, 1968; Karamata, 1968, 1970) presently occur as dissected sheets overlying or within Jurassic eugeosynclinal rocks (the diabase-hornstein formation) which overlie in turn Paleozoic basement and its mantle of early Mesozoic shelf carbonates. This situation is strongly reminiscent of that of the ophiolites of western Newfoundland (Stevens, 1970). In both cases the ophiolites represent gravity slides which have slid into a migrating flysch trough (Stevens, 1970). Consequently, ophiolites associated with olistostromes are commonly disrupted and often only part of the full ophiolite sequence is preserved. Such ophiolites have been interpreted as blocks of oceanic lithosphere incorporated into trench mélanges (Dewey and Bird, 1970). However, stratigraphic relations preclude such an interpretation for the ilistostromes of the Alps and the Appalachians (e.g. the Dunnage Formation of Newfoundland, Horne and Helwig, 1969; the St. Daniel Formation, St. Julien, 1968). Furthermore, within both the Appalachian and Dinaride ophiolite zones, blueschist metamorphic rocks associated with mélanges, an association considered by Dewey and Bird to indicate that the mélanges are trench deposits, are absent. Even in areas such as Turkey and the Sesia Lanzo zone of the Western Alps where ophiolite and glaucophane schists occur together, it has been shown that the ophiolite was emplaced prior to the onset of blueschist metamorphism and nappe formation (Nicolas, 1967; Van der Kaaden, 1970). Andesitic volcanism, the appearance of which is considered to mark the development of a subduction zone and initiation of destruction of oceanic crust beneath an island arc, also makes its appearance in the Dinarides (Upper Cretaceous-Miocene) much later than the emplacement (Jurassic) of ophiolite. Similarly, in the Appalachians, calc-alkaline volcanism was initiated later than the emplacement of ophiolite, and continued until late Middle Ordovician time. It therefore seems unlikely that ophiolite emplacement marks subduction zone activity as is potentially represented by the serpentine and eclogite bearing Franciscan mélange of California, or continental collision marked by orogenic events late during the tectonic cycle. (It should perhaps be stated that it is not entirely clear whether the ophiolite components in the Franciscan mélange are really primary trench material derived from oceanic lithosphere being subducted in the immediate vicinity of the trench – as in the Dewey and Bird 1970 interpretation – or parts of an olistostrome composed of material derived from an easterly terrain of older ophiolite and blueschist metamorphic rocks (cf. Hsu, 1971).)

In the Mediterranean Alpine system, ophiolites preserved relatively near to their sites of primary emplacement may be present on the Isle of Elba and in the Sesia Lanzo zone of the Western Alps (Nicolas, 1967). In the Circum-Pacific region, ophiolites preserved in their positions of primary emplacement overlying blueschist metamorphic rocks occur in Papua (Davies, 1968; Coleman, 1971, p. 1216) and New Caledonia (Routhier, 1953, fig. 22; Avias, 1967; Guillon, 1969). It is probable that the Circum-Pacific ophiolites represent overthrust sheets of 'cold' oceanic lithosphere derived from an adjacent major ocean basin (Pacific). However ophiolites of the intrasialic Alpine and Appalachian systems generally have, where preserved, high-temperature basal contact aureoles, and the origin of ophiolite as overthrust plates of 'cold' oceanic lithosphere emplaced during the closing of a major ocean basin is therefore not entirely satisfactory.

Significance of the basal contact aureoles of ophiolites

The high-temperature, yet narrow, contact aureoles of ophiolites record their primary emplacement history. The contact aureoles indicate that the ophiolites were emplaced as high-temperature solids, the narrowness of the aureoles precluding their intrusion as liquids. In places the contact minerals have undergone granulation and serpentinization, and their formation is therefore independent of any process involving the formation of serpentine. The two most viable explanations for the formation of the aureoles are:

(1) the aureoles formed as a result of frictional heating produced during overthrusting of oceanic lithosphere (or underthrusting of a continental plate).

(2) the heat for the metamorphism is inherent, the ophiolites having been emplaced relatively soon after their formation at the oceanic ridge. This may have been accomplished either by the ridge having migrated into a position marginal to the continental plate during a phase of ocean closing, or, by the ridge having originated within a continental sialic plate such that 'hot' ophiolite sheets were emplaced directly onto the continental margins during an early stage in the formation of an ocean basin. Evaluation of these hypotheses is at an early stage and requires further reasearch both in the field and laboratory, and theoretical evaluation of the frictional heating hypothesis.

Models for the origin of Appalachian ophiolites

With regard to the specific mode of formation and emplacement of the Appalachian ophiolites a number of alternatives can be considered:

(1) The ophiolites are the dissected remains of a large single sheet which, during the early Ordovician, following the deformation of the marginal clastic wedge represented by the Fleur de Lys, Caldwell and Chain Lakes metamorphic complexes, covered a large part of the Appalachians between Newfoundland and Vermont, and possibly farther south (Stevens, Church, and St. Julien, 1969).

(a) the ophiolites were emplaced as a result of underthrusting of continental margin and adjacent oceanic crust beneath oceanic lithosphere during the closing of a *Cambrian oceanic basin* along a southeasterly (present geographic co-ordinates) dipping subduction zone. The source area of the ophiolites is now delineated by the Lukes Arm or Dildo fault zones, and the contact aureoles were formed as a result of frictional heating during thrusting. The Ordovician calc-alkaline volcanic activity of the Burlington Peninsula-Notre Dame Bay region of Newfoundland, New Brunswick (Tetagouche volcanic rocks), Maine and Vermont, is related to subduction of oceanic crust beneath oceanic lithosphere now represented by the ophiolites.

(b) the ophiolites of western Newfoundland (Bay of Islands-Hare Bay) were emplaced during the formation of an *early Ordovician ocean basin*. The contact aureoles were formed as a result of the migration of hot peridotite and gabbro from an ocean-producing ridge directly onto the continental margin. The Baie Verte and Betts Cove ophiolites (also the Ballantrae ophiolite of Scotland) may have been emplaced in a similar manner, or alternatively, emplaced as 'cold' oceanic crust at a slightly later date. In the latter case the emplacement could be related to the development of a southeasterly dipping subduction zone which brought Arenig age oceanic lithosphere over previously emplaced Tremadocian oceanic rocks now represented by the allochthonous ophiolites of the Bay of Islands. Ordovician calc-alkaline volcanism of the Appalachian eugeosyncline is related to this event.

(2) The ophiolites of the Bay of Islands-Hare Bay, Baie Verte-Eastern Townships, and Betts Cove-Chain Lakes belts represent independent small ocean basins formed within a distending sialic plate.

(a) all three ophiolite belts were formed and emplaced during a phase of *early Ordovician ocean* formation.

(b) the ophiolites of western Newfoundland (Bay of Islands-Hare Bay) were emplaced as 'hot' oceanic lithosphere at the time of formation of an *early Ordovician small ocean basin* of Japan Sea-type within the Fleur de Lys metamorphic complex, now delineated by the White Bay fault zone, during the closing of a major Cambrian ocean basin east of the Fleur de Lys as in case (1a).

Early history of the Appalachian geosyncline

The distribution on both sides of the Appalachian-Caledonide orogen of rock types which uniquely characterize certain periods of the Proterozoic and early Phanerozoic of the North Atlantic region (Figure 3) clearly indicates that the Appalachian system was initiated on a Precambrian sialic basement. This view is supported by the proven existence of Precambrian basement beneath thick late Proterozoic-Cambrian clastic sequences in the Appalachians and the British and Norwegian Caledonides. The clastics were probably deposited in several fault-bounded linear troughs or rifts. Evidence of rapid distension of the basement is provided by the existence of a latest Proterozoic-early Cambrian mafic dyke swarm within the Precambrian of the Long Range Peninsula of western Newfoundland (Williams and Stevens, 1969). (This event may correlate with the late Proterozoic-Cambrian Pan African and Cadomian orogenies of Africa and Western Europe.) However, the recent discovery of late Cambrian ? (post-Fleur de Lys Supergroup-pre-Ordovician) peralkaline granite and subalkalic-peralkaline volcanic rocks in the Burlington Peninsula (Cockburn, 1971) and the distribution of peralkaline granites in the North Atlantic region (Figure 3) suggest that rifting of the continent had, by late Cambrian times, not exceeded a stage represented at the present time by the Red Sea rift. The existence of similar age (c. 500 m.y.) peralkaline silicic rocks in the vicinity of the East African-Middle East rift system also suggests that Cambrian crustal distension and development of a system of major crustal fractures was not a local phenomenon but may have reflected a major though largely abortive attempt at continental fragmentation. This view is supported by the apparent absence of oceanic lithosphere in the form of ophiolite from the southern Appalachians, implying that distension of continental crust in this region was of limited magnitude. Oceanic lithosphere may therefore have been developed only in the northern Appalachians, and the first appearance of recognizable oceanic crust may not have taken place until early Ordovician (Tremadocian) time (Bay of Islands Ophiolite). Whether the ophiolites were emplaced directly onto the margin of the basin of deposition, as is suggested by the existence of contact aureoles welded onto the base of the ophiolites, or were emplaced significantly later than their formation at an oceanic ridge, or whether both types of ophiolite exist (hypothesis 1b) is not at present resolved. However, the continuity of sedimentation throughout the Ordovician, and even into the Silurian in the region south of the Lukes Arm fault (cf. Kay, 1969) can only be explained by assuming that the 'North American' (Long Range - Fleur de Lys) plate was subducted beneath the ophiolites (that is, the continental plate underthrusts the oceanic crust) rather than vice versa as in the Bird and Dewey 1969 model in which the Newfoundland ophiolites are not interpreted as oceanic lithosphere.

Conclusions

The stratiform ultramafic-mafic complexes of the northern Appalachians may

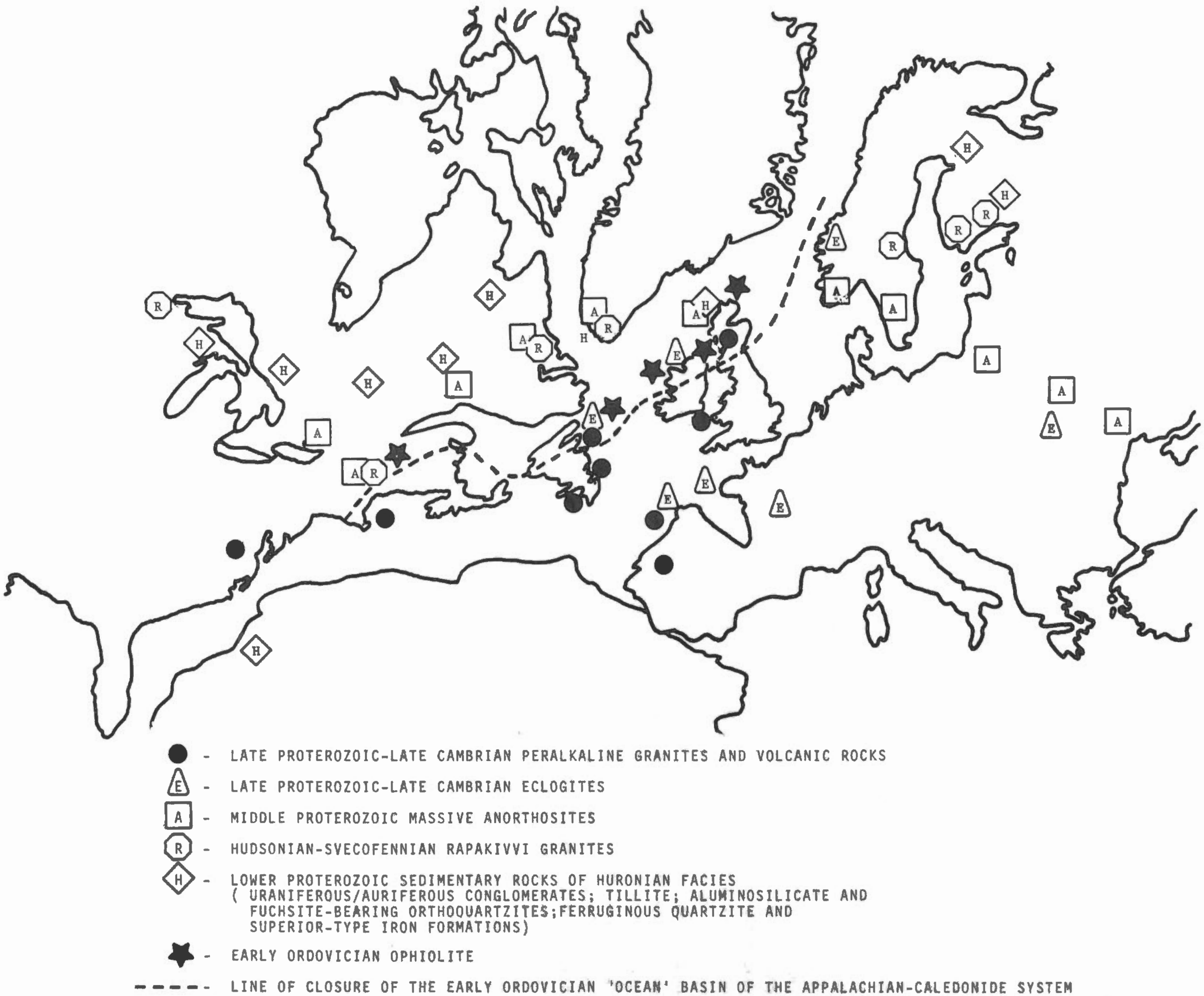

Figure 3. Sketch map showing the pre-Mesozoic distribution in the North Atlantic of various rock types which characterize the early and middle Proterozoic, and the late Proterozoic-early Phanerozoic, relative to the proposed line of closure of the intrasialic early Ordovician 'Proto-Atlantic Ocean' of the Appalachian-Caledonide system. Distribution of anorthosite after Herz (1969).

represent not only the oldest but possibly the only true alpine-type ophiolites in eastern North America. The apparent absence of ophiolites in North American Precambrian orogens such as the presently intra-continental circum-Superior Province fold belts (Penokean - Labrador Trough - Cape Smith - Belcher Island - Setting Lake - Moak Lake) should also be taken into consideration in any attempt to apply plate tectonic theory to the Precambrian (cf. Church, 1971; Gibb and Walcott, 1971).

Acknowledgments

This paper is based on the results of research work carried out in the Burlington Peninsula of Newfoundland and western Newfoundland by the author and graduate students of the University of Western Ontario. The work on the ophiolites of western Newfoundland was carried out in partnership with R.K. Stevens of Memorial University, Newfoundland, to whom should be accorded joint credit for many of the ideas expressed in this paper. G. Cockburn, L. Riccio and T. Schroeter are thanked for their help in elucidating the nature of the ophiolites at Tilt Cove, Betts Cove, and Nippers Harbour, respectively. The author also wishes to record his thanks to Professor S. Karamata for his demonstration of the nature and stratigraphic relations of the ophiolites of Yugoslavia during the 1970 AZOPRO field excursion, to Dr. E. Boudette for discussions on the geology of the Chain Lakes region of Maine during the 1970 New England Intercollegiate Field Conference, and to Dr. P. St. Julien for introducing him to the geology of the Eastern Townships of Quebec.

Financial support was provided by the National Research Council of Canada and the Geological Survey of Canada, and is gratefully acknowledged.

Selected bibliography

Abbate, E., V. Bortolotti, P. Passerini, and M. Sagri. 1970. The northern Appenines geosyncline and continental drift. *Sedim. Geol.*, 4, 637-642.

Anonymous 1968. Symposium "zone Ivrea-Verbano". *Schweiz. Mineral. Petrog. Mitt.* 48, 3-355.

——— 1969. Deep-seated foundations of geological phenomena. *Tectonophysics* 7, 437-523.

Aubouin, J. 1964. Geosynclines: Developments in geotectonics I. Elsevier, New York, 335 p.

Aumento, F. and H. Loubat. 1971. The Mid-Atlantic Ridge near 45°N: XV Serpentinized ultramafic intrusions (preprint). *Can. J. Earth Sci.* 8, 631-663.

Avé Lallemant, H.G. 1967. Structural and petrofabric analysis of an "alpine-type" peridotite: the lherzolite of the French Pyrénées. *Leidse Geol. Mededel.* 42, 1-57.

Avias, J. 1967. Overthrust structures of the main ultrabasic New Caledonian massives. *Tectonophysics* 4, 531-541.

Bailey, E.B. and W.J. McCallien. 1953. Serpentine lavas, the Ankara mélange and the Anatolian thrust. *Roy. Soc. Edinburgh*, Trans. 62, pt. 2, 403-442.

Barret, D.L. and F. Aumento. 1970. The Mid-Atlantic Ridge near 45°N: XI Seismic velocity, density, and layering of the crust. *Can. J. Earth Sci.* 7, 1117-1124.

Beeson, M.H. and E.D. Jackson. 1969. Chemical and mineralogical trends during fractional melting of the mantle beneath Oahu. *Prog. Geol. Soc. Amer.*, Ann. Meet. Atlantic City, 8-9.

Benson, W.N. 1926. The tectonic conditions accompanying the intrusion of basic and ultrabasic igneous rocks. *Nat. Acad. Sci.*, Mem. 19, mem. 1, 90 p.

Bezzi, A. and G.B. Piccardo. 1971. Structural features of the Ligurian ophiolites: petrologic evidence for the "oceanic" floor of the Northern Appenines geosyncline; a contribution to the problem of the alpine-type gabbro-peridotite associations. *Mem. Soc. Geol. Italiana*, 10, 53-63.

Bilgrami, S.A. 1963. Further data on the chemical composition of Zhob Valley chromites. *Amer. Mineral.*, 48, 573-587.

Bird, J.M. and J.F. Dewey. 1969. Lithosphere plate: continental margin tectonics and the evolution of the Appalachian orogen. *Geol. Soc. Amer.* Bull. 81, 1031-1059.

Bloxam, T.W. and J.B. Allen. 1959. Glaucophane-schist, eclogite, and associated rocks from Knockormal in the Girvan-Ballantrae complex, South Ayrshire. *Trans. Roy. Soc. Edinburgh* 54, 1-31.

Bonatti, E., J. Honnorez and G. Ferrara. 1970. Equatorial Mid-Atlantic Ridge: petrologic and Sr isotopic evidence for an alpine-type rock assemblage. *Earth Plan. Sci.*, 9, 247-256.

Borchert, H. 1961. Zusammenhange zwischen Lagerstattenbildung, Magmatismus und Geotektonik. *Geol. Rundschau* 50, 131-165.

Bortolami, G. and G.V. Dal Piaz. 1970. Il substrato cristallino dell'anfiteatro morenico di Rivoli-Avigliana (Prov. di Tor ino) ed alcune considerazioni sull'evoluzione paleogeografica e strutturale della eugeosinclinale piemontese. *Mem. Soc. It. Sci. Nat. Mus. Civ. St. Nat.*, Milano, 17.

Boudette, E.L. 1970. Pre-Silurian rocks in the Boundary Mountains anticlinorium, northwestern Maine, p. C1-C21 in Guide Book for field trips in the Rangeley Lakes-Dead River Basin region, western Maine: *New England Intercoll. Geol. Conf.*, 62nd Ann. Meet., Rangeley, Maine.

Bowen, N.L. 1920. Differentiation by deformation. *Proc. Nat. Acad. Sci.*, 6, 159-162.

———1927. The origin of ultrabasic and related rocks. *Amer. J. Sci.*, 14, 89-108.

Bowin, C.O. 1966. Geology of Central Dominican Republic (a case history of part of an island arc). *Geol. Soc. Amer.* Mem. 98, 84 p.

Brunn, J.H. 1954. Les éruptions ophiolitiques dans le Nord-Ouest de la Grèce: leurs relations avec l'orogenèse. *19th Int. Geol. Cong.* Algiers, Sec. XV, fasc. XVII, 19-27.

——— 1960. Mise en place et differentiation de l'association plutovolcanique du cortège ophiolitique. *Rev. Geogr. Phys. Geol. Dyn.* 3, 115-132.

Cann, J.R. and B.M. Funnell. 1967. Palmer Ridge: a section through the upper part of the ocean crust? *Nature*, 213, 661-664.

Carter, J.L. 1970. Mineralogy and chemistry of the Earth's Upper Mantle based on the partial fusion – partial crystallization model. *Geol. Soc. Amer.* Bull. 81, 2021-2034.

Challis, G.A. 1965. Origin of New Zealand ultramafic intrusions. *J. Petrol.* 6, 322-364.

——— 1969. Discussion on the paper "The origin of ultramafic and ultrabasic rocks" by P.J. Wyllie. *Tectonophysics*, 7, 495-505.

———and W.R. Lauder. 1966. The genetic position of "Alpine" type ultramafic rocks. *Bull. Volcanol.* 29, 283-306.

Chapman, C.A. 1968. A comparison of the Maine Coastal Plutons and the magmatic central complexes of New Hampshire. In Studies of Appalachian Geology, Northern and Maritime, Zen E-An, White W.S., Hadley, J.B., and Thompson, J.B. (editors) Interscience Pub., New York, 385-396.

Chidester, A.H. 1968. Evolution of the ultramafic complexes of northwestern New England. In Studies of Appalachian Geology Northern and Maritime, Zen, E-an, White, W.S., Hadley, J.B., and Thompson, J.B. (editors) Interscience Pub., New York, 343-354.

Christensen, N.I. 1970. Composition and evolution of the oceanic crust. *Marine Geol.*, 8, 139-154.

Church, W.R. 1966. Comparative mineralogical and chemical composition of ariégite and eclogite. *Prog. Geol. Soc. Amer.*, Ann. Meet., San Francisco, 39-40.

———1968. Eclogites. In Basalts: the Poldervaart treatise on rocks of basaltic composition, Hess, H.H. (editor) Interscience Pub., New York, 755-798.

———1969. Metamorphic rocks of Burlington Peninsula and adjoining areas of Newfoundland, and their bearing on continental drift in the North Atlantic. In North Atlantic Geology and Continental Drift, M. Kay (editor) *Amer. Assoc. Petrol. Geol.*, Mem. 12, 212-233.

——— 1971. Nature and evolution of Proterozoic and Phanerozoic orogenic belts. Abst. of Papers, *Geol. Assoc. Can.* Min. Assoc. Canada Ann. Meet., Sudbury, 14-15.

Church, W.R. and R.K. Stevens. 1970(a). Mantle peridotite and the early Paleozoic ophiolite complexes of the Newfoundland Appalachians. *Dept. Geol. Univ. Western Ont.*, Prel. Rpt. 175, 3 p.

———1970(b). Mantle peridotite and the early Paleozoic ophiolite complexes of the Newfoundland Appalachians. *Prog. Int. Symp. Mech. Properties.* Processes in the Mantle, Flagstaff, Abst. 7-6, 38-39.

———1971. Early Paleozoic ophiolite complexes of the Newfoundland Appalachians as Mantle-Oceanic Crust sequences. *J. Geophys. Res.* 76, 1460-1466.

Cockburn, G.H. 1971. Peralkaline granite and associated plutonic rocks of the Eastern Division of the Fleur de Lys Metamorphic Complex of Newfoundland. Abst. *Prog. Geol. Soc. Amer.* Meet., Northeastern Sect., Hartford, 22-23.

Coleman, R.G. 1971. Plate tectonic emplacement of upper mantle peridotite along continental edges. *J. Geoph. Res.* 76, 1212-1222.

Collée, A.L.G. 1962. A fabric study of lherzolites with special reference to ultrabasic nodular inclusions in the lavas of Auvergne (France). *Leidse Geol. Med.* 28, 102 p.

Conquéré, F. 1971. La lherzolithe à amphibole du gisement de Caussou (Ariège, France). *Cont. Min. Petr.* 30, 296-313.

Cooper, J.R. 1936. Geology of the southern half of the Bay of Islands Igneous Complex. *Nfld. Dept. Nat. Res. Geol. Sec.* Bull. 4, 62 p.

Davies, H.L. 1968. Papuan ultramafic belt. *Int. Geol. Congr.* Rpt., 23rd Session, Proc., Sect. 1, 209-220.

Decandia, F.A. and P. Elter. 1969. Riflessioni sul problema delle ofioliti nell'Appennino settentrionale (nota preliminare). *Atti. Soc. Sci. Nat.*, Mem. Ser. A, 76, 1-9.

Den Tex, E. 1965. Metamorphic lineages of orogenic plutonism. *Geol. en Mijn.*, 44, 105-132.

———1969. Origin of ultramafic rocks their tectonic setting and history: a contribution to the discussion of the paper "The origin of ultramafic and ultrabasic rocks" by P.J. Wyllie. *Tectonophysics* 7, 457-488.

de Roever, W.P. 1957. Sind die Alpinotypen peridotitmassen vielleicht tektonisch verfrachtete Brüchstucke der Peridototschale? *Geol. Rundschau* 46, 137-146.

Dewey, J.F. and J. Bird. 1970. Mountain belts and the new global tectonics. *J. Geoph. Res.*, 75, 2625-2647.

Dickinson, W.R. 1971. Plate tectonic models of geosynclines. *Earth Plan. Sci.* Letters 10, 165-174.

Dietz, R.S. 1963. Alpine serpentines as oceanic rind fragments. *Geol. Soc. Amer.* Bull. 74, 947-952.

Dubertret, L. 1955. Géologie des roches vertes du nord-ouest de la Syrie et du Hatay (Turquie). Notes et Mem. sur le Moyen-Orient, *Mus. Nat. d'Hist, Naturelle*, Paris, 6, 5-224.

Forestier, F.H. 1968. Discussion sur l'article de P.J. Wyllie "The origin of ultramafic and ultrabasic rocks". Prog. Symposium on Deep-seated Foundations of Geological Phenomena, *23rd Int. Geol. Congr.*, Prague, 28-30.

Gannser, A. 1959. Ausseralpine ophiolith probleme. *Eclogae. Geol. Helv.*, 52, 659-680.

———1966. The Indian Ocean and the Himalayas. A geological interpretation. *Eclogae. Geol. Helv.*, 59, 831-848.

Gass, I.G. 1968. Is the Troodos-Massif of Cyprus a fragment of Mesozoic ocean floor? *Nature*, 220, 39-42.

Gibb, R.A. and R.I. Walcott. 1971. A Precambrian suture in the Canadian Shield. *Earth Planet. Sci.* Letters 10, 417-422.

Green, D.H. 1964. The petrogenesis of the high-temperature peridotite intrusion in the Lizard area, Cornwall. *J. Petrol.*, 5, 134-188.

———1970. Peridotite-gabbro complexes as keys to petrology of mid-oceanic ridges: Discussion. *Geol. Soc. Amer.* Bull. 81, 2161-2166.

Guillon, J.H. 1969. Le grand massif péridotitique du sud de la Nouvelle Caledonie. *Caheirs ORSTOM Geol.* 1, 7-25.

Hamilton, W. 1969. Mesozoic California and the underflow of Pacific Mantle. *Geol. Soc. Amer.* Bull. 80, 2409-2430.

Hernandez-Pacheco, A. 1967. Estudio petrografico y geoguimico del macizo ultramafico de Ojen (Malaga). *Estudios Geologicos*, 23, 85-143.

Hertz, N. 1969. Anorthosite belts, continental drift and the anorthosite event. *Science*, 164, 944-947.

Hess, H.H. 1955. Serpentines, orogeny, and epeirogeny, *Geol. Soc. Amer.* Special Paper 62, 391-407.

———1964. The oceanic crust, the upper mantle and the Mayaguez serpentinized peridotite. In a study of serpentine; the AMSOC core hole near Mayaguez, Puerto Rico. *Nat. Acad. Sci.*, Nat. Res. Council Pub. 1188, 169-175.

———1965. Mid-oceanic ridges and tectonics of the sea floor. In Colston papers No. 17, submarine Geology and Geophysics, Whittard, W.F. and Bradshaw, R. (editors) Butterworth, London, 317-334.

Horne, G.S. and J. Helwig. 1969. Ordovician stratigraphy of Notre Dame Bay, Newfoundland. In North Atlantic Geology and Continental Drift, M. Kay (editor). *Amer. Assoc. Petrol. Geol.* Mem. 12, 212-233.

Hsu, K.J. 1970. Franciscan mélanges as a model for eugeosynclinal sedimentation and underthrusting tectonics. *J. Geoph. Res.* 76, 1162-1169.

Hutchinson, R.W., R.H. Ridler and G.G. Suffel. 1971. Metallogenic relationships in the Abitibi Belt, Canada: a model for Archean Metallogeny. *G.I.M.M.* Bul. 64, 48-57.

——— and T.J. Dhonau, 1969. Deformation of an Alpine ultramafic association in Darvel Bay, East Sabah. Malaysia. *Geol. en Mijn.* 48, 481-494.

Igi, S. 1953. Petrographical studies on the Peridotite in the Horoman region at the southern end of the Hidaka Mountain Range Hokkaido. *J. Geol. Soc.*, Japan, 59, 111-121.

Irwin, W.P. 1964. Late Mesozoic orogenies in the ultramafic belts of northwestern California and southwestern Oregon. *U.S. Geol. Surv.*, Prof. Paper 501-C, p. C1-C9.

Jackson, E.D. and T.L. Wright. 1970. Xenoliths in the Honolulu volcanic series Hawaii. *J. Petrol.*, 11, 405-430.

Karamata, S. 1968. Zonality in contact metamorphic rocks around the ultramafic mass of Brezovica (Serbia, Yugoslavia). Rpt. 23rd Sess. *Int. Geol. Congr.*, Sect. 1, 197-208.

———1970. Guide for the AZOPRO excursion: Part B, Ultramafic Rocks, Yugoslavia. *Univ. Beograd*, 6 p.

Kay, M. 1969. Silurian of northeast Newfoundland coast. In North-Atlantic – Geology and continental drift, M. Kay (editor). *Amer. Assoc. Petrol. Geol.* Mem. 12, 414-424.

Kornprobst, J. 1969. Le massif ultrabasique de Beni Bouchera (Rif Interne, Maroc): Etude des péridotites de haute température et de haute pression, et des pyroxenolites, à grenat ou sans grenat, qui leur sont associées. *Contr. Miner. and Petrol.* 23, 283-322.

Kozary, M.T. 1968. Ultramafic rocks in thrust zones of northwestern Oriente Province, Cuba. *Amer. Assoc. Petrol., Geol.* Bull. 52, 2298-2317.

Lamarche, R.Y. 1971. Ophiolites of southern Quebec (this volume).

Laubscher, H. 1969. Mountain building. *Tectonophysics* 7, 551-563.

MacKenzie, D.B. 1960. High-temperature alpine-type peridotite from Venezuela. *Geol. Soc. Amer.* Bull. 71, 303-317.

Maxwell, J.C. 1969. "Alpine" mafic and ultramafic rocks– the ophiolite suite: a contribution to the discussion of the paper "The origin of ultramafic and ultrabasic rocks" by P.J. Wyllie. *Tectonophysics* 7, 489-494.

McTaggart, K.C. 1971. On the origin of ultramafic rocks. *Geol. Soc. Amer.* Bull. 82, 23-42.

Milovanovic, B. and B. Ciric. 1968. Geologic map of the Socialist Republic of Serbia –

ZVORNIK-TITOVO UZICE region, Scale 1:200,000. *Research Inst. Geol. Geophys.*, Geokarta, Beograd.

Moores, E.M. 1969. Petrology and structure of the Vourinos ophiolitic complex of Northern Greece. *Geol. Soc. Amer.* Spec. Paper No. 118, 74 p.

———1970. Ultramafics and orogeny with models of the U.S. Cordillera and the Tethys. *Nature*, 228, 837-842.

Myashiro, A. 1966. Some aspects of peridotite and serpentinite in orogenic belts. *Jap. J. Geol. Geg.* 37, 45-61.

Myashiro, A., F. Shido and M. Ewing. 1970. Crystallization and differentiation in abyssal tholeiites and gabbros from mid-oceanic ridges. *Earth Plan. Sci.* Letters 7, 361-365.

Nicolas, A. 1967. Géologie des Alpes piémontaises entre Dora Maira et Grand Paradis. *Travaux Lab. Géol.*, Fac. Sci. Grenoble 43, 139-167.

———1969. Une vue unitaire concernant l'origine des massifs ultrabasiques des Alpes occidentales internes. *C. R. Acad. Sci.*, Paris, 269, 1831-1834.

Peters, T.J. 1969. Rocks of the Alpine ophiolitic suite: discussion on the paper "The origin of ultramafic and ultrabasic rocks" by P.J. Wyllie. *Tectonophysics* 7, 507-509.

Pratt, J.H. and J.V. Lewis. 1905. Corundum and peridotites of western North Carolina. *North Carolina Geol. Surv.*, Rpt. 1, 464 p.

Ragan, D.M. 1963. Emplacement of the Twin Sisters Dunite, Washington. *Amer. J. Sci.*, 261, 549-565.

Raleigh, C.B. 1965. Structure and petrology of an Alpine peridotite on Cypress Island, Washington, *U.S.A. Beitr. Min. Petrol.*, 11, 719-741.

Ravier, J. 1959. Le métamorphisme des terrains secondaires des Pyrénées. *Soc. Géol. France*, Mem. 86, 250 p.

———1964. Ariégite et eclogite. *Soc. franc. Miner. Crist.*, Bull. 87, 212-215.

Reinhardt, B.M. 1969. On the genesis and emplacement of ophiolites in the Oman Mountains Geosyncline. *Schweitz. Mineral. Petrog.*, Mitt. 49, 1-30.

Ricou, L-E. 1971. Le métamorphisme au contact des péridotites de Neyriz (Zagros interne, Iran): développement de skarns à pyroxene. *C. R. Somm. Séances.* Soc. Géol. France 1, p. 43.

Rocci, G. and T. Juteau, 1968. Spilite-keratophyre et ophiolite, influence de la traversée d'un socle sialique sur le magmatisme initial. *Géol. en Mijn.*, 47, 330-339.

Rost, F. von 1968. Vergleich der Ultramafitite der Ivrea-Zone mit Peridotiteinschaltungen im europaischen kristallinen Grundgebirge. *Schweitz. Mineral. Petrog.*, Mitt. 48, 165-173.

Routhier, P. 1946. Volcano-plutons sous-marins du cortège ophiolitique. *C.R. Acad. Sci.*, 222, 192-194.

———1953. Étude géologique du versant occidental de la Nouvelle Caledonia entre le cola de Boghen et la Pointe d'Arana. *Soc. Géol. France*, Mem. 67, 271 p.

Smith, C.H. Bay of Islands igneous complex, western Newfoundland. *Geol. Surv. Can.*, Mem. 290, 132 p.

Southwick, D.L. 1970. Structure and petrology of the Harford County part of the Baltimore-State Line gabbro-peridotite complex. In Studies of Appalachian geology – central and southern, G.W. Fisher, F.J. Pettijohn, J.C. Reed, Jr., and K.N. Weaver (editors). Interscience Pub., New York, 397-416.

Steinmann, G. 1905. Geologische Beobachtungen in den Alpen. II: Die Schardt'sche Uberfaltungstheorie und die geologishe Bedeutung der Tiefseeabsatze und der ophiolithischen Massengesteine. *Ber. Nat. Ges.*, Freiburg, I, Bd. 16, 44-65.

———1927. Die ophiolithischen Zonen in dem mediterranean Kettengebirgen. *14th Internat. Geol. Congr.*, Madrid, C.R. 2, 638-667.

Stevens, R.K. 1970. Cambro-Ordovician flysch sedimentation and tectonics in western Newfoundland, and their possible bearing on a proto-Atlantic Ocean. In Flysch Sedimentology in North America, Lajoie, J. (editor). *Geol. Assoc. Can.*, Spec. Paper 7, 165-178.

———, W.R. Church and P. St. Julien. 1969. Age of the ultramafic rocks in the northwestern Appalachians (Abst.) Program, *Geol. Soc. Amer.* Ann. Meet., Atlantic City, 215-216.

St. Julien, P. 1968. Les "Argilles à Blocs" du sud-ouest des Appalaches du Québec. *Naturaliste Canadienne* 95, 1345-1356.

Suess, E. 1909. Das Antlitz der Erde, Vienna. F. Tempsky, 789 p.

Thayer, T.P. 1960. Some critical differences between alpine-type and stratiform peridotite-gabbro complexes. *Int. Geol. Congr.*, 21st Sess., Rpt. 13, 247-259.

———1963.Flow layering in alpine peridotite-gabbro complexes. *Mineral. Soc. Amer.* Spec. Paper 1, 55-61.

———1967. Chemical and structural relations of ultramafic and feldspathic rocks in alpine intrusive complexes. In Ultramafic and Related Rocks, P.J. Wyllie, (editor). Wiley and Sons Inc., New York, 222-239.

———1969. Alpine-type sensu stricto (ophiolitic) peridotites: refractory residues from partial melting or igneous sediments? A contribution to the discussion of the paper "The origin of ultramafic and ultrabasic rocks" by P.J. Wyllie. *Tectonophysics* 7, 511-516.

———1969. Peridotite-gabbro complexes as keys to petrology of mid-ocean ridges. *Geol. Soc. Amer.* Bull. 80, 1515-1522.

———and G.R. Himmelberg. 1968. Rock succession in the alpine-type mafic complex at Canyon Mountain Oregon. *Int. Geol. Congr.*, Rpt., 23rd Sess., Proc. Sect. 1, 175-186.

Trumpy, R. 1960. Paleotectonic evolution of the central and western Alps. *Geol. Soc. Amer.* Bull. 71, 843-908.

Van der Kaaden, G. 1962. The different concepts of the genesis of alpine-type emplaced ultrabasic rocks and their implications on chromite prospection. *Mineral Res. Explor. Inst.*, Turkey, Bull. 61, 41-56.

———1970. Chromite-bearing ultramafic and related gabbroic rocks and their relationship to "ophiolitic" extrusive rocks and diabases in Turkey. In Symposium on the Bushveld igneous complex and other layered intrusions. *Geol. Soc. South Africa*, Spec. Pub. 1, 511-531.

Vuagnat, M. 1968. Quelques réflexions sur le complexe basique-ultrabasique de la zone d'Ivrée et les ultramafites alpinotypes. *Schweiz. Mineral. Petrog.*, Mitt. 48, 157-164.

———and E. Cogulu. 1968. Quelques réflections sur le massif basique-ultrabasique du Kizil Dagh, Hatay, Turquie. *C.R. Sc. Soc. Phys. Hist. Nat.* Genève, N.S. 2, 210-216.

Williams, H. and R.K. Stevens. 1969. Geology of Belle Isle – northern extremity of the deformed Appalachian miogeosynclinal belt. *Can. J. Earth Sci.*, 6, 1145-1158.

Wolfe, W.J. 1965. The Blue River ultramafic intrusion, Cassiar District, British Columbia. *Geol. Surv. Can.*, Paper 64-48, 15 p.

Wyllie, P.J. (editor) 1967. Ultramafic and related rocks. Wiley and Sons Inc., New York, 464 p.

Yoshino, G. 1961. Structural-petrological studies of peridotite and associated rocks of the Higashiakaishiyama District, Shikoku, Japan. *J. Sci. Hiroshima Univ.*, (ser. C) 3, 343-402.

———1964. Ultrabasic mass in the Higashiakaishiyama District, Shikoku, southwest Japan. *J. Sci. Hiroshima Univ.*, (ser. C) 4, 333-364.

No. 7

paleomagnetism and the kinematic history of mafic and ultramafic rocks in fold mountain belts

E. IRVING
Earth Physics Branch
Department of Energy, Mines and Resources, Ottawa

R.W. YOLE
Department of Geology
Carleton University
Ottawa

Abstract. Mafic and ultramafic rocks commonly occur in orogenic belts, and some can be regarded as remnants of oceanic lithosphere trapped in a subduction zone at the edge of oceanic plate. If this is so, then the opposing plate edges must have moved towards one another. The initial (pre-movement) positions of the plate margins can be calculated if there are paleomagnetic results from both margins pertaining to at least two different periods (different field configurations) prior to the movements. Only a few paleomagnetic results relevant to Canadian ultramafic complexes are available. However, the kinematic framework of most Phanerozoic examples could be studied using existing paleomagnetic techniques, and, as an illustration, results from the Pacific Ocean and the Pacific rim of North America are described. These results do not yet meet the full technical requirements, so accurate reconstructions cannot be made, but nevertheless they indicate that since the Triassic the crust of the Pacific Ocean and the western margin of the Cordillera were displaced northwards by several thousand kilometres relative to the main body of North America, and hence that the ultramafic rocks of the Cordillera could be fragments of intervening oceanic lithosphere driven into the continent from the south. Data are insufficient for comparisons relevant to Canadian ultramafic complexes older than late Paleozoic to be made, but a review of the problems allows two conclusions to be made. The first is that the problem of determining the kinematic framework of the Appalachian ophiolites is experimentally accessible and could be readily obtained; such a study could be a test case of the hypothesis of plate tectonics for the Lower Paleozoic. The second conclusion is that in order to determine the kinematic framework of Precambrian occurrences it will almost certainly be necessary to make general use of late orogenic secondary magnetization.

Introduction

The purpose of this paper is to discuss the ways in which paleomagnetism may be used to determine the kinematic framework of some ultramafic and mafic rocks with particular reference to Canadian occurrences (*see* Frontispiece).

In the application of the hypothesis of plate tectonics to orogenic belts many mafic and ultramafic complexes (particularly those that have associated submarine extrusive rocks) have been interpreted as fragments of ridge-generated oceanic lithosphere which have been trapped in an orogen as an oceanic lithospheric plate passes down a subduction zone into the mantle (for example Temple and Zimmerman 1969; Moores, 1970; Dewey and Bird, 1970). If this hypothesis is accepted, then the under-riding plate must have moved a great distance relative to the over-riding plate. Therefore, a necessary condition for this tectonic interpretation of such mafic and ultramafic occurrences, is that paleomagnetic directions from rocks which predate the period of movement should show large differences between plates. Discrepancies (expressed as differences between paleomagnetic poles) of 30° to 90° have been observed between either side of Tethys in late Paleozoic and Mesozoic sequences on the present-day fragments of Gondwanaland and Laurasia, so that for the Alpine ophiolites this condition is fulfilled. However, before plate tectonics can be applied with any confidence to the interpretation of pre-Alpine mafic and ultramafic rocks there is a need for similar quantitative evidence, independent of the hypothesis itself, of motions between opposed plates of lithosphere. The geometrical and magnetic requirements are given first, followed by a discussion of how paleomagnetism may be applied to the ultramafic occurrence within the orogenic belts of Canada.

Two hypothetical ways in which oceanic lithosphere may be emplaced into orogenic belts are shown in Figure 1. On the left (after Moores, 1970) the subduction zone dips away from the continent Y. The continent is buoyant and cannot descend, so movement ceases and a further cycle of sinking commences at another site. Fragments of oceanic crust (X) together with deformed sediments become part of continent Y. On the right the subduction zone dips under the continent C, and oceanic lithosphere becomes incorporated into the trench and later into the continent perhaps as huge slivers as Dewey and Bird (1970) have shown in their diagrams. Similar displacements between opposed plates could occur in both models, but the displacement between trapped oceanic lithosphere and continent depends on the direction of dip of the subduction zone, and the method of incorporation of oceanic material into the continental margins. In principle, this feature could be a means of determining the direction of dip of subduction zones.

Should no paleomagnetic discrepancies be observed, then plate models requiring large displacements can be discounted. However, if discrepancies are found, then the past arrangement of

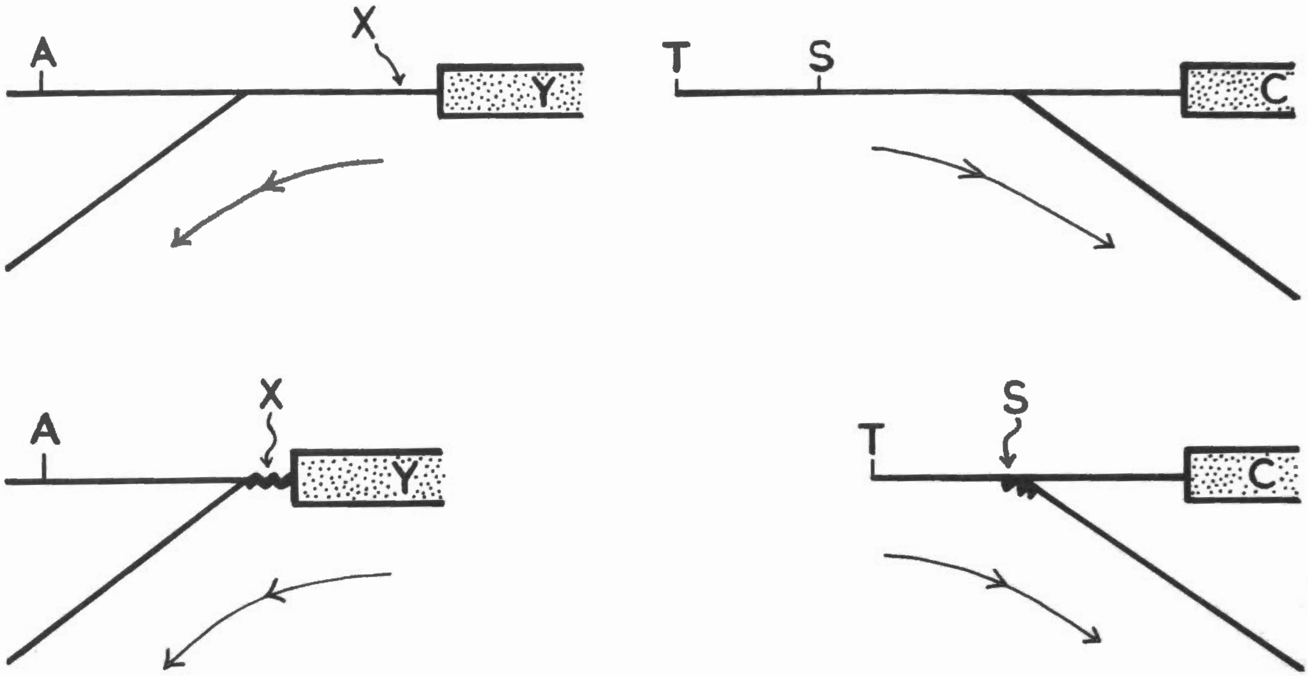

Figure 1. Models for the emplacement of oceanic crust within a continent. On the left (modified after Moores, 1970) the down-going plate dips away from the continent (Y). The continent is prevented from descending by its buoyancy, and oceanic crust (X) may become incorporated in the marginal zone. On the right the down-going plate dips beneath the continent (C) and oceanic crust from it is incorporated into the inner wall of the trench, and eventually becomes incorporated into new continental crust.

plates needs to be determined. In order to do this it is necessary to obtain from each plate, paleomagnetic poles which can be referred to at least two different field configurations prior to the period of movement. Suppose that we wish to determine the relative movement of localities R and S (Figure 2) from which paleomagnetic poles A to D have been obtained (A and C from S, and B and D from R) then the movement of S relative to R (which is assumed fixed) is described by a rotation about a point (called a pivot point) on the earth's surface. Thus the technical problem in paleogeographic reconstructions is to determine the pivot points and rotations appropriate to each plate (Runcorn, 1956). If only one pair of contemporaneous poles are known (say only A and B) then the pivot point lies anywhere on a line PX equidistant from A and B, but it is determined uniquely by the intersection of a second line PY defined by a second pair of poles (C and D) assigned to a later field configuration, provided the observing localities (R and S) have not moved relative to one another between the two periods of time. Once the pivot point is determined, the angle (SPS′) through which S must be rotated to bring the poles into agreement can be calculated, and the position (S′) prior to movement determined.

Paleomagnetic evidence can be obtained in either of two ways. The first and usual way is to study the directions at primary magnetization (magnetization acquired when the rock was formed) of undeformed, chemically unaltered rocks which lie superficially on the earth's crust. This method is generally applicable to the study of the tectonic framework of ultramafic and mafic occurrences in Phanerozoic fold mountain belts, because it is commonly possible to obtain the primary magnetization of late Precambrian and younger rocks; but this is probably not so for most Archean rocks whose presently detectable magnetization was acquired long after formation. If their magnetization (secondary magnetization) was acquired during cooling (say by uplift after a period of deep burial) then it will be a type of thermoremanent magnetization. If it was acquired during recrystallization of the iron minerals at temperatures below the Curie temperature, then it will be a chemical remnant magnetization. The age of such secondary magnetization probably corresponds, to a first approximation, to the apparent K-Ar age reset at the time regional heating ceased. In the Phanerozoic many examples of primary magnetization being replaced by stable secondary magnetization during some identifiable later regional process are known. For example, the Silurian Bloomsburg formation in the Valley and Ridge Province of the Appalachians has a strong stable secondary magnetization acquired at the close of the Appalachian orogeny (late Carboniferous or Permian) presumably as a result of cooling during uplift following a time of deep burial and regional heating (Roy *et al.,* 1968). Thus the only source of paleomagnetic information in very old altered rocks is stable secondary magnetization of known age; instead of applying the usual paleomagnetic method of studying the primary magnetization of unaltered superficial rocks, it will be necessary, in order to determine the

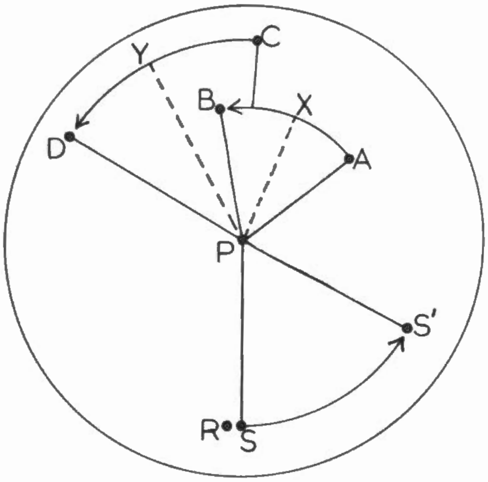

Figure 2. Geometrical requirements for determining past relative position of two sampling localities R and S. Poles A and C are observed from S, and B and D from R. The poles A,B refer to the same time period (field configuration). The poles C,D also refer to the same field configuration as each other but different from that of A,B. In order to bring B and D into agreement with A and C locality S is rotated about a pivot point P by and angle SPS'. The past position of S' relative to R is then fixed uniquely. For convenience P is taken to be at the centre.

tectonic history of ultramafic rocks in Precambrian orogenic belts, to study the stable secondary magnetization acquired during uplift or metamorphism of basement complexes.

The paleomagnetic requirements for determining the kinematic history of pre-Alpine mafic and ultramafic orogenic complexes may now be summarized: (1) remnant magnetization directions of known age from both margins of an orogen, and, if possible, from supposed remnants of oceanic lithosphere within it, and (2) sufficient data to furnish at least two pole pairs pertaining to two different field configurations prior to the movements.

Through lack of study, the paleomagnetic data do not yet fully satisfy these requirements for any Canadian examples. The youngest ultramafic rocks (late Paleozoic and early Mesozoic) in Canada are in the Cordillera (localities 1 to 9 of the Frontispiece) and the following discussion is concerned mainly with paleomagnetic data from the Pacific rim of North America which is relevant to them. However, in the long term, the main challenge will be the study of the kinematic history of older ultramafic and mafic rocks, particularly those of the Canadian Shield, because they are economically so important, and because they span such an enormous length of time, and hence provide an excellent opportunity for the application of plate tectonics to the remote history of the earth. Therefore, although the data relevant to them are few, a discussion is also given of how paleomagnetism may be applied to older examples.

Previous work from the Pacific Ocean and the Pacific Rim of North America

Magnetic surveys of Cretaceous seamounts from a wide area of the Pacific have given paleomagnetic poles near northern Europe with a mean at 016E,61N (error (P = 0.05) = 8°; Francheteau *et al.*, 1970). The seamounts typically have declinations near zero or 180°, and inclinations that are consistent with a position south of their present position. The good agreement among seamount poles and the presence of reversals indicates that the magnetization is stable. The mean Cretaceous pole for the main body of North America is at 176W,69N (error (P = 0.05) = 3°), and differs from the Pacific seamount poles by 49°.

Paleomagnetic studies of the Pacific rim of mainland North America began with the work of Cox (1957) on the Siletz River Volcanic Series of Oregon (locality *S* of Figure 3), which is of Eocene age. These rocks have easterly declinations with a pole in the Atlantic (mean direction 070,+55; error (P = 0.5) = 7°; pole 050W,37N). Cox studied samples from eight sites spaced over a distance of about 60 km and a stratigraphic thickness of about 1000 m. The original attitude of each flow was determined from bedding in associated sediments, and thermal demagnetization studies and the application of Graham's bedding tilt test (Graham, 1949) showed the magnetization to be stable.

Some years later, results were reported by Grommé and Gluskotter (1965) from three large bodies of pillow basalt and diabase in the Franciscan Formation (late Jurassic to late Cretaceous; locality F_1 of Figure 3). These bodies were sampled over a distance of about 20 km just north of San Francisco. Directions were obtained (mean 078,+47 based on seven collecting localities; error (P = 0.05) = 14°; pole 050W,26N) with large easterly declinations, strongly discordant with results from rocks of comparable age from North America (Table I). The original attitudes of the beds were determined from the shape of the lava pillows. The stability of magnetization was established by demagnetization studies.

More recently Saad (1969) has studied Franciscan ultramafic rocks from Red Mountain to the southeast of San Francisco. He found three distinct groups of directions. Saad's group 3 (mean direction 090,+11; error (P = 0.05) = 27°; pole 036W,03N) which he considers to have been acquired "during or immediately after emplacement", gave a pole in the Atlantic, not far from that just described from Franciscan pillow basalt and diabase. Saad's group 2 directions (mean 350,+75; error (P = 0.05) = 6°; pole 132W,66N) occurred in dunite "emplaced and magnetized at a much later time". They gave a pole in Alaska in good

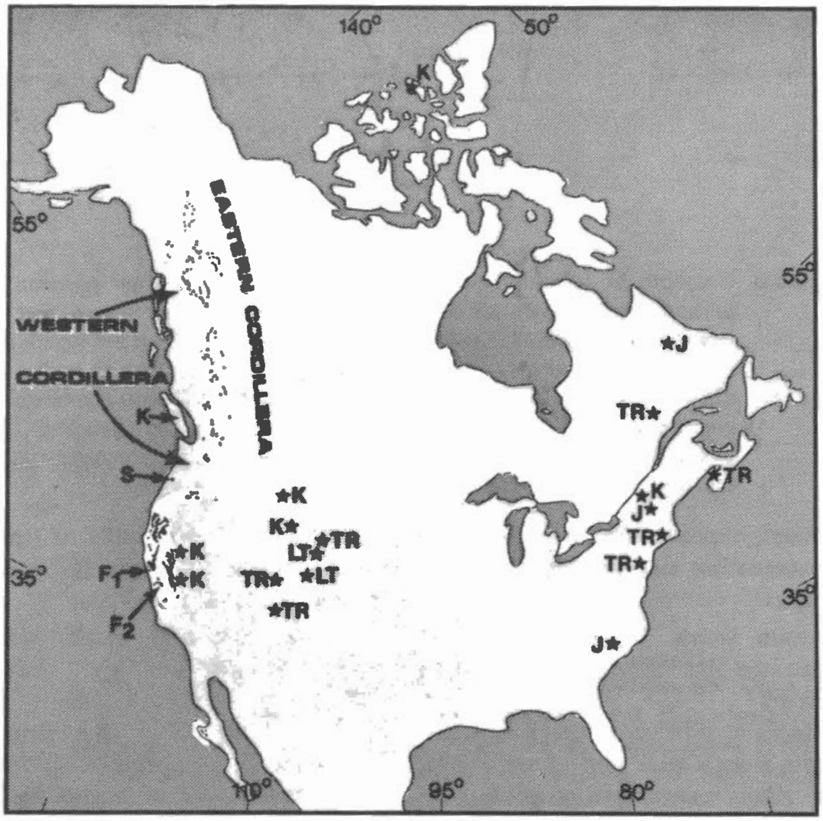

Figure 3. Paleomagnetic sampling localities from the Mesozoic and Paleogene of North America. Localities giving concordant results for the same geological period are indicated by stars and labelled LT (Paleogene), K (Cretaceous), J (Jurassic) and TR (Triassic). Localities giving discordant results (Table I) are indicated by arrows.

Table I
Differences between poles from the Pacific rim and the main body of North America

	Rock Unit	Δ°
S	Siletz volcanics (Eocene)	57
F_1	Franciscan spilites and diabase (Upper Jurassic or Cretaceous)	69,84
F_2	Franciscan ultramafics (Upper Jurassic or Cretaceous)	86,75
K	Karmutsen (Upper Triassic)	55

Δ is the difference in degrees between the corresponding poles for the rock unit and that for stable North America. The error associated with these values is about 10°, on average, and never exceeds 20°. In entries F_1 and F_2 two values are given, which refer to Jurassic and Createaceous poles respectively. The results in F_2 refer to Saad's group 3.

agreement with Cretaceous poles from elsewhere in North America. Saad's group 1 directions occurred in the main peridotite body (mean 045,+59; error (P = 0.05) = 4°; pole 050W,56N). They gave a pole intermediate between those for groups 3 and 2. Saad considered the group 1 directions to have been acquired after the magnetization of group 3. The Red Hill intrusion is thought to have the form of a sill or laccolith folded into a syncline; original attitudes were calculated by Saad from the regional geology by an interpolation technique. The method seems to be justified in that after correction the directions within each group are, with few exceptions, in good agreement.

New results from Vancouver Island

The Karmutsen Volcanic Group (locality *K* of Figure 3) of Vancouver Island comprises over 4000 m of mainly basaltic and andesitic flows (some pillowed), diabase sills, pyroclastic rocks, and sediments. Upper Triassic fossils (late Karnian, Tozer, 1967) occur in the upper part. The sequence is intruded by Jurassic and younger granitic plutons. The Karmutsen has been sampled in the Buttle Lake area (125.6°W,49.7°N) at 11 sites, (three in diabase (D specimens) and eight from lavas (L specimens)) spanning much of the exposed thickness.

Reliable "bedding" attitudes are not easily obtained at the sampling sites, because of the massive nature of most flows and diabases, the abundance of minor faults and joints, and the absence of easily recognizable interlava sediments. At those sites where structural attitudes could not be gained from local sedimentary bedding, pillow lava configurations or flow boundaries, local attitudes were interpolated from regional geological maps.

The magnetization directions after thermal and alternating field (a.f.) cleaning are plotted in Figure 4. There are two distinct sets. The first set (group *A* comprising most samples), even after cleaning, shows high within-site dispersion, all except one site having Fisher (Fisher, 1953) precision indices (k) less than 3. The site mean directions are also poorly grouped (k = 12). The overall mean

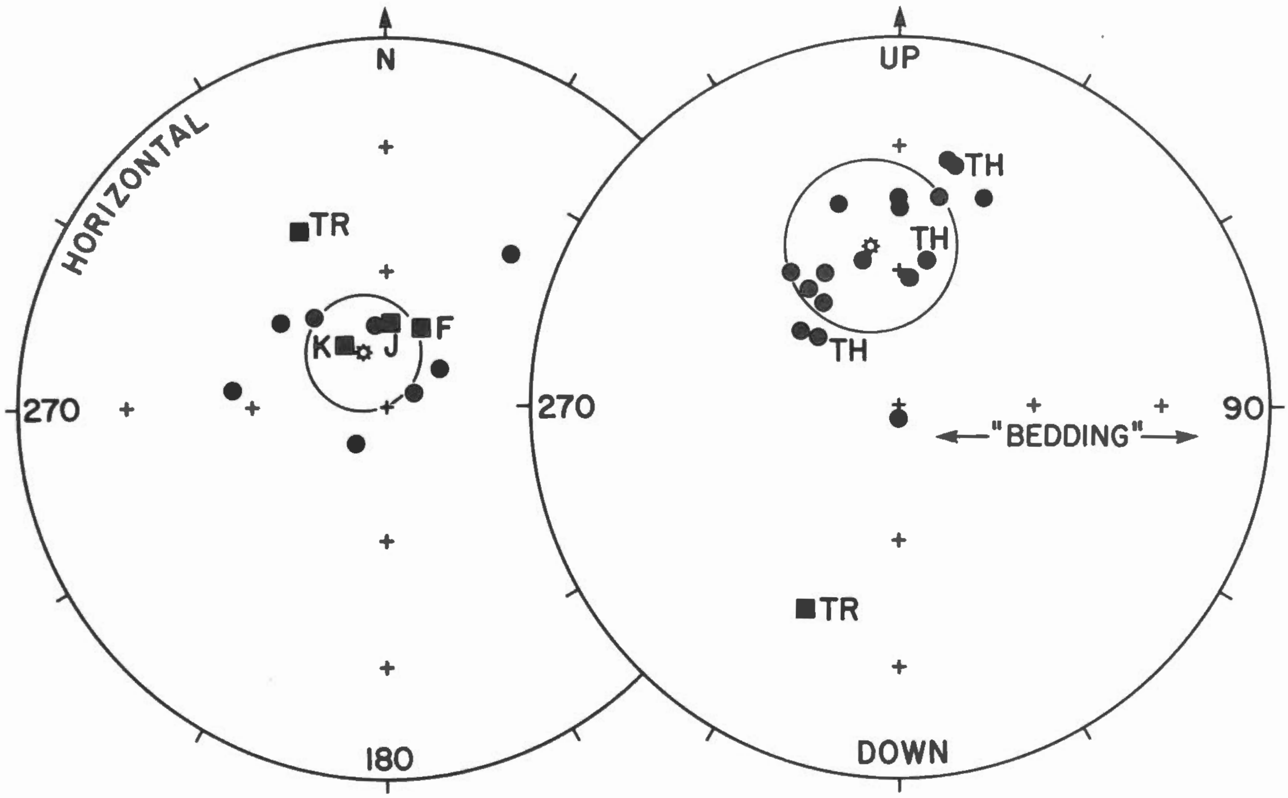

Figure 4. Directions of remanent magnetization in the Karmutsen samples after magnetic cleaning at 150 oersted and thermal cleaning (TH) at 500°C. On the left, means of eight sites (group *A*) are given, the primitive being the horizontal plane. On the right, all the specimen directions of group *B* are given, the primitive being the east-west meridian plane. These differing plotting conventions are adopted to avoid interference between directions on the upper and lower hemispheres. The means and error circles are indicated by stars. The squares labelled TR, J, K, and F are the expected Triassic, Jurassic, Cretaceous and present field directions.

direction with respect to present horizontal (337,+77; error (P = 0.05) = 17°) does not differ significantly from the expected Jurassic and Cretaceous fields; and is only marginally different from the present field. The stability of group *A* is generally very low. The a.f. demagnetization curves fall rapidly and directional stability is poor (Specimen L1 of Figure 5). The mean coercivity (the a.f. required to reduce the n.r.m. intensity by one half) is 60 oersted, which is very low. The blocking temperatures are also low, the decay under thermal demagnetization being rapid and sometimes erratic (Specimens L4 and D2 of Figure 6).

The second group of directions (group *B*) have negative (upward) inclination. The agreement among samples from the same site is good, the mean within-site Fisher precision being 64. The magnetizations are stable, and the mean coercivity is 190 oersted. Under a.f. demagnetization the directions are generally little changed up to 400 oersted (Specimen D3 of Figure 5). The blocking temperatures are high (mostly above 500°C), and the thermal decay curves are square-shouldered and typical of fine-grained magnetite (Specimens L6 and D3 of Figure 6). A further characteristic which distinguishes these two sets is that whereas in *B* the demagnetization curves of anhysteretic remanent magnetization (a.r.m.) and n.r.m. are similar, as is found in recent stably magnetized pillow basalts, in group *A* the two are grossly different (Figure 6) indicating that any original magnetization has been lost (Park and Irving, 1970).

Polished sections of all samples have been studied. The high coercivity, high blocking temperature rocks of group *B* contains iron mineral grains (skeletal in lava L6) commonly ranging in size up to 60μm. They contain well-developed very fine intergrowths of magnetite and ilmenite whose thicknesses range down from 5μm to below the limit of resolution (1μm). The low coercivity, low blocking temperature lavas of group *A* contain grains (commonly skeletal) ranging up to 60μm in which there are no visible intergrowths. These grains contain irregular widely-spaced (10μm spacing is characteristic) cracks, and have granular surfaces and corroded margins. The dolerite of group *A* (D2) contains very large (100 to 1000μm) grains, with intergrowths of ilmenite and magnetite whose thicknesses usually exceed 10μm. Thus, the effective grain size of the magnetic minerals of group *A* rocks is generally in excess of 10μm, whereas that of group *B* rocks is less, commonly very much less, than 5μm. The stability of magnetization of iron minerals depends on grain size, and it seems clear that the unstable

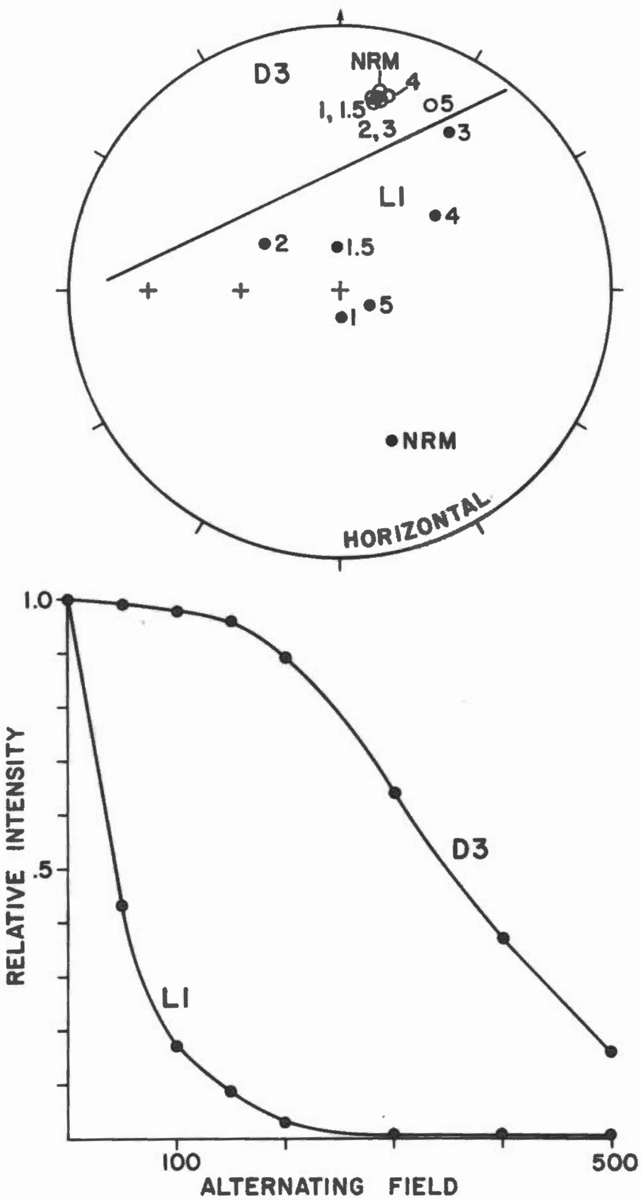

Figure 5. Stability (a.f.) of the Karmutsen groups *A* and *B*. Above, the variation in directions, and below, the decay of intensity, versus strength of alternating field (in oersted peak values). Circles (D3) denote negative (upward) inclinations, and dots (L1) positive inclinations. The numbers in the top diagram denote the field strengths in hundreds of oersted. The contrast between the very rapid decay and wide scatter of the unstable *A* group specimen, and the slow decay and small scatter of the stable *B* group specimen are clearly shown.

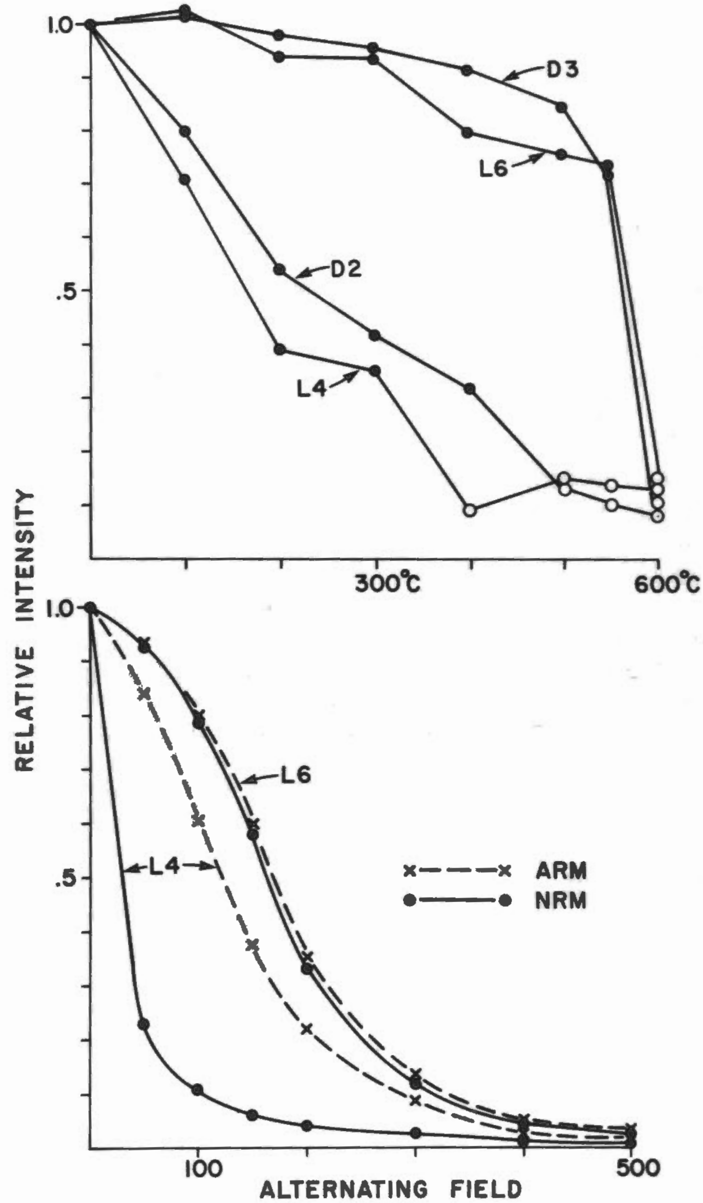

Figure 6. Above is shown the thermal stability of the Karmutsen groups *A* and *B*. L6 and D3 belonging to group (*B*) and D2 and L4 to group *A*. Open circles denote the point at which all the original magnetization has been destroyed and the directions become random. Below, the different rates of decay versus alternating magnetic fields for two of these specimens are shown, together with the comparison of the decay of a.r.m.

magnetization of group *A* is due to the large effective grain size. Although the group *A* magnetizations are generally scattered, they are, on average, directed along a late Mesozoic field (Figure 4), and it seems reasonable to suppose that they were acquired at the time of granite intrusion in the Jurassic when there may have been mild regional heating. The high stability of the Group *B* magnetizations is presumably due to the presence of very fine-grained intergrowths of magnetite. The intergrowth textures are original cooling textures, and hence the group *B* magnetization was probably acquired at the time of formation and is indicative of the field in the Upper Triassic. The mean direction of group *B* with respect to bedding is 354,-35 (error (P = 0.05) = 19°) and the corresponding pole is at 061E,21N. The error is large because the number of sites (three) is small, but the mean is significantly different from the expected Triassic field (Figure 4, Table I). Dips average about 20° to the north over the sampling area.

Discussion of results relevant to the Cordillera

The results from the Pacific seamounts indicate that the latitude of the Pacific plate has increased by about 30° since the Cretaceous whereas the results from the main body of North America indicate, if anything, a decrease in latitude since that time; that is, the Pacific plate has moved northwards with respect to the North America plate by about 3,000 km. Their relative longitudinal movement cannot yet be calculated.

Of the results from the Pacific rim of North America, only those from the Siletz volcanics are straightforward, presumably because they are the youngest rocks and have been the least subject to secondary changes. The discrepancy between the results from Oregon and those of Torreson *et al.* (1949) from Eocene sediments in Colorado, can be accounted for by assuming a clockwise rotation of the Siletz region by 70° relative to the main body of North America (Irving, 1959), a rotation which is similar to that suggested by Carey (Carey, 1958; Ivring, 1964, fig. 10.4) on geological grounds.

In order to explain the discordance between their results from Franciscan mafic rocks and those of comparable age from other parts of the continent, Grommé and Gluskotter listed three possible causes: (1) a clockwise rotation of the entire rock unit by about 70°, (2) the occurrence at that time (late Jurassic or early Cretaceous) of a predominantly non-dipole field, and (3) a temporary excursion of the pole of the dipole field, from its customary late Mesozoic position near the Bering Strait, into the central Atlantic. When discussing his own more complicated results Saad (1969) favoured the latter explanation. He argued that his discordant group 3 directions were acquired at about the time of emplacement during a polar excursion, that his group 2 directions were acquired later when the pole was in its usual position, and that his intermediate group 1 directions were acquired while the pole was in the process of moving. However, Saad's observations are also consistent with the first hypothesis of Grommé and Gluskotter; that the Franciscan region has been rotated clockwise by about 70°. On this view his group 3 directions (since they were acquired at about the time of emplacement) are the only reliable data, and the group 1 and 2 directions, which Saad acknowledges to be secondary and due to a high degree of serpentinization, were acquired during or after rotation.

Similar arguments apply to the Karmutsen results. Those directions that are stable and paleomagnetically reliable are strongly discordant with Triassic data from the rest of North America, whereas those directions that are generally unstable are concordant with later fields. Again it can be argued, either that the stable magnetizations represent a true tectonic discordance, or that they reflect an aberrant field. Although the latter possibility cannot be disproved, it seems to us that the tectonic hypothesis is the more reasonable.

In the four instances from the Pacific rim of North America, representing at least three independent points in time, in which there is evidence that the magnetization was acquired at the time of formation, large significant discordances in direction are found, whereas in the two instances (Saad's group 1 and Karmutsen group *A*) in which the magnetization is of unstable type, the directions have a configuration appropriate to a younger field and are probably secondary. Furthermore, *all* four localities show major discordances, whereas *none* of the 18 Mesozoic and Lower Tertiary units from elsewhere in North America show them; for example, the Cretaceous poles observed at localities spaced from the Sierra Nevada to the eastern and northern coasts of the continent are in excellent agreement (Larochelle, 1968).

The paleomagnetic evidence therefore suggests that the Pacific plate was displaced southward with respect to the North America plate, so that the zone of mafic and ultramafic rocks in the Cordillera (Figure 1) could be parts of oceanic crust trapped in the subduction zone between them. The details of the displacements will not become clear until very much more data are available. However, it is notable that the discrepancies are of two types. The Siletz and Franciscan discrepancies are largely (but not entirely) in declination, so that they can be explained, to a first approximation, by a clockwise twist (rotation about a pivot point near their present location). The discrepancy in Pacific seamounts and in the Karmutsen rocks, however, is largely in inclination, implying a large displacement of several thousand kilometres relative to North America without any gross twist.

The Triassic latitude expected for Vancouver Island from the paleomagnetic data from the main body of North America is 27N, whereas that calculated from the Karmutsen result is 19S, estimates which could be in error by 15°. The implied northward movement of Vancouver Island is consistent with the occurrence, between the Western and Eastern Cordillera, of large post-Triassic faults (the Tintina Trench for example) on which right-lateral transcurrent movements have occurred (Roddick, 1967). Also Tozer (1970) has suggested on faunal grounds "that the warm-water Triassic deposits of the Western Cordillera were originally deposited south of the latitude of the contemporaneous rocks in the Eastern Cordillera". Presumably it was this motion, which in Vancouver Island was terminated by the Nassian orogeny (and therefore occurred within the Jurassic), which realtes to the emplacement of ultrabasic rocks in the Canadian Cordillera. The general northward movement of the Pacific plate relative to the main body of North America continued (Vancouver Island now being part of the North American plate) through the Cretaceous and Tertiary to the present, as the paleomagnetic poles from the Pacific seamounts and as the dextral strike slip motion on the San Andreas and Queen Charlotte Island faults show. Assuming the Jurassic to be of 40 m.y. duration, the relative velocity (north-south component) prior to the Nassian orogeny is of the order 10 cm/yr., which is comparable to that occurring beneath modern ocean trenches.

Appalachian occurrences

If plate tectonic models for the emplacement of Appalachian ophiolites (sites 20 to 26 of the Frontispiece) are correct, then there should be large paleomagnetic discrepancies among the bordering cratons. The opening of the Atlantic during the Mesozoic did not occur exactly along the line of the Caledonian geosyncline so that the comparisons of late Proterozoic results can be made in three ways: (1) within Canada, by comparing results from the Avalon peninsula and the Canadian Shield, (2) within Europe, by comparing results from the Lewisian platform and the Baltic Shield, and (3) by comparing results from the Canadian and Baltic Shields after restoration to their late Paleozoic positions. Should all comparisons show agreement (disagreement) between their late Proterozoic polar paths, then the Caledonian geosyncline was not (was) the site of a wide ocean. Of all the tests applicable (in part) to Canadian terrain this one regarding the emplacement of the Appalachian ophiolites is experimentally the most accessible, because suitable late Proterozoic rocks occur on all six crustal elements, and because the paleomagnetic directions that have been observed from them are roughly perpendicular to the trend of the orogen, which is geometrically the optimum configuration for measuring crustal movements. The first two comparisons are particularly powerful, since they involve no assumptions about post-Caledonian movements.

Franklinian occurrences

There are ultrabasics in northern Ellesmere Island (*see* Irvine and Findlay this volume) associated with Ordovician rocks folded during the Devonian. If these are remnants of Lower Paleozoic oceanic crust then a literal interpretation in terms of plate tectonics would imply that the Franklinian geosyncline was once a wide ocean. The problem may be stated in another way: do the Precambrian rocks which outcrop in northwestern Ellesmere Island represent the re-emergence (from beneath the Franklinian geosyncline) of a northern prolongation of the Canadian Shield, or are they an exotic remnant of continental crust which was formerly displaced by many thousands of kilometres from the Canadian Shield? The problem could be studied by obtaining paleomagnetic observations from northwestern Ellesmere Island and comparing them with results from the Canadian Shield. The task will be a difficult one technically, because the rocks are altered and stable secondary magnetizations will have to be sought.

Precambrian occurrences

A useful starting point for the discussion of the kinematic history of the Canadian Shield is to consider the question of the origin of the Churchill Province. The Churchill Province consists of a series of Aphebian (earliest Proterozoic) geosynclines containing Archean fragments (McGlynn, 1970, fig. 14). These could have been the sites of a successive series of subduction zones (Gibb and Walcott, 1970) which during Aphebian time consumed oceanic lithosphere, so narrowing the wide ocean that formerly separated the Archean Superior and Slave Provinces and the Superior and eastern Nain Provinces. As the oceans contracted, and as the Slave and Nain continental cratons neared the subduction zone peripheral to the Superior craton, buoyancy would prevent their descent, and the resulting continental collision closed the ocean, caused the Hudsonian orogeny (1800 m.y), sealed the intervening rocks into what is now the Churchill Province, and terminated the Aphebian Era. Those parts of the Chruchill Province peripheral to the Superior Province (Manitoba Nickel Belt, Fox River Region, Belcher Islands, Cape Smith Belt, Labrador Trough, *see* Frontispiece), contain mafic and ultramafic rocks with abundant pillow basalt, and it is these that suggest that former existence of a wide ocean between the Archean cratons. These rocks could once have been oceanic lithosphere, which sank beneath a deep ocean trench peripheral to the Superior craton and which became trapped during the Hudsonian orogeny, and sealed into the Canadian Shield.

Such reconstructions are interesting as speculations but have no firm foundation until quantitative estimates of the displacements have first been made. The problem therefore is to measure, paleomagnetically, the pre-Hudsonian relative positions of the Slave and Superior Provinces, of the eastern Nain and Superior Provinces, and of the Archean fragments within the Churchill Province. It may eventually be possible to obtain abundant data on pre-Hudsonian primary magnetization (particularly from late Archean intrusive rocks) but this will undoubtedly be a very difficult task because of the generally altered nature of such old rocks. Another experiment which may be performed on the geographical scale appropriate to the problem, is to study the general phenomenon in metamorphic terrain of secondary magnetization (of Kenoran age in particular) with a time scale provided by the apparent (reset) K-Ar ages. Before this idea can be exploited, basic research into the magnetic properties of metamorphic rocks is needed.

Acknowledgments

Grateful acknowledgment is made to J.K. Park for magnetic measurements and to Dr. J. McGlynn for helpful discussion.

References

Bergeron, R. 1957. *Roy. Soc. Can.*, Spec. Pub. 2, 101-111.

Carey, S.W. 1958. Continental Drift, *Univ. Tasmania*, 177-358.

Cox, A. 1957. *Nature*, 179, 685-686.

Dewey, J.F. and J.M. Bird. 1970. *J. Geophys. Res.*, 75, 2625-2647.

Fisher, R.A. 1953. *Proc. Roy. Soc. Lond.*, 217, 195-305.

Francheteau, J., C.G.A. Harrison, J.G. Sclater and M.L. Richards. 1970. *J. Geophys. Res.*, 75, 2035-2061.

Gibb, R.A. and R.I. Walcott. 1970. Abs. *Geol. Assoc. Can.* Annual meeting Winnipeg, p. 25.

Graham, J.W. 1949. *J. Geophys. Res.*, 54, 131-167.

Grommé, C.S. and H.J. Gluskotter. 1965. *J. Geol.*, 73, 74-94.

Irving, E. 1959. *Geophys. J.*, 2, 51-79.

———1964. Paleomagnetism, Wiley and Sons Inc., New York, 399.

Larochelle, A. 1968. *J. Geophys. Res.*, 73, 3239-3246.

Moores, E. 1970. *Nature*, 228, 837-842.

McGlynn, J.C. 1970. Geology and Economic Minerals of Canada, R. Douglas (editor) *Geol. Surv. Can.* Econ. Geol. Ser. 1, p. 85.

Park, J.K. and E. Irving. 1970. *Can. J. Earth Sci.*, (in press).

Roddick, J.A., 1967. *J. Geol.*, 75, p. 23.

Roy, J.L., N.D. Opdyke and E. Irving. 1968. *J. Geophys. Res.*, 72, 5075-5085.

Runcorn, S.K. 1956. *Proc. Geol. Assoc. Can.*, 8, 77-85.

Saad, A.M. 1969. *J. Geophys. Res.*, 74, 6567-6578.

Torreson, O.W., T. Murphy, and J.W. Graham. 1949. *J. Geophys. Res.*, 54, 111-129.

Tozer, E.T. 1967. *Geol. Surv. Can.* Bull., 156, p. 82.

———1970. Geology and Economic Minerals of Canada, R. Douglas (editor) *Geol. Surv. Can.*, Econ. Geol. Ser. 1, p. 635.

Temple, P.G. and J. Zimmerman. 1969. Abs. *Proc. Geol. Soc. Amer.*, 221.

No. 8

alpine-type peridotite with particular reference to the bay of islands igneous complex

T.N. IRVINE and T.C. FINDLAY
Geological Survey of Canada
Ottawa

Abstract. The characteristics of alpine-type peridotite are reviewed, and some comparisons are made with other kinds of olivine-rich ultramafic rocks. Information is summarized which indicates that such peridotite is rare, if present at all, in the Canadian Shield and only infrequently has associated Ni-sulphide deposits. In some occurrences the mineralogical and chemical relationships suggest that the rock at stage just prior to its final consolidation consisted of olivine, subordinate orthopyroxene, and minor chromite, in association with variable amounts of interstitial picritic liquid.

In the Bay of Islands Igneous Complex in western Newfoundland, alpine-type peridotite forms the floor of a rudely stratiform intrusion in which cumulate feldspathic ultramafic rocks and gabbro have precipitated from a K-poor, Ti-poor, tholeiite magma of low silica activity emplaced into basaltic roof rocks. However, the peridotite itself appears to have been through a partial melting process and to have solidified at considerably greater depths than the feldspathic rocks. It may therefore be residual mantle material. These features are consistent with current opinion that complexes of this type represent sections of oceanic crust and upper mantle.

Acknowledgments

This paper reviews a large number of analytical data on various kinds of ultramafic rocks obtained in studies sponsored by the Geological Survey of Canada in the past 10 years (Tables 1-8). Appreciation is expressed to the Survey Laboratories that provided the data, with particular thanks going to J.A. Maxwell, S. Abbey, S. Courville, W.H. Champ, K.A. Church, D.A. Brown, and R.N. Delabio. Sources of information are indicated throughout the text, but special acknowledgment is given for data used from a thesis dissertation by W.J. Wolfe (1966). Chemical analyses illustrated for Mount Albert rocks are from samples collected by C.H. Smith and I.D. MacGregor. The Bay of Islands data were obtained by the second author; the review section of the paper was prepared by the first author. The manuscript was critically read by W.R.A. Baragar, O.R. Ekstrand, T.M. Gordon, H. Helmstaedt, G.B. Skippen and D.R.E. Whitmore, whose comments and suggestions have contributed substantially to its improvement. E. Froese also gave helpful consultation.

Introduction

Although it is widely believed that the alpine-type peridotite of Phanerozoic orogenic belts was largely solid when emplaced in its exposed positions (Smith, 1958; Moores, 1969; Wyllie, 1970), opinions differ greatly as to its origin. Two interpretations have received most attention. One, advocated especially by Thayer (1964, 1967, 1969), is that the peridotite, together with associated chromitite, pyroxenite, and gabbro, formed by magmatic differentiation, at least in part by crystal settling in intrusions in the deep crust or upper mantle (see also Challis, 1965). The other, which has become increasingly popular along with the concept of plate tectonics, is that the peridotite is the depleted residue of more primitive mantle material from which basaltic and other materials have been removed by partial fusion (e.g. Hess, 1964; Green and Ringwood, 1967; Dickey, 1970; Dewey and Bird, 1970; Bonnatti, Honnorez and Ferrara, 1970). Despite their great difference, these possibilities are not easily distinguishable petrologically because they involve the same kinds of crystal-liquid equilibria. In this paper, we first summarize several criteria that appear useful in making the distinction. This section serves also to introduce the terminology and certain of the concepts involved. The characteristics of alpine-type peridotite are then reviewed.

Finally we present and discuss data from the Bay of Islands Igneous Complex in western Newfoundland that appear relevant to the problem.

Criteria for distinguishing products of fractional crystallization from residues of partial melting

The postulate that an ultramafic rock is an accumulation of mafic minerals settled from magma does not necessarily require that the minerals be formed by progressive fractional crystallization (they might, for example, have settled from a suspension), although this is likely if there has been appreciable differentiation. The evidence that some ultramafic rocks are products of fractional crystallization comes mainly from stratiform layered intrusions, like the Stillwater and Muskox intrusions, in which the rocks are precipitates from basaltic magmas. The evidence is principally of three types:

(1) Layering structures and textural features that show that the rocks consist of settled (cumulus) crystals cemented together by a later (post-cumulus) generation of materials crystallized from pore (intercumulus) magma (Hess, 1960; Wager, Brown and Wadsworth, 1960; Jackson, 1961; Irvine, 1965a).

(2) Layer sequences, such as peridotite-pyroxenite-gabbro, in which the succes-

TABLE 1. MAJOR CHEMICAL CONSTITUENTS IN ROCKS FROM THE MOUNT ALBERT ULTRAMAFIC COMPLEX.

			WEIGHT PERCENT												
SAMPLE	FOOTAGE	ROCK	SIO2	AL2O3	FE2O3	FEO	MGO	CAO	NA2O	K2O	TIO2	P2O5	MNO	NIO	CR2O3
57- 8		ALP PD	38.7	3.2	0	8.6	37.0	1.7	.1	0	.01	0	.15	.25	.28
57- 17		ALP PD	35.6	2.5	0	7.7	37.8	.7	.1	0	0	0	.12	.32	.23
57- 25		ALP PD	36.6	.8	0	6.5	41.4	.2	.1	0	0	0	.11	.29	.29
57- 41		ALP PD	36.6	2.8	0	6.4	40.8	.4	.1	0	0	0	.11	.28	.42
57- 44		ALP PD	35.4	3.8	0	6.8	41.1	.2	.1	0	0	0	.12	.29	.85
57- 45		ALP PD	35.2	2.6	0	7.4	38.8	.3	.1	0	0	0	.15	.22	.58
57- 52		ALP PD	37.0	2.7	0	6.8	39.7	.3	.1	0	0	0	.14	.32	.29
57- 56		ALP PD	38.7	2.6	0	6.7	38.2	.4	.1	0	0	0	.12	.24	.32
57- 57		ALP PD	39.5	3.3	0	7.7	35.2	.8	.1	0	0	0	.17	.29	.29
57- 60		ALP PD	36.0	2.4	0	7.1	40.3	.4	.1	0	0	0	.14	.39	.23
57- 91		ALP PD	40.0	2.6	0	7.4	38.9	.5	.1	0	0	0	.15	.33	.29
57- 95		OL OPXN	48.1	7.4	0	6.0	29.9	2.4	.1	0	.42	0	.16	.28	.84
57- 105		ALP PD	39.7	4.0	0	7.6	36.1	1.5	.1	0	.01	0	.15	.38	.32
57- 117		ALP PD	39.4	4.0	0	7.9	38.4	1.6	.1	0	.01	0	.15	.29	.36
57- 118		ALP PD	41.0	3.5	0	7.5	36.3	1.8	.1	0	.01	0	.15	.31	.34
57- 124		ALP PD	40.9	4.7	0	7.4	34.3	2.2	.1	0	.01	0	.14	.34	.41
57- 126		ALP PD	37.5	2.1	0	6.7	37.7	.5	.1	0	0	0	.11	.46	.23
57- 131		ALP PD	40.1	3.5	0	7.6	34.8	1.7	.1	0	.01	0	.14	.28	.32
57- 144		ALP PD	38.7	3.2	0	6.8	34.9	.7	.1	0	0	0	.13	.46	.04
57- 150		ALP PD	40.7	3.2	0	6.8	36.6	1.9	.1	0	.01	0	.12	.18	.04
57- 165		ALP PD	39.5	3.1	0	7.6	37.0	1.0	.1	0	0	0	.14	.23	.35
57- 186		ALP PD	38.1	2.3	0	7.6	37.8	.7	.1	0	0	0	.13	.32	.31
57- 246		ALP PD	39.4	2.9	0	6.7	35.2	.9	.1	0	0	0	.12	.33	.50
57- 262		ALP PD	38.6	2.1	0	5.1	36.2	.4	.1	0	0	0	.08	.38	.29
57- 268		ALP PD	33.7	2.3	0	6.4	39.9	.4	.1	0	0	0	.10	.31	.35
57- 269		ALP PD	34.8	2.8	0	7.4	38.7	.4	.1	0	0	0	.12	.36	.41
57- 270		ALP PD	35.3	2.0	0	6.4	36.3	.4	.1	0	0	0	.11	.37	.28
57- 504		ALP PD	37.5	1.8	0	6.8	41.5	.8	.1	0	.01	0	.11	.33	.39
57- 528		ALP PD	39.3	2.1	0	7.3	42.8	.8	.1	0	.01	0	.12	.34	.25
57- 570		ALP PD	35.9	1.7	0	7.4	39.9	.5	.1	0	.01	0	.13	.36	.32
57- 612		ALP PD	39.1	2.5	0	7.5	37.9	1.0	.1	0	.03	0	.13	.36	.47
57- 621		ALP PD	38.8	3.1	0	7.0	37.7	1.9	.1	0	.01	0	.13	.32	.53
57- 628		ALP PD	36.2	1.8	0	6.7	39.9	.5	.1	0	0	0	.13	.23	.31

NOTES.

1. ALL SAMPLE NUMBERS HAVE A SDM-PREFIX.
2. SYMBOLS. ALP PD = ALPINE-TYPE PERIDOTITE, OL OPXN = OLIVINE ORTHOPYROXENITE.
3. FEO REPRESENTS TOTAL IRON. FE2O3 NOT DETERMINED.
4. NA2O NOT DETERMINED. ASSUMED TO BE 0.1 PERCENT FOR CALCULATION PURPOSES.
5. K2O AND P2O5 NOT DETERMINED.
6. TIO2, NIO AND CR2O3 BY EMISSION SPECTROGRAPHIC METHODS.
7. OTHER CONSTITUENTS BY X-RAY FLUORESCENCE.
8. ANALYSES BY THE ANALYTICAL CHEMISTRY SECTION, GEOLOGICAL SURVEY OF CANADA.

TABLE 2. MAJOR CHEMICAL CONSTITUENTS IN ROCKS FROM
BAY OF ISLANDS IGNEOUS COMPLEX, TABLE MOUNTAIN PLUTON

SAMPLE	FOOTAGE	ROCK	SIO2	AL2O3	FE2O3	FEO	MGO	CAO	NA2O	K2O	TIO2	P2O5	MNO	NIO	CR2O3
			WEIGHT PERCENT												
64- 87K	2678	FELD DN	37.7	5.6	3.6	4.7	33.1	3.3	.1	0	.41	.01	.12	.24	.31
64- 87J	2670	FELD DN	34.0	4.9	4.0	4.1	34.2	1.9	.1	0	.45	.01	.12	.29	.52
64- 87I	2665	FELD DN	34.4	4.8	3.4	4.6	35.3	2.2	.1	0	.18	.01	.11	.27	.70
64- 87F	2650	FELD DN	38.3	8.5	2.5	5.8	27.2	5.8	.2	0	.09	.01	.13	.12	.56
64- 87E	2645	FELD DN	39.0	6.4	3.2	5.5	32.0	5.3	.2	0	.12	.01	.12	.18	.57
64- 87B	2628	TROCT	40.2	14.5	2.3	4.7	20.9	9.1	.5	0	.07	0	.10	.02	.05
64- 95	2710	GABBRO	45.6	18.1	1.1	3.8	7.2	14.3	1.0	0	.17	.01	.08	.02	.11
64- 87N	2688	OL GABB	43.8	17.5	.7	2.4	8.5	15.4	1.2	.18	.12	0	.03	.03	.17
64- 87H	2658	OL GABB	40.1	20.5	.2	2.5	7.9	18.4	.6	0	.41	.01	.01	.03	.14
64- 87G	2651	OL GABB	39.3	20.4	.3	2.5	7.9	18.1	.5	0	.04	.01	.02	.02	.08
64- 87D	2644	OL GABB	38.6	18.5	.3	3.6	9.6	17.8	.4	.17	.18	.01	.03	.02	.15
64- 87C	2636	OL GABB	40.7	18.6	0	3.7	11.9	18.2	.2	0	.09	0	.03	.02	.11
64- 87A	2627	OL GABB	42.1	22.7	.5	2.8	9.2	15.5	1.1	0	.07	0	.03	.03	.08
64- 96	2565	OL GABB	45.9	17.2	.9	4.8	5.5	12.6	3.1	.15	.33	0	.09	.02	.06
64-111C	2367	OL GABB	39.8	16.6	2.9	3.1	16.2	9.3	2.6	0	.13	0	.08	.02	.07
64-111B	2365	OL GABB	44.4	21.1	0	4.3	4.5	13.9	.8	0	.04	0	.06	.06	.07
64-111A	2362	OL GABB	41.7	23.2	.4	2.7	7.1	15.5	.8	0	.07	0	.02	.04	.06
64- 99	2340	OL GABB	44.1	22.1	.5	3.6	8.1	13.3	1.7	0	.09	0	.05	.02	.06
64-113B	2308	OL GABB	42.4	19.4	.9	5.3	11.2	10.9	1.6	0	.04	0	.06	.04	.02
64-112	2300	OL GABB	46.1	21.3	.9	3.5	5.4	13.3	2.5	0	.18	0	.04	.01	.04
64- 61	2270	OL GABB	46.2	20.6	.1	3.5	9.1	13.9	2.1	0	.14	0	.02	.03	.11
64- 60B	2252	OL GABB	46.3	21.2	.5	3.3	6.4	14.9	1.9	0	.17	0	.05	.02	.04
64- 58	2237	GABBRO	44.4	18.3	.1	3.3	8.2	14.9	1.7	0	.11	0	.04	.02	.07
64- 56	2193	OL GABB	45.5	18.9	.8	3.2	12.3	13.5	1.0	0	.11	0	.05	.04	.28
64- 52	2158	OL GABB	48.0	19.4	.2	3.2	6.2	16.0	1.5	0	.18	0	.06	.01	.10
64- 55B	2151	FELD DN	34.9	6.2	2.9	4.5	32.3	2.4	2.6	0	.08	0	.12	.13	.54
64- 55A	2150	OL GABB	38.0	21.7	0	5.3	10.2	15.3	.9	.20	.20	0	.06	.01	.03
64- 48D	2113	OL GABB	46.1	21.6	.6	2.8	8.1	14.8	1.1	0	.08	0	.05	.03	.15
64- 48A	2105	OL GABB	42.1	19.7	.5	3.0	11.7	12.0	.9	0	.03	0	.06	.04	.16
64- 48B	2108	TROCT	45.7	21.7	.2	2.9	8.1	14.7	1.6	0	.09	0	.05	.02	.16
64- 49	2096	OL CPXN	48.8	4.3	.3	4.8	21.8	16.9	.2	0	.10	0	.10	.04	.37
64- 50A	2082	OL CPXN	51.3	3.0	.4	4.8	17.7	18.0	.1	0	.06	0	.11	.05	.44
64- 50B	2078	FELD DN	32.0	2.9	5.2	4.3	36.8	.5	.1	0	.01	0	.12	.14	.75
64- 47	2075	FELD DN	38.8	3.1	2.7	4.8	37.7	1.1	.1	0	0	0	.11	.23	.32
64- 50C	2073	ALP PD	38.3	2.3	3.6	3.8	38.5	.9	.1	0	0	0	.11	.32	.32
64- 51	2060	ALP PD	36.6	2.5	2.9	4.4	36.2	1.0	.1	0	0	0	.12	.24	.39

TABLE 2. CONTINUED.

SAMPLE	FOOTAGE	ROCK	SIO2	AL2O3	FE2O3	FEO	MGO	CAO	NA2O	K2O	TIO2	P2O5	MNO	NIO	CR2O3
					WEIGHT PERCENT										
64- 44	1895	ALP PD	37.3	2.3	2.8	3.9	37.2	.8	.1	0	0	0	.10	.30	.28
64- 43	1839	ALP PD	38.4	2.2	2.4	4.4	37.5	.9	.1	0	0	0	.10	.34	.57
64- 42	1695	ALP PD	36.4	1.9	3.3	3.8	37.5	1.0	.1	0	0	0	.11	.23	.35
64- 41	1618	ALP PD	34.9	1.6	2.9	3.0	38.1	.7	.1	0	0	0	.08	.23	.34
64- 40	1472	ALP PD	34.4	1.9	4.5	2.7	32.7	.9	.1	0	0	0	.10	.25	.41
64- 34	1228	ALP PD	35.4	2.0	3.7	3.4	37.7	.4	.1	0	0	.01	.10	.27	.31
64- 31A	1148	ALP PD	37.2	2.4	4.5	3.3	39.1	.6	.1	0	0	0	.10	.28	.37
64- 29	963	ALP PD	39.7	1.9	4.8	2.7	41.5	.8	.1	0	0	0	.10	.23	.44
64- 28	875	ALP PD	39.5	2.8	3.7	3.4	40.3	.5	.1	0	0	.01	.11	.20	.37
64- 27	786	ALP PD	39.3	2.2	3.3	3.3	44.9	.5	.1	0	0	0	.08	.28	.26
64- 26A	745	ALP PD	37.3	2.0	4.7	2.5	41.9	.4	.1	0	0	0	.10	.23	.31
64- 25	532	ALP PD	38.7	2.4	4.2	3.0	40.6	.8	.1	0	0	0	.09	.23	.44
64- 24A	415	ALP PD	36.9	1.8	3.8	3.4	41.9	.6	.1	0	0	0	.09	.28	.23
64- 16A	370	ALP PD	37.4	2.5	4.1	3.3	37.6	.8	.1	0	0	0	.10	.38	.32
64- 18	350	ALP PD	38.2	2.3	3.3	3.6	42.4	.7	.1	0	0	0	.08	.38	.37
64- 15	105	ALP PD	36.6	1.4	4.2	3.2	41.1	.5	.1	0	0	0	.10	.17	.13
64- 12A	80	ALP PD	41.3	2.4	2.7	4.4	40.0	.7	0	0	0	0	.10	.23	.29

NOTES.

1. ALL SAMPLE NUMBERS HAVE A FJBT-PREFIX.
2. THE ≠FOOTAGE≠ VALUES ARE IN ARBITRARY UNITS PROGRESSING FROM SOUTHEAST TO NORTHWEST ACROSS THE PLUTON. THEY SERVE GENERALLY TO PUT THE SAMPLES IN APPROXIMATE STRATIGRAPHIC SEQUENCE, BUT THE TOP OF THE PLUTON IS REACHED AT 2367 AND THE REMAINING SAMPLES CONSTITUTE A SEQUENCE BACK DOWN INTO THE CRITICAL ZONE.
3. ROCK SYMBOLS. ALP PD = ALPINE-TYPE PERIDOTITE, FELD DN = FELDSPATHIC DUNITE, OL CPXN = OLIVINE CLINOPYROXENITE, TROCT = TROCTOLITIC GABBRO, OL GABB = OLIVINE GABBRO, GABBRO = OLIVINE-FREE GABBRO, HB GABB = HORNBLENDE GABBRO, CONT RK = CONTACT OR COUNTRY ROCK, AB GRAN = ALBITE GRANITE. SOME OF THE GABBROIC ROCKS ARE ALTERED TO THE EXTENT THAT IT IS UNCERTAIN WHETHER THEY CONTAINED OLIVINE. HOWEVER, OLIVINE GABBRO IS PREDOMINANT AMONG THE LESS ALTERED SAMPLES, THEREFORE IN CASES OF DOUBT IT IS ASSUMED TO HAVE BEEN THE ORIGINAL ROCK.
4. FEO DETERMINED CHEMICALLY.
5. NA2O BY FLAME PHOTOMETRY.
6. TIO2, NIO AND CR2O3 BY EMISSION SPECTROGRAPHIC METHODS.
7. TOTAL IRON AND OTHER CONSTITUENTS BY X-RAY FLUORESCENCE METHODS.
8. ANALYSES BY THE ANALYTICAL CHEMISTRY SECTION, GEOLOGICAL SURVEY OF CANADA.

TABLE 3. MAJOR CHEMICAL CONSTITUENTS IN ROCKS FROM
BAY OF ISLANDS IGNEOUS COMPLEX, NORTH ARM MOUNTAIN, WEST

SAMPLE	FOOTAGE	ROCK	SIO2	AL2O3	FE2O3	FEO	MGO	CAO	NA2O	K2O	TIO2	P2O5	MNO	NIO	CR2O3
			WEIGHT PERCENT												
64-651C	3595	OL GABB	47.7	15.5	2.5	6.7	7.5	13.6	3.6	0	1.67	.09	.13	.01	.04
64-651A	3562	OL GABB	47.3	17.4	.7	4.4	5.0	15.4	3.7	.17	1.37	.07	.06	0	.03
64-640	3463	OL GABB	46.7	18.8	1.5	4.6	8.6	12.4	2.8	.11	.47	0	.08	0	.03
64-614	3432	AB GRAN	75.5	13.2	1.5	1.3	1.2	1.1	6.0	.11	.17	.02	.05	0	0
64-639	3398	OL GABB	44.5	25.9	1.5	2.4	5.1	13.0	2.1	0	.16	0	.02	.02	.02
64-638	3305	GABBRO	49.1	21.6	1.5	4.4	4.9	12.0	2.9	.22	.18	0	.16	.01	.05
64-636	3070	OL GABB	43.2	21.6	.7	4.3	9.5	12.4	1.7	0	.27	.01	.07	.01	.04
64-634	2822	OL GABB	46.2	20.1	.4	4.3	7.7	11.7	3.1	.10	.28	.01	.07	.01	.05
64-632	2632	OL GABB	48.4	18.3	1.5	5.0	9.4	13.1	2.5	0	.27	.01	.12	.01	.05
64-737	2448	OL GABB	45.9	22.7	.7	4.6	8.2	13.1	2.3	0	.20	.01	.09	.02	.05
64-546A	2230	OL GABB	46.3	20.7	.6	4.0	11.8	13.5	1.9	0	.17	.01	.06	.03	.06
64-537	2090	GABBRO	50.6	21.5	.9	2.8	4.7	15.6	2.6	0	.15	0	.09	.01	.01
64-540	1930	OL GABB	45.3	24.5	.7	2.3	6.1	16.1	1.8	0	.09	0	.05	.01	.02
64-745	1762	GABBRO	48.2	22.9	.5	4.8	7.1	14.7	.9	0	.14	0	.11	.01	.04
64-746	1692	GABBRO	47.4	20.2	.3	5.6	8.6	12.9	1.4	.31	.08	.01	.12	0	.01
64-747	1537	ALP PD	37.6	2.0	4.3	3.4	39.9	1.1	.1	0	0	0	.12	.23	.04
64-710	1338	ALP PD	34.7	1.5	3.6	3.7	40.3	.8	.1	0	0	0	.10	.29	.31
64-721	1262	ALP PD	37.3	2.6	3.5	3.4	41.8	.8	.1	0	0	0	.11	.29	.35
64-723	1082	ALP PD	36.8	2.4	3.9	3.4	40.8	.6	.1	0	0	0	.12	.42	.32
64-715	798	ALP PD	35.3	1.8	4.0	3.6	41.1	.5	.1	0	0	0	.12	.28	.37
64-716	670	ALP PD	35.2	2.1	4.5	3.4	41.0	.7	.1	0	0	.01	.12	.31	.32
64-717	614	ALP PD	35.4	1.9	4.7	3.4	38.4	1.4	.1	0	0	0	.12	.32	.32
64-797	445	ALP PD	39.1	2.8	3.0	3.8	44.4	.7	.1	0	0	0	.12	.19	.31
64-796	285	ALP PD	39.2	2.7	3.0	4.5	41.2	1.4	.1	0	0	.01	.13	.18	.34
64-779	262	ALP PD	39.1	2.3	2.2	4.1	41.1	1.9	.1	0	0	0	.10	.32	.34
64-777	213	ALP PD	39.7	2.8	3.2	4.9	38.4	1.6	.1	0	0	.01	.15	.33	.35
64-775	188	ALP PD	37.0	2.3	4.1	4.2	41.8	.9	.1	0	0	0	.13	.35	.02
64-895	177	ALP PD	37.2	2.4	3.3	3.8	38.1	1.8	.5	0	0	.01	.11	.31	.31
64-896	162	CONT RK	47.9	14.7	.5	11.2	11.0	8.3	3.5	.84	1.50	.11	.27	.01	.02
64-894	154	CONT RK	48.2	17.4	1.9	7.6	7.7	10.3	3.8	1.21	1.17	.14	.18	.01	.03
64-893A	142	CONT RK	47.2	21.0	3.1	5.6	4.7	9.8	4.4	1.23	.85	.13	.14	.01	.03
64-878	92	CONT RK	70.8	16.2	.6	4.2	2.2	.6	2.5	2.50	.70	.08	.14	0	.01
64-874	53	CONT RK	78.7	12.4	1.0	2.2	2.9	.4	1.7	2.62	.50	.04	.05	0	0

NOTES.

1. ALL SAMPLE NUMBERS HAVE A FJBN-PREFIX.
2. THE ≠FOOTAGE≠ VALUES ARE IN ARBITRARY UNITS PROGRESSING FROM SOUTHEAST TO NORTHWEST ACROSS THE PLUTON. THEY SERVE GENERALLY TO PUT THE SAMPLES IN APPROXIMATE STRATIGRAPHIC SEQUENCE.
3. FOR OTHER RELEVANT NOTES SEE TABLE 2.

TABLE 4. MAJOR CHEMICAL CONSTITUENTS IN ROCKS FROM
BAY OF ISLANDS IGNEOUS COMPLEX, NORTH ARM MOUNTAIN, EAST.

						WEIGHT PERCENT									
SAMPLE	FOOTAGE	ROCK	SIO2	AL2O3	FE2O3	FEO	MGO	CAO	NA2O	K2O	TIO2	P2O5	MNO	NIO	CR2O3
64-505	2195	HB GABB	42.7	13.2	2.2	7.0	10.0	10.8	2.7	.58	1.22	0	.14	.02	.02
64-511	1902	HB GABB	46.8	19.8	.8	5.2	5.6	12.7	3.4	0	.73	.06	.08	0	.03
64-513	1680	OL GABB	45.3	25.7	.6	1.6	4.8	14.2	2.1	.10	.08	0	.01	.02	.05
64-525	1445	OL GABB	46.7	15.4	.9	5.8	7.6	13.2	2.4	0	.37	0	.11	.02	.10

NOTES.

1. ALL SAMPLE NUMBERS HAVE A FJBN-PREFIX.
2. FOR OTHER RELEVANT NOTES SEE TABLE 3.

TABLE 5. MINERALOGICAL DATA AND TRACE ELEMENT ABUNDANCES FOR ROCKS FROM THE MOUNT ALBERT ULTRAMAFIC COMPLEX.

SAMPLE	FOOTAGE	ROCK	MOL. PCT FO IN OLIVINE	Å CHROMITE CELL EDGE	BA	CO	CR	CU	NI	SC	SR	V	ZN	ZR
					PARTS PER MILLION									
57- 8		ALP PD	91.2	8.150	13	94	1900		2000	0		36		
57- 17		ALP PD	90.2	8.170	12	120	1500		2500	0		0		
57- 25		ALP PD	90.6	8.320	0	77	2000		2300	0		0		
57- 41		ALP PD	91.6	8.275	0	76	2900		2200	0		37		
57- 44		ALP PD	90.5	8.315	12	87	5800		2300	0		0		
57- 45		ALP PD	90.6	8.310	0	65	4000		1700	0		0		
57- 52		ALP PD	91.2	8.315	0	97	2000		2500	0		0		
57- 56		ALP PD	90.9	8.270	0	90	2200		1900	0		0		
57- 7		ALP PD		8.225	0	120	2000		2300	0		0		
57- 60		ALP PD	90.5	8.240	0	140	1600		3100	0		0		
57- 91		ALP PD	91.0	8.290	0	160	2000		2600	0		16		
57- 95		OL OPXN		8.145	0	130	5800		2200	59		64		
57- 105		ALP PD		8.170	0	160	2200		3000	0		63		
57- 117		ALP PD	89.6	8.150	0	96	2500		2300	0		68		
57- 118		ALP PD		8.155	8	170	2300		2400	0		71		
57- 124		ALP PD	89.7	8.155	0	170	2800		2700	0		31		
57- 126		ALP PD	91.2	8.280	0	200	1600		3600	0		79		
57- 131		ALP PD	90.0	8.145	0	130	2200		2200	0		64		
57- 144		ALP PD	89.7	8.215	0	220	240		3500	0		32		
57- 150		ALP PD	90.0	8.160	0	55	290		1400	0		26		
57- 165		ALP PD		8.220	10	64	2400		1800	0		40		
57- 186		ALP PD		8.280	10	100	2100		2500	0		0		
57- 246		ALP PD	90.0	8.225	12	100	3400		2600	0		0		
57- 262		ALP PD	90.6	8.295	0	110	2000		3000	0		0		
57- 268		ALP PD	91.2	8.315	0	110	2400		2400	0		0		
57- 269		ALP PD	90.1	8.265	8	100	2800		2800	0		0		
57- 270		ALP PD		8.300	0	0	1900		2900	0		0		
57- 504		ALP PD	90.6	8.150	8	100	2700		2600	0		37		
57- 528		ALP PD	89.4	8.200	16	140	1700		2700	0		0		
57- 570		ALP PD	90.6	8.260	0	0	2200		2800	0		0		
57- 612		ALP PD	89.0	8.150	18	210	3200		2800	0		0		
57- 621		ALP PD	89.5	8.160	13	170	3600		2500	0		62		
57- 628		ALP PD	91.2	8.280	0	120	2100		1800	0		0		

NOTES.

1. ALL SAMPLE NUMBERS HAVE A SDM-PREFIX.
2. SYMBOLS. ALP PD = ALPINE-TYPE PERIDOTITE, OL OPXN = OLIVINE ORTHOPYROXENITE.
3. OLIVINE COMPOSITIONS AND CHROMITE CELL EDGE DATA BY X-RAY METHODS. DATA FROM MACGREGOR AND SMITH (1962).
4. TRACE ELEMENT DATA BY EMISSION SPECTROGRAPHIC METHODS. FOR SENSITIVITY VALUES SEE TABLE 6.
5. ANALYSES BY THE ANALYTICAL LABORATORIES OF THE GEOLOGICAL SURVEY OF CANADA.

TABLE 6. MINERALOGICAL DATA AND TRACE ELEMENT ABUNDANCES FOR ROCKS FROM BAY OF ISLANDS IGNEOUS COMPLEX, TABLE MOUNTAIN PLUTON

SAMPLE	FOOTAGE	ROCK	MOL PCT FO IN OLIVINE	Å CHROMITE CELL EDGE	BA	CO	CR	CU	NI	SC	SR	V	ZN	ZR
					PARTS PER MILLION									
64- 87K	2678	FELD DN	86.8	8.251	0	160	2100	44	1900	0	0	57	55	0
64- 87J	2670	FELD DN	89.3		0	140	3600	14	2300	0	0	52	50	0
64- 87I	2665	FELD DN	87.5	8.233	0	150	4800	70	2100	0	0	40	50	0
64- 87F	2650	FELD DN	83.7	8.280	9	74	3800	66	910	0	0	100	70	0
64- 87E	2645	FELD DN	84.6		12	85	3900	56	1400	0	0	140	70	0
64- 87B	2628	TROCT	84.6		13	0	320	200	120	55	170	87	60	0
64- 95	2710	GABBRO			12	0	720	50	160	0	160	95	50	0
64- 87N	2688	OL GABB			14	0	1200	60	240	0	220	110	20	0
64- 87H	2658	OL GABB			20	0	960	4	210	0	240	64	20	0
64- 87G	2651	OL GABB			13	0	550	6	140	0	340	88	20	0
64- 87D	2644	OL GABB			23	0	1000	8	150	0	160	140	20	0
64- 87C	2636	OL GABB			12	0	770	24	190	0	56	110	40	0
64- 87A	2627	OL GABB			14	0	530	48	260	0	280	64	30	0
64- 96	2565	OL GABB			24	0	400	50	160	0	230	170	40	0
64-111C	2367	OL GABB			16	0	490	14	140	0	190	120	25	0
64-111B	2365	OL GABB	83.4		13	69	460	16	500	0	120	0	30	0
64-111A	2362	OL GABB			17	0	440	42	300	0	270	55	25	0
64- 99	2340	OL GABB			17	0	430	40	160	0	270	0	30	0
64-113B	2308	OL GABB			25	0	120	112	290	0	220	0	50	0
64-112	2300	OL GABB			16	0	320	52	110	0	210	97	40	0
64- 61	2270	OL GABB			10	50	750	80	230	0	110	140	45	0
64- 60B	2252	OL GABB	77.2		8	37	280	66	140	0	70	150	30	0
64- 58	2237	GABBRO	0		20	0	470	190	190	0	91	160	40	0
64- 56	2193	OL GABB	86.3		13	0	1900	76	310	0	57	140	40	0
64- 52	2158	OL GABB	78.6		20	0	710	64	110	0	110	180	30	0
64- 55B	2151	FELD DN	90.0	8.253	11	53	3700	12	1000	0	0	71	50	0
64- 55A	2150	OL GABB			28	62	200	4	110	100	2500	220	20	0
64- 48D	2113	OL GABB			11	0	1000	76	220	0	51	91	50	0
64- 48A	2105	OL GABB	84.9		10	20	1100	70	320	0	180	50	45	0
64- 48B	2108	TROCT			15	43	1100	8	190	0	190	11	35	0
64- 49	2096	OL CPXN	84.2		9	0	2500	36	300	120	0	19	45	0
64- 50A	2082	OL CPXN	83.7		111	0	3000	330	410	140	0	18	65	0
64- 50B	2078	FELD DN	84.7	8.266	5	130	5100	4	1100	0	0	40	55	0
64- 47	2075	FELD DN	89.9	0	0	95	2200	4	1800	0	0	65	50	0
64- 50C	2073	ALP PD	91.4	8.206	4	120	2200	4	2500	100	0	57	50	0
64- 51	2060	ALP PD	90.7	8.194	0	73	2700	6	1900	0	0	52	45	0

TABLE 6. CONTINUED.

SAMPLE	FOOTAGE	ROCK	MOL PCT FO IN OLIVINE	Å CHROMITE CELL EDGE	PARTS PER MILLION BA	CO	CR	CU	NI	SC	SR	V	ZN	ZR
64- 44	1895	ALP PD	90.9	8.208	0	160	1900	4	2400	0	0	63	50	0
64- 43	1839	ALP PD	87.8	8.207	0	150	3900	2	2700	0	0	83	50	0
64- 42	1695	ALP PD	89.0	8.220	0	130	2400	4	1800	0	48	78	45	0
64- 41	1618	ALP PD	91.0	8.223	0	100	2300	4	1800	0	0	0	40	0
64- 40	1472	ALP PD	88.5	8.221	0	120	2800	2	2000	0	0	54	40	0
64- 34	1228	ALP PD	90.2	8.273	0	130	2100	4	2100	0	0	43	50	0
64- 31A	1148	ALP PD	88.3	8.259	0	130	2500	4	2200	0	0	47	50	0
64- 29	963	ALP PD	91.3	8.219	0	83	3000	2	1800	0	0	0	60	0
64- 28	875	ALP PD	89.8	8.224	0	66	2500	4	1600	0	0	60	45	0
64- 27	786	ALP PD	90.8	8.215	0	96	1800	4	2200	0	0	31	50	0
64- 26A	745	ALP PD	90.0	8.263	0	85	2100	2	1800	0	0	40	60	0
64- 25	532	ALP PD	92.2	8.227	0	88	3000	2	1800	0	0	52	50	0
64- 24A	415	ALP PD	91.2	8.227	0	110	1600	4	2200	0	0	54	55	0
64- 16A	370	ALP PD	91.4	8.234	0	190	2200	8	3000	0	0	60	55	0
64- 18	350	ALP PD	90.7	8.228	0	170	2500	4	3000	0	0	43	50	0
64- 15	105	ALP PD	90.0	8.244	0	68	920	4	1300	0	0	21	60	0
64- 12A	80	ALP PD	90.4	8.262	0	75	2000	4	1800	0	0	38	55	0

NOTES.

1. ALL SAMPLE NUMBERS HAVE A FJBT-PREFIX.
2. FOR EXPLANATION OF THE FOOTAGE VALUES, SEE TABLE 2.
3. FOR EXPLANATION OF THE ROCK-NAME SYMBOLS, SEE TABLE 2.
4. OLIVINE COMPOSITIONS AND CHROMITE CELL EDGE DATA BY X-RAY METHODS.
5. CU AND ZN BY CHEMICAL METHODS. SENSITIVITIES (IN PPM) - CU(4), ZN(5). PB WAS LESS THAN 5 PPM IN ALL SAMPLES.
6. OTHER TRACE ELEMENT DATA BY EMISSION SPECTROGRAPHIC METHODS. SENSITIVITY VALUES (IN PPM) AS FOLLOWS - BA(10), CO(20), CR(30), NI(20), SC(40), SR(40), V(30), ZR(40). A ZERO VALUE SIGNIFIES THAT THE ELEMENT WAS BELOW ITS DETECTION LIMIT.
7. ANALYSES BY THE ANALYTICAL LABORATORIES OF THE GEOLOGICAL SURVEY OF CANADA.

TABLE 7. MINERALOGICAL DATA AND TRACE ELEMENT ABUNDANCES FOR ROCKS FROM BAY OF ISLANDS IGNEOUS COMPLEX, NORTH ARM MOUNTAIN, WEST

SAMPLE	FOOTAGE	ROCK	MOL PCT FO IN OLIVINE	Å CHROMITE CELL EDGE	BA (PARTS PER MILLION)	CO	CR	CU	NI	SC	SR	V	ZN	ZR
64-651C	3595	OL GABB			19	0	250	12	50	120	210	380	40	50
64-651A	3562	OL GABB			23	0	200	10	43	0	450	250	20	0
64-640	3463	OL GABB			16	0	200	24	38	0	210	200	25	0
64-614	3432	AB GRAN			110	0	0	14	0	0	28	0	60	190
64-639	3398	OL GABB			29	0	150	40	170	0	200	0	40	0
64-638	3305	GABBRO			30	0	350	10	130	0	170	64	70	0
64-636	3070	OL GABB			15	0	270	68	89	0	190	87	40	0
64-634	2822	OL GABB			19	0	330	52	55	0	190	120	30	0
64-632	2632	OL GABB			16	0	330	18	88	0	140	110	40	0
64-737	2448	OL GABB			13	0	320	72	120	55	170	87	60	0
64-546A	2230	OL GABB	78.6		25	0	380	72	230	0	140	100	40	0
64-537	2090	GABBRO			21	0	87	34	58	0	83	110	40	0
64-540	1930	OL GABB			8	0	140	54	41	0	90	83	25	0
64-745	1762	GABBRO			0	0	240	250	97	0	110	130	60	0
64-746	1692	GABBRO			17	0	47	32	26	0	140	190	40	0
64-747	1537	ALP PD	91.8	8.214	0	90	290	12	1800	0	0	0	40	0
64-710	1338	ALP PD	90.4	8.240	0	95	2100	4	2300	0	0	0	40	0
64-721	1262	ALP PD	91.7	8.221	0	0	2400	4	2300	0	0	0	40	0
64-723	1082	ALP PD	90.5	8.216	0	0	2200	4	3300	0	0	0	40	0
64-715	798	ALP PD	89.5	8.272	0	0	2500	4	2200	0	0	0	40	0
64-716	670	ALP PD	89.4	8.226	0	0	2200	4	2400	0	0	0	40	0
64-717	614	ALP PD	89.4	8.210	0	0	2200	4	2500	0	0	0	40	0
64-797	445	ALP PD	90.9	0	0	50	2100	8	1500	0	0	0	40	0
64-796	285	ALP PD	90.2	8.176	0	60	2300	8	1400	0	0	0	45	0
64-779	262	ALP PD	89.4	8.175	0	130	2300	4	2500	0	0	0	45	0
64-777	213	ALP PD	90.8	0	0	150	2400	4	2600	0	0	0	40	0
64-775	188	ALP PD	90.3	8.189	0	170	170	4	2800	0	0	0	45	0
64-895	177	ALP PD	89.8	8.177	0	120	2100	8	2400	0	0	0	20	420
64-896	162	CONT RK			410	0	120	72	55	0	320	370	230	0
64-894	154	CONT RK			120	50	190	124	73	0	180	230	40	30
64-893A	142	CONT RK			170	0	200	4	55	0	90	70	90	0
64-878	92	CONT RK			430	0	47	16	30	0	36	74	80	130
64-874	53	CONT RK			520	0	0	12	0	0	33	0	40	0

NOTES.

1. ALL SAMPLE NUMBERS HAVE A FJBN-PREFIX.
2. FOR EXPLANATION OF THE FOOTAGE VALUES, SEE TABLE 3.
3. FOR OTHER RELEVANT NOTES SEE TABLE 6.

TABLE 8. MINERALOGICAL DATA AND TRACE ELEMENT ABUNDANCES FOR ROCKS FROM BAY OF ISLANDS IGNEOUS COMPLEX, NORTH ARM MOUNTAIN, EAST.

SAMPLE	FOOTAGE	ROCK	MOL PCT FO IN OLIVINE	Å CHROMITE CELL EDGE	BA	CO	CR	CU	NI	SC	SR	V	ZN	ZR
					PARTS PER MILLION									
64-505	2195	HB GABB			24	0	180	8	180	100	190	390	65	0
64-511	1902	HB GABB			20	0	220	8	39	0	230	200	40	0
64-513	1680	OL GABB			78	0	350	46	120	0	0	71	0	0
64-525	1445	OL GABB	69.6		19	0	700	54	120	0	100	170	40	0

NOTES.
1. ALL SAMPLE NUMBERS HAVE A FJBN-PREFIX.
2. FOR OTHER RELEVANT NOTES SEE TABLE 7.

sion and modal proportions of the main minerals correlate closely with experimentally based fractional crystallization models for the type of magma represented in the chilled margins of the intrusions (Irvine and Smith, 1967; Irvine, 1970). In such stratiform intrusions these sequences are commonly repeated (due to the periodic influx of fresh magma; Irvine and Smith, 1967) and are called cyclic units (Jackson, 1961).

(3) Chemical grading or cryptic layering (i.e. chemical trends in the cumulus minerals, and in the rocks themselves) corresponding to the order in which the pertinent constituents are known to be extracted from basic magma during fractional crystallization. Relevant examples are trends of (a) iron enrichment as expressed by a decrease of the ratio $Mg/(Mg + Fe^{+2})$, of (b) Ni depletion as reflected in its abundance in solid solution in olivine and pyroxene, and of (c) Cr depletion as reflected in either the amount of chromite in the rock or the abundance of the element in pyroxene (Irvine and Smith, 1969).

Criteria for identifying the residue of a partial fusion process are more tenuous, as they generally involve some assumption regarding the nature of the original rock, or the nature of the process; they tend to be negative criteria. In general, the rock should be fairly refractory with a "reduced" content of highly "fusible" constituents such as the alkalies and sulphide minerals. Fractional or partial fusion of an ultramafic rock will ordinarily increase its Mg/(Mg+Fe) ratio (e.g. Carter, 1970), and, in a case of broad-scale melting under relatively gentle thermal gradients (as one might anticipate for alpine-type peridotite), this ratio should probably also be fairly uniform. The constraints imposed on the modal composition of a rock during fractional fusion can lead to appreciably different products than those developed by fractional crystallization (Presnall, 1969), and one might expect this to be reflected in certain trace-element relations. Also, partial melting is probably less apt to produce spatially systematic rock sequences and chemical or mineralogical trends, than fractional crystallization. However, it is emphasized that all these criteria are provisional and it is not difficult to visualize circumstances in which they would not be valid: for example, systematic chemical trends might persist from an earlier stage of differentiation.

Characteristics of alpine-type peridotite

In this paper the term "alpine-type peridotite" is applied only to a very particular kind of ultramafic rock. This rock spans certain of the boundaries ordinarily drawn in petrographic classifications of ultramafic rocks, but, as a unit, it is characterized by a combination of features by which it can generally be identified (quite independently of genetic considerations) provided it is not too altered. It is commonly associated with other kinds of ultramafic rocks and may even be found with other types of peridotite. On the continents it typically occurs in Phanerozoic mountain belts in the bodies here referred to as "alpine ultramafic complexes". These are variously described in the literature as discrete intrusions, as parts of more varied plutonic bodies containing gabbroic and other intrusive rocks, and as members of ophiolite complexes in which they bear a definite relation to volcanic and sedimentary rocks. The peridotite as described below is the characteristic rock of these bodies, the principal features of which are as follows:

1. **Occurrence:** They are found in large numbers along certain orogenic belts, such as the Appalachians and the Coast ranges of California. In Canada, they are the principal kind of ultramafic body in the Cordillera, and they occur in a discontinuous belt from the Eastern Townships to the north coast of western Newfoundland (Figure 1). Interestingly, however, the exact kind of peridotite discussed here is rare, if present at all, among the large numbers of ultramafic bodies in the Canadian Shield (see below).

2. **Size:** In terms of area of exposure at least, alpine ultramafic complexes comprise many of the largest bodies of olivine-rich ultramafic rocks in the world; in fact, it appears that the only occurrence of greater extent is the Great Dyke of Rhodesia, a stratiform intrusion. The largest example in Canada is the Nahlin complex in northern British Columbia, which is more than 50 miles long and has an area of about 140 square miles (Smith, 1962). Several of the other bodies in the Cordillera are 50 - 80 square miles in size. In the Appalachians, the ultramafic rocks of the Bay of Islands Igneous Complex, consisting, in large part of alpine-type peridotite, have a composite area of about 130 square miles (Smith, 1958). The great majority of the bodies are intermediate or small in size, but the large ones are distinctive, and, as Smith (1962) pointed out, are much larger than anything found in the Canadian Shield.

A related point is that none of the large stratiform intrusions contain coherent masses of olivine-rich rocks to compare with those found in the alpine complexes. The layers of dunite and peridotite in stratiform intrusions, although extensive laterally, are rarely more than a few hundred feet thick, being closely interstratified with major layers of pyroxenite and gabbro. By contrast, in alpine-type bodies, the peridotite and associated dunite may be virtually the sole rock types throughout mountain masses having thousands of feet of relief and extending over many square miles.

On the other hand, geophysical studies, particularly gravity surveys, have (so far as we are aware) failed to show that any Canadian alpine ultramafic complex extends to depths of more than a few miles, and there seems no evidence that any of them are directly "rooted" in the mantle.

3. **Conditions of emplacement:** As already noted, it is generally accepted that alpine-type peridotites were largely solid when emplaced in their present country rocks. Some complexes have well developed contact metamorphic aureoles (Green, 1964a; Challis, 1965), and it is evident that the peridotite was very hot when emplaced. Some Canadian examples with aureoles are the Bay of Islands

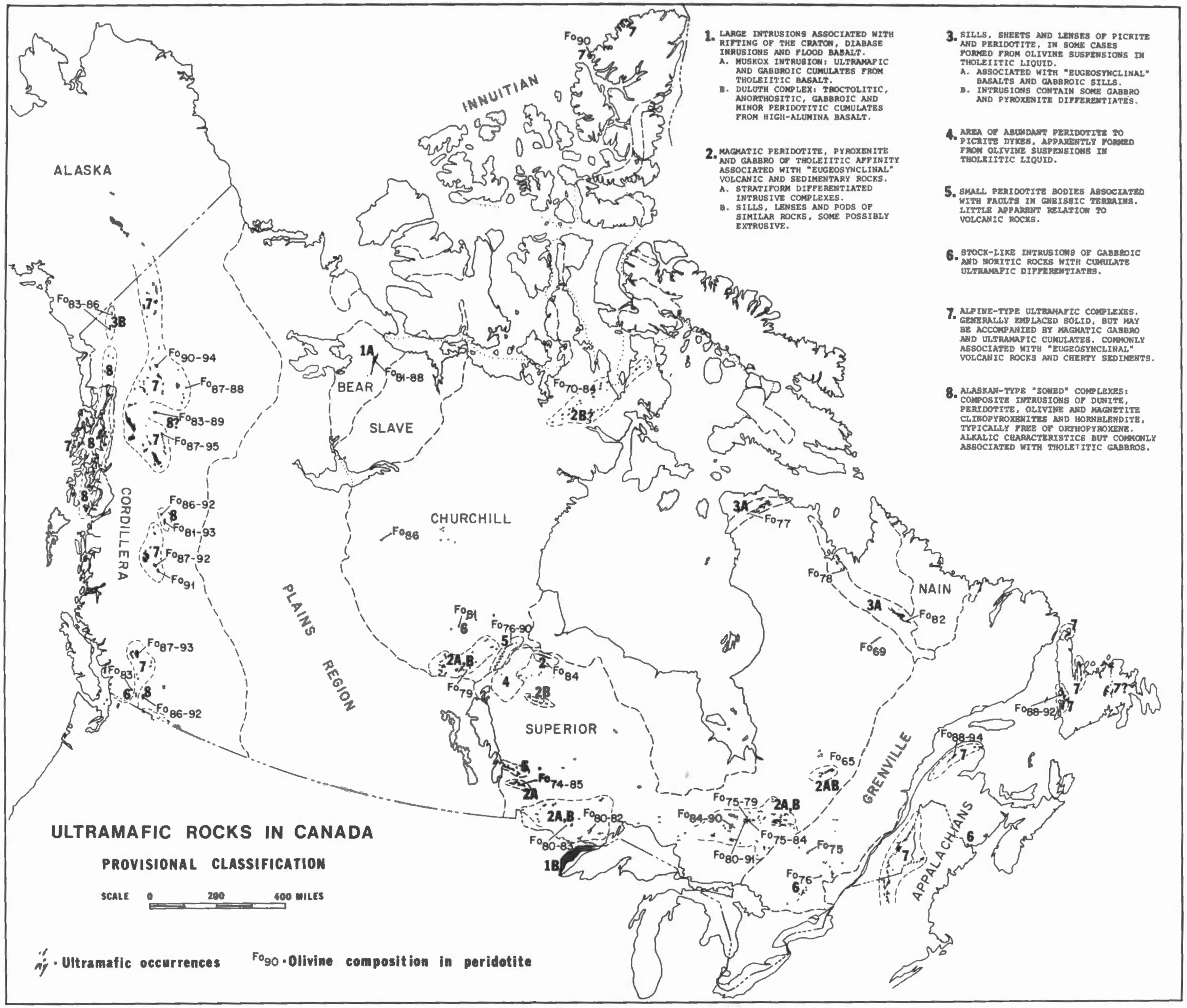

Figure 1. Map showing a partial, very generalized classification of ultramafic and related rocks in Canada and adjoining U.S.A., with some data on the composition of olivine in the peridotitic rocks.

Complex (Smith, 1958), the Mount Albert intrusion in the Gaspé (MacGregor,1962, 1964a), and the Blue River intrusion in northern British Columbia (Wolfe, 1966). More commonly, however, contact metamorphism is absent or inconspicuous, and the peridotite bodies have serpentinized and talcose margins, and are bounded by, or associated with, major faults, so that they appear to have been emplaced "cold" through the action of faulting (Hess, 1955). It is notable, however, that while the Mount Albert body has a beautifully developed metamorphic aureole around one side, it is bounded by a major fault on the other (MacGregor, 1962). Also, in a general petrographic comparison, the peridotite in the "hot" intrusions is not conspicuously different from that in the "cold" ones, unless perhaps that it shows more penetrative deformation.

4. Petrography of alpine-type peridotite: Alpine-type peridotite is generally a spinel peridotite in the harzburgite-dunite range, grading in places to lherzolite. Typically it is a partly to completely serpentinized assemblage of 60 - 90 per cent olivine, 5 - 35 per cent orthopyroxene and 1 - 7 per cent clinopyroxene (Figure 2), plus $^{1}/_{2}$–2 per cent chromium-bearing spinel (chromite). Uncommon minor phases are amphibole (Green, 1964a) and, very rare in North America at least, pyrope garnet (Church, this volume). Plagioclase may occur in associated peridotite, but is not generally found in the alpine-type. (An exceptional occurrence of plagioclase-bearing alpine-type peridotite is described by Walcott, 1969.) The olivine occurs as coarse spheroidal to polygonal grains if it is undeformed, but commonly it is strained and granulated and shows two distinct sizes of anhedral grains all in a foliated fabric. (e.g. Ragan, 1967; Moores, 1969). Compositionally, its range is small, generally between Fo_{87} and Fo_{94}, and its variation in particular occurrences may be even smaller – for example, most of the olivine in the Mount Albert and Bay of Islands peridotites is between Fo_{89} and Fo_{92} (Tables 5 - 8). The pyroxenes show similarly high Mg/(Mg+Fe) ratios. In some complexes the pyroxenes contain 5 - 7 per cent Al_2O_3 (Green, 1963, 1964) but such large amounts are not universal (e.g. Challis, 1965, Table 6). The orthopyroxene generally appears as blocky prisms that are prominent on weathered surfaces and persist in the deformed rocks as augen with conspicuously bent cleavages. It may be partly grown around the olivine grains but shows little evidence of having formed by reaction from olivine, and rarely is it poikilitic like the pyroxene oikocrysts common to olivine cumulates in stratiform intrusions. (Challis (1965) compared peridotite containing poikilitic orthopyroxene in the Red Hill alpine complex, New Zealand with Stillwater cumulates, but Walcott (1969) considered the same rock to be formed by replacement and recrystallization.) Some of the clinopyroxene forms exsolution lamallae in the orthopyroxene, but much of it occurs as small grains "interstitial" to the olivine and orthopyroxene. The chromite shows a large compositional range, particularly in Cr/Al ratio (MacGregor and Smith, 1963; Irvine, 1967) and, if undeformed, differs in habit accordingly. At one extreme is an opaque to deep red, Cr-rich, subhedral-euhedral type, that looks much like the cumulus chromite in stratiform intrusions. At the other, apparently gradational in all respects with the Cr-rich type, are olive to green Al-rich spinels that generally appear interstitial or micropoikilitic (Figure 3; see also Smith, 1958, Pl. X).

Serpentinization of the peridotite variously produces a host of serpentine minerals, talc, brucite, carbonates, secondary magnetite, native Ni and Fe alloys, and other minerals. There has been much controversy as to whether the alteration occurred as a "constant composition" process, except for the addition of volatiles, that caused expansion of the rock, or as a "constant volume" process marked by major chemical changes (e.g. Hostetler *et al.*, 1966; Thayer, 1966). However, there appear to be valid arguments on both sides, and probably both interpretations have some application.*

The peridotite commonly shows a rude layering on the scale of inches owing to thin bands alternately enriched in olivine and orthopyroxene. The layering is generally steeply dipping, and, while it may have broadly regular strike over large areas, commonly shows local irregularity and folding (e.g. Leech, 1953; Smith, 1958). In the Mount Albert intrusion it defines a broad fold pattern that appears to be indicative of diapiric emplacement (MacGregor, 1962). The layering has frequently been interpreted as flow banding (Smith, 1958; Dickey, 1970), but it occasionally shows grading and other features suggestive of crystal-settling and current-sorting. In some of the examples that we have seen, the pyroxenes appear to be oriented normal to the layering, a feature that is difficult to explain by flow. Dickey (1970) distinguished between "tectonic-type" layers, described as occurring in several cross-cutting generations, and "magmatic-type" layers considered to have formed from a basic magma produced by partial fusion of the peridotite.

5. Associated dunites: Although the peridotite commonly grades to dunite, there is also associated coarse-grained dunite, in sharply defined bodies ranging from "veins" less than an inch wide, to irregular masses measurable in hundreds of feet (e.g. Leech, 1953; Smith, 1958; Burch, 1969). These occasionally contain

*All the chemical analyses of ultramafic rocks illustrated graphically in the present paper, including trace element data, have been adjusted for effects of serpentinization on the "constant composition" model by converting Fe_2O_3 to FeO (except for an arbitrary 0.5 per cent such as generally is found in unaltered ultramafic rocks) and normalizing to 100 per cent without H_2O and CO_2. Most of the analyzed rocks are only partly serpentinized, and a comparison with the primary mineralogy shows good correlation between $Mg/(Mg+Fe^{+2})$ variations of the primary olivine and the adjusted analyses, and between original modal compositions as inferred partly from textures and calculated modes based on a "spinel peridotite norm" in which Al_2O_3 is assigned to chromite (with Cr_2O_3) and the pyroxenes.

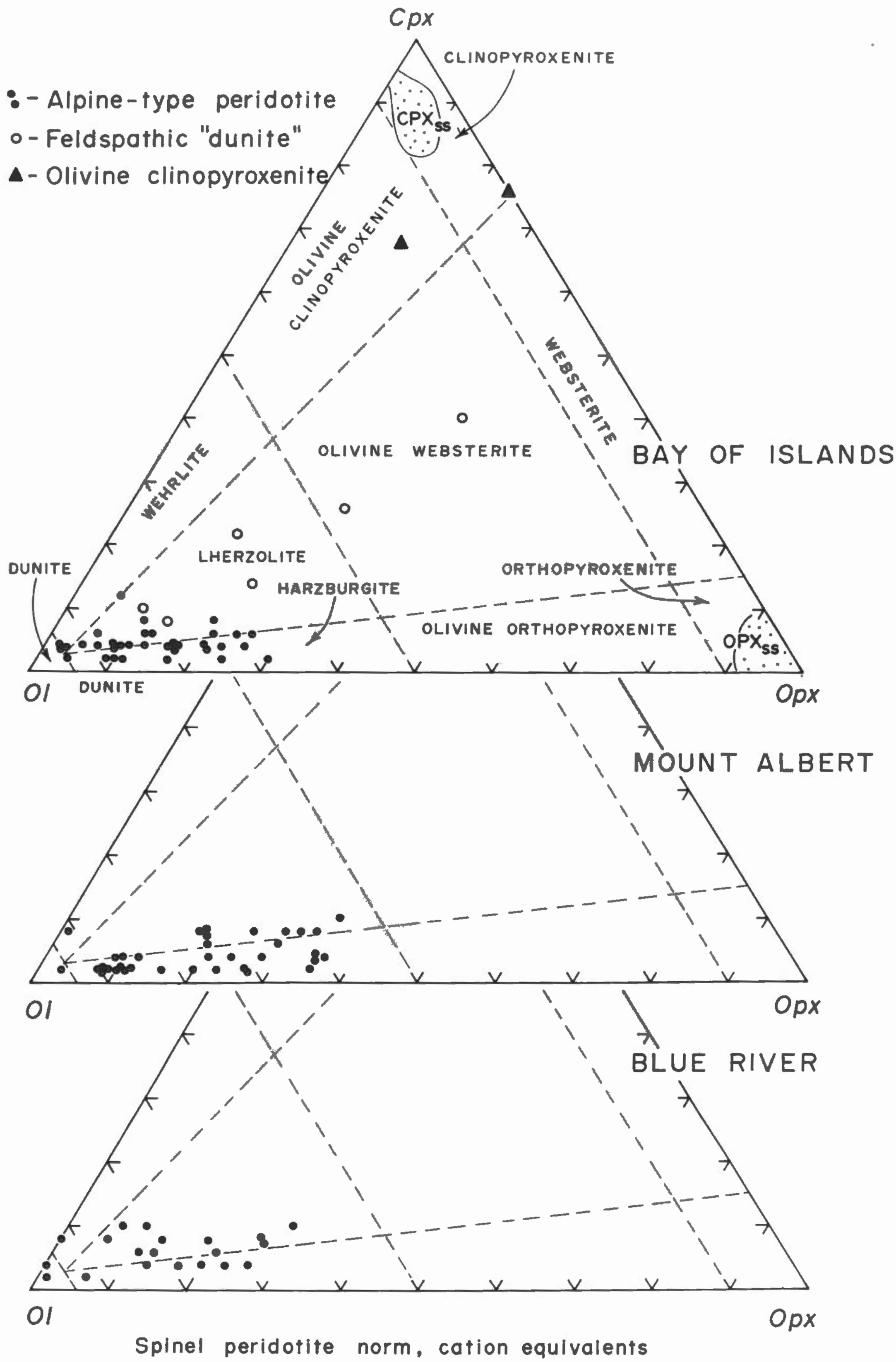

Figure 2. Ternary plots of *Ol, Cpx* and *Opx* in three alpine ultramafic complexes, based on a spinel peridotite norm. Provisional fields for conventional petrographic classification of feldspar-free ultramafic rocks are indicated.

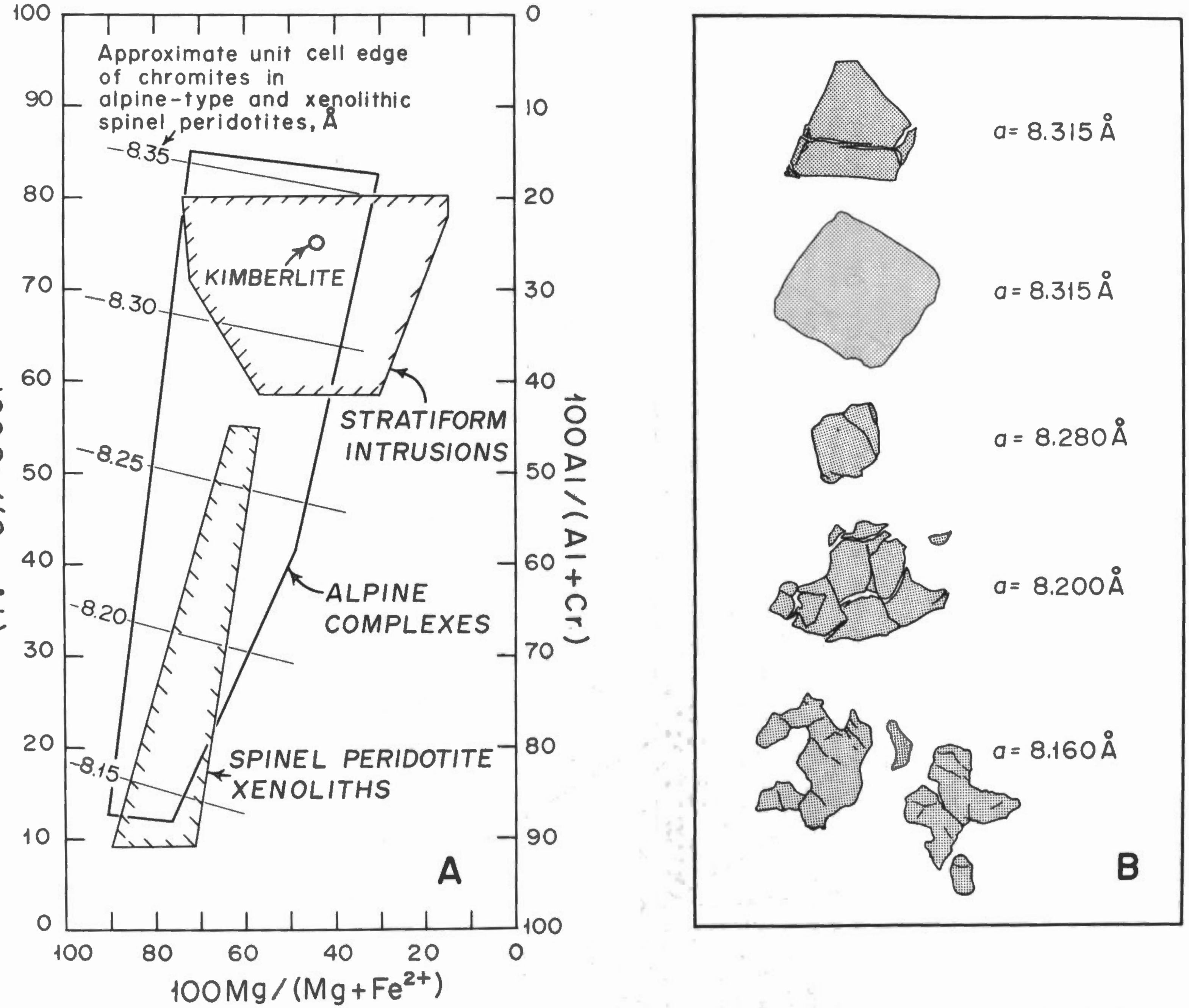

Figure 3. A. Plot comparing the compositional fields of chromite in alpine ultramafic complexes, stratiform intrusions, spinel peridotite xenoliths from basaltic lavas, and kimberlite (one sample only), after Irvine (1967). The indicated cell edge values will not generally apply to chromites in stratiform intrusions because they tend to be fairly rich in Fe_2O_3, which acts strongly to increase cell size. B. Textural variants of chromite in the Mount Albert complex. Cell edge data from MacGregor and Smith (1963).

small chromite deposits varying from thin median zones in the veins (Smith, 1958) to irregular pods and vein-like accumulations in the larger bodies (Thayer, 1963a). The veins are frequently interpreted as having formed due to the removal of silica by an aqueous fluid phase. However, this implies a volume reduction, whereas in the Shulaps Complex in British Columbia, for example, fairly large dunite bodies of this type can be seen to transgress layering in peridotite in a way that suggests that they have formed by volume-for-volume replacement.

Still other dunite occurs in major, roughly "conformable" zones, which in some complexes occur between the peridotite and adjoining gabbro (Thayer, 1960, 1964, 1967). This type of dunite commonly contains layered deposits of chromite, and it is from these deposits that Thayer (1969) has gathered much of his most convincing textural and structural evidence of crystal settling. Two of the principal occurrences cited by Thayer are in the Camaquey Complex in Cuba and the Zambales Complex in the Phillipines. Canadian examples are to be found in the Bay of Islands Complex (Smith, 1958), and in the vicinity of the abandoned chromite mines on Colline Provincial near Thetford Mines, Quebec.

6. Other rock associations: Other rocks associated with alpine-type peridotite are pyroxenite, gabbro, quartz-diorite, and albite granite (Thayer, 1963, 1967; Moores, 1969). Some of the pyroxenite occurs in "dykes" or "veins" and pegmatitic pods; but the main masses, which are usually websterite or olivine clinopyroxenite, range from irregular "blocks" a few feet in size, to rude layers up to a few hundred feet in thickness or even several miles in length, to still more extensive bodies or areas of no distinctive shape. The larger bodies tend to occur around the apparent top of the peridotite (e.g. Thayer, 1963; Moores, 1969). Among the gabbroic rocks are olivine gabbro, clinopyroxene gabbro, and norite, but perhaps of more frequent occurrence are the highly-altered types in which hornblende, actinolite, epidote, albite, and other secondary minerals predominate. Diorite and granite occur in minor quantities as small late plutons and dykes.

The idealized ophiolite sequence is as follows: peridotite at the base, overlain by pyroxenite and gabbro, followed by pillowed lavas and associated diabase dykes, the whole overlain by chert-rich sediments (e.g. Maxwell, 1969). This succession is now considered by many to represent a section of the oceanic crust and part of the upper mantle (e.g. Gass, 1968; Dewey and Bird, 1970; Church, this volume). Thayer (1967) stressed that the same lithological association is common to many alpine complexes, and his descriptions, and those of Moores (1969), emphasize the structural and petrological complexities that can be involved (*see also* Walcott, 1969). Many authors now apply the term ophiolite in a broader sense to any ensemble of alpine-type peridotite and these other rocks.

7. Chemical characteristics: Alpine-type peridotite ordinarily shows only a very limited range of chemical composition (e.g. Tables 1 - 8; Hess, 1964). The major constituents (SiO_2, MgO, FeO and Fe_2O_3) essentially reflect the modal abundance and composition of the olivine and orthopyroxene, and the nature and extent of their serpentinization. As a rule, Al_2O_3 is between 0.5 and 4 per cent, CaO is between 0.5 and 2.5 per cent, and TiO_2 is less than 0.03 per cent. Na_2O and K_2O are generally less than 0.3 and 0.02 per cent, respectively, and both may be extremely low (Hamilton and Mountjoy, 1965; Stueber and Goles, 1965). BaO, P_2O_5, Cu, Zr, and S are also very low, and Frey (1970) has interpreted rare-earth element abundances as indicating that the peridotite is a depleted residue after basalt magma formation. Our data show that NiO is slightly higher than in the peridotitic cumulates of the Muskox Intrusion, whereas Cr_2O_3 is generally only half to two-thirds as abundant (Figure 4).

8. Sr-isotope characteristics: Several occurrences of alpine-type peridotite have exceptionally high Sr^{87}/Sr^{86} ratios compared to oceanic basalts and other magmatic materials believed to come directly from the mantle, and regression lines based on the ratio Rb/Sr, tracing the isotope ratios back in time, suggest that the analyzed rocks were isolated from the present magma-producing parts of the mantle long before their times of emplacement. However, a between-laboratory discrepancy in the abundance of Sr has left a large uncertainty as to when the separation occurred (Hurley, 1967). Stueber and Murthy (1966) suggested from their data that the peridotite is a residue of melting that occurred in early Archean times at a stage when most of the continental crust was being formed, whereas Roe, Pinson and Hurley (1965) placed the time of separation in the latter half of earth history (at about 730 m.y. for their particular samples). Bonnatti, Honnorez and Ferrara (1970) recently reported data for peridotite of alpine-type character from the Mid-Atlantic Ridge in agreement with Stueber and Murthy's results, and they interpret their findings as indicating the presence of a very ancient zone of depleted mantle beneath the Atlantic.

9. Absence from the Canadian Shield: Alpine-type peridotite does not occur in any abundance, if at all, in the Canadian Shield. The absence there of bodies of comparable size to the large alpine-type complexes has already been noted: the largest Shield peridotite bodies are a series of sills in the Labrador Trough and Cape Smith-Wakeham Bay fold belts (Smith, 1962), but structural, textural, mineralogical and chemical data from those bodies that have been studied in detail (Fahrig, 1962; Baragar, 1967; Wilson *et al.,* 1969) all show clearly that the peridotite is not alpine-type. The next largest Shield bodies occur as layers and sills associated with stratiform complexes, particularly in the Muskox Intrusion (Smith, 1962), in the Abitibi region (Naldrett and Mason, 1968; MacRae, 1969), and in several areas in Manitoba (Scoates, 1969). But again, in those occurrences familiar to us, or for which reasonably detailed information is available, no alpine-type peridotite can be recognized. It appears that in most Shield peridotites: plagioclase (now generally much altered) or hornblende are

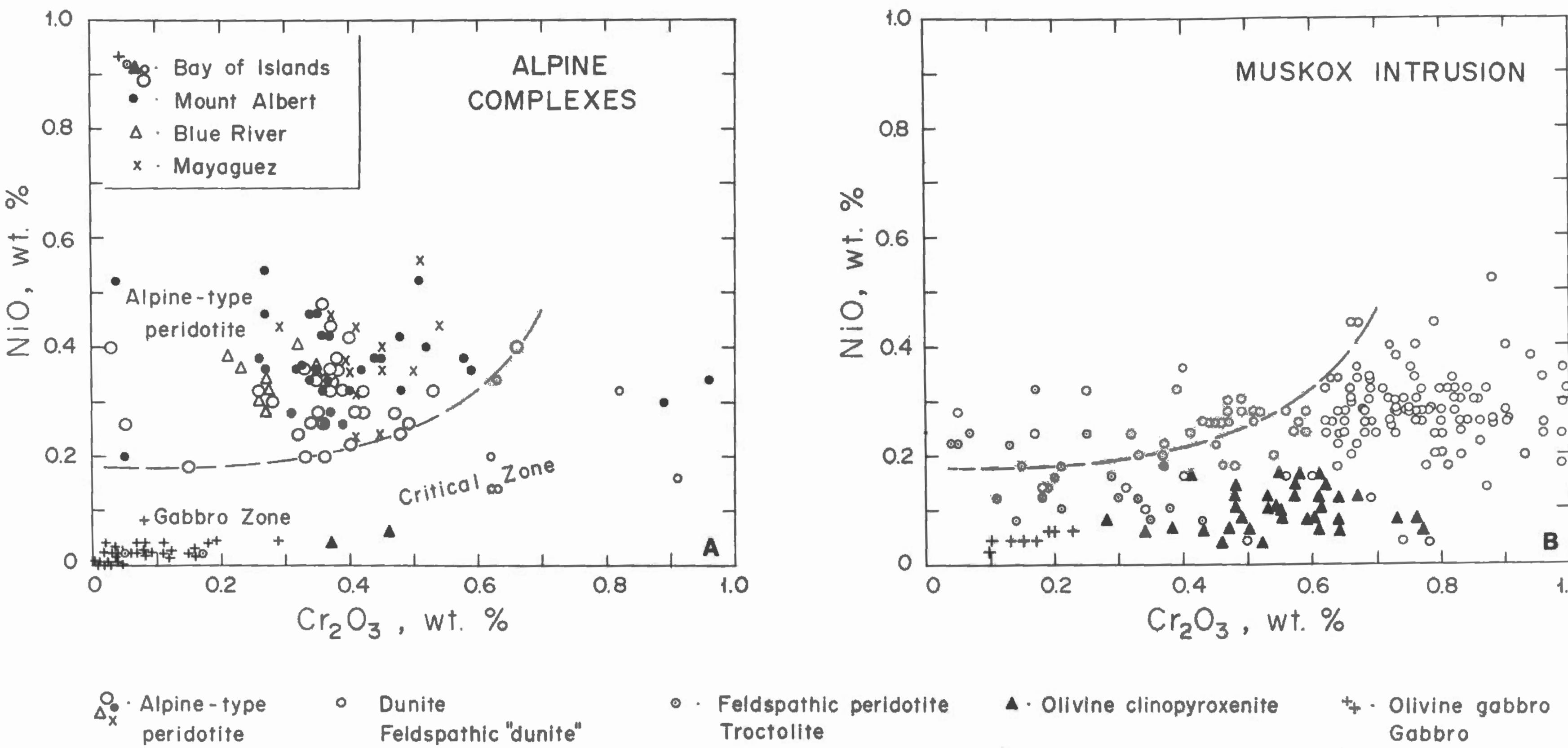

Figure 4. Plots showing the relative abundances of NiO and Cr_2O_3 in (A) four alpine complexes, and (B) the lower half of the Muskox layered series. The dashed line effectively separates the alpine-type peridotite from the rocks of the Critical and Gabbro Zones at Bay of Islands and from most of the cumulate rocks in the Muskox Intrusion. Mayaguez (Puerto Rico) data from Hess (1964); Blue River data from Wolfe (1966).

important constituents; cumulate-type textures featuring poikilitic pyroxenes and reaction replacement of olivine by pyroxene are common; the associated chromite is more generally opaque than in alpine-type peridotite; and much of the olivine either has a lower Fo-content or ranges to lower Fo-values (Figure 1). The data on which the last point is based are still scanty, but the same pattern is shown by Mg/(Mg+Fe) ratios calculated from more than a thousand unpublished chemical analyses obtained by Cameron, Siddley and Durham (1971) in an extensive geochemical survey of Canadian Precambrian ultramafic rocks.

One area in the Shield where alpine-type peridotite might be present is along the Manitoba Nickel Belt. Coats (1966) described rocks from this belt consisting of magnesian olivine and orthopyroxene, and transparent chromite, having the same general chemical composition as alpine-type peridotite; and the tectonic setting close to the boundary of the Superior and Churchill Provinces might suggest a similar association with faulting. However, the rock does not appear to show the same kind of deformation found in alpine peridotite, and Coats' data and illustrations demonstrate clearly that other kinds of peridotite are present; consequently there is some uncertainty.

10. Paucity of associated Ni-sulphide deposits: In connection with the last point it is recalled that Smith (1962) noted an important difference between Shield ultramafic rocks and those in the Cordillera and Appalachians that Ni-sulphide deposits are much more numerous in the former than in the latter. It is now evident that this difference, which is essentially confirmed by Chamberlain and Johnson's (1970) recent compilation map of Ni-deposits in Canada, represents in large degree a contrast between undoubted alpine-type peridotite and other kinds of ultramafic rocks. There are exceptions (for example, the Eastern Metals deposit in the Eastern Townships is associated with alpine-type peridotite), but it is particularly notable, that among the relatively few Ni-sulphide deposits found with Cordilleran ultramafic bodies, at least three of the main ones (the Giant Mascot orebody in southern British Columbia, and two deposits in the Kluane ranges in the western Yukon) accompany peridotites that are definitely not alpine in type (Figure 1). The difference would appear to reflect a generally lower level of sulphur in the alpine-type rock, although different processes of origin may also be a factor.

Some general genetic considerations

1. Temperatures of formation or equilibration: Information on the temperatures at which alpine-type peridotite has formed comes mainly from an experimental study of a natural peridotite by Ito and Kennedy (Figure 5), and from data on a few "high-temperature" intrusions. Metamorphic grades in the contact aureoles of the Lizard and Mount Albert Intrusions indicate that they were emplaced at close to solidus temperatures (Green, 1964b; MacGregor, 1964). Challis (1965) considered that the New Zealand high-temperature intrusions formed from basaltic magma at liquidus temperatures. Green (1964a) showed that the relative distribution of Mg and Fe^{+2} between coexisting pyroxenes in the Lizard Intrusion was the same as found in pyroxenes formed from basaltic magmas, and O'Hara (1967) estimated near solidus temperatures for the peridotites of several complexes on the basis of the distribution of Ca amongst coexisting pyroxenes.

2. Pressures of formation or equilibration: Experimental data relevant to defining the pressures at which alpine-type peridotite may have formed are summarized in Figure 5 together with a semi-quantitative illustration of the interrelation of Cr/Al ratio, mineral assemblage, and chromite composition.

Some alpine-type peridotite has clearly formed at moderately high pressures (Green, 1964a; O'Hara, 1967) although exact values are still rather uncertain. The essential evidence is that the Al_2O_3 in the rock is contained in pyroxenes and spinel rather than in plagioclase, with minimum pressures being determined essentially by the reaction

Anorthite + Forsterite ⇌ Aluminous enstatite + Aluminous diopside + Spinel ($MgAl_2O_3$)

For the pure system, the right side of the reaction is favoured above $7^1/_2$ - $8^1/_2$ kb at 1000 - 1300°C (Kushiro and Yoder, 1966). However, the reaction boundary is strongly affected by Cr_2O_3 and Fe_2O_3, which act to stabilize the spinel phase, and in fact, at high Cr/Al ratios, plagioclase-free "spinel" peridotite may be stable at pressures right down to one atmosphere (Figure 5; see also Ito and Kennedy, 1967). Therefore, in the absence of detailed mineralogical data, a high-pressure origin can be inferred for alpine-type peridotite only if the rock contains olive to green Al-rich chromite in association with olivine and two pyroxenes (Figure 5). This assemblage probably indicates a minimum pressure somewhere in the range 5 - 7 kb.

Na_2O also has a considerable effect on the above reaction, as it tends to stabilize plagioclase. Green and Hibberson (1970) found that, starting with Cr-free mixtures of olivine and a sodium-bearing plagioclase (An_{59}) at 1200°C, spinel did not appear until 9 kb, and all five phases involved in the reaction persisted together to 10 - 14 kb, depending on starting composition. This effect is not critical to the immediate discussion, as alpine-type peridotite is generally very low in Na_2O, but it is pertinent to the Bay of Islands data presented below.

An upper pressure limit for the crystallization of most alpine-type peridotite is set by the appearance of garnet, essentially by the reaction (MacGregor, 1964).

Aluminous enstatite + Spinel ⇌ Pyrope garnet + Olivine

Important additional constituents in this case are CaO, which stabilizes the garnet and causes the appearance of clinopyroxene as an extra phase (Kushiro and Yoder, 1966), and Cr_2O_3, which continues to stabilize the spinel (MacGregor, 1970). In the natural peridotite studied

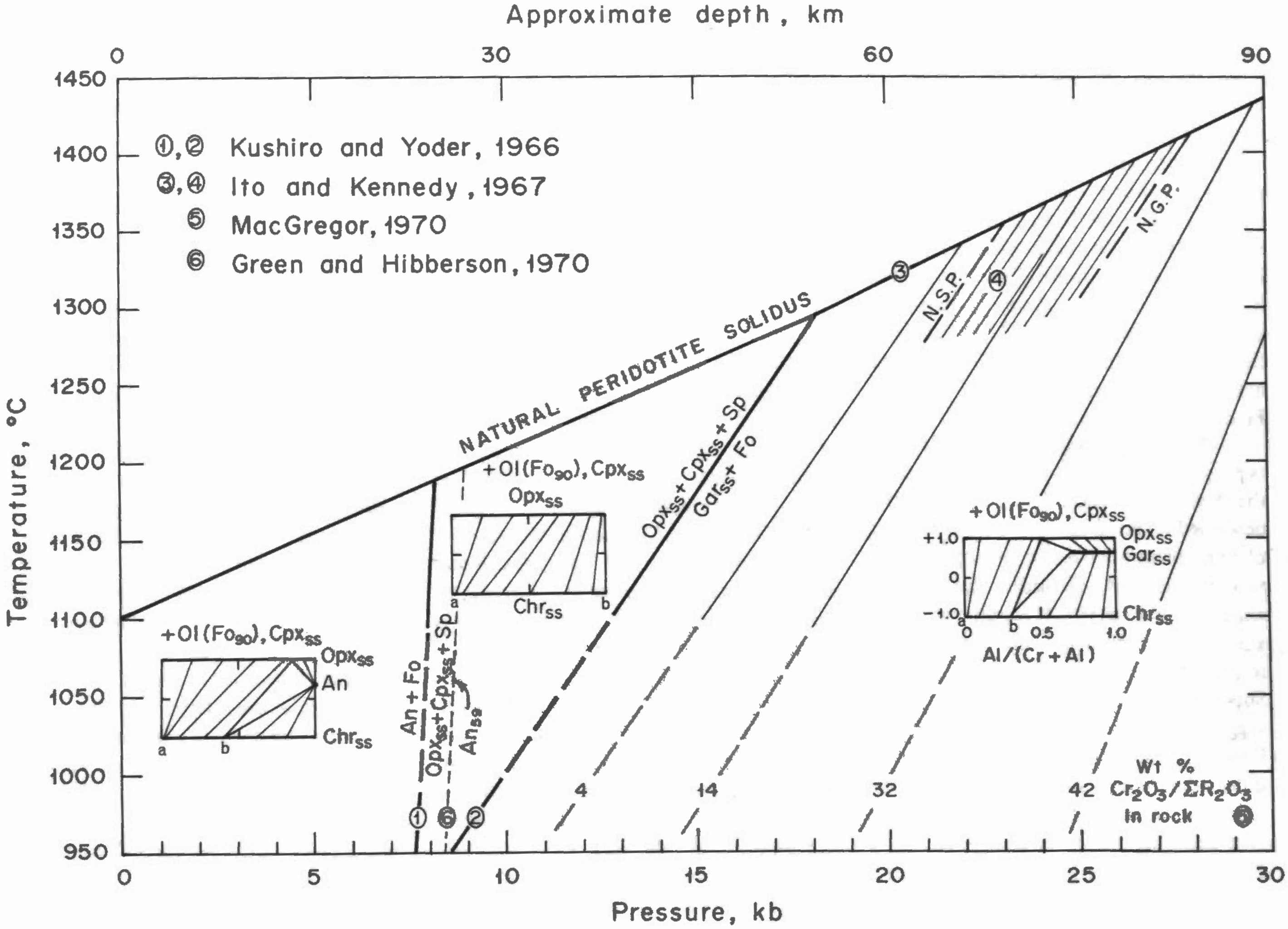

Figure 5. Diagram summarizing experimental data relating to pressures and temperature of formation of peridotitic rocks. Abbreviations: Ol — olivine; Fo — forsterite; Cpx — clinopyroxene; Opx — orthopyroxene; Chr — chromite; Sp — spinel; Gar — garnet; An — anorthite; SS — solid solution; N.S.P. — natural spinel peridotite; N.G.P. — natural garnet peridotite. The lines labelled 4, 14, 32, 42 mark the appearance of garnet as a function of the R_2O_3 composition of the rock. The dashed line "An_{59}" illustrates the effect of Na_2O on the appearance of spinel in a Cr-free system. The inset diagrams are projections showing the possible mineral assemblages that may coexist with olivine (Fo_{90}) and clinopyroxene in a Na_2O-free system. Assuming idealized compositions for the olivine and clinopyroxene, the vertical coordinate of the projections is the molecular ratio:

$$\frac{SiO_2 - \frac{1}{2}(MgO + FeO) - 1\frac{1}{2}\,CaO}{SiO_2 - \frac{1}{2}(MgO + FeO) - 1\frac{1}{2}\,CaO + Al_2O_3 + Cr_2O_3 + Fe_2O_3}$$

The horizontal coordinate is strictly applicable only to the plotted mineral compositions: to project rock compositions, the amount of Al and Cr contained in clinopyroxene must first be subtracted. The solid solution ranges shown for the minerals are roughly consistent with data on natural assemblages; and the slopes of the tie lines are consistent with observed distribution coefficients for Cr and Al. Note how the possible compositional range, a-b, of chromite in association with olivine and two pyroxenes first expands with increased pressure and then contracts. This compares with the data summarized in Figure 3A, and at very high pressures would be expected to give extremely Cr-rich chromites and garnets like the inclusions found in diamonds by Meyer and Boyd (1970). Similar projections showing the phase relations of clinopyroxene, chromite, plagioclase and garnet coesixting with olivine and orthopyroxene can be constructed by plotting Ca/(Ca+Al) against Al/(Cr+Al).

by Ito and Kennedy (1967) – which had a representative content of CaO (1.76 per cent), Al_2O_3 (2.05 per cent) and Cr_2O_3 (0.48 per cent) for alpine-type peridotite (cf. Figure 6 and Hess, 1964) – the first appearance of garnet was established at the solidus (1350°C) at 23 kb. However, the reaction zone is expected to have large positive slope (*see* Figure 5) in which case garnet could form at appreciably lower pressures, depending on temperature. If the reaction is kinetically significant in nature at temperatures as low as 1100°C, as seems likely from the experimental studies, then a common upper limit for equilibration pressures in alpine-type peridotite should be around 16 - 20 kb.

More precise definition of pressures of formation requires quantitative data on mineral chemistry, with the Al_2O_3 content of the pyroxenes being especially important (Green, 1964a; Boyd, 1970). O'Hara (1967) set up a provisional scale based on the sum (Al_2O_3+Cr_2O_3+Fe_2O_3) in clinopyroxene as variously contained in plagioclase, spinel, and garnet peridotites. The scale shows that with increasing pressure at constant temperature, this quantity should gradually increase until garnet begins to form, and then gradually decrease. The scale appears fairly reliable (Boyd, 1970) although control data are rather sparse and no systematic testing has been done on the effects of Cr_2O_3 and Fe_2O_3. O'Hara estimated equilibration pressures for alpine ultramafic complexes ranging from less than 1 kb for the New Zealand occurrences, to as high as about 17 kb for the Lizard Intrusion and rocks from the Pyrénées. He noted that his results were generally consistent with inferences made previously from detailed petrological studies of the rocks. The indication of low pressures for the New Zealand rocks is qualitatively consistent with Walcott's (1969) more recent observation that much of the Red Hill peridotite contains small amounts of anorthitic plagioclase.

3. Observations relating to the possibility of an origin by cumulus processes: An important question in establishing that alpine-type peridotite is a cumulate is, can its composition be simulated by a fractional crystallization model based on phase equilibria data? Where the rock is relatively free of penetrative deformation, its modal composition and texture and, in particular, the makeup of the layers in which there is some suggestion of gravitative sorting would seem to require that, if it has formed by crystal settling, it be a cumulate of both olivine and orthopyroxene precipitated in proportions of about $Ol_{85}Opx_{15}$. Such a precipitate would not be expected to form at pressures less than about 5 kb because of the well known magmatic reaction relation between olivine and orthopyroxene at low pressures which prevents them from crystallizing simultaneously, and indeed cumulates of this constitution do not occur in large quantity in any of the better known stratiform intrusions. Olivine and orthopyroxene were precipitated together for short periods during formation of some of the cyclic units in the Stillwater, Bushveld, and Great Dyke Intrusions (Jackson, 1970), apparently because they were at pressures just high enough for the two minerals to have a temporary cotectic relation (Irvine, 1970), but the cumulates produced contain a maximum of only about 50 per cent olivine and grade rapidly upwards into pure orthopyroxene cumulates. On the other hand, there appears to be a possibility within the rather loose framework of liquidus relationships presently available for higher pressures (Green and Ringwood, 1967; Ito and Kennedy, 1968; O'Hara, 1968), that olivine and orthopyroxene might coprecipitate in the proportions $Ol_{85}Opx_{15}$ from a liquid of tholeiitic picrite composition at pressures somewhere in the range 10 - 20 kb. However, the data are still far from definitive.

The NiO-Cr_2O_3 relations shown in Figure 4 also seem critical in deciding whether or not alpine-type peridotite is a cumulate. A comparative study indicates that the relation shown by the Muskox peridotite is a characteristic pattern for fractionation of olivine and chromite from basaltic liquids at low pressures. Thus, if the pattern revealed for alpine-type peridotite in Figure 4 is also due to crystal fractionation, then either the liquid was considerably different from basalt, or the crystallization occurred under very different conditions (the most likely possibility being higher pressures). The low Cr_2O_3 values might, for example, reflect fractionation of a relatively aluminous spinel at high pressures rather than Cr-rich chromites of the type common to stratiform intrusions. But another, perhaps more attractive possibility is that the level of Cr_2O_3 was basically established by fractionation of chromian pyroxenes and garnet (cf. O'Hara, 1968) and was then somewhat modified (most probably slightly increased) by the extraction of basaltic melt during a subsequent episode of fractional fusion, with the existing chromite being produced at that time as a refractory, residual product. In stratiform intrusions, there is commonly evidence of crystallization reaction relations of the type (Irvine, 1967)

Chromite + Liquid → Chromian pyroxene

The melting reaction suggested here would, in effect, be the reverse

Chromian pyroxenes + Chromian garnet → Chromite + Liquid

4. Relation of spinel composition to bulk rock composition: In attempting to understand further the large compositional range of the chromite in alpine-type peridotite, we have compared its Al/(Cr+Al) ratio as indicated by its unit cell size against the bulk composition of its host rock using data from three different intrusions (Figure 6). The results show no significant correlation with Cr_2O_3 and only a vague dependency on Al_2O_3 (the Blue River Complex excepted). However, there is a rather surprising correlation with CaO (Plot B), which must be largely contained in clinopyroxene (Plot D). Since the clinopyroxene and aluminous chromite both tend to be "interstitial", a possible interpretation is that the correlation is due to the original presence of differing percentages of a liquid component (such as basalt) containing fairly definite amounts of CaO and Al_2O_3 in a crystal aggregate of olivine, orthopyroxene, and minor Cr-rich chromite. When the liquid solidified, it could have precipitated the clinopyroxene and reacted with the

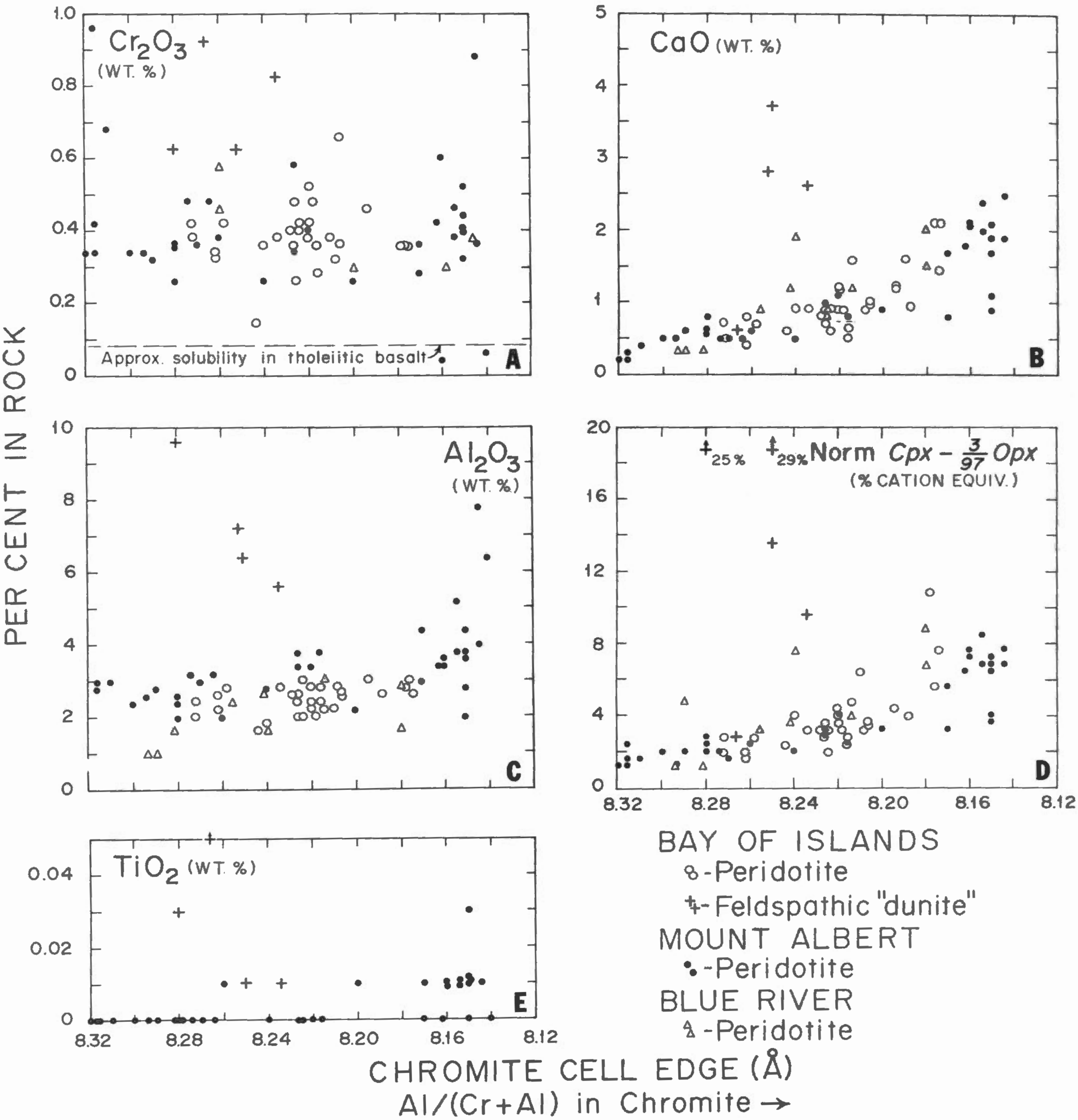

Figure 6. Plots relating the unit cell edge of chromite in alpine ultramafic complexes to the bulk composition of its host rock. In plot D, *Opx* and *Cpx* are based on a spinel peridotite norm (see text); the vertical coordinate is an estimate of the amount of *Cpx* occurring as modal clinopyroxene, assuming the orthopyroxene contains 3 per cent in solid solution. Blue River data from Wolfe (1966). The indicated solubility level for Cr_2O_3 in tholeiitic basalt is from Irvine and Smith (1969). The cell edge of the chromite is approximately the inverse of the ratio Al/(Cr+Al) (see Figure 3A).

chromite to produce the more aluminous spinel (Irvine, 1967).* This interpretation is consistent with the slightly higher TiO_2 content of these Mount Albert rocks having the more aluminous chromite (Plot E) inasmuch as natural magmas are generally slightly enriched in TiO_2 compared to derived olivine, pyroxenes, and chromite. For the rocks examined, the range of CaO is about $1^1/_2$ per cent; hence if the inferred liquid was basaltic with a typical line content of 10 – 12 per cent, its amount would be indicated to have varied over about 15 per cent. Alternatively, if the liquid were picritic, the variation could have been considerably larger, perhaps to as high as 20 or 25 per cent. The latter possibility is considered important because several studies have shown that the first liquid to be derived by partial fusion of peridotite of alpine-type composition at high pressures under anhydrous conditions is picritic rather than basaltic (O'Hara, 1965; Ito and Kennedy, 1967, 1968; Green and Ringwood, 1967). Therefore, accepting that a liquid phase was involved, two questions are raised: (1) Which of the two kinds of liquid just mentioned is the more probable? and (2) Was the liquid the pore magma of the cumulate, or undrained liquid in a residue of partial fusion? These are examined below on the basis of data from Bay of Islands.

Bay of Islands Igneous Complex

The structure and igneous geology of the Bay of Islands Igneous Complex have been described by Cooper (1936) and Smith (1958), and its tectonic setting by Rodgers and Neale (1963) and Stevens (1970). Only a few of its main features are mentioned here, with the emphasis on our petrologic observations.

As exposed, the complex is a discontinuous north-south belt of layered ultramafic and gabbroic rocks, about 60 miles long and 15 miles wide, contained within an allocthonous plate of a major thrust system (Rodgers and Neale, 1963). It embodies four principal segments or "plutons" in which it appears as a rude "sheet" divisible into a lower Ultramafic Zone, $2^1/_2$ to 4 miles thick, and an upper Gabbro Zone of variable thickness to a maximum possibly of 3 miles. The sheet is emplaced within basic volcanic rocks that show contact metamorphism along both its roof and floor (Smith, 1958). The volcanic rocks in the roof are partly pillowed and are locally cut by numerous basic dykes; small intrusions of quartz diorite are associated; and minor bodies of albite granite are found in the Gabbro Zone (Smith, 1958). The association therefore has the essential earmarks of an ophiolite complex, and several authors have suggested that it represents a section of ancient oceanic lithosphere (Stevens, 1970; Moores, 1970; Church, this volume).

Ultramafic Zone. Through most of its thickness this zone consists of alpine-type peridotite and dunite. Layering on the scale of inches is widely developed in the peridotite. The layers in places show modal grading suggesting mineralogical sorting by magmatic currents. However, the microscopic evidence for cumulate textures is not conclusive, and there are no obvious major layers or cyclic units as in the better known stratiform intrusions. Also, while the layering is broadly conformable with the overall structure of the complex, it locally has undergone "plastic" folding, and Smith (1958) suggested that it was due to solid flow. Penetrative deformation is common in the peridotite, especially near the base of the zone (Smith, 1958).

Gabbro Zone. This zone consists largely of rocks that are readily classified as cumulates on the basis of small-scale layering, lamination, and detailed textural features. The principal rock is olivine gabbro, which is a plagioclase-clinopyroxene-olivine cumulate. Less common is a one-pyroxene gabbro, generally a plagioclase-clinopyroxene cumulate, while relatively massive (non-cumulate?) hornblende gabbro is found locally in at least one of the main "plutons" (North Arm Mountain).

A peculiarity of the gabbroic rocks is that they only rarely contain orthopyroxene, a feature that is also evident in their chemistry in that they commonly show normative nepheline rather than hypersthene (Figure 7). This is in such contrast to the mineralogy of the alpine-type peridotite of the Ultramafic Zone, where orthopyroxene is a major phase, as to suggest a fundamental difference in genesis – if not in mechanism of formation, then in composition of parent magma or depth of crystallization. Moreover, it indicates that the gabbroic rocks were precipitated from magma of relatively low silica activity, similar perhaps to the "transitional" type of tholeiite (transitional to alkali basalt) found along the Mid-Atlantic Ridge (e.g. Muir and Tilley, 1964). Like the transitional tholeiite, the gabbroic rocks are very poor in K_2O and TiO_2 (Table 2 - 4).

In the few specimens of gabbro in which we have found orthopyroxene, olivine is absent – an antipathy that could develop during fractional crystallization by virtue of the reaction relation, olivine → orthopyroxene. It is of interest to know if this relation was effective as this might place some limit on depth of crystallization. In the "simple basalt systems" studied in the laboratory, the reaction relation obtains under anhydrous conditions only at pressures less than 5 – 6 kb, giving way at higher pressures to a cotectic relation (Boyd and Davis, 1964). Unfortunately we have not as yet been able to establish whether orthopyroxene ever occurs as reaction rims around the olivine grains, or, alternatively, whether the two minerals have ever precipitated together. However, comparison of the chemical composition of the rocks with the inferred liquidus relations in Figure

*An alternative interpretation is that the clinopyroxene and the critical part of the Al_2O_3 content of the chromite were derived from Ca-Tschermaks "molecule" in solid solution in orthopyroxene by reaction with olivine: $CaAl_2SiO_6 + Mg_2SiO_4 \rightarrow CaMgSi_2O_6 + MgAl_2O_4$. However, this is not supported by textural relationships in that the clinopyroxene and spinel appear quite independent of the orthopyroxene. Also, there is no clear correlation between either the amount of CaO or the composition of the spinel and the amount of orthopyroxene in the rocks.

In the preferred interpretation, it is considered that the rock must initially have contained some chromite because its Cr_2O_3 content is generally more than four times the common solubility limit of Cr_2O_3 in basaltic magmas (Figure 6A) and therefore probably far exceeded the amount that could have been contained in the postulated interstitial liquid.

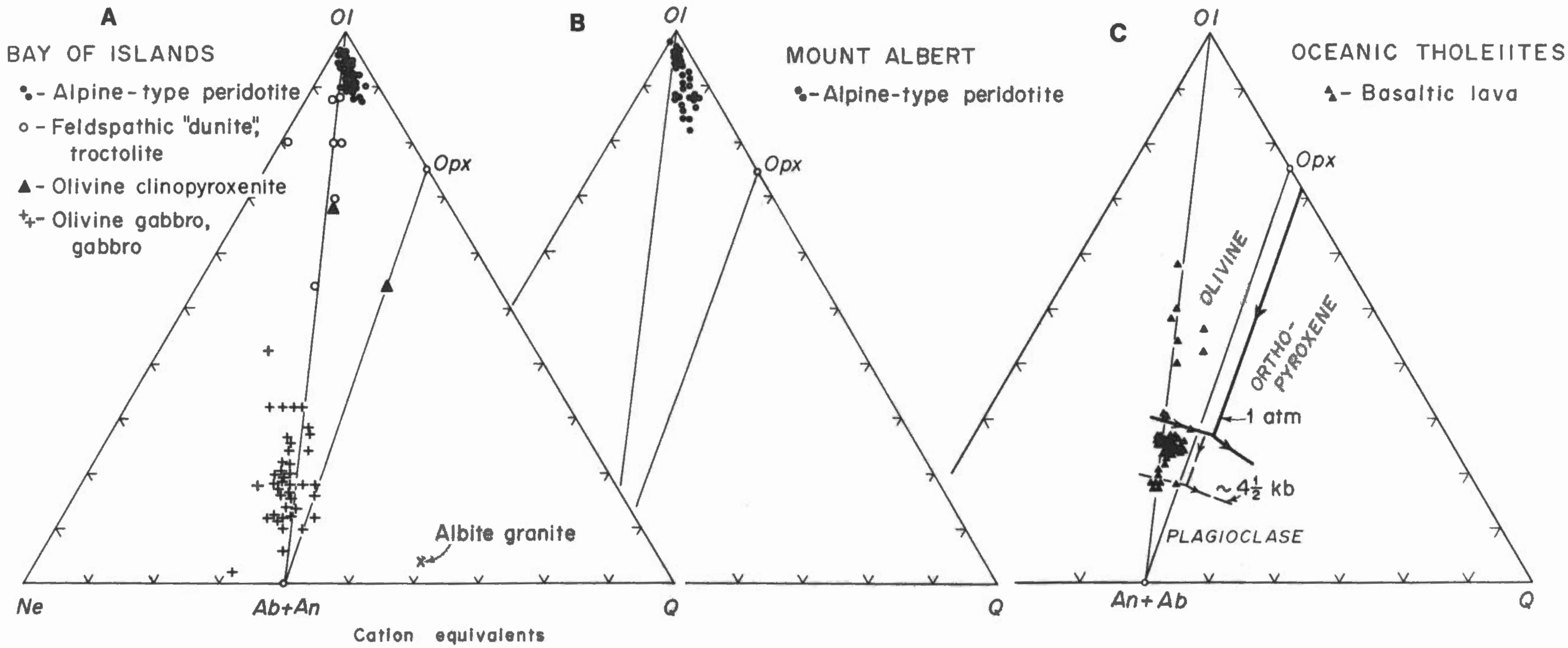

Figure 7. Ternary plots of normative *Ol, Ne* and *Q*, with *An* and *Ab* combined. Cation norm based on CIPW conventions. Note that the alpine-type peridotite contains large amounts of *Opx* whereas most of the Bay of Islands Critical and Gabbro Zone rocks contain *Ne*. Plot C shows approximate liquidus boundaries for basaltic melts at 1 atmosphere and $4^1/_2$ kb (after Irvine, 1970).

7C suggests that they may have formed at pressures of about 5 kb.

Critical Zone. The contact of the Ultramafic and Gabbro Zones is marked by a seemingly transitional unit, termed the Critical Zone, consisting of feldspathic "dunite" and olivine gabbro with complexly interbanded layers and lenses of olivine clinopyroxenite, troctolitic, and anorthositic rocks. The "dunite" (which actually ranges in composition to feldspathic peridotite) is a typical olivine-chromite cumulate with minor postcumulus clinopyroxene and poikilitic growths of plagioclase (now much altered). According to Smith (1958), it contains the main deposits of chromite at Bay of Islands. The olivine clinopyroxenite forms one major "layer", three miles long and up to several hundred feet thick, and numerous smaller "lenses" and thin layers (Smith, 1958). The troctolite is gradational to both dunite and gabbro, while the anorthosite occurs in thin layers that are almost certainly formed by the sorting and concentration of plagioclase through the action of magmatic currents. The Critical Zone does not have a well defined "stratigraphy" that can be traced for any distance along its length, and according to Smith (1958) some of the layers and lenses are slightly discordant to the general contact trend of the Ultramafic and Gabbro Zones. However, the layering and repetition of contrasting rock types are typical of stratiform intrusions, and in our experience the zone is particularly reminiscent of a complexly interstratified sequence of compositionally and texturally almost identical rocks in the middle of the Muskox Intrusion (Layers 10 and 11; Findlay and Smith, 1965). This latter sequence formed by accumulation of olivine, clinopyroxene and plagioclase precipitated in different proportions by fractional crystallization of basaltic magma at shallow depths during a period when fresh magma was repeatedly introduced into the intrusion (Irvine, 1970). While the Bay of Islands Critical Zone is thicker and structurally more complicated, we feel that it must have much the same origin. Notable in this respect is that NiO-Cr_2O_3 relations in the Critical Zone are the same as observed in the ultramafic cumulates of the Muskox Intrusion (Figure 4).

Compositionally, the rocks of the Critical Zone appear more closely tied to the Gabbro Zone than to the alpine-type peridotite that underlies them. Besides containing feldspar, they are like the gabbro in that they rarely contain orthopyroxene. The chemical data suggest that the base of the Critical Zone is a discontinuity in that it is the first level in the complex at which Na_2O, TiO_2, Ba, Sr, Sc and Cu were detected with certainty by the analytical methods used (Tables 2 - 4 and 6 - 8). Moreover, the chromite in the Critical Zone is different from that in the alpine-type peridotite immediately beneath in that it is opaque rather than red and has a larger unit cell size (Figure 8), possibly indicating a lower Al/(Cr+Al) ratio. This last feature, if correctly inferred, together with the presence of feldspar, suggests that the Critical Zone solidified at appreciably lower pressures than the peridotite (*see* Figure 5). However, confirmation of this inference must await a quantitative study of the mineral chemistry and an evaluation of the effect of the slightly higher Na_2O content of the Critical Zone.

The contrast between the Critical and Ultramafic Zones appears to be of major importance in view of Smith's (1958) suggestion, based mainly on structural relations, that the Bay of Islands Complex was emplaced with the ultramafic rocks largely solid and the gabbro in a much more fluid state. From present knowledge and observations, it seems clear that the alpine-type peridotite was the solid part, and that the ultramafic and other rocks of the Critical Zone are early differentiates of the gabbro parent magma precipitated during the general period of instability that accompanied its intrusion. The problem is whether the peridotite is a still earlier differentiate of the same magma, formed at some appreciably greater depth and then remobilized when the complex was emplaced in its present country rocks, or whether it is a block of residual mantle material, perhaps having no direct compositional relation to the gabbroic magma, that in some way came to serve as the floor on which the overlying cumulates were deposited. Since the peridotite is layered in a fairly regular manner, the first possibility can be tested by looking for effects of fractional crystallization. This matter is now considered.

Mineralogical and chemical variations through the complex: Figure 8 shows olivine and whole rock $Mg/(Mg+Fe^{+2})$ ratios for samples collected across two of the plutons in the Bay of Islands Complex, together with data on the NiO and Cr_2O_3 contents of the rocks, the unit cell size of the chromite, and the amount of CaO in the Ultramafic Zone. The sample interval is too large to give good definition of possible "stratigraphic" trends (especially within the Critical Zone), but the data indicate certain broad features, and since both the main zones appear relatively uniform in the field we tentatively accept the illustrated features as representative.

The $Mg/(Mg+Fe^{+2})$ ratios show distinct (although very irregular) trends of upward decrease through the rocks of the Critical and Gabbro Zones – as they should if the rocks are cumulates formed by fractional crystallization. However, in the alpine-type peridotite of the Ultramafic Zone their total range of variation is only about 3 percentage units, and possible overall trends, even if real, are extremely slight. At Table Mountain, the ratios of both olivine and whole rock show some indication of upward decrease, but the maximum change that could possibly be suggested from the data is only about 2 percentage units through what may be as much as four miles of section. In the North Arm Mountain pluton the Mg/(Mg+Fe) ratio of the rock is essentially constant while that of olivine appears to *increase* upwards, the opposite of a fractional crystallization trend.

NiO and Cr_2O_3 decrease sharply from the ultramafic to the gabbroic rocks, as in many intrusions; and a slight increase in their concentrations about a third the way up the North Arm Mountain gabbro may signify an addition of "fresh" magma, as is common in strati-

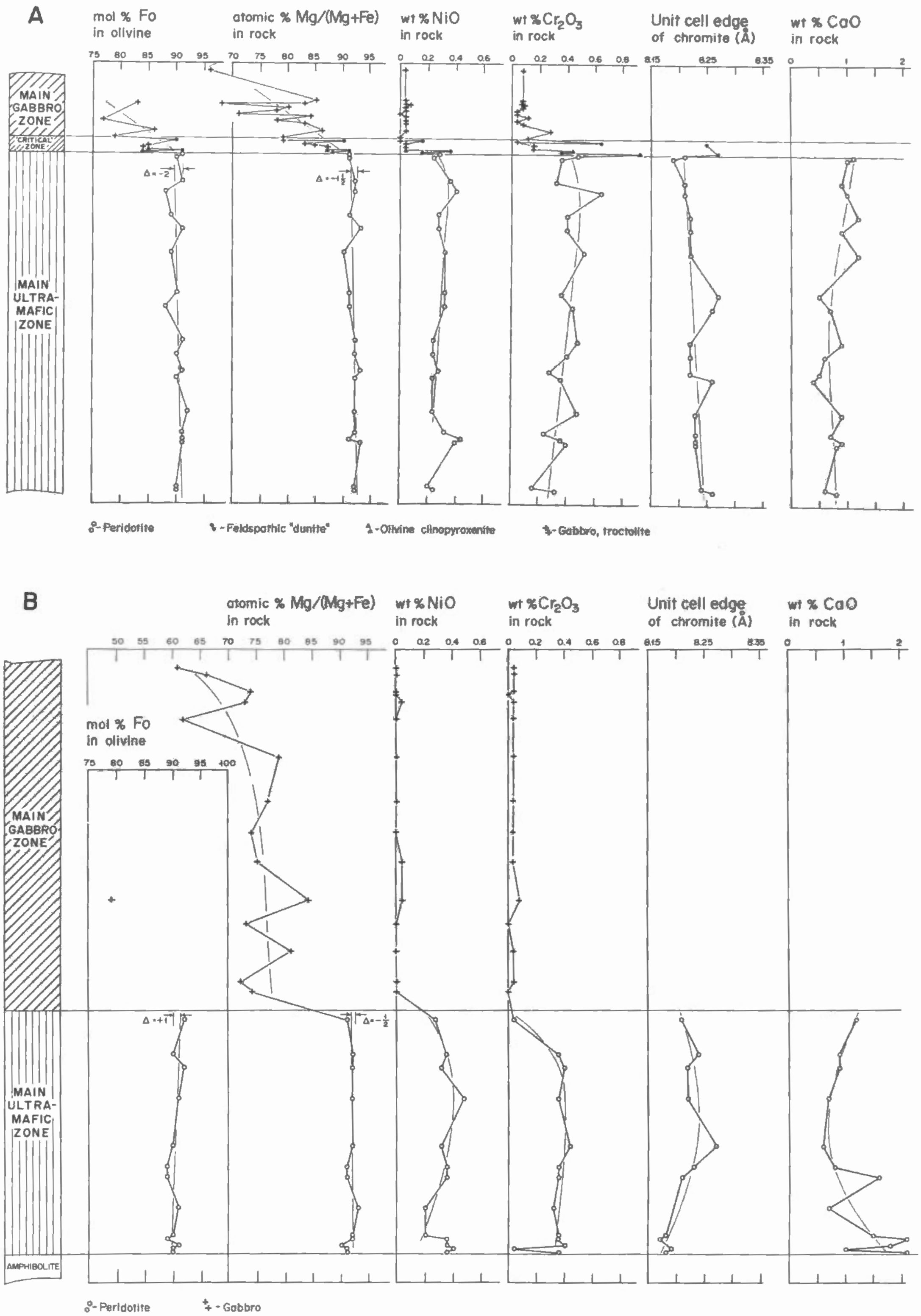

Figure 8. Mineralogical and chemical variations through the Bay of Islands Complex. A. Table Mountain; B. North Arm Mountain. In each section the Ultramafic Zone is about three miles thick. The light "trend lines" (and the Δ – values) are intended only to facilitate comparison; they are not fitted statistically, and they may not be significant genetically. Olivine compositions were determined by the x-ray method of Jambor and Smith (1964).

form intrusions. In the Ultramafic Zone, local variations are large, but overall trends of upward increase are suggested for both NiO and Cr_2O_3 at Table Mountain – again, the inverse of the trends expected from fractional crystallization, at least of basaltic magmas. As noted previously, the relation of NiO and Cr_2O_3 is not typical of established cumulate peridotites (Figure 4).

The data therefore do not support an hypothesis that the alpine-type peridotite was formed by fractional crystallization; in fact, on the basis of the criteria suggested earlier, they favour the alternative, that the peridotite is a residue of a partial fusion process. However, it is not unknown in layered intrusions for stratigraphic trends of $Mg/(Mg+Fe^{+2})$ to be weak, non-systematic, or the inverse of the trend expected from fractional crystallization. Thick sections of ultramafic cumulates in the Duke Island Ultramafic Complex, Alaska, show no strong trends of variation (Irvine, 1959); and inverse trends are shown by cumulus olivine in the lower parts of the Muskox Intrusion (Smith and Kapp, 1963) and Stillwater Complex (Jackson, 1970), and by cumulus hypersthene near the lower (outer) edge of the Sudbury Irruptive (Naldrett *et al.,* 1970). The following analysis of the problem is therefore undertaken before drawing conclusions.

Discussion of the Mg-Fe variations: Among the factors that might affect the $Mg/(Mg+Fe^{+2})$ ratios of mafic minerals in igneous rocks are two principal ones that can be examined on a more or less quantitative basis: (1) crystal fractionation, and (2) reaction with trapped interstitial (e.g. intercumulus) liquid. The first is illustrated in Figure 9A, which shows theoretical fractionation curves for olivine where the first crystals have the compositions given by the abscissa intercepts. The curves are calculated assuming a distribution coefficient

$$K_D = \left(\frac{Mg}{Fe^{+2}}\right)^{liquid} / \left(\frac{Mg}{Fe^{+2}}\right)^{solid} = 0.3$$

as was found by Roeder and Emslie (1970) to be characteristic of olivine-liquid equilibria over a wide range of liquid compositions and temperatures. Fractionation curves for the pyroxenes should be very similar, because the coefficients describing the distribution of Mg and Fe^{+2} between olivine and pyroxene at magmatic temperatures are close to unity (Nafziger and Muan, 1967). The light curves with Δ labels indicate the differences in composition between crystals precipitated as fractionation progresses and the first crystals. In the simple case of olivine crystallizing from an olivine melt, the ordinate is per cent solidification. However, in natural situations the liquid will generally have a different percentage content of $(Mg+Fe^{+2})$ than the minerals that crystallize from it, and more than one mineral may precipitate at a time; consequently to obtain per cent crystallization, the ordinate scale must be adjusted by multiplying it by the ratio

$$(Mg+Fe^{+2})_{\text{initial liquid}} / (Mg+Fe^{+2})_{\text{fractionated solids}}$$

where the denominator is a constant. Thus, for olivine precipitating from basaltic liquid, the adjustment factor is about 20/67 (see inset, Figure 9A), and if a second mineral such as plagioclase were subsequently to join the olivine, then it would be necessary to define a new factor based on the *bulk* $(Mg+Fe^{+2})$ content of the precipitate and the *current* composition of the liquid, and to start over again in terms of per cent solidification of the *remaining* liquid using the fractionation curve appropriate to the *current* $Mg/(Mg+Fe^{+2})$ ratio of the olivine.

Considering the fractionation curves in reference to the present problem, it is notable that, if the percentage ratio $Mg/(Mg+Fe^{+2})$ of the first crystals is greater than 90, then the rate of change in the composition of subsequent crystals with solidification will for a time be appreciably slower than for a value of 87, the common upper limit for cumulus olivine in some stratiform intrusions formed from basaltic magmas (e.g. the Stillwater and Muscox Intrusions). If we add to this the possibility that the more magnesian olivine might have precipitated from a picritic liquid containing, say, 40 per cent $(Mg+Fe^{+2})$ (equivalent to about 40 per cent normative olivine) rather than from basalt, then we see what might be at least a partial explanation of why there is such relatively little variation in the composition of olivine in alpine-type peridotite. However, the percentage amount of olivine that can be derived even in the more magnesian system without causing appreciable change in the fractionating crystals is still relatively small. For example, if the first crystals were Fo_{93} and the liquid contained 40 per cent $(Mg+Fe^{+2})$, the Fo-content of later crystals should be lower by 2 percentage units by the time the liquid was only 18 per cent solidified. Thus, applied to the Table Mountain section (Figure 8A) even those rather optimum conditions would require that the Ultramafic Zone represent less than a fifth of its parent magma, whereas the unit forms well over half the volume of the Bay of Islands Complex as presently exposed. It is perhaps possible that a large amount of a residual liquid was lost from the complex – for example while it was being emplaced (reintruded?) with the peridotite solidified – but the whole situation is rather unprecedented, especially from the viewpoint that none of the well know stratiform-type layered intrusions contain such large volumes of peridotitic cumulates without showing conspicuous cyclic units defined by major layers of pyroxenite or gabbro. (The ultramafic cumulates of the Great Dyke provide some parallel, consisting as they do of highly magnesian olivine and orthopyroxene, but they feature a great deal of cyclic repetition, cf. Worst (1960); Jackson (1970).) However, a still more critical point arising directly from our data is that it appears likely that the 2 – 3 per cent variation in the $Mg/(Mg+Fe^{+2})$ ratios of the Bay of Islands peridotite – including the apparent "inverse trend" shown by olivine at North Arm Mountain – is largely due to variations in amount of trapped interstitial liquid. This, if true, leaves little basis on which even to attempt to apply the fractionation curves.

The effect of equilibration with trapped interstitial liquid can be evaluated by means of Figure 9B. Examining first the main diagram, where the fractionation curves now serve simply to

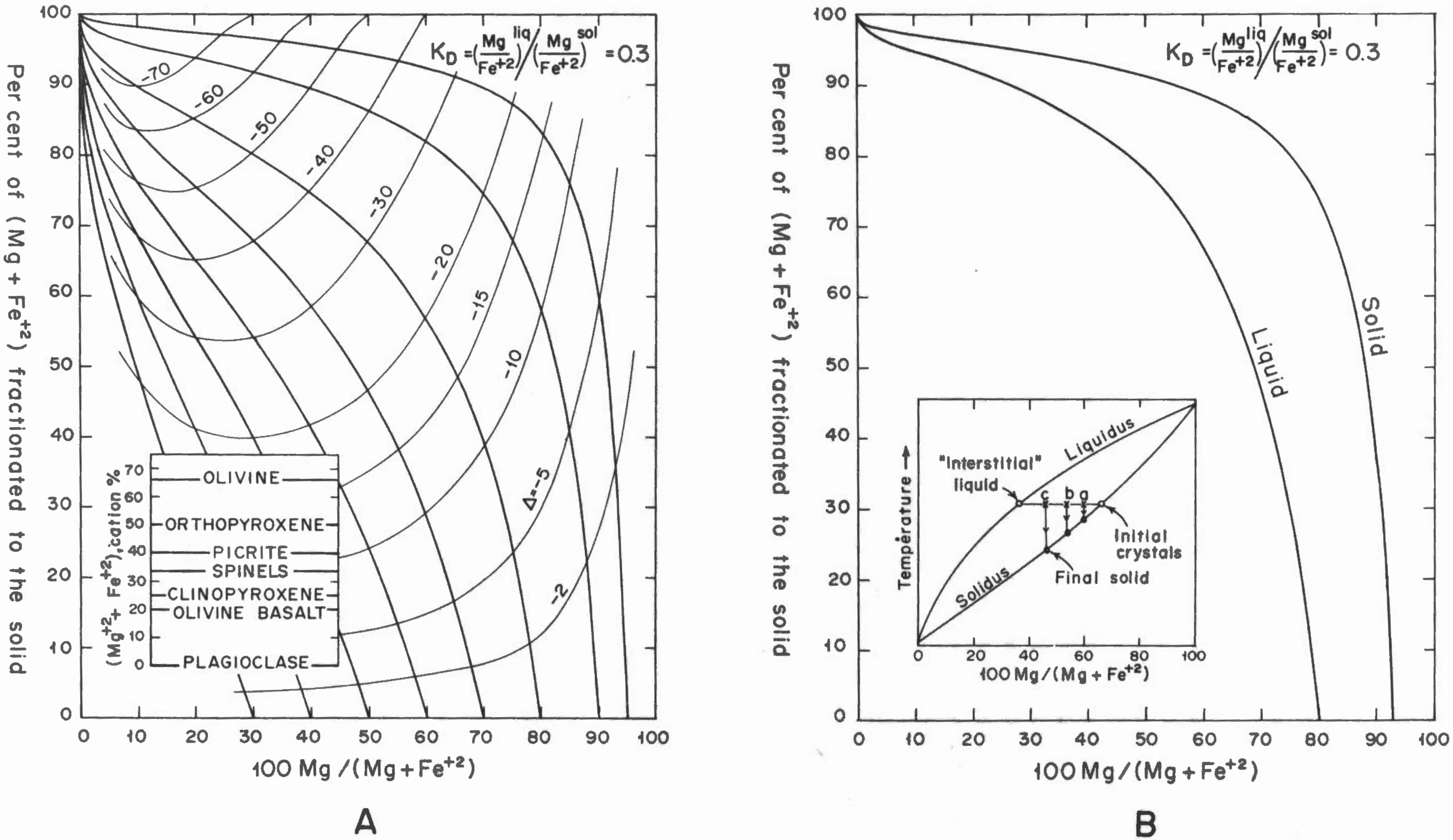

Figure 9. Curves showing the theoretical effect of fractional crystallization on $Mg/(Mg + Fe^{+2})$ in olivine and its parent liquid in a system "closed" or "unbuffered" with respect to oxygen. For explanation, see text.

illustrate the equilibrium compositions of coexisting olivines and liquids, it is seen that for olivine in the range Fo_{89} to Fo_{92}, such as found in alpine-type peridotite, the $Mg/(Mg+Fe^{+2})$ ratio of the liquid should be lower by some 13 percentage units. The phase diagram in the inset shows schematically how an increased proportion of the liquid (represented in the succession of "mixtures" a-b-c) can cause the olivine to become increasingly enriched in iron. In natural situations, the critical factor is not just the proportions of liquid and solid, but the ratio:

$$\frac{\text{Per cent liquid x per cent } (Mg+Fe^{+2}) \text{ in the liquid}}{\text{Per cent liquid x per cent } (Mg+Fe^{+2}) \text{ in the solid}}$$

Hence, other things being equal, a picritic liquid should have more affect than basaltic liquid, and basaltic liquid should have more affect in gabbroic rocks than in ultramafic rocks.

Quantitative application of Figure 9B to the Bay of Islands Complex shows that to change the Fo-content of the olivine in the peridotite by 2 percentage units would require about 40 per cent of interstitial basaltic liquid. From textural relations and the low Na_2O content of the peridotite, it is clear that this amount is too large. However, the same change could be effected by only 20-25 per cent picritic liquid (Na-poor), and, although this quantity is perhaps also rather high, it is the same amount as was suggested earlier for picritic liquid from the correlation between CaO and chromite cell edge. Moreover, the data in Figure 8 show that the $Mg/(Mg+Fe^{+2})$ ratios of the peridotite and its olivine do bear the appropriate relation to the CaO content of the rock and the cell edge of the chromite. As a rule, if these ratios are low, CaO is high and cell edge is low (implying the presence of a relatively large amount of liquid); if they are high, the opposite obtains. These correlations are not strong, but this is not surprising considering that the variations are so small and that there might be other complicating factors*. The evidence therefore seems reasonably good that the inferred effect is significant and has lowered the $Mg/(Mg+Fe^{+2})$ ratios of the samples richest in CaO by 1 – 2 percentage units.

Differences in amount of trapped interstitial (intercumulus) liquid are probably also partly responsible for the erratic $Mg/(Mg+Fe^{+2})$ variations in the Gabbro Zone. In the compositional range of the Gabbro the ratios of the liquid and the cumulus mafic minerals should have differed by 25 – 30 percentage units, and accordingly, equilibration of the crystals with 15 per cent of the liquid should have lowered their ratio by about 5 percentage units. If the equilibration was incomplete, still lower ratios could have resulted.

Conclusions

On the basis of the foregoing discussion the following conclusions appear valid for the Bay of Islands alpine-type peridotite, and probably apply also to the peridotites at Mount Albert and Blue River:

(1) Prior to its final solidification, the peridotite was an aggregate of olivine, subordinate orthopyroxene and minor Cr-rich chromite with a variable content, from 0 to about 20 per cent, of interstitial liquid, probably of picritic composition.

(2) At this stage, the Fo-content of the olivine was virtually constant at a value close to its present upper limit – that is, in the approximate range $Fo_{90.5}$ to Fo_{92}.

These features would suggest that the peridotite is the residue of a fractional melting process in which it was subjected to prolonged heating under very gentle thermal gradients, with the melt being slowly filtered off so that, through reaction, it had a homogenizing effect.

This interpretation does not eliminate the possibility that the alpine-type peridotite was originally a cumulate; in fact, it would even allow that the melt was partly composed of intercumulus liquid. However, it does seem clear that the peridotite has had a very different sub-liquidus history from the feldspathic dunite and other ultramafic rocks that overlie it, with several features suggesting that it solidified at considerably greater depths. On this basis, therefore, the rock could be regarded as a block of mantle material quite independent in origin from the cumulates of the Critical and Gabbro Zones, except for being the floor on which they accumulated. Moreover, since the roof of the Gabbro Zone is basalt, a possible extension of this postulate is that the gabbro magma was intruded along the interface between the mantle and crust. In an oceanic environment, the situation would be essentially like that pictured by Dewey and Bird (1970, fig. 4C) in their model of oceanic lithosphere.

We have no strong convictions in respect to these last interpretations – their evaluation requires detailed knowledge of the regional structure of the Bay of Islands area. An obvious problem is the presence of contact metamorphosed basalt beneath the Ultramafic Zone, but possibly this is in some way accounted for in the process of transfer of the complex from an oceanic to the continental regime.

Our main point is that the complex comprises two distinct kinds of olivine-rich ultramafic rocks of apparently two distinct origins – one, the feldspathic "dunite" of the Critical Zone, undoubtedly a cumulate, and the other, the alpine-type peridotite of the Ultramafic Zone, probably a residue of partial fusion solidified at considerably greater depths. Several authors have suggested that the Bay of Islands Igneous Complex is "intermediate" or "transitional" between stratiform and alpine complexes. It would seem more accurate to say that it is a *combination* of a rudely stratiform intrusion *with* alpine-type peridotite.

It is intriguing to speculate that such a combination might be fairly common in alpine ultramafic complexes. This could account for many of the seemingly dichotomous features and relations that have lead to the conflicting interpretations expressed in the literature. For example, could it be that the small irregular bodies of dunite with associated

*For example, the discussion here assumes that the system was "closed". It is not unlikely, however, that there was some migration of the liquid while it was solidifying.

pods and veins of chromite found within alpine-type peridotite are residual materials, recrystallized and to some extent redistributed during partial fusion and degassing of the mantle, while the larger zones of dunite with layered deposits of chromite are cumulates in adjoining intrusions? If the cumulates formed at fairly great depths, they might show similar mineralogy and be subject to the same deformation as the peridotite. Also, the interface between a peridotitic mantle and basaltic crust would seem a very likely site for emplacement of stratiform intrusions. Being a major structural and density discontinuity, it would be somewhat analogous to the unconformities between crystalline basement rocks and overlying sedimentary deposits that are commonly the locus of major basaltic and diabasic intrusions in the continents.

In reference to the specific problem posed for this symposium – the identification of ancient oceanic lithosphere – two observations from this study seem particularly significant:

(1) The Bay of Islands Critical and Gabbro Zones comprise the kinds of cumulates that would be expected to form from a K-poor, Ti-poor "transitional tholeiite" magma of the type common to the mid-ocean ridges. The objection has been made that ophiolite complexes thought to represent oceanic lithosphere do not contain this kind of basalt (Engel and Fisher, 1969) but this does not seem appropriate to Bay of Islands.

(2) There is little if any alpine-type peridotite in the Canadian Shield. An intriguing possibility is that there might be a distinctly different, "Precambrian alpine-type peridotite" representative of a very early, more primitive mantle, but at the moment we cannot point to a specific ultramafic body in the Shield that would seem to fit such a category. An alternative, of course, is that tectonic conditions or processes were sufficiently different in Precambrian times that solid mantle material was not emplaced into the continental crust.

Finally, it is suggested that the difference between cumulate and alpine-type peridotites revealed by the plots of NiO vs Cr_2O_3 in Figure 4 may be a useful additional criterion for distinguishing these rocks among altered materials dredged from the ocean floor. The discrimination is not unequivocal, but an examination of many data besides those illustrated indicates that it is very good on a percentage basis. The difference may also prove to be one of the more useful clues toward defining the nature and origin of alpine-type peridotite before it underwent partial fusion, if indeed this has been one of the stages in its development.

References

Baragar, W.R.A. 1967. Wakuach Lake map-area, Quebec-Labrador. *Geol. Surv. Can.*, Mem. 344, 174 p.

Bonnatti, E., J. Honnorez and G. Ferrara. 1970. Equatorial Mid-Atlantic Ridge: Petrologic and Sr isotopic evidence for an alpine-type rock assemblage. *Earth Plante. Sci. Lett.*, Vol. 9, 247-256.

Boyd, F.R. 1970. Garnet peridotites and the system $CaSiO_3$-$MgSiO_3$-Al_2O_3. *Amer. Mineral.* Spec. Paper No. 3, 63-75.

Boyd, F.R. and B.T.C. Davis. 1964. Effects of pressure on the melting and polymorphism of enstatite, $MgSiO_3$. *J. Geophys. Res.*, Vol. 69, 2101-2109.

Burch, S.J. 1969. Tectonic emplacement of the Burro Mountain ultramafic body, Santa Lucia Range, California. *Geol. Soc. Amer.*, Bull., Vol. 79, 527-544.

Cameron, E.M., G. Siddley and C.C. Durham. 1971. Distribution of ore elements in rocks for evaluating ore potential: Nickel, copper, cobalt and sulphur in ultramafic rocks of the Shield. *Can. Inst. Min.*, Spec. Vol. No. 11, 1-17.

Challis, G.A. 1965. The origin of New Zealand ultramafic intrusions. *J. Petrology*, Vol. 6, 322-364.

Carter, J.L. 1970. Mineralogy and chemistry of the Earth's Upper Mantle based on the partial fusion – partial crystallization model. *Geol. Soc. Amer.* Bull., Vol. 81, 2021-2034.

Chamberlain, J.A. and A.G. Johnston. 1970. Nickel in Canada. *Geol. Surv. Can.*, Map 1258A.

Coats, C.J.A. 1966. Serpentinized ultramafic rocks of the Manitoba Nickel Belt. Unpubl. Ph. D. thesis, Univ. Manitoba, 280 p.

Cooper, J.R. 1936. Geology of the southern half of the Bay of Islands igneous complex. *Newfoundland Dept. Nat. Res.*, Geol. Sec. Bull. 4.

Dewey, J.F. and J.M. Bird. 1970. Mountain belts and the new global tectonics. *J. Geophys. Res.*, Vol. 75, 2625-2648.

Dickey, J.S. 1970. Partial fusion products in alpine-type peridotites: Serrania de la Ronda and other examples. *Mineral. Soc. Amer.* Spec. Paper 3, 33-49.

Engel, C.G. and R.L. Fisher. 1969. Lherzolite, anorthosite, gabbro and basalt dredged from the Mid-Indian Ocean Ridge. *Science*, Vol. 166, 1136.

Fahrig, W.F. 1962. Petrology and geochemistry of the Griffis Lake ultrabasic sill of central Labrador Trough, Quebec. *Geol. Surv. Can.*, Bull. 77, 39 p.

Findlay, D.C. and C.H. Smith. 1965. The Muskox drilling project. *Geol. Surv. Can.*, Paper 64-44, 1-170.

Frey, F. 1970. Rare earth abundances in alpine ultramafic rocks. *Phys. Earth Planet. Interiors*, Vol. 3, 323-330.

Gass, I.G. 1968. Is the Troodos Massif of Cyprus a fragment of Mesozoic ocean floor. *Nature*, Vol. 220, 39-42.

Green, D.H. 1963. Alumina content of enstatite in a Venezuelan high-temperature peridotite. *Geol. Soc. Amer.* Bull., Vol. 74, 1397-1402.

————1964a. The petrogenesis of the high-temperature peridotite intrusion in the Lizard area, Cornwall. *J. Petrol.*, Vol. 5, 134-188.

————1964b. The metamorphic aureole of the peridotite at the Lizard, Cornwall. *J. Geol.*, Vol. 72, 543-563.

———— and W. Hibberson, 1970. The instability of plagioclase in peridotite at high pressure. *Lithos*, Vol. 3, 209-222.

————and A.E. Ringwood. 1967. The genesis of basaltic magma. *Contrib. Mineral. Petrol.*, Vol. 15, 103-109.

Hamilton, W. and W. Mountjoy. 1965. Alkali content of alpine ultramafic rocks. *Geochim. Cosmochim. Acta*, Vol. 29, 661-671.

Hess, H.H. 1955. Serpentines, orogeny and epeirogeny. *Geol. Soc. Amer.*, Spec. Paper, Vol. 62, 391-408.

————1960. Stillwater igneous complex, Montana, a quantitative mineralogical study. *Geol. Soc. Amer.*, Mem. 80, 230 p.

————1964. The oceanic crust, the upper mantle and Mayaguez serpentinized peridotite. *Nat. Acad. Sci. Nat. Res. Counc. Publ.*, 1118, 169-175.

Hostetler, P.B., R.G. Coleman, F.A. Mumpton and B.W. Evans. 1966. Brucite in alpine serpentinites. *Amer. Mineral.*, Vol. 51, 75-98.

Hurley, P.M. 1967. Rb^{87}-Sr^{87} relationships in the differentiation of the mantle. In Ultramafic and related rocks, P.J. Wyllie (editor), Wiley and Sons Inc., New York, 372-375.

Irvine, T.N. 1959. The ultramafic complex and related rocks of Duke Island, Alaska Ph. D. thesis, Calif. Inst. Technology, Pasadena, Calif., 320 p.

————1965a. Sedimentary structures in

igneous intrusions, with particular reference to the Duke Island ultramafic complex. *Soc. Econ. Paleontol. Mineral.* Spec. Publ. 12, 220-232.

———1965b. Chromian spinel as a petrogenetic indicator: Part 1, Theory. *Can. J. Earth Sci.*, Vol. 2, 648-672.

———1967. Chromian spinel as a petrogenetic indicator: Part 2, Petrologic applications. *Can. J. Earth Sci.*, Vol. 4, 71-103.

———1970. Crystallization sequences in the Muskox intrusion and other layered intrusions: I, Olivine-pyroxene-plagioclase relations. *Geol. Soc. Africa* Spec. Publ. 1, 441-476.

———and C.H. Smith. 1967. The ultramafic rocks of the Muskox intrusion, Northwest Territories, Canada. In Ultramafic and related rocks, P.J. Wyllie (editor), Wiley and Sons Inc., New York, 38-49.

———1969. Primary oxide minerals in the layered series of the Muskox intrusion. *Econ. Geol.* Monograph 4, 76-94.

Ito, K. and G.C. Kennedy, 1967. Melting and phase relations in a natural peridotite to 40 kilobars. *Amer. J. Sci.*, Vol. 265, 519-538.

———1968. Melting and phase relations in the plane tholeiite-basanite-lherzolite-nepheline basanite to 40 kilobars with geological implications. *Contrib. Mineral. Petrol.*, Vol. 19, 177-211.

Jackson, E.D. 1961. Primary textures and mineral associations in the ultramafic zone of the Stillwater complex, Montana. *U.S. Geol. Surv.* Prof. Paper 358, 106 p.

———1970. The cyclic unit in layered intrusions – a comparison of repetitive stratigraphy in the ultramafic parts of the Stillwater, Muskox, Great Dyke and Bushveld complexes. *Geol. Soc. S. Africa.* Spec. Publ. 1, 391-424.

Jambor, J.L. and C.H. Smith. 1964. Accurate determination of olivine compositions with small-diameter x-ray powder cameras. *Mineral. Mag.*, Vol. 33, 730-748.

Kushiro, I. and H.S. Yoder, Jr. 1966. Anorthite-forsterite and anorthite-enstatite reactions and their bearings on the basalt-eclogite transformation. *J. Petrol.*, Vol. 7, 337-362.

Leech, G.B. 1953. Geology and mineral deposits of the Shulaps Range. *B.C. Dept. Mines*, Bull. No. 32, 61 p.

MacGregor, I.D. 1962. Geology, petrology and geochemistry of the Mount Albert and associated ultramafic bodies of central Gaspé, Quebec. Unpubl. M.Sc. thesis, Queen's University, Kingston, Ontario, 288 p.

———1964a. A study of the contact metamorphic aureole surrounding the Mount Albert ultramafic intrusion. Unpubl. Ph.D. thesis, Princeton Univ., Princeton, N.J., 195 p.

———1964b. The reaction 4 enstatite + spinel ⇌ forsterite + pyrope. *Carnegie Inst. Washington, Yearbook* 63, 157.

———1970. The effect of CaO, Cr_2O_3, Fe_2O_3 and Al_2O_3 on the stability of spinel and garnet peridotites. *Phys. Earth Planet. Interiors*, Vol. 3, 372-377.

———and C.H. Smith. 1963. The use of chrome spinels in petrographic studies of ultramafic intrusions. *Can. Mineral.*, Vol. 7, 403-412.

MacRae, N.D. 1969. Ultramafic intrusions of the Abitibi area, Ontario. *Can. J. Earth Sci.*, Vol. 6, 281-304.

Maxwell, J.C. 1969. "Alpine" mafic and ultramafic rocks – The ophiolite suite: A contribution to the discussion of the paper "The origin of ultramafic and ultrabasic rocks" by P.J. Wyllie. *Tectonophysics*, Vol. 7, 489-494.

Meyer, H.O.A. and F.R. Boyd. 1970. Inclusions in diamonds. *Carnegie Inst. Washington, Yearbook* 68, 315-320.

Moores, E.M. 1969. Petrology and structure of the Vourinos Ophiolitic Complex of Northern Greece. *Geol. Soc. Amer.* Spec. Paper 118, 73 p.

———1970. Ultramafics and orogeny, with models of the U.S. Cordillera and the Tetheys. *Nature*, Vol. 228, 837-842.

Muir, I.D. and C.E. Tilley. 1964. Basalts from the northern part of the rift zone of the Mid-Atlantic Ridge. *J. Petrol.*, Vol. 5, 499-434.

Nafziger, R.H. and A. Muan, 1967. Equilibrium phase compositions and thermodynamic properties of olivines and pyroxenes in the system MgO-FeO-SiO_2. *Amer. Mineral.*, Vol. 52, 1364-1385.

Naldrett, A., J.G. Bray, E.L. Gasparrini, T. Podolsky and J.C. Rucklidge. 1970. Cryptic variation and the petrology of the Sudbury Nickel irruptive. *Econ. Geol.*, Vol. 65, 122-155.

Naldrett, A.J. and G.D. Mason. 1968. Contrasting Archean ultramafic igneous bodies in Dundonold and Clergue Townships, Ontario. *Can. J. Earth Sci.*, Vol. 5, 111-143.

O'Hara, M.J. 1965. Primary magmas and the origin of basalts. *Scot. J. Geol.*, Vol. 1, 19-40.

———1967. Mineral paragenesis in ultrabasic rocks. In Ultramafic and related rocks, P.J. Wyllie (editor), Wiley and Sons Inc., New York, 393-403.

———1968. The bearing of phase equilibria studies in synthetic and natural systems on the origin and evolution of basic and ultrabasic rocks. *Earth Sci. Rev.*, Vol. 4, 69-133.

Presnall, D.C. 1969. The geometrical analysis of partial fusion. *Amer. J. Sci.*, Vol. 217, 1178-1194.

Ragan, D.M. 1967. The Twin Sisters dunite, Washington. In Ultramafic and related rocks, P.J. Wyllie (editor), Wiley and Sons Inc., New York, 160-167.

Roe, G.D., W.H. Pinson and P.M. Hurley. 1965. Rb-Sr evidence for the origin of peridotites. *Trans. Amer. Geophys. Un.* 46, 186 (Abstr.).

Roeder, P.L. and R.F. Emslie. 1970. Olivine-liquid equilibrium in basaltic melts. *Contrib. Mineral. Petrol.*, Vol. 29, 275-289.

Rogders, J. and E.R.W. Neale. 1963. Possible "Taconic" klippen in western Newfoundland. *Amer. J. Sci.*, Vol. 261, 713-730.

Ross, C.S., M.D. Foster and A.T. Myers. 1954. Origin of dunites and olivine-rich inclusions in basaltic rocks. *Amer. Mineral.*, Vol. 39, 693-737.

Scoates, R.F.J. 1969. Ultramafic rocks of Manitoba. *Manitoba Dept. Mines Nat. Resources.* Preliminary Map 1969A.

Smith, C.H. 1958. Bay of Islands igneous complex, western Newfoundland. *Geol. Surv. Can.*, Mem. 290, 132 p.

———1962. Ultramafic intrusions in Canada and their significance to Upper Mantle studies. *Can. Geophys. Bull.*, Vol. 14, 157-169.

———and H.E. Kapp. 1963. The Muskox intrusion, a recently discovered layered intrusion in the Coppermine River area, Northwest Territories, Canada. *Mineral. Soc. Amer.* Spec. Paper 1, 30-35.

Stevens, R.K. 1970. Cambro-Ordovician flysch sedimentation and tectonics in west Newfoundland and their possible bearing on a Proto-Atlantic Ocean. *Geol. Assoc. Can.* Spec. Paper. 7, 165-177.

Stueber, A.M. and V.R. Murthy. 1966. Strontium isotope and alkali element abundances in ultramafic rocks. *Geochim. Cosmochim. Acta*, Vol. 30, 1243-1259.

Stueber, A.M. and G.G. Goles. 1965. Abundances of Na, Mn, Cr, Sc, and Co on ultramafic rocks. *Geochim. Cosmochim. Acta*, Vol. 31, 75-93.

Thayer, T.P. 1960. Some critical differences between alpine-type and stratiform peridotite-gabbro complexes. *21st Internat. Geol. Congr.*, Copenhagen, Repts. Part 13, 247-259.

———1963a. The Canyon Mountain complex, Oregon, and the alpine mafic magma stem. *U.S. Geol. Surv.* Prof. Paper 475-C, C82-C85.

———1963b. Flow layering in alpine peridotite-gabbro complexes. *Mineral. Soc. Amer.* Spec. Paper 1, 55-61.

———1964. Principal features and origin of podiform chromite deposits, and some observations on the Guleman-Soridag District, Turkey. *Econ. Geol.*, Vol. 59, 1497-1524.

———1966. Serpentinization considered as a constant volume metasomatic process. *Amer. Mineral.*, Vol. 51, 685-710.

———1967. Chemical and structural relations of ultramafic and feldspathic rocks in alpine intrusive complexes. In Ultramafic and related rocks, P.J. Wyllie (editor), Wiley and Sons Inc., New York, 222-239.

————1969a. Alpine-type sensu stricto (ophiolitic) peridotites: refractory residues from partial melting or igneous sediments? *Tectonophysics,* Vol. 7, 511-516.

————1969b. Gravity differentiation and magmatic replacement of podiform chromite deposits. *Econ. Geol.* Monograph 4, 132-146.

————1969c. Peridotite-gabbro complexes as keys to the petrology of mid-ocean ridges. *Geol. Soc. Amer.* Bull., Vol. 80, 1515-1522.

Wager, L.R., G.M. Brown and W.J. Wadsworth. 1960. Types of igneous cumulates. *J. Petrol.,* Vol. 1, 73-85.

Walcott, R.I. 1969. Geology of the Red Hill Complex, New Zealand. *Trans. Roy. Soc. N.Z. Earth Sciences,* Vol. 7, 57-88.

Wilson, H.D.B., L.C. Kilburn, A.R. Graham and K. Ramlal. 1969. Geochemistry of some Canadian nickeliferous ultrabasic intrusions. *Econ. Geol.* Monograph 4, 294-309.

Wolfe, W.J. 1966. Petrology, mineralogy and geochemistry of the Blue River ultramafic intrusion, Cassiar District, British Columbia. Unpubl. Ph.D. thesis, Yale University, New Haven, Conn., 174 p.

Worst, B.G. 1960. The Great Dyke of southern Rhodesia. *Geol. Surv. S. Rhodesia* Bull., Vol. 47, 234 p.

Wyllie, P.J. 1970. Ultramafic rocks and the upper mantle. *Mineral. Soc. Amer.* Spec. Paper 3, 3-32.

No. 9

some physical and chemical aspects of precambrian volcanic belts of the canadian shields

W.R.A. BARAGAR
Geological Survey of Canada
Ottawa

Abstract. This paper reviews some of the physical and chemical characteristics of Precambrian greenstone belts of the Canadian Shield; mainly those of Noranda, Yellowknife, and Uchi Lake (Archean) and of the Grenville Province (Proterozoic). The greenstone belts are thick, mainly conformable successions of volcanic rocks characterized by a cyclic, upward change in lithology and composition from basic to acid. Basic and ultrabasic sills and iron-formation are commonly present, particularly in the basic and acid fractions respectively. The boundary relationships of the greenstone belts are generally obscured by intrusive granites, but the Labrador Trough and possibly the Yellowknife belt, appear to be founded upon continental crust. The composition of the basaltic fraction of the greenstone assemblages is similar to oceanic tholeiite except for slightly higher potash content, iron-magnesium ratio, and lower alumina content. The intermediate to acidic fraction resembles the calo-alkaline succession of the circumpacific belt except for generally lower potash contents and contrasting alumina differentiation trends. In circumpacific successions alumina is characteristically depleted with differentiation from high-alumina basalts to low-alumina felsites, whereas in Precambrian successions, which commence with low-alumina basalts, it may be either enriched, maintained at about the same level, or depleted with differentiation.

The characteristics of Precambrian greenstone belts taken together, contrast markedly with those of oceanic-ridge assemblages. It might be supposed that the basic fraction of the greenstone belts was generated at the ridge and the acid fraction at the subduction zone. If so, the continuous sequential transition from basic to acidic rocks, the repetition of basic to acid cycles, and the compositional distinctions manifest between Precambrian greenstone assemblages and their supposed oceanic and circumoceanic counterparts, would be difficult to explain.

Introduction

The purpose of this symposium, to survey the continents for possible remnants of ancient ocean crusts, limits the scope of this paper to the greenstone belts, a term that will be used throughout this paper. The plateau basalts of Coppermine River. Lake Superior, and Seal Lake regions are subaerial for the most part and were deposited on the continents. They could not, therefore, have been oceanic crust. Most of the material herein is drawn from the Archean belts near Yellowknife, Uchi Lake, and Noranda, and from the Proterozoic belts near Kaladar in the Grenville Province, and the Labrador Trough. The purpose is to review the principal physical and chemical properties of Precambrian greenstone belts so that they may be compared with those of oceanic deposits.

Physical aspects of Precambrian greenstone belts

Greenstone belts, a name reflecting the generally low-grade metamorphic character of the volcanic rocks, are widely scattered in the Canadian Shield. They are generally linear in form with the exception, principally, of the Yellowknife Group which appears to have formed in a broad basin. Volcanic rocks typically form the basal and predominant part of the greenstone belts. Exceptions are the Yellowknife Group where sedimentary rocks predominate, and the Labrador Trough where volcanic rocks are late in the sequence. The volcanic rocks are mostly or entirely of submarine deposition and are commonly interlayered with thin cherty beds. Pillowed lavas are characteristic of the volcanic assemblage. Quartzose greywackes, impure quartzites and slates appear to be the principal associated sediments. According to some authors (Goodwin and Shklanka, 1967; Ridler, 1970; Ayres, 1969) such sediments are mainly volcanogenic. However, Donaldson and Jackson (1965) and McGlynn and Henderson (in press) find that sediments associated with volcanic belts in northwestern Ontario and Mackenzie District respectively contain a higher proportion of coarse quartz than is consistent with a volcanogenic origin. In addition, associated conglomerates contain at least subordinate quantities of granitoid boulders. Thus, they conclude that the sediments are partly derived from pre-existing sialic basement.

Volcanic sequences in the greenstone belts are typically thick; 30,000 – 50,000 feet being not uncommon (e.g. Goodwin, 1967; Baragar, 1966, 1968; Ridler, 1969). Less is known about the accompanying sediments, which are more readily deformed and accordingly less easily measured.

The volcanic rocks of the greenstone belts are predominantly basaltic. Baragar and Goodwin (1969) estimated the relative proportions of the main volcanic classes in four well-studied Archean belts as: basalts – 60 per cent; andesites – 28 per cent; and remaining salic rocks – 12 per cent.

Metamorphic grades are generally low – mainly greenschist or low amphibolite facies – and structures in the volcanic rocks are commonly little deformed.

The stratigraphy of Precambrian volcanic assemblages in the greenstone belts is exemplified by the four stratigraphic sections given in Figure 1. Three Archean belts – Uchi Lake (Goodwin, 1967); Yellowknife (Henderson and Brown, 1966; Baragar, 1966); and Noranda (Baragar, 1968); – and one Proterozoic belt (Grenville, Sethuraman, 1970) are represented. The Grenville section is a synthesis of two partial sections but it is believed that they can be joined together as shown here with little misfit (Sethuraman, 1970).

The principal features of the stratigraphy are as follows:

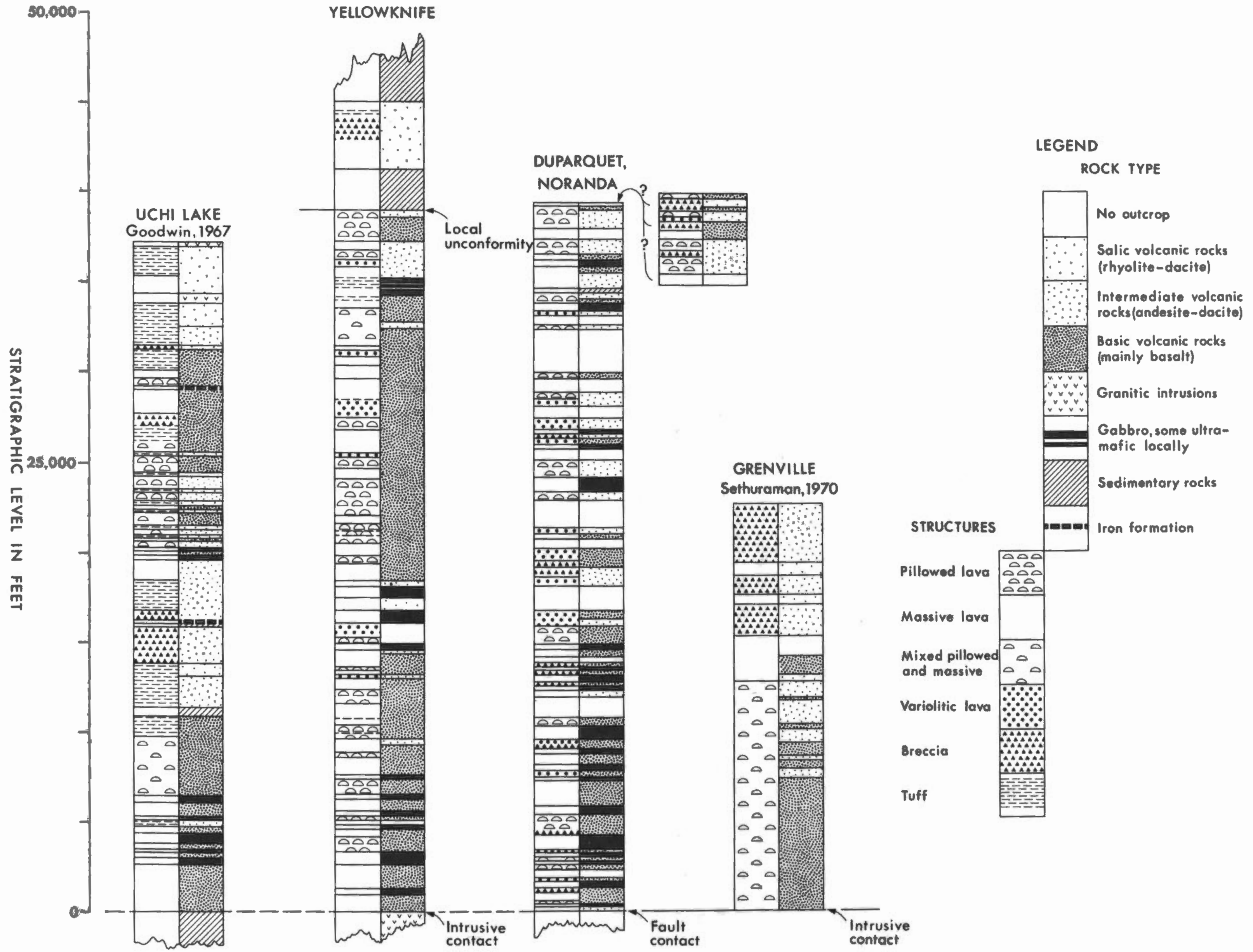

Figure 1. Comparison of stratigraphic sections characteristic of four Precambrian greenstone belts. The stratigraphic position of the offset segment of the Duparquet section is uncertain, but it is at least partly younger than the main section.

(1) The lithology changes systematically from basic to salic upward in the succession. The change is not generally abrupt but takes place over a stratigraphic range of varying thickness by interlayering of flows of different composition.

(2) More than one mafic to acid cycle may be present in any one succession. Examples shown here are Yellowknife and Uchi Lake. Ridler (1969) recognizes parts of three cycles in the Kirkland Lake region.

(3) The entire succession of a greenstone belt, regardless of number of cycles, is generally conformable. An exception is in the Yellowknife section where an unconformity occurs high in the upper cycle. However, elsewhere in the Yellowkife Group no unconformity is recognized at this level.

(4). The mafic fractions of the volcanic sequences are dominated by pillowed and massive flows whereas the salic or acid fractions are dominated by fragmental rocks.

(5) The mafic rocks show repeated evidence throughout the sections of submarine deposition but the salic rocks rarely show evidence of either submarine or subaerial deposition.

(6) Mafic sills with compositions similar to their host rocks are generally abundant in the lower parts of the volcanic sequences.

(7) Iron-formation, although present only in the Uchi Lake section of Figure 1, is a characteristic component of Precambrian volcanic belts. It commonly occurs near the tops of the volcanic cycles or in the immediately overlying sediments. Examples are the Bee Lake and Michipicotin belts described by Goodwin and Shklanka (1967), the Timmins-Kirkland Lake-Noranda belt described by Goodwin (1965a) and Ridler (1970a) and the Ennadai-Tavani belt observed recently by Ridler (1970, personal communication).

(8). Ultramafic sills are not shown separately in Figure 1. Although not present in most of these sections, they are a common associate of the greenstone belts and commonly appear with the mafic fraction (Naldrett and Mason, 1968; MacRae, 1969). Whether or not they occupy a distinctive stratigraphic position in most greenstone belts is not known. In the Labrador Trough they are late components of the volcanic succession.

Most of the Precambrian greenstone belts are bounded by intrusive granites. Accordingly the bases of the successions are rarely preserved and the nature of their floors is generally unknown. An exception is the Aphebian Labrador Trough which is clearly founded on Archean continental crust (Baragar, 1967; Dimroth *et al.*, in press). Among Archean belts some evidence exists that the Yellowknife Group was similarly deposited upon continental crust (Baragar, 1966; Heywood and Davidson, 1969; McGlynn and Henderson, 1970). Because of the importance of this point to the present discussions some of the evidence might be briefly reviewed here.

In the Cameron River area about 45 miles east of Yellowknife volcanic rocks of the lower Yellowknife Group (there about 9,000 feet thick) are bounded on the west side by the conformably overlying greywacke and slates and on the east side by granitic gneisses. The contact between the gneisses and flows is generally concordant with the attitude of the flows but no clear evidence is present as to the nature of the contact. A swarm of closely-spaced mafic dykes roughly parallel in attitude to the contact, intrudes both gneisses and flows in great profusion but does not penetrate the overlying sediments. A few miles farther east a younger, generally massive granite invades the gneisses and the dykes that intrude them. The mafic dyke swarm can reasonably be assumed to be the subsurface expression of the Yellowknife volcanic rocks and, if so, the granitic gneisses are clearly basement to the Yellowknife Group. Green (1968), on the basis of Rb-Sr ages has disputed this conclusion. Nevertheless, some 80 miles to the east a similar relationship between gneisses intruded by mafic dykes and structurally overlying Yellowknife volcanic rocks led Heywood and Davidson (1969) to the same conclusion. McGlynn and Henderson (in press) citing, in addition, Stockwell's (1933) evidence of a basal conglomerate in the Yellowknife Group at Point Lake generally concur in this interpretation.

Chemical properties of the greenstone belts

Three aspects of the chemistry of Precambrian greenstone belts are presented in this section: the bulk compositions; the variation of composition with time in the eruptive sequence; and the relative variation between chemical components of each succession.

Bulk compositions

The most characteristic bulk composition of a volcanic sequence is probably that of the basalts erupted early in the sequence. These can be expected to be close to the parent magma in composition.

Table I shows the average compositions of basalts from a number of Precambrian greenstone belts. The Archean and Grenville averages are from systematically sampled sequences and are probably representative of basalts in these sequences. The average basalt of the Labrador Trough comprises analyses from widely scattered localities and a number of sources. Nevertheless because of the general similarity of most of the individual analyses it too is probably close to a representative result. An average of 25 oceanic tholeiites is given for comparison.

The method of classifying analyses as basalts is that followed by Baragar and Goodwin (1969) utilizing normative colour index and plagioclase composition, but including both the basalt and Type A categories of that publication. Thus all analyses that comprise the averages of Table I have been selected by the same criteria.

The average basalts of Table I are remarkably similar although the oceanic tholeiite is slightly more primitive. That is to say, the usual measures of differentiation – potash content, iron-magnesium ratio – are somewhat lower. The most significant differences between the oceanic tholeiite and the Precambrian basalts are

Table I

Comparison of average analyses of Precambrian basalts with an average of some oceanic basalts

	No. of analyses	SiO_2	Al_2O_3	Fe_2O_3	FeO	CaO	MgO	Na_2O	K_2O	TiO_2	P_2O_5	MnO	CO_2	H_2O	$CO_2 + H_2O$	
1. Birch-Uchi	56	48.7	15.0	2.57	8.60	8.82	5.83	2.30	.36	.95		.20			5.35	Archean
2. Lake of the Woods Wabigoon	181	50.0	14.5	2.72	9.05	8.60	5.95	2.45	.40	1.01	.26	.21			5.10	Archean
3. Timmins - Noranda	141	50.2	14.4	2.32	9.13	9.39	6.01	2.68	.26	1.24	.13	.20	1.23	3.32	4.55	Archean
4. Yellowknife	69	50.1	15.0	2.78	9.38	9.50	6.50	2.24	.34	1.11		.18	.30			Archean
5. Labrador Trough	22	48.8	14.1	2.36	9.78	10.07	7.28	2.52	.22	1.08	.10	.22	.22	3.14	3.36	Aphebian
6. Grenville	29	48.0	14.7	1.89	10.30	9.83	8.12	3.27	.20	1.06	.10	.19	1.64	1.63	3.27	Neohelikian
7. Oceanic Tholeiites	25	49.29	16.89	2.06	6.79	11.55	7.46	2.81	.18	1.37	.12	.16		1.12		

Averages 1-4 are from Baragar and Goodwin, 1969 but modified so as to be classified on the same basis as basalts from the Labrador Trough and Grenville. Average 5, Dimroth *et al.* (in press). Average 6 produced on the basis of results reported in Sethuraman, 1970. Average 7 for analyses reported by Nicholls *et al.*, 1964; Engel and Engel, 1963; Engel, Engel, and Havens, 1965; Engel, Fisher, and Engel, 1965, Cann and Vine, 1966; Engel and Fisher, 1969.

the lower alumina, and less markedly, lime and titania contents of the latter.

Note that there is no evidence of an evolution in basaltic composition with time in these averages. Fahrig (1970) and Mueller (1970) found a consistent potash enrichment in Precambrian diabase dykes of diminishing age and Mueller, in addition, found parallel enrichment in titania and impoverishment in magnesia.

Variations of composition with time in the eruptive sequence

The variation of lava composition with time in an eruptive sequence has been examined in a few thick, closely sampled stratigraphic sections in the Yellowknife, Noranda, and Grenville volcanic belts (Baragar, 1966, 1968; Sethuraman, 1970). In Figure 2 results from the three sections are presented. Samples in each section were generally taken at 400- or 500-foot stratigraphic intervals but to eliminate local scattering the results have been averaged over intervals of chiefly 3,000 (Grenville) and 5,000 (Yellowknife, Noranda) feet. Salic rocks in the Yellowknife section have been averaged separately. The average analysis of each interval has been plotted at the mid-point of the interval. The two segments of the Grenville section have been joined to give a continuous section as is believed appropriate on the basis of field work (Sethuraman, 1970).

Note that the Yellowknife section includes two basic to acidic cycles each of about the same thickness as the Grenville section. The Noranda section, on the other hand, although nearly as thick as the two Yellowknife cycles together does not span a complete cycle in that acidic rocks are virtually absent. Minor amounts of salic fragments are found in the upper parts of the Noranda section and these are thought to be stratigraphically equivalent to major acidic units farther east.

The major features to be noted from Figure 2 are:

(1) The rocks become progressively less mafic with time; that is, upward in the volcanic sequence. This is represented in a gross way by the colour index and in more detail by the marked upward decline in iron, magnesia, and to lesser degree, titania contents.

(2) The rocks become more alkalic and siliceous with time. The proportion of lime generally diminishes while that of alkalis and silica rises. In the case of Noranda, which is an extended mafic part of the cycle, the changes are less marked.

(3) The alumina content of both Noranda and Grenville sequences increases steadily with increasing stratigraphic level. The upper cycle of the Yellowknife section tends towards a similar trend.

The changes in composition with stratigraphic level illustrated by these three sections are probably characteristic of Precambrian greenstone belts in general, as evident in studies by Goodwin in the Birch-Uchi (1967) and Lake of the Woods-Wabigoon (1965) areas and by Ridler (1969) in the Kirkland Lake area. The salient feature of the changing composition is the mafic to acidic eruptive cycle.

Relative variations between chemical components

The chemical characteristics of magmatic provinces are generally distinguished by the manner in which their constituents vary with respect to one another. In Figures 3 to 6 are illustrated some of the variations that may be characteristic of Precambrian greenstone belts.

Figure 3 shows projections onto the base of the Diopside-Olivine-Nepheline-Quartz tetrahedron of average analyses from the Uchi Lake, Yellowknife, Noranda, and Grenville sections of Figure 1. The last three sections are represented

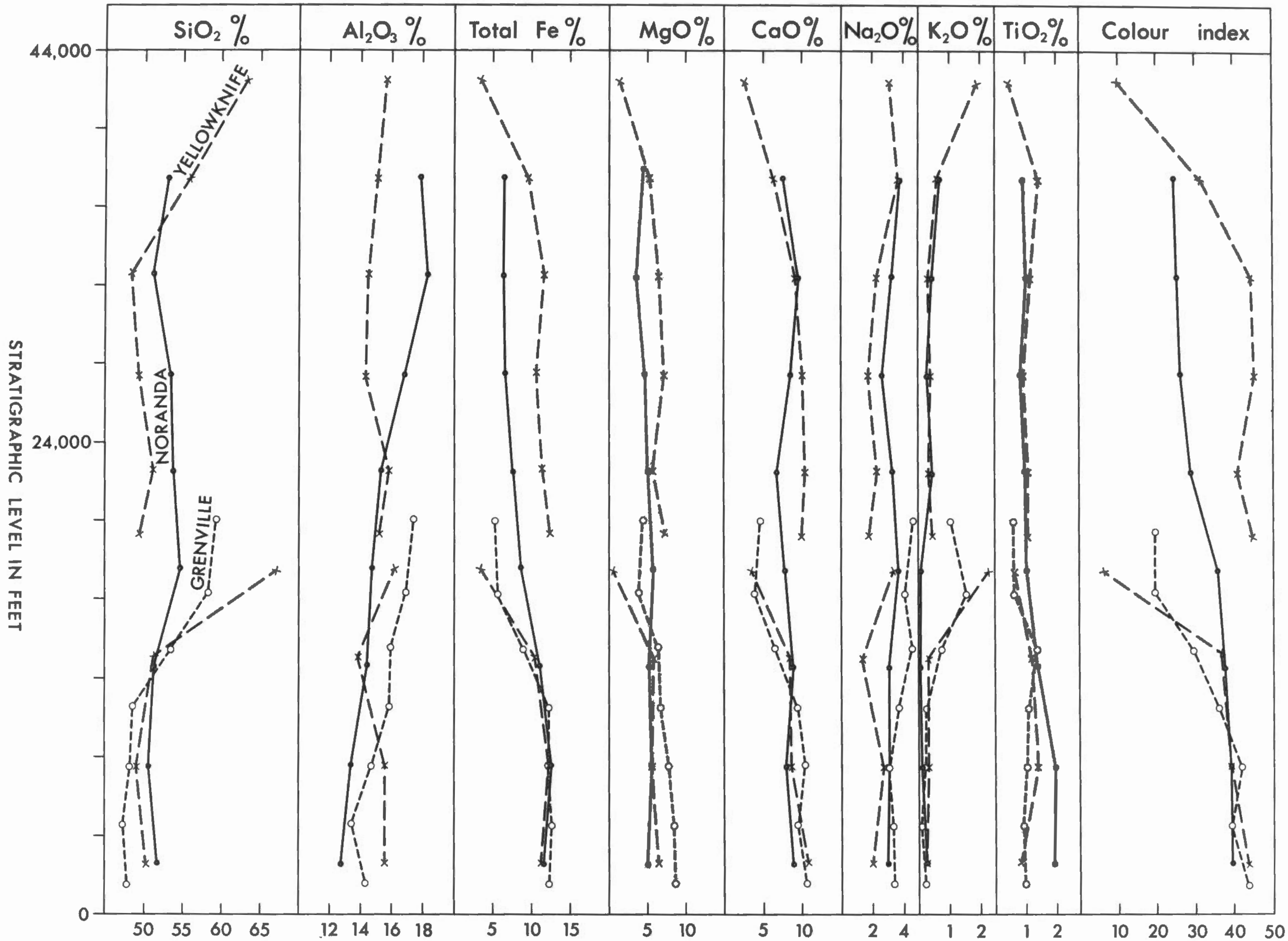

Figure 2. The variation of volcanic compositions with stratigraphic level in well-sampled sections of three Precambrian greenstone belts. Sample interval is 400 – 500 feet stratigraphically but the plotted points are average analyses for each 3,000-foot (Grenville) or 5,000-foot (Yellowknife and Noranda) stratigraphic interval. Acidic rocks in the Yellowknife section are averaged separately.

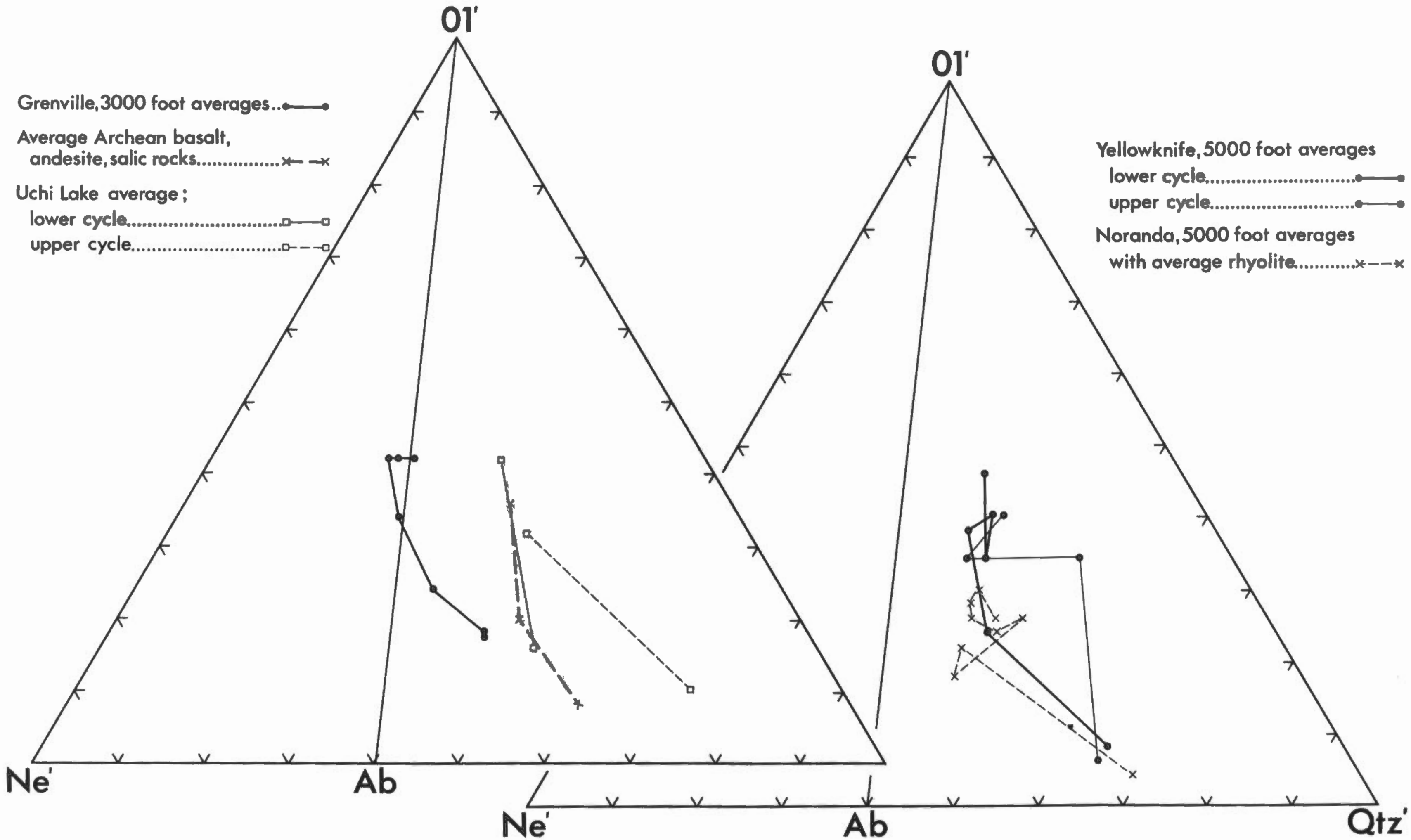

Figure 3. Projections on to the base of the basalt tetrahedron (normative Ol'-Ne'-Qtz'-Di') of average analyses representing successive stages in the evolution of a number of Precambrian greenstone belts. The rhyolitic stage of the Noranda belt is represented by an average of a number of rhyolite analyses from the region (Sakrison, 1966) since salic rocks are virtually absent in the Duparquet section.

by the 5,000-foot and 3,000-foot averages of Figure 2, and the Uchi section by average analyses of the basic and acidic segments of each cycle (Goodwin, 1967). In addition are plotted the average basalt, andesite, and salic rock for the Archean of the Canadian Shield as determined by Baragar and Goodwin (1969). In these plots the analyses are totally recast into normative olivine, nepheline, and quartz. The purpose of the diagrams is to show clearly the contrast between trends leading to feldspathoidal, and to quartz enrichment, respectively.

The trends of the Precambrian sequences are all sharply directed towards the quartz apex. Most of them originate well within the tholeiitic field but the Grenville sequence does commence on the alkali basalt side of the plane of critical undersaturation. Clearly the major trend of the Precambrian sequences is towards silica enrichment. This contrasts with what we know of trends along much of the mid-ocean ridges where tholeiitic substructures are commonly topped by feldspathoidal rocks of the islands (Engel *et al.,* 1965).

One exception to the general Precambrian trend of silica enrichment is the Timiskaming feldspathoid-bearing volcanic rocks at Kirkland Lake (Cooke and Moorehouse, 1969). Ridler (1969) has suggested that these form the upper part of the greenstone succession of that region rather than a discrete volcanic episode unrelated to the greenstones.

Another aspect of the chemistry of Precambrian greenstone belts is shown in the alkali-iron-magnesium diagrams of Figure 4. In each of the three greenstone belts (Yellowknife, Grenville, Noranda) represented in the figure two trends of differentiation are evident. One represents enrichment in iron relative to magnesia— the tholeiitic trend—; the other represents enrichment in alkalis with negligible enrichment in iron – the calc-alkaline trend. The former is the common differentiation trend of mafic intrusions crystallizing at shallow depths. Indeed, the trends of differentiated mafic sills from each of the Yellowknife and Noranda sections shown in the diagram, parallel the tholeiitic trend of the lavas. Thus it seems reasonable to attribute this trend to fractional crystallization of the mafic magma in high-level reservoirs such as the accompanying sills.

The other trend is that which may be traced upward through the stratigraphic successions (Figure 2) and is evidently a more fundamental attribute of the volcanism. It is similar to calc-alkaline trends of the circumpacific belt but differs in some important respects which will be noted in the next two diagrams.

Figure 5 shows plots of normative An-Ab-Or for Yellowknife and Noranda rocks. Because the sections sampled at Noranda contained few acidic volcanic rocks these are not well represented in the diagram. The diagrams illustrate two features of Precambrian greenstone belts: the lack of a coherent trend, and a general impoverishment in orthoclase relative to rocks of the circumpacific* belt. Possibly two trends are distinguishable; a main trend with little enrichment in potash and a subsidiary trend similar to that of the circumpacific belt.

The distinction between Precambrian volcanic belts and the circumpacific belt is more apparent in the alumina-colour-index plots of Figure 6. These show the contrasting behaviour of alumina with differentiation in the two environments. In the upper diagram the density of analyses from several localities along the circumpacific belt is represented by contours. The trends of several Precambrian greenstone belts are shown by lines joining average analyses representing successive segments of each trend. The main features are presented in the simplified lower diagram. Circumpacific volcanic rocks form a smooth trend from high-alumina basalts at the mafic end to low-alumina salic rocks at the acidic end of the sequence. Precambrian volcanic rocks of the greenstone belts originate with low-alumina basalt and proceed along one of three trends: (1) enrichment in alumina (Noranda, Grenville); (2) maintenance of original alumina content (Yellowknife, lower cycle of Uchi section, average Archean basalt, andesite, salic); and (3) impoverishment in alumina (upper cycle of Uchi section). The second trend is thought to be the major one.

*Circumpacific magma compositions are represented by analyses from the North American Cordilleran and Aleutian arc compiled from a number of sources by Dr. T.N. Irvine. The original references are to be found in Irvine and Baragar (in press).

Summary of chemical properties

(1) Basalts of Precambrian greenstone belts are generally similar to oceanic basalts except for lower alumina, slightly lower titania, and higher potash contents and higher iron-magnesia ratio.

(2) Precambrian greenstone assemblages characteristically evolve from mafic to acidic compositions with time in the eruptive sequence. More than one such cycle may be present in a continuous, conformable sequence.

(3) The Precambrian greenstone successions lack simple, coherent differentiation trends. Elements of both tholeiitic and calc-alkaline trends are recognized. The tholeiitic trend, attributable to differentiation in high-level reservoirs, is superimposed upon the major calc-alkaline trend.

(4) The calc-alkaline trend of the Precambrian greenstone successions differs from that of the circumpacific belt in the behaviour of alumina and in the generally lower levels of potash present. Alumina is characteristically depleted during differentiation of circumpacific lava sequences from high-alumina basalt to low-alumina salic rocks. In contrast Precambrian successions commence with low-alumina basalts and either gain, maintain or lose alumina during differentiation.

Precambrian greenstone belts as remnants of oceanic crust?

It will be readily apparent from the previous descriptions that there is little resemblance between the Precambrian greenstone belts of the Canadian Shield as they exist today and volcanic sequences of the oceanic ridges. The Precambrian successions typically evolve from mafic to acidic rocks, alkali basalts are rare, and feldspathoidal lavas are known only at Kirkland Lake. In contrast, acidic rocks are rare on the oceanic ridges and feldspathoidal rocks seem to be the principal end products of the eruptive sequence.

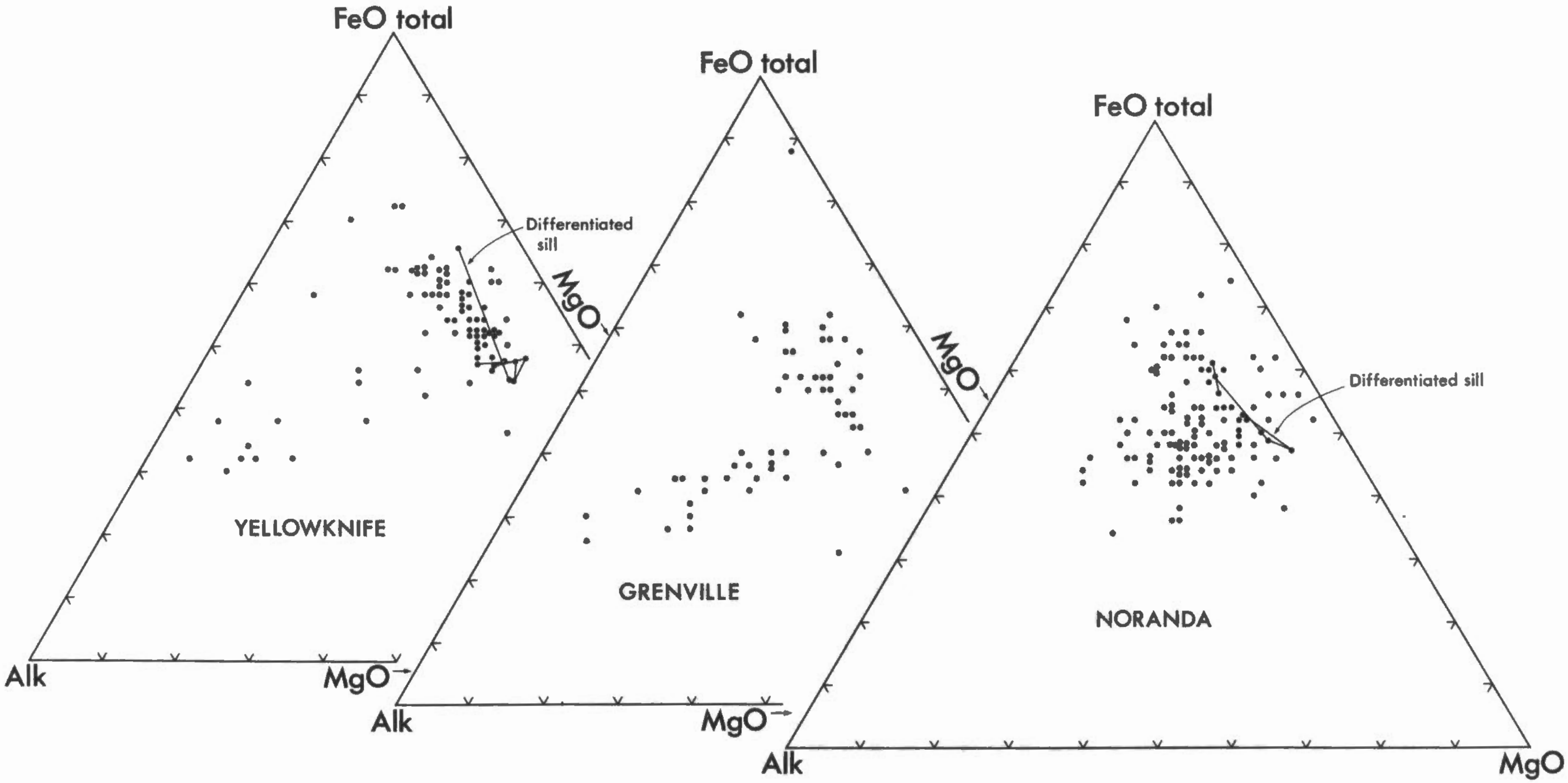

Figure 4. AFM diagram of individual analyses from sampled sections of the Grenville, Yellowknife, and Noranda greenstone belts (cf. Figure 2). Also shown are successive samples from differentiated sills (joined by lines) associated with the Yellowknife and Noranda volcanic assemblages.

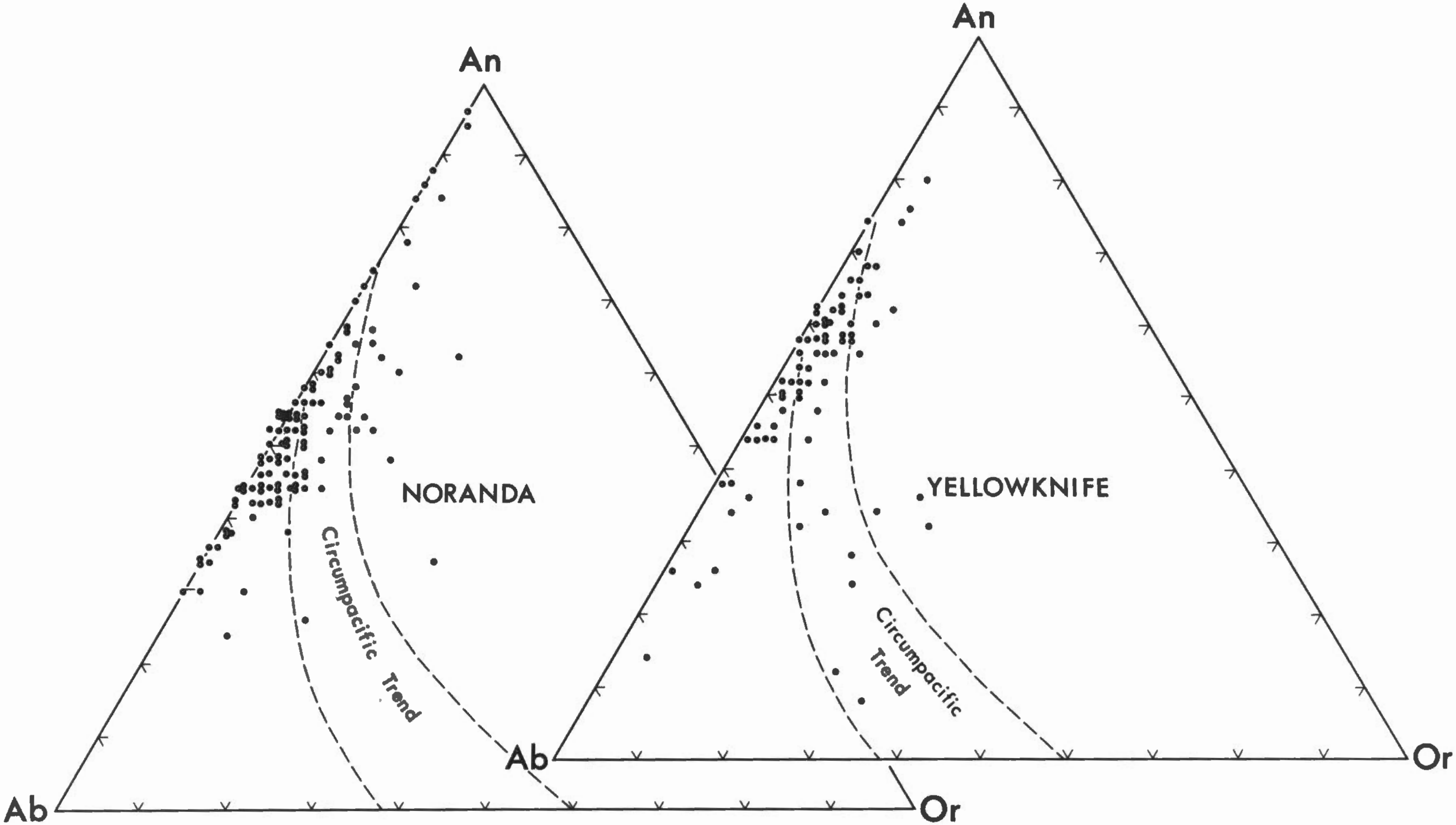

Figure 5. Normative An-Ab-Or plots of analyses from the sampled sections at Yellowknife and Noranda. The trend of circumpacific magmas is shown for comparison.

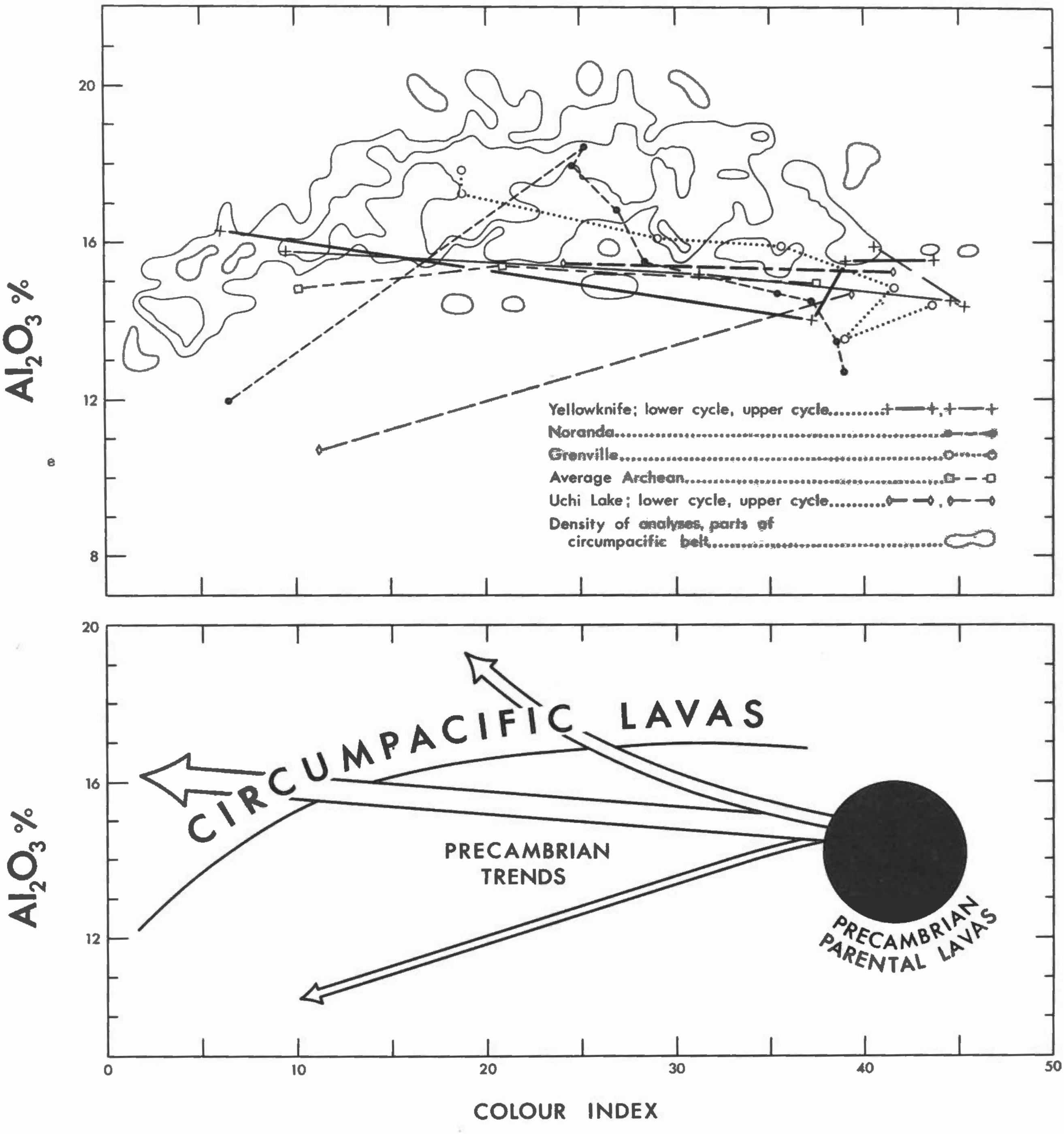

Figure 6. The upper diagram compares the variation trends of alumina with colour index (representing differentiation) of a number of Precambrian greenstone belts and the circumpacific belt. The Precambrian belts are represented by average analyses of successive stratigraphic fractions and the circumpacific belt by summary contours of the density of analyses. Also shown are an average Archean basalt, andesite, and salic fraction. The Noranda analyses have been supplemented by an average analysis of rhyolite from the district (Sakrison, 1966). The lower diagram is a generalized version of the trends displayed in the upper diagram. The lower limit of circumpacific lavas shown is the limit of densest concentration of analyses.

An additional possibility that might be considered is that the greenstone belts are a combination of volcanic rocks formed at the oceanic ridge and in the subduction zone. According to this view tholeiites in the lower parts of the sequences would represent the ridge effusions and the overlying calc-alkaline rocks the contributions of the subduction zone.

At first sight there appears to be some support for this view. Tholeiitic basalts in the lower parts of Precambrian sequences are generally similar to oceanic tholeiites. Where ultramafic rocks are present they are commonly in the tholeiitic part of the sequence. The AMF and An-Ab-Or diagrams suggest the presence of two superimposed trends; the tholeiitic and the calc-alkaline trends. Rocks of the calc-alkaline part of the sequence are roughly similar to those of the present circum-pacific belt.

However there are major obstacles to this point of view. If a tholeiitic sequence is formed at the ridge, rafted to the subduction zone, scraped on to the walls of the trench and covered with calc-alkaline rocks one would certainly expect to find a major break between each part of the sequence. Instead, in the sections examined the rocks are conformable throughout and even interlayered where they pass from tholeiites to andesites. In some sequences certain elements vary so smoothly and consistently throughout the sequence that it is difficult to imagine that different parts of the sequence were derived from different sources. Alumina in the Grenville and Noranda sections is one example.

The superposition of more than one mafic to acidic volcanic cycle is also difficult to explain in this way.

Precambrian greenstone successions have some distinctive chemical features that are unmatched by oceanic tholeiites on the one hand and calc-alkaline rocks of the circumpacific belt on the other. The generally low alumina content of their initial basalts is an example. The rarity of alkaline, subsilicic volcanic rocks in the greenstone belts in contrast to their relative abundance on the ocean ridges remains a major obstacle to the hypothesis.

Finally the possibility that some of the greenstone belts may have been deposited upon continental crust invokes a feeling of caution towards the view that they originated at the oceanic ridges. The Precambrian assemblage that most closely resembles the oceanic tholeiites in composition, that of the Labrador Trough, seems to be indisputably underlain by continental crust.

Acknowledgments

It is regretted that shortage of time in preparation necessitated drawing more heavily on personal experience than the subject deserves. However, acknowledgment is particularly made to the work of Drs. A.M. Goodwin, R. Ridler, and K. Sethuraman which have been drawn on quite freely in this account; and to Dr. T.M. Irvine for the use of several plotting programs.

References

Ayres, L.D. 1969. Early Precambrian metasandstone from Lake Superior Park, Ontario, Canada, and implications for the origin of the Superior Province. *Geol. Soc. Amer.*, pt. 7, Abstracts of Meetings, 5.

Baragar, W.R.A. 1966. Geochemistry of the Yellowknife volcanic rocks. *Can. J. Earth Sci.* 3, 9-30.

———1967. Wakuach Lake map-area, Quebec-Labrador (23O). *Geol. Surv. Can.*, Mem. 344.

———1968. Major-element geochemistry of the Noranda volcanic belt, Quebec-Ontario. *Can. J. Earth Sci.* 5, 773-790.

———and Goodwin, A.M. 1969. Andesites and Archean volcanism of the Canadian Shield. Proc. Andesite Conference, Oregon Dept. Geol. Miner. Industries, Bull. 65, 121-149.

Cann, J.R. and F.J. Vine. 1966. An area on the crest of the Carlsberg ridge: Petrology and magnetic survey. *Phil. Trans. Roy. Soc. London* 259, 198-217.

Cooke, D.L. and W.W. Moorehouse. 1969. Timiskaming volcanism in the Kirkland Lake area, Ontario, Canada. *Can. J. Earth Sci.* 6, 117-132.

Dimroth, E., W.R.A. Baragar, R. Bergeron, and G.D. Jackson. 1970. The filling of the Circum-Ungava geosyncline. In A.J. Bear, editor. Symposium on basins and geosynclines of the Canadian Shield, *Geol. Surv. Can.*, Paper 70-40, 45-142.

Donaldson, J.A. and G.D. Jackson. 1965. Archean sedimentary rocks of North Spirit Lake area, northwestern Ontario. *Can. J. Earth Sci.* 2, 622-647.

Engel, C.G. and A.E.J. Engel. 1963. Basalts dredged from the northeastern Pacific Ocean. *Science* 140, 1321-1324.

———R.L. Fisher and A.E.J. Engel. 1965. Igneous rocks of the Indian Ocean floor. *Science* 150, 605-610.

———and R.L. Fisher. 1969. Lherzolite, anorthosite, gabbro, and basalt dredged from the Mid-Indian Ocean Ridge. *Science* 166, 1136-1141.

Engel, A.E.J., C.G. Engel, and Havens, R.G., 1965. Chemical characteristics of oceanic basalts and the upper mantle. *Geol. Soc. Amer.* Bull. 76, 719-734.

Fahrig, W.F. 1970. Diabase dyke swarms; chapter 4, Geology of the Canadian Shield; In Geology and Economic Minerals of Canada, R.J.W. Douglas, (editor) p. 131-134.

Goodwin, A.M. 1965a. Mineralized volcanic complexes in the Porcupine-Kirkland Lake-Noranda region, Canada. *Econ. Geol.* 60, 955-971.

———1965b. Preliminary report on volcanism and mineralization in the Lake of the Woods-Manitou Lake-Wabigoon region of Northwestern Ontario. *Ont. Dept. Mines*, Prelim. Rept. 1965-2.

———1967. Volcanic studies in the Birch-Uchi Lakes area of Ontario. *Ont. Dept. Mines.* Miscellaneous Paper 6.

——— and R. Shklanka. 1967. Archean Volcano-Tectonic basins: form and pattern. *Can. J. Earth Sci.* 4, 777-795.

Green, D.C. 1968. Precambrian geology and geochronology of the Yellowknife area, N.W.T. Univ. Alberta, Unpubl. Ph.D. thesis.

Henderson, J.F. and I.C. Brown. 1966. Geology and structure of the Yellowknife greenstone belt, District of Mackenzie. *Geol. Surv. Can.*, Bull. 141.

Heywood, W.W. and A. Davidson. 1969. Geology of Benjamin Lake map-area, District of Mackenzie. *Geol. Surv. Can.*, Mem. 361.

Irvine, T.N. and W.R.A. Baragar. 1971, in press. A guide to the classification of the common volcanic rocks. *Can. J. Earth Sci.*

MacRae, N.D. 1969. Ultramafic intrusions of the Abitibi area, Ontario. *Can. J. Earth Sci.*, Vol. 6, 281-303.

McGlynn, J.C. and J.B. Henderson. 1970. Archean volcanism and sedimentation in the Slave Province. In A.J. Baer, editor. Symposium on basins and geosynclines of the Canadian Shield. *Geol. Surv. Can.*, Paper 70-40, 31-44.

Mueller, P.A. 1970. Secular variations in the mafic rocks of the Southern Beartooth Mountains, Montana and Wyoming. *Geol. Soc. Amer.* Abstracts of Annual Meeting, Milwaukee, 632.

Naldrett, A.J. and G.D. Mason. 1968. Contrasting Archean ultramafic igneous bodies in Dundonald and Clergue Townships, Ontario; *Can. J. Earth Sci.*, Vol. 5, 111-143.

Nicholls, G.D., A.J. Nalwalk and E.E. Hays. 1964. The nature and composition of rock samples dredged from the Mid-Atlantic Ridge between 22°N. and 52°N. *Marine Geology* 1, 333-343.

Ridler, R.H. 1969. The relationship of mineralization to volcanic stratigraphy in the Kirkland Lake area, northeastern Ontario, Canada. Univ. Wisconsin, Unpubl. Ph.D. thesis.

———1970a. Relationship of mineralization to volcanic stratigraphy in the Kirkland-Larder Lakes area, Ontario. *Geol. Assoc. Can.*, Proc. 21, 33-42.

———1970b. Volcanic stratigraphy and metallogeny of the Kaminak Group. *Geol. Surv. Can.*, Report of Activities, Paper 71-1A, 142-148.

Sakrison, H.C. 1966. Chemical studies of the host rocks of the Lake Dufault Mine, Quebec. McGill Univ. Unpubl. Ph.D. Thesis.

Sethuraman, K. 1970. Petrology of Grenville metavolcanic rocks in the Bishop Corners – Donaldson Area, Ontario. Carleton Univ., Unpubl. Ph.D. thesis.

Stockwell, C.H. 1933. Great Slave Lake-Coppermine River Area, Northwest Territories. *Geol. Surv. Can.*, Summ. Rept. 1932, pt. C. 37-63.

No. 10

archean ultramafic rocks

A.J. NALDRETT
University of Toronto
Toronto, Ontario

Introduction

Classification of ultramafic bodies

Bodies of ultramafic and related mafic rocks fall into a number of natural classes based on the composition of their magma, the form (shape) of the bodies and the timing of their emplacement in relation to the tectonic history of the area in which they occur. These factors are related to one another and reflect the conditions under which the magma involved was generated and then crystallized. In devising a classification scheme, (Naldrett and Gasparrini, 1971) it is logical to put particular emphasis on the tectonic environment in which the body was emplaced because this exerts a considerable influence on the other two factors.

With our present very imperfect knowledge of Precambrian tectonic processes, it is convenient to make the major division in the classification between those bodies emplaced in orogenic belts and those in non-orogenic (generally cratonic) areas. Ultramafic bodies in orogenic belts can be subdivided on the basis of the timing of their final emplacement with regard to the development of the orogen; namely into

(1) those that were emplaced and crystallized before major folding affected their enclosing rocks,

(2) those whose final emplacement occurred during folding (so-called "Alpine-type" ultramafic bodies), and

(3) those whose emplacement occurred during the final stages of orogenesis, after the most intense folding but before the main period of batholith intrusion. Examples of this class include the concentrically zoned ultramafic bodies of Alaska, British Columbia and the southern Urals of the U.S.S.R. (Taylor, 1967; Irvine, 1967).

Classes of Archean ultramafic bodies

The different classes of ultramafic bodies that are common in Canadian Archean greenstone belts are well represented in that portion of the Superior Province designated as the Abitibi orogenic belt (Figure 1) by Goodwin and Ridler (1970). Three main classes are present: All of these classes are conformable in a broad sense with their enclosing rocks. Where gravity-stratified layers are present, these are parallel to stratification in the surrounding rocks. All classes therefore belong to subdivision (1) of the orogenic division of the scheme outlined above; that is they were emplaced prior to folding.

The classes are:

(1) Large (20 – 50 miles long, > 20,000 feet thick) igneous complexes such as the Dore Lake complex (1 on Figure 1) described by Allard (1970); the Bell River complex (2 on Figure 1) described briefly by Sharp (1965); and possibly the large body of gabbroic rocks located 15 miles west of Timmins (3 on Figure 1). These complexes consist primarily of anorthositic gabbro and are notably rich in titaniferous magnetite and ilmenite. Although they contain pyroxenitic layers, they are mafic rather than ultramafic in overall composition and are not discussed further in this analysis.

(2) Smaller (1 – 10 miles long, up to 5,000 feet thick) gravity-stratified sills such as the Dundonald sill (4 on Figure 1) described by Naldrett and Mason (1968) and the Munro Lake, Garrison and Ghost Range (5 on Figure 1) sills described by MacRae (1969). These sills are well developed in a narrow belt running east-southeast from just south of Cochrane.

(3) Lenses of peridotite and pyroxenite (ranging from 10 × 200 feet to 4,000 × 20,000 feet surface dimensions) that show no evidence of gravity stratification. These lenses appear to be developed throughout the Abitibi orogen.

The small sills and lenses (classes 2 and 3) are the subject of the remainder of this paper.

Gravity-stratified sills

Canadian examples

The Dundonald sill is a typical example of this class. It is composed of a basal zone of serpentinized peridotite (1,100 feet thick) that was originally an olivine cumulate, with up to 80 modal per cent olivine enclosed poikilitically by augite; this is successively overlain by 500 feet of an augite cumulate and 1,200 feet of gabbro composed of cumulus augite, plagioclase and titaniferous magnetite; a localized zone of granophyre occurs close to the upper contact. Cryptic variation with enrichment of iron in augite and sodium in plagioclase is well developed. Figure 2 is a reconstruction of a vertical cross-section through the sill as it was before folding.

The other sills of the Abitibi belt resemble the Dundonald sill although some of them show additional complexities. The Munro Lake sill has a lower contact zone of hornblende peridotite and is remarkable in being composed of seven cyclical units involving the sequences, peridotite-clinopyroxenite, and peridotite-clinopyroxenite-gabbro. Following Irvine and Smith (1967), MacRae attributes this cyclic development to the intrusion of seven pulses of magma with concomitant expulsion of the residual magma of the previous pulse. Some of the smaller sills of the belt are wholly ultramafic while others are wholly gabbroic.

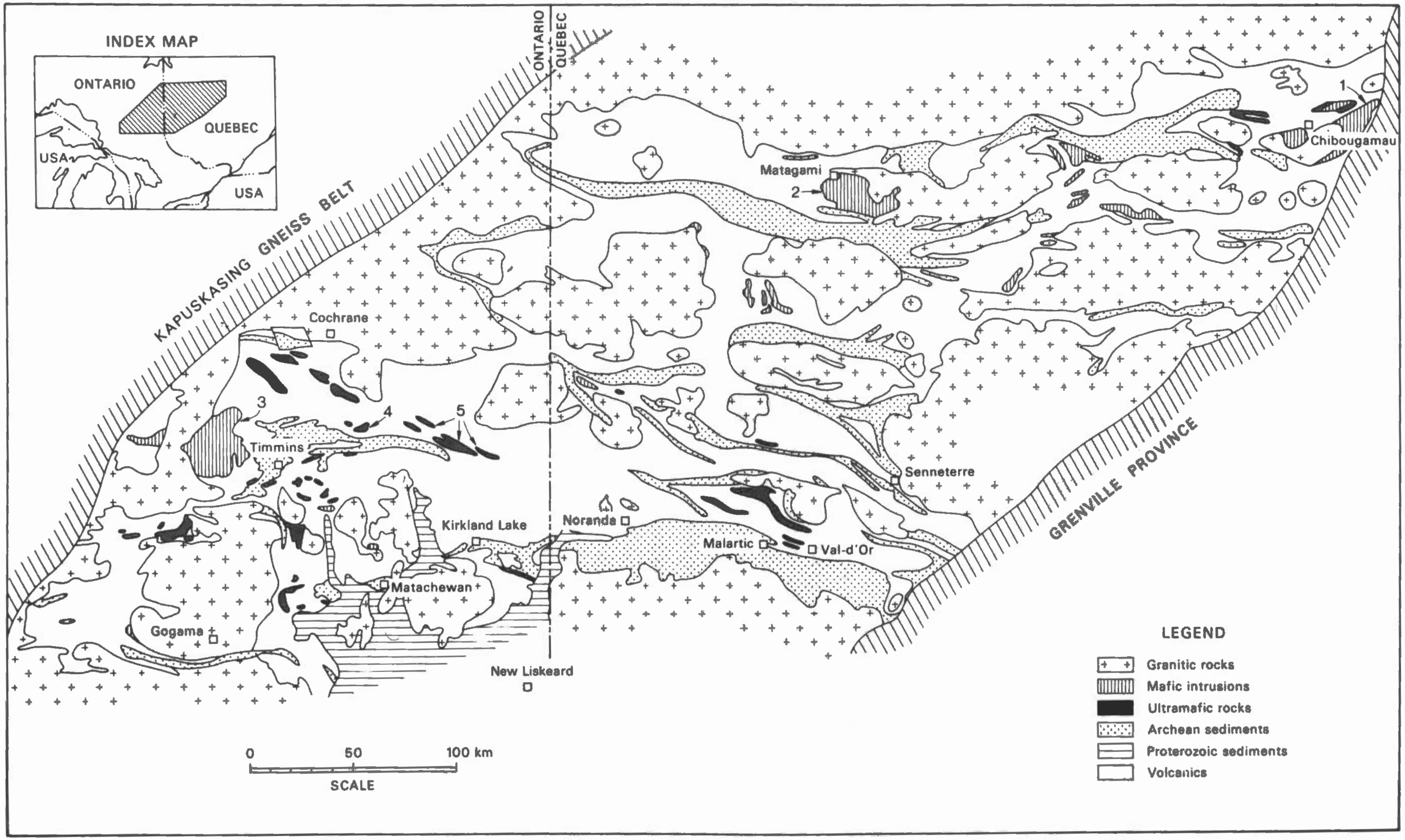

Figure 1. The Abitibi orogenic belt modified after Goodwin and Ridler (1970).

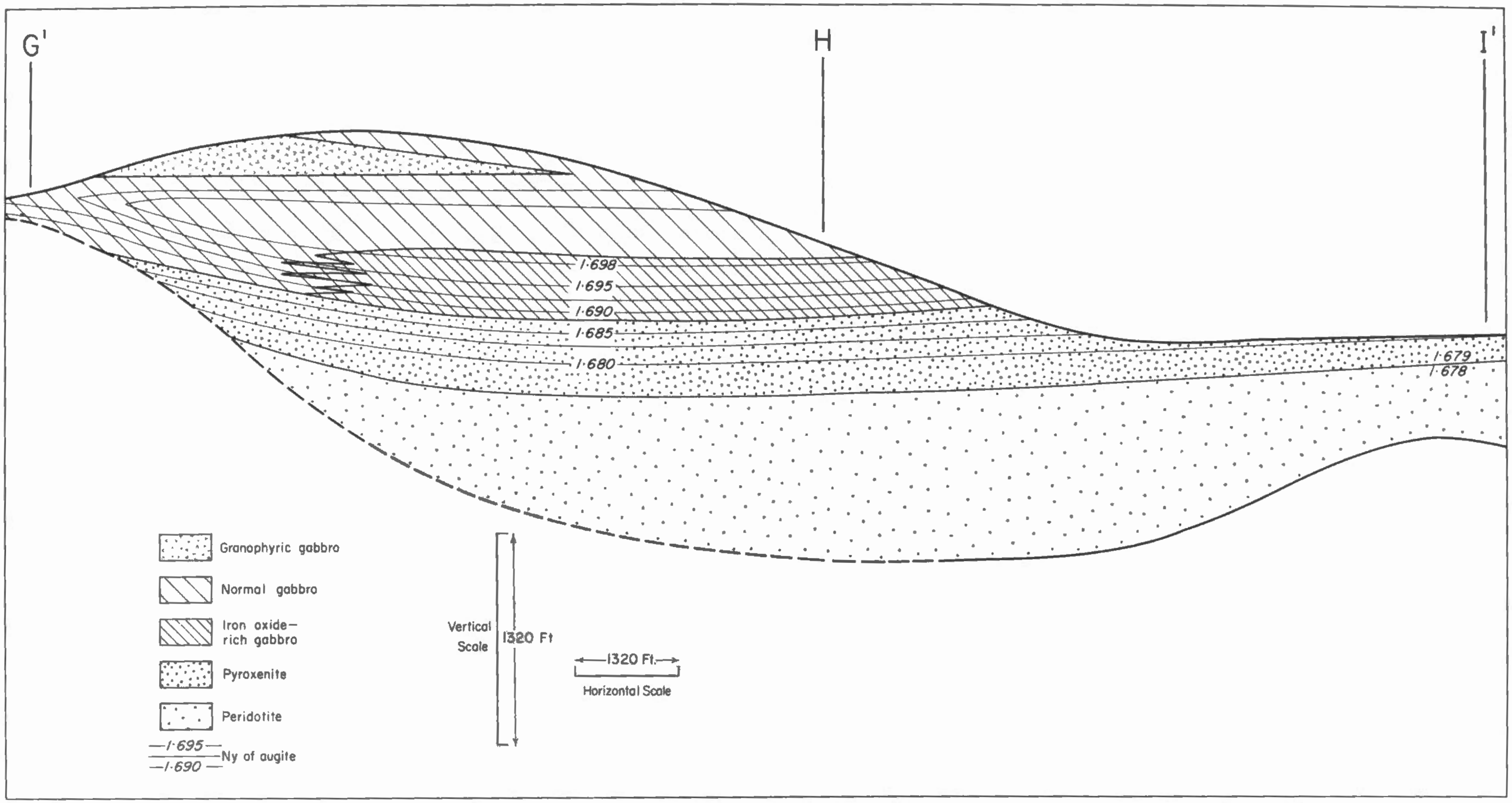

Figure 2. A vertical section through the Dundonald sill as it was before folding. Points G′, H and I′ relate to a plan of the sill in its unfolded state given by Naldrett and Mason (1968) Figure 8.

Calcium-rich pyroxene (augite) predominates in the sills of the Abitibi belt. No fresh calcium-poor pyroxene has been identified although MacRae interprets serpentine pseudomorphs as indicating that it was present as an intercumulus mineral in most of the sills that he studied. However, predominance of calcium-rich pyroxene is probably not a characteristic of this class of sills throughout Canada generally. Ridler (1965) describes the ultramafic portion of one of a similar group of sills from the Kakagi Lake area, south of Kenora, Ontario, as being composed predominantly of harzburgite.

Examples from outside Canada

Viljoen and Viljoen (1970) describe a group of layered ultramafic sills from the Kaapmuiden area of the Barberton geosyncline in South Africa that have all of the characteristics of the class under discussion. The sills have been intruded conformably between silicate iron-formation and pillowed basalts and have differentiated to give rise to a basal zone of dunite overlain successively by layers of orthopyroxenite, websterite and gabbro. Cyclical units such as these found in the Munro Lake sill are developed in a number of the Kaapmuiden sills.

Similar layered sills are common in the greenstone belts of the Eastern Goldfields area of the Western Australian shield. Two examples form the Norseman area are the Mount Thirsty and Mission Sills (McCall, 1970). These both consist of a basal zone or dunite or harzburgite overlain by a bronzite cumulate and then a gabbro capped by localized zones of granophyre. Both sills occur conformably within a thick sequence of pillowed basalts, banded iron-formation and clastic sediments and have been tightly folded with these rocks.

General remarks and the chemical composition

An estimate of the bulk composition of any of the sills of this class is very difficult because of the periodic influxes and effluxes of magma that have apparently given rise to the numerous cyclic units in some of the more complex sills, and also because of the migration of residual magma during crystallization of even the simpler sills that has resulted in the "offlap – onlap" relationship such as that illustrated in Figure 2. Naldrett and Mason have attempted a very rough estimate of the overall composition of the Dundonald sill which appears in column 1 of Table I; this composition is distinctly ultramafic. They point out, however, that a large proportion of the olivine in the sill was apparently carried in suspension and their estimate for the liquid portion at the moment of intrusion (Table I, column 2), which is based on the relative proportion of the rock types of the sill apart from the peridotite, is mafic rather than ultramafic.

MacRae, assuming that his vertical section through the Munro Lake sill is representative of the whole, calculates the overall composition of the magma, after deposition of the magma, after deposition of the basal peridotite, to be that shown in column 3 of Table I. This is higher in alumina and soda and lower in calcium than Naldrett and Mason's estimate, reflecting the difference in the weight given to granophyre, gabbro and diopsidic pyroxenite in the different averages. Despite this difference, the estimates are both broadly tholeiitic in their affiliation. It seems clear that the sills of this class are the result of the intrusion of tholeiitic or olivine tholeiitic magma

Table I

	1	2	3	4	5	6
SiO_2	44.7	52.7	51.2	45.4	45.6	46.2
Al_2O_3	2.90	8.29	11.2	10.2	8.75	
Fe_2O_3	1.74	2.33	2.78	4.68		
FeO	11.8	9.53	11.9	8.14(12.4)*	12.2*	13.0
MgO	32.9	10.4	7.99	20.6	23.0	22.4
CaO	3.61	13.1	9.94	10.1	7.73	18.4
Na_2O	0.49	1.96	3.08	0.78		
K_2O	0.05	0.20	0.25	0.13		
TiO_2	0.42	1.09	1.30		0.48	
MnO	0.22	0.20	0.20		0.22	
NiO	0.33	0.018			0.11	
Cr_2O_3	0.88	0.23			0.48	
CIPW Norm						
Quartz		1.8				
Orthoclase	0.3	1.2	1.5	0.8(0.8)*		
Albite	4.1	16.6	26.1	6.6(6.6)*		
Anorthite	5.6	13.2	16.0	23.9(23.9)*	24.4	
Salic	10.1	32.8	43.6	31.3(31.3)*	24.4	
Augite	9.8	41.9	27.6	20.8(21.2)*	11.7	
Hypersthene	22.3	19.5	17.4	12.8(3.7)*	31.0	
Olivine	53.2		4.9	28.3(43.5)*	31.3	
Magnetite	3.8	3.7	4.0	6.8(0)*	0.7	
Ilmenite	0.8	2.1	2.5		0.9	
Mafic	89.9	67.4	56.4	68.7(68.7)*	75.6	

*Total Fe calculated as FeO

Column 1. Estimated bulk composition of Dundonald sill after Naldrett and Mason (1968).
2. Estimated composition of liquid portion of Dundonald sill magma at the time of intrusion (Naldrett and Mason, 1968).
3. Estimated composition of Munro Lake sill apart from peridotite (after MacRae, 1969).
4. High lime basic silicate liquid, recalculated to eliminate H_2O, after Drever and Johnston (1966), Table 1, analysis 5.
5. Average composition of quench rocks from Dundonald township after Naldrett and Mason (1968).
6. Composition of experimental charge from Presnall (1966).

carrying a considerable, although variable, proportion of olivine phenocrysts in suspension.

Ultramafic lenses

Canadian examples

Although these lenses apparently occur widely throughout the Abitibi orogen and in other greenstone belts of the Superior Province (for example the Shebandowan area, 60 miles west of Thunder Bay), the most intensive study has been given to those in the Dundonald area and also those south of Timmins, Ontario. These studies include those of Naldrett and Mason (1968) and Pyke (1970).

In their simplest form the lenses consist of a central core (10 – 1,000 feet thick) rich in olivine or serpentine pseudomorphous after olivine (75 – 90 per cent original olivine) with minor pyroxene and accessory chrome spinel. The core is surrounded by a marginal zone, 10 – 100 feet wide, over which pyroxene increases steadily at the expense of olivine toward the contact with enclosing rocks. The pyroxene consists of calcium-poor and/or calcium-rich pyroxene and occurs interstitial to the equant olivine grains as bladed or acicular crystals, sometimes showing a radiating or sheaf-like development; this contrasts strongly with the poikilitic texture of the ultramafic portion of the gravity-stratified sills just described. Naldrett and Mason have attributed the central concentration of olivine in these simple lenses to flowage differentiation of the type described by Bhattacharji (1967). In some of the lenses the olivine, pyroxene, chrome spinel and occasional plagioclase found in the marginal portions have developed distinctive skeletal forms identical with those shown by rapidly chilled experimental charges. This material, which will be referred to as quench rock, reaches its ultimate development in complex lenses in which a series of lens-like zones rich in normal equant olivine are separated by thin, less olivine-rich bands with the quench textures.

The best exposed complex lens is in southern Langmuir township where a body of ultramafic rock, 4,000 feet wide by 4 miles long, strikes in conformity with the enclosing volcanic rocks. The lens-like zones with normal olivine vary in thickness from 15 feet to more than 150 feet and are separated by 2 – 15-feet-thick bands of quench rock. A weathered sample of this material is shown in Figure 3. With the rather limited detailed mapping undertaken so far, it has not been possible to trace individual lenses for more than 500 feet although it is very probable that they have a much greater strike-length than this, possibly several thousand feet. Most of the bands of quench rock appear to be as continuous as the olivine-rich lenses although occasional bands feather out into a series of disjointed blocks of quench material in normal peridotite and others pinch out altogether (Figure 4). The normal peridotite is sometimes foliated, particularly adjacent to bands of quench rock, where it commonly contains elongated blocks similar to the quench rock. Thin (2 – 6-inch) veins of quench material have also been observed cutting the normal peridotite.

Two complex lenses are also known to exist in the Dundonald area. Exposure is much more restricted here than in Langmuir township, but this disadvantage is offset by the availability of drill core and the much better state of preservation of the textures; all of the available analyses of quench rock also come from this area. In general, the zones of normal peridotite are richer in olivine in Dundonald than in Langmuir township (65 – 80 as compared with 45 – 60 modal per cent). The bands of quench rock contain between zero and 50 modal per cent skeletal olivine. Figure 5 illustrates some of this material in drill core. Figure 6(a) illustrates the skeletal olivine of Figure 5(c) in thin section, and 6(b) the interstitial quench pyroxene from the same sample.

Despite close similarity in the forms, the natural skeletal textures are very much coarser grained than those produced experimentally. Very occasionally, books of parallel plates similar to those in Figure 5a are as much as 3 feet long. The coarse grain size has led some investigators to discount quenching as the origin and to conclude that the textures result from metamorphism. In this regard, it is instructive to note the similar textures that have developed in the slag from the International Nickel Company's slag pile at Copper Cliff, Ontario. Figures 7a, b and c are of this material and show skeletal crystals of fayalite developing from an iron-rich silicate glass. The scale of these textures is very similar to that of those in the majority of the natural quench rocks.

Examples from outside Canada

Ultramafic lenses associated with zones and patches of quench rock comprise more than 30 per cent of the total stratigraphic thickness in the lower half of the Onverwacht volcanic sequence in the Barberton mountainland of South Africa (Viljoen and Viljoen, 1969). The lenses interfinger with pillowed basalts, and rare pillow structures have been reported in the ultramafic rocks themselves. The writer has examined these reputed pillows and, bearing in mind the tendency of ultramafic rocks to develop a joint pattern that looks remarkably like pillows, is unable to accept them as such without more detailed work, particularly on the pillow selvages.

Simple and complex lenses of ultramafic rock are also common in the Eastern Goldfields area of Western Australia where they are hosts to at least 95 per cent of the recent discoveries of nickel ore. The lenses occur at intervals throughout the large thickness of pillowed basalt that is also host to the stratified sills described previously. An interesting feature of the Australian rocks is that thin bands of fine-grained siliceous or argillaceous sediment, many of them rich in iron sulphides and graphite, occur within the complex lenses. The bands are conformable with the lenses, occur at as many as four different horizons within a given complex, and extend for as much as 2,000 feet along strike.

General remarks including a discussion of the chemical composition

As mentioned previously, the simple lenses are thought to have been emplaced as magma carrying a very high proportion of equant olivine grains in suspension.

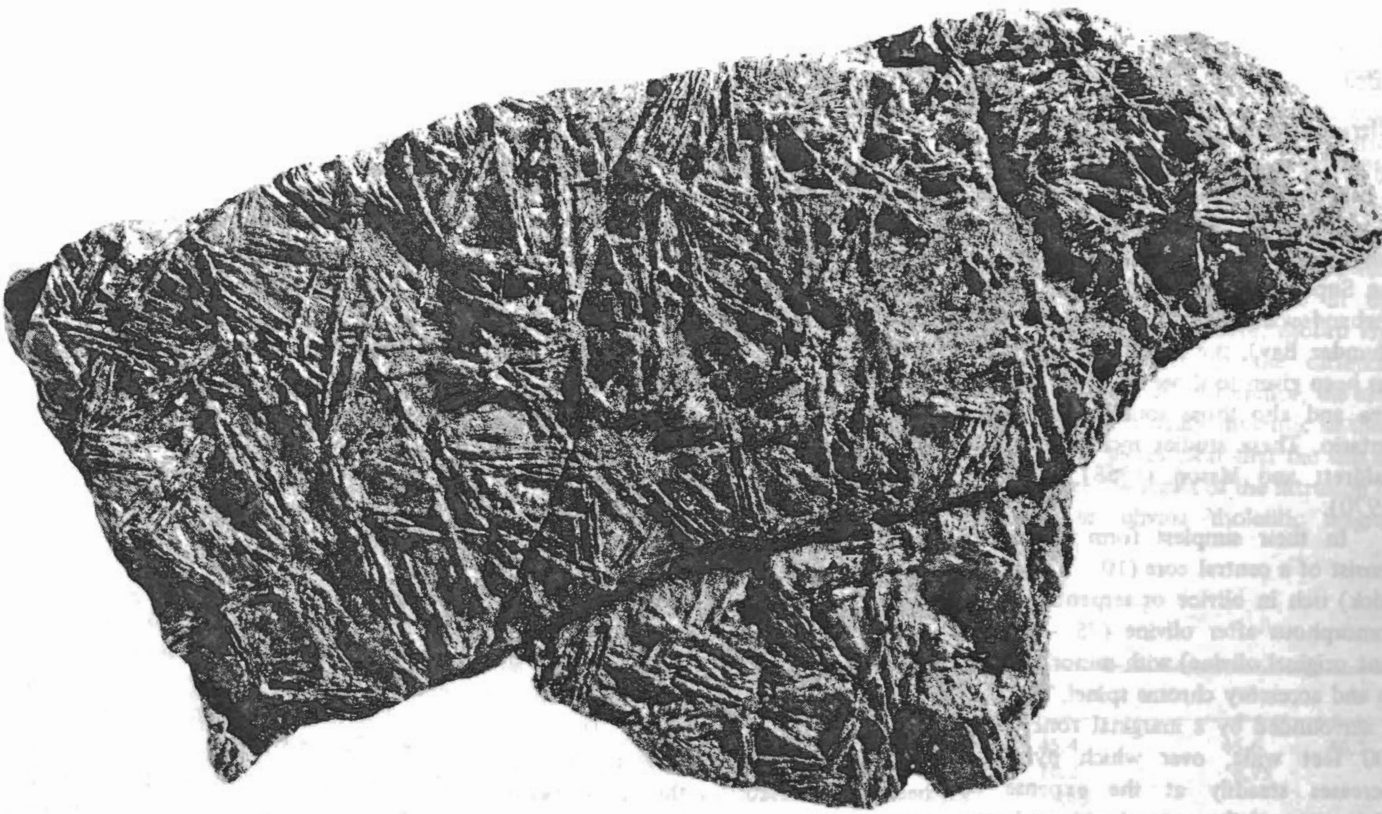

Figure 3. Sample of weathered "quench rock" from Langmuir township, Ontario. The sample is 9 inches long.

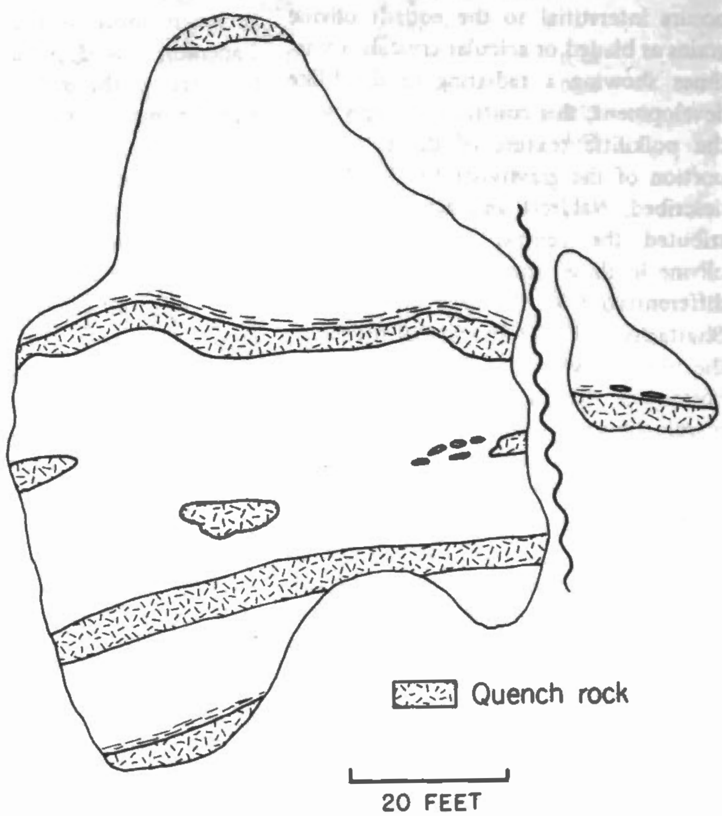

Figure 4. Sketch of a small outcrop showing interbanding between normal peridotite with equant olivine (unshaded area) and quench rock. The dashed lines indicate zones over which the rock shows marked foliation. The outcrop is in southern Langmuir township, 30 miles southeast of Timmins.

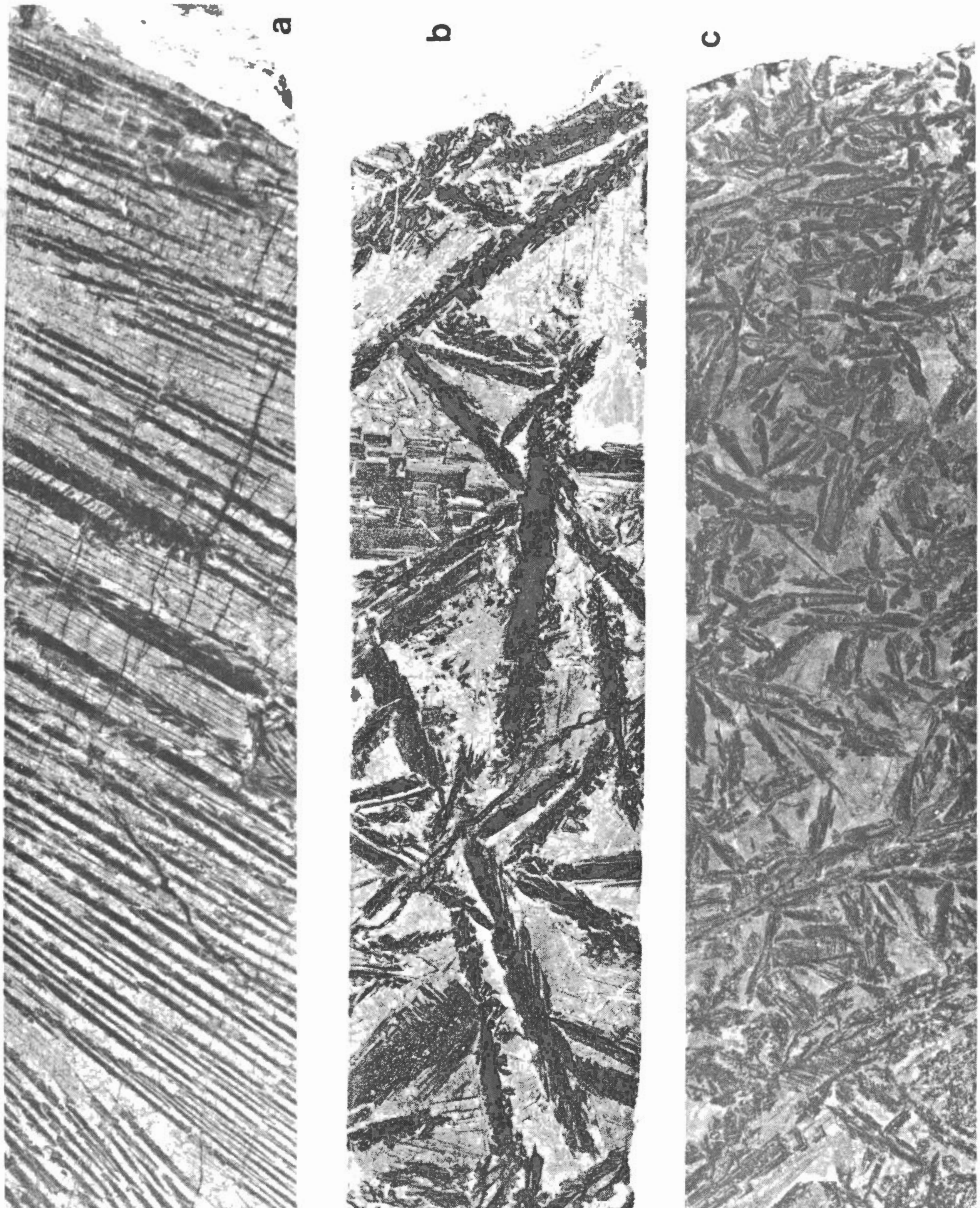

Figure 5. Samples of "quench rock" in which the serpentine pseudomorphous after olivine stands out in strong contrast to the pyroxene-rich groundmass. The core samples are 6 inches long.

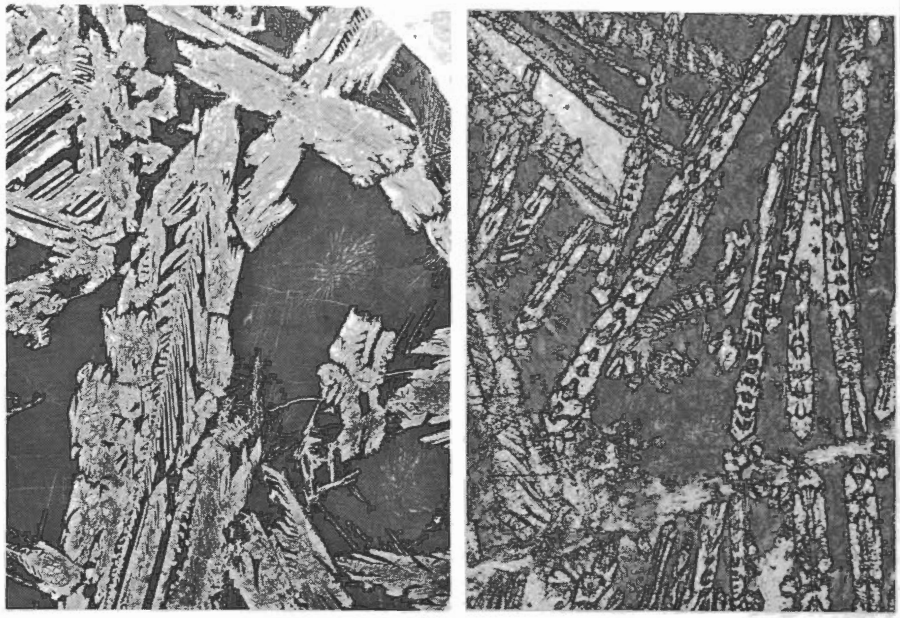

a b

Figure 6.
a) Thin section showing serpentine after skeletal olivine cut from the sampel shown as Figure 5(b) above. Plane polarized light. 6X.
b) Thin section showing acicular, skeletal crystals of augite in the material interstitial to the olivine illustrated in Figure 6(a). Plane polarized light. 100X.

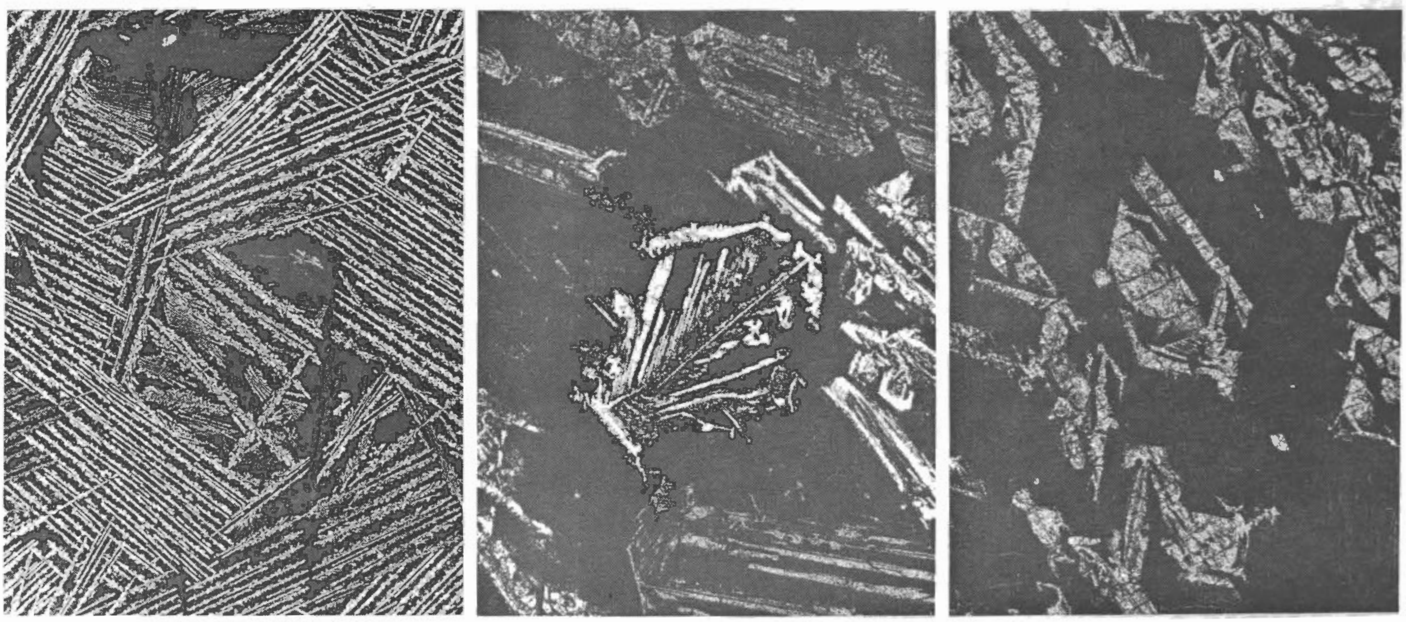

a b c

Figure 7. a) Skeletal growths of fayalite in smelter slag. 4X.
b) and c) Details of skeletal crystals from sample shown as 7(a).
b) Crossed nicols. 100X.
c) Plane polarized light. 100X.

These olivine phenocrysts presumably crystallized under the conditions of slow cooling common to many peridotites. The contrast between this olivine and the skeletal material developed in the marginal zones suggests that the latter crystallized subsequently in a much cooler environment, and raises the question of whether some of the lenses may be extrusive.

The complex lenses, consisting of thin sheets of quench rock interleaved between thicker, stratiform sheets of normal peridotite are readily interpreted as a series of submarine flows in which the quench material represents the rapidly chilled top or base of a single flow. It is difficult to conceive how a single intrusion, or possibly a series of multiple intrusions, could give rise to such a sequence of parallel lenses with well developed sheets of quenched material between each. The Australian examples, in which the sulphide-rich sediments are also laminated within the complex lenses, lend further support to the extrusion hypothesis. These sediments are very similar to the banded zones of cherty or tuffaceous material that are a common feature between, for example, volcanic flows of the Noranda district and that are interpreted as forming during quiescent periods during the volcanism. If the Australian ultramafic rocks are regarded as intrusive, one has to postulate that a series of intrusions invaded the sedimentary horizon, each splitting off a thin band of sediment between itself and its neighbour without disrupting the sediments in any other way.

Viljoen and Viljoen conclude that much of the ultramafic material in the Onverwacht formation is extrusive. They suggest that this is due to the thin crust prevailing at this early stage in the earth's history (3.4 billion years ago) and point out that the Barberton rocks (both mafic and ultramafic) have a unique composition. They characterize this crust as having a high Fe:Mg ratio and an unusually high CaO/Al_2O_3 ratio, both factors implying an unusually large proportion of normative diopside. They consider that the rocks are members of a previously unrecognized igneous rock suite to which they give the name "Komartiite".

The $CaO:(CaO+Al_2O_3)$ and $FeO:(FeO+MgO)$* ratios of both ultramafic and basaltic Komartiites from Barberton are compared with Wilson *et al.'s* (1965) average for Canadian Archean basalts, Baragar's (1968) rocks from the Noranda area, and Engel, Engel and Havens' (1965) and Aumento's (1968) oceanic tholeiites in Figure 8. The high CaO/Al_2O_3 ratio of the Barberton rocks is very apparent. Also shown are Naldrett and Mason's (1968) analyses of samples from the ultramafic lenses of the Dundonald area. Although overlapping with some of the Barberton rocks, in general these have a distinctly lower CaO/Al_2O_3 ratio and do not appear to be part of the Komartiite suite. The large cross indicates the average (column 5, Table I) for the quench rocks of the Dundonald area. This figure, being of rocks carrying no olivine phenocrysts, is representative of the liquid portion of the lenses; it has a distinctly higher MgO:FeO ratio than any of the Archean or oceanic basalts shown in the figure. It is interesting to note, however, that the average is remarkably similar to the most mafic of the high lime basic silicate liquids that Drever and Johnston (1966) describe from Skye (Table I, column 4). Furthermore, in Figure 8, other liquids described in Drever and Johnston's paper (solid squares) bridge the gap between the Dundonald average and oceanic basalts. It is quite possible that as the ultramafic lenses are studied in greater detail more rocks similar to those from Skye, and spanning the gap between existing analyses and basalts, will be found.

As can be seen from Table I, the average composition of the liquid portion of the Dundonald lenses is distinctly ultramafic. This raises the question of the temperature required for this composition to be liquid. In a brief note, Clark and Fyfe (1961) reported the results of melting experiments under water pressures of 500 – 1,000 kb on charges with the composition of serpentine. The first suggestion of melting was obtained at about 1,300°C and the samples were nearly entirely molten at 1,400°C. No further data on these experiments have been published and one cannot attach too much weight to them until this is done. Presnall (1966) reports that, under dry conditions at 1 atm. confining pressure, an experimental charge with the composition listed in column 6 of Table I has a liquidus temperature of 1,450°C. On cooling it first crystallizes olivine, with diopside joining olivine at 1,330°C. This experimental composition is close to the estimate for the Dundonald liquid, if one counts the alumina in the latter as calcium. It is a reasonable assumption that the effect of 500 – 1,000 kb of water pressure, the substitution of some alumina for calcium, and the addition of small amounts of alkali might lower the experimentally determined liquidus temperature by as much as 100°C, suggesting a possible temperature of about 1,350°C for extrusion of the Dundonald lenses.

*Total Fe calculated as FeO.

Conclusions

In conclusion, most ultramafic rocks of Archean greenstone belts are of two types, gravity-stratified sills and ultramafic lenses, that were emplaced within eugeosynclinal volcanic rocks either during the volcanism or very shortly afterwards. Although more work remains to be done, there is much evidence to suggest that some of the lenses are the result of extrusion of ultramafic lava.

In some areas bodies of both types are particularly rich in normative diopside but, for the most part, the bodies appear to have formed from magmas composed of silicate liquids ranging in composition from tholeiite to distinctly ultramafic, olivine-rich picrite, and carrying varying quantities of olivine phenocrysts in suspension.

Except that they carry olivine phenocrysts, the bodies are essentially autochthonous and were emplaced in a sequence of volcanic and sedimentary rocks that was relatively undisturbed. They differ, therefore, from the alpine-type peridotites and ophiolite complexes of Phanerozoic orogenic belts, whose final emplacement was largely allochthonous and occurred in a tectonically dynamic environment.

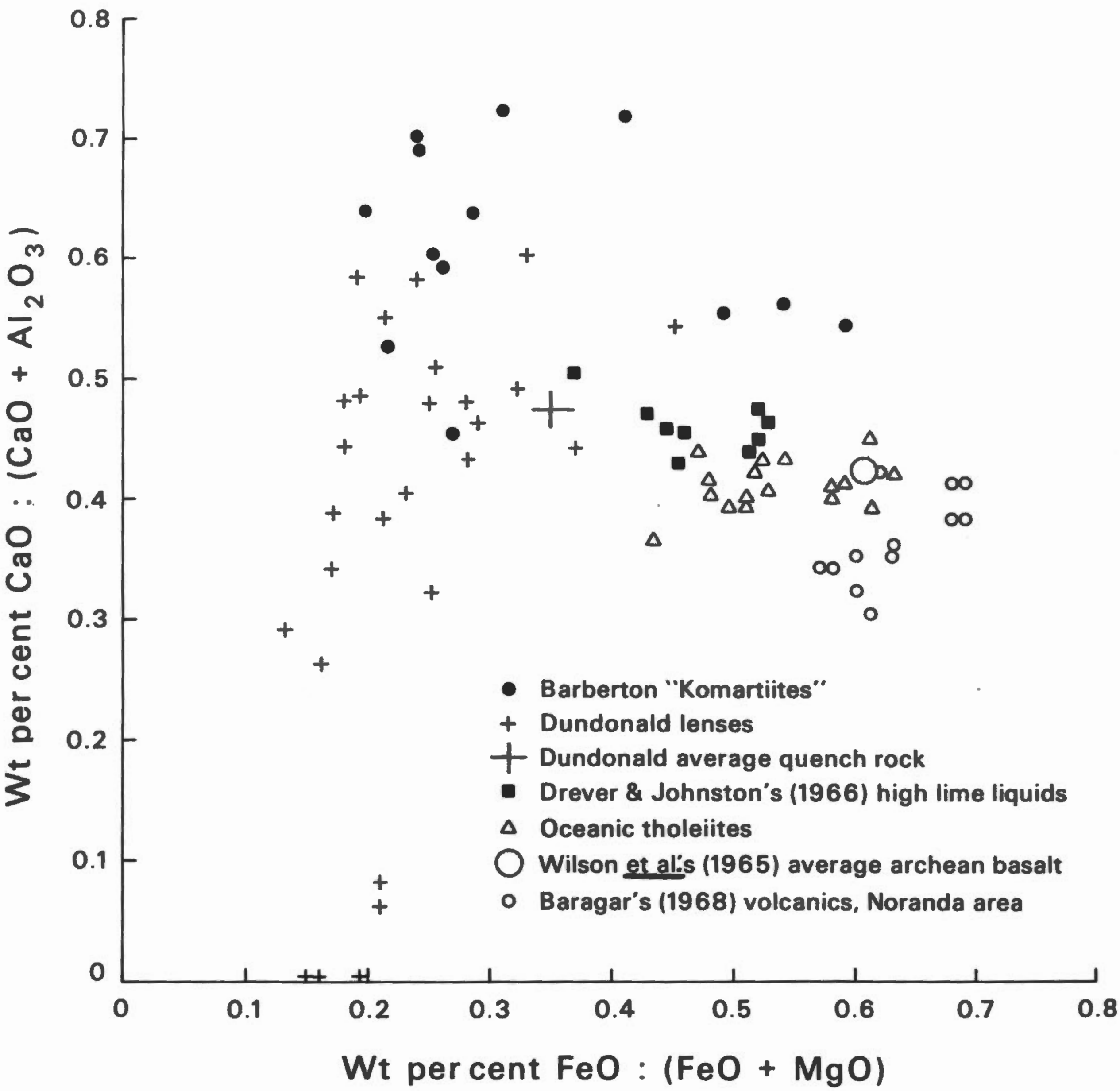

Figure 8. Plot of wt per cent CaO: (CaO+Al_2O_3) against wt per cent Fe: (FeO+MgO) for a number of rocks including those of the Dundonald area.

As claimed by some authors in this publication, it is possible that some Phanerozoic ultramafic bodies are fragments of oceanic crust that have been rafted into the debris collecting in the trench at the top of a subduction zone. The geology of the Archean bodies is not consistent with this interpretation. Archean bodies belong to a distinctive synvolcanic class that may not be present in Phanerozoic orogens. The presence of this class, coupled with the apparent restriction of ultramafic lavas to the Archean, is support for the view that tectonic processes may have been quite different in the early Precambrian to those in younger eons.

References

Allard, G.O. 1970. The Dore Lake complex of Chibougamau, Quebec – a metamorphosed Bushveld-type layered complex. Symposium on the Bushveld and other layered intrusions. *Geol. Soc. S. Africa*, Spec. Publ. 1, 477-491.

Aumento, F. 1968. The Mid-Atlantic Ridge near 45°N. II. Basalts from the area of Confederation Peak. *Can. J. Earth Sci.*, 5, 1-21.

Baragar, W.R.A. 1968. Major element geochemistry of the Noranda volcanic belt, Quebec-Ontario. *Can. J. Earth Sci.*, 5, 773-790.

Bhattacharji, S. 1967. Scale model experiments on flowage differentiation insills. Ultramafic and related rocks, P.J. Wyllie (editor), Wiley and Sons Inc., New York, 69-71.

Clark, R.H. and W.S. Fyfe. 1961. Ultrabasic liquids. *Nature*, 191, 158-159.

Drever, H.I. and R. Johnston. 1966. A natural high-lime silicate liquid more basic than basalt. *J. Petrol.*, 7, 414-420.

Engel, A.E.J., C.G. Engel and R.G. Havens. 1965. Chemical characteristics of oceanic basalts and upper mantle. *Geol. Soc. Amer.*, Bull. 76, 719-734.

Goodwin, A.M. and R.H. Ridler. 1970. Abitibi orogenic belt. *Geol. Surv. Can.* Paper 70-40 (in press).

Irvine, T.N. 1967. The Duke island ultramafic complex, southeastern Alaska. Ultramafic and related rocks P.J. Wyllie (editor). Wiley and Sons Inc., New York, 84-97.

——— and C.H. Smith. 1967. The ultramafic rocks of the Muskox Intrusion, Northwest Territories, Canada. Ultramafic and related rocks, P.J. Wyllie (editor), Wiley and Sons Inc., New York, 38-49.

McCall, G.H.H. 1970. The Archean rocks. Field excursion guide book for Geol. Soc. Australia General Meeting and Symposium on the "Archean Rocks", Perth, May 1970.

McRae, N.D. 1969. Ultramafic intrusions of the Abitibi area, Ontario. *Can. J. Earth Sci.*, 6, 281-304.

Naldrett, A.J. and E.L. Gasparrini. 1971. Archean nickel sulphide deposits in Canada: their classification, geological setting and genesis with some suggestions as to exploration. *Geol. Soc. Australia, Spec. Publ.* 3 (in press).

——— and G.D. Mason. 1968. Contrasting Archean ultramafic igneous bodies in Dundonald and Clergue townships, Ontario. *Can. J. Earth Sci.*, 5, 111-143.

Pyke, D. 1970. The geology of Langmuir and Blackstock townships. Ontario Dept. Mines Report (in press).

Presnall, D.C. 1966. The forsterite-diopside-iron oxide join and its bearing on the crystallization of basaltic and ultramafic magmas. *Amer. J. Sci.*, 264, 753-809.

Ridler, R.H. 1965. Petrographic study of a Crow Lake ultrabasic sill, Keewatin volcanic belt, northwestern Ontario. Unpubl. M.A.Sc. Thesis, University of Toronto.

Shapr, J.I. 1965. Field relations of Matagami sulphide masses bearing on their disposition in time and space. *Trans. Can. Inst. Min. Met.*, 68, 265-278.

Taylor, H.P. Jr. 1967. The zoned ultramafic complexes of southeastern Alaska. Ultramafic and related rocks, P.J. Wyllie (editor). Wiley and Sons Inc., New York.

Viljoen, M.J. and R.P. Viljoen. 1969. Evidence of the existence of a mobile extrusive peridotitic lava from the Komati formation of the Onverwacht group. Preprint, South African Upper Mantle Symposium, Pretoria.

Viljoen, R.P. and M.J. Viljoen. 1970. The geology and the geochemistry of the layered ultramafic bodies of the Kaapmuiden area, Barberton Mountain Land. Symposium on the Bushveld and other layered intrusions, *Geol. Soc. S. Africa, Spec. Publ.* 1, 661-688.

Wilson, H.D.B., P. Andrews, R.L. Moscham and K. Rambel. 1965. Archean volcanism in the Canadian Shield. *Can. J. Earth Sci.* 2, 161-175.

No. 11

oceanic crust and the identification of ancient oceanic crust on the continents: a summary

R.F. EMSLIE
Geological Survey of Canada
Ottawa

Introduction

One of the major principles underlying reconstruction of the earth's history is that of uniformitarianism which has proved serviceable in explaining many processes that produced ancient rocks. The emergence in recent years of convincing evidence for sea-floor spreading and plate tectonics in geologically young rocks, however, has raised questions as to whether such processes can be assumed to have operated from the earliest history of the earth. No one doubts that the earth's crust and mantle have evolved through time and this in itself is sufficient reason to question whether sea-floor spreading and plate tectonics may be consequences of the evolutionary process and thus be confined to the latter part of earth history.

Enquiry into the potential significance of plate tectonics and ocean-floor spreading in past geological eras provided the stimulus for this symposium volume. Although it is concerned chiefly with Canadian examples, these span a wide variety of geological ages and settings. The following summary is an attempt to distill briefly some of the features of importance and problems that arise in attempting to trace evidence for plate tectonics and ocean-floor spreading from modern examples back through geological time.

Characteristics of modern oceanic crust and criteria for recognition of ancient oceanic crust-mantle rocks

A review of the characteristics of a modern dynamic ridge system based primarily on studies of the Mid-Atlantic Ridge at 45°N latitude is presented by Aumento. A typical oceanic crustal section is interpreted as comprising about 5 km of mafic extrusive and intrusive rocks whose metamorphism increases with depth from negligible through zeolite facies to amphibolite facies. These rocks are pierced locally by diapiric serpentinites and the whole is overlain by a thin veneer of sediments. The mafic rocks range from quartz tholeiites through alkali basalts with olivine tholeiites being dominant. Large layered intrusive/extrusive mafic lopolithic complexes are believed to be emplaced in the vicinity of the ridge axis. Small bodies of hornblende quartz diorite, trondjhemite and albite granite are closely associated with ultramafic rocks. Certain geochemical parameters such as Fe_2O_3/FeO, U and H_2O content, O^{18}/O^{16} and Sr^{87}/Sr^{86} are known to vary with distance from the ridge axis. However, some or all of these may be too ephemeral in character to be useful criteria in the search for older oceanic crustal rocks: Kay, Hubbard, and Gast (1970) conclude that olivine tholeiite basalts with low SiO_2, low K, and generally high but variable Al_2O_3 with characteristic dispersed element patterns (rare earth abundances, Sr, Ni) are distinguishing features of rocks formed in the axial zone of an ocean ridge. It is important to note, however, that oceanic ridges are sites of oceanic plate accretion and not sites of basinal sedimentation or continental growth. Description of the characteristics of oceanic crustal sections in marginal and inter-arc basins (Karig, 1971a, 1971b) will be anticipated with great interest.

Alpine-type peridotite is now widely believed to be an excellent indicator of the presence of oceanic crust-mantle. Irvine and Findlay provide a detailed review of comparisons and contrasts of alpine-type peridotite with other ultramafic rocks. In Canada, alpine-type peridotites are found in the Cordillera and in the northern Appalachians; they have not been identified among the ultramafic bodies of the Precambrian Shield. Some of the better defined features brought out are:

(1) Typical alpine-type (spinel) peridotites consist of a more or less serpentinized assemblage with 60 - 90 per cent olivine, 5 - 35 per cent orthopyroxene, 1 - 7 per cent clinopyroxene, and 0.5 - 2 per cent chromium-bearing spinel. Additional minerals that may occur are amphibole, pyrope-rich garnet, and plagioclase.

(2) In general the bodies appear to have been largely solid when emplaced; "cold" contacts seem to be most common but substantial contact metamorphism has been found in places.

(3) Ni-sulphide deposits seem to be rarely associated with alpine-type peridotites.

(4) Temperatures of equilibration of alpine-type peridotite mineral assemblages commonly lie in the range from basalt liquidus temperatures to temperatures of the peridotite solidus. Pressures of equilibration appear to range from 1 atmosphere to about 17 kb.

(5) Plots of NiO vs. Cr_2O_3 are believed to be potentially useful for distinguishing alpine-type peridotites from ultramafic cumulates of basaltic magmas.

(6) The ultimate origin of alpine-type peridotite is not satisfactorily resolved but its production as a residue of partial melting processes has gained favour over an origin by fractional crystallization.

The characteristics and significance of ophiolites are discussed by Church who recommends a more restricted usage of the term to those complexes with complete "ophiolite stratigraphy" i.e. a lower alpine-type peridotite member overlain by gabbroic rocks followed by pillow basalts and then cherty sediments. Sheeted diabase intrusions seem commonly to have been injected between the pillow lavas and underlying gabbro. Ophiolites are believed to be emplaced early in an alpine-type tectonic cycle rather than during the main orogenic phase. There is considerable controversy about the nature of ophiolite emplacement and whether it can be explained by: differentiation of large mafic submarine extrusions; upwelling and partial melting of the mantle to form a composite subsea laccolith; tectonically incorporated allochthonous fragments of ocean floor, etc. Regardless of the mechanism of emplacement, the present level of knowledge strongly suggests that ophiolite complexes represent oceanic crust-mantle.

Evidence bearing on the existence of old oceanic crustal rocks in Canada

The subject matter of most of the contributions can be broken down conveniently into three groups which deal with: 1) the Cordillera, 2) the Appalachians, and 3) the Precambrian Shield.

The Cordilleran belt

Souther states that the existence of oceanic crustal rocks is unknown in Tertiary and Mesozoic sequences of the Canadian Cordillera. In the western Cordillera andesitic volcanic arcs existed and migrated westward during the first half of the Mesozoic. West of these arcs contemporaneous thick piles of tholeiitic pillow basalts and pyroclastics were deposited. Eruptions of large volumes of silicic volcanics including rhyolites, rhyodacites, dacite ash-flows, and ignimbrites took place in late Cretaceous and early Tertiary. Mid-Tertiary and younger volcanic activity comprised plateau and central vent eruption of mainly alkali basalt. The volcanic history can be related to plate tectonic interpretations of Cordilleran geology.

Monger discusses the tectonic implications of some upper Paleozoic rock sequences in the light of possible oceanic-continental plate interactions. Alpine-type peridotites are spatially associated with upper Paleozoic rocks. The association of peridotite, basalt, and chert has been reported but the existence of classical ophiolites has yet to be verified. Permo-Carboniferous basalts with their associated deep water sediments, alpine-type peridotites and serpentinites in the McDame map-area (Gabrielse, 1963) and adjacent parts of northern British Columbia comprise one assemblage that bears closer examination as a possible representative of oceanic crust-mantle.

The Appalachian belt

Lamarche reviews the geological setting of the ultramafic rocks of the Eastern Townships of Quebec and discusses their origin. The rocks are contained within a fairly closely defined stratigraphic interval in the Lower Ordovician. The lower contacts lie unconformably on schistose, folded, eugeosynclinal deposits. Contacts of the complexes range from apparently "cold" to ones with pronounced metamorphic effects on the underlying rocks only. In addition to the mafic-ultramafic components of these complexes, Lamarche believes that dioritic, syenitic, and granitic intrusions are genetically related and that the whole suite originated by submarine extrusion on a eugeosynclinal floor.

Irvine and Findlay discuss the geology of the Bay of Islands Complex and its interpretation. The complex consists of a lower Ultramafic Zone 2.5 – 4 miles thick, an upper Gabbro Zone up to 3 miles thick and is emplaced into basic volcanics, partly pillowed, with contact metamorphic effects on both roof and floor. It is intruded by basic dykes and small bodies of quartz diorite and albite granite. Consideration of the mineralogy, spinel compositions, $Mg/Mg{+}Fe^{2+}$ in olivines and rocks, and NiO and Cr_2O_3 contents of rocks leads to the tentative conclusions that the alpine-type peridotite of the Ultramafic Zone is the residue of a fractional melting process and the overlying feldspathic dunite is a cumulate from fractional crystallization of the magma that produced the Gabbro Zone. The rock assemblage has the essential earmarks of an ophiolite complex and probably represents oceanic crust-mantle.

Church considers the general characteristics of ultramafic-mafic associations in the northern Appalachians. He believes that these suites in the Bay of Islands – Hare Bay belt, the Baie Verte belt, and the Betts Cove belt all show characteristics of alpine-type ophiolite complexes and as such may represent Early Ordovician or older oceanic crust-mantle. At present, these seem to be the oldest probable ophiolites recognized on the North American continent.

The Precambrian Shield

Baragar deals with the physical and chemical characteristics of lava sequences at Noranda, Yellowknife, Uchi Lake (Archean) and at Kaladar (Proterozoic). These cover a substantial time interval and are geographically widely dispersed yet they show many similarities. Volcanic successions commonly have thicknesses of 30,000 to 50,000 feet and have associated substantial thicknesses of sediments comprising principally quartzose greywacke, impure quartzite, and slate. Basalt, andesite and silicic volcanics occur in estimated relative proportions of about 6:3:1. A characteristic common to all belts is the conformable succession of one or more mafic to felsic cycles. Evidence concerning the floors on which these sequences were deposited is largely now inaccessible but it is probable that the Yellowknife and Labrador Trough belts were laid down upon pre-existing continental basement. Precambrian basaltic sequences have similarities to modern oceanic tholeiites but tend to have lower Al_2O_3 and TiO_2 and higher K_2O and Fe/Mg. The overall trend shown by the successions is calc-alkaline, although the tendency toward high Na_2O/K_2O ratios suggests a possible relationship to differentiation trends that produce the trondjhemite-keratophyre association in oceanic crustal rocks and ophiolites.

Naldrett classifies the common occurrences of ultramafic rocks in the Canadian Precambrian as:

(1) ultramafic cumulates associated with large layered gabbroic complexes,

(2) smaller layered ultramafic sills intruded into Archean greenstone belts and

(3) still smaller peridotite and pyroxenite lenses that are layered but may be zoned, also associated with greenstone belts. The latter two types are of most frequent occurrence and some type 3 examples have textures resembling quench textures thus implying that they formed from ultramafic liquids some of which may have been extrusive. Naldrett finds no evidence to support interpretations of allochthonous ultramafic material introduced into Archean sequences.

Paleomagnetism

Measurement and interpretation of paleomagnetic properties of rocks is the single most powerful tool available for investigation of the direction and magnitude of plate motions during Paleozoic and earlier times.

Irving and Yole concern themselves primarily with relative plate motions and only incidentally with the direct identification of fossil oceanic crust. Nevertheless, as these authors point out, the two approaches are intimately connected and provide independent criteria for recognition of continental-oceanic plate interactions.

The principles involved in determination of plate motions by paleomagnetic methods are discussed and several examples dealing with Mesozoic and younger rocks of the Pacific margin of North America are described. Potential applications of paleomagnetism to plate motion studies are outlined for the Appalachians, the Franklinian geosyncline and Precambrian structural provinces. Primary magnetization is probably fairly common in rocks as old as Paleozoic but in still older rocks it is expected that heavier reliance will have to be placed on measurements of secondary magnetizations. Analysis of possible plate motions back through the Paleozoic should be fairly readily attainable. The major challenge, however, will be in detection and measurement of plate motions in the Precambrian.

Concluding remarks

There is agreement that the northern Appalachians contain a number of examples of probable ophiolite complexes emplaced entirely or in part allochthonously. These rocks are likely representatives of Ordovician or older oceanic crust-mantle.

Alpine-type ultramafic bodies are emplaced into upper Paleozoic rocks in the Cordillera. None is yet established as being associated with an ophiolite complex and further investigation is required to determine their exact nature.

Evidence of fossil oceanic crust-mantle rock within the Canadian Precambrian Shield has not yet been discovered. Alpine-type peridotites, if they exist, must be rare. Tools for accurate identification of ocean floor basalts are not yet available and it is not possible to verify any Precambrian basalts as oceanic. Ultramafic rocks associated with thick basaltic sequences appear to have solidified in place and are not allochthonous.

As Irving and Yole point out, a major challenge exists in evaluating plate motions in the Precambrian. An equally exciting and closely related challenge lies in unravelling the history of tectonic development in the Precambrian. It is widely believed that the major period of evolution of the earth's crust and mantle took place prior to the end of the Archean i.e. before about 2.5 b.y. ago. By that time large plates of continental crust had stabilized and little has affected parts of them since. If this is so, one might expect Proterozoic tectonism to be similar to that of Paleozoic and younger eras. To a degree this seems to be true, e.g. the Labrador Trough – Cape Smith belt has many similarities to younger orogenic belts yet it contains no alpine-type peridotites and no syntectonic or post-tectonic granites. Possibly both these aspects can be related to its development as an intracontinental basin.

A popular conception of Archean greenstone belts is that they have a characteristic and relatively simple tectonic style comprising essentially synformal keels enclosed within granitoid terranes part of which may, or may not, represent pre-existing basement rocks. This simple tectonic style and apparent lack of alpine-type ultramafic rocks seems impossible to reconcile in any fashion with current concepts of Alpine orogenic processes and modern continental-oceanic plate interactions.

The western Superior Province represents, for the most part, a relatively shallow level of erosion. The Superior Province of northwestern Quebec, on the other hand, shows clear evidence of deeper erosional levels in which greenstone belts give way to relict amphibolites and then disappear altogether in dominantly granulitic terranes. This constitutes a strong argument that the rocks of the granulite terranes formed a basement upon which greenstone successions were deposited. It follows that these belts were deposited in intracontinental basins which accords with evidence cited by Baragar for deposition of at least some greenstone belts on continental crustal rocks. The calc-alkaline volcanic trends, however, suggest that some sort of oceanic crust consumption was involved. It is tempting to consider analogies with marginal basins of the modern western Pacific region. Karig (1971a, 1971b) believes these basins are of extensional origin which formed at continental-oceanic interfaces behind island arc systems and subsequently migrated oceanward. If these basins are indeed extensional and thus floored by oceanic crust then we have an important inconsistency with at least some continentally-floored Archean basins. An alternative is that Archean greenstone belts may have formed in sites akin to modern intracontinental small ocean basins (Menard, 1967). The modern examples accumulate up to 20 km of sediment in deep water and evidently are not subsequently strongly deformed. Archean basins may have formed in a similar manner but were filled with larger volcanic contributions.

Some of the major geosutures on the Precambrian Shield, the structural province boundaries, seem to provide natural loci in the search for ancient oceanic crustal rocks which may have been caught up during closing of an ocean. The Churchill-Superior boundary in Manitoba, with its complex structural and lithologic relations and a peridotite belt, seems especially worthy of closer examination.

For good reason, the paradigm of plate tectonics has fired the imaginations of earth scientists of many disciplines working with rocks of all ages. It is clear that careful and detailed studies will be required to evaluate the extent to which these processes contributed to shaping the geological record in ancient rocks.

Acknowledgments

I am grateful to J.O. Wheeler for contributing some useful comments on this summary and to my colleagues for helpful discussion.

References

Gabrielse, H. 1963. McDame map-area, Cassiar district, British Columbia. *Geol. Surv. Can.* Mem. 319, 138 p.

Kay, R., N.J. Hubbard and P.W. Gast. 1970. Chemical characteristics and origin of oceanic ridge volcanic rocks. *J. Geophy. Res.*, Vol. 75, 1585-1613.

Karig, D.E. 1971a. Origin and development of marginal basins in the western Pacific. *J. Geophy. Res.*, Vol. 76, 2542-2561.

———1971b. Structural history of the Mariana island arc system. *Geol. Soc. Amer.* Bull. Vol. 82, 323-344.

Menard, H.W. 1967. Transitional types of crust under small ocean basins. *J. Geophy. Res.*, Vol. 72,3061-3073.

PUBLICATIONS of the EARTH PHYSICS BRANCH

VOLUME 42–NO. 4

polar magnetic substorms 03 – 06, u.t. december 5, 1968

E. I. LOOMER and G. JANSEN VAN BEEK

DEPARTMENT OF ENERGY, MINES AND RESOURCES

OTTAWA, CANADA 1972

Contents

157 Abstract
157 Introduction
157 Analysis of data
159 Sequence of magnetic events
160 Development of the westward surge
161 Velocity of the westward surge and rotation of the oval
162 Identification of trigger bays
163 The extent of the auroral electrojet
163 Auroral information
164 Conclusions
165 References

polar magnetic substorms 03 – 06, u.t. december 5, 1968

E. I. LOOMER and G. JANSEN VAN BEEK

Abstract. Magnetic effects associated with a westward travelling surge are illustrated by analysis of simple bays which occurred during three moderately weak substorms, 03 - 06 U.T. on December 5, 1968.

South of the electrojet centre, at $\Phi=57^\circ$, magnetic effects are shown to be attributable solely to the auroral electrojet and its return currents.

The azimuth of the Thule current vector, previously shown to reflect the westward extension of the electrojet in the auroral oval, is used to identify individual substorms, to estimate the rate of westward rotation of the oval, and to distinguish between trigger and main bays. All storms show a rapid decay and eastward swing in the final phase. The westward rotation of the oval, deduced from the azimuth of the Thule vector and the velocity of the D demarcation line, is found to be highly irregular.

Résumé. Les effects magnétiques associés à un sursaut se propageant en direction de l'ouest sont illustrés par l'analyse des baies simples qui se sont produites au cours de trois sous-orages modérément faibles, entre 3 et 6 h. (temps universel) le 5 décembre 1968.

Au sud du centre de l'electrojet, à $\Phi=57^\circ$, on constate que les effets magnétiques sont attribuables seulement au jet auroral et à ses courants de retour.

L'azimut du vecteur du courant de Thule, qui indiquait auparavant le prolongement vers l'ouest du jet de particules électrisées dans l'ovale auroral, est utilisé pour reconnaître les sous-orages individuels, évaluer la vitesse de rotation vers l'ouest de l'ovale et distinguer le sursaut précurseur des principales baies. Tous les orages présentent un décroissement rapide et un mouvement vers l'est au cours de la phase finale. On constate que la rotation vers l'ouest de l'ovale, déduite de l'azimut du vecteur de Thule et de la vitesse de la ligne de démarcation D, est très irrégulière.

Introduction

There are certain advantages in selecting relatively weak magnetic substorms of simple form for analysis. With a satisfactory distribution of observatories such analyses can be expected to reveal details in the morphology of substorms which would be lost in larger disturbances.

A weak substorm developed in the midnight sector around 03 U.T. on December 5, 1968. The largest H perturbation was 500 gammas, recorded at Baker Lake, and the electrojet was apparently confined in longitude to the sector bounded by Leirvogur and Baker Lake. The greatest width of the electrojet was probably not more than 4 degrees. At this time, the number of observatories located in and near the auroral oval was sufficient to give a reasonably clear picture of several interesting features of the storm: in particular, the development at the northern edge of the oval of a travelling westward surge, and the identification of the trigger bays postulated by Rostoker (1970).

The intense negative H(X) bays frequently observed in the early evening hours at Baker Lake were explained by Akasofu and Meng (1967) as resulting from the westward extension of the polar electrojet which follows the travelling auroral surge along the auroral oval. Two very distinct negative bays occurred in X at Baker Lake during the weak substorm activity of 03 - 06 U.T. An analysis of these bays and the associated changes in Y and Z have clearly illustrated the magnetic effects associated with a westward travelling surge at a station in the evening sector inside the auroral zone.

Rostoker (1970) has suggested that a substorm consists of a trigger bay and a main bay, with the amplitude of the trigger bay appreciable only close to the centre of the disturbance. According to his hypothesis, the trigger bay is generated by the short-circuiting of the quiet-time ring current, and the resulting collapse of the field lines is seen as a signal propagating back into the tail. After about 07 - 10 min this signal reaches the region of the tail where it may trigger reconnection of field lines. The reconnected field lines will move inward and rejoin the inner dipole configuration. The plasma brought in by the freshly reconnected field lines may overload the ring current again, and its subsequent collapse is associated with the main bay and the development of a westward surge. The average time delay between trigger and main bays is thus 15 - 20 min. The process may repeat itself, causing substorm regeneration with a periodicity of 15 - 20 min. If the initial signal does not cause reconnection of field lines in the tail, only the trigger bay and the northward movement of the auroral arcs will be observed; the westward surge will not develop.

The azimuth of the Thule current vector has been found to reflect very closely the development of polar magnetic substorms (Loomer and Jansen van Beek, 1971). In particular, by identifying the periods in a substorm characterized by a westward extension of the electrojet in the auroral oval, the azimuth plot provides one method of distinguishing between trigger and main bays.

Analysis of data

The 03 U.T. storm has been analyzed using the magnetograms from 19 observatories (Figure 1 and the table). The method of analysis is essentially that described previously by Loomer and Jansen van Beek (1971). Deflections of X(H), Y(D), Z from the baseline were measured at approximately 9-minute

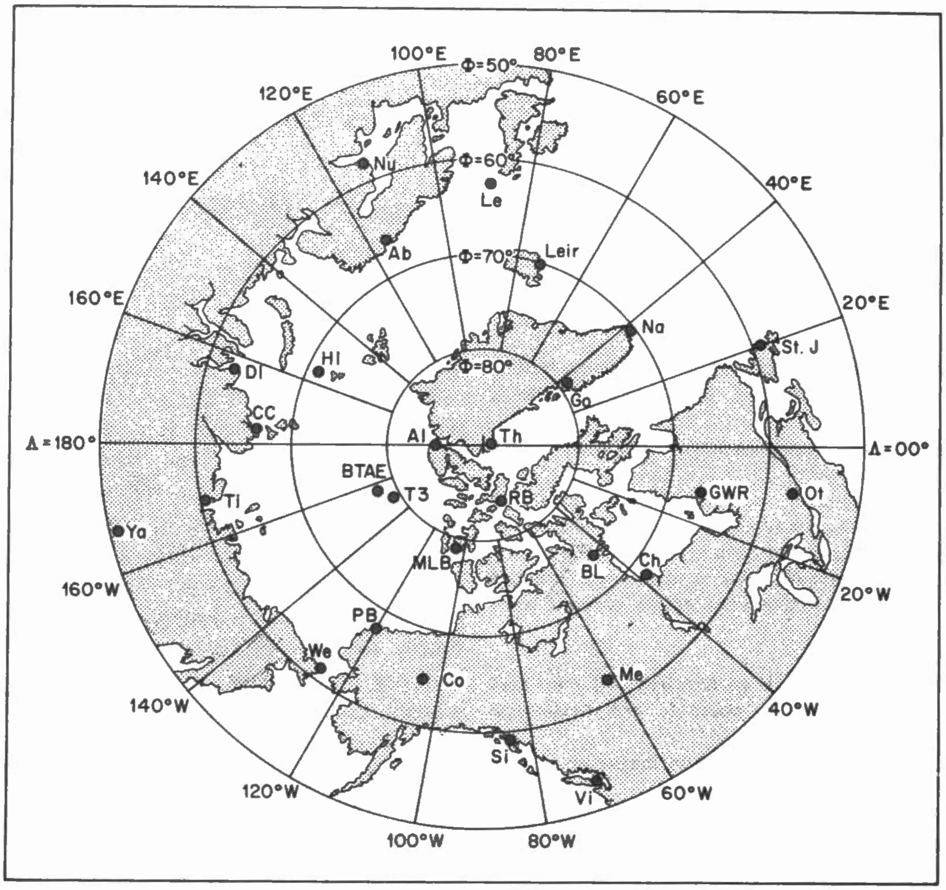

Figure 1. Map in geomagnetic coordinates showing the stations used for this analysis.

intervals from 02 to 06 U.T. Perturbations from the midnight level of the quiet day (December 14) were then expressed in the geomagnetic coordinate system X′, Y′, Z. Plots of equivalent line currents, calculated from the three perturbation vectors ΔX′, ΔY′, ΔZ for a height of 112 km (equivalent to 1 degree of latitude) were drawn for several instants of time during the storm (Figure 2). H perturbation vectors for the four observatories – Narssarssuaq, Great Whale River, Fort Churchill, Baker Lake – for selected intervals of the storm, are shown in Figure 3. The orientation of the Thule current vector for the period 0225 to 0600 is given in Figure 4. Magnetogram traces for selected observatories are reproduced in Figure 5.

The Kp indices for the 8 three-hour U.T. intervals of this day were 3- 3o 5+ 5o 4o 3- 3+ 3-. Dst had a small positive maximum of 3 gammas at 08 U.T. and a minimum of -48 gammas at 01 U.T. on December 6. The AE indices showed 4 distinct maxima: 235 gammas at 05 U.T., 356 gammas at 10 U.T., 511 gammas at 13 U.T. and 155 gammas at 18 U.T.

Auroral data available for this storm from the National Research Council, Ottawa, were limited. All sky camera (ASCA) records for Churchill were not usable owing to cloud cover, and a full moon limited the usefulness of the ASCA records at Great Whale River. No ASCA records were available for this period from Narssarssuaq, Sondrestrom, and Godhavn. Auroral radar plots were available for Thompson, Ottawa, Great Whale River and Churchill, but unfortunately azimuth indicators were missing on the Churchill records.

		Geomag. Lat.N.	Coords. Long.E	Ψ_E	U.T. of local midnight (hrs)			Geomag. Lat.N	Coords. Long.E	Ψ_E	U.T. of local midnight (hrs)
Th	Thule	89.2	357.4	2.4	04.61	Ab	Abisko	65.9	115.3	330.2	22.75
Al	Alert	85.7	168.7	197.7	04.17	Co	College	64.6	256.1	27.6	09.86
RB	Resolute Bay	83.1	287.7	47.1	06.33	DI	Dixon Is.	62.8	161.7	347.0	18.63
Go	Godhavn	80.0	33.1	341.8	03.56	Le	Lerwick	62.5	89.0	336.0	00.07
MLB	Mould Bay	79.1	255.4	55.3	07.96	Me	Meanook	61.9	300.7	17.5	07.55
BL	Baker Lake	73.9	314.8	19.4	06.40	We	Welen	61.6	236.8	24.8	11.32
Na	Narssarssuaq	71.4	37.3	345.2	03.02	Ti	Tixie Bay	60.3	192.6	351.9	15.40
HI	Heiss Is.	71.1	156.3	330.0	20.13	Si	Sitka	60.0	275.0	21.8	09.02
Leir	Leirvogur	70.3	71.6	333.8	01.45	Nu	Nurmijarvi	59.6	114.4	336.4	22.36
Ch	Fort Churchill	68.8	322.5	13.8	06.27	St.J	St. John's	58.7	21.4	353.7	03.51
PB	Point Barrow	68.4	240.7	33.5	10.45	Ot	Ottawa	57.0	351.5	2.4	05.04
GWR	Great Whale River	66.8	347.2	4.5	05.18	Vi	Victoria	54.3	292.7	16.4	08.23
CC	Chelyuskin Is.	66.1	176.5	356.6	17.05	Ya	Yakutsk	50.8	193.8	5.9	15.35

Note: Ψ_E, the angle between geographic and geomagnetic meridians at a station is measured eastward from the geographic meridian.

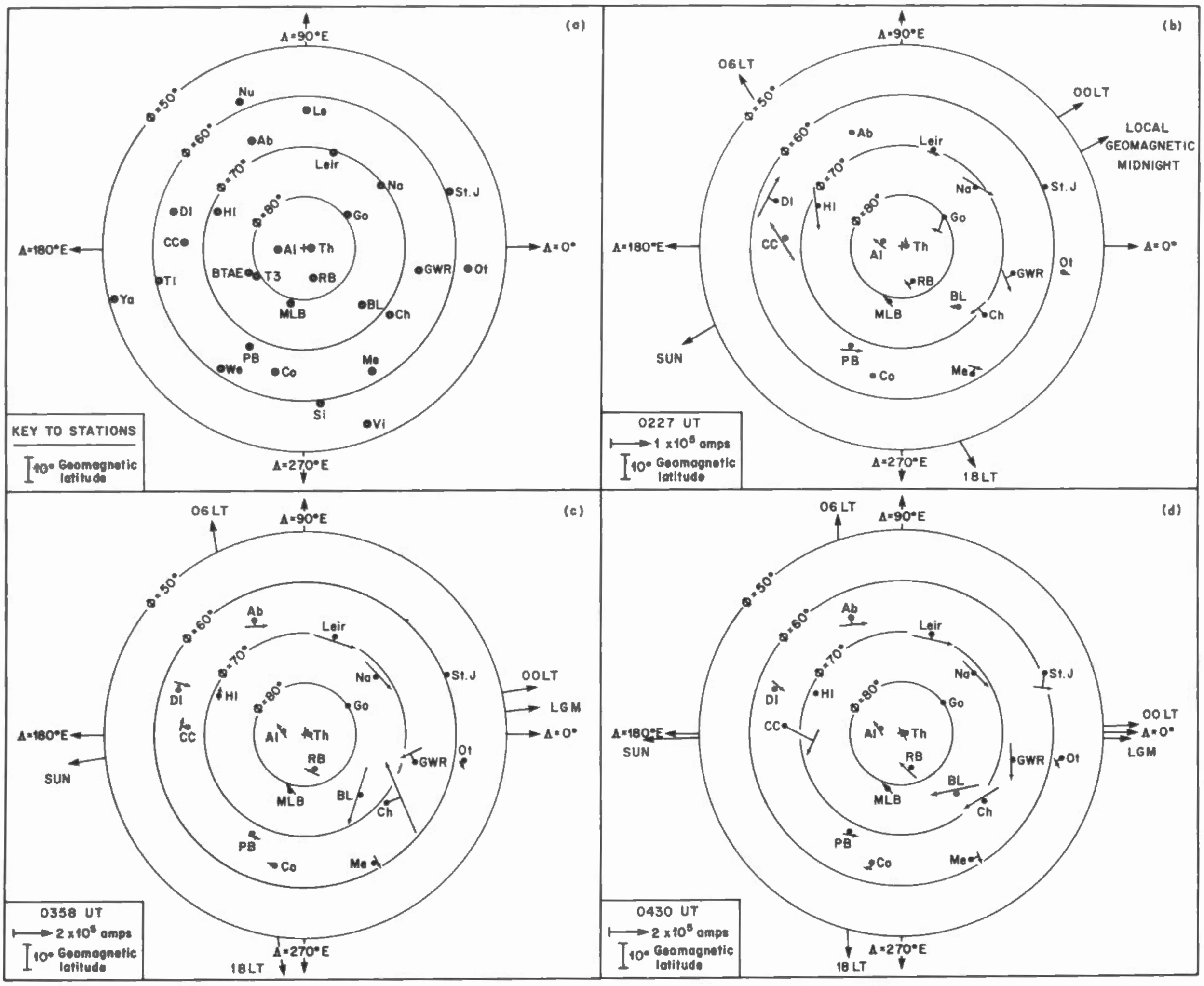

Figure 2. Current vector plots for 0227 U.T. (Figure 2b), 0358 U.T. (Figure 2c), 0430 U.T. (Figure 2d). Key to location of stations is shown in Figure 2a.

Sequence of magnetic events

The magnetograms (Figure 5) indicate that a disturbance was developing in the Na area shortly after 02 U.T., with sharp impulses in all elements at 0225, 0238 and 0258. At 0327 magnetic effects were evident at all observatories in and near the auroral oval. The main negative H bay at Na and Leir and a gradual bay at BL in H (negative) and Z (positive) began at this time. However, the largest magnetic effects were recorded at GWR where large perturbations occurred in all elements, and at Ch where the gradual negative movement in H was abruptly indented with a large positive bay. The storm activity was most intense at BL, where the sharply increased negative movement in X, beginning 0339, reached its maximum value of 500 gammas at 04 U.T. The effects of this disturbance had disappeared by 0447, and another storm, beginning 0500, was recorded on the BL magnetogram.

At St. J and Ot, south of the oval in the late evening sector, magnetic effects were very small with maxima less than 25 gammas in -ΔX′, ΔY′, and less than 50 gammas in -ΔZ. At Me, geomagnetically south of BL, ΔX′ was slightly negative (less than 20 gammas) from 0330 to 0500, and ΔY′ was maximum east (70 gammas) at 04 U.T. ΔZ at Me was positive but did not exceed 30 gammas.

In the daytime sector magnetic perturbations were less than 100 gammas. Small positive H bays and negative Z bays were recorded at PB and CC from 0300 to 0600. During this interval negative H bays were observed at Co, Si, Ya, Ti and We, and ΔZ was generally positive. ΔH was slightly negative at HI and positive at DI until 0500. Following this the sign of the H perturbation at these stations was reversed. No effect was evident in Z at HI until 0430, after which ΔZ became slightly negative.

The outstanding magnetic events are thus the sharp impulses at Na at 0225 and 0238, followed by the larger impulse (-270γ in ΔH, -69γ in ΔZ) at 0258; the extensive magnetic effects observed at 0327; the abrupt movement in all elements at BL at 0339, and the new disturbance beginning there at 0500.

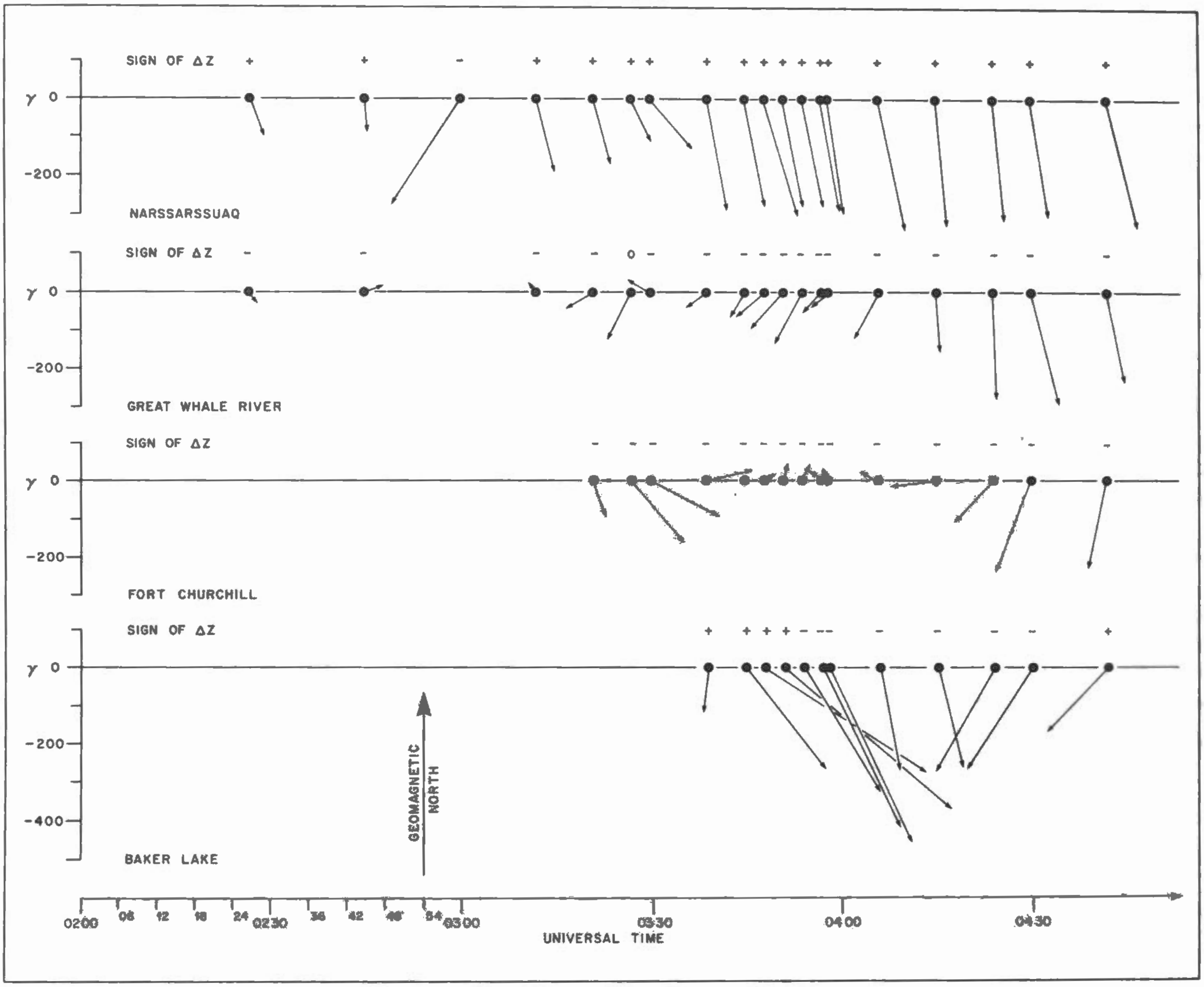

Figure 3. H perturbation vectors and the sign of ΔZ for selected intervals at Na, GWR, Ch, BL.

Development of the westward surge

In his discussion of transitional bays at middle latitudes, Rostoker (1966) defined a demarcation line which divided the region of the return current south of the oval into two parts: a western part, where ΔD is always east, and an eastern part, with ΔD always west (Figure 6). The Y transitional bays at Baker Lake and Churchill and the less regular changes in D at GWR and Na similarly define a demarcation line in the return current flow immediately south of the electrojet, although not necessarily the same as that observed at middle latitudes. The information given by the changes in D (or Y′) is conveniently summarized in the ΔH vector plots, based on ΔX′, ΔY′, (Figure 3).

The effects at Na associated with the large impulse at 0258 indicate a rapid movement of the current system to the north of the station, placing Na in the return flow south of the main electrojet. However, it is not possible to determine if a western travelling surge developed at this time. ΔY′ is west, suggesting that the demarcation line was to the west of the station at 0258. Following the impulse, the equivalent current vector, much enhanced, is again south of Na (Figure 2).

At CH, from 0321 to 0440, the ΔH vector swings 330 degrees in an anti-clockwise direction. At 0358 the demarcation line passes over Churchill as the station moves from ΔY′ east to ΔY′ west in the return current south of the oval (Figure 2). A gradual negative bay in X, typical of a station just south of the oval in the evening sector (Akasofu, 1968), begins at 0215 (Figure 5). This is indented suddenly at 0327 with a large positive bay which peaks at 0405 and lasts until 0442. A negative Z bay begins at 0327. These effects imply a rapid movement of the electrojet northward at 0327.

The changes in the H perturbation vector at GWR from 0227 to 0327 are similar to those at Ch. ΔY′ changes from east to west at 0312 as the demarcation line passes over the station. From 0327 to 0330 thc ΔH vector swings sharply to the north through 90 degrees. This would result from the rapid northward movement of the electrojet noted at CH at 0327, causing both CH and GWR to be located farther south in the return current system (Figure 6) and indicates the passage of a westward travelling surge north of GWR and Ch at this time.

BL remains in the polar cap return current until 0345 (Figure 2), when the positive Z bay is abruptly indented with an intense negative bay, which peaks at 0406 and ends abruptly at 0447 (Figure 5). The station comes under the influence of the main electrojet as early as 0327, when the negative X bay begins. At 0339 a rapid negative movement begins in X, and Y suddenly increases to the east. ΔZ still moves in the positive direction, but at an increased rate until 0345. These effects can be understood as resulting from the close approach of the electrojet to the station from the east at 0339, and simultaneously its rapid movement to the north of the station, effectively moving the station out of the polar cap into the anti-clockwise circulation of the leakage current south of the oval. ΔY′ is maximum east at 0348, changing to west at 0424, and reaching its westerly maximum at 0432. The electrojet remains north of the station until 0432, after which the auroral bulge has passed to the west of the station and BL is again located in the polar cap flow.

These effects are clearly illustrated in Figure 7, which is a synthesis of equivalent current vector plots for several instants during the storm. The effect of the surge is represented schematically by a westward travelling bulge of the electrojet, which leads the westward advance of the primary current flow in the dark sector of the auroral oval (Akasofu and Meng, 1967; Rostoker *et al.*, 1970). This is a development of the model proposed by Rostoker (1966). The equivalent current system is regarded as fixed in space with relation to the earth. The movement of BL (Φ~74°) relative to the current system for the interval 0321 to 0442 is shown by the dashed line. Values of the BL perturbation vectors for several instants during the storm are given with the figure.

The magnetic effects are closely repeated in miniature at BL during the smaller storm 0500 - 0545. However, for this period, since the demarcation line is now to the west of the station, Baker Lake passes south of the electrojet into the east half of the return current cell associated with ΔD west (or -ΔY′). The effects of this storm can be explained by a surge causing an explosive poleward shift of the electrojet west of BL with the bulge approaching close to the station from the west shortly after 0500, causing ΔD to swing farther west and ΔZ to increase in the positive direction (Figure 7). At 0510, as the station comes under the eastward edge of the expanding bulge, the negative movement begins abruptly in Z. D is maximum west at 0512 and -ΔH is maximum at 0520. Following 0527 the station is south of the electrojet. The negative bay ends abruptly in Z at 0545. The abrupt ending of the Z bay in this and the preceding storm is explained by the passage of the electrojet over the station, as the main current returns to the south. The effects of the second surge are over at 0546 after which the station is again in the polar cap return.

Velocity of the westward surge and rotation of the oval

The approximate speed of the surge which developed north of GWR and Ch at 0327 and was detected at BL at 0339 may be estimated as follows. The current vector plot (Figure 2) suggests that the electrojet is at dipole latitude $\Phi = 70°$ at this time. The difference in geomagnetic longitude between BL and the point midway between Ch and GWR is 20 degrees. The distance along the 70° geomagnetic parallel is 38.185 km/degree of geomagnetic longitude Λ. This distance must be reduced by approximately $\Delta t/4 \times 38.185$ to correct for the rotation of the earth, where Δt is the time difference in minutes between the surge effects at the two locations. Then, if y is the speed of the surge in km/sec

y (Δt min x 60) sec = (ΔΛ - Δt/4) 38.185
and $y = 0.9$ km/sec

This calculation can only be approximate owing to the uncertainty in locating the point of origin of the surge and in reading the time of events on normal magnetograms. The commonly

Figure 4. Graph of change with time of geomagnetic azimuth of Th current vector.

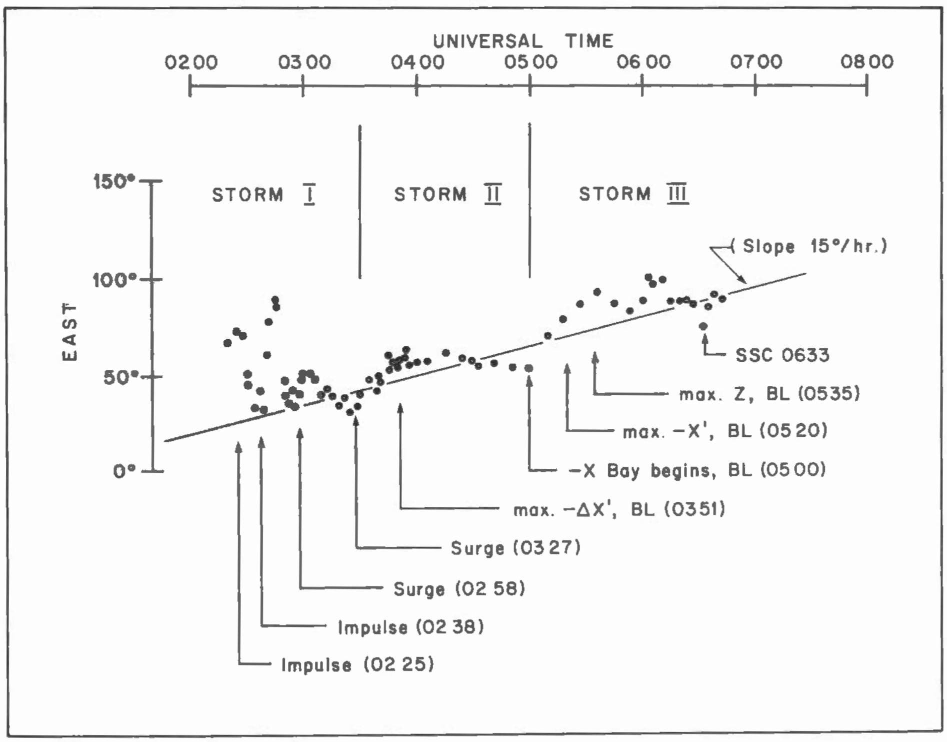

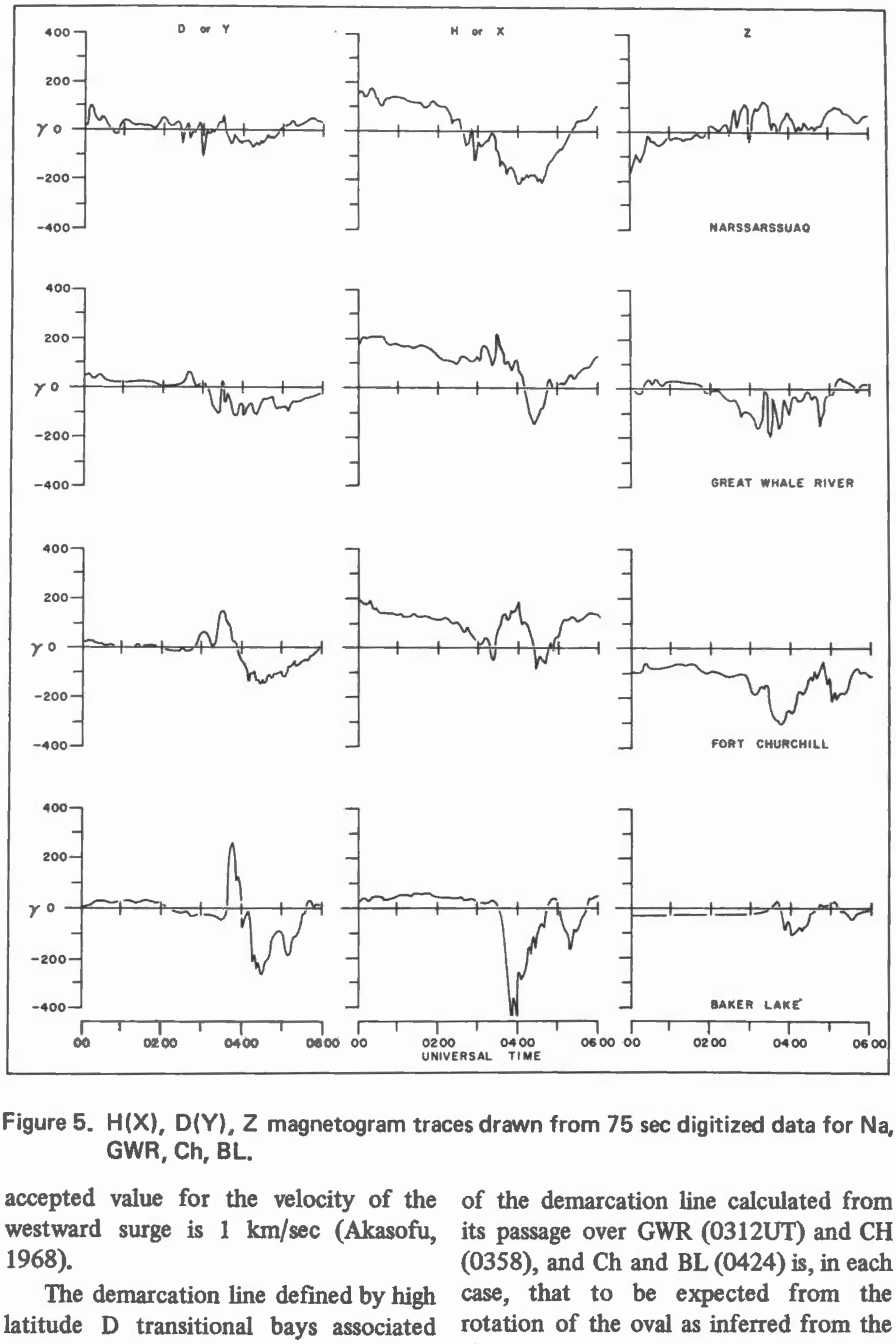

Figure 5. H(X), D(Y), Z magnetogram traces drawn from 75 sec digitized data for Na, GWR, Ch, BL.

accepted value for the velocity of the westward surge is 1 km/sec (Akasofu, 1968).

The demarcation line defined by high latitude D transitional bays associated with surge activity, does not move westward at a consistent rate. This is in contrast to the movement of the demarcation line calculated by Rostoker *et al.* (1970) for transitional D bays at mid-latitudes, in which the demarcation line was found to move west with respect to the sun-earth line at about 0.9 km/sec at the latitude of the polar electrojet in the case of two geomagnetic arrays located at 45°N and 53°N. The velocity of the demarcation line calculated from its passage over GWR (0312UT) and CH (0358), and Ch and BL (0424) is, in each case, that to be expected from the rotation of the oval as inferred from the change in orientation of the Th current vector (Figure 4) which is discussed in the following section. Figure 4 suggests that the oval rotated to the west at a rate just slightly greater than 15°/hr (equivalent to 0.16 km/sec at $\Phi = 70°$) between 0312 and 0358. The corresponding velocity of the demarcation line was 0.18 km/sec. The velocity of the demarcation line from Ch to BL is 0.03 km/sec; the change in azimuth of the Th current vector between 0358 and 0424 implies that the oval has moved to the west in this interval at a rate of 3°/hr or 0.03 km/sec. These comparisons underline the significance of the orientation on the Th current vector in determining the westward rotation of the oval.

Identification of trigger bays

As shown in an earlier paper (Loomer and Jansen van Beek, 1971), the changing orientation of the current vector at Thule, near the geomagnetic pole, reflects very closely the extension of the polar electrojet which follows the westward surge along the oval. However, the Thule current vector would be quite insensitive to a purely poleward movement of the electrojet, and could be expected to distinguish between trigger bays and the main bay, if a westward surge develops only with the main bay.

A plot of the azimuth of the Thule current vector is shown in Figure 4. Since the azimuth is derived from arc tan $\Delta Y'/\Delta X'$, values become quite uncertain for small $\Delta X'$, $\Delta Y'$. In practice this precludes use of the azimuth information prior to 0220 U.T. when $\Delta X'$, $\Delta Y'$ were generally small and oscillated about the adopted quiet level. For the period shown in Figure 4 the uncertainty of the azimuth values does not exceed 3 degrees.

The impulsive negative H bays at Na at 0225 and 0238 could be interpreted as trigger bays. These bays are also observed at Leir, and the 0238 bay may be identified on the Ch record as a small negative X bay.

It can be argued that the westward surge which was identified on the Churchill and BL magnetograms developed north of GWR and Ch at 0327, and is thus connected with the main negative H bay beginning at that time. If a surge, travelling westward along the oval at 1 km/sec, developed north of Na at 0258, it could be expected to appear north of GWR at about 0327. The effect would be felt to the east at Leir at about the same time. However, it is reasonably certain that the surge observed north of GWR and Ch developed in that area at 0327, and did not originate earlier in Na. The occurrence of negative H bays at stations along the active part of the oval at 0327 indicates that a significant new disturbance began at that time. This is confirmed by the change in azimuth of the Th current vector around 0330.

The graph of the Th current vector in Figure 4 suggests that three distinct substorms occurred in the interval 03 - 06 U.T. The first was very short-lived, and decayed soon after its onset around 0258. The second and third lasted much longer, and reached maximum intensity (as inferred from the maximum geomagnetic east azimuth of the Th current vector) at 0348-0354 and 0536 respectively. The storms show the rapid decay and pronounced eastward swing of the storm centre noted previously by Loomer and Jansen van Beek (1971) for the storms of 08 U.T. and 11 U.T.

There is no evidence from Figure 4 of a westward extension of the electrojet following the impulse at 0225. There is a suggestion that a short-lived substorm developed after the 0238 impulse, although the anomalously large increase in azimuth between 0240 and 0250 does not resemble the usual substorm signature. It is possible that the abrupt increase in azimuth at this time, which is also observed at Resolute Bay, results from a local disturbance in the polar cap and does not reflect a westward extension of the jet in the auroral oval.

It is concluded that the bay at 0225 is a trigger bay. Lacking evidence of a westward surge in the Na area at 0238, it is not possible to establish whether the bay which began at that time is a second trigger bay or the beginning of a small substorm. If the latter interpretation is correct, then the bays at 0258 and 0327 result from the periodic regeneration of substorms discussed by Rostoker (1970), although the delay of 29 minutes is significantly longer than the 15-20 minutes which he postulated.

The extent of the auroral electrojet

The auroral electrojet did not attain a large east-west extent during these disturbances, and was probably confined at its most intense to a sector between Leir and a point slightly west of BL (about 120° in geomagnetic longitude) in which the flow was estimated to lie between 71.5°N and 75.5°N at 0358 (Figure 2). In the daytime sector at 0227 a weak eastward current flowed at HI and PB, with a westward current south of CC and DI. At 0358 and 0430 HI is in the polar cap return flow. By 0518 an eastward current flowed south of HI, CC and PB, and north of DI. Only very small effects were observed at stations south of the active part of the oval at Ot, St. J and Me.

Fukushima (1969) has shown that the geomagnetic effect of the auroral electrojet return current is confined practically to a rather small area in high latitudes, and does not extend down to low latitudes, if the electrojet flows in a narrow latitude range within several degrees. For a station at the latitude of Ot on the meridian passing through the auroral electrojet centre, the calculated effect for an auroral electrojet of 4 degrees width would be 63 gammas for an electrojet of 120 degrees longitudinal extent. The calculation applies to the case where the maximum field change under the jet is 1000 gammas. At 0358 the total maximum effect at BL was about 500 gammas. The effect measured at Ot, slightly east of the central meridian, was 36 gammas. This agrees closely with the value predicted from Fukushima's model and implies that in this case the geomagnetic effect observed at Ot can be attributed solely to the westward auroral electrojet and its return currents. The calculation is relatively insensitive to the longitudinal extent of the electrojet.

Auroral information

As already noted, the auroral information for this period was very limited. From 0200 to 0500 quiet homogeneous arcs directed approximately east-west were visible to the north of GWR. These were located typically at 32 degrees from the zenith. Double arcs were observed occasionally. In addition to the

Figure 6. Rostoker's equivalent current system for a polar magnetic substorm.

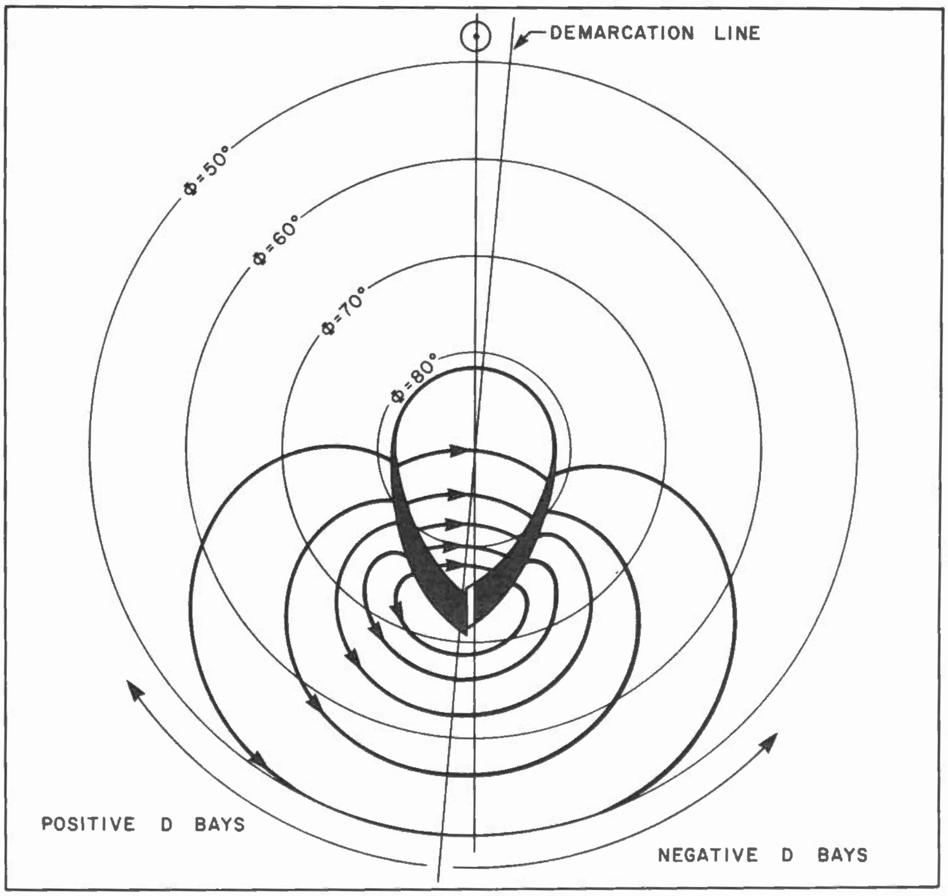

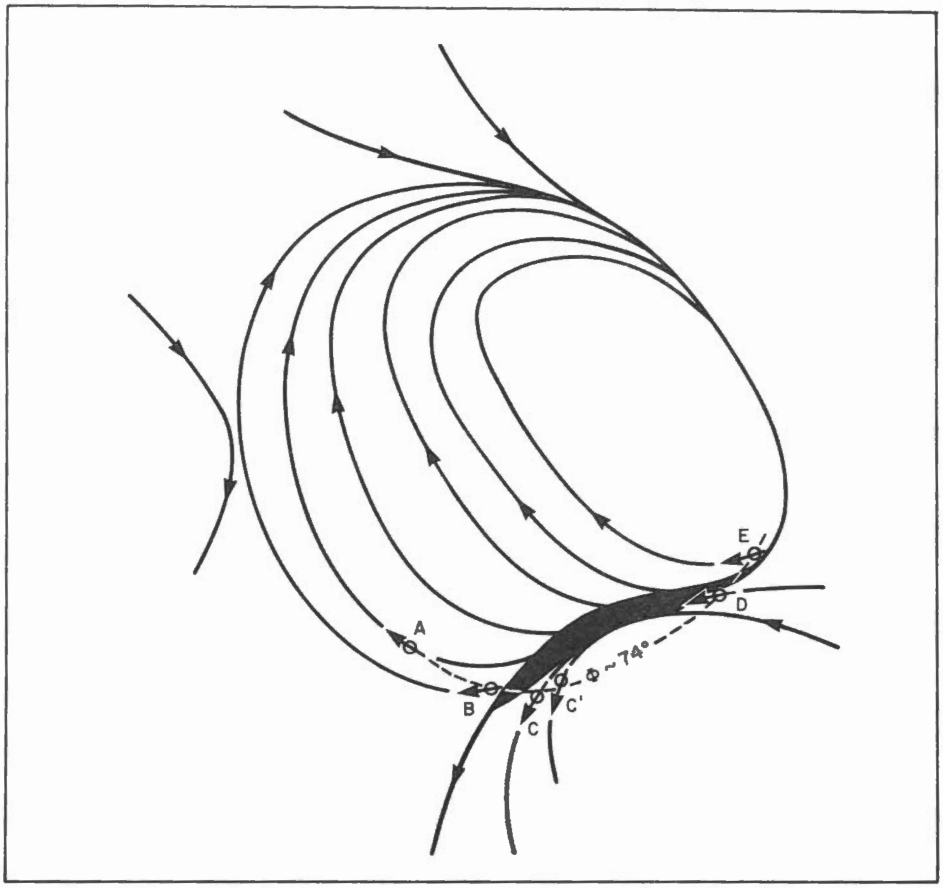

Figure 7. Schematic representation of westward surge effect at Baker Lake (Φ~74°) for storms 0327-0447 and 0500-0545.

Storm (0327-0447)					Storm (0500-0545)				
		ΔX'	ΔY'	ΔZ			ΔX'	ΔY'	ΔZ
A	0321	U.T. -52γ	-31γ	20γ	E	0500U.T.	-159γ	-141γ	196γ
B	0339	-113	-16	118	D	0527	-205	-97	-39
C	0354	-320	197	-301	E	0554	-17	-8	52
C'	0358	-451	215	-85					
D	0424	-268	-159	-275					
E	0442	-168	-166	92					

weak homogeneous arcs, additional auroral activity in the form of patches was observed northeast of the station at 0221 and 0223, at 0238 - 0240, at 0301, and at 0331. At 0405 - 0407 patches were visible to the north-northwest and moved west at 0407, disappearing at 0413. The patches were generally preceded by brightening of the arcs. Unfortunately GWR was too far south of the oval to see the effects of the surge which developed to the north around 0327. The weak homogeneous arc less than 15 degrees above the northern horizon was observed to brighten in the northeast at 0330, followed by a patch about 35 degrees from the zenith at 0331. This activity was doubtless associated with the magnetic effects of 0327.

Since ionized patches do not always give rise to radar echoes, it is difficult to correlate the auroral radar records with magnetic effects. At GWR and Thompson (Φ65.N, Λ317.5E) these echoes were always observed to move in a counter-clockwise direction from the south to a position east or north of the station, returning again to the south. Echoes were observed due east, or north of east, of GWR within 400 km of the station at 0238, 0300, 0330 and 0445. The echoes were structured in all cases except th first, and were especially bright at 03[illegible]. Although this information adds little to the understanding of the magnetic storms in this period, it does not conflict with the interpretation which has been presented.

Conclusions

The magnetic effects associated with a westward travelling surge at a high latitude (Φ = 74°) station in the evening hours have been clearly illustrated by the analysis of the simple bays which occurred at BL during the weak substorms of December 5, 1968. In particular, the smoothly varying transitional bays in D (or Y') and the sharply defined negative indentations of Z, lasting about an hour, have been interpreted by means of a simple model to show the rapid movement of the electrojet to the north, west and east.

The storm developed east of the midnight sector in the vicinity of Na. In the interval 03 - 06 U.T. three distinct substorms were identified, each initiated by the rapid poleward shift and the westward extension of the electrojet characteristic of the auroral surge. The longitudinal extension of the electrojet was limited to approximately 120° for the largest of the three substorms (0327 - 0447), and current flow, as given by the equivalent current vectors, was confined between geomagnetic latitudes 71.5° and 75.5°N approximately. Magnetic effects south of the oval at Ot and St. J were very small and apparently can be attributed solely to the auroral electrojet and its return currents. The largest effects in the daytime sector were about 1/5 of the maximum observed for the storm.

The velocity of the 0327 surge inferred from magnetic effects was 0.9 km/sec, in good agreement with values found in the literature (Loomer and Jansen van Beek, 1971). The westward rotation of the oval, deduced from the change in azimuth of the Th current vector and confirmed by the calculated velocity of the D (Y′) demarcation line, was found to be highly irregular. The usefulness of the azimuth plot of the Th current vector for identifying individual substorms and for estimating the rate of rotation of the oval was again illustrated. The rapid swing of the oval to the east during the decay phase of substorms, first noted for the intense substorm of 08 U.T., was again evident in the orientation plot of the Th vector for the weak substorms of 03 - 06 U.T.

The negative H bay which occurred at Na at 0225 and was visible also with reduced intensity on the Leir record, was identified by means of the Th azimuth plot as a trigger bay. However, it was not possible to clearly establish whether the impulse at Na at 0238 was associated with a second trigger bay, or marked the beginning of the main bay of a weak substorm. Although the sensitivity of the orientation of the Thule current vector to the westward extension of the electrojet is useful in distinguishing between trigger and main bays, the unambiguous identification of the trigger bay is clearly very difficult.

References

Akasofu, S.I. 1968. Polar and magnetospheric substorms. *Astrophysics and Space Science Library*, 2, D. Reidel Publishing Co., Dordrecht, Holland.

Akasofu, S.I. and C.I. Meng. 1967. Intense negative bays inside the auroral zone. Part I: The evening sector. *J. Terr. Phys.*, 29, 965-973.

Fukushima, N. 1969. Spatial extent of the return current of the auroral zone electrojet, Part I. *Rep. Ionos. Space Res. Japan*, 23, 209-218.

Loomer, E.I. and G. Jansen van Beek. 1971. Magnetic substorms, December 5, 1968. *Pub. Earth Phys. Br.*, Vol. 41, No. 10.

Rostoker, G. 1966. Midlatitude transition bays and their relation to the spatial movement of overhead current systems. *J. Geophys. Res.*, 71, 79-95.

Rostoker, G. *et al.* 1970. Development of a polar magnetic substorm current system. Report of Univ. of Alberta, Killam Earth Sciences, May 8.

Rostoker, G. 1970. Polar substorms and the dynamics of the magnetosphere. Proceedings of Upper Atmospheric Currents and Electric Fields Symposium. *ESSA Technical Memorandum ERLTM - ESL12*, 358-366. Published by U.S. Department of Commerce.

PUBLICATIONS of the EARTH PHYSICS BRANCH

VOLUME 42 - NO. 5

an astatic magnetometer with negative feedback

J. L. ROY, J. REYNOLDS and E. SANDERS

DEPARTMENT OF ENERGY, MINES AND RESOURCES

OTTAWA, CANADA 1972

Cat. No: M70-42/5

Contents

168 Introduction

168 Part I – Theory of design
168 1. The magnet system
168 2. Period limitations
169 3. Patio P/I
169 4. Magnetic materials

169 Part II – Experimental design
169 1. The magnet system
171 2. Magnet system housing
171 3. Field compensation
172 4. Response of an astatic magnetometer
172 5. Calibration
172 6. Specimen table

174 Part III – Torsion method
174 1. Performance
174 2. Measurements

174 Part IV – Magnetic control method
175 1. Principle of operation
176 2. Characteristics of the system
177 3. Sensitivities
178 4. Design variations
178 5. Measuring method (direct read)
179 6. Disturbances
180 7. Zeroing
180 8. Performance

182 Acknowledgments

182 References

an astatic magnetometer with negative feedback

J. L. ROY, J. REYNOLDS and E. SANDERS

Abstract. This paper describes an astatic magnetometer designed for the measurement of weakly magnetized rock specimens with special reference to a magnetic control method as a means of improving both the performance and efficiency of the instrument.

In the first section, it is shown that for high sensitivity and rapid response, the two magnets should be long and thin, magnetized perpendicular to the long axis, and that the moment of inertia of each magnet should be 1/4 the moment of inertia of the whole suspended system. In general, magnetic materials of high coercive force give the best design.

The second section describes in detail the construction of an astatic magnetometer according to the above principles, including a method of astatizing without the use of trimmer magnets. Following a discussion on the size, shape and positioning of the rock specimen, a cylindrical specimen (height/diameter $=\pi^{1}/_{2}/2$) placed directly beneath the lower magnet is chosen. A specimen table and a method for accurate determination of the distance between specimen and magnetometer are described.

The third section describes the procedure for measuring three orthogonal components of magnetization of a specimen. When the instrument is operated in the conventional manner, that is with the restoring torque provided by the suspension fibre, with a period of 14 seconds the sensitivity is 1×10^{-8} oe/mm deflection on a scale 5 m distant. This sensitivity permits the measurement of specimens magnetized to an intensity of 1×10^{-6} e.m.u.

The fourth section describes the use of negative feedback to improve the performance and efficiency of the instrument. Here, in addition to the torque of the suspension, a magnetic restoring torque is provided by a small solenoid connected to a pair of photo resistors centred on the light beam. Measurements can be made in terms of current or voltage with a variety of electrical instruments. High sensitivity (0.56×10^{-9} oe/mv) can be obtained while maintaining a short period (5.1 sec). The sensitivity and the period can be lowered instantly through 11 steps down to 1.2×10^{-7} oe/mv and 1.2 sec. The quick response permits the direct measurement of the direction and total intensity of magnetization of the specimen, rather than computing them from three components. This eliminates much calculation and increases the accuracy, especially with weakly magnetized rocks. The range of the instrument provides for accurate measurement of specimens magnetized to an intensity of 1×10^{-7} to 5×10^{-3} e.m.u.; the time required for a measurement of direction and intensity is eight and three minutes, respectively. The period and damping of the system can be altered in many ways to suit particular conditions and requirements. Disturbances affecting the instrument and means of avoiding or reducing them are discussed.

Résumé. Les auteurs décrivent un magnétomètre astatique servant à mesurer l'intensité d'aimantation, généralement très faible, d'échantillons de roches; ils insistent tout particulièrement sur une méthode de contrôle par champ magnétique permettant d'améliorer la sensibilité et le rendement de l'appareil.

Dans la première partie, ils démontrent que, dans un système astatique à deux aimants, il est préférable d'utiliser des aimants longs et étroits aimantés perpendiculairement à leur axe longitudinal; en outre, le moment d'inertie de chaque aimant devrait être égal au 1/4 de celui de l'ensemble de l'équipage mobile. En général, ce sont les matériaux magnétiques à haute coercitivité qui répondent le mieux à ces conditions.

Dans la deuxième partie, les auteurs décrivent en détail la construction d'un magnétomètre astatique conçu suivant les principes énoncés précédemment, et la méthode employée pour le rendre astatique sans utiliser des aimants compensateurs. Après avoir discuté des dimensions, de la forme et du positionnement de l'échantillon, ils fixent leur choix sur un échantillon cylindrique (hauteur/diamètre $= \pi^{1}/_{2}/2$) placé directement sous l'aimant inférieur. Ils décrivent ensuite le porte-échantillon ainsi que la méthode permettant de déterminer avec précision la distance optimale entre échantillon et magnétomètre.

Dans la troisième partie, les auteurs énoncent la procédure à suivre pour mesurer trois composantes orthogonales de l'intensité d'aimantation d'un échantillon. Quand l'appareil fonctionne suivant le mode habituel, c'est-à-dire quand le couple de rappel du fil de torsion correspond à une période d'oscillation de 14 secondes, la sensibilité est de 1×10^{-8} oersted pour une déflection de 1 mm sur une mire graduée distante de 5 m. Cette sensibilité permet de mesurer l'intensité d'aimantation d'échantillons présentant des intensités aussi faibles que 1×10^{-6} gauss.

Dans la quatrième partie, les auteurs décrivent le procédé par lequel ils améliorent la sensibilité et le rendement de l'appareil à l'aide d'un système de rétroaction négative. On ajoute au couple de torsion du fil de suspension un couple de rappel électromagnétique fourni par un petit solénoïde connecté à deux photorésistances encadrant le faisceau lumineux. Les mesures se font en termes d'intensité ou de tension, à l'aide d'appareils électriques variés. Grâce à la méthode indiquée ci-dessus, on peut obtenir une haute sensibilité (0.56×10^{-9} oersted/millivolt), tout en conservant une courte période d'oscillation (5.1 sec.). On peut réduire instantanément la sensibilité et la période, en 11 étapes successives jusqu'à 1.2×10^{-7} oersted/millivolt et 1.2 seconde. Le temps de réponse très court ainsi obtenu permet la mesure directe de la direction et de l'intensité de l'aimantation de l'échantillon sans avoir à les calculer à partir de trois composantes. Ceci élimine une grande partie des calculs et améliore la précision, en particulier dans le cas des roches faiblement aimantées. L'appareil permet une mesure précise sur des échantillons dont l'intensité est comprise entre 1×10^{-7} et 5×10^{-3} gauss; il faut 8 et 3 minutes respectivement, pour mesurer la direction et l'intensité de l'aimantation. Il est possible de modifier à volonté la période et l'amortissement de l'équipage mobile pour répondre aux conditions et aux exigences particulières qui pourraient se présenter. Les auteurs examinent enfin les perturbations pouvant affecter l'appareil et indiquent la façon de les éviter ou d'en atténuer les conséquences.

Introduction

Astatic magnetometers have been used extensively for the measurements of the remanent magnetization of rock specimens since Blackett (1953) showed them to be well suited for measuring weak fields. Blackett's magnetometers were designed to measure the weakest field possible without regard to the time taken, and instrument periods were as long as 60 to 70 seconds. In paleomagnetic work, a large number of measurements are required and shorter period instruments are desirable. Various designs for maximum sensitivity at a limited period have been described (e.g. Collinson *et al.*, 1957; As, 1960; Collinson and Creer, 1960; Roy, 1963). Owing primarily to new manufacturing processes of magnetic materials, it has been possible over the last two decades to improve the design and consequently the performance of astatic magnetometers. The performance of a magnetometer constructed according to the design theory given by Roy (1963) and using Platinax II magnets shows that the instrument can accurately measure the components of magnetization of a rock specimen magnetized to an intensity of 1×10^{-6} e.m.u. with an acceptable response time of 14 seconds. With a change of the suspension fibre, the response time can be shortened to, say, 4 to 5 seconds; the corresponding reduced sensitivity (≈ a tenfold reduction) is still adequate to measure intensities of 1×10^{-5} e.m.u. These performances are obtained when using the conventional torsion control method of measuring (by means of lamp mirror and scale) the deflection produced by a magnetized specimen placed near the instrument. When using the instrument in this mode, the deflection of the magnet system should be entirely controlled by the torsion of the fibre. For this reason, by changing the suspension, the instrument can be made into a high sensitivity magnetometer *or* a quick-response magnetometer; however, the two characteristics (high sensitivity and quick response) cannot be combined because an increase of one is accompanied by a reduction of the other.

The range of intensities found in rock specimens is large (≈ 1×10^{-7} to 1×10^{-2} e.m.u.) and an instrument with multiple sensitivities is desirable for reasons of efficiency. Changing suspension fibres to attain this objective is most impractical. Because of the high risk of breaking the fibre, such changes are usually avoided. Furthermore, the time required for re-alignment of the system would defeat the purpose. An alternative would be to have several magnetometers of different sensitivities. However, because it is preferable to operate these instruments in field-free spaces, an array of such spaces far apart one from the other (to avoid interference) would be required. Such a proposition would be costly and not the most practical for obvious reasons, such as the time spent travelling from one instrument to the other.

Part IV describes a method by which the same instrument can be converted into a multiple sensitivities magnetometer. By using a feedback system, the sensitivity can be changed electrically to different preset values. In this way, the measuring range of the instrument can be expanded and, with the proper choice of sensitivities, the magnetometer can be operated at maximum efficiency whatever the intensity of the specimen. The performance (both sensitivity and speed of operation) can also be greatly improved. The sensitivity attainable with the present magnetometer is 10 times greater in the magnetic control mode than in the torsion control mode; at the same time the response is markedly quickened and kept below 6 seconds for all sensitivities. This rapid response permits the use of a direct-read method of determining the direction and total intensity of the magnetization of a rock specimen. Because two measuring procedures (three-component and direct-read) can be used with this instrument, both are described.

Part I — Theory of design

1. The magnet system

An astatic magnetometer consists essentially of two magnets fixed to a vertical rod which is suspended by a fibre or ribbon. The magnets of nearly equal moments are set with their directions of magnetization horizontal and antiparallel, and with one a distance L above the other. A mirror fixed to the rod permits one to measure the angular deflections of the suspended system about a vertical axis. To avoid susceptibility effects and to increase the sensitivity of the instrument, the magnetometer is usually placed in a quasi-zero field. The earth's field can be reduced by means of a magnetic-shielded room such as described by Patton (1967) or compensated for by means of a system of Helmholtz (or a similar type) coils. The choice of shielding or compensating coils does not alter the basic design but could possibly affect performance.

When a magnetized specimen is placed under the bottom magnet and oriented so that its direction of magnetization is not parallel to the axis of magnetization of the magnet, the deflection of the suspended system in a zero field is given by

$$\theta = \Delta HP / \sigma \quad \ldots . \text{(1)}$$

where ΔH is the vector subtraction of the fields produced at the bottom and upper magnets, P is the horizontal moment of a magnet and σ is the torsion constant of the fibre. The period is given by

$$T^2 = \frac{4\pi^2 I}{\sigma} = \frac{4\pi^2 (2I_1 + I_2)}{\sigma} \quad \ldots . \text{(2)}$$

where I, I_1 and I_2 are the moments of inertia of the system, of one magnet and of the system without the magnets, respectively.

From (1) and (2), we find the sensitivity is

$$\frac{\theta}{\Delta H} = \frac{T^2}{4\pi^2} \cdot \frac{P}{I} = \frac{T^2}{4\pi^2} \cdot \frac{P}{2I_1 + I_2} \quad \ldots . \text{(3)}$$

showing that the sensitivity can be increased by increasing the period and the ratio P/I.

2. Period limitations

Three considerations limit the increase of T. The first is the efficiency of the instrument. With critical damping, as is usually the case, the time taken for an observation may be taken as equal to the period. For routine measurements, because of the number of observations required (6 or 12 for each specimen), 30 seconds is normally regarded as the maximum period allowed.

The second limitation is due to the fact that a system cannot be made and remain truly astatic. The astaticism A is defined as the ratio of P/P' where P' is the residual moment of the system and can be written

$$A = P/P' = P/(P'^2_A + P'^2_S)^{1/2} \quad \ldots . \text{(4)}$$

where $P'_S = P_B - P_M$

$$P'_A = \alpha P_B = \alpha P_U$$

P_B and P_U being the dipole moments of the lower and upper magnets and α the angular departure from antiparallelism. Although an astaticism of 5,000 or even 10,000 can be obtained, it is unlikely to remain for any length of time owing to changes with time and temperature; changes which affect the whole system and particularly the magnetic properties of the magnets. For periods of months or years, it is more realistic to consider an astaticism of about 1,000. This is normally sufficient for accurate measurements on a magnetically quiet day. However, the error introduced in the readings owing to variations on disturbed days may be large and, for this reason, it is usually preferable to keep the period short. This source of error can be practically eliminated by using a negative feedback fluxgate system (Roy, 1963) which automatically detects and compensates for the diurnal variation.

The third limitation arises from the effect of changes in the dimensions and shape of any part of the apparatus, mainly of the compensating coils. These changes, which become more serious as the sensitivity is increased, may originate from different sources such as vibration and ambient temperature changes. Distortion or relative displacements of the compensating coils produce different field changes at the upper and lower magnets. Since the astaticism cannot reduce the effect of this type of disturbance, the drifts that occur might be considerable. This is exemplified in Part IV. These disturbances can be reduced by rigid construction of the coil system and good temperature control and their effect minimized with short periods.

3. Ratio P/I

This ratio which should be made as large as possible is given by

$$P/I = m\,J(\beta)\,/\,(2I_1 + I_2) \quad \ldots . \text{(5)}$$

where m is the mass of one magnet. $J(\beta)$ is the specific intensity of magnetization of a rectangular magnet of square cross section where $\beta = w/h$ = width/height.

Although the $J(\beta)$ of many materials increases asymptotically to a maximum value as β increases, it is found (Roy, 1963) that, because I_2 cannot be neglected (5), the maximum P/I is usually obtained for $\beta < 1$, that is, when the magnet is magnetized transversely or parallel to the short side. $J(\beta)$ is then ($0 < \beta < 1$) almost independent of shape (or β) and as a first approximation $J(\beta)$ can be treated as a constant. Under this condition, it can be shown that P/I is maximum for

$$I_1 = I_2/2 \quad \ldots . \text{(6)}$$

and from (5), we get

$$P/I = m\,J(\beta)/2I_2 \quad \ldots . \text{(7)}$$

I_2 should therefore be made as small as possible keeping in mind the necessity of a mirror large enough to provide a good light beam and a structure rigid enough to maintain high astaticism.

The dimensions of the magnet can be obtained from

$$I_2 = \rho\, hw^4/3 \quad \ldots . \text{(8)}$$

where ρ is the density of the magnetic material or from

$$I_2 = \pi\rho\, hd^4/16 \quad \ldots . \text{(8a)}$$

for an upright cylindrical magnet of diameter d.

From (7) and (8), one finds that P/I is inversely proportional to w^2 for rectangular magnets and to d^2 for cylindrical magnets indicating that the magnets be made high and thin. However, depending on the positioning of the specimen with respect to the magnet system, a practical limit of h usually has to be set. For example, when the specimen is placed under the bottom magnet, h should be small compared to the distance z between magnet and specimen; otherwise only part of the magnet would be reacting to a field produced by a nearby specimen. In general, h should be kept < 1 cm.

4. Magnetic materials

New manufacturing processes have made available magnetic materials well suited for astatic magnetometers; products of ceramic barium ferrite ($Ba\,Fe_{12}\,O_{19}$) such as Magnadur II, Magnadur III, Indox V and Arnox Va, and cobalt-platinum alloys such as Platinax II have very high coercive forces and their specific intensity of magnetization is almost independent of shape. The P/I curves of these materials are comparable and the performance of a magnet system built with any of these materials would be approximately the same (Deutsch *et al.*, 1967). Platinax II, however, is a very hard material that can be easily machined and is not as friable as the ceramic material. The Platinax II P/I curve is given in Figure 1 for different practical values of I_2. The I_2 of the system described next is $0.0019 \leqslant I_2 \leqslant 0.0025$ gm.cm^2. The uncertainty arises from the limits of error in calculating the moment of inertia of each component of the system. For this I_2, the maximum P/I requires 0.18 cm diameter magnets while ours are 0.2 cm. The reason for the discrepancy is that the exact value of I_2 cannot be determined in advance.

Part II – Experimental design

1. The magnet system (Figure 2)

The separation L (centre to centre) between the magnets (height = 0.8 cm) is 7.68 cm. The glass connecting rod (0.90 cm dia.) is inserted and cemented into the aluminum holder (wall thickness = 0.03

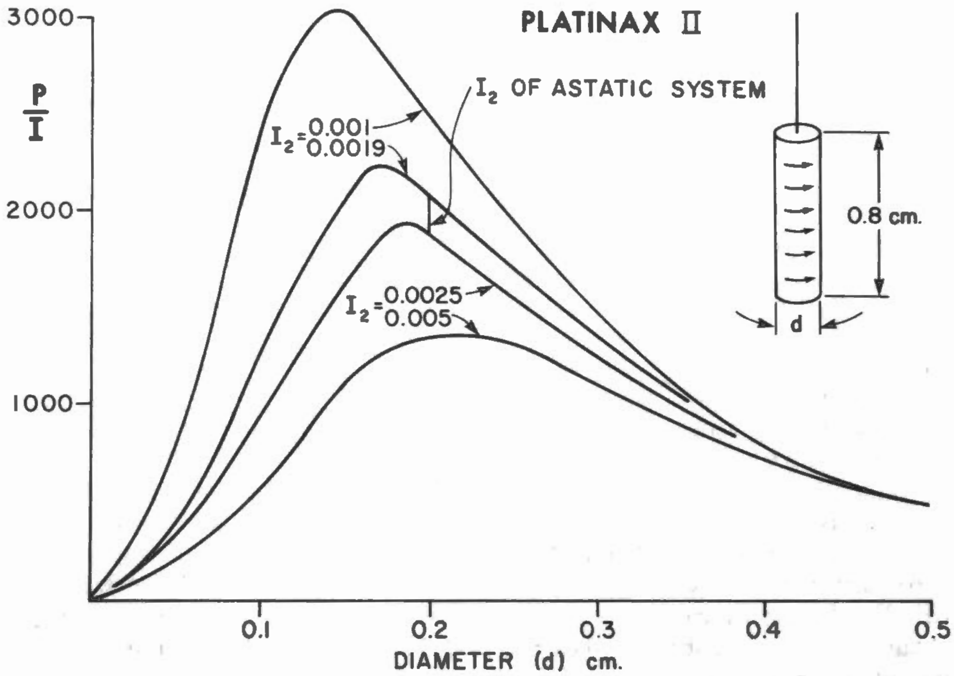

Figure 1. Values of P/I plotted against the diameter of transversely magnetized cylindrical magnets (height = 0.8 cm) for fixed I_2 and calculated from (7). ρ = 15.5. The calculated I_2 of the astatic system described in Part II is indicated.

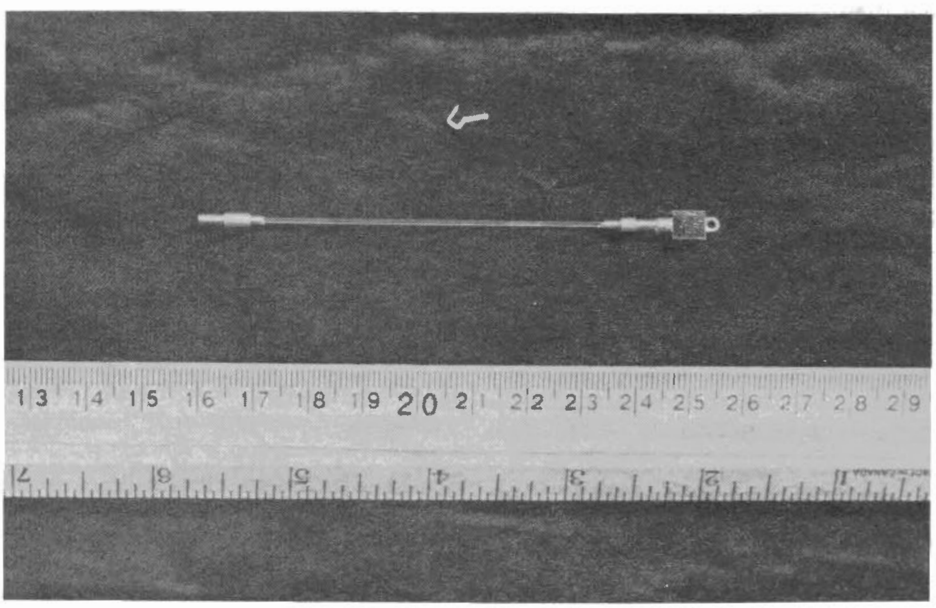

Figure 2. Astatic system of Platinax II magnets as described in Part II.

cm). The upper magnet is inserted and cemented into its holder (wall thickness = 0.025 cm). The mirror (side = 0.5 cm, thickness = 0.001 cm) is cemented into a depression of the top holder in order to maintain the dynamic balance of the system. The cross section of the bottom of the hook is of the knife edge type to avoid relative angular displacement between the magnet system and the suspension. The bottom magnet is pressure fitted into the slotted bottom holder so that with the aid of the rig described here it is possible to obtain high astaticism without the use of trimmer magnets that would add substantially to the moment of inertia. The magnets were first chosen out of a lot of 20 by comparing their magnetic moments using a commercial oerstedmeter. With repeat measurements at different distances from the probe, two magnets could be matched to better than 0.002 for an astaticism A_S ($=P/P'_S$; eq. 4) > 500. The final A_S (1000) was obtained by rubbing down the bottom magnet with an emery cloth. An azimuthal astaticism A_A ($=P/P'_A$; eq. 4) of 2200 was obtained with the following method. The bottom holder (with its magnet) is loosely clamped into an expansible hole (by means of a set screw) made at the end of a long pointer (25 cm). The pointer and the magnet system are placed onto a plate where an expansible hole receives the protruding bottom magnet which is then securely clamped. The pointer is moved in the required direction on a graduated scale drawn on the plate; in this way, the upper part of the system (carrying the upper magnet) can be accurately rotated while the bottom magnet is held in place. With such controlled rotations, a high astaticism can be obtained in a few (≈4) trials. A_A and A_S were determined by producing uniform fields parallel to (for A_A) and perpendicular to (for A_S) the direction of magnetization of the magnets. It is preferable to do both astaticisms at the same time as they become large. Unless the applied field is exactly parallel (or perpendicular) to the axis of magnetization of the upper magnet, and this usually is not the case when astatizing (because the system is taken in and out so often), the field will not be applied solely to P'_A or P'_S but to a component of each. If P'_S is much larger than P'_A, for example, part of it can easily be mistaken for a P'_A with the result that the magnet will be rotated the wrong way.

2. Magnet system housing (Figure 3)

The system is suspended by a 30-cm long phosphor bronze strip attached to a threaded rod passing through a circular plate which closes the upper end of an aluminum tube (length 23.5 cm; diameter 2.5 cm). The threaded rod and circular plate permit height adjustment of the magnet system. The tube is fixed to a 3-point aluminum plate resting on a wooden tripod. Levelling screws permit plumb adjustment of the tube. Under the plate, a rectangular box (height 18.7 cm; sides 7.6 and 3.2 cm) is attached. The short sides are made of aluminum and hold a nylon bottom plate. On the centre of this plate, a threaded holder carrying an aluminum disc (diameter 2.5 cm; thickness 0.15 cm) can be height adjusted for critical damping. The long sides are closed by detachable Perspex windows. The width of the box facilitates the installation and removal of the magnet system from the suspension hook. Two sides and the bottom are of nonmetallic materials to avoid eddy currents. Lenses of different focal lengths can be easily installed on the window facing west. The mirror has been set facing west so that the light beam is not in the direction of the operator.

3. Field compensation

The magnetometer is installed in the centre of a set of three orthogonal pairs of square (side = 244 cm) coils, which is part of an array of five identical sets (Roy *et al.*, 1969). The set (Figure 3) is located at the south end of a 3 x 12 meters building oriented along the magnetic meridian. Each component (vertical Z, horizontal along H_H and perpendicular to H_D the meridian) of the earth's field are compensated for by two circuits. Constant fields produced by constant currents compensate the mean field and a negative feedback fluxgate system compensates the diurnal variations. An additional winding on the coils is used to produce nearly uniform fields when astatizing the magnet system.

The system is oriented with the north pole of the bottom magnet pointing north. The effective compensation of the diurnal variations are 0.998 ± 0.0002 for H_H and 1.000 ± 0.0002 for H_D. Since the astaticisms are A_A = 2200 and A_S = 1000, the ratio of apparent uniform disturbing field is 10^{-6} for north-south and 2 x 10^{-7} for east-west disturbances.

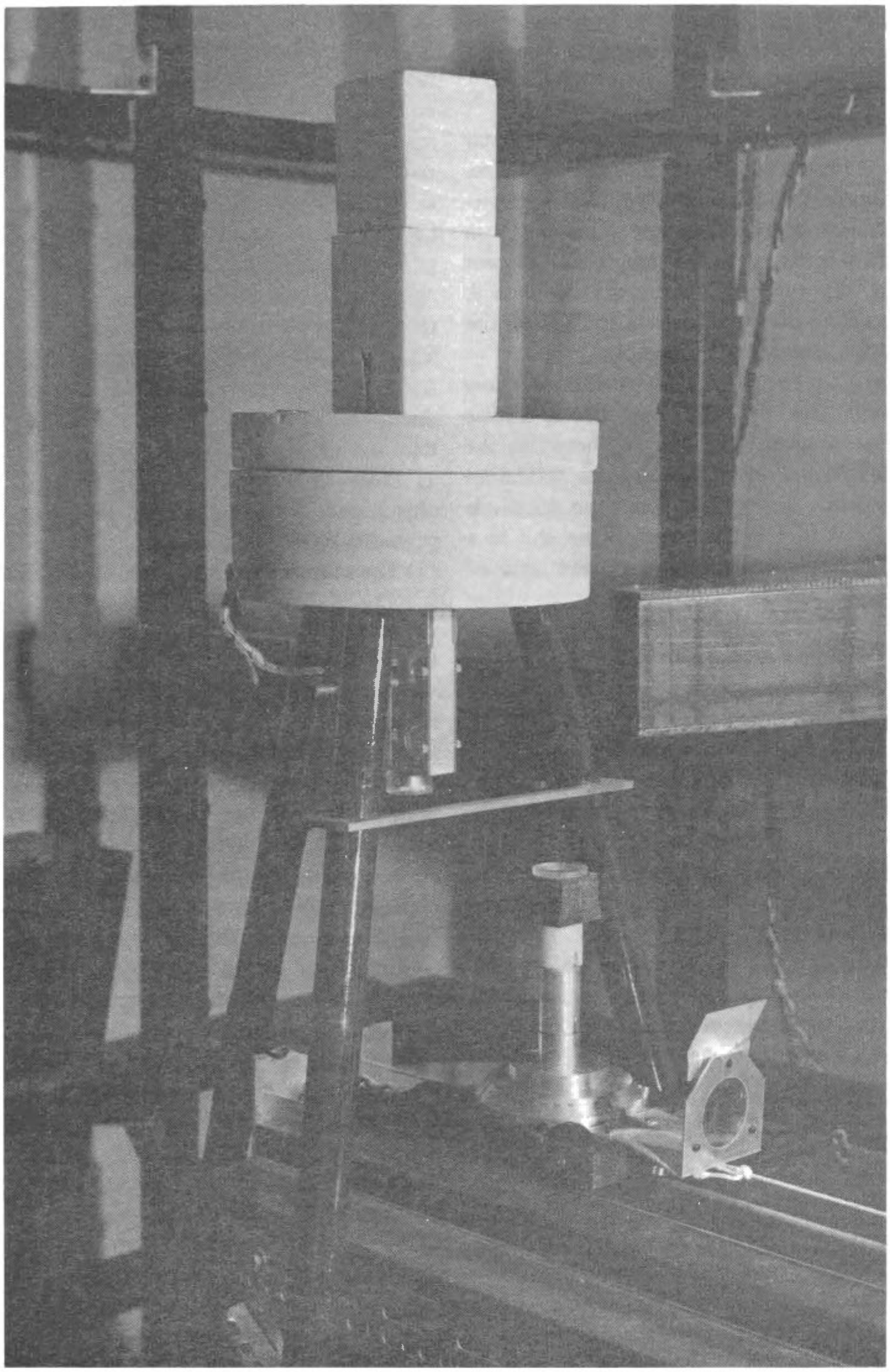

Figure 3. Astatic magnetometer with styrofoam head and specimen presentation table. Descriptions are given in Part II.

This means that for a change of say 100 γ in the north-south component, the deflection of the magnet system would correspond to a field of 10^{-9} Oe applied to the bottom magnet. At the location, the diurnal variations on a normal day are in the 60-70 γ range and on a disturbed day, they average about 200 γ. The instrument drift due to diurnal variations is therefore negligible.

4. Response of an astatic magnetometer

The amplitude of the angular deflection of the magnet system to the magnetization of a rock sample depends (1) on the positioning of the sample with respect to the system, (2) on the distance L between the two magnets and (3) on the shape and size of the sample.

(1) The sample can be positioned many ways (see Collinson and Creer, 1960). For a given distance (z) between the sample and one of the magnets, maximum response is obtained when the sample is placed in the horizontal plane and in a direction perpendicular to the axis of magnetization of the magnet (position A). Another position (B) is the placing of the sample on the axis of rotation of the system and below the lower magnet. The response of the instrument is about twice as large for position A as for position B. However, for practical considerations, position B is usually favoured. Technically, with a more sophisticated magnet system housing design, it is possible to make z as small for position A as for position B. However, because the presentation of the sample must be done by remote control (to avoid magnetic and other disturbances caused by the operator) safety devices to protect against accidentally hitting the instrument must be added. For position B, such devices (aluminum clamp on Figure 3) can be installed without increasing z since the sample and holder slide under the instrument. For position A, the sample has to be pushed toward or alongside the instrument. Since it is useful to be able to vary the distance (for measuring different intensities) the latter case should have a transverse motion. Therefore, in both cases, the sample has to be pushed toward the instrument and a protective screen must be installed, and z increased. Because the field reduces as the third power of the distance, a small increase of z will considerably reduce the instrument response. So, in practice, it is found that there is little to choose between the two positions. Position B was chosen because only one component (horizontal) of magnetization is measured in a single reading. In position A, the vertical component produced a field at the upper magnet; the deflection produced by this component is nulled by inverting the sample and averaging.

(2) The sensitivity of the instrument depends on L since the field produced at the oppositely magnetized upper magnet reduces the deflection. L should then be made large. On the other hand, the larger L is, the larger are the deflections produced by magnetic disturbances other than diurnal variations; disturbances such as those caused by a nearby magnetic object and distortion of the field compensating coils.

(3) The standard size specimen used in our laboratory is an upright cylinder of 2.5 cm diameter and 2.2 cm height for a ratio height/diameter = $\pi^{1/2}/2$. A larger ratio would increase the response of the magnetometer (Roy, 1967). However, since the specimen is of finite size and not a dipole point, corrections as calculated by Papapetrou (see Blackett, 1953) must be applied. When the specimen is cut according to the above ratio, the corrections are quite small (2% for $z = 3.6$ cm) and the same whether the specimen is upright or on its side (Roy, 1966); thereby, the errors due to shape are small and the computation of results simplified.

A larger deflection would be obtained by using a larger specimen even if, for small z, the increase in deflection is not equal to the increase in volume. To make room for the larger specimen, z must be increased by $\Delta z = (V_x^{1/3} - V_s^{1/3})/2$ where V_s and V_x are the volumes of the standard and larger specimens respectively. The increase of the ratio deflection/volume varies with the increase in volume; for a typical z = 3 to 4 cms, the ratio increase would amount to 0.6 – 0.8 of a two- to four-fold increase in volume or about a 3-times larger deflection for a 4-times larger volume. There are many hindrances to using too large a specimen; for example, as the size is increased, the effects of inhomogeneity increase, larger coring equipment is required, etc. The main consideration is that, in rock magnetism, a specimen is often fitted into different apparatuses. Because other pieces of equipment such as alternating field demagnetizer favour small specimens, a medium-size specimen must be adopted as a standard.

5. Calibration

The system is calibrated by means of a coil suspended from the ceiling. The distances from the centre of the coil to the centres of the magnets are 122.27 and 129.95 cm. The 91 turns are tapped on the fifth turn to provide two field-producing sources for calibration of high (5 turns) and low (91 turns) sensitivities. The difference of field ΔH at the magnets is 1.010×10^{-8} Oe/ma for the 5 turns (diameter = 16.76 cm) and 0.6794×10^{-7} Oe/ma for the 91 turns (diameter = 15.98 cm).

6. Specimen table (Figure 3 and 4)

The specimen is placed in a graduated (10° spacing) Perspex cylinder which has been bored so that the specimen fits snugly. The cylinder fits into a rectangular piece of laminated wood veneer (permali). The dimensions of the cylinder and the wood holder are such that the distance between the centre of the specimen and all faces of the holder is constant so that z remains constant for all attitudes of the specimen. Holes in the bottom and two sides of the holder fit onto a pin in the centre of a small table for accurate centring of the specimen. Ridges on each side of the table maintain the orientation of the holder. The table is attached to a female tapered post which fits onto a male tapered post in the centre of a disc (diameter = 14 cm) whose perimeter is graduated in degrees. The assembly is installed on a three-wheeled carriage which is rolled under the magnetometer by means of string and pulleys. When the assembly is against its stop, gear coupling (ratio 4 to 1; 1 turn = 90°) permits rotating the assembly from a distance of two meters. The orientation

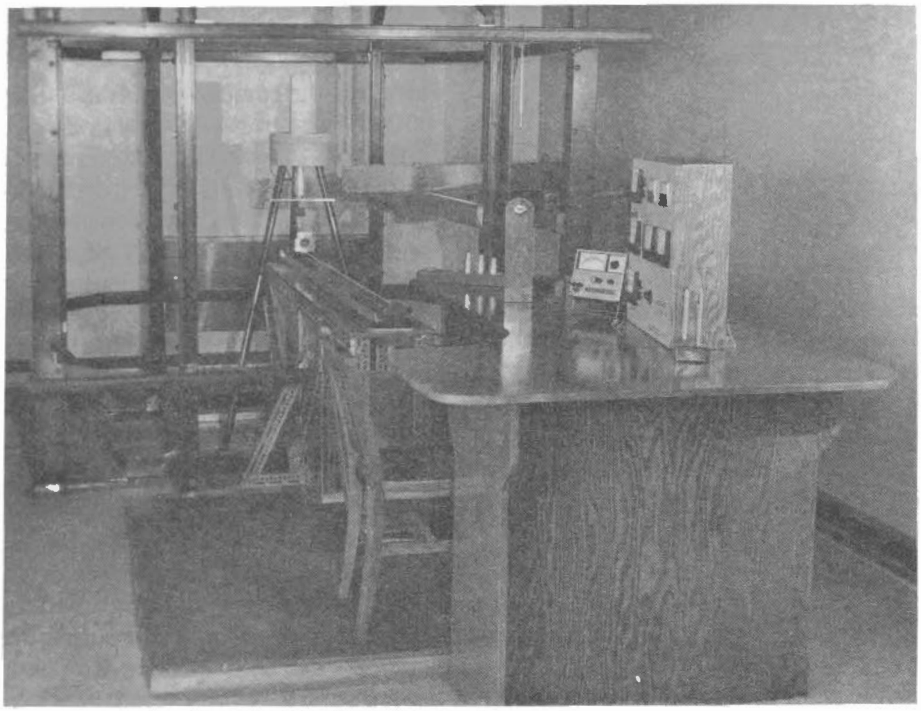

Figure 4. General view of astatic magnetometer and accessories.

of the specimen given by the graduated circle is read through a lens.

Centring and levelling of the holder table was accomplished by means of a small coil producing vertical fields. The carriage table is moved and tilted on the stationary table until the magnet system remains undeflected when a large field is applied in different azimuthal directions. A levelling to within 0.5° and a centring to within 0.3 mm could be obtained. Five different z's are provided by inserting tapered spacers (shown on the desk) under the holder table. The alignment of all parts is maintained by a slot and a pin at the bottom and top of the spacers. The distance z between each position and the bottom magnet is measured by means of magnetic fields; this is more accurate than direct readings of the distance. For each position a small two-turns coil (diameter = .503 cm) is placed with its axis perpendicular to the axis of magnetization of the magnet. A field is produced by passing a calibrated current through the coil. The difference of field ΔH at the bottom and upper magnets (for large A) is given by

$$\Delta H = \pi N i C_c r^2 \, 10^{-4} \times \left[\frac{C_B}{(r^2+z^2)^{3/2}} - \frac{C_U}{\{r^2(z+L)^2\}^{3/2}} \right] \quad \ldots . \; (9)$$

where i is the current in milliampere, N is the number of turns and r the radius of the coil. C_c, C_B and C_U are the corrections for the shape of the coil, bottom and upper magnets respectively. These corrections are to compensate for the differences between the physical and effective centres of coil and magnets; differences that are not negligible when z is comparable to the dimensions of these components.

The angular deflection θ of the system produced by ΔH is measured by the deflection (defl.) of the light spot reflected from the mirror. Using a scale at a distance D',

$$\Delta H = \frac{H_s \times \text{defl. (mm)}}{2D'\theta} = S \times \text{defl. (mm)} \quad . . (10)$$

where S is the sensitivity expressed in Oe/mm defl. and is defined as the difference of field H_s required to deflect the light spot by 1 mm at a distance D'. From (9) and (10) we find that

$$\frac{C_c\, i}{\text{defl. (mm)}} \times \left[\frac{C_B}{[r^2+z^2]^{3/2}} - \frac{C_U}{\{r^2+(z+L)^2\}^{3/2}} \right] = C \quad \ldots . (11)$$

where

$$C = \frac{10^4 S}{\pi N r^2} \quad \ldots . (12)$$

Taking measurements at the different positions different i, z must be determined so that C in (11) is a constant. It is found that with precise measurements of i and defl. (the two large variables), z can be determined to within 0.3 mm. The method also provides an excellent check on the sensitivity (12) obtained from the calibration coil. The agreement between the two methods of calibrating is within 1 per cent.

The ratio of P/I can be checked experimentally. From (3) and (10), we get

$$P/I = 2\pi^2/D'ST^2 \quad \ldots . (13)$$

The P/I obtained by measuring T is 1975 and in agreement with the theoretical value (Figure 1).

Part III – Torsion method

1. Performance

The system was first tested by placing a graduated scale at $D' = 1.7$ meters. Using suspensions of different torsional constants, the following sensitivities and periods were determined

$S = 13.5 \times 10^{-8}$ Oe/mm defl. $T = 6.6$ sec.
$S = 3.37 \times 10^{-8}$ Oe/mm defl. $T = 13.2$ sec.
$S = 1.94 \times 10^{-8}$ Oe/mm defl. $T = 17.4$ sec.

On a scale at $D' = 5$ meters, the deflection would be about three times larger. The system could then be used as a moderately high sensitivity magnetometer (4.6 x 10^{-8} Oe/mm defl.) with a low period (6.6 sec) or as a high sensitivity (6.6 x 10^{-9} Oe/mm defl.) with a period of 17.4 sec.

2. Measurements

The magnetic moment of a specimen is often determined by measuring its three orthogonal components; p_x p_y and p_z. Since this measuring method can be used with the torsion and the magnetic control methods, a brief account of the procedure is given.

The specimen is placed upright with its orientation mark on 0° azimuth of the table to obtain p_x; p_y is obtained by rotating the table by 90°; p_z is obtained by placing the specimen on its side and with its axis perpendicular to the axis of magnetization of the bottom magnet. The components of magnetization are obtained (A being large) from

$$p_x = B_x S \left[\frac{E_{Bx}C_B}{z^3} - \frac{E_{Ux}C_U}{(z+L)^3}\right]^{-1} \quad \ldots . (14)$$

$$p_y = B_y S \left[\frac{E_{Bx}C_B}{z^3} - \frac{E_{Ux}C_U}{(z+L)^3}\right]^{-1} \quad \ldots . (15)$$

$$p_z = B_z S \left[\frac{E_{Bz}C_B}{z^3} - \frac{E_{Uz}C_U}{(z+L)^3}\right]^{-1} \quad \ldots . (16)$$

where E is a specimen shape correction which depends on the distances (z and $z+L$) to the bottom (E_B) and upper (E_U) magnets and on the presentation of the specimen: upright (E_x) or on its side (E_z). B_x, B_y and B_z are the scale deflections. For large L, E_U and C_U can be neglected and we have

$$p_x = B_x S z^3 \left[E_{Bx}C_B - \left(\frac{z}{z+L}\right)^3\right]^{-1} \quad \ldots (17)$$

$$p_z = B_y S z^3 \left[E_{Bx}C_B - \left(\frac{z}{z+L}\right)^3\right]^{-1} \quad \ldots (18)$$

$$p_z = B_z S z^3 \left[E_{Bz}C_B - \left(\frac{z}{z+L}\right)^3\right]^{-1} \quad \ldots (19)$$

Since z is constant, it is more convenient to determine the corrections in terms of the different positions used so that

$$p_x = B_x S\, C_x \quad \ldots . (20)$$

$$p_y = B_y S\, C_x \quad \ldots . (21)$$

$$p_z = B_z S\, C_z \quad \ldots . (22)$$

where all the corrections are included in C_x and C_z which can be readily obtained from tables. In a rock collection, most specimens are long enough to be cut to standard length (2.2 cm); z and the volume are then constant and $C_x = C_z$. The intensities (Int.) of each component are then given by

$$\text{Int.}_x = B_x E \quad \ldots . (23)$$

$$\text{Int.}_y = B_y E \quad \ldots . (24)$$

$$\text{Int.}_z = B_z E \quad \ldots . (25)$$

where E is the constant correcting factor multiplied by the sensitivity and divided by the volume. The directions (D and I) and the total intensity of magnetization are determined from these components. The effects of inhomogeneity of magnetization are reduced by averaging readings 180° apart and also by averaging readings of upright and inverted positions of the specimen. In the side position (Int.$_z$), the holder is rotated 180° about its axis.

Part IV – Magnetic control method

The performance and efficiency of a torsion-controlled astatic system can be improved by using magnetic fields to control and measure the deflection. This is illustrated by using as an example the previously described system, two photo resistors and an electrical circuit which provides an automatic negative feedback. The circuit (Figure 5) has been designed to suit specific conditions that will be discussed. However, it can be easily modified for different conditions and requirements, and great freedom is left to the designer.

By comparing the two methods, the magnetic control is preferred. For example, it permits, while maintaining short periods, sensitivities not possible with the torsion method since the period would then be too long to meet the requirements. As opposed to the torsion method where the sensitivity and period are set by the suspension fibre, the magnetic control method allows quick switching among several different sensitivities and associated periods. This increases the working range and efficiency of the magnetometer since the more strongly magnetized specimens can be measured at much lower period and therefore in less time. Because of the quick response, the system can be used as a null detector and the direction of magnetization can be determined directly. The direct-read method in turn allows taking full advantage of the flexibility of the instrument, thereby increasing the accuracy of results achieved with the three-component method. Problems arising as the sensitivity is increased and precautions to be taken will be discussed.

1. Principle of operation

When the horizontal field is equal at the upper and lower magnets ($\Delta H = O$), the light spot (diameter 2.1 cm) illuminates equally two photo resistors (diameter 2.5 cm) placed side by side at a distance of 90 cm from the magnet system. The current through each photo resistor is 6 ma, the lower branch of the circuit (Figure 5) is in balance, and no current flows in the upper branch. When a magnetized specimen is brought under the magnet system ($\Delta H \neq O$), the spot is deflected, the resistance of one photo resistor decreases, the resistance of the other increases, and a current flows through the upper part of the circuit and one of the seven solenoids, depending on the switch position. The solenoid is located near the upper magnet and in the same horizontal plane (Figures 3 and 4) with its axis perpendicular to the axis of magnetization of the magnet. It is wired so that the torque it produces on the upper magnet tends to reduce the deflection. If, in a particular switch position, the circuit gives a current through the solenoid of K_1 ma/radian deflection, and the solenoid produces a field of K_2 Oe/ma at the upper magnet, the feedback torque for a small deflection θ is $PK_1K_2\theta$. When the system has come to rest

$$P\Delta H = PK_1K_2\theta + \sigma\theta \qquad \ldots.(26)$$

writing

$$PK_1K_2/\sigma = G \qquad \ldots.(27)$$

where G is the (magnetic/torsion) control ratio

$$\Delta H = K_1K_2\left(1 + \frac{1}{G}\right)\theta \qquad \ldots.(28)$$

The deflection θ is determined by taking the reading n in millivolts as measured across a precision resistor R inserted in the feedback circuit and is given by

$$n\,(\text{mv}) = K_1R\theta \qquad \ldots.(29)$$

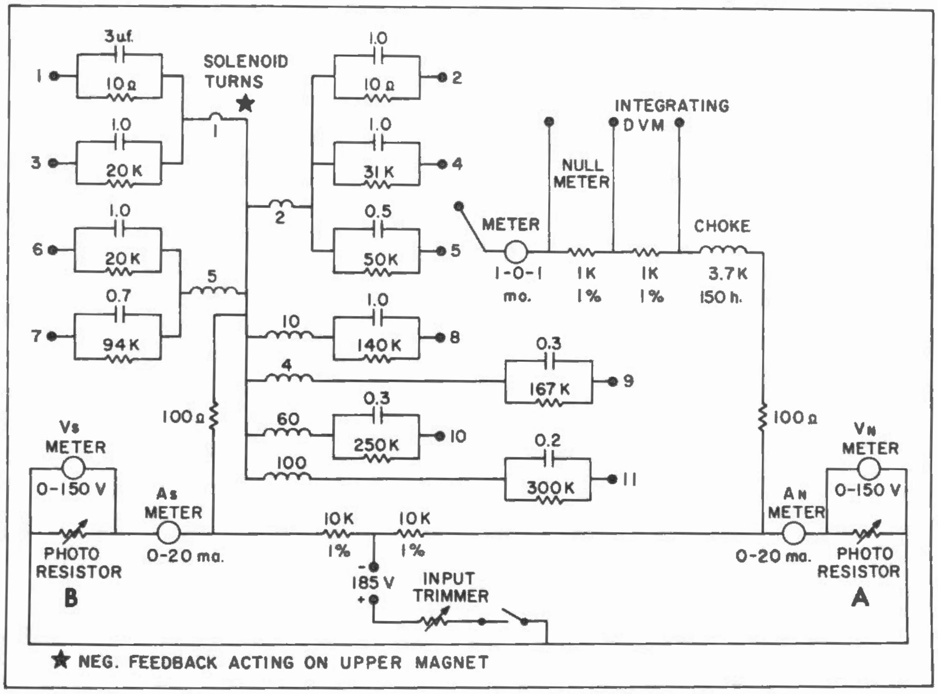

Figure 5. Circuit used to provide negative feedback from signal picked up by the photo resistors.

and from (28)

$$n\,(\text{mv}) = \frac{R\Delta H}{K_2\left(1 + \frac{1}{G}\right)} \qquad \ldots.(30)$$

The sensitivity S in oersted per millivolt is then given by

$$S\,(\text{Oe/mv}) = \frac{\Delta H}{n} = \frac{K_2\left(1 + \frac{1}{G}\right)}{R} \qquad \ldots.(31)$$

The factor K_2 can be calculated from the geometry:

$$K_2 = \frac{\pi N\, 10^{-4}}{l} \times \left[\frac{x + l}{\{(x + l)^2 + r^2\}^{1/2}} - \frac{x - l}{\{(x - l)^2 + r^2\}^{1/2}}\right] \qquad \ldots.(32)$$

where l is the half-length of the solenoid, r its radius, x its distance from the magnet, and N the number of turns.

The control ratio G can be determined by comparing the deflection produced by a given ΔH with and without feedback. However, it is difficult to obtain an accurate estimate in this way, and it is preferable to measure the sensitivity first by means of the calibration coil (III, 5), and then derive G from (31):

$$G = \left[\frac{R\,S}{K_2} - 1\right]^{-1} \qquad \ldots.(33)$$

The sensitivity can be accurately determined by measuring in mv the deflection caused when a ΔH is applied. The application of progressively higher ΔH permits one to determine the operating range of the photo resistors and the accuracy of the readings (i.e. the near linearity of the curve $\Delta H/n$) within that range.

The period of the undamped system is

$$T_c = 2\pi\left[\frac{I}{\sigma + K_1K_2P}\right]^{1/2} = 2\pi\left[\frac{I}{\sigma(G + 1)}\right]^{1/2} \qquad \ldots.(34)$$

by analogy to (2). Both the aluminum damping disc (II, 2) and the capacitors shown in Figure 5 are used for damping the system. The damping disc is adjusted for critical damping at a period T_c of 5 sec. The additional damping provided by the capacitors reduces both the time required to take a reading and the oscillations of the magnet system caused by vibrations of the ground. The frequency of these oscillations varies (about a 4 cycles/sec frequency) depending on the disturbing conditions. Without electrical damping, oscillations would occasionally build up (especially when operating the instrument at lower sensitivities where the magnetic control is large and T_c short $\cong$ 2 to 3 sec) until the light spot was driven out of the range of the photo resistors. The values of the capacitors were determined empirically, and a variety of time constants provided to meet different conditions.

2. Characteristics of the system

The light source is a Pye (W.G. Pye Co. Ltd.) lamp outfit (#8122). The light bulb (4V-1A) and the optical system is placed at 1.1 m from the magnetometer. The transformer (117/4V) is magnetic and placed 10 meters away. A lens (1 m focal length) is placed at 1.6 cm from the mirror. The light beam is received on two cadmium sulphide photo resistors (NSL 4972; Dwg 5472; National Semiconductors Ltd.) mounted on a brass carriage (at $D' = 90$ cm) that can be remotely displaced (± 3 cm) in a horizontal direction perpendicular to the direction of the light beam. The photo resistors are housed in a tapered rectangular box which projects to within 25 cm of the magnet system; the inside of the box has been painted black and the instrument can be operated in a lighted room. The photo resistors (shown on the table; Figure 6) were specially manufactured without a metal case and the magnetization of the pins produces a negligible field at the magnet system. Their rated characteristics are max power = 1 watt, max voltage = 420V, resistance at 100 foot-candles = 140 ohms and in darkness = 2.3 meg ohms. In the system described, when the light spot is directed on one photo resistor, the resistance is 2.1 K on the lighted photo resistor and

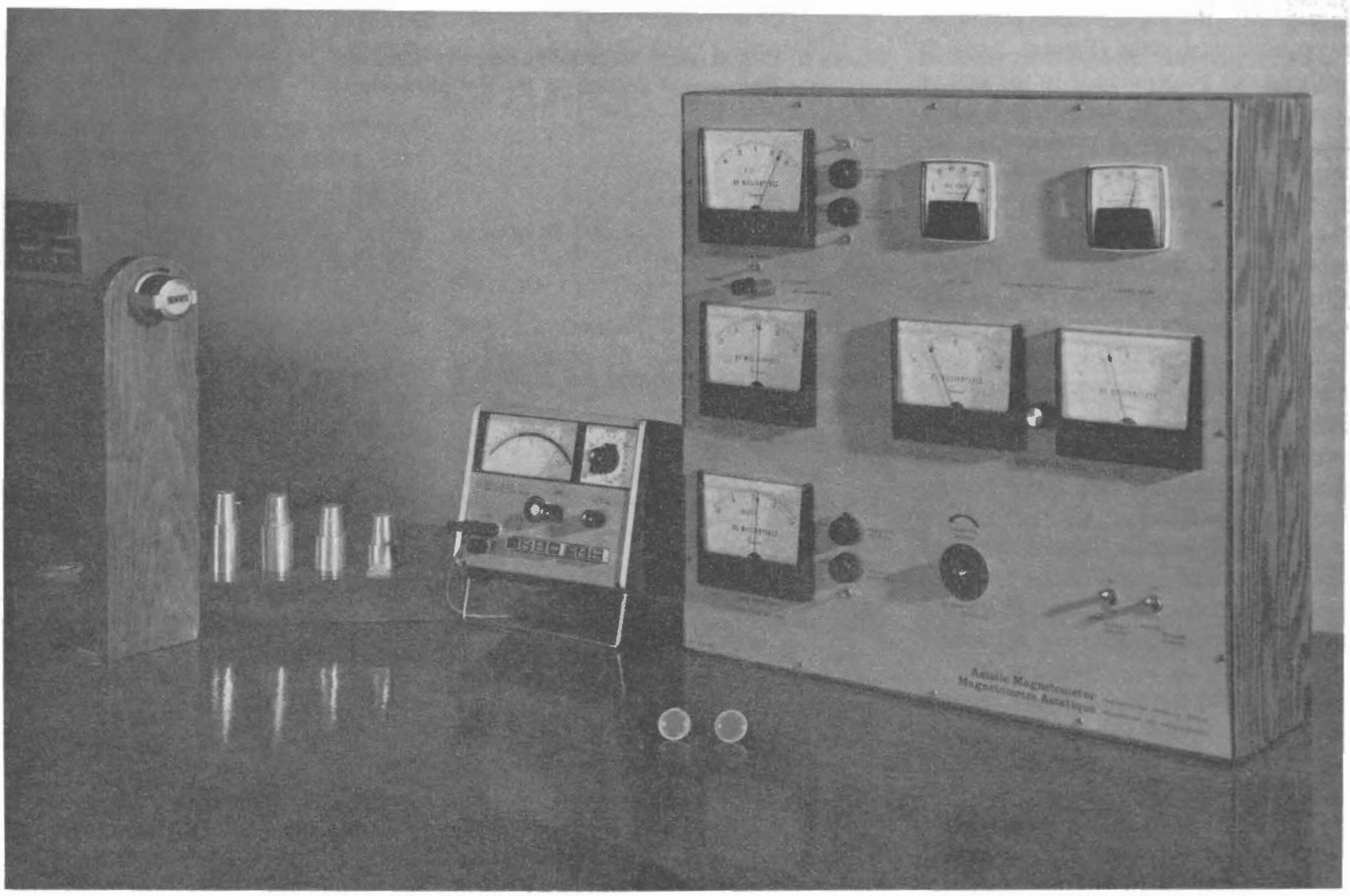

Figure 6. Control panel as described in Part IV. The deflection shown has been obtained by passing a current through the calibration coil. The dial indicating the alignment of the magnet system is shown on the left. The aluminum spacers used to obtain different distances are also shown. On the table are photo resistors of the type used.

200 *K* on the other giving a max/min ratio of about 100. Among several types of photo resistors tested, this type gave the highest ratio. Since the deflection ratio mv/mm increases with this ratio, the photo resistors should be chosen accordingly. When the spot is equally split onto the two photo resistors, the resistance of each is about 17 *K*.

A 185-volts power source is trimmed so that on zero deflection of the magnetic system a current of 6 ma (base current) flows through the photo resistors. Owing to long term changes in the circuit and light intensity changes due to voltage variations and dirt on the lenses, the input voltage might have to be changed slightly to obtain the right base current. This is done by trimming down a constant voltage source set slightly higher than required, and which is placed at the other end of the room because of its magnetic properties. The voltage across and the power through the photo resistors are about 100 volts and 0.6 watt. With a rated power of 1 watt, the current (and sensitivity) could be increased by 25 per cent if necessary. However, as a precaution and for longer life of the photo resistors, all calibrations have been performed on the 6 ma base current and therefore hereafter parameters such as *D*, *G* and working range, which depend on the base current, are given on this basis.

The negative feedback can be switched to one of the seven solenoids (radius = 0.4 cm). Their number of turns with the mean distance (given in cm in brackets) from the upper magnet are in descending order of sensitivity 1(7.6), 2(7.6), 5(7.5), 10(7.2), 4(3.7), 60(6.1) and 100(4.6). The deflections are measured in mv across a 1-*K* resistor by means of a DC null voltmeter (Hewlett Packard; 419A) and/or an integrating digital voltmeter (H.P. 2401-C).

Different spacings between the photo resistors were tried. As the spacing is increased (from 0.2 to 1 cm from side to side) the sensitivity increases slightly (5-10%) and the overall working range remains about the same; the portion of the range, where $\Delta H/n$ is almost linear, decreases. In practice, the feedback current increases with the angular deflection until the spot is fully (or centred) on one of the photo resistors. However, for the feedback current to be practically linear with respect to the deflection, i.e. ratio (current/deflection) constant, the spot must be on *both* photo resistors. Once the spot has left one photo resistor but keeps moving onto the other the ratio (current/deflection) becomes smaller and smaller (from 100% to 90%) resulting in a decrease in sensitivity. Therefore, in order to minimize the sensitivity variations within a given range, the photo resistors have been placed as close as possible to each other, that is 0.2 cm for these caseless photo resistors.

3. Sensitivities

Without magnetic control, and with a suspension giving $\sigma = 5.5 \times 10^{-3}$ dyne cm/radian, the period of the system is 6.6 sec and the sensitivity is 2.55×10^{-7} Oe/mm at $D' - 90$ cm. Table I gives the eleven sensitivities (S 1 to S 11) available with the magnetic control. They were measured with the aid of the calibration coil over a range of ΔH values (IV, 1), and the table shows the range of output readings for each switch position within which the sensitivity is constant to 3 per cent and 1 per cent respectively.

Table I also gives the factor *G*, calculated from (33), the ratio

$$f_c = 1/(1 + \frac{1}{G}) \quad \text{. . . . (35)}$$

which is the fraction of ΔH measured by magnetic control, and the period of the system T_c, calculated from (34).

S 1, S 2, S 6, S 8, S 9, S 10 and S 11 are regarded as the primary sensitivities, and are generally used, because of their larger *G* and f_c values, and smaller T_c. The instrument can measure (on S 11) fields as large as 3×10^{-5} Oe and it can detect (on S 1) fields as low as the disturbing conditions at the location permit. The disturbances affecting the instrument are discussed in (IV, 6); under the best conditions at the site, magnetizations producing fields as small as 2×10^{-9} Oe at the lower magnet can be detected. One advantage of the photoelectric system can be seen from the following comparison. To obtain a sensitivity of 0.56×10^{-9} Oe/mm deflection on a scale at a distance D' of 5 meters, the system without feedback would have a period of 60 seconds, which would be impractical because of disturbance problems.

The control panel is shown in Figure 6. The meters on the right-hand side indicate at all times the voltages across and the currents through the photo resistors. On zero deflection a large change in voltage from 100 volts would be indicative of a lighting or photo resistor problem. The input current trimmer is located between the two milliammeters and is the only adjustment required for

Table I. Particulars of the system for each of the 11 circuits shown in Figure 5.

	Sensitivity $\times 10^{-9}$ Oe/mv	G	f_c	T_c (sec)	RANGE LIMIT (mv.) 3 per cent accuracy	3 per cent accuracy
S 1	0.56	0.64	0.40	5.1	3000	2500
S 2	0.68	1.50	0.60	4.2	2400	2000
S 3	0.88	0.35	0.26	5.7	1500	1200
S 4	1.17	0.58	0.36	5.2	1200	900
S 5	1.48	0.42	0.30	5.5	1000	700
S 6	1.77	2.00	0.67	3.9	1500	1250
S 7	3.15	0.58	0.37	5.2	550	450
S 8	5.30	1.03	0.51	4.6	450	350
S 9	13.30	2.78	0.69	3.4	400	325
S 10	29.40	9.10	0.90	2.1	300	275
S 11	120.00	28.50	0.97	1.2	275	250

G is the control ratio (magnetic/torsion) given by (33).

f_c is the fraction of ΔH measured (35).

Without magnetic control, the period of the magnetometer is 6.6 seconds.

intensity measurements (no adjustments are required for direction determinations). The milliammeter in the upper left-hand corner is used for calibration. In this photograph, a current is applied to the calibration coil to deflect the system off zero. A digital ammeter of high resolution can be used by switching to the terminals below the meter. The high or low sensitivity calibration coil can be selected by a switch. The milliammeter (centre left) indicates the deflection of the magnet system during measurement and is useful because its response is quicker (no damping) than that of the nullmeter shown on the left of the panel. For direction finding, the milliammeter is used to find an approximate zero and fine zeroing is accomplished using the nullmeter which has a large scale and is easier to read. The other meter (bottom left) is an indicator for the zeroing procedure (when $\Delta H = 0$) that will be explained later.

4. Design variations

Under this heading, we consider the possibility of extending the measuring range of a magnetically controlled astatic magnetometer beyond the limits imposed by the present requirements and the disturbing conditions (described in IV, 6) existing at this particular site.

The upper limit has been set so that, with the present specimen table and specimen size, most weakly magnetized (intensity $\leqslant 4 \times 10^{-3}$ e.m.u.) rock specimens can be measured; the direction and intensity of specimens of larger intensity are quickly measured by means of a fluxgate magnetometer especially adapted for this purpose. Thus, in this instance, the largest field (3×10^{-5} Oe) the instrument can measure is adequate; however, for other applications or with a different setting, it might be desirable to design an instrument which could measure higher fields. The upper limit can easily be raised and it is not necessary to open the housing (III, 2) of the magnetometer.

When the instrument is operated at lower sensitivities, G is large (Table I), and (31) shows that S is then almost independent of G and proportional to K_2. Therefore, the sensitivity can be reduced (more Oe per mv) by simply adding turns to the solenoid or reducing the distance between the solenoid and the upper magnet. From (27), (31) and (34), it is found that the reduction of T_c^2 is then almost proportional to the reduction of S. Thus, without changing the suspension, the measuring range can be extended upwards so that the instrument can also be used as a low sensitivity and short period magnetometer.

Under the present disturbing conditions discussed in IV, 6, the measuring range of this particular instrument cannot be extended downwards. Higher sensitivities would not increase the performance unless the disturbances or their source (mainly temperature changes) can be better controlled or damped. However, under the assumption that this can be done and as a matter of interest to people designing a magnetometer for operation under more favourable conditions, the extension of the measuring range downwards is now considered.

Equations (27) and (31) show that higher sensitivities (less oersted per mv) can be obtained by reducing either K_2 or σ. However, because, at high sensitivity, G is usually small, the change of S obtained by changing K_2 *or* σ is not readily visualized from the equations and may be illustrated by an example. Using S 1 of Table I as a base for comparison, the calculated sensitivities (S_x) and periods (T_x) obtained by changing K_2 and σ to arbitrary K_x and σ_x are given in Table II. In the calculations, f_c has been kept equal or larger than 0.20 so that a reasonable fraction of ΔH is measured. The table shows that a small improvement in sensitivity can be optionally obtained by reducing K_2 or σ; changes of suspension can therefore be avoided by using a different solenoid to change the sensitivity. Table II also shows that to obtain a large increase of S_x, both K_2 and σ must then be reduced. In Nos. 6, 7 and 8 where G_x is kept constant, the increase of both S_x and T_x is proportional to the reduction of K_x.

The sensitivity could also be increased by increasing K_1. An increase of K_1 would increase the control ratio K_1 (27) which in turn would increase S (31). K_1 could be increased in a number of ways, e.g. light beam of stronger intensity and photo resistors with a higher power rating. The use of a stronger magnet cannot increase the sensitivity and, as in the torsion method, the magnet system must be designed according to the theory given in Part I. From (27), (31) and (34), we find

$$S = \frac{1}{RK_1}\left(\frac{2\pi}{T_c}\right)^2 \cdot \frac{I}{P} \qquad \ldots.(36)$$

showing that the sensitivity increases as P/I increases.

5. Measuring method (direct read)

Because of the quick response, the instrument is used to read directly the

Table II. Calculated periods (T_x) and sensitivities (S_x) obtained by changing G, K_2, σ and f_c of S 1 (Table I) to arbitrary G_x, K_x, σ_x and f_x. See Part IV – 4. Design variations.

NO	G_x/G	K_x/K_2	σ_x/σ	G_x	f_x	T_x sec	S_x X 10^{-9} Oe/mv.
S 1	1.	1.	1.	0.64	0.39	5.1	0.56
1	3.00	3.00	1.00	1.92	0.65	3.8	1.02
2	3.00	1.00	0.33	1.92	0.65	6.6	0.34
3	2.00	1.00	0.50	1.28	0.56	6.1	0.40
4	0.39	0.39	1.00	0.25	0.20	5.8	0.43
5	0.39	1.00	2.56	0.25	0.20	3.6	1.09
6	1.00	0.67	0.67	0.64	0.39	6.3	0.37
7	1.00	0.50	0.50	0.64	0.39	7.3	0.28
8	1.00	0.33	0.33	0.64	0.39	8.8	0.19

direction of magnetization. The specimen is placed in the holder so that its orientation mark is towards the 0° azimuth on the graduated circle and the assembly is rolled under the instrument (as in Figure 4). It is then rotated until a zero deflection is obtained on the nullmeter. This occurs when the mean direction of the horizontal component of magnetization is parallel to the axis of magnetization of the bottom magnet. The angle D_1 between this direction and the mark is read directly on the graduated circle. The assembly is then rotated until a second zero giving D_2 is encountered at approximately (D_1 + 180°). Averaging of the two readings reduces the effect of inhomogeneity. With weakly magnetized specimens, the first reading is usually repeated (and used for averaging) for eventual drift. The sense of the direction is obtained from the positive or negative reading on 0° azimuth. The same procedure is followed with the specimen in an inverted position. The declination D is obtained by averaging the four readings. The graduated Perspex cylinder containing the specimen is rotated in its wooden holder so that, when the specimen is placed on its side, the horizontal component of magnetization lies in the horizontal plane. The assembly is then rotated until a zero reading is obtained on the nullmeter; this occurs when the mean direction of (the total) magnetization is parallel to the axis of magnetization of the bottom magnet. The angular reading on the graduated circle is that of the direction of magnetization with respect to the axis of the specimen, i.e. the inclination I'. I'' is obtained at about 180° from I' and the average of the two readings gives I_1. The assembly is rotated to $I_1 - 90°$ and then $I_1 + 90°$ so that the direction of total magnetization is at right angle to the axis of magnetization of the bottom magnet and two intensity readings are measured on the integrating DVM (not shown). The holder is then rotated 180° about its horizontal axis and the procedure is repeated; I_2 is obtained and $I_2 - 90°$ and $I_2 + 90°$ are measured. I_1 and I_2 are averaged to obtain I and the four intensity readings averaged to get the total intensity (Int.). Whether I is positive or negative is determined from the direction of the deflection on 0° azimuth.

Using the spacers (Figure 5), the specimen can be placed at five different distances (z = 3.58; 4.08; 5.08; 6.08; 11.08 cms) from the bottom magnet. These five positions (Pos. 5 to Pos. 1) and the 11 sensitivities permit to measure specimens of different intensities. From (19) the intensity is given by

$$\text{Int.} = S \text{ defl. (mv) } z^3 / \left[E_{Bz}C_B - \left(\frac{z}{z+L}\right)^3\right] V \quad \ldots (37)$$

where V is the volume of the specimen. Writing

$$K = S\,z^3 / \left[E_{Bz}C_B - \left(\frac{z}{z+L}\right)^3\right] V \quad \ldots (38)$$

where the constant K is determined for each Pos. and S we get

$$\text{Int.} = K \times \text{defl. (mv)} \quad \ldots (39)$$

For convenience, the 55 different K are tabled on the measuring sheet (Pos. vs S).

When a specimen is not of standard height (≠ 2.2 cm), a correction must be added to the intensity measurements. This correction depends on the volume of the specimen and on the inclination I and, for a given Pos., is given by

$$C'_Z = \frac{\left[E_{Bz}C_B - \left(\frac{z}{z+L}\right)^3\right] V}{\left[C_I C_B - \left(\frac{z}{z+L}\right)^3\right] V'} \quad \ldots (40)$$

where C is the correction owing to the shape and orientation of the specimen and V' is the volume of the (non-standard) specimen. For $z > 3$ and L much larger than z, the effect of $(z/z + L)^3$ is negligibly small and we can write

$$C'_Z = \frac{C_s V}{C_I V'} \quad \ldots (41)$$

where C_s is written for E_{Bz}, the correction applicable to a standard specimen. C_I is obtained from

$$C_I = \{C_V^2 \sin^2 I + C_W^2 \cos^2 I\}^{1/2} \ldots (42)$$

where C_V is the correction to be applied when I = 90°; the axis of the specimen is then horizontal and perpendicular to the axis of magnetization of the bottom magnet. C_W is the correction when I = 0°; the small dimension (height) is then parallel to the axis of magnetization of the magnet and no additional correction is required so that $C_W = C_s$. Since the volume ratio V/V' = 2.2 cm/height, the correction is then given by

$$C'_Z = 2.2/\text{height}\,\{(C_V \sin I/C_s)^2 + \cos^2 I\}^{1/2} \quad \ldots (43)$$

The intensity of a non-standard specimen is obtained from

$$\text{Int. (n.s.)} = K\,C'_Z \times \text{defl. (mv)} \quad \ldots (44)$$

C'_Z has been tabled (h vs I) for the 5 Pos.

The largest value on the K table is 1975 x 10^{-8} Oe/mv. Since the range at S 11 is ± 250 mv (1% accuracy; Table I), intensities up to 4.9 x 10^{-3} e.m.u. can be measured. The smallest K is 0.261 x 10^{-8} Oe/mv which means that an intensity of magnetization (of a standard specimen) = 1 x 10^{-7} e.m.u. will produce a deflection (at S 1) of 38 mv. The accuracy of the reading is discussed in IV, 6.

6. Disturbances

Certain precautions must be taken when working at high sensitivities (S 1 to S 5 to measure intensities of 1 to 10 x 10^{-7} e.m.u.). Otherwise, vibrations and temperature changes may cause noise and drift large enough to render the instrument useless for measuring intensities <10^{-6} e.m.u. Seismic vibrations of 4 cycles/sec cause the magnet system to oscillate about its axis at the same frequency. The instrument is set on an anti-vibration pier which was built at the same time as the building. It consists of a concrete slab (1.05 x 1.05 x 0.15 meter) resting on crushed stone and sand to a depth of 1.5 meters. It is detached from the floor of the building. Measurements (by F. Lombardo of the Seismology Division) taken on the floor and on the pier show that the amplitudes are 3 times smaller on the pier. The transmission of these low frequency oscillations to the electrical circuit can be controlled to a certain extent by the filters but cannot be cancelled. It is then difficult to measure directly the current passing through the negative feedback solenoids and much easier to measure the voltage across a precision resistor. The zero deflections (for *D* and *I*) are measured by means of the DC nullvoltmeter which is normally left on the 100 mv range. The input resistance is high (100 MΩ) and the response time is less than 1 sec. The remaining small oscillations are not a serious problem. Indeed, since the deflection must be zero, it is relatively easy to rotate the specimen until the oscillations are equally divided on both sides of the scale centre. The intensities are measured on the integrating DVM which is normally set on a 2-sec integrating time.

The room temperature must be carefully controlled, especially when working at high sensitivity. The magnetometer head is quite sensitive to any temperature change. Such changes will cause expansion of the aluminum plate and vertical tube supporting the suspension; large drifts will then occur. To prevent this, a styrofoam cover (Figure 3) was made and at least 5 cm of insulation protects any part of the head. The shape of the compensating coils system is temperature dependent. As the room temperature changes, the coil system is either distorted or tilted. Although the distortion (or tilt) may be small, the changes in fields at the upper and bottom magnets are different and a drift will occur; a drift that may be large since the astaticism is of little help against this type of disturbance. The amplitude of the drift depends on the source of heat and on the location of this source with respect to the coil system.

The room is heated by 5 electric radiant heaters (2000 watts) controlled by 3 thermostats: (1) 2 heaters (1 thermostat) at the south end of the building; (2) 1 heater in the middle of the west wall and 1 at the north end of the building (1 thermostat); (3) 1 heater (1 thermostat) in a vestibule. About 20 minutes after switching on any of these groups, an irregular but oscillating drift starts. Recordings show the zero drifting one way for about 6 sec, then regressing by 70 per cent in 5 seconds before drifting again in the original direction by the same amount; this fairly regular pattern repeats until about 20 minutes after switching off this group of heaters. The amplitude of the drift (in one peak-to-peak oscillation) depends on the source or group that is switched on: (1) 2×10^{-7} Oe; (2) 6×10^{-8} Oe; (3) 4×10^{-9} Oe. These values correspond to the field required at the bottom magnet to reproduce the drift recorded.

When the building is allowed to cool with the heaters off, the oscillating drift disappears and a regular drift of about 2×10^{-7} Oe/°C takes place. Therefore, it seems reasonable to assume that the oscillating drift is caused by heat convection currents around the compensating coil system thereby producing shape changes. It is intended to install additional bracing in an attempt to reduce the oscillating drift. The drifts would probably be smaller for a smaller *L* and they would not occur if a magnetic-shielded room was used.

However, by taking certain precautions the instrument can still be used at full sensitivity. Since the amplitude of the drift is dependent on the location of the source, and 3 heaters are sufficient to maintain the room temperature constant, source (1) is never used. When measuring on S 1 to S 8, source (2) is switched off and when measuring on S 1 to S 5, source (3) is also switched off. The maximum decrease of temperature in winter without heat is 4°C/hour (in general it is 1 to 2°C/hour). The drift is then 8×10^{-7} Oe/hr or 1.3×10^{-8}/min. Since a set of three readings (D_1, D_2, D_1) can be taken in 30 seconds, it is estimated that the error introduced in the mean by drift and noise is probably not much greater than 3×10^{-9} Oe. This amounts to 5-6 mv on S 1. The estimate agrees with experimental results such as C84A (Table III) where the individual directions (of a 0.37×10^{-6} e.m.u. intensity) are all within 3° of the mean.

The magnetization of the specimen holder should be thoroughly checked. It should not produce fields larger than 1 to 2×10^{-9} Oe at the bottom magnet. The permali holder used can easily be contaminated and it must often be washed with soap or alcohol and magnetically cleaned in alternating fields of 3000 Oe. Another prevention against drift is to insulate the damping disc; otherwise, specimen and holder which are not at room temperature because of previous warm up (by handholding for example) will produce a temperature change at the bottom magnet resulting in a drift. To prevent this, a Perspex cup (Figure 3) has been glued to the damping disc (the rest of the case bottom is of nylon).

7. Zeroing

The instrument can be zeroed in two ways: mechanical and electrical. The photo resistor carriage can be displaced by remote control and its position is indicated on a dial (Figure 6; on the left). The alignment of the magnet system with respect to the 0° azimuth of the specimen holder is indicated by this dial. When the dial reads 000.0, the two are aligned to within 0.002° of arc; a reading of 001.0 corresponds to a misalignment of 0.2′ of arc. The dial is normally kept between 950.0 and 050.0 so that the misalignment of the magnet system is ≤ 10′ of arc.

The electrical zeroing is accomplished by passing a calibrated current in a 2-turns coil on the feedback solenoid holder. No misalignment of the magnet system occurs when this method of zeroing is used. A meter (Figure 6; bottom left) graduated (1° – 0° – 1°) indicates the angular displacement if no electrical compensation was used.

8. Performance

Table III gives the results of routine measurements taken from different rock collections. It is divided into two parts. The first part shows the results of progressive thermal or chemical demagnetization. To check the accuracy of the direction determination, specimens with stable magnetizations are chosen to avoid large direction changes inherent to the specimen. Small direction changes between different demagnetization steps may be owing to real changes of directions or to measurement errors. However, the regularity of the changes

Table III. (a) Measurements taken on the same specimen after each thermal (at x°C) or chemical (during x hours immersion in Hcl) demagnetization.

	H 134B		H 2A		H 2B	
°C	D,I	INT. X 10^{-6} e.m.u.	D,I	INT. X 10^{-6} e.m.u.	D,I	INT. X 10^{-6} e.m.u.
20	168,−34	4.5	184,+05	9.6	191,+08	9.3
100	168,−35	4.5	185,+01	9.0	186,+02	9.6
300	168,−35	3.8	185,+00	8.7	187,+01	9.0
400	169,−34	3.4	185,+00	6.3	187,+01	7.1
500	169,−32	2.7	188,+00	4.9	190,−01	5.4
550	169,−33	2.5	189,−05	2.2	196,+01	3.9
600	168,−33	1.9	I.M.		198,−01	2.4
650	168,−33	1.2			I.M.	

I.M. = Large instantaneous magnetizations, acquired when the specimen is subjected to the field (0.20e) of the magnetometer, render the readings meaningless.

	C 23 B		C 34 B		C 54 B	
Hours	D,I	INT. X 10^{-6} e.m.u.	D,I	INT. X 10^{-6} e.m.u.	D,I	INT. X 10^{-6} e.m.u.
00	037,+67	13.0	075,+57	4.9	045,+43	19.1
29	037,+66	9.5	080,+55	1.8	045,+40	15.1
100	040,+70	6.3	073,+60	1.2	046,+45	10.9
241	046,+69	2.7	076,+63	0.8	050,+48	4.8
423	042,+73	1.5	070,+72	0.9	045,+54	3.3
790	054,+79	1.3	073,+73	0.9	048,+55	3.2

(b) Repeat measurements taken on inhomogeneously magnetized specimens. The measurements are often taken at different distances as indicated by Pos.

Specimen	D,I	INT. X 10^{-6} e.m.u.	POS.	Specimen	D,I	INT. X 10^{-6} e.m.u.	POS.
C84A	143,+00	0.35	4	H152A	147,+00	1.6	4
	145,+05	0.37	4		145,+00	1.5	3
	147,+03	0.38	4	H166	261,+36	5.2	2
	145,+04	0.36	4		260,+36	5.0	3
	142,+02	0.37	4	690371	162,+34	11.7	2
H8A	115,+33	5.8	3		160,+35	12.8	3
	118,+33	5.9	2		162,+34	13.3	3
H9A	318,+13	4.7	4	690372	184,+23	20.2	2
	320,+13	4.7	3		185,+23	20.2	3
H108*	074,+68	1.7	4	690373	181,+16	54.6	2
	074,+69	1.9	4		181,+16	54.4	3
H151	128,−26	2.2	4	690082	050,+37	46.3	3
	128,−26	2.2	4		049,+37	44.9	2
					048,+35	46.8	1

*Non standard specimens — height = 1.2 cm

between 100°C and 600°C for H2B for example, suggests that most of the changes can be attributed to direction changes.

The second part consists of repeat measurements taken on the same specimen because the magnetization was very inhomogeneous and the two directions (D_1 and D_2) of a set of readings were far from 180° apart. In such cases, intensity permitting, the repeat measurements are taken at different distances and the position is indicated. Only specimens of low intensities are listed. Repeat measurements on specimens of intensities > 10^{-4} e.m.u. normally agree to 1°; readings are taken to the closest degree. Results indicate that the direction of intensity = 1 x 10^{-7} e.m.u. can be determined to within 9° on S 1 as estimated from the ratio noise/deflection = 6 mv/38 mv, and the direction of intensity of 3 x 10^{-7} e.m.u. (such as C 84 A) to within 3°. The direction of 1 x 10^{-6} e.m.u. intensities can be determined on S 6 to within 2°. These values can, of course, be improved upon by taking repeat measurements.

For intensities $< 10^{-6}$ e.m.u., about 8 specimens can be measured in an hour; this includes repeat measurements that may be required because of intermittent increases in the disturbance level. About 12 specimens of intensities in the 10^{-6} e.m.u. range can be measured per hour. When the intensities are $> 10^{-4}$ e.m.u. the measurements can be done on S 10 and S 11 and because of the quick response, 15 to 20 specimens are normally measured in an hour. It is found that about 2/3 of the time is spent in handling the specimens, changing spacers and working out the averages of *D, I* and Int. so that for weakly magnetized specimens repeat measurements can be taken without unduly increasing the total time.

The system could be used to measure three orthogonal components of magnetization. However, for many reasons, it is preferable to measure *D, I* and Int. as described. Time is saved by eliminating the necessity of computing the results as required in the three-component method. Accuracy obtained with the direct method is greater; in the three-component method, each determination is performed on a fraction of the total intensity while in the direct method *I* and Int. are determined from the total intensity. The determination of *D* is obtained from the total horizontal intensity and its accuracy can be further improved by reducing the distance used for *I* and Int. or by using a higher sensitivity. Indeed, since only Int. depends on *K*, both Pos. and *S* can be changed at any time for the determination of *D* and *I*. A change of distance (or Pos.) is usually avoided in the three-component method because of complications in computation; different *z* and shape correcting factors must then be used for p_x and p_y and p_z.

The direct method also provides an instant estimate of the inhomogeneity of magnetization. The direction readings (D_1, D_2) of an inhomogeneously magnetized specimen will not be 180° apart. However, measurements taken at different distances show that the mean reading (upright and inverted) is representative of the mean direction of magnetization.

It should be noted that the *mean* direction of magnetization is not necessarily parallel to the direction of the magnetizing field. For example, if a change of direction or polarity of the field occurs while a sedimentary formation is gradually deposited and consolidated, the direction of magnetization of the upper part of a specimen (2.2 cm thickness formed during that change) is different from that of the lower part. Such an occurrence is readily determined by the inequality of D_1 and D_2 since D_1 (upright position) is then biased towards the direction of the latter field and D_2 (inverted position) towards the direction of the former. In paleomagnetic work, it is normally assumed that the field at the time of magnetization was a dipole field and that the direction of magnetization obtained after adequate cleaning is representative of the direction of the earth's field at that time. However, if a specimen is highly inhomogeneously magnetized, the mean direction and intensity of magnetization measured may be the resultant vector of two magnetizations acquired in two different fields and therefore that vector is non-representative of a particular field. By comparing D_1 and D_2, and I_1 and I_2, the direct read method of measuring provides means of assessing if during magnetization the direction of the field remained in the same direction with respect to the orientation and attitude of the specimen. The method has been used successfully to detect the presence of a composite magnetization of the Seal Lake and Croteau Groups sediments (Roy and Fahrig; in preparation).

Acknowledgments

We are indebted to G. Massie for his valuable assistance in setting up the apparatus and the construction of components, E. Gelinas for the photographs and J.K. Park for his help with the specimens used for chemical demagnetization. Critical reading of the manuscript by P.H. Serson and E. Irving was greatly appreciated, and we owe special thanks to P.H. Serson for assistance in editing. The photo resistors were supplied by National Semiconductors Ltd. and we wish to thank Messrs. Pankau and Clifton for their interest in this project.

References

As, J.A. 1960. Instruments and measuring methods in paleomagnetic research, *Mededel. Verhandel. K.N.M.I*, Vol. 78, 1-56.

Blackett, P.M.S. 1953. A negative experiment relating to magnetism and the earth's rotation, *Phil. Trans. Roy. Soc. London*, Ser. A, Vol. 245, 309-370.

Collinson, D.W., and K.M. Creer. 1960. Measurements in paleomagnetism, in *Methods and Techniques in Geophysics 1*, S.K. Runcorn, ed. Interscience Publishers, New York, 168-210.

———K.M. Creer, E. Irving, S.K. Runcorn. 1957. Paleomagnetic investigations in Great Britain. 1. The measurement of the permanent magnetization of rocks. *Phil. Trans. Roy. Soc. London*, Ser. A, Vol. 250, 73-82.

Deutsch, E.R., J.L. Roy, and G.S. Murthy. 1967. An improved astatic magnetometer for paleomagnetism. *Can. J. Earth Sci.*, Vol. 5, 1270-1273.

Patton, B.J. 1967. Magnetic shielding, in *Methods in paleomagnetism*, D.W. Collinson, K.M. Creer and S.K. Runcorn, eds. Elsevier Press, Amsterdam, 568-588.

Roy, J.L. 1963. The measurement of the magnetic properties of rock specimen. *Pub. Dom. Obs.* Ottawa, Vol. 27, 420-439.

———1966. Désaimantation thermique et analyse statistique des directions de sédiments carbonifères de l'est du Canada. *Can. J. Earth Sci.*, Vol. 3, 139-161.

———1967. Shape and size of weakly magnetized rock specimens, in *Methods in Paleomagnetism*, D.W. Collinson, K.M. Creer and S.K. Runcorn, eds. Elsevier Press, Amsterdam, 192-195.

———W.A. Robertson, C. Keeping. 1969. Magnetic "field free" spaces for paleomagnetism, rock magnetism, and other studies. *Can. J. Earth Sci.*, Vol. 6, 1312-1316.

PUBLICATIONS of the EARTH PHYSICS BRANCH

VOLUME 42 – NO. 6

the ottawa PZT observations—1956-70, their comparison with BIH values by graphical, spectral and fourier analyses

E. G. WOOLSEY

DEPARTMENT OF ENERGY, MINES AND RESOURCES

OTTAWA, CANADA 1972

Cat. No: M70-42/6

Contents

183 Introduction
183 History
184 Star catalogue
184 Preparation of data
184 Preparation of summary values
185 Values at one-twentieth of a year
185 Ten-day smoothed values
185 Description of observations
187 Comparison with BIH
189 Apparent secular change in latitude
189 Conclusion
189 Bibliography
191 Appendix A
197 Appendix B
209 Appendix C

the ottawa PZT observations—1956-70, their comparison with BIH values by graphical, spectral and fourier analyses

E. G. WOOLSEY

Abstract. Results of measurements of latitude and time made with the Ottawa Photographic Zenith Tube (PZT) from 1956 to 1970 are given. The observations, on magnetic tape, are available to recognized scientific organizations at nominal cost.

The observations are shown to produce values of the variation in latitude and longitude with a probable error of ″.01. They were compared to the published results of the Bureau International de l'Heure. The residuals so formed were subjected to a spectral analysis and it is demonstrated that the PZT was not capable of detecting secular motions of 10 cm or less. No motion was found for Ottawa.

The star catalogue is published to contribute to the knowledge of stellar positions.

Résumé. La présente publication donne les résultats de mesures de la latitude et du temps effectuées à l'aide de la lunette photographique zénithale d'Ottawa (PZT) de 1956 à 1970. Les observations, enregistrées sur bande magnétique, sont disponibles et seront communiquées aux organismes scientifiques reconnus, pour un coût nominal.

Les observations sont données de manière à indiquer les valeurs de la variation de latitude et de longitude avec une erreur possible de ″.01. Elles ont été comparées aux résultats publiés par le Bureau International de l'Heure. Les données résiduelles ainsi obtenues ont été soumises à une analyse spectrale et il a été démontré que la lunette (PZT) ne peut détecter des mouvements séculaires de 10 cm ou moins. Aucun mouvement n'a été décelé pour Ottawa.

Le catalogue des étoiles est publié comme contribution à la connaissance de la position des étoiles.

Introduction

The PZT (Photographic Zenith Tube) is basically a fixed telescope that observes stars within 15 minutes of arc of the zenith. The light from a star passes through the lens, is reflected by a dish of mercury which establishes the vertical and is brought to focus on a photographic plate placed at just a sufficient distance below the lens to allow room for the plate holder. Each star is photographed four times during transit; the plate is driven to produce point images and is rotated 180° between each exposure. Each exposure is accurately timed.

The photographic plates are measured in two coordinates. Since we know the positions of the stars, in one coordinate we are able to record the latitude in relation to our star catalogue and, in the other coordinate, record the difference between observed and calculated times of transit of the star over our meridian. Clock comparisons are made daily (in our case with WWV and CHU).

These measures are used to determine the position of the pole and the rate of rotation of the earth. In order to do this we must adopt a coordinate system (x,y) for the position of the pole. By international agreement x is measured as the displacement of the pole toward Greenwich, and y the displacement of the pole toward 90° west of Greenwich. The origin adopted is the Conventional International Origin (CIO). Both x and y are measured in seconds of arc.

Our measures become:

$$\phi = \phi_0 + x \cos \lambda_0 + y \sin \lambda_0$$

$$\Delta T = (-x \sin \lambda_0 + y \cos \lambda_0) \tan \phi + t$$

where ϕ is our observed latitude and ΔT our observed difference in time, in seconds of mean solar time; ϕ_0 and λ_0 are our adopted latitude and west longitude. The values to be determined are x and y for the position of the pole and t the time correction measured in seconds of mean time in respect to our reference clock. Thus at any instant we have two equations and three unknowns. It is only by introducing results from other stations that a solution can be found.

Such a solution is regularly carried out by the BIH (Bureau International de l'Heure) using observations from many stations around the world. When the observations from any individual station are compared to the values published by the BIH (Guinot, 1967-70), the major part of the observed variations in latitude and time correspond to the variations in x, y and t of the BIH and therefore must be features of the earth as a whole. There are, however, small residuals at each station that appear to be periodic and a phenomenon of that station. The study of both these types of variation reveals properties of the earth.

History

This article deals with results only. No effort will be made to describe the instrument in technical detail, which has already been done by Thomson (1955).

The Ottawa PZT was brought into operation in 1952. During the early years it was mounted in the transit annex of the Dominion Observatory, which was a stone, brick and concrete addition on the west side of the main building. In 1960 it was moved about 100 metres southeast to its own light, insulated building. At the end of January 1968 the 10-inch (25-cm) PZT was replaced with a new 8-inch (20-cm) instrument. The former was moved to Calgary to be on the same latitude as the Herstmonceux PZT of the Royal Greenwich Observatory. Finally, in January 1970 the Ottawa PZT was moved to a new site 16 kilometres due west. This is the terminal point of this report.

The Ottawa PZT plates from the years 1956 to 1960 inclusive were previously remeasured. The observations in latitude were published in *Time & Latitude Bulletin*, A45, of the Dominion Observatory, (Tanner, 1967), from which the following notes have been extracted.

"The principal changes within the period which still may effect the results are:

(1) From 1956 to 1959 inclusive, observations consisted of two, two-hour groups from a 160-star catalogue, centred near 2200 hours local time; from 1960 onwards observations were made from dusk to dawn.

(2) The instrument was moved in the period May 7 to May 25, 1960, to the new observing hut 1″.252 south and 0ˢ.275 east of its earlier location. The 0ˢ.275 was allowed for in the calculation of time so there is no apparent discontinuity in this coordinate.

(3) From 1962 onwards the catalogue consists of 80 stars in eight, three-hour groups.

"It has not been considered profitable to rework the 1952-1955 results for three reasons; the larger scatter, the smaller number of stars in common with the current catalogue, and the lack of an atomic standard of time comparison."

Star catalogue

The star catalogues are essentially on the FK4 basis with an epoch of observation about 1962. The positions were amended in 1966 by R.W. Tanner of this Branch, and incorporate the PZT observations to that date. They are relatively free from error and any adjustments made in the future will have litte effect on the results being considered.

In order to have a permanent record, and to assist astronomers forming star catalogues, the catalogues employed for the two periods are published in Appendix A. The 160-star catalogue was used from 1956 to 1961 and the 80-star catalogue from 1962 to 1970.

The star catalogues require little explanation since they follow current practice. The star number is made up of two parts, the hundreds define the group, the tens and units the number of the star within the group. The photographic magnitude and spectral class have been copied from the other publications, principally the *Henry Draper Catalogue.* The right ascension and declination are presented for the year 1950 and the proper motions are centennial. The BD number is given to provide identification of the star and cross-reference to other star catalogues.

Preparation of data

Since observations were available on punched cards, it was only necessary to bring them to a uniform basis and decide how to collect and present them in the most usable form for future investigations. The latitude is given directly and presents no problem.

In the time coordinate the readings are the difference between observed and calculated time of transit of a star recorded as differences with the time broadcast by WWV. In the past, time was related to the mean rotation of the earth; with the advent of atomic clocks time was maintained by adopting a constant annual rate and applying step corrections to keep radio transmitted time within 0.1 sec. of mean solar time. The annual rate was changed several times in the period considered. An obvious uniform time is atomic time and the most easily available atomic time was A1 (the U.S. Naval Observatory atomic standard) for which they had already published comparisons with WWV. Our observations are published as ΔT = UTO − A1, the difference between our observed time of transit and the time of the atomic standard A1.

The other adjustment required to bring the observations to a uniform basis was to correct the earlier years for the change in aberration adopted in 1968.

The observations were collected by star groups and comparisons with the original summaries were made to insure that the values were free from errors. Our raw results are available on magnetic tape to recognized scientific organizations at a nominal cost. The tape gives:

Ottawa date of observation – year, month, day.
Julian day to two decimals.
Star group number.
Observed time minus atomic time 'A1'.
Observed latitude – seconds of latitude, omitting the 45°23′.
Number of stars observed.
Our night or reference number.

Preparation of summary values

Rather than publish our raw data, which would be of use to few investigators, summary values have been derived at intervals of one-twentieth of a year and ten-day intervals. The use of summary values reduces the night-to-night dispersion and provides values that can be compared directly with those published by the BIH.

The information on the raw data tape is similar to that sent to the BIH; the observations are arranged as average of star groups. These star groups originated in the star catalogue and contained about ten stars balanced north and south of the zenith. Unfortunately, it is the exception rather than the rule that complete groups are observed. Also, each night's work is on one plate, and the plate constants are derived from the mean of all stars observed. It therefore seemed preferable to use the average of all stars observed on one night as an observation.

In order to reduce night-to-night dispersion, the nights were grouped to form summary values. The grouping of nights was done in such a manner as to produce values at one-twentieth of a year and at ten-day intervals to facilitate comparisons with the published BIH (1968) values. Two different numerical methods were used, one for the one-twentieth of a year and the second for the ten-day intervals. Both schemes appear to represent our observations equally well.

The summary values are listed in Appendix B, giving time of observation in Besselian years from 1900 for the .05 year values and in Julian days for the ten-day smoothed values. The latitude, (ϕ), is in seconds only; the 45°23′ has been omitted. The time coordinate is observed minus atomic time A1 and is called 'UTO-A1'.

Values at one-twentieth of a year

The method of combining observations as suggested by Jeffreys (1960, 1961) was used to calculate the values for each twentieth of a year. The night values were weighted one for all nights with ten or more observations, one-half for all nights with five to nine stars, and zero for all nights with less than five stars observed. The various nights were divided into ten groups per year to yield values near .05, .10, etc., parts of a Besselian year. Care was taken to ensure that each group had a weight of at least ten, thus each group included a minimum of 10 nights on which observations were successfully carried out. To form values for the exact periods, the three term Lagrange interpolation formula for unequal intervals was used.

A second solution was made by grouping half the nights from each set to form a new series of ten groups per year. The average of the solutions has been adopted as the value at one-twentieth of a year.

This solution lent itself to the calculation of standard deviations. The standard deviations for each star were obtained on each night (as part of the routine calculations) from differences between the observed values and the mean value for the night. The standard deviations for each night and each summary value were obtained using the least-square solution of Jeffreys' formula. The averages of these errors are the values quoted in Table I.

In order to ensure that these standard deviations were indeed correct, a standard deviation for each night was determined from the differences between the observed value and a value for the night determined by straight line interpolation between the two adjacent summary values. This gave standard deviations in latitude and time respectively of $''.090$ and $0^s.0165$ for 1956 to 1959 and $''.050$ and $^s.0045$ for 1962 to 1967. These standard deviations are not significantly different from those of the first solution.

Table I. Standard deviations

Epoch	Each star Lat.	Time	Each night Lat.	Time	Each summary values Lat.	Time
1956-59	$''.15$	$^s.021$	$''.088$	$^s.0162$	$''.027$	$^s.0062$
1962-67	$''.11$	$^s.013$	$''.051$	$^s.0045$	$''.015$	$^s.0013$

The standard deviation for a summary value was checked by comparing the two solutions. The root mean sum of the differences was the same as before.

There is a considerable improvement of the results with the change of location in 1960. In order to indicate the reliability of the results the standard deviations using a representative period for each site are as shown in Table I.

These are considered internal standard deviations since they are formed by comparing results among themselves.

The method of weighting and combining observations is somewhat arbitrary but the considerations leading to the method adopted may be of interest. From our experience, it should never be assumed (without investigation) that precision increases with the square root of the number of observations; there appears to be a limiting accuracy which cannot be improved significantly merely by increasing the number of observations.

Markowitz (1960) has pointed out that "On account of systematic effects no great increase in precision is gained by observing a large number of stars in any one night ... the weight of an observation with 16 stars is about 1.5 times as great as one with 6 stars."

We concur with his reasoning but have solved the problem by graphic means. We graphed the root mean square of residuals formed by subtracting our night values from the curve of best fit through the night values against the number of observations as ordinate. We found that after a certain number of observations the curve becomes a horizontal line.

Examining our night corrections in this manner we found that when ten stars were observed, we were approaching the values $''.05$ and $^s.005$, which was about 90 per cent of the limit. There was no justification for a more elaborate weighting scheme than a simple one, two ratio (1. and .5).

The summary values became asymptotic at about $''.015$ and $^s.0015$, but the value was not approached until 18 or 20 nights were combined. The minimum number of ten nights was set rather by the number of nights available.

Ten-day smoothed values

The ten-day smoothed values were calculated by a less sophisticated method. The earlier years were adjusted for the move in 1960 by subtracting $1''.252$ from the latitude. Running means for ten successive plates were formed. Values for the ten-day Julian dates were interpolated linearly from two adjacent values. The final listing was formed from these ten-day values by parabolic smoothing in groups of five.

Both methods produce comparable values and are in good agreement except at the beginning of 1968 where there is a period of thirty days with no observations, then four days observing followed by a gap of nine days. Neither method can be expected to bridge gaps so large.

Description of observations

Very little can be said about the observations until they are compared to the BIH. However, they have been graphed to give a visual representation to the reader. Figure 1 shows our readings in latitude and time.

As already stated the main part of each variation is common to all stations and these graphs resemble those in other publications.

In the lower or latitude curve the beat period of about six years between the Chandler and annual terms is obvious and during this period the amplitude of the Chandler term appears to be decreasing.

It is not practical to graph the time coordinate in the same manner. The large rate difference between observed and

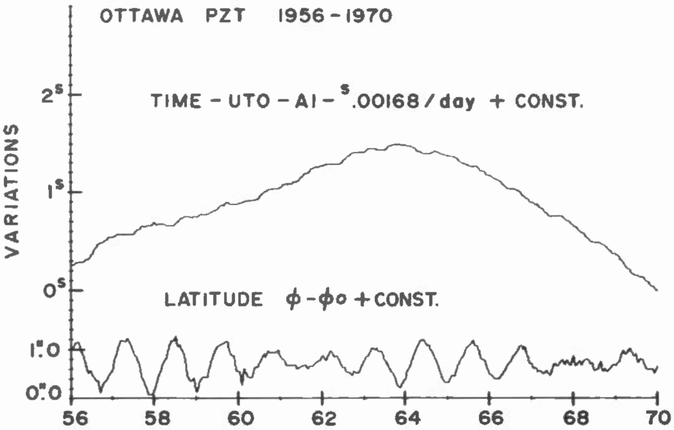

Figure 1.

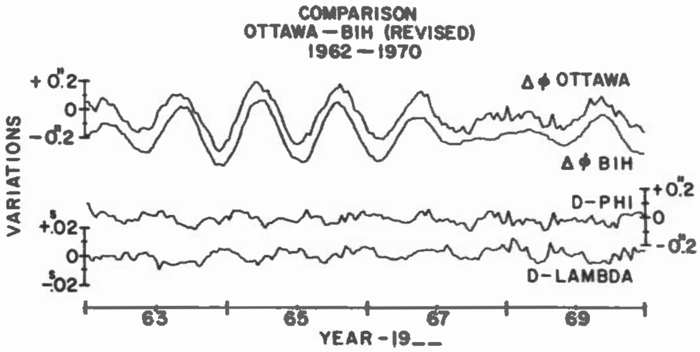

Figure 4.

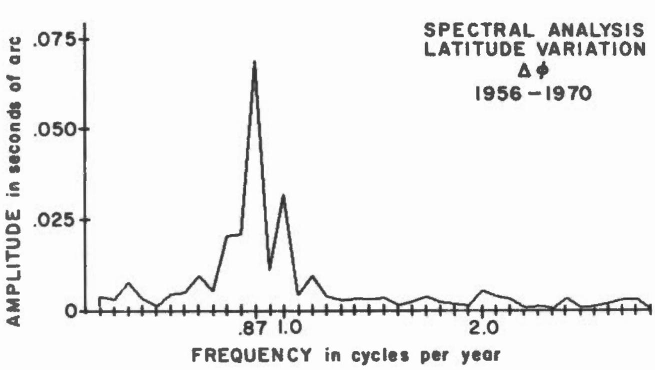

Figure 2.

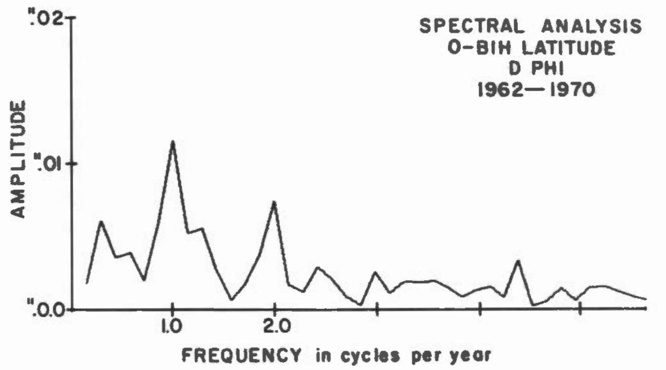

Figure 5.

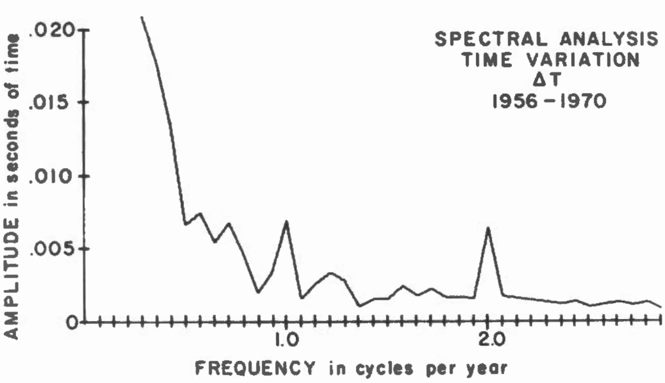

Figure 3.

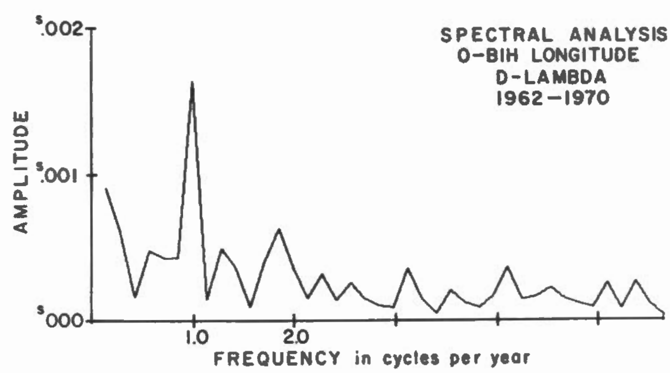

Figure 6.

atomic time would require the scale to be greatly reduced and thus obscure variations. By subtracting an average rate for the period, of $^s.00168$ per day, the changes in rate are more easily seen and the graph draws attention to the fact that the rate of rotation of the earth is far from constant. This graph is similar to that shown by Markowitz (1969). Even with this method of showing the time, scale has been reduced by a factor of 10, that is, each division of the time graph is approximately equal to ten in latitude. The graph draws attention to the significant change in the rate of rotation of the earth (more than 100 parts in 10^{10} i.e. more than a millisecond per day) that occurred in the short period 1964-1966.

A spectral analysis may show better what is actually happening. Figure 2 shows the amplitude in latitude plotted against frequency.

Table II.

Frequency cycles per year	Period in days	Power $(''.01)^2$
.73	511	5
.75	465	5
.87	426	49
1.00	365	11
2.00	183	.3

The principal features are:

1. A few long terms that may be related to the short period examined (i.e. frequences .73 and .75).
2. A large Chandler term. The values given in Table II confirm other findings, that the power of the Chandler term is about four times the annual term.
3. An annual term, and a semi-annual term barely distinguishable from the noise.
4. Amplitude of the noise level is taken as a little over $''.003$ or 10 cm.
5. The value of Q, the figure of merit (cf. electronic circuits), was calculated for the Chandler term as greater than 5. A much longer period would have to be studied to improve this value.

The spectral analysis of the time coordinate is given in Figure 3.

The principal features are:

1. Long-term variations had amplitudes too large to be included in the graph.
2. They are due to the major changes in the rate of rotation of the earth (the cause of which is still unknown). This can be more effectively studied by employing the BIH values, and has been adequately done by Markowitz (1969).
3. The period is too short to show any two- or four-year variations as suggested by some writers.
4. The annual and semi-annual terms of amplitude $^s.0070$ and $^s.0065$ dominate the rest of the spectrum.
5. The noise level is about four times as large as that found in latitude.
6. The scale used in the time graph is 1/4 that used to show variations in latitude.

Comparison with BIH

As stated in the introduction the BIH has solved equations similar to

$$\Delta\phi = \phi - \phi_0 = x \cos \lambda_0 + y \sin \lambda_0$$

$$\Delta T = (-x \sin \lambda_0 + y \cos \lambda_0) \tan \phi + t$$

by assigning latitude, longitudes, and weights to the various stations around the world. In their solution differences in time are expressed with respect to another uniform time, UTC, rather than atomic time. UTC is the coordinated universal time approximating the rotation of the earth and is essentially the same as WWV. It is maintained at a constant rate for the short periods required by their calculations but is not uniform over the longer period used in this report. Their method of calculation is described in detail in their annual reports (Guinot, 1967-70) and it suffices to say it provides the best reference to which we may compare our results (The International Latitude Service (ILS) and International Polar Motion Service (IPMS) only publish values of x and y.). The BIH report provides values of x, y and UT1 and UT2-UTC, and comparisons of UTC with various atomic times. From their tables we are able to calculate our value for t, the correction to atomic A1 at any instant.

Comparison of our observations with the BIH are given in Appendix C under the headings of D-PHI and D-LAMBDA, the values being given in the sense observed minus computed. The latitude differences (D-PHI) were formed by adopting a latitude of 45°23′37″ (as a convenience to give decimals of a second only), so that the D-PHI values are observed corrections to this adopted latitude. The interpretation of the D-LAMBDA term is not as obvious. Our observed time values were based on an adopted west longitude of $5^h2^m51^s.94$, which entered directly into the calculation. If we had chosen a slightly smaller longitude, our recorded observed time would be increased by exactly the same amount. Thus the differences (D-LAMBDA) are observed corrections to our adopted longitude. The values used in the comparisons are the values for each twentieth of a year compared to the BIH unsmoothed values on the 1968 system which are only available back to 1962.

As expressed in the introduction "When the observations from any individual station are compared to the BIH . . . there are small residuals at each station that appear to be periodic and a phenomenon of that station." These residuals will now be examined by graph, spectral analysis and analytical solution.

Figure 4 provides a picture of these observations. The upper two graphs show the similarity of our latitude observations to those calculated for Ottawa using the BIH published values of x and y. The upper graph is $\Delta\phi = (\phi - \phi_0)$ Ottawa and the lower one $\Delta\phi = x \cos \lambda_0 + y \sin \lambda_0$. The time coordinate has been omitted because the scale required would mask all differences. The two lower graphs show D-PHI and D-LAMBDA, the variations in latitude and longitude of Ottawa compared to the BIH. At a latitude near 45°, $''.01$ is nearly equal to $^s.001$ so that the variations are essentially on the same scale. There is no significance to the spacing of the graphs which have been designed to show variations with time. We will now proceed to examine these latter two curves.

The spectral analysis of D-PHI and

D-LAMBDA are given in Figure 5 and Figure 6. They have been graphed to essentially the same scale so that variations in latitude and longitude may be compared in amplitude and frequency. In order to have enough observations the ten-day smoothed values were used.

The noticeable features are:

1. In latitude there is an annual term of amplitude $''.012$ and a semi-annual term of amplitude $''.007$ and the noise level has remained unchanged at $''.003$ or 10 cm.
2. In longitude there is an annual term of amplitude $^{s}.0016$ and no semi-annual term. The amplitude of the noise level is about $^{s}.0004$, i.e. near 10 cm.
3. The large reduction in the noise when our results are compared to the BIH shows that this was a feature of the earth as a whole. It was very encouraging to find our error in determining longitude is again the same order as that for latitude.

The small annual and semi-annual terms as shown by the spectral analysis suggest that we submit our results to a Fourier analysis. This is precisely the practice followed by the BIH. Although the semi-annual term is not present in the D-LAMBDA, there appears no harm in following the BIH and treating both coordinates in the same manner.

The analytical solutions for each year are given in Table III. There is a year-to-year variation but on the average in latitude the amplitude of the annual term is double the semi-annual, and in longitude the annual term is predominant.

The constant terms from the analytical solutions provide corrections to our adopted latitude and longitude. Therefore, we can say the observed mean values (1962-70) for the latitude and longitude of Ottawa in the BIH (1968) system are:

Latitude	45°23′	$37''.132$
Longitude	$5^{h}02^{m}$	$51^{s}.9525$

The BIH adopted values: 45°23′ 37.121 and 5^{h} 2^{m} 51.950 were based on our observations made in 1967. Our calculated values for the same period are: 45° 23′ 37.122 and 5^{h} 2^{m} 51.9506. The difference is considered negligible and is probably due to the method of grouping.

An analysis of the variation of the constant terms *a* and *a′* (Table III) with time should yield the secular motion or continental drift of Ottawa (or an error in the proper motions of our star catalogue). Our solutions give:

Secular variation of		
latitude	$-''.11$	$\pm''.46$ per century
longitude	$-^{s}.042$	$\pm^{s}.060$ per century

As would be expected for so short a period, the motion can hardly be called significant.

According to Munk and MacDonald (1960), the local variation described by the variations in D-PHI and D-LAMBDA after the removal of the corrections to the adopted latitude and longitude is "related to wind, pressure, and other meteorological variables." The verification of this is beyond the scope of this report.

The standard deviations obtained by comparing $(\phi - \phi_0)$ Ottawa $- \Delta\phi$ BIH without adjustment for the annual terms yields values of $''.036$ and $^{s}.0038$ for latitude and longitude respectively. However, when these annual variations are applied, the standard deviations reduce to $''.022$ and $^{s}.0019$ which are one and half times the calculated internal values of $''.015$ and $^{s}.0013$. It is hoped that these differences can be reduced when local effects are studied.

Although the published values for the variation in latitude by the IPMS (Yumi, 1962-68) have not been adjusted for the new aberrational constant, it is interesting to compare our results. In order to avoid our values at the beginning of 1968, only six years, 1962 to 1967, were used. The Ottawa values are not adjusted for any annual term.

Table III. Comparison with BIH revised Fourier analysis

D-PHI: $\Delta = a + b \sin 2\pi\theta + c \cos 2\pi\theta + d \sin 4\pi\theta + e \cos 4\pi\theta$

θ is in decimals of a Besselian year

D-LAMBDA: $\Delta = a' \pm b' \sin 2\pi\theta \pm c' \cos 2\pi\theta \pm d' \sin 4\pi\theta \pm e' \cos 4\pi\theta$

θ is in decimals of a Besselian year

	D-PHI	Units $''.001$				D-LAMBDA	Units $^{s}.0001$			
Year	*a*	*b*	*c*	*d*	*e*	*a′*	*b′*	*c′*	*d′*	*e′*
1962	148	7	35	− 1	− 8	137	7	5	4	9
1963	117	− 6	41	24	1	159	39	−16	28	14
1964	133	25	20	15	−17	129	36	−25	17	0
1965	138	− 9	28	10	−11	117	36	−23	0	−11
1966	142	−12	20	5	−19	118	29	−25	− 1	− 1
1967	122	−34	13	18	−21	106	25	−34	− 9	5
1968	119	− 7	19	− 6	− 8	104	4	−32	−44	7
1969	137	−30	21	− 1	−22	132	40	−17	3	−10
8 years	132	− 8	25	8	−13	125	27	−20	− 3	1

Mean errors *a* ± 5
b, c, d, e ± 7

Mean errors *a′* ± 5
b′, c′, d′, e′ ± 7

The CIO origin was chosen to make the pole of the BIH and IPMS coincide on the average for the years 1964-1966. The Ottawa observations appear to favour the BIH position of the pole. No case is made for the standard deviations since all differences are known to contain systematic terms.

Table IV.

	Average	Standard deviation
$\Delta\phi$(BIH) – $\Delta\phi$(IPMS)	".004	".028
ϕ–ϕ_0 (OTTAWA) – $\Delta\phi$(BIH)	".001	".034
ϕ–ϕ_0 (OTTAWA) – $\Delta\phi$(IPMS)	".005	".028

Apparent secular change in latitude

The secular change of latitude was investigated by averaging the latitudes at one-twentieth of a year over a period of six years. This should remove most of the annual and Chandler terms. The values for the earlier years were adjusted by subtracting 1".252. In Table V the decimals of a second only are listed along with their differences from the mean.

The solution gives the secular drift in latitude as 0".08 ± 0".13 per century. This table was formed on the assumption that the Chandler term has a period of exactly 1.2 years, which is not exactly true; the small uncertainty was obtained by assuming each six-year period as independent, which is also not exactly true. The value is about equal and opposite in sign to that obtained by comparing Ottawa with the BIH for the years 1962 to 1970. The only conclusion is that there is no evidence of secular drift.

Conclusion

The Ottawa PZT has produced results of high order, by determining the variation in latitude and longitude with a probable error of ".01. This instrument has now been moved to Calgary and is observing the same list of stars as Herstmonceux. We expect the Calgary results to duplicate the accuracy of Ottawa 1962-1967.

The results were examined and no secular motion of Ottawa was determined. The analysis shows that the Ottawa PZT cannot detect variations or motions of 10 cm or less. Although observations can be investigated for weather, tidal effects or corrections to the star catalogue, the noise level inherent in the observations makes it unlikely that any improvement will be made in the final results.

Table V.

Period	Average latitude	Difference from mean
1956 to 1961 inclusive	.357	-.007
1957 1962	.364	.000
1958 1963	.361	-.003
1959 1964	.366	.002
1960 1965	.368	.004
1961 1966	.369	.005
1962 1967	.364	.000
1963 1968	.361	-.003
1964 1969	.369	.005

Bibliography

Guinot, B. 1967-70. *Rapports Annuels*, Bureau International de l'Heure.

Jeffreys, H. 1961. *Theory of Probability*, Oxford University Press, p. 223.

———1960. *Bull. Geod.* No. 59, p. 43, item 2.

Markowitz, W.M. 1960. *Telescopes* G.P. Kuiper and Barbara Middlehurst, eds. University of Chicago Press.

———1969. *Earthquake Displacement Fields and the Rotation of the Earth*, L. Mansinha, D.E. Smylie and A.E. Beck, – eds. Reidel Publishing Co.

Munk, W.H. 1960, and G.J.F. MacDonald, 1960. *The Rotation of the Earth*, Cambridge University Press.

Tanner, R.W. 1967. *Time and Latitude Bulletin*, No. A45 Dom. Obs.

Thomson, M.M. 1955. *Pub. Dom. Obs.*, Vol. 15, No. 4.

Yumi, S. 1962-68. *Annual Reports of the International Polar Motion Service.*

APPENDIX A

OTTAWA PZT CATALOGUE 80 STARS IN 8 GROUPS

NO	MAG	SP	RA 1950	PM	DEC 1950	PM	BD NO
101	8.3	K0	22 59 17.438	+0.26	45 14 27.72	+02.1	44 4307
102	7.7	K0	23 08 31.452	-0.75	45 14 40.47	-27.5	44 4347
103	6.3	B9P	23 15 34.807	+0.24	45 12 56.46	-00.9	44 4373
104	8.7	K0	23 26 03.189	+0.02	45 25 03.86	-00.4	44 4424
105	8.1	A2	23 36 53.550	-0.06	45 26 34.76	-00.9	44 4464
106	8.4	F0	00 13 06.819	+0.15	45 15 58.75	-01.1	44 50
107	7.5	F5	00 17 53.264	+0.59	45 13 54.48	-00.6	44 62
108	7.4	F5	00 58 27.340	+0.96	45 11 00.60	-01.5	44 215
109	8.4	K2	01 16 06.745	-0.02	45 26 35.63	+01.8	44 279
110	8.5	K0	01 25 43.133	+0.58	45 22 31.21	+00.3	44 312
201	8.1	A5	01 54 49.045	-0.14	45 21 22.59	+00.7	44 392
202	8.4	A0	02 19 32.511	-0.07	45 16 56.77	+00.4	44 473
203	7.8	G5	02 21 50.218	-0.23	45 25 22.39	-07.8	44 483
204	8.3	F8	02 38 28.567	+0.86	45 16 54.33	-03.0	44 558
205	8.0	F8	02 41 28.822	-0.18	45 23 21.23	-04.4	44 569
206	7.5	B8	03 18 04.408	-0.06	45 12 28.61	+01.0	44 677
207	7.2	B8	03 22 11.257	-0.01	45 20 25.39	+00.2	44 695
208	8.4	K0	03 50 29.504	+0.03	45 21 53.86	-02.9	45 836
209	8.3	G5	04 07 34.442	+0.16	45 16 24.54	-04.0	45 887
210	7.6	A0	04 17 17.985	+0.22	45 20 46.01	-02.8	45 921
301	7.8	A0	04 44 15.199	+0.07	45 24 05.58	-03.3	45 987
302	7.5	B9	04 57 39.232	-0.09	45 22 25.23	-00.8	45 1023
303	8.5	A0	05 21 38.178	+0.04	45 11 04.07	+00.2	45 1115
304	8.3	G5	05 29 03.048	+0.11	45 27 22.43	-01.9	45 1132
305	8.0	F3	05 45 02.924	-0.02	45 13 17.65	-02.2	45 1178
306	7.4	A0	05 57 36.672	-0.02	45 09 35.81	-01.1	45 1225
307	7.4	A2	06 00 51.730	+0.04	45 35 24.79	-05.5	45 1235
308	7.8	A0	06 04 37.163	-0.07	45 33 44.46	-02.0	45 1248
309	8.7	K0	07 07 13.727	-0.12	45 19 48.00	-00.8	45 1394
310	7.5	K0	07 11 59.681	-0.08	45 29 52.45	-02.9	45 1408
401	8.3	K0	07 40 45.666	0.00	45 29 20.85	-02.9	45 1476
402	8.3	K0	08 08 24.269	+0.31	45 21 32.48	-00.4	45 1550
403	7.8	F0	08 30 49.208	-0.28	45 22 07.77	-02.3	45 1601
404	8.2	F5	08 40 29.395	-0.23	45 38 07.02	-05.2	45 1624
405	7.1	K0	08 48 48.223	-0.11	45 30 06.29	-03.4	45 1649
406	7.4	K0	09 18 06.177	-0.07	45 35 00.26	-03.0	45 1708
407	7.7	K0	09 43 31.098	+0.48	45 20 51.76	-13.0	45 1762
408	8.1	F2	09 47 19.985	-0.78	45 19 08.45	-09.1	45 1769
409	7.2	K0	09 54 48.110	+0.05	45 39 12.71	-03.4	46 1566
410	7.8	K0	10 25 36.216	-0.19	45 28 05.74	-02.3	45 1832

APPENDIX A

OTTAWA PZT CATALOGUE 80 STARS IN 8 GROUPS

NO	MAG	SP	RA 1950	PM	DEC 1950	PM	BD NO
501	9.2	K0	10 49 38.791	-0.71	45 33 11.54	-03.6	46 1671
502	7.8	K0	10 56 08.877	-0.48	45 27 58.78	-03.7	45 1879
503	8.4	G0	11 12 20.111	-0.48	45 20 05.54	-06.1	45 1903
504	8.2	A2	11 19 05.622	-0.56	45 36 23.76	-01.5	46 1717
505	8.1	MB	11 25 06.823	-0.07	45 27 38.85	-02.3	45 1924
506	7.5	F2	11 37 09.720	+0.15	45 26 01.66	-01.4	45 1952
507	7.8	A3	12 29 13.744	-0.26	45 30 05.68	-01.4	46 1791
508	7.5	F2	12 36 10.645	-1.35	45 29 31.93	-03.8	46 1805
509	6.7	K0	13 03 37.467	-0.18	45 32 07.59	+02.5	46 1847
510	9.0	F5	13 17 05.553	-1.38	45 21 45.35	-03.4	45 2104
601	8.4	F5	13 33 51.762	-0.44	45 16 12.86	-01.8	45 2120
602	8.8	F5	13 46 33.442	-0.35	45 25 06.48	+01.0	45 2131
603	8.4	G5	14 39 16.606	-1.10	45 37 44.50	-19.2	46 1981
604	7.1	F0	14 42 38.338	+0.52	45 23 47.74	-02.0	45 2214
605	8.0	F5	14 52 37.590	-0.62	45 30 00.78	+05.4	45 2233
606	7.4	K2	15 22 23.836	-0.16	45 26 48.66	-00.3	45 2284
607	8.2	F0	15 37 32.744	+0.27	45 16 42.39	+01.4	45 2317
608	9.0	G5	15 42 27.953	-0.41	45 28 18.99	+03.1	45 2325
609	8.2	K0	16 06 25.425	-0.03	45 30 41.78	+00.9	45 2374
610	8.4	G5	16 23 47.715	-0.64	45 29 27.16	+01.7	45 2404
701	7.9	K2	17 10 12.145	-0.01	45 23 01.21	-01.2	45 2504
702	7.3	B3	17 12 00.269	-0.12	45 25 45.49	-01.1	45 2509
703	6.9	F0	17 18 23.795	-0.36	45 21 24.36	+08.6	45 2521
704	7.9	G0	17 36 37.733	+0.02	45 35 02.75	+04.7	45 2573
705	8.6	G5	17 53 14.164	+0.41	45 33 39.90	+02.2	45 2620
706	8.2	A0	17 53 17.771	-0.07	45 13 27.28	+00.4	45 2621
707	6.2	B9	17 57 26.447	-0.07	45 28 40.95	+02.5	45 2635
708	7.7	B9	17 59 41.018	-0.11	45 21 00.40	+01.4	45 2643
709	6.9	G0	18 14 06.184	-0.81	45 11 34.49	-11.2	45 2684
710	7.3	F0	18 47 08.243	+0.26	45 12 10.34	08.5	45 2777
801	8.4	K0	19 52 12.069	-0.09	45 20 19.21	+00.1	45 3001
802	7.7	A2	20 00 11.300	+0.28	45 20 10.19	+02.3	45 3038
803	8.1	K2	20 14 58.124	+0.03	45 11 00.79	+01.6	44 3414
804	7.2	F5	20 18 11.258	+0.18	45 12 19.84	-02.0	44 3429
805	6.3	B3	20 37 41.827	-0.03	45 29 21.48	+00.2	45 3233
806	7.7	K5	20 45 37.771	-0.02	45 23 43.18	-01.8	45 3275
807	7.7	G0	21 05 05.640	-0.08	45 28 25.57	-01.0	45 3410
808	6.7	A0	21 09 27.750	-0.08	45 28 07.49	-00.6	45 3438
809	6.8	B5	21 28 08.531	-0.02	45 16 26.73	-00.5	44 3840
810	7.0	MC	21 34 08.259	+0.59	45 09 00.09	+00.9	44 3877

APPENDIX A

OTTAWA PZT CATALOGUE 160 STARS IN 12 GROUPS

NO	MAG	SP	RA 1950	PM	DEC 1950	PM	BD NO
101	8.0	F0	00 13 06.819	+0.15	45 15 58.75	-01.1	44 50
102	7.0	F5	00 17 53.264	+0.59	45 13 54.48	-00.6	44 62
103	8.5	MA	00 34 53.232	+0.12	45 19 45.53	+01.5	45 128
104	7.8	A3	00 43 40.231	-0.21	45 09 12.94	+00.5	44 162
105	8.8	A5	00 49 56.700	-0.35	45 10 13.18	-01.7	44 186
106	6.2	K0	00 54 49.201	+0.07	45 34 10.05	-00.5	45 237
107	7.0	F5	00 58 27.340	+0.96	45 11 00.60	-01.5	44 215
108	8.7	F8	01 07 03.176	+0.54	45 28 53.63	-01.5	44 252
109	7.5	K2	01 16 06.745	-0.02	45 26 35.63	+01.8	44 279
110	8.1	K0	01 25 43.133	+0.58	45 22 31.21	+00.3	44 312
111	6.3	A0	01 35 30.437	-0.16	45 08 45.40	+00.8	44 341
112	8.1	A5	01 54 49.045	-0.14	45 21 22.59	+00.7	44 392
113	8.1	A3	02 00 00.257	+0.04	45 32 14.69	-00.5	45 523
201	8.8	A0	02 19 32.511	-0.07	45 16 56.77	+00.4	44 473
202	7.6	G5	02 21 50.218	-0.23	45 25 22.39	-07.8	44 483
203	7.3	G5	02 27 10.353	+0.05	45 12 36.31	-00.8	44 512
204	8.4	F8	02 38 28.567	+0.86	45 16 54.33	-03.0	44 558
205	8.1	F8	02 41 28.822	-0.18	45 23 21.23	-04.4	44 569
206	8.6	K2	03 08 17.963	-0.19	45 33 01.83	-01.7	45 721
207	6.4	MA	03 12 40.017	+0.28	45 09 45.02	-03.0	44 648
208	7.5	B8	03 18 04.408	-0.06	45 12 28.61	+01.0	44 677
209	7.6	B8	03 22 11.257	-0.01	45 20 25.39	+00.2	44 695
210	8.1	K2	03 31 35.567	-0.13	45 16 59.78	-00.1	44 744
211	8.1	K0	03 48 07.130	-0.10	45 18 15.14	+00.3	45 828
212	7.9	K0	03 50 29.504	+0.03	45 21 53.86	-02.9	45 836
213	8.6	A0	03 56 23.122	+0.14	45 33 25.26	-01.2	45 858
301	7.8	G5	04 07 34.442	+0.16	45 16 24.54	-04.0	45 887
302	7.6	A0	04 17 17.985	+0.22	45 20 46.01	-02.8	45 921
303	7.7	B9	04 30 27.468	0.00	45 31 54.87	-01.0	45 955
304	7.7	A0	04 44 15.199	+0.07	45 24 05.58	-03.3	45 987
305	7.8	B9	04 57 39.232	-0.09	45 22 25.23	-00.8	45 1023
306	8.5	A0	05 21 38.178	+0.04	45 11 04.07	+00.2	45 1115
307	7.8	F8	05 28 57.611	-0.06	45 30 07.03	-03.5	45 1131
308	7.9	G5	05 29 03.048	+0.11	45 27 22.43	-01.9	45 1132
309	8.1	G5	05 35 20.203	+0.70	45 25 18.24	-10.8	45 1150
310	8.0	F3	05 45 02.924	-0.02	45 13 17.65	-02.2	45 1178
311	6.6	A0	05 55 42.894	-0.01	45 37 00.50	-01.6	45 1216
312	7.6	A0	05 57 36.672	-0.02	45 09 35.81	-01.1	45 1225
313	7.2	A2	06 00 51.730	+0.04	45 35 24.79	-05.5	45 1235

APPENDIX A

OTTAWA PZT CATALOGUE 160 STARS IN 12 GROUPS

NO	MAG	SP	RA 1950	PM	DEC 1950	PM	BD NO
401	7.3	A0	06 04 37.163	-0.07	45 33 44.46	-02.0	45 1248
402	7.4	K0	06 18 03.542	+0.05	45 38 07.59	-01.5	45 1289
403	8.0	K5	06 20 52.448	+0.13	45 11 41.50	+00.3	45 1296
404	8.7	G5	06 40 22.174	+0.09	45 24 50.05	-03.2	45 1346
405	9.0	A2	06 50 50.710	-0.12	45 14 51.16	-04.1	45 1363
406	8.9	A0	06 59 55.120	-0.02	45 30 01.47	-00.7	45 1380
407	7.8	K0	07 07 13.727	-0.12	45 19 48.00	-00.8	45 1394
408	6.7	K0	07 11 59.681	-0.08	45 29 52.45	-02.9	45 1408
409	7.6	F2	07 14 24.115	-0.08	45 13 13.09	-06.9	45 1415
410	8.1	G5	07 27 57.558	-0.08	45 13 06.75	-02.3	45 1441
411	7.6	K0	07 40 45.666	0.00	45 29 20.85	-02.9	45 1476
412	8.0	K2	07 46 59.001	+0.09	45 28 04.63	-01.0	45 1496
413	8.1	A3	07 53 21.691	-0.19	45 35 03.40	-01.1	45 1509
501	7.8	K0	08 08 24.269	+0.31	45 21 32.48	-00.4	45 1550
502	8.1	K0	08 19 05.887	-0.37	45 30 45.09	-07.3	45 1568
503	7.8	F0	08 30 49.208	-0.28	45 22 07.77	-02.3	45 1601
504	8.1	G5	08 37 33.122	0.00	45 19 40.22	+01.5	45 1613
505	8.1	F5	08 40 29.395	-0.23	45 38 07.02	-05.2	45 1624
506	6.1	K0	08 48 48.223	-0.11	45 30 06.29	-03.4	45 1649
507	8.4	G5	09 03 59.561	-0.58	45 22 41.90	-04.9	45 1680
508	6.6	K0	09 18 06.177	-0.07	45 35 00.26	-03.0	45 1708
509	6.8	K0	09 43 31.098	+0.48	45 20 51.76	-13.0	45 1762
510	8.0	F2	09 47 19.985	-0.78	45 19 08.45	-09.1	45 1769
511	8.7	G5	09 52 36.884	+0.16	45 25 08.06	-00.9	45 1778
512	6.5	K0	09 54 48.110	+0.05	45 39 12.71	-03.4	45 1566
513	7.5	F2	10 04 02.073	-0.07	45 18 15.91	-00.6	45 1798
601	7.8	K2	10 11 08.518	-0.09	45 20 07.72	+00.4	45 1811
602	7.4	F5	10 13 27.840	-0.13	45 17 34.24	+02.3	45 1814
603	7.8	G5	10 14 27.401	-0.63	45 16 09.23	-02.0	45 1819
604	6.5	K0	10 25 36.216	-0.19	45 28 05.74	-02.3	45 1832
605	8.4	K5	10 32 46.110	-0.22	45 30 56.13	+01.6	46 1643
606	8.0	K0	10 49 38.791	-0.71	45 33 11.54	-03.6	46 1671
607	7.0	K0	10 56 08.877	-0.48	45 27 58.78	-03.7	45 1879
608	9.0	G5	11 01 40.650	+0.09	45 25 37.76	-02.6	45 1890
609	7.5	G0	11 12 20.111	-0.48	45 20 05.54	-06.1	45 1903
610	7.9	A2	11 19 05.622	-0.56	45 36 23.76	-01.5	46 1717
611	*	MB	11 25 06.823	-0.07	45 27 38.85	-02.3	45 1924
612	8.4	G0	11 36 07.336	-5.62	45 23 06.63	+01.4	45 1947
613	7.9	F2	11 37 09.720	+0.15	45 26 01.66	-01.4	45 1952

* 611, MAG 6.5 TO 7.3

APPENDIX A

OTTAWA PZT CATALOGUE 160 STARS IN 12 GROUPS

NO	MAG	SP	RA 1950	PM	DEC 1950	PM	BD NO
701	8.8	F8	12 08 12.935	+0.30	45 27 13.91	-06.5	45 2001
702	7.7	A3	12 29 13.744	-0.26	45 30 05.68	-01.4	46 1791
703	8.0	F0	12 35 10.360	+0.15	45 31 41.96	+01.2	46 1802
704	7.1	F2	12 36 10.645	-1.35	45 29 31.93	-03.8	46 1805
705	6.7	K0	13 03 37.467	-0.18	45 32 07.59	+02.5	46 1847
706	8.6	F5	13 12 12.560	-0.02	45 26 41.46	-01.0	45 2096
707	8.7	F5	13 17 05.553	-1.38	45 21 45.35	-03.4	45 2104
708	8.3	F5	13 33 51.762	-0.44	45 16 12.86	-01.8	45 2120
709	8.0	K2	13 38 14.810	+0.03	45 14 24.05	-01.1	45 2124
710	8.9	F5	13 41 17.137	+0.06	45 35 46.83	-01.8	46 1894
711	8.6	F5	13 46 33.442	-0.35	45 25 06.48	+01.0	45 2131
712	8.6	F8	13 55 33.197	-0.08	45 23 55.73	+00.1	45 2140
713	6.1	K0	13 59 10.965	+0.17	45 31 36.54	-00.8	45 2148
801	9.1	G5	14 22 45.835	-1.45	45 22 22.42	+03.4	45 2178
802	8.4	F8	14 35 54.203	-0.07	45 32 45.40	-01.7	45 2203
803	7.7	G5	14 39 16.606	-1.10	45 37 44.50	-19.2	46 1981
804	6.8	F0	14 42 38.338	+0.52	45 23 47.74	-02.0	45 2214
805	8.5	F8	14 49 57.387	-0.68	45 22 33.50	+06.8	45 2230
806	7.9	F5	14 52 37.590	-0.62	45 30 00.78	+05.4	45 2233
807	8.7	G5	15 10 23.099	-0.86	45 20 56.51	+15.4	45 2266
808	7.9	K0	15 16 56.988	-0.39	45 11 52.82	+00.9	45 2277
809	6.2	K2	15 22 23.836	-0.16	45 26 48.66	-00.3	45 2284
810	8.8	K2	15 34 00.418	+0.15	45 36 45.90	-02.1	45 2307
811	7.9	F0	15 37 32.744	+0.27	45 16 42.39	+01.4	45 2317
812	8.0	G5	15 42 27.953	-0.41	45 28 18.99	+03.1	45 2325
813	8.7	F2	15 58 07.352	-0.27	45 35 35.49	-00.5	45 2355
901	7.4	K0	16 06 25.425	-0.03	45 30 41.78	+00.9	45 2374
902	7.4	G5	16 23 47.715	-0.64	45 29 27.16	+01.7	45 2404
903	8.4	G5	16 43 41.730	-0.28	45 11 37.83	-00.5	45 2446
904	8.4	G0	16 47 27.468	-0.33	45 17 12.85	-00.7	45 2453
905	6.9	K2	17 10 12.145	-0.01	45 23 01.21	-01.2	45 2504
906	7.4	B3	17 12 00.269	-0.12	45 25 45.49	-01.1	45 2509
907	6.6	F0	17 18 23.795	-0.36	45 21 24.36	+08.6	45 2521
908	8.3	K0	17 23 11.751	-0.06	45 23 44.14	+01.3	45 2531
909	7.3	G0	17 36 37.733	+0.02	45 35 02.75	+04.7	45 2573
910	8.2	G5	17 53 14.164	+0.41	45 33 39.90	+02.2	45 2620
911	8.0	A0	17 53 17.771	-0.07	45 13 27.28	+00.4	45 2621
912	6.2	B9	17 57 26.447	-0.07	45 28 40.95	+02.5	45 2635
913	5.9	K2	17 58 30.393	-0.05	45 30 09.87	-03.0	45 2638
914	7.4	B9	17 59 41.018	-0.11	45 21 00.40	+01.4	45 2643

APPENDIX A

OTTAWA PZT CATALOGUE 160 STARS IN 12 GROUPS

NO	MAG	SP	RA 1950	PM	DEC 1950	PM	BD NO
1001	8.5	F0	18 08 22.099	+0.02	45 36 21.48	-01.8	45 2667
1002	6.3	G0	18 14 06.184	-0.81	45 11 34.49	-11.2	45 2684
1003	7.9	A0	18 16 45.251	-0.01	45 08 07.24	+00.8	45 2690
1004	8.1	A0	18 21 37.358	0.00	45 11 34.56	+03.0	45 2704
1005	8.5	K0	18 29 41.225	+0.33	45 25 10.42	+00.2	45 2731
1006	8.0	F0	18 35 47.805	-0.10	45 37 38.61	+01.1	45 2747
1007	6.8	F0	18 47 08.243	+0.26	45 12 10.34	+08.5	45 2777
1008	8.9	F5	19 02 16.826	+0.18	45 31 58.28	-00.9	45 2824
1009	7.3	A0	19 13 56.282	+0.10	45 14 48.09	-01.0	45 2865
1010	8.6	K	19 18 55.970	-0.07	45 29 58.90	+00.6	45 2877
1011	7.5	K0	19 44 44.962	-0.04	45 36 45.24	-00.8	45 2971
1012	7.8	K0	19 52 12.069	-0.09	45 20 19.21	+00.1	45 3001
1013	7.5	A2	20 00 11.300	+0.28	45 20 10.19	+02.3	45 3038
1014	8.1	G5	20 06 32.283	-0.12	45 23 48.25	-03.3	45 3066
1101	7.5	K2	20 14 58.124	+0.03	45 11 00.79	+01.6	44 3414
1102	7.0	F5	20 18 11.258	+0.18	45 12 19.84	-02.0	44 3429
1103	7.3	B9	20 27 09.446	0.00	45 33 04.86	-00.5	45 3191
1104	6.5	G3	20 37 41.827	-0.03	45 29 21.48	+00.2	45 3233
1105	6.7	K5	20 45 37.771	-0.02	45 23 43.18	-01.8	45 3275
1106	7.5	A0	20 46 42.881	+0.04	45 15 58.32	+00.1	44 3590
1107	8.2	G7	20 51 47.539	+0.14	45 11 36.86	+00.1	44 3622
1108	7.3	G0	21 05 05.640	-0.08	45 28 25.57	-01.0	45 3410
1109	6.7	A0	21 09 27.750	-0.08	45 28 07.49	-00.6	45 3438
1110	7.6	B9	21 14 09.125	-0.03	45 31 20.27	-00.7	45 3476
1111	8.5	G0	21 26 15.499	-0.01	45 21 34.44	-03.7	44 3825
1112	7.0	B5	21 28 08.531	-0.02	45 16 26.73	-00.5	44 3840
1113	*	MC	21 34 08.259	0.59	45 09 00.09	00.9	44 3877
1114	6.5	MB	21 40 13.484	-0.07	45 32 13.60	-01.7	45 3637
1201	6.5	G5	22 06 39.422	-0.56	45 29 45.59	05.1	45 3813
1202	7.3	A2	22 24 54.875	-0.25	45 32 03.82	-01.5	45 3941
1203	8.2	K2	22 27 45.273	-0.05	45 29 17.24	00.5	45 3958
1204	7.9	K0	22 35 36.991	-0.19	45 08 52.98	00.5	44 4183
1205	7.1	F8	22 36 02.557	-1.05	45 34 11.50	-16.9	45 4002
1206	8.3	K2	22 41 01.671	0.06	45 15 57.76	1.7	44 4209
1207	8.1	K0	22 50 58.151	-0.02	45 25 37.18	0.1	44 4263
1208	8.4	F8	22 53 55.366	-0.16	45 31 29.35	-03.7	45 4094
1209	7.9	K0	22 59 17.438	0.26	45 14 27.72	2.1	44 4307
1210	8.8	F5	23 01 58.620	0.17	45 12 42.42	0.8	44 4320
1211	7.1	K0	23 08 31.452	-0.75	45 14 40.47	-27.5	44 4347
1212	6.3	B9	23 15 34.807	0.24	45 12 56.46	-00.9	44 4373
1213	7.9	K0	23 26 03.189	0.02	45 25 03.86	-00.4	44 4424
1214	7.8	A2	23 36 53.550	-0.06	45 26 34.76	-00.9	44 4464

* 1113, MAG 5.0 TO 6.7

APPENDIX B
OTTAWA PZT OBSERVATIONS 1956 TO 1970
VALUES AT 1/20 YEAR

EPOCH	LATITUDE	UTO-A1	EPOCH	LATITUDE	UTO-A1
56.05	38.768	.7958	58.55	38.777	-0.3096
56.10	38.820	.7910	58.60	38.792	-0.3044
56.15	38.831	.7634	58.65	38.742	-0.3283
56.20	38.821	.7330	58.70	38.718	-0.3440
56.25	38.722	.7032	58.75	38.645	-0.3684
56.30	38.692	.6786	58.80	38.473	-0.4031
56.35	38.630	.6700	58.85	38.429	-0.4511
56.40	38.503	.6497	58.90	38.450	-0.4696
56.45	38.536	.6367	58.95	38.459	-0.4922
56.50	38.500	.6307	59.00	38.320	-0.5329
56.55	38.464	.6394	59.05	38.361	-0.5498
56.60	38.425	.6451	59.10	38.444	-0.5624
56.65	38.433	.6378	59.15	38.478	-0.6023
56.70	38.309	.6352	59.20	38.465	-0.6376
56.75	38.401	.5993	59.25	38.469	-0.6573
56.80	38.428	.5882	59.30	38.551	-0.6791
56.85	38.447	.5590	59.35	38.625	-0.6951
56.90	38.488	.5610	59.40	38.680	-0.7140
56.95	38.516	.5145	59.45	38.741	-0.7393
57.00	38.541	.5001	59.50	38.790	-0.7478
57.05	38.646	.4757	59.55	38.792	-0.7638
57.10	38.737	.4665	59.60	38.812	-0.7686
57.15	38.820	.4356	59.65	38.812	-0.8168
57.20	38.851	.3950	59.70	38.836	-0.8208
57.25	38.838	.3614	59.75	38.838	-0.8426
57.30	38.827	.3298	59.80	38.732	-0.8914
57.35	38.869	.2967	59.85	38.687	-0.9192
57.40	38.808	.2671	59.90	38.683	-0.9533
57.45	38.763	.2479	59.95	38.540	-0.9825
57.50	38.704	.2228	60.00	38.528	-1.0108
57.55	38.673	.2190	60.05	38.529	-1.0373
57.60	38.638	.2086	60.10	38.386	-1.0559
57.65	38.582	.1764	60.15	38.554	-1.0791
57.70	38.467	.1750	60.20	38.482	-1.1014
57.75	38.405	.1371	60.25	38.464	-1.1347
57.80	38.355	.1179	60.30	38.468	-1.1647
57.85	38.301	.0909	60.35	37.232	-1.1862
57.90	38.284	.0565	60.40	37.326	-1.2140
57.95	38.298	.0390	60.45	37.325	-1.2402
58.00	38.341	.0277	60.50	37.345	-1.2583

APPENDIX B

OTTAWA PZT OBSERVATIONS 1956 TO 1970

VALUES AT 1/20 YEAR

EPOCH	LATITUDE	UT0-A1	EPOCH	LATITUDE	UT0-A1
58.05	38.388	-0.0244	60.55	37.394	-1.2645
58.10	38.474	-0.0457	60.60	37.451	-1.2677
58.15	38.551	-0.0782	60.65	37.427	-1.2852
58.20	38.612	-0.1151	60.70	37.484	-1.2986
58.25	38.649	-0.1513	60.75	37.462	-1.3235
58.30	38.690	-0.1929	60.80	37.471	-1.3488
58.35	38.776	-0.2219	60.85	37.465	-1.3760
58.40	38.836	-0.2499	60.90	37.481	-1.4074
58.45	38.845	-0.2719	60.95	37.497	-1.4356
58.50	38.882	-0.2875	61.00	37.427	-1.4571
61.05	37.409	-1.4667	63.55	37.367	-2.6277
61.10	37.387	-1.4938	63.60	37.318	-2.6402
61.15	37.348	-1.5127	63.65	37.279	-2.6552
61.20	37.336	-1.5423	63.70	37.240	-2.6781
61.25	37.348	-1.5727	63.75	37.187	-2.7044
61.30	37.337	-1.5977	63.80	37.129	-2.7370
61.35	37.342	-1.6187	63.85	37.103	-2.7721
61.40	37.301	-1.6469	63.90	37.130	-2.8063
61.45	37.314	-1.6611	63.95	37.183	-2.8388
61.50	37.330	-1.6712	64.00	37.192	-2.8751
61.55	37.330	-1.6766	64.05	37.293	-2.9115
61.60	37.349	-1.6894	64.10	37.332	-2.9466
61.65	37.304	-1.7072	64.15	37.403	-2.9866
61.70	37.330	-1.7181	64.20	37.459	-3.0287
61.75	37.323	-1.7341	64.25	37.519	-3.0731
61.80	37.341	-1.7539	64.30	37.556	-3.1157
61.85	37.364	-1.7736	64.35	37.593	-3.1586
61.90	37.386	-1.8015	64.40	37.603	-3.2048
61.95	37.399	-1.8257	64.45	37.576	-3.2408
62.00	37.449	-1.8521	64.50	37.533	-3.2658
62.05	37.417	-1.8790	64.55	37.544	-3.2913
62.10	37.385	-1.8984	64.60	37.486	-3.3171
62.15	37.448	-1.9263	64.65	37.463	-3.3396
62.20	37.486	-1.9544	64.70	37.410	-3.3636
62.25	37.465	-1.9859	64.75	37.343	-3.4025
62.30	37.428	-2.0167	64.80	37.280	-3.4435
62.35	37.435	-2.0489	64.85	37.226	-3.4836
62.40	37.400	-2.0791	64.90	37.176	-3.5220
62.45	37.349	-2.0998	64.95	37.159	-3.5605
62.50	37.317	-2.1073	65.00	37.164	-3.5930

APPENDIX B

OTTAWA PZT OBSERVATIONS 1956 TO 1970

VALUES AT 1/20 YEAR

EPOCH	LATITUDE	UT0-A1	EPOCH	LATITUDE	UT0-A1
62.55	37.312	-2.1179	65.05	37.185	-3.6270
62.60	37.269	-2.1319	65.10	37.238	-3.6647
62.65	37.250	-2.1440	65.15	37.221	-3.7029
62.70	37.234	-2.1574	65.20	37.284	-3.7442
62.75	37.273	-2.1799	65.25	37.354	-3.7932
62.80	37.267	-2.2025	65.30	37.394	-3.8422
62.85	37.254	-2.2340	65.35	37.421	-3.8864
62.90	37.277	-2.2630	65.40	37.450	-3.9263
62.95	37.333	-2.2939	65.45	37.519	-3.9662
63.00	37.397	-2.3237	65.50	37.543	-4.0019
63.05	37.432	-2.3390	65.55	37.565	-4.0395
63.10	37.439	-2.3618	65.60	37.592	-4.0731
63.15	37.481	-2.3853	65.65	37.533	-4.0999
63.20	37.512	-2.4156	65.70	37.535	-4.1408
63.25	37.496	-2.4492	65.75	37.486	-4.1888
63.30	37.513	-2.4853	65.80	37.402	-4.2346
63.35	37.486	-2.5228	65.85	37.388	-4.2800
63.40	37.482	-2.5572	65.90	37.363	-4.3248
63.45	37.454	-2.5865	65.95	37.292	-4.3700
63.50	37.385	-2.6108	66.00	37.242	-4.4120
66.05	37.235	-4.4503	68.05	37.330	-6.1874
66.10	37.202	-4.4977	68.10	37.356	-6.2368
66.15	37.206	-4.5399	68.15	37.383	-6.2919
66.20	37.194	-4.5800	68.20	37.348	-6.3391
66.25	37.226	-4.6291	68.25	37.397	-6.3835
66.30	37.254	-4.6785	68.30	37.400	-6.4460
66.35	37.283	-4.7304	68.35	37.391	-6.4979
66.40	37.323	-4.7779	68.40	37.353	-6.5468
66.45	37.354	-4.8179	68.45	37.361	-6.5895
66.50	37.387	-4.8543	68.50	37.289	-6.6279
66.55	37.438	-4.8839	68.55	37.296	-6.6586
66.60	37.459	-4.9174	68.60	37.301	-6.6847
66.65	37.489	-4.9555	68.65	37.380	-6.7312
66.70	37.526	-4.9999	68.70	37.276	-6.7727
66.75	37.543	-5.0478	68.75	37.303	-6.8139
66.80	37.503	-5.1020	68.80	37.270	-6.8619
66.85	37.520	-5.1554	68.85	37.295	-6.9131
66.90	37.422	-5.2066	68.90	37.312	-6.9620
66.95	37.356	-5.2516	68.95	37.349	-7.0077
67.00	37.356	-5.2926	69.00	37.334	-7.0541

APPENDIX B
OTTAWA PZT OBSERVATIONS 1956 TO 1970
VALUES AT 1/20 YEAR

EPOCH	LATITUDE	UTO-A1	EPOCH	LATITUDE	UTO-A1
67.05	37.302	-5.3354	69.05	37.364	-7.0973
67.10	37.310	-5.3724	69.10	37.378	-7.1479
67.15	37.276	-5.4212	69.15	37.440	-7.2016
67.20	37.281	-5.4712	69.20	37.496	-7.2581
67.25	37.253	-5.5211	69.25	37.448	-7.3167
67.30	37.266	-5.5718	69.30	37.477	-7.3771
67.35	37.289	-5.6233	69.35	37.512	-7.4326
67.40	37.251	-5.6712	69.40	37.467	-7.4885
67.45	37.234	-5.7111	69.45	37.436	-7.5385
67.50	37.296	-5.7437	69.50	37.450	-7.5736
67.55	37.350	-5.7745	69.55	37.368	-7.6127
67.60	37.334	-5.8007	69.60	37.409	-7.6517
67.65	37.353	-5.8326	69.65	37.383	-7.6820
67.70	37.385	-5.8678	69.70	37.348	-7.7294
67.75	37.390	-5.9091	69.75	37.299	-7.7811
67.80	37.340	-5.9546	69.80	37.294	-7.8265
67.85	37.393	-6.0023	69.85	37.307	-7.8820
67.90	37.337	-6.0511	69.90	37.295	-7.9299
67.95	37.351	-6.1014	69.95	37.255	-7.9804
68.00	37.442	-6.1515	70.00	37.321	-8.0356

APPENDIX B

OTTAWA PZT OBSERVATIONS 1956 TO 1970
10 DAY SMOOTHED VALUES

JULIAN DAY	LATITUDE	UTO-A1	JULIAN DAY	LATITUDE	UTO-A1
2435509.5	38.822	.7910	2436009.5	38.742	.2390
2435519.5	38.834	.7782	2436019.5	38.712	.2284
2435529.5	38.835	.7597	2436029.5	38.695	.2206
2435539.5	38.832	.7450	2436039.5	38.669	.2181
2435549.5	38.803	.7280	2436049.5	38.645	.2163
2435559.5	38.771	.7109	2436059.5	38.619	.2073
2435569.5	38.741	.6940	2436069.5	38.605	.1894
2435579.5	38.723	.6808	2436079.5	38.563	.1775
2435589.5	38.689	.6743	2436089.5	38.512	.1706
2435599.5	38.641	.6702	2436099.5	38.452	.1628
2435609.5	38.574	.6664	2436109.5	38.412	.1465
2435619.5	38.524	.6547	2436119.5	38.388	.1340
2435629.5	38.521	.6430	2436129.5	38.364	.1217
2435639.5	38.532	.6366	2436139.5	38.321	.1103
2435649.5	38.518	.6342	2436149.5	38.291	.0938
2435659.5	38.493	.6346	2436159.5	38.288	.0804
2435669.5	38.473	.6351	2436169.5	38.285	.0663
2435679.5	38.446	.6402	2436179.5	38.288	.0565
2435689.5	38.432	.6455	2436189.5	38.325	.0428
2435699.5	38.438	.6465	2436199.5	38.371	.0280
2435709.5	38.431	.6426	2436209.5	38.407	.0091
2435719.5	38.375	.6378	2436219.5	38.420	-0.0101
2435729.5	38.343	.6318	2436229.5	38.434	-0.0283
2435739.5	38.362	.6160	2436239.5	38.448	-0.0444
2435749.5	38.399	.6043	2436249.5	38.487	-0.0612
2435759.5	38.418	.5894	2436259.5	38.533	-0.0792
2435769.5	38.420	.5759	2436269.5	38.566	-0.0975
2435779.5	38.440	.5648	2436279.5	38.590	-0.1142
2435789.5	38.459	.5625	2436289.5	38.621	-0.1333
2435799.5	38.476	.5552	2436299.5	38.654	-0.1572
2435809.5	38.490	.5427	2436309.5	38.679	-0.1830
2435819.5	38.507	.5272	2436319.5	38.708	-0.2019
2435829.5	38.523	.5111	2436329.5	38.752	-0.2162
2435839.5	38.551	.4984	2436339.5	38.804	-0.2299
2435849.5	38.584	.4864	2436349.5	38.833	-0.2450
2435859.5	38.633	.4730	2436359.5	38.846	-0.2599
2435869.5	38.686	.4621	2436369.5	38.853	-0.2722
2435879.5	38.746	.4560	2436379.5	38.856	-0.2802
2435889.5	38.793	.4453	2436389.5	38.823	-0.2896
2435899.5	38.828	.4250	2436399.5	38.796	-0.3003

APPENDIX B
OTTAWA PZT OBSERVATIONS 1956 TO 1970
10 DAY SMOOTHED VALUES

JULIAN DAY	LATITUDE	UTO-A1	JULIAN DAY	LATITUDE	UTO-A1
2435909.5	38.843	.4018	2436409.5	38.782	-0.3072
2435919.5	38.840	.3810	2436419.5	38.785	-0.3070
2435929.5	38.851	.3647	2436429.5	38.784	-0.3084
2435939.5	38.846	.3476	2436439.5	38.758	-0.3206
2435949.5	38.841	.3296	2436449.5	38.712	-0.3384
2435959.5	38.850	.3097	2436459.5	38.670	-0.3507
2435969.5	38.870	.2930	2436469.5	38.652	-0.3554
2435979.5	38.854	.2767	2436479.5	38.601	-0.3652
2435989.5	38.807	.2627	2436489.5	38.534	-0.3830
2435999.5	38.772	.2493	2436499.5	38.480	-0.4097
2436509.5	38.455	-0.4345	2437009.5	38.489	-1.1041
2436519.5	38.450	-0.4534	2437019.5	38.469	-1.1223
2436529.5	38.454	-0.4598	2437029.5	38.460	-1.1413
2436539.5	38.461	-0.4668	2437039.5	38.463	-1.1572
2436549.5	38.456	-0.4824	2437049.5	38.465	-1.1695
2436559.5	38.416	-0.5082	2437059.5	38.489	-1.1828
2436569.5	38.382	-0.5297	2437069.5	38.519	-1.1967
2436579.5	38.365	-0.5443	2437079.5	37.305	-1.2120
2436589.5	38.392	-0.5506	2437089.5	37.320	-1.2262
2436599.5	38.419	-0.5570	2437099.5	37.332	-1.2380
2436609.5	38.444	-0.5673	2437109.5	37.342	-1.2466
2436619.5	38.467	-0.5876	2437119.5	37.366	-1.2530
2436629.5	38.468	-0.6118	2437129.5	37.388	-1.2584
2436639.5	38.469	-0.6316	2437139.5	37.411	-1.2623
2436649.5	38.447	-0.6452	2437149.5	37.437	-1.2661
2436659.5	38.470	-0.6559	2437159.5	37.449	-1.2726
2436669.5	38.519	-0.6676	2437169.5	37.439	-1.2825
2436679.5	38.555	-0.6805	2437179.5	37.446	-1.2908
2436689.5	38.580	-0.6896	2437189.5	37.464	-1.2988
2436699.5	38.618	-0.6960	2437199.5	37.478	-1.3094
2436709.5	38.650	-0.7049	2437209.5	37.470	-1.3238
2436719.5	38.688	-0.7202	2437219.5	37.471	-1.3382
2436729.5	38.718	-0.7333	2437229.5	37.467	-1.3521
2436739.5	38.750	-0.7403	2437239.5	37.465	-1.3669
2436749.5	38.778	-0.7462	2437249.5	37.470	-1.3829
2436759.5	38.789	-0.7533	2437259.5	37.483	-1.3991
2436769.5	38.807	-0.7582	2437269.5	37.491	-1.4145
2436779.5	38.814	-0.7617	2437279.5	37.483	-1.4307
2436789.5	38.817	-0.7752	2437289.5	37.469	-1.4448
2436799.5	38.798	-0.7959	2437299.5	37.450	-1.4536

APPENDIX B
OTTAWA PZT OBSERVATIONS 1956 TO 1970
10 DAY SMOOTHED VALUES

JULIAN DAY	LATITUDE	UT0-A1	JULIAN DAY	LATITUDE	UT0-A1
2436809.5	38.797	-0.8116	2437309.5	37.432	-1.4595
2436819.5	38.815	-0.8195	2437319.5	37.414	-1.4698
2436829.5	38.837	-0.8286	2437329.5	37.396	-1.4827
2436839.5	38.820	-0.8442	2437339.5	37.374	-1.4946
2436849.5	38.774	-0.8631	2437349.5	37.360	-1.5059
2436859.5	38.728	-0.8844	2437359.5	37.348	-1.5209
2436869.5	38.712	-0.9023	2437369.5	37.340	-1.5366
2436879.5	38.701	-0.9196	2437379.5	37.342	-1.5527
2436889.5	38.576	-0.9355	2437389.5	37.346	-1.5684
2436899.5	38.632	-0.9531	2437399.5	37.343	-1.5837
2436909.5	38.588	-0.9705	2437409.5	37.337	-1.5959
2436919.5	38.545	-0.9871	2437419.5	37.338	-1.6079
2436929.5	38.526	-1.0021	2437429.5	37.334	-1.6207
2436939.5	38.525	-1.0174	2437439.5	37.327	-1.6346
2436949.5	38.521	-1.0318	2437449.5	37.320	-1.6458
2436959.5	38.485	-1.0435	2437459.5	37.314	-1.6553
2436969.5	38.450	-1.0536	2437469.5	37.311	-1.6636
2436979.5	38.471	-1.0642	2437479.5	37.324	-1.6699
2436989.5	38.505	-1.0768	2437489.5	37.334	-1.6729
2436999.5	38.510	-1.0894	2437499.5	37.329	-1.6763
2437509.5	37.332	-1.6819	2438009.5	37.319	-2.2874
2437519.5	37.337	-1.6894	2438019.5	37.354	-2.3050
2437529.5	37.327	-1.6990	2438029.5	37.381	-2.3208
2437539.5	37.306	-1.7086	2438039.5	37.405	-2.3315
2437549.5	37.315	-1.7149	2438049.5	37.422	-2.3403
2437559.5	37.324	-1.7202	2438059.5	37.434	-2.3514
2437569.5	37.320	-1.7291	2438069.5	37.446	-2.3651
2437579.5	37.320	-1.7401	2438079.5	37.467	-2.3779
2437589.5	37.335	-1.7509	2438089.5	37.492	-2.3917
2437599.5	37.350	-1.7616	2438099.5	37.505	-2.4069
2437609.5	37.358	-1.7732	2438109.5	37.507	-2.4250
2437619.5	37.371	-1.7866	2438119.5	37.509	-2.4440
2437629.5	37.384	-1.8011	2438129.5	37.513	-2.4638
2437639.5	37.390	-1.8155	2438139.5	37.509	-2.4835
2437649.5	37.399	-1.8290	2438149.5	37.496	-2.5040
2437659.5	37.426	-1.8434	2438159.5	37.486	-2.5249
2437669.5	37.443	-1.8585	2438169.5	37.485	-2.5436
2437679.5	37.426	-1.8723	2438179.5	37.477	-2.5609
2437689.5	37.397	-1.8842	2438189.5	37.457	-2.5767
2437699.5	37.388	-1.8954	2438199.5	37.435	-2.5915

APPENDIX B
OTTAWA PZT OBSERVATIONS 1956 TO 1970
10 DAY SMOOTHED VALUES

JULIAN DAY	LATITUDE	UTO-A1	JULIAN DAY	LATITUDE	UTO-A1
2437709.5	37.409	-1.9089	2438209.5	37.410	-2.6050
2437719.5	37.445	-1.9244	2438219.5	37.383	-2.6166
2437729.5	37.480	-1.9403	2438229.5	37.361	-2.6261
2437739.5	37.486	-1.9556	2438239.5	37.343	-2.6330
2437749.5	37.473	-1.9722	2438249.5	37.321	-2.6401
2437759.5	37.455	-1.9897	2438259.5	37.294	-2.6477
2437769.5	37.440	-2.0072	2438269.5	37.267	-2.6570
2437779.5	37.436	-2.0241	2438279.5	37.251	-2.6684
2437789.5	37.431	-2.0412	2438289.5	37.229	-2.6816
2437799.5	37.414	-2.0578	2438299.5	37.202	-2.6963
2437809.5	37.395	-2.0736	2438309.5	37.171	-2.7119
2437819.5	37.374	-2.0877	2438319.5	37.139	-2.7298
2437829.5	37.356	-2.0982	2438329.5	37.110	-2.7490
2437839.5	37.334	-2.1051	2438339.5	37.112	-2.7689
2437849.5	37.321	-2.1093	2438349.5	37.138	-2.7874
2437859.5	37.320	-2.1138	2438359.5	37.151	-2.8053
2437869.5	37.308	-2.1204	2438369.5	37.158	-2.8240
2437879.5	37.289	-2.1277	2438379.5	37.174	-2.8420
2437889.5	37.268	-2.1349	2438389.5	37.182	-2.8611
2437899.5	37.249	-2.1418	2438399.5	37.205	-2.8805
2437909.5	37.231	-2.1485	2438409.5	37.252	-2.9011
2437919.5	37.236	-2.1569	2438419.5	37.306	-2.9209
2437929.5	37.255	-2.1675	2438429.5	37.328	-2.9412
2437939.5	37.269	-2.1791	2438439.5	37.358	-2.9616
2437949.5	37.273	-2.1909	2438449.5	37.392	-2.9827
2437959.5	37.266	-2.2054	2438459.5	37.424	-3.0051
2437969.5	37.257	-2.2221	2438469.5	37.456	-3.0292
2437979.5	37.257	-2.2388	2438479.5	37.490	-3.0537
2437989.5	37.268	-2.2550	2438489.5	37.521	-3.0775
2437999.5	37.288	-2.2706	2438499.5	37.541	-3.1007
2438509.5	37.564	-3.1239	2439009.5	37.542	-4.1245
2438519.5	37.583	-3.1476	2439019.5	37.538	-4.1484
2438529.5	37.598	-3.1723	2439029.5	37.508	-4.1735
2438539.5	37.600	-3.1972	2439039.5	37.462	-4.1988
2438549.5	37.596	-3.2199	2439049.5	37.425	-4.2235
2438559.5	37.574	-3.2387	2439059.5	37.394	-4.2487
2438569.5	37.549	-3.2535	2439069.5	37.379	-4.2746
2438579.5	37.535	-3.2660	2439079.5	37.360	-4.2998
2438589.5	37.547	-3.2803	2439089.5	37.340	-4.3239
2438599.5	37.534	-3.2955	2439099.5	37.324	-4.3478

APPENDIX B
OTTAWA PZT OBSERVATIONS 1956 TO 1970
10 DAY SMOOTHED VALUES

JULIAN DAY	LATITUDE	UTO-A1	JULIAN DAY	LATITUDE	UTO-A1
2438609.5	37.509	-3.3099	2439109.5	37.299	-4.3721
2438619.5	37.489	-3.3225	2439119.5	37.276	-4.3958
2438629.5	37.475	-3.3347	2439129.5	37.258	-4.4181
2438639.5	37.439	-3.3466	2439139.5	37.245	-4.4399
2438649.5	37.406	-3.3607	2439149.5	37.223	-4.4621
2438659.5	37.389	-3.3791	2439159.5	37.210	-4.4873
2438669.5	37.356	-3.4002	2439169.5	37.209	-4.5127
2438679.5	37.306	-3.4222	2439179.5	37.205	-4.5357
2438689.5	37.274	-3.4455	2439189.5	37.198	-4.5569
2438699.5	37.252	-3.4682	2439199.5	37.191	-4.5798
2438709.5	37.217	-3.4897	2439209.5	37.204	-4.6054
2438719.5	37.188	-3.5109	2439219.5	37.231	-4.6325
2438729.5	37.168	-3.5323	2439229.5	37.243	-4.6606
2438739.5	37.151	-3.5526	2439239.5	37.256	-4.6884
2438749.5	37.154	-3.5722	2439249.5	37.267	-4.7161
2438759.5	37.167	-3.5893	2439259.5	37.297	-4.7431
2438769.5	37.173	-3.6066	2439269.5	37.312	-4.7692
2438779.5	37.194	-3.6264	2439279.5	37.329	-4.7934
2438789.5	37.228	-3.6474	2439289.5	37.343	-4.8147
2438799.5	37.236	-3.6676	2439299.5	37.351	-4.8349
2438809.5	37.227	-3.6882	2439309.5	37.372	-4.8538
2438819.5	37.242	-3.7089	2439319.5	37.405	-4.8713
2438829.5	37.278	-3.7312	2439329.5	37.436	-4.8877
2438839.5	37.313	-3.7560	2439339.5	37.451	-4.9057
2438849.5	37.342	-3.7839	2439349.5	37.474	-4.9257
2438859.5	37.368	-3.8115	2439359.5	37.494	-4.9467
2438869.5	37.389	-3.8377	2439369.5	37.503	-4.9680
2438879.5	37.405	-3.8620	2439379.5	37.514	-4.9917
2438889.5	37.419	-3.8856	2439389.5	37.542	-5.0172
2438899.5	37.436	-3.9086	2439399.5	37.535	-5.0458
2438909.5	37.460	-3.9297	2439409.5	37.511	-5.0750
2438919.5	37.494	-3.9514	2439419.5	37.504	-5.1047
2438929.5	37.525	-3.9731	2439429.5	37.516	-5.1333
2438939.5	37.539	-3.9932	2439439.5	37.501	-5.1629
2438949.5	37.543	-4.0126	2439449.5	37.456	-5.1904
2438959.5	37.558	-4.0344	2439459.5	37.408	-5.2161
2438969.5	37.574	-4.0563	2439469.5	37.373	-5.2407
2438979.5	37.593	-4.0713	2439479.5	37.358	-5.2650
2438989.5	37.573	-4.0844	2439489.5	37.348	-5.2884
2438999.5	37.547	-4.1018	2439499.5	37.329	-5.3109

APPENDIX B

OTTAWA PZT OBSERVATIONS 1956 TO 1970

10 DAY SMOOTHED VALUES

JULIAN DAY	LATITUDE	UTO-A1	JULIAN DAY	LATITUDE	UTO-A1
2439509.5	37.318	-5.3333	2440009.5	37.362	-6.5615
2439519.5	37.307	-5.3553	2440019.5	37.355	-6.5851
2439529.5	37.298	-5.3785	2440029.5	37.329	-6.6074
2439539.5	37.277	-5.4034	2440039.5	37.295	-6.6280
2439549.5	37.268	-5.4297	2440049.5	37.299	-6.6457
2439559.5	37.267	-5.4565	2440059.5	37.307	-6.6600
2439569.5	37.271	-5.4834	2440069.5	37.309	-6.6742
2439579.5	37.261	-5.5108	2440079.5	37.313	-6.6931
2439589.5	37.255	-5.5382	2440089.5	37.337	-6.7175
2439599.5	37.262	-5.5665	2440099.5	37.335	-6.7424
2439609.5	37.270	-5.5944	2440109.5	37.305	-6.7655
2439619.5	37.290	-5.6218	2440119.5	37.298	-6.7872
2439629.5	37.276	-5.6486	2440129.5	37.292	-6.8103
2439639.5	37.249	-5.6739	2440139.5	37.282	-6.8354
2439649.5	37.235	-5.6965	2440149.5	37.272	-6.8627
2439659.5	37.254	-5.7167	2440159.5	37.286	-6.8903
2439669.5	37.285	-5.7349	2440169.5	37.290	-6.9185
2439679.5	37.313	-5.7521	2440179.5	37.295	-6.9451
2439689.5	37.331	-5.7682	2440189.5	37.311	-6.9710
2439699.5	37.339	-5.7829	2440199.5	37.325	-6.9962
2439709.5	37.340	-5.7977	2440209.5	37.327	-7.0217
2439719.5	37.341	-5.8153	2440219.5	37.328	-7.0465
2439729.5	37.343	-5.8345	2440229.5	37.334	-7.0709
2439739.5	37.360	-5.8531	2440239.5	37.348	-7.0952
2439749.5	37.388	-5.8724	2440249.5	37.373	-7.1211
2439759.5	37.401	-5.8942	2440259.5	37.393	-7.1495
2439769.5	37.389	-5.9180	2440269.5	37.415	-7.1788
2439779.5	37.376	-5.9422	2440279.5	37.444	-7.2078
2439789.5	37.378	-5.9669	2440289.5	37.477	-7.2379
2439799.5	37.384	-5.9937	2440299.5	37.468	-7.2705
2439809.5	37.367	-6.0218	2440309.5	37.443	-7.3030
2439819.5	37.338	-6.0495	2440319.5	37.441	-7.3355
2439829.5	37.334	-6.0763	2440329.5	37.462	-7.3683
2439839.5	37.364	-6.1027	2440339.5	37.491	-7.4006
2439849.5	37.389	-6.1288	2440349.5	37.506	-7.4302
2439859.5	37.394	-6.1541	2440359.5	37.498	-7.4607
2439869.5	37.398	-6.1798	2440369.5	37.466	-7.4915
2439879.5	37.398	-6.2054	2440379.5	37.460	-7.5187
2439889.5	37.391	-6.2308	2440389.5	37.461	-7.5409
2439899.5	37.383	-6.2569	2440399.5	37.457	-7.5617

APPENDIX B

OTTAWA PZT OBSERVATIONS 1956 TO 1970

10 DAY SMOOTHED VALUES

JULIAN DAY	LATITUDE	UTO-A1	JULIAN DAY	LATITUDE	UTO-A1
2439909.5	37.372	-6.2830	2440409.5	37.425	-7.5833
2439919.5	37.356	-6.3092	2440419.5	37.401	-7.6045
2439929.5	37.356	-6.3378	2440429.5	37.393	-7.6259
2439939.5	37.371	-6.3625	2440439.5	37.409	-7.6459
2439949.5	37.384	-6.3869	2440449.5	37.401	-7.6634
2439959.5	37.343	-6.4169	2440459.5	37.381	-7.6820
2439969.5	37.409	-6.4522	2440469.5	37.353	-7.7054
2439979.5	37.414	-6.4831	2440479.5	37.340	-7.7334
2439989.5	37.396	-6.5105	2440489.5	37.322	-7.7615
2439999.5	37.371	-6.5373	2440499.5	37.308	-7.7876
2440509.5	37.289	-7.8130	2440549.5	37.298	-7.9258
2440519.5	37.284	-7.8403	2440559.5	37.289	-7.9536
2440529.5	37.293	-7.8697	2440569.5	37.273	-7.9801
2440539.5	37.298	-7.8980	2440579.5	37.278	-8.0085

APPENDIX C
COMPARISON WITH BIH REVISED VALUES AT 1/20 YEAR 1962 - 1970

EPOCH	D-PHI	D-LAMBDA
62.00	.235	.0139
62.05	.173	.0169
62.10	.139	.0138
62.15	.178	.0158
62.20	.186	.0129
62.25	.163	.0136
62.30	.140	.0129
62.35	.150	.0133
62.40	.118	.0154
62.45	.107	.0154
62.50	.093	.0111
62.55	.123	.0110
62.60	.109	.0155
62.65	.121	.0162
62.70	.117	.0118
62.75	.177	.0118
62.80	.168	.0103
62.85	.155	.0128
62.90	.150	.0139
62.95	.152	.0161
63.00	.186	.0227
63.05	.185	.0171
63.10	.139	.0183
63.15	.147	.0194
63.20	.152	.0196
63.25	.098	.0189
63.30	.092	.0179
63.35	.077	.0180
63.40	.060	.0169
63.45	.073	.0169
63.50	.053	.0173
63.55	.088	.0213
63.60	.111	.0190
63.65	.132	.0147
63.70	.135	.0130
63.75	.132	.0097
63.80	.117	.0109
63.85	.089	.0085
63.90	.128	.0093
63.95	.153	.0084

EPOCH	D-PHI	D-LAMBDA
64.50	.064	.0128
64.55	.106	.0138
64.60	.103	.0154
64.65	.122	.0119
64.70	.134	.0068
64.75	.131	.0087
64.80	.122	.0083
64.85	.117	.0112
64.90	.111	.0102
64.95	.102	.0103
65.00	.123	.0074
65.05	.152	.0097
65.10	.196	.0142
65.15	.138	.0144
65.20	.150	.0140
65.25	.149	.0136
65.30	.141	.0178
65.35	.093	.0183
65.40	.087	.0155
65.45	.106	.0132
65.50	.095	.0112
65.55	.101	.0134
65.60	.158	.0144
65.65	.111	.0064
65.70	.174	.0085
65.75	.158	.0114
65.80	.122	.0099
65.85	.162	.0081
65.90	.190	.0063
65.95	.156	.0067
66.00	.149	.0082
66.05	.168	.0067
66.10	.159	.0130
66.15	.162	.0145
66.20	.137	.0135
66.25	.146	.0146
66.30	.129	.0156
66.35	.119	.0157
66.40	.123	.0150
66.45	.110	.0138

APPENDIX C
COMPARISON WITH BIH REVISED
VALUES AT 1/20 YEAR 1962 - 1970

EPOCH	D-PHI	D-LAMBDA	EPOCH	D-PHI	D-LAMBDA
64.00	.126	.0092	66.50	.103	.0160
64.05	.187	.0108	66.55	.109	.0133
64.10	.180	.0114	66.60	.119	.0124
64.15	.183	.0143	66.65	.139	.0106
64.20	.169	.0156	66.70	.177	.0091
64.25	.174	.0179	66.75	.190	.0087
64.30	.132	.0167	66.80	.155	.0082
64.35	.141	.0162	66.85	.205	.0091
64.40	.146	.0199	66.90	.135	.0085
64.45	.104	.0165	66.95	.108	.0102
67.00	.132	.0091	68.50	.053	.0164
67.05	.116	.0098	68.55	.065	.0126
67.10	.136	.0051	68.60	.100	.0029
67.15	.111	.0092	68.65	.186	.0106
67.20	.120	.0121	68.70	.097	.0106
67.25	.091	.0139	68.75	.138	.0065
67.30	.103	.0154	68.80	.115	.0103
67.35	.101	.0134	68.85	.130	.0125
67.40	.062	.0150	68.90	.131	.0132
67.45	.042	.0157	68.95	.152	.0111
67.50	.093	.0141	69.00	.118	.0112
67.55	.139	.0156	69.05	.131	.0098
67.60	.132	.0113	69.10	.109	.0147
67.65	.148	.0074	69.15	.141	.0186
67.70	.189	.0075	69.20	.166	.0168
67.75	.192	.0088	69.25	.103	.0176
67.80	.140	.0081	69.30	.112	.0179
67.85	.180	.0074	69.35	.127	.0155
67.90	.103	.0052	69.40	.092	.0171
67.95	.109	.0082	69.45	.078	.0184
68.00	.195	.0102	69.50	.116	.0112
68.05	.080	.0002	69.55	.069	.0125
68.10	.114	.0022	69.60	.155	.0154
68.15	.129	.0084	69.65	.176	.0072
68.20	.091	.0097	69.70	.174	.0100
68.25	.135	.0065	69.75	.163	.0155
68.30	.123	.0145	69.80	.175	.0064
68.35	.127	.0154	69.85	.192	.0098
68.40	.102	.0181	69.90	.191	.0083
68.45	.114	.0169	69.95	.150	.0092

APPENDIX C
COMPARISON WITH BIH REVISED
10 DAY SMOOTHED VALUES 1962-1970

JULIAN DAY	D-PHI	D-LAMBDA	JULIAN DAY	D-PHI	D-LAMBDA
2437669.5	.223	.0153	2438169.5	.070	.0179
2437679.5	.191	.0164	2438179.5	.068	.0167
2437689.5	.153	.0158	2438189.5	.062	.0159
2437699.5	.139	.0146	2438199.5	.062	.0158
2437709.5	.151	.0148	2438209.5	.064	.0164
2437719.5	.177	.0151	2438219.5	.066	.0185
2437729.5	.198	.0150	2438229.5	.078	.0207
2437739.5	.190	.0133	2438239.5	.094	.0211
2437749.5	.172	.0128	2438249.5	.109	.0202
2437759.5	.155	.0134	2438259.5	.116	.0170
2437769.5	.146	.0135	2438269.5	.119	.0145
2437779.5	.148	.0125	2438279.5	.128	.0133
2437789.5	.147	.0123	2438289.5	.134	.0122
2437799.5	.135	.0125	2438299.5	.135	.0110
2437809.5	.124	.0129	2438309.5	.128	.0096
2437819.5	.115	.0141	2438319.5	.117	.0096
2437829.5	.110	.0147	2438329.5	.097	.0089
2437839.5	.101	.0146	2438339.5	.102	.0083
2437849.5	.102	.0127	2438349.5	.126	.0083
2437859.5	.117	.0112	2438359.5	.134	.0089
2437869.5	.122	.0122	2438369.5	.135	.0087
2437879.5	.121	.0140	2438379.5	.140	.0076
2437889.5	.116	.0157	2438389.5	.129	.0080
2437899.5	.113	.0161	2438399.5	.131	.0084
2437909.5	.108	.0152	2438409.5	.156	.0096
2437919.5	.123	.0140	2438419.5	.187	.0102
2437929.5	.151	.0129	2438429.5	.182	.0118
2437939.5	.171	.0115	2438439.5	.180	.0127
2437949.5	.177	.0100	2438449.5	.177	.0135
2437959.5	.169	.0107	2438459.5	.170	.0138
2437969.5	.156	.0119	2438469.5	.164	.0155
2437979.5	.150	.0126	2438479.5	.162	.0170
2437989.5	.148	.0136	2438489.5	.159	.0174
2437999.5	.148	.0141	2438499.5	.145	.0166
2438009.5	.150	.0148	2438509.5	.139	.0158
2438019.5	.163	.0177	2438519.5	.137	.0159
2438029.5	.169	.0213	2438529.5	.142	.0168
2438039.5	.174	.0205	2438539.5	.141	.0187
2438049.5	.171	.0184	2438549.5	.136	.0190
2438059.5	.159	.0178	2438559.5	.109	.0170

APPENDIX C
COMPARISON WITH BIH REVISED
10 DAY SMOOTHED VALUES 1962-1970

JULIAN DAY	D-PHI	D-LAMBDA	JULIAN DAY	D-PHI	D-LAMBDA
2438069.5	.143	.0193	2438569.5	.081	.0141
2438079.5	.143	.0202	2438579.5	.071	.0123
2438089.5	.153	.0203	2438589.5	.096	.0134
2438099.5	.151	.0187	2438599.5	.106	.0152
2438109.5	.135	.0189	2438609.5	.109	.0162
2438119.5	.118	.0190	2438619.5	.114	.0151
2438129.5	.105	.0189	2438629.5	.125	.0136
2438139.5	.091	.0180	2438639.5	.118	.0101
2438149.5	.078	.0180	2438649.5	.120	.0076
2438159.5	.071	.0187	2438659.5	.140	.0072
2438669.5	.143	.0069	2439169.5	.167	.0144
2438679.5	.124	.0068	2439179.5	.161	.0155
2438689.5	.121	.0079	2439189.5	.149	.0146
2438699.5	.124	.0103	2439199.5	.133	.0140
2438709.5	.115	.0110	2439209.5	.133	.0137
2438719.5	.111	.0106	2439219.5	.145	.0140
2438729.5	.109	.0103	2439229.5	.137	.0151
2438739.5	.096	.0101	2439239.5	.126	.0160
2438749.5	.104	.0096	2439249.5	.114	.0158
2438759.5	.123	.0077	2439259.5	.124	.0152
2438769.5	.135	.0070	2439269.5	.117	.0149
2438779.5	.160	.0091	2439279.5	.112	.0147
2438789.5	.191	.0125	2439289.5	.102	.0140
2438799.5	.188	.0139	2439299.5	.087	.0146
2438809.5	.159	.0148	2439309.5	.087	.0153
2438819.5	.148	.0140	2439319.5	.097	.0155
2438829.5	.157	.0133	2439329.5	.108	.0143
2438839.5	.164	.0134	2439339.5	.113	.0140
2438849.5	.161	.0143	2439349.5	.131	.0135
2438859.5	.152	.0147	2439359.5	.146	.0128
2438869.5	.138	.0162	2439369.5	.153	.0108
2438879.5	.117	.0168	2439379.5	.163	.0091
2438889.5	.094	.0171	2439389.5	.191	.0083
2438899.5	.079	.0165	2439399.5	.184	.0094
2438909.5	.083	.0135	2439409.5	.161	.0096
2438919.5	.095	.0122	2439419.5	.158	.0099
2438929.5	.107	.0120	2439429.5	.182	.0093
2438939.5	.101	.0115	2439439.5	.185	.0101
2438949.5	.093	.0116	2439449.5	.160	.0092
2438959.5	.106	.0148	2439459.5	.131	.0081

APPENDIX C
COMPARISON WITH BIH REVISED
10 DAY SMOOTHED VALUES 1962-1970

JULIAN DAY	D-PHI	D-LAMBDA	JULIAN DAY	D-PHI	D-LAMBDA
2438969.5	.125	.0183	2439469.5	.115	.0097
2438979.5	.157	.0145	2439479.5	.117	.0100
2438989.5	.152	.0084	2439489.5	.124	.0104
2438999.5	.143	.0060	2439499.5	.125	.0102
2439009.5	.159	.0080	2439509.5	.132	.0099
2439019.5	.179	.0100	2439519.5	.129	.0092
2439029.5	.171	.0105	2439529.5	.125	.0090
2439039.5	.147	.0105	2439539.5	.109	.0098
2439049.5	.134	.0096	2439549.5	.104	.0109
2439059.5	.130	.0093	2439559.5	.106	.0118
2439069.5	.145	.0092	2439569.5	.110	.0124
2439079.5	.156	.0079	2439579.5	.100	.0134
2439089.5	.166	.0057	2439589.5	.092	.0142
2439099.5	.174	.0052	2439599.5	.097	.0151
2439109.5	.170	.0063	2439609.5	.108	.0143
2439119.5	.167	.0089	2439619.5	.108	.0130
2439129.5	.169	.0100	2439629.5	.088	.0134
2439139.5	.174	.0089	2439639.5	.059	.0148
2439149.5	.166	.0083	2439649.5	.043	.0154
2439159.5	.163	.0109	2439659.5	.060	.0153
2439669.5	.087	.0149	2440129.5	.144	.0057
2439679.5	.108	.0150	2440139.5	.139	.0048
2439689.5	.122	.0150	2440149.5	.141	.0067
2439699.5	.127	.0136	2440159.5	.163	.0094
2439709.5	.133	.0112	2440169.5	.173	.0120
2439719.5	.138	.0101	2440179.5	.177	.0124
2439729.5	.138	.0095	2440189.5	.185	.0127
2439739.5	.158	.0093	2440199.5	.178	.0129
2439749.5	.192	.0088	2440209.5	.155	.0133
2439759.5	.205	.0092	2440219.5	.134	.0135
2439769.5	.191	.0094	2440229.5	.118	.0138
2439779.5	.176	.0082	2440239.5	.109	.0131
2439789.5	.176	.0065	2440249.5	.115	.0129
2439799.5	.177	.0065	2440259.5	.120	.0140
2439809.5	.148	.0072	2440269.5	.128	.0145
2439819.5	.104	.0069	2440279.5	.141	.0129
2439829.5	.093	.0073	2440289.5	.162	.0112
2439839.5	.119	.0083	2440299.5	.137	.0124
2439849.5	.134	.0099	2440309.5	.100	.0140
2439859.5	.133	.0103	2440319.5	.088	.0152

APPENDIX C
COMPARISON WITH BIH REVISED
10 DAY SMOOTHED VALUES 1962-1970

JULIAN DAY	D-PHI	D-LAMBDA	JULIAN DAY	D-PHI	D-LAMBDA
2439869.5	.136	.0105	2440329.5	.102	.0155
2439879.5	.134	.0102	2440339.5	.126	.0153
2439889.5	.125	.0095	2440349.5	.139	.0140
2439899.5	.119	.0091	2440359.5	.133	.0154
2439909.5	.111	.0082	2440369.5	.105	.0180
2439919.5	.100	.0066	2440379.5	.105	.0175
2439929.5	.101	.0090	2440389.5	.115	.0136
2439939.5	.119	.0092	2440399.5	.121	.0104
2439949.5	.135	.0095	2440409.5	.101	.0105
2439959.5	.143	.0080	2440419.5	.100	.0112
2439969.5	.156	.0129	2440429.5	.122	.0123
2439979.5	.159	.0173	2440439.5	.173	.0124
2439989.5	.147	.0198	2440449.5	.200	.0100
2439999.5	.133	.0210	2440459.5	.209	.0075
2440009.5	.137	.0196	2440469.5	.208	.0081
2440019.5	.140	.0173	2440479.5	.209	.0108
2440029.5	.122	.0184	2440489.5	.198	.0109
2440039.5	.096	.0212	2440499.5	.191	.0090
2440049.5	.106	.0193	2440509.5	.177	.0068
2440059.5	.119	.0138	2440519.5	.176	.0061
2440069.5	.126	.0080	2440529.5	.189	.0066
2440079.5	.133	.0063	2440539.5	.199	.0068
2440089.5	.162	.0092	2440549.5	.200	.0076
2440099.5	.165	.0114	2440559.5	.189	.0083
2440109.5	.141	.0109	2440569.5	.170	.0077
2440119.5	.143	.0081	2440579.5	.173	.0084

PUBLICATIONS of the EARTH PHYSICS BRANCH

VOLUME 42 – NO. 7

magnetic anomaly maps of british columbia and the adjacent pacific ocean

G. V. HAINES and W. HANNAFORD

DEPARTMENT OF ENERGY, MINES AND RESOURCES

OTTAWA, CANADA 1972

Cat. No: M70-42/7

Contents

215 Introduction
215 The data
215 Representation of the anomaly field
217 Acknowledgments
217 References

magnetic anomaly maps of british columbia and the adjacent pacific ocean

G. V. HAINES and W. HANNAFORD

Abstract. A three-component aeromagnetic survey of British Columbia and the northeastern Pacific Ocean was carried out in early 1969. The survey data are in the form of averages over 30 seconds of time, or roughly 3.5 km of flight track. The International Geomagnetic Reference Field (IGRF) was removed from these data, and the resulting residuals plotted as profiles. A 3rd-degree polynomial was fitted to the survey data by least-squares to determine how well the IGRF represents the average regional field over the survey area. The polynomial was also used to obtain vector residuals, which require a residual mean close to zero. Lines of zero gradient in the component parallel to the flight tracks are also given.

Résumé. Un relevé aéromagnétique à trois composantes de la Colombie-Britannique et du nord-est de l'océan Pacifique a été effectué au début de 1969. Les données obtenues se présentent sous forme de moyennes sur 30 secondes de temps, ou approximativement sur 3.5 km de ligne de vol. On a soustrait de ces données la valeur du champ géomagnétique international de référence (International Geomagnetic Reference Field – IGRF), et les données rédisuelles ont été tracées sous forme de profils. Un polynome du 3^e degré a été appliqué aux données du levé par la méthode des moindres carrés afin de vérifier dans quelle mesure la valeur de IGRF représente bien la valeur du champ régional moyen dans la région étudiée. Le polynome a également servi à obtenir des données résiduelles de vecteurs, ce qui demande une moyenne résiduelle située près de zéro. On donne également les lignes de gradient zéro dans la composante parallèle aux lignes de vol.

Introduction

In 1969, between January 26 and March 20, the Dominion Observatory (now the Earth Physics Branch), Department of Energy, Mines and Resources, carried out a three-component aeromagnetic survey of British Columbia and the northeastern Pacific Ocean. An index map of the survey area is shown in Figure 1. The aircraft used was a DC 6, chartered from Pacific Western Airlines. The fluxgate magnetometer and direction-reference system have been described by Serson, *et al.* (1957) and Hannaford, *et al.* (1967).

The total number of line-kilometres flown was approximately 90,000 (of which about 15,000 were ferry and calibration flights) and the area covered was 3.4×10^6 square kilometres. The average flight-line spacing was 37 km (20 naut. mi.) over British Columbia and 74 km (40 naut. mi.) over the adjacent ocean. Flight altitudes ranged from 4.6 to 6.8 km, the average altitude being 5.5 km.

The data

A gyro-stabilized fluxgate magnetometer produced values of the declination D, the horizontal intensity H, and the vertical intensity Z. A Barringer OM-104 proton precession magnetometer measured the total field F. Because of the high accuracy of the proton magnetometer the fluxgate measurements of Z were discarded whenever H and F were available, and a new Z was calculated. This was possible because the error in Z resulting from an error in H is proportional to H/Z, and for the survey area this ratio was only about 0.3. The analysis of the aircraft fields, altitude corrections to sea level, and a discussion of various other problems will be given by Hannaford and Haines (1972).

Representation of the anomaly field

An anomaly field was obtained by subtracting from the $^1/_2$-minute average values of the International Geomagnetic Reference Field (IGRF). This spherical harmonic reference field has been described by the International Association of Geomagnetism and Aeronomy Commission 2 Working Group 4 (1969). Means and standard deviations of the differences, or residuals, are given in Table I. They are, however, not too meaningful.

To see how well the IGRF represents the average regional field over the survey area a 3rd-degree polynomial was fitted, in three orthogonal components, to 5-minute averages of the survey data. The coefficients of this polynomial and the appropriate formulas for their use are given in Table II. Means and standard deviations for the differences between the $^1/_2$-minute averages and the 3rd-degree polynomial are given in Table III. The means of Table III are not exactly zero because not every $^1/_2$-minute average forms part of a 5-minute average. The sample size used in Table I is larger than that used in Table III because many of the observations lie outside the main survey area to which the polynomial was fitted.

The 3rd-degree polynomial of Table II was subtracted from the IGRF, and the resulting difference field was contoured in Figure 2 for the geographic north component X, the geographic east component Y, the vertical downward component Z, the declination D, the horizontal intensity H, and the total force F. It is immediately evident that the IGRF does not accurately represent the average field over the region. This is particularly noticeable in the case of Z and F where there is a feature approximately 2000 km in wavelength and over 300γ in amplitude which is not present in the IGRF. (Indeed, the lowest wavelength which can be represented in a spherical harmonic expansion of degree 8 is 5000 km.) The horizontal components of the IGRF seem to fit much better, with differences generally being less than 100γ.

Figure 2 shows why the means and standard deviations of Table I are not very meaningful. When the residuals in one quarter of the survey area, for example, differ systematically from the residuals in another quarter, the over-all mean has little significance. It could be made to equal zero by choosing appropriate boundaries for the survey area. The over-all standard deviation is also misleading, since it is affected by the non-zero regional means and depends on the choice of the survey boundaries. This demonstrates a basic difficulty in specifying the goodness of fit of a smooth reference field, such as the IGRF, to survey data from an area even as large as several million square kilometres.

Although it is felt the 3rd-degree polynominal field of Table II would be a much better reference field than the IGRF, in that much smaller wavelengths (in this case, of appreciable amplitude) can be represented, it was decided to use the IGRF for plotting residual profiles (Figures 3-8). The IGRF was favoured because it is an international standard, and residuals from any other overlapping survey can be compared directly with those of this survey if they too are derived from the IGRF. This of course was one of the main reasons for the adoption of an international reference field. For deriving and plotting residual vectors (Figures 9-10), however, the polynomial reference field was used since zero means in all components are necessary. For the zero-gradients of Figure 11 the IGRF was used.

The $^1/_2$-minute residuals were plotted, in Figures 3-11, on a Lambert conformal conic map with standard parallels 37° and 65° N and convergence 0.785. The flight lines are parallel to the Greenwich meridian so this direction was chosen as the x-axis of the map. The y-axis is then parallel to 90° divided by the convergence, or 114° 36′W on the map.

In Figures 3-8, the IGRF-subtracted residuals were plotted in profile form, parallel to the y-axis. A residual was plotted toward the top of the map when positive and toward the bottom when negative. The polynomial-subtracted residuals were represented as two-dimensional vector residuals in the horizontal plane (Figure 9) and in a vertical plane parallel to the x-axis (Figure 10). Their directions follow the same convention as those of the profiles: positive components of the residual vector are plotted toward the top of the map, negative components toward the bottom.

Table I. Means and standard deviations of the observed minus IGRF field

	D	H	X	Y	Z	F
Sample size	20679	20679	20679	20679	20690	20694
Mean	−.06°	45γ	46γ	1γ	126γ	137γ
Standard deviation	.52	144	143	142	182	168

Table II. 3rd-degree polynomial reference field from least-squares fit of survey data

θ = colatitude λ = east longitude

$$a = -\tan(\theta/2)\cos(\lambda+117^\circ) + .3072$$
$$b = \tan(\theta/2)\sin(\lambda+117^\circ) + .0709$$

$$U = \sum_{1}^{10} u_i x_i \qquad V = \sum_{1}^{10} v_i x_i \qquad Z = \sum_{1}^{10} z_i x_i$$

$$X = U\cos(\lambda+117^\circ) - V\sin(\lambda+117^\circ)$$
$$Y = U\sin(\lambda+117^\circ) + V\cos(\lambda+117^\circ)$$

i	x_i	u_i	v_i	z_i
1	1	1.2239+4	1.0364+4	5.5262+4
2	a	−6.2556+4	−1.0855+4	3.7613+4
3	b	−6.5451+3	−6.1180+4	5.6891+4
4	a^2	6.3980+3	−4.9853+4	−1.7066+5
5	ab	−1.4139+5	−4.8740+4	−4.6326+4
6	b^2	−2.7125+4	−6.1475+4	−1.2595+5
7	a^3	4.3951+5	1.4481+5	−2.0118+5
8	a^2b	−1.6407+5	−9.0320+4	−7.1641+5
9	ab^2	−9.2440+4	6.1401+4	−1.9050+5
10	b^3	7.4499+4	1.1052+5	−2.3696+5

Note: Coefficients are in floating-point notation, a decimal fraction followed by a power of ten.

Table III. Means and standard deviations of the observed minus polynomial field

	D	H	X	Y	Z	F
Sample size	19751	19751	19751	19751	19791	19795
Mean	.00°	−2γ	−3γ	0γ	1γ	0γ
Standard deviation	.48	134	130	135	144	136

Figure 11 shows contour-segments of the residuals of the geomagnetic component in the direction of the x-axis. Suppose this component is called X′ and the component in the y-direction is called Y′. Their respective residuals will be called ΔX′ and ΔY′. Then, since the flight lines lie parallel to the x-axis the partial gradients $\partial(\Delta X')/\partial x$ and $\partial(\Delta Y')/\partial x$ are both known. If the field is derivable from a potential, $\partial(\Delta X')/\partial y = \partial(\Delta Y')/\partial x$, and the gradient of ΔX′ is given by

$$\text{grad}\,(\Delta X') = \frac{\partial(\Delta X')}{\partial x}\,\mathbf{i} + \frac{\partial(\Delta X')}{\partial y}\,\mathbf{j}$$

$$= \frac{\partial(\Delta X')}{\partial x}\,\mathbf{i} + \frac{\partial(\Delta Y')}{\partial x}\,\mathbf{j}$$

where **i** and **j** are unit vectors in the x and y directions, respectively. Rotating this gradient vector 90° counterclockwise gives the vector plotted in Figure 11:

contour − segment

$$= -\frac{\partial(\Delta Y')}{\partial x}\,\mathbf{i} + \frac{\partial(\Delta X')}{\partial x}\,\mathbf{j}$$

These contour-segments give the direction of the contour lines of ΔX′ as they intersect the flight lines.

When the distance between adjacent flight tracks is much larger than the distance between successive measurements on the tracks themselves, the contour-segments give additional information about the behaviour of $\Delta X'$ between the flight lines. The method, in fact, is equivalent to an extrapolation (or continuation) of the field beyond the actual point of measurement. The advantage of this representation is that linear and other trends, and changes in trends, are immediately apparent.

A contoured Z-residual map, comparable to Figure 7, has been published by Haines, *et al.* (1971), with an interpretation in terms of geology and tectonics.

Acknowledgments

The authors wish to thank student assistants J.A. Dunn, D.G. Smith and L.J. Watts for scaling $^1/_2$-minute averages of D, H and F from the strip-chart records and preparing the data for computer analysis; and Dr. P.H. Serson for his help and guidance and also for reviewing the manuscript.

The data were collected by Dominion Observatory personnel F. Andersen, G.L. Carr and the authors.

References

Haines, G.V., W. Hannaford and R.P. Riddihough. 1971. Magnetic anomalies over British Columbia and the adjacent Pacific Ocean. *Can. J. Earth Sci.*, Vol. 8, No. 3, pp. 387-391.

Hannaford, W., F. Andersen and P.H. Serson. 1967. A new three-component airborne magnetometer. Presented at the IUGG 1967. (Abstract only, *Int. Assoc. Geomag. and Astronomy*, Bull. No. 24, p. 48, Paris, 1967.).

Hannaford, W. and G.V. Haines. 1972. A three-component aeromagnetic survey of British Columbia and the adjacent Pacific Ocean. In preparation.

International Association of Geomagnetism and Aeronomy Commission 2 Working Group 4. 1969. International Geomagnetic Reference Field 1965.0. *J. Geophys. Res.*, Vol. 74, No. 17, pp. 4407-4408.

Serson, P.H., S.Z. Mack and K. Whitham. 1957. A three-component airborne magnetometer. *Pub. Dom. Obs.*, Vol. XIX, No. 2, pp. 15-97.

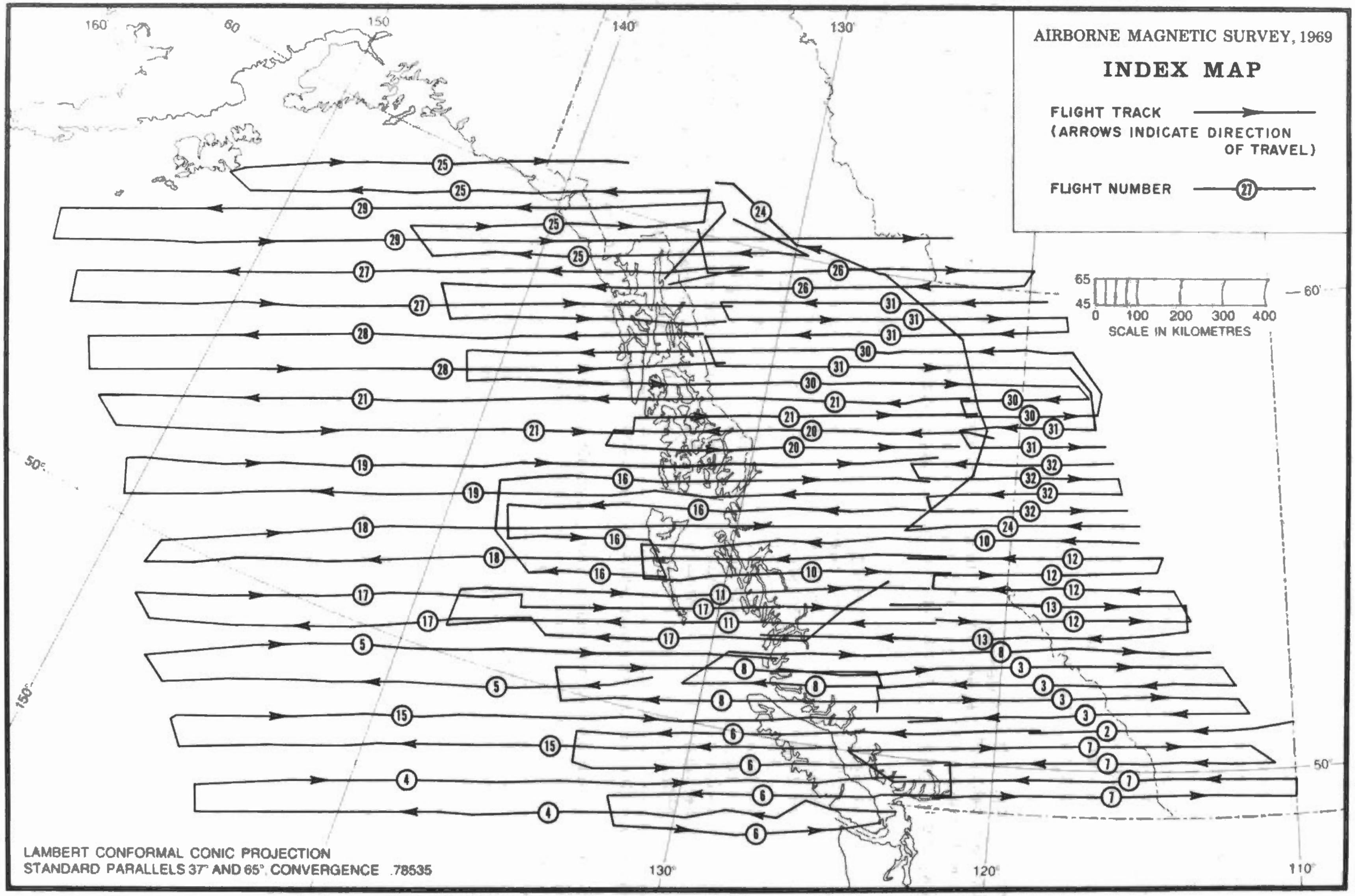

Figure 1. Flight lines of the British Columbia-northeastern Pacific Ocean aeromagnetic survey, 1969. Flight numbers are circled and arrowheads indicate direction of travel.

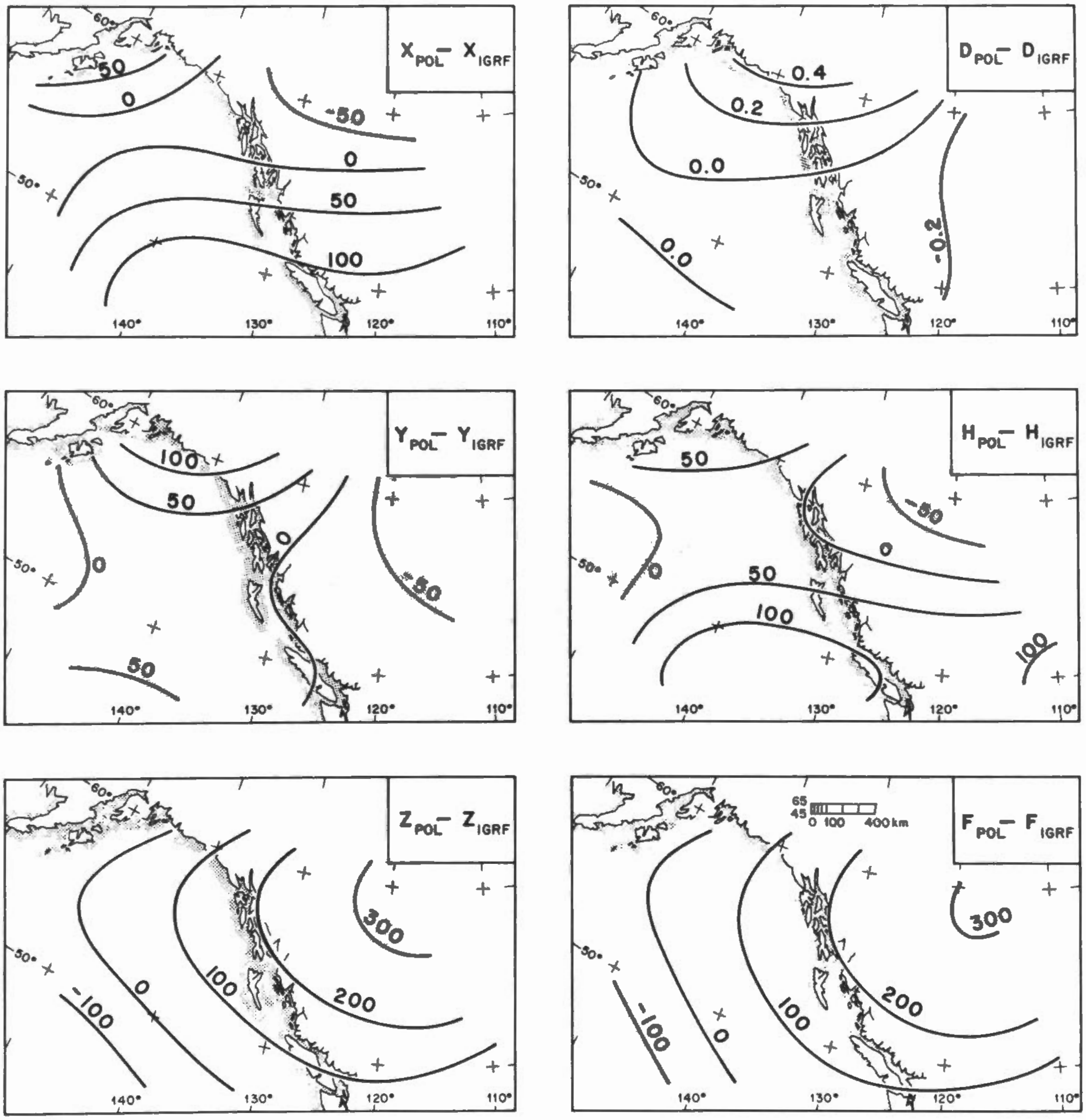

Figure 2. Comparison of International Geomagnetic Reference Field (IGRF) with 3rd-degree polynomial (POL). Declination D is in degrees; all other components are in gammas.

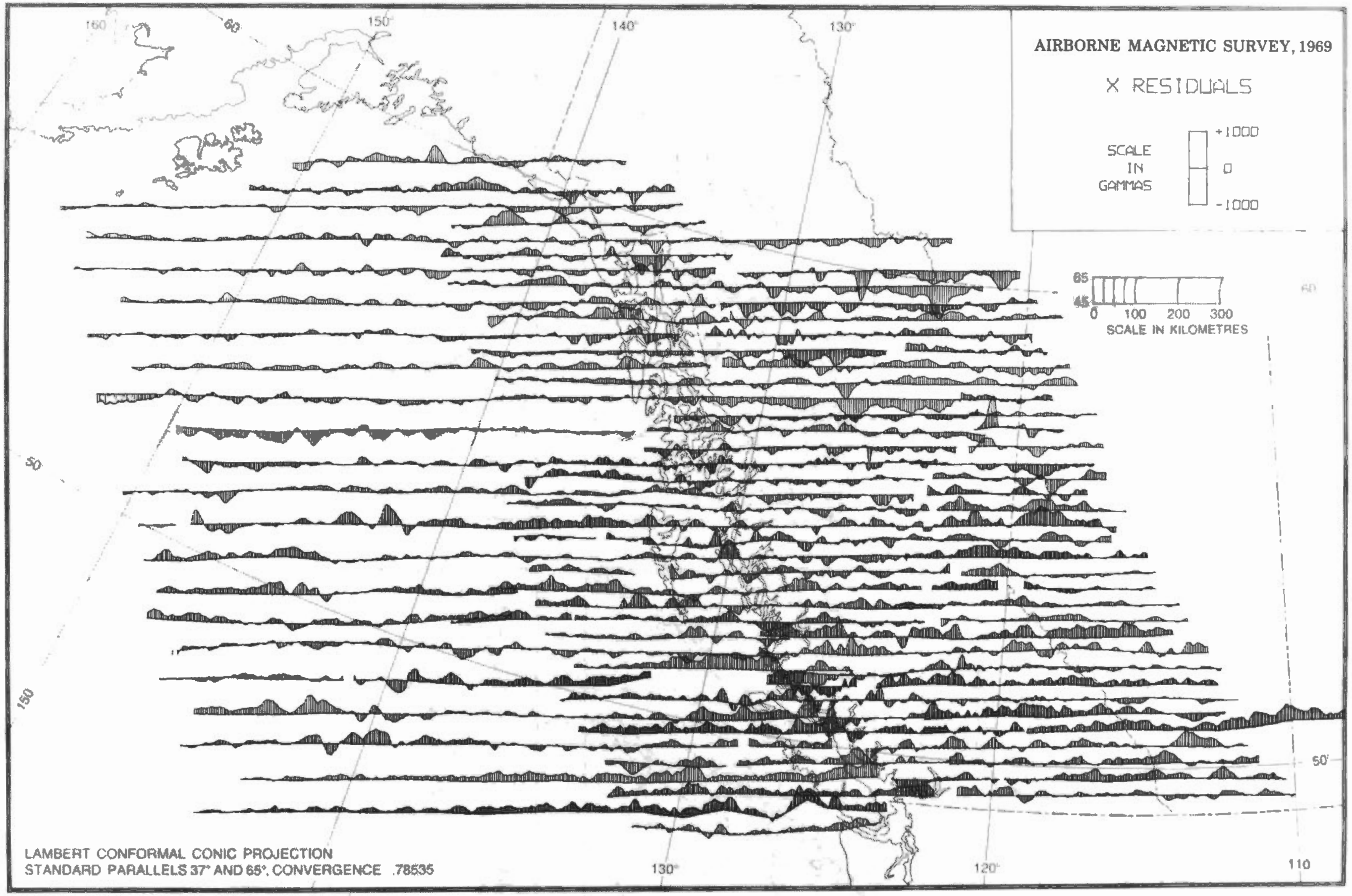

Figure 3. Residual profiles of the geographic north component of the earth's magnetic field, relative to the International Geomagnetic Reference Field (IGRF). A residual is an observed value minus the reference-field value.

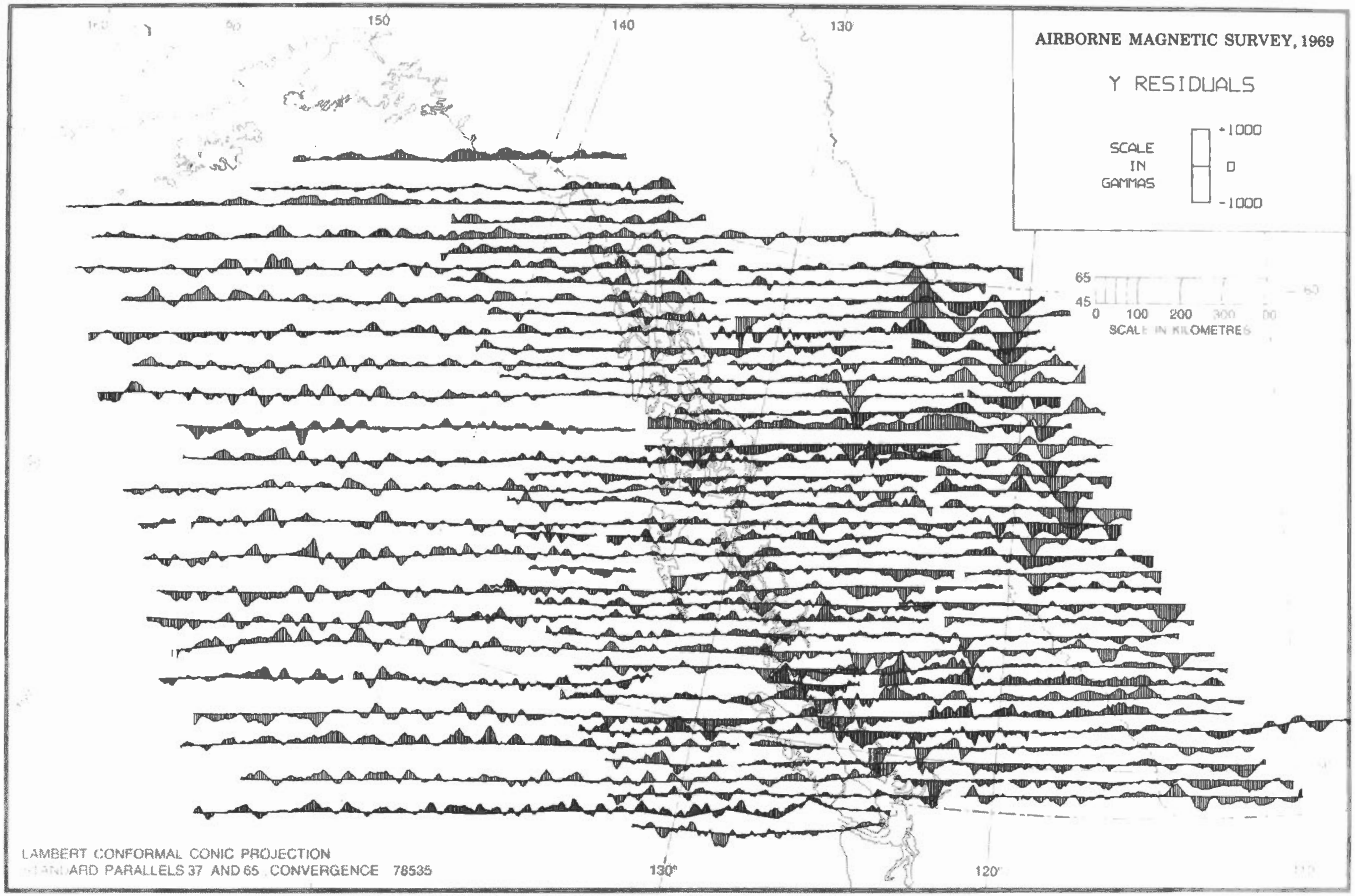

Figure 4. Residual profiles of geographic east component, relative to the IGRF.

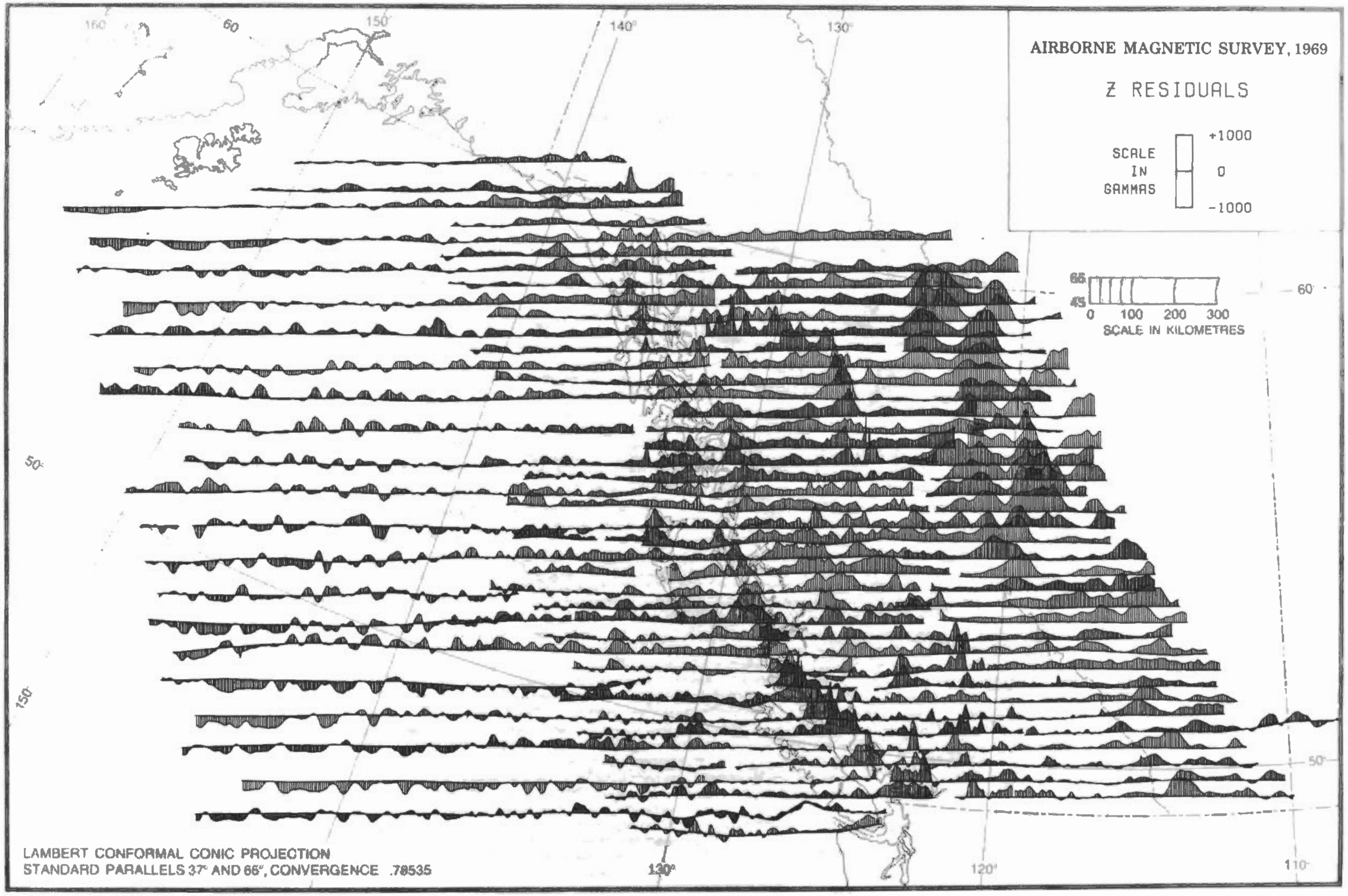

Figure 5. Residual profiles of vertical downward component, relative to the IGRF.

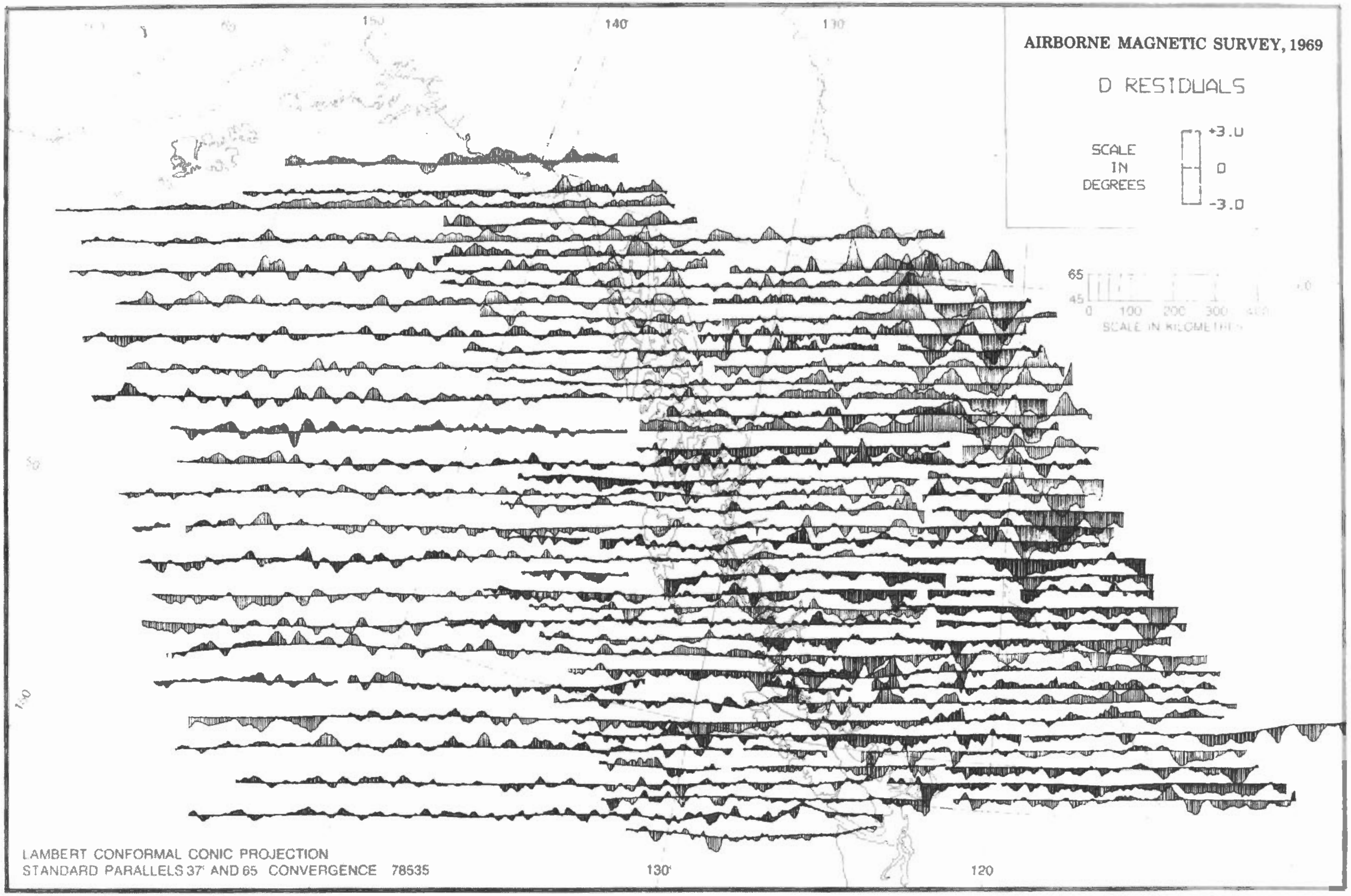

Figure 6. Residual profiles of declination, relative to the IGRF.

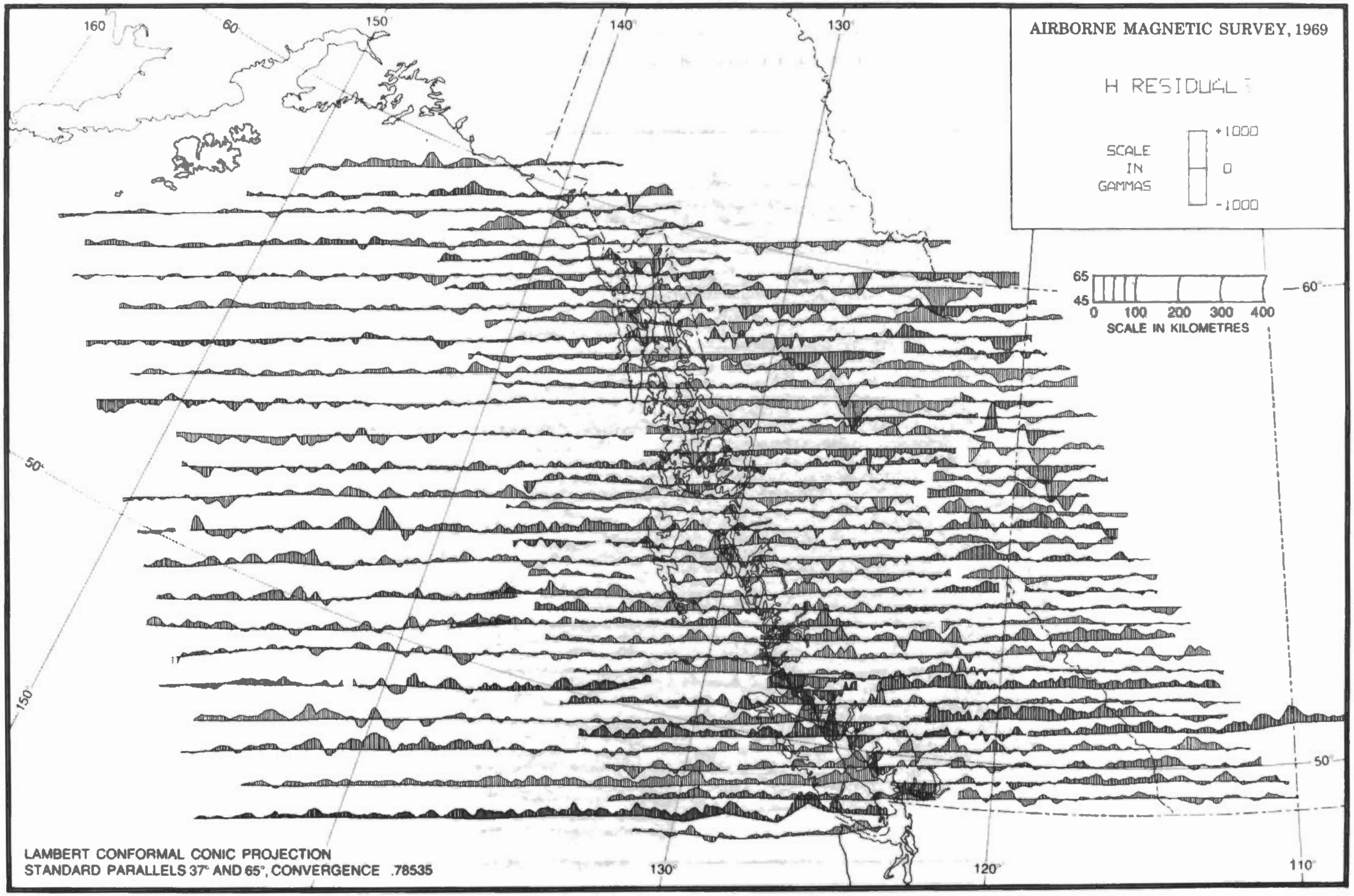

Figure 7. Residual profiles of horizontal intensity, relative to the IGRF.

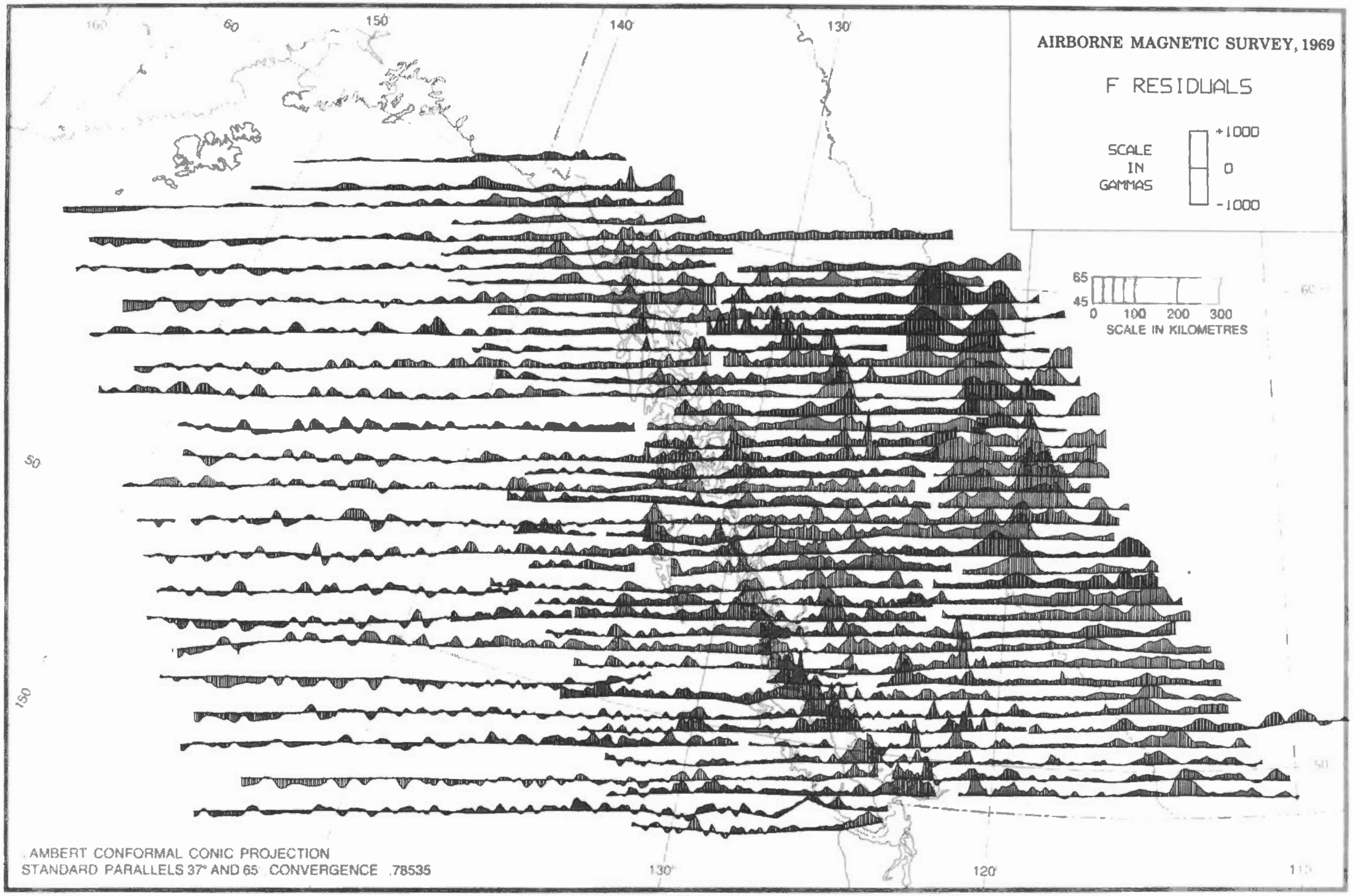

Figure 8. Residual profiles of total force, relative to the IGRF.

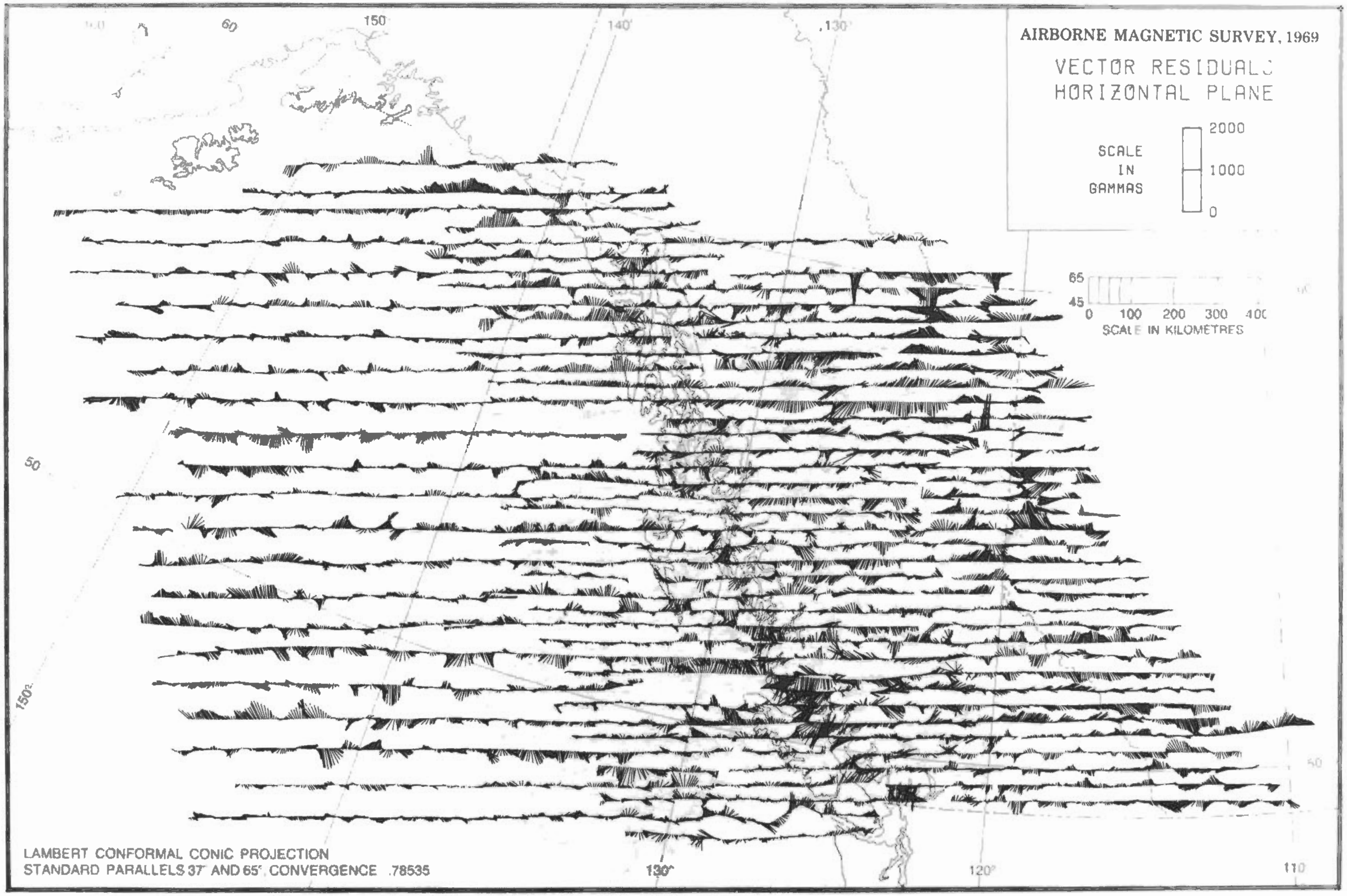

Figure 9. Projection of total residual vector onto horizontal plane. Residual vector is taken relative to 3rd-degree polynomial of Table II.

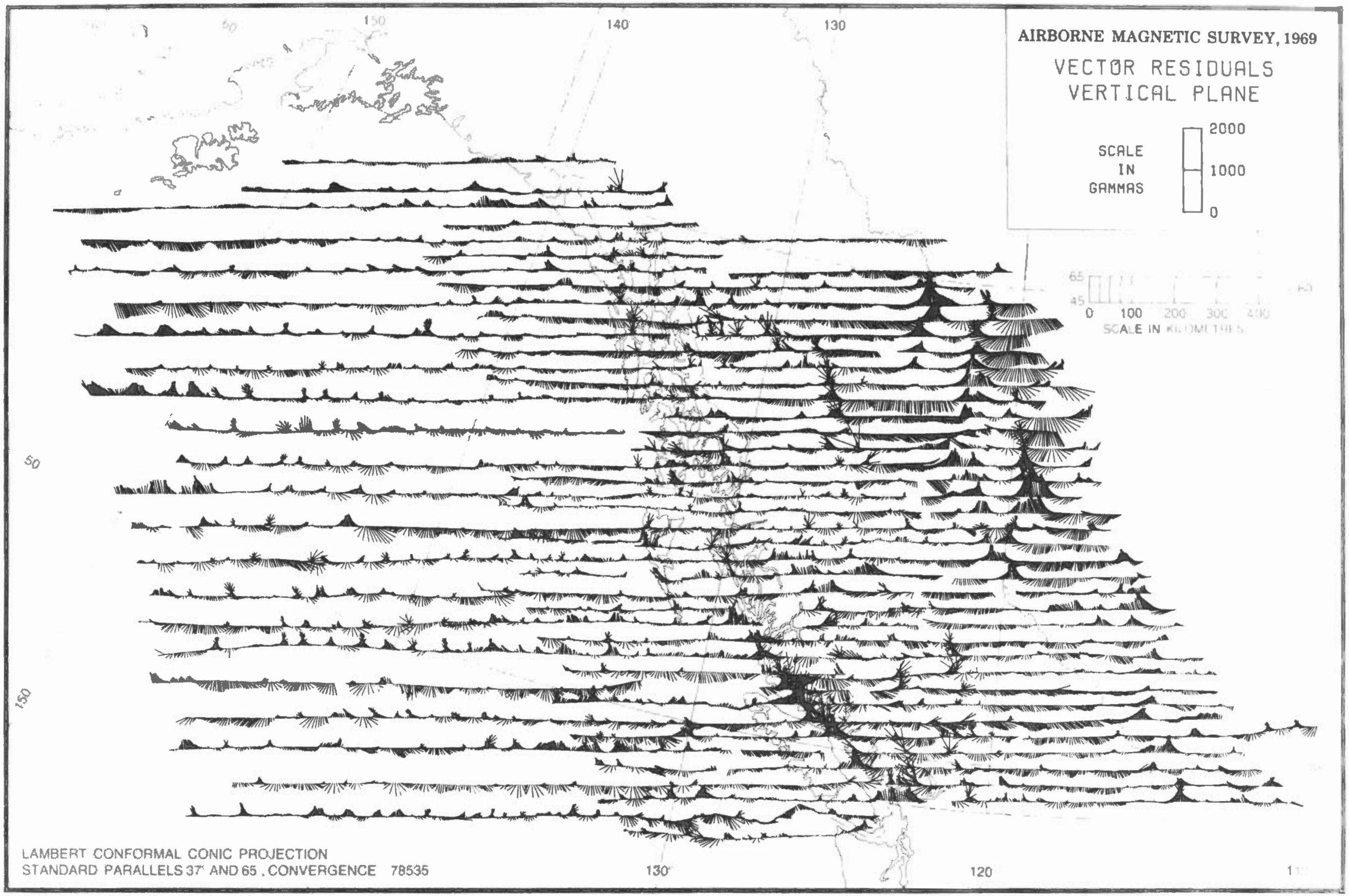

Figure 10. Projection of total residual vector onto vertical plane parallel to *x*-axis (from left to right, in figure). Residual vector relative to 3rd-degree polynominal.

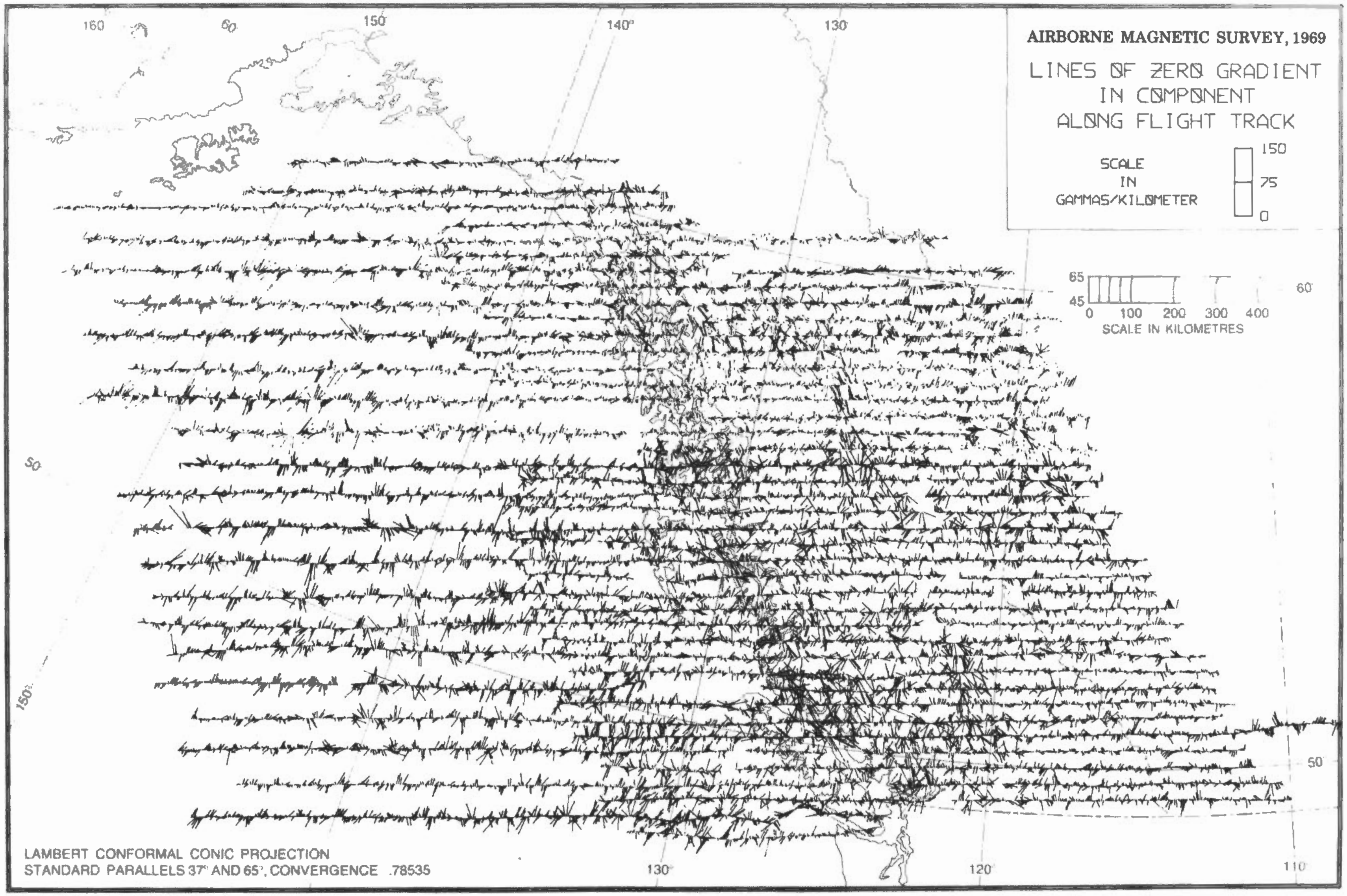

Figure 11. Contour line segments of the magnetic component parallel to the *x*-axis (from left to right, in figure). Rotating line segments 90° clockwise would give gradient vector.

PUBLICATIONS of the EARTH PHYSICS BRANCH

VOLUME 42 - No 8

un four électrique pour l'étude des propriétés magnétiques des roches

J.-L. ROY, E. SANDERS et J. REYNOLDS

DEPARTMENT OF ENERGY, MINES AND RESOURCES

OTTAWA, CANADA 1972

N° de Cat.: M70-42/8F

Table des matières

229 Introduction
229 Construction d'un four
231 Description du four a) et b)
232 Champ nul b)
233 Uniformité du champ
234 Matériaux employés b)
234 Élément de chauffage et composante magnétique b) et c)
235 Contrôle de température d) et g)
235 Uniformité de température e) et f)
236 Rendement
236 Remerciements
236 Information
237 Bibliographie

un four électrique pour l'étude des propriétés magnétiques des roches

J.-L. ROY, E. SANDERS et J. REYNOLDS

Résumé. Les auteurs décrivent la construction, les caractéristiques et le fonctionnement d'un four électrique (diamètre: 30.5 cm, hauteur: 20.3 cm), et font état des matériaux «non magnétiques» employés à sa construction. Le four peut recevoir 120 échantillons cylindriques (diamètre: 2.5 cm, hauteur: 2.2 cm) dans un champ magnétique d'intensité $<6\gamma$ dont 45 dans un champ d'intensité $<1\gamma$. Le champ magnétique et la température sont contrôlés automatiquement.

Abstract. The construction, characteristics, and performance of an electric oven (diameter 30.5 cm, height 20.3 cm) are described. The "non-magnetic" materials used are discussed. The oven can accommodate 120 cylindrical samples (diameter 2.5 cm, height 2.2 cm) within a magnetic field $<6\gamma$; 45 of which are within a field $<1\gamma$. The magnetic field and the temperature are controlled automatically.

Introduction

Depuis nombre d'années, les chercheurs sur les propriétés magnétiques des roches ou des terres cuites font amplement usage de traitements thermiques. Entre autres, les travaux pratiques de Thellier (1938) et de Thellier et Thellier (1959) et les travaux théoriques de Néel (1955) ont beaucoup contribué à l'étude de certaines lois d'aimantation des roches. Ainsi, il a été démontré que lorsqu'une roche est laissée à refroidir dans l'intervalle de température T_1 et T_2 ($T_1 > T_2$), situé entre le point de curie (T_c) le plus élevé de ses constituants et T_{20} = 20°C, elle acquiert une aimantation thermorémanente partielle (ATRP) d'intensité proportionnelle à celle du champ magnétique ambiant si celui-ci est faible; les directions du champ ambiant et de l'ATRP sont habituellement parallèles. Cette ATRP restera imperméable à tout réchauffement inférieur à T_2, mais pourra être remplacée totalement, ou en partie, par une nouvelle ATRP par un réchauffement à température $T \geqslant T_2$, où $T_2 < T < T_1$, et un refroidissement subséquent. Il en sera ainsi pour chaque intervalle $T_2 - T_3 - \ldots T_n$ compris entre T_c et T_{20}. La somme vectorielle des aimantations de tous ces intervalles constitue l'aimantation thermorémanente dite totale (ATR).

Une ATR peut donc être simple ou composée suivant que la roche a refroidi dans un champ constant ou non. Ainsi, une roche qui, à la suite d'un refroidissement initial à partir de T_c, a été soumise à un réchauffement jusqu'à $T < T_c$ et à un refroidissement dans un champ différent du premier possédera deux aimantations bien distinctes. Heureusement, grâce à la propriété de la roche de retenir à quelle température chaque ATRP a été acquise, il reste possible, dans bien des cas, de retracer l'évolution de l'aimantation fossile de telle ou telle roche. Pour y parvenir, il s'agit de soumettre la roche à des réchauffements progressifs et à des refroidissements en champ magnétique connu. De cette façon, on efface une aimantation inconnue pour la remplacer par une ATRP acquise dans des conditions connues. En comparant les vecteurs précédant et suivant le traitement thermique, on peut alors déterminer le vecteur de cette aimantation inconnue. Une telle comparaison de vecteurs est de beaucoup simplifiée si le traitement thermique a lieu en champ nul puisque alors on n'a fait qu'effacer l'aimantation fossile sans la remplacer par quoi que ce soit; une simple soustraction de vecteurs est donc suffisante. Afin de profiter de cette simplification dans l'analyse des résultats, il est donc avantageux d'effectuer les traitements thermiques en champ nul.

Le but principal de l'étude de l'aimantation des roches est d'identifier les aimantations contenues dans la roche et d'isoler une aimantation qui peut donner des renseignements sur la direction et l'intensité du champ magnétique terrestre ancien.

Cette méthode systématique de traitements thermiques peut aider à atteindre ce but. Ainsi, un réchauffement à basse température permet d'éliminer toute aimantation visqueuse ou de traînage (AVR) que la roche peut avoir acquis récemment. Un réchauffement à $\simeq$100°C (Thellier et Thellier, 1959) est habituellement suffisant pour éliminer ces aimantations parasites. Des réchauffements à températures plus élevées (de 100° à 500°C) permettent de déceler d'autres aimantations qui peuvent être à la fois des AVR et des ATRP et qui ont été acquises au cours d'une longue période à température basse ou modérée comme dans le cas de roches qui peuvent avoir été enfouies pendant un certain temps. Par ce procédé d'élimination, on peut arriver à isoler une aimantation qui persiste jusqu'au point de curie. En effectuant d'autres tests (de plissement par exemple), il est souvent possible de déterminer à quelle période de l'évolution de la roche l'aimantation appartient. Il n'est donc point surprenant que la désaimantation thermique soit devenue une technique de base pour les recherches archéo- et paléo-magnétiques.

Construction d'un four

Un four est d'autant plus employé et conforme aux besoins requis qu'il répond aux exigences suivantes:

a) avoir un refroidissement rapide, une longue existence, une grande capacité et être facile d'accès
b) opérer en champ nul
c) atteindre au moins 700°C
d) être précis en température absolue
e) avoir une température uniforme
f) exiger peu de surveillance
g) pouvoir garder la température et le champ constants pendant de longues périodes.

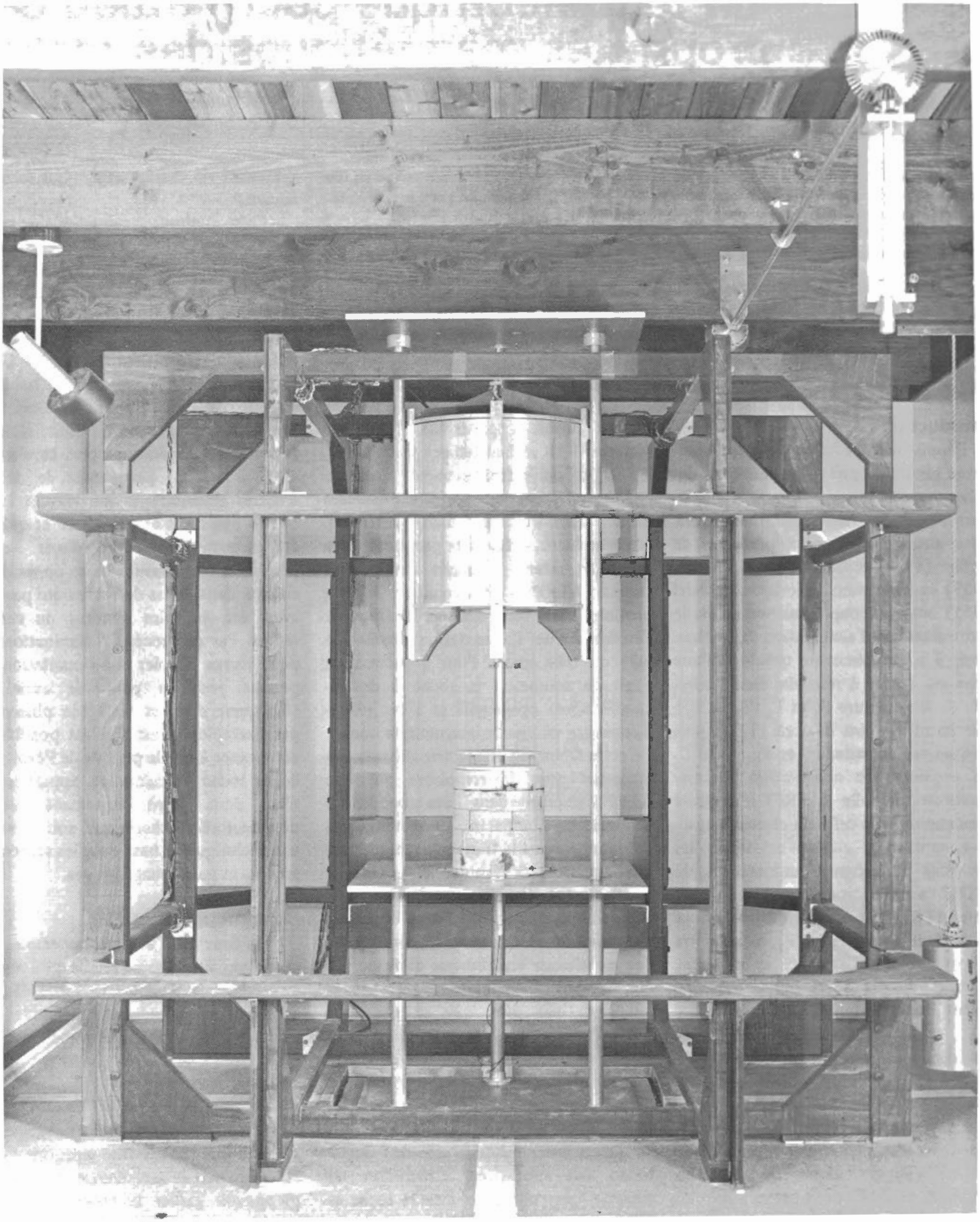

Figure 1. Le four électrique.

En a) le refroidissement rapide est nécessaire afin d'éviter les changements chimiques qui pourraient être causés en gardant longtemps l'échantillon à une température élevée; sa grande capacité est indispensable afin de désaimanter plusieurs échantillons simultanément tout en les espaçant suffisamment pour prévenir des interactions magnétiques. L'exigence g) est afin de pouvoir effectuer des expériences en conditions connues. Si l'on espère pouvoir identifier certaines aimantations, il peut être nécessaire de reproduire certaines conditions.

Le four a donc été construit afin d'approcher le plus possible ces conditions idéales. La façon avec laquelle chacune des exigences a été traitée est indiquée dans l'étude par la lettre correspondante.

Description du four a) et b)

Le four (fig. 1 et 2) est du type mobile qu'on peut élever et abaisser (Irving et coll., 1961). De cette façon, les échantillons refroidissent beaucoup plus rapidement que dans le cas des fours fixes. L'accès aux échantillons est facile et si le four est quelque peu aimanté, le champ magnétique transmis aux échantillons sera d'autant plus petit que la distance est plus grande.

L'intérieur du four est constitué d'un tube d'alumine de 30.5 cm de diamètre intérieur, de 20.3 cm de haut, de 1.8 cm d'épaisseur, et fermé en haut. Le fil de

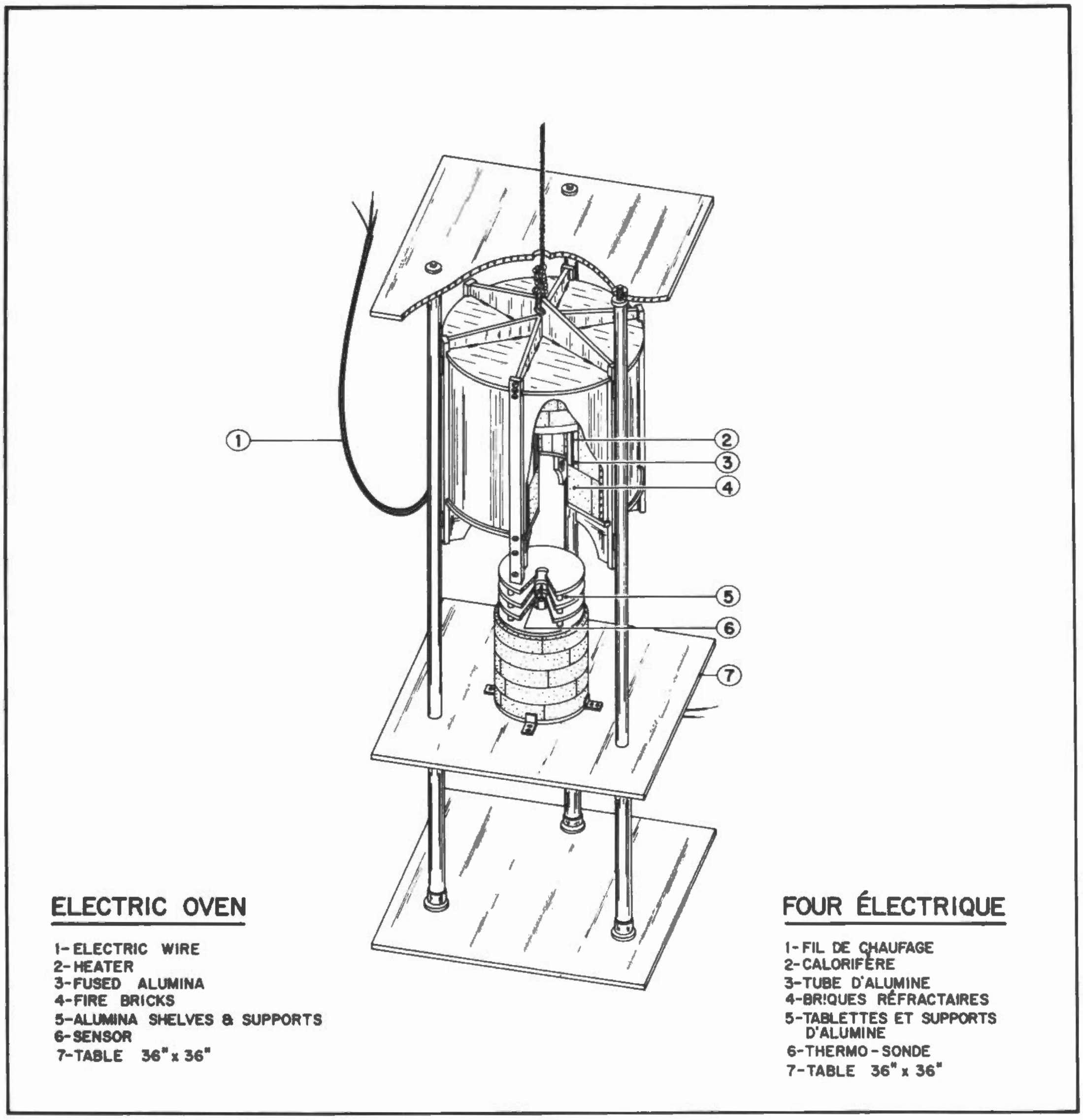

Figure 2. Dessin schématique du four.

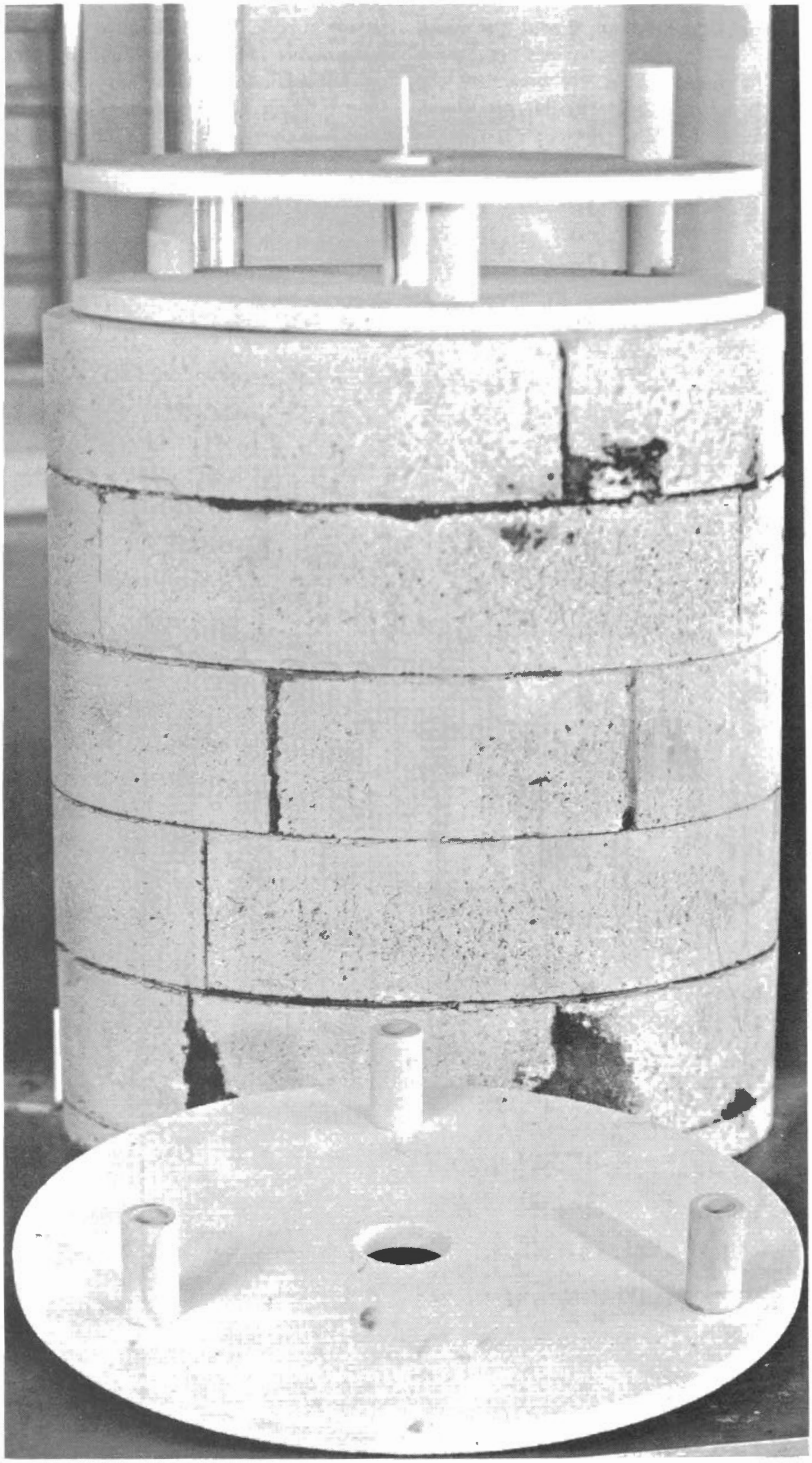

Figure 3. Tablettes et supports d'alumine. La thermo-sonde apparaît au centre.

chauffage a été placé autour du tube et cimenté en 56 rangées, espacées de 1.9 cm et parallèles à l'axe du four selon la méthode de Thellier (1938). Le courant de chauffage qui circule par une rangée revient donc par la rangée adjacente. Ainsi, des champs égaux et opposés tendent à se compenser mutuellement. Un deuxième tube d'alumine, d'un diamètre intérieur de 35.6 cm et de 1.3 cm d'épaisseur, entoure le calorifère afin de maintenir les rangées en place. Les extrémités du double tube sont scellées avec du ciment afin d'éviter tout contact avec l'air environnant et prolonger ainsi l'existence du calorifère. Des briques réfractaires de 11.5 cm d'épaisseur entourent le double tube; l'isolant du dessus est formé d'une épaisseur de 19 cm de briques. Le double tube et l'isolant reposent sur un anneau formé de briques, aux dimensions de 20 cm de haut et de 15 cm de large. Une feuille d'aluminium supportée par un anneau d'aluminium de 1.3 cm d'épaisseur entoure l'ensemble. Six supports d'aluminium (1.9 x 3.8 cm) encastrés et vissés dans l'anneau inférieur et la plaque supérieure (1.3 cm d'épaisseur) relient le poids à cette dernière qui est soulevée à l'aide d'une corde de nylon (1.3 cm de diamètre).

Le four est contrebalancé par un poids égal (143 kg) de plomb et l'ascension et la descente peuvent être accomplies sans heurts au moyen d'une manivelle (fig. 1). Le déplacement est guidé par trois piliers (3.8 cm de diamètre) et des coussinets de nylon rendent l'opération plus régulière. Quatre tablettes d'alumine (fig. 3) de 28 cm de diamètre et de 1.0 cm d'épaisseur peuvent être superposées; le four peut alors recevoir 120 échantillons (2.5 cm de diamètre et 2.2 cm de haut) tout en maintenant une distance minimum de 2.5 cm entre eux.

Champ nul b)

Pour obtenir un espace où le champ magnétique est «pratiquement» nul, il faut: 1) réduire ou compenser le champ magnétique terrestre; 2) n'employer que des matériaux à très faible teneur magnétique dans la construction du four et de ses accessoires. En employant un matériau à haute perméabilité, tel que du mumétal, dans la construction d'un bouclier magnétique, il est possible de réduire la majeure partie du champ magnétique terrestre. Ainsi, Patton (1967) rapporte qu'à l'intérieur d'une chambre cubique en mumétal de 244 cm de côté un champ magnétique de 50,000γ est réduit à 35γ. A l'aide d'un champ compensateur, le champ magnétique résiduel peut être maintenu à quelques γ près de zéro. Dans le cas présent, cependant, un gros four dans un local clos est peu pratique en raison de la chaleur dégagée.

Une compensation du champ terrestre est obtenue en produisant un champ dans le sens contraire de manière que les deux champs magnétiques soient égaux et opposés. Une pratique très courante d'effectuer cette compensation est d'employer trois paires de bobines placées orthogonalement de façon à compenser pour chacune des trois composantes du champ magnétique terrestre: vertical (Z), horizontal nord-sud magnétique (H_H) et horizontal est-ouest magnétique (H_D). Les bobines peuvent être circulaires (type helmholtz, Chapman et Bartels, 1940) ou à section carrée (Parry, 1967). Ce dernier type de bobines (244 cm de côté) est celui que nous employons pour compenser le champ magnétique au four.

Ces bobines (fig. 1) font partie d'un réseau de cinq ensembles identiques au centre desquels le champ magnétique est compensé automatiquement à 1γ près (2γ lors d'un orage magnétique) (Roy et coll., 1969); la compensation étant effectuée à l'aide d'un système de solénoïdes à noyau saturable placé au centre de l'un des ensembles.

Un troisième enroulement de fil sur chaque bobine permet de créer et de maintenir des champs magnétiques constants de 0 à 1 oersted dans n'importe quelle direction g).

Uniformité du champ

Le champ magnétique résiduel à l'intérieur et autour du four est montré graphiquement à la figure 4. Les courbes ont été calculées d'après les équations données par Parry (1967) et en prenant

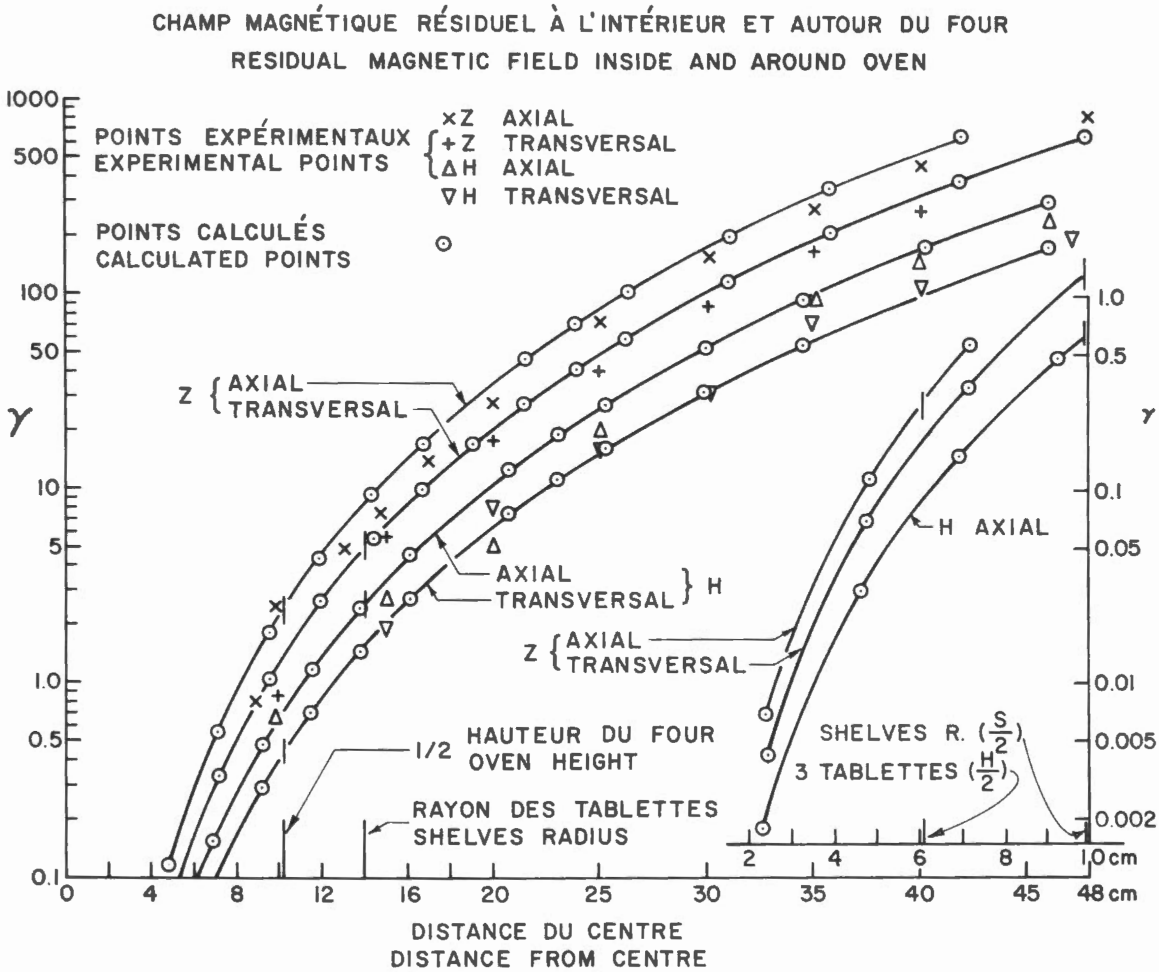

Figure 4. Champ magnétique résiduel (vertical et horizontal) à partir du centre des bobines. Les dimensions du four sont indiquées par des lignes verticales.

les valeurs locales 0.56 oe pour Z et 0.15 oe pour H_H (H_D = O). Les points expérimentaux ont été mesurés par W.A. Robertson et E. Irving à l'aide d'un appareil millioersted dont la résolution est de 1γ. Les points expérimentaux ont tendance à être un peu plus petits que ceux de la courbe calculée. Ceci est probablement dû au fait que la sonde à double tête (deux solénoïdes de 3.5 cm espacés de 2 cm) de l'appareil mesure le champ magnétique dans un volume fini et non pas à un point précis.

La compensation de Z est évidemment moins uniforme que celle de H_H puisque Z est quatre fois plus grand. En même temps, la compensation est meilleure transversalement qu'axialement. Il s'ensuit que le four a été construit plus large que haut afin de bénéficier du plus petit champ résiduel possible. Lorsque le four est utilisé à pleine capacité, tous les échantillons se trouvent dans un champ <6γ. En employant trois tablettes et la moitié de la surface (fig. 4, partie droite), 45 échantillons espacés de 2.5 cm peuvent être placés dans un champ ⩽ 1γ.

Matériaux employés b)

Le champ magnétique maximum transmis à un échantillon par le moment magnétique A d'un constituant du four peut être exprimé ainsi

$$H = 2A/x^3 = 2(A_R + A_S)/x^3 \quad .... 1$$

où x est la distance entre l'échantillon et le matériau magnétique, A_R est l'aimantation rémanente du matériau et A_S est l'aimantation causée par le champ magnétique F agissant sur ce matériau; A_S est donc égal à χ F où χ est la susceptiblité du matériau. L'emploi de matériaux diamagnétiques ou paramagnétiques suffit à rendre négligeable le deuxième énoncé de l'expression ($2\chi F/x^3$). En effet, la susceptibilité de ces matériaux est de l'ordre de 10^{-5} – 10^{-6} u.é.m. Toutes les parties du four se trouvent dans un champ faible (10^{-5} – 10^{-3}oe, fig. 4) et, sauf pour les tablettes, x est de plusieurs centimètres. Le champ magnétique causé par A_S est donc extrêmement faible, soit ⩽ 10^{-10} oe. L'x des tablettes où reposent les échantillons est petit étant de 0 à 2.2 cm; cependant $\chi = 1 \times 10^{-7}$ u.é.m. et F ⩽ 6×10^{-5} oe (fig. 4) et, en conséquence, le champ magnétique sur l'ensemble de l'échantillon est faible; par exemple, au centre de l'échantillon (x = 1.1 cm), le champ magnétique causé par l'A_S des tablettes est 5×10^{-12} oe et même à une distance de 1 mm, il n'est que 6×10^{-9} oe.

Dans la construction, on s'est limité à l'emploi des matériaux suivants: aluminium, alumine, briques réfractaires, mortier, nylon, platine, laiton et nichrome. L'aimantation rémanente d'échantillons de chacun de ces matériaux a été mesurée à l'aide d'un magnétomètre astatique. Les deux derniers matériaux ont démontré une aimantation plus prononcée que les autres. Leur effet est décrit ci-dessous.

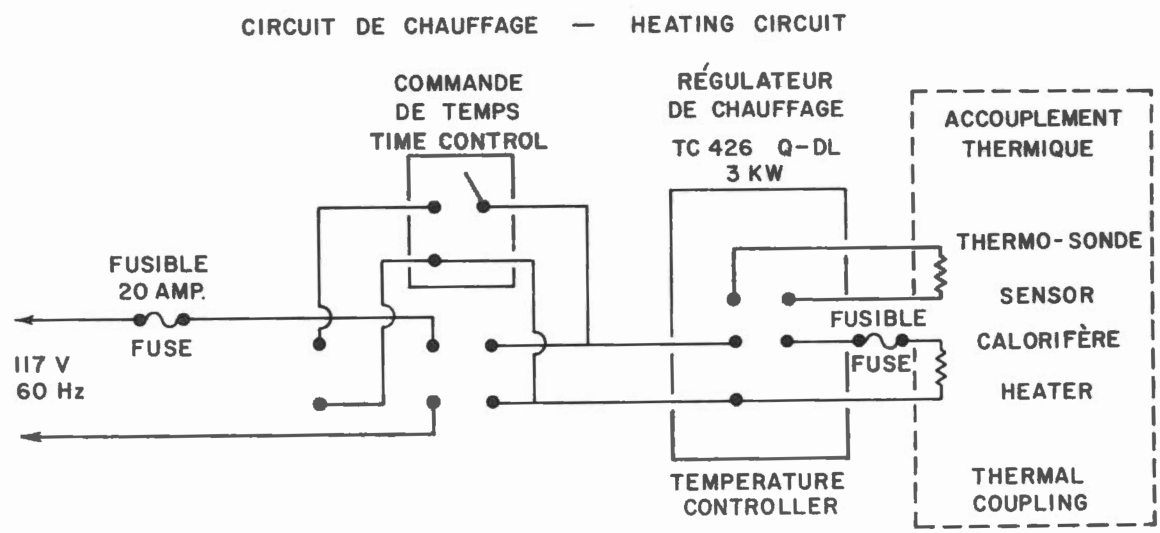

Figure 5. Circuit de chauffage.

Élément de chauffage et composante magnétique b) et c)

On a utilisé un fil de nichrome (80 Ni, 20 Cr, tophet A, de calibre n° 14 B et S, 0.163 cm de diamètre, *voir* Information). Long de 1.14 m, il a une résistance de 7.3 ohms à 20°C et 7.75 à 700°C. Sur un circuit de 117 V.A.C., le courant, qui au départ est de 16 A, est réduit sous l'effet du chauffage à 15 A qui donnent alors 1,750 W. Le point de fusion de cet alliage est ≃ 1,400°C. Du fait que le fil est encastré dans une masse d'alumine dont la conductivité thermique est bonne, la différence de température entre l'élément et le four demeure en principe petite.

Un alliage de nichrome peut être plus ou moins aimanté. L'aimantation rémanente de plusieurs échantillons de ce tophet A nichrome a donc été mesurée. La valeur moyenne du moment magnétique par cm de longueur est de 1.1×10^{-8} u.é.m. (l'aimantation la plus grande étant 2×10^{-8} u.é.m.). La plus proche distance

(d) qu'un échantillon puisse être d'une rangée verticale de fil est de 3 cm. Le champ magnétique maximum (h) que ce fil peut transmettre à l'échantillon est

$$h = 2m\,\ell d/(d^2 + \ell^2)^2 \ldots . 2$$

où m = moment/cm de fil n° 14, ℓ = longueur, h est alors égal à 1.4×10^{-9} oe. Si l'on y additionne les champs magnétiques transmis par les fils des rangées adjacentes et en supposant toutes ces aimantations dirigées dans le même sens, h maximum est encore $< 1 \times 10^{-8}$ oe. Ce nichrome donne donc une intensité (moment/volume) moyenne de 1.3×10^{-7} u.é.m., ce qui est moindre que l'intensité du laiton commercial qui varie beaucoup, d'après nos mesures, autour de 2×10^{-5} u.é.m.

L'emploi du laiton a été limité aux boulons qui servent à fixer les différentes parties du four. Bien que l'intensité de cet alliage soit relativement forte, le champ produit à l'intérieur du four sera négligeable si on prend soin de choisir les boulons les moins aimantés ($< 2 \times 10^{-5}$ u.é.m.). En effet, les plus gros boulons ont 1.1 cm^3 et la distance de n'importe quelle partie du four est > 20 cm. Donc, le champ magnétique transmis par un boulon est au maximum 3×10^{-9} oe. Bien qu'une soixantaine de boulons soient employés, le champ en un endroit donné ne peut dépasser 1×10^{-7} oe et est vraisemblablement beaucoup plus petit.

Contrôle de température d) et g)

La température est contrôlée automatiquement au moyen d'un régulateur de chauffage (*voir* Information). La thermosonde (fig. 5) est accouplée thermiquement avec le calorifère. La température désirée est signalée sur un indicateur gradué en degrés C. Au début, dès que l'interrupteur est fermé, le calorifère chauffe à pleine puissance. La résistance en platine de la thermo-sonde est alors continuellement comparée à celle qui a été déterminée d'après l'indicateur. Lorsque les valeurs de ces deux résistances approchent l'une de l'autre, la puissance diminue graduellement jusqu'à ce que les deux résistances soient égales. Le régulateur laisse alors passer juste le courant nécessaire au maintien de cette température. Une minuterie automatique permet de régler l'interrupteur, ce qui signifie qu'un chauffage peut avoir lieu en l'absence d'un opérateur. La thermosonde a été calibrée à 1°C près au moyen d'un thermo-couple de platine et de platine à 10 p. 100 de rhodium et la correction applicable est donnée à la table 1. Du fait de la dimension du four et du fait que le calorifère est encastré dans les tubes d'alumine, il existe un décalage de temps entre la température perçue par la thermo-sonde et la chaleur émise par le calorifère. Ce décalage amène la température, au permier cycle, à dépasser la température signalée. La correction à faire pour compenser cet effet est donnée à la table 1.

Table I. Température et sa variation* d'après le réglage

Réglage °C	Température °C	Variation* Max.	Min.
50	53	+10	00
100	103	+10	00
150	153	+10	-01
200	202	+09	-03
250	252	+08	-04
300	301	+07	-04
350	351	+06	-04
400	400	+05	-05
450	450	+05	-05
500	499	+04	-04
550	547	+04	-04
600	596	+03	-03
650	644	+03	-03
700	692	+03	-03
740	732	+03	-03

*Cette variation s'effectue au cours d'une heure environ à 100°C et en 20 minutes à 700°C. Après ce cycle initial, la température demeure constante à 1°C près.

Uniformité de température e) et f)

Bien que l'encastrement du calorifère contribue au décalage de temps, il est fort possible que cette masse d'alumine réchauffée soit une source de chaleur plus uniforme que le serait un élément exposé. La température est uniforme (fig. 6) à quelques degrés près, excepté pour les 5 cm du haut (4e tablette) où elle est de 5 à 10°C plus basse.

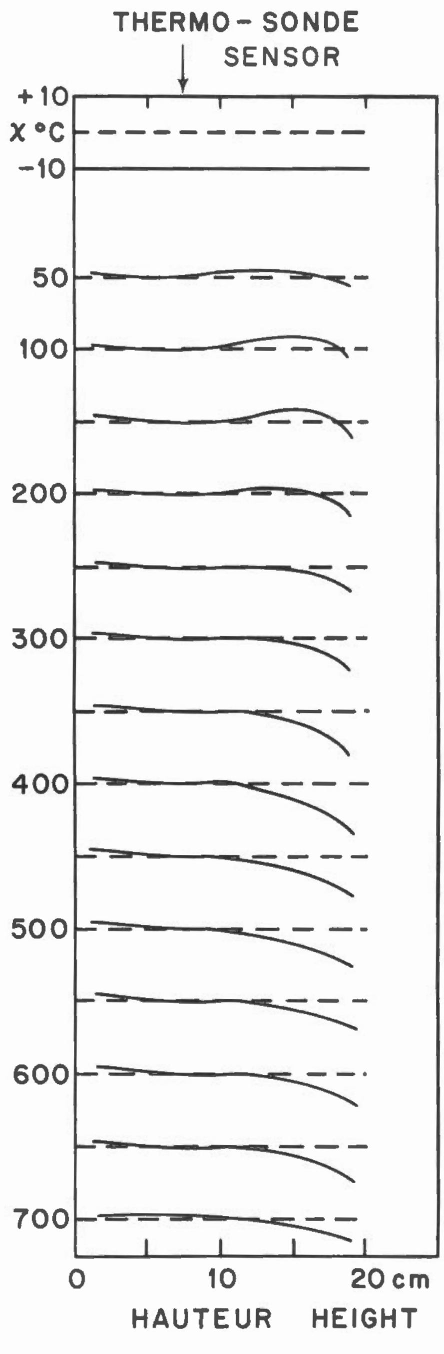

Figure 6
Thermo-sonde placée à l'intérieur du four à 7.5 cm de la base. La variation de température est en fonction de la hauteur intérieure du four dans les cinq premières minutes après avoir atteint la température désirée. Par la suite, les variations diminuent d'environ 50 p. 100.

L'élévation de la température à l'intérieur du four débute à 2°C/min. et baisse graduellement à 0.75°C/min. lorsque la température atteint 700°C. Ainsi, une température de 600°C peut être atteinte en 5 1/2 heures.

Rendement

Après plus de deux années d'usage, nombre de courbes ont été obtenues et plusieurs ont déjà parues dans différentes publications (Park, 1970; Brooke et coll., 1970; Park et Irving, 1970). Le décroissement régulier d'intensité jusqu'à zéro, que l'on remarque dans plusieurs de ces courbes, témoigne de l'efficacité de la désaimantation thermique en champ quasi nul. A la figure 7 sont données les courbes de désaimantation d'une aimantation rémanente naturelle (ARN) (A) et d'une ATR (B) obtenue en laissant l'échantillon refroidir de 700°C à 20°C dans un champ mangétique vertical de 0.57 oe. Entre l'aimantation et la désaimantation, l'échantillon a été soumis à une désaimantation par champ alternatif de 2,900 oe. La courbe B provient d'une étude de Park (1970) et la courbe A, d'une étude d'Irving et Park (non publiée) effectuée sur une roche sédimentaire du Grand lac de l'Ours. Étant donné que l'aimantation de B est unique, puisqu'elle est provoquée et qu'elle est plus forte que celle de A (ce fait diminue les erreurs des mesures), la courbe B doit être plus représentative du rendement du four.

Remerciements

Les auteurs tiennent à remercier E. Irving pour ses nombreux conseils. Ils sont reconnaissants à R. Harvey pour son dessin schématique du four (fig. 2) et à E. Gélinas pour les photos (fig. 1 et 3).

Information

Adresses des manufacturiers des divers matériaux et accessoires employés à la construction du four. Plusieurs publient des catalogues sur la construction de fours.

Alumine - Norton Company of Canada Ltd., Box 3008, Station B, Hamilton, Ontario.

Bobines - Permali (Canada) Ltd., 2870 Slough St., Malton, Ontario.

Briques réfractaires-Standard Refractories Ltd., 1185 Walkers Line N., Burlington, Ontario.

Nichrome - Canadian Wilbur B Driver Co. Ltd., 85 King St. E., Toronto 1, Ontario.

Régulateur de chauffage - Harrel Incorporated, 16 Fitch St., East Norwalk, Connecticut, U.S.A.

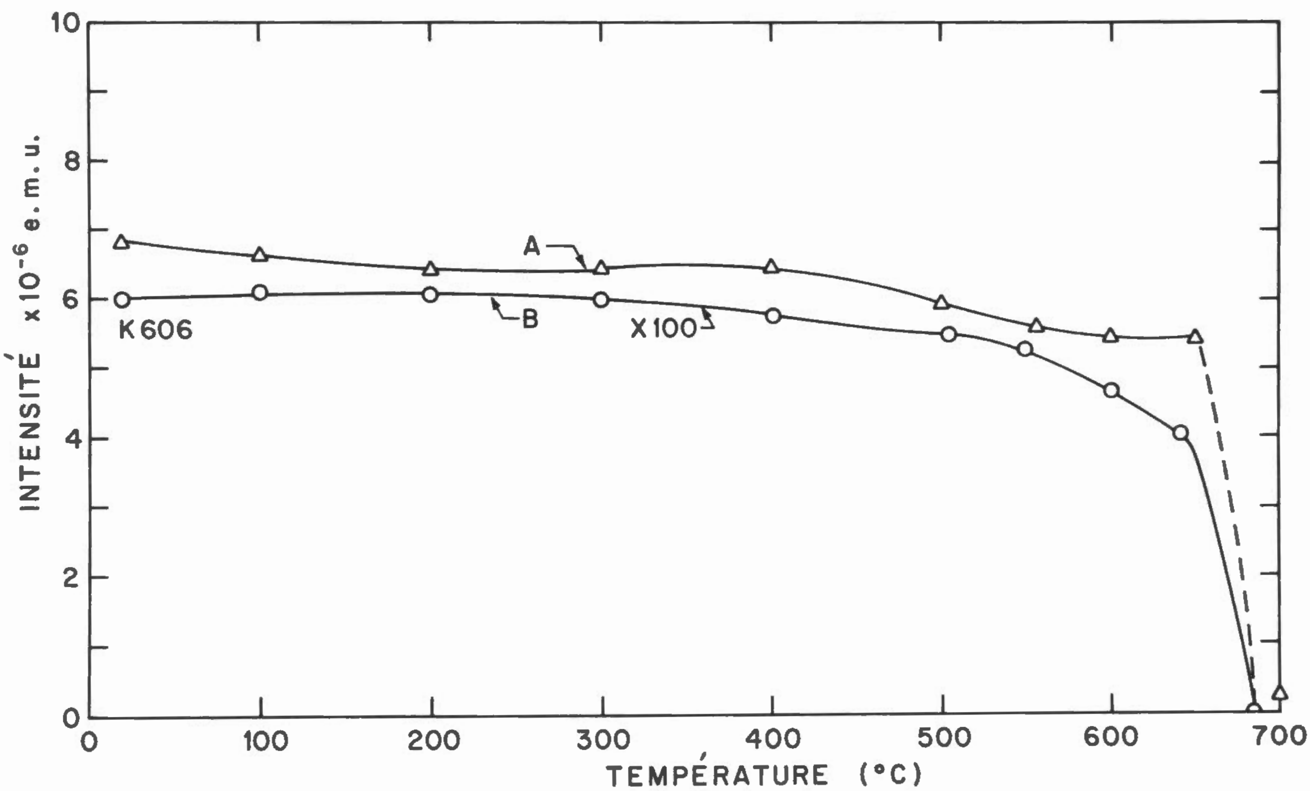

Figure 7. Courbes de désaimantation d'après les résultats d'une étude de Park (1970) et d'une étude d'Irving et Park (non publiée).

Bibliographie

Brooke, J., Irving, E. et Park, J.K., 1970. The Mid-Atlantic Ridge near 45°N XI magnetic properties of basalt base-core. *Can. J. Earth Sci.*, vol. 7, pp. 1515-1527.

Chapman, S. et Bartels, J., 1951. *Geomagnetism*, p. 83.

Irving, E., Robertson, W.A., Stott, P.M., Tarling, D.H. et Ward, M.A., 1961. Treatment of partially stable sedimentary rocks showing distribution of direction of magnetization. *J. Geophys. Res.*, vol. 66, pp. 1927-1933.

Néel, L., 1955. Some theorical aspects of rock magnetism. *Phil. Mag. Supp. Adv. Phys.*, vol. 4, pp. 191-243.

Park, J.K., 1970. Acid leaching of red beds and the relative stability of the red and black magnetic components. *Can. J. Earth Sci.*, vol. 7, pp. 1086-1092.

Park J.K. et Irving, E., 1970. The Mid-Atlantic Ridge near 45°N XII coercivity, secondary magnetization, polarity and thermal stability of dredge samples. *Can. J. Earth Sci.*, vol. 7, pp. 1499-1514.

Parry, J.H., 1967. Helmholtz coils and coil desing. *Dans* Methods in palaeomagnetism, Elsevier, Amsterdam, pp. 551-567.

Patton, B.J., 1967. Magnetic shielding. *Dans* Methods in palaeomagnetism, Elsevier, Amsterdam, pp. 568-588.

Roy, J.-L., Robertson, W.A. et Keeping, C., 1969. Magnetic "field free" spaces for paleomagnetism, rock magnetism and other studies. *Can. J. Earth Sci.*, vol. 6, pp. 1312-1316.

Thellier, E., 1938. Sur l'aimantation des terres cuites et ses applications géophysiques. *Ann. de l'Institut de Phys. du Globe*, Univ. Paris., vol. 16, pp. 157-302.

Thellier, E. et Thellier, O., 1959. Sur l'intensité du champ magnétique terrestre dans le passé historique et géographique. *Ann. géophys.*, vol. 15, pp. 285-376.

PUBLICATIONS of the EARTH PHYSICS BRANCH

VOLUME 42 – NO. 9

record of observations at meanook magnetic observatory 1969

A. B. COOK and S. J. SPRYSAK

DEPARTMENT OF ENERGY, MINES AND RESOURCES

OTTAWA, CANADA 1972

Cat. No.: M70-42/9

Contents

239 Introduction
239 Equipment
239 Variometers
239 Absolute instruments
239 Absolute observations and baseline values
240 Notes on the tables
241 Mean annual values
242 References

Tables

1 – 36 Hourly values of horizontal intensity, declination and vertical intensity; hourly, daily and monthly means
37 – 45 Mean hourly values H, D and Z, for month and year; all days, international quiet days and disturbed days
46 Three-hour range indices in H, D and Z and K-indices

record of observations at meanook magnetic observatory 1969

A. B. COOK and S. J. SPRYSAK

Geographic Coordinates: 54° 37′N; 113° 20′W
Geomagnetic Coordinates: 61.8°N; 301°E

Officer-in-Charge: Anne B. Cook
Assistant: Steven J. Sprysak

Introduction

Meanook magnetic observatory was established in July 1916, 85 miles north of the city of Edmonton, Alberta, 11 miles south of the town of Athabasca, Alberta. The observatory is controlled by the Division of Geomagnetism of the Earth Physics Branch, Ottawa, Canada.

Equipment

Variometers. Three sets of photographic variometers are operated continuously at Meanook: standard-sensitivity Ruska variometers, and standard-sensitivity la Cour and low-sensitivity la Cour variometers. The Ruska variometers were adopted as standard recorders on October 1, 1963. The paper speed is 20 mm/hr for the Ruska and 15 mm/hr for the la Cour. The temperature of the variometer rooms is maintained constant to 1°C by thermostatic controls.

The scale values are determined monthly in the case of the Ruska recorders, less frequently for the la Cour, by applying known fields to the variometers by means of Helmholtz coils.

On August 5, 1969, a major adjustment of the Ruska variometers was carried out. The bench supporting the variometers was rotated by approximately 90° in order that the H and D calibration coils could be left in the calibration position at all times. (Previously, it was necessary to move the Helmholtz coils between calibrations to avoid blocking light beams during large magnetic disturbances.) The normal direction of the magnetic meridian was first established in the variometer room, using portable fluxgate magnetometer No. TA-8. With the axes of the H and D calibration coils perpendicular to their normal orientation, the H and D variometer magnets were aligned to give no visible deflection when a direct current of 20 ma was sent through the corresponding coil. The coils were then fixed in the calibration position. The temperature-compensating magnet was not reinstalled on the H variometer, since it had affected the other variometers, and good thermostatic control made it unnecessary. The Z variometer was levelled by visual inspection of the magnet, and then the desensitizing magnet was installed.

The shift of baseline values and changes in sensitivity of the Ruska variometers resulting from these adjustments are shown in the tables following. The scale values per mm adopted for the la Cour variometers were constant throughout the year, as follows:

	H	D	Z
la Cour standard	7.18γ	0.93′	10.36γ
la Cour low-sensitivity	21.67γ	2.35′	37.47γ

In addition to the photographic variometers, a three-component recording fluxgate magnetometer[1] provides a visible record of X, Y and Z at a chart speed of 20 mm per hour. The scale value is normally 8.3γ per mm, corresponding to a full-scale range of 1000γ in each component. By means of a limit switch and a relay, the sensitivity of the recorder is cut in half whenever any element exceeds full-scale indication, thus automatically converting the instrument into a storm recorder.

Absolute instruments. The absolute instruments used at Meanook during 1969 were: Cooke magnetometer No. 15 (with correction of −0.3′) for declination; quartz horizontal intensity magnetometer No. 259[2] (with correction of $-0.00013H$) for horizontal intensity; Ruska earth inductor No. 6540 (with correction of 0.0′) for inclination; and a Dominion Observatory proton precessionn magnetometer[3,5] (4257.60 cps/oersted) for total intensity. A Dominion Observatory portable fluxgate magnetometer[4] was used as a standby instrument for determining declination, inclination and total intensity and for Meanook field surveys.

Absolute observations and baseline values

Absolute observations were made twice a week, on the average. Baseline values for the vertical intensity were computed from the readings of the proton precession magnetometer and the earth inductor by the formula $Z = F \sin I$.[5]

Notes on the tables

Universal time (U.T.) is used throughout. Tables 1 - 36 show the mean values of D, H and Z for the intervals of 60 minutes centred on the half hour.

Reductions. The hourly values of D, H and Z are manually scaled and punched on cards. The tables were calculated by a CDC 3100 computer. The computer was programmed so that the output was compatible with offset printing techniques.

Table 46 lists three-hour range indices and K-indices for Meanook. Lower limit K_9 is 1500γ. Throughout the year, these indices are sent twice a month to De Bilt, Netherlands, and Göttingen, Germany, for use in preparation of planetary K-indices published by the International Association of Geomagnetism and Aeronomy. The magnetograms were read each month for magnetic phenomena and the results were sent to the I.A.G.A.

Maximum hourly ranges in all components were also scaled. Copies of hourly ranges, three-hour indices and magnetograms were sent upon request to Defence Research Telecommunication Establishment. Copies of magnetograms were supplied to researchers during the year 1969.

H Baselines γ				H Scale Value γ/mm	
		Adopted	Observed		Adopted
Jan.	1–27	12825	12825	Jan.	11.07
	28–31	12824			
Feb.	1–28	12824	12824	Feb.	11.07
Mar.	1–10	12824	12820	Mar.	11.07
	11–31	12825			
Apr.	1–10	12825	12828	Apr.	11.07
	11–30	12826			
May	1–11	12826	12823	May	11.07
	12–31	12827			
June	1–30	12827	12828	June	11.07
July	1–8	12827	12826	July	11.07
	9–31	12826			
			Shift July 31(0724)		
*Aug.	1–4(2315)			Aug. 1–5(1109)	
		13087			11.07
	5(1109)–9		13081	5(1109)–9	
		13082			10.29
	10–31	13081		10–31	10.29
			Shift Aug. 5(1109)		
Sept.	1–22	13080	13079	Sept.	10.29
	23–30	13079			
Oct.	1–12	13079	13079	Oct.	10.29
			Shift Oct. 13		
	13–22	13069	13069		10.29
	23–31	13068	13068		
Nov.	1–3	13068	13066	Nov.	10.29
	4–12	13067			
	13–23	13066			
	24–30	13065			
Dec.	1–3	13065	13063	Dec.	10.29
	4–14	13064	13063		
	15–25	13063	13063		
	26–31	13062	13063		

*No Ruska Trace Aug. 4(2315) – 5(1109)

D Baselines				D Scale Value ′/mm	
		Adopted 23°E+	Observed 23°E+		Adopted
		′	′		
Jan.	1–6	33.5	33.1	Jan.	1.67
	7–31	33.6	33.1		
Feb.	1–22	33.6	33.1	Feb.	1.67
	23–28	33.7	33.1		
Mar.	1–31	33.7	33.7	Mar.	1.67
Apr.	1–6	33.7	33.7	Apr.	1.67
			Shift		
	7–8	35.0	34.9		
	9–17	34.9			
	18–27	34.8			
	28–30	34.7			
May	1–6	34.7	34.6	May	1.67
	7–28	34.6			
	29–31	34.7			
June	1–13	34.7	34.8	June	1.67
	14–30	34.8			
July	1–7	34.8	34.9	July	1.67
	8–31	34.9			
			Shift July 31(0724)		
Aug.	1–4(2315)			Aug. 1–5(1109)	
		13.2			1.67
	*5–16	11.0	11.0	5(1109)–16	
					1.61
	17–31	10.9			1.61
			Shift Aug. 5(1109)		
Sept.	1–14	10.9	10.8	Sept.	1.61
	15–30	10.8			
Oct.	1–12	10.8	10.8	Oct.	1.61
	13–17	9.7	9.7		
	18–21	9.6	9.7		
	22–25	9.5	9.7		
	26–28	9.4	9.7		
	29–31	9.3	9.7		

*No Ruska Trace Aug. 4(2315) – Aug. 5(1109)

D Baselines / **D Scale Value ′/mm**

		Adopted 23°E+	Observed 23°E+		Adopted
Nov.	1	9.3	8.9	Nov.	1.61
	2–5	9.2	8.9		
	6–9	9.1	8.9		
	10–11	9.0			
	12–19	8.9			
	20–25	9.0			
	26–30	9.1			
Dec.	1–5	9.2	9.4	Dec.	1.61
	6–11	9.3			
	12–21	9.4			
	22–30	9.3			
	31	9.2			

Z Baselines γ / **Z Scale Value γ/mm**

		Adopted	Observed		Adopted
Jan.	1–2	58571		Jan.	12.04
	3–6	58572			
	7–10	58573			
	11–14	58574			
	15–31	58575			
Feb.	1–11	58575		Feb.	12.04
	12–28	58576			
Mar.	1–11	58576		Mar.	12.04
	12–31	58577			
			New proton precession magnetometer installed		
Apr.	1–8	58577		Apr.	12.04
	9–22	58578	58578		
	22–30	58577			
May	1–31	58577	58577	May	12.04
June	1–11	58577	58578	June	12.04
	12–17	58578			
	18–30	58577			
July	1–3	58577	58576	July	12.04
	4–21	58576			
	22–31	58575			
			Shift July 31(0724)		
Aug.	1(0000–1706)	58565			
	1(1706)–4(2315)	58590		Aug.	1–5(1109) 12.04
	*5(1109–1848)	58523	58537	Aug.	5(1109)–31 9.42
	5(1848)–23	58537			
	24–31	58538			

*No Ruska Trace Aug. 4(2315) – 5(1109)

Z Baselines γ / **Z Scale value γ/mm**

		Adopted	Observed		Adopted
			Shifts Aug. 1(1706), 5(1109), 5(1848)		
Sept.	1–19	58538	58538	Sept.	9.42
	20–30	58539			
Oct.	1–11	58539	58538	Oct.	9.42
			Shift Oct. 13		
	12–16	58495	58496		9.42
	17-21	58494			
	22–24	58493			
	25–28	58492			
	29–30	58491			
	31	58490			
Nov.	1–4	58490	58486	Nov.	9.42
	5–7	58489			
	8–11	58488			
	12–13	58487			
	14–15	58486			
	16–23	58487			
	24–30	58488			
Dec.	1	58488	58490	Dec.	9.42
	2–9	58489			
	10–15	58490			
	16–18	58491			
	19–20	58492			
	21–22	58493			
	23–24	58494			
	25–26	58495			
	27–28	58496			
	29–30	58497			
	31	58498			

Mean annual values

Year	D(E)	H	Z	X*	Y*(E)	I*(N)	F*
	′	γ	γ	γ	γ	′	γ
1957	24°23.1	12921	58801	11768	5335	77°36.4	60204
1958	15.0	943	819	801	16	35.4	226
1959	13.0	960	787	819	16	34.1	198
1960	09.7	985	774	848	16	32.5	192
1961	06.1	13022	748	887	18	30.1	175
1962	02.7	054	723	921	18	28.1	156
1963	23°58.7	076	711	949	14	26.5	150
1964	54.9	103	694	978	12	24.9	139
1965	51.7	130	672	12008	12	23.1	123
1966	49.6	150	663	029	12	21.9	119
1967	47.2	170	663	051	12	20.8	123
1968	45.0	197	659	079	15	19.4	125
1969	42.1	234	662	118	20	17.2	136

*X, Y, I, F are derived from annual means D, H and Z.

References

[1] Serson, Paul H. 1967. An electrical recording magnetometer. *Can. J. Phys.*, Vol. 35, pp. 1387-1394.

[2] la Cour, D., and E. Sucksdorff. 1936. Le quartz-magnetomètre QHM, Commun. No. 15, 22 pp., No. 16, 11 pp. *Danish Meteorol. Inst. Copenhagen.*

[3] Serson, Paul H. 1962. A simple proton precession magnetometer. *Report Dominion Observatory, Ottawa,* 13 pp.

[4] Serson, P.H., and W.L.W. Hannaford. 1956. A portable electrical magnetometer. *Can. J. Technology,* Vol. 1, No. 28, pp. 232-243.

[5] U.G.G.I., Helsinki. 1960. Résolution N° 66, *Comptes Rendus de la XII^e Assemblée générale.*

HORIZONTAL INTENSITY

TABLE 1 MEANOOK   H = 12500 PLUS TABULAR VALUES IN GAMMAS   JANUARY 1969

HOUR UT DAY		0 TO 1	1 TO 2	2 TO 3	3 TO 4	4 TO 5	5 TO 6	6 TO 7	7 TO 8	8 TO 9	9 TO 10	10 TO 11	11 TO 12	12 TO 13	13 TO 14	14 TO 15	15 TO 16	16 TO 17	17 TO 18	18 TO 19	19 TO 20	20 TO 21	21 TO 22	22 TO 23	23 TO 24	MEAN
1		737	733	724	729	727	724	724	724	714	698	681	737	732	717	702	735	728	718	719	724	722	717	722	727	721
2		727	727	731	724	724	733	733	729	729	732	731	728	727	727	724	721	727	721	720	721	722	722	724	727	726
3	Q	733	735	736	736	735	736	736	736	736	738	741	739	738	735	732	732	727	724	722	724	720	717	720	724	731
4		725	727	732	733	733	733	733	733	735	730	726	721	731	735	736	735	731	725	717	715	716	716	720	724	728
5		726	733	733	729	729	731	730	735	735	735	735	735	735	733	735	735	728	720	714	712	716	722	722	724	728
6	Q	727	732	732	732	728	727	727	726	727	730	730	733	733	733	732	727	722	712	707	707	712	722	726	731	726
7		735	735	736	739	738	742	743	737	735	721	717	669	614	715	743	740	728	712	697	691	717	725	722	724	720
8		729	730	729	736	733	738	738	702	718	726	733	727	727	725	724	724	725	720	710	700	701	705	710	707	722
9		726	735	735	732	738	735	732	733	727	727	726	726	726	726	724	727	721	709	701	701	702	711	714	722	723
10	Q	727	735	735	735	736	735	735	733	732	727	728	727	712	731	735	735	724	712	709	710	714	722	726	727	727
11		731	733	735	736	737	735	731	726	724	735	733	732	733	733	724	737	736	722	708	702	709	712	722	728	727
12		735	735	738	736	738	733	736	731	726	727	687	716	724	735	708	732	731	712	706	704	709	714	720	725	723
13	Q	727	733	733	733	733	733	733	731	731	727	721	720	733	733	736	735	731	721	711	711	712	719	722	731	727
14		725	719	727	732	731	732	735	712	712	735	701	735	743	735	735	735	727	722	715	714	714	711	701	722	724
15	D	730	733	749	757	749	745	743	733	731	737	724	736	727	732	746	739	737	724	680	670	709	716	717	725	729
16		731	728	733	740	747	758	747	746	735	716	706	735	687	586	694	745	742	725	717	720	722	724	726	720	722
17	D	707	735	747	757	770	789	751	736	707	679	662	726	679	711	733	727	725	699	688	688	714	712	709	720	720
18	D	716	722	742	735	746	736	712	632	722	675	695	433	705	735	725	722	716	696	701	702	716	709	711	724	701
19		725	731	738	738	743	737	736	731	705	623	648	720	714	699	728	735	729	720	701	702	[illegible]	701	704	725	714
20		735	738	733	721	737	736	737	737	726	722	722	722	710	719	722	720	718	708	706	707	712	716	712	717	722
21		735	740	725	738	745	738	726	732	736	724	711	737	738	737	737	735	728	719	710	714	721	724	725	725	729
22		730	732	735	737	740	737	735	735	719	710	736	735	735	735	735	733	728	721	716	712	716	714	718	724	728
23		732	735	736	738	736	735	733	733	735	735	735	732	728	742	742	739	735	729	724	722	726	728	726	733	733
24		739	738	741	741	741	741	741	741	741	741	741	741	732	689	694	678	700	720	699	693	680	694	706	733	721
25	D	737	756	748	733	735	738	690	660	463	380	388	412	438	579	707	745	655	662	705	667	681	724	731	726	644
26	D	757	779	737	748	746	727	722	720	724	724	724	588	480	677	710	764	733	722	716	715	716	716	712	717	711
27		727	736	735	735	733	727	725	693	668	607	644	628	638	602	705	724	710	716	704	701	701	715	721	712	696
28		723	726	731	734	734	734	732	731	731	725	725	724	725	727	728	731	726	721	709	708	713	710	711	719	724
29	Q	725	730	734	732	732	732	732	732	732	727	727	729	732	736	741	741	736	725	711	704	704	710	720	731	727
30		724	727	735	735	726	723	725	730	724	697	664	747	745	744	742	737	732	723	719	715	716	723	724	727	725
31		734	737	738	739	741	737	734	731	728	719	710	709	720	714	744	736	725	735	726	715	711	717	721	723	727
MEAN	A	729	734	735	736	737	737	732	724	716	704	702	700	701	712	726	732	725	717	709	706	711	716	718	724	720
MEAN	Q	728	733	734	734	733	733	733	732	732	730	730	730	730	734	735	734	728	719	712	711	712	718	723	729	728
MEAN	D	729	745	745	746	749	747	724	696	669	639	638	579	606	687	724	739	713	700	698	689	707	715	716	722	701

DECLINATION

TABLE 2 MEANOOK D = 23.5 DEGREES EAST PLUS TABULAR VALUES IN MINUTES JANUARY 1969

HOUR UT / DAY		0 TO 1	1 TO 2	2 TO 3	3 TO 4	4 TO 5	5 TO 6	6 TO 7	7 TO 8	8 TO 9	9 TO 10	10 TO 11	11 TO 12	12 TO 13	13 TC 14	14 TO 15	15 TO 16	16 TO 17	17 TO 18	18 TO 19	19 TO 20	20 TC 21	21 TO 22	22 TC 23	23 TO 24	MEAN
1		12.5	14.7	16.7	15.2	14.2	13.5	15.2	18.0	13.5	14.9	8.3	16.7	13.9	13.7	13.7	17.2	13.0	8.7	10.2	13.0	11.8	13.2	14.4	14.2	13.8
2		14.0	13.7	14.5	15.4	21.2	13.4	12.4	12.2	12.9	13.0	13.0	13.9	14.5	14.7	15.4	14.9	16.9	17.2	16.9	15.4	13.7	13.5	13.5	13.5	14.6
3	Q	13.4	13.4	13.5	13.5	13.4	13.0	12.9	12.4	13.0	13.0	13.2	13.5	13.5	14.0	14.9	15.7	17.2	16.9	15.2	15.2	14.7	14.4	14.4	14.4	14.1
4		13.9	13.4	13.0	12.7	12.7	12.4	12.7	12.2	12.0	13.5	15.4	16.9	16.9	17.0	16.5	15.5	15.4	13.9	13.5	13.4	13.5	13.4	13.2	13.2	14.0
5		13.4	13.4	13.4	13.5	15.2	12.9	11.8	12.4	13.0	13.4	13.5	13.4	13.2	13.2	15.4	16.4	17.2	17.2	12.5	14.9	13.5	13.0	13.0	12.4	13.8
6	Q	12.4	12.4	13.4	13.5	13.2	13.0	12.4	12.7	13.2	13.5	13.5	14.2	15.2	16.4	15.7	16.7	17.5	18.5	17.2	15.4	13.5	12.0	11.8	12.0	14.1
7		12.5	13.1	13.6	13.8	13.8	13.1	12.6	12.5	15.6	15.1	20.5	21.6	28.5	27.5	22.5	20.1	18.5	18.3	15.1	4.8	4.1	6.9	11.4	11.9	15.3
8		12.3	13.6	14.8	13.3	11.9	13.8	12.5	5.8	16.8	14.3	13.8	15.8	15.6	17.0	16.6	16.8	19.0	18.6	16.8	15.3	11.8	10.6	10.8	10.3	14.1
9		10.8	12.1	14.0	14.8	13.8	13.6	12.5	13.8	13.6	13.6	13.8	14.8	15.3	15.5	17.0	17.5	18.6	18.6	16.6	14.1	12.5	12.3	11.8	11.4	14.3
10	Q	12.5	13.1	14.1	14.1	13.8	13.8	13.6	13.6	13.8	13.3	14.3	16.8	14.0	17.1	18.6	19.3	19.0	17.1	15.3	12.3	11.4	11.8	11.8	11.9	14.4
11		11.9	12.3	13.0	13.5	13.5	13.1	13.3	13.5	14.1	13.1	14.6	15.6	16.1	18.0	14.1	18.6	18.0	15.3	15.0	12.1	10.9	10.1	9.8	10.4	13.7
12		11.4	13.3	13.8	13.6	13.6	13.8	13.6	12.5	11.8	14.0	20.1	18.6	21.8	24.0	20.6	20.1	20.3	12.5	12.5	14.0	13.8	13.1	13.1	13.1	15.4
13	Q	13.3	13.0	13.6	13.8	14.1	13.6	13.5	13.6	13.5	14.3	15.8	17.0	15.0	14.1	15.3	16.5	18.6	18.5	16.6	15.1	13.6	11.9	11.4	10.8	14.4
14		11.8	12.8	15.1	14.5	15.1	19.0	16.6	14.3	17.1	16.5	15.5	16.6	15.3	16.1	15.6	17.1	18.1	17.6	15.5	13.5	10.1	10.4	8.4	10.4	14.7
15	D	11.6	10.6	10.4	9.6	11.8	13.5	12.3	15.0	15.0	18.3	18.3	19.0	19.6	16.6	15.5	18.3	16.8	18.5	16.0	7.4	7.6	9.1	10.6	12.6	13.9
16		12.5	12.5	13.6	13.1	14.0	7.3	14.8	11.6	12.5	12.1	13.8	17.3	24.0	8.6	22.6	21.8	17.1	15.6	15.1	13.5	11.9	12.1	11.6	10.9	14.2
17	D	13.3	12.3	10.9	8.6	8.1	12.8	11.9	12.5	13.8	3.4	23.3	17.8	15.1	12.5	16.6	17.6	18.5	15.3	12.6	9.9	12.5	12.3	13.5	13.0	13.3
18	D	11.8	13.3	13.8	13.8	15.8	12.8	9.3	1.4	15.6	13.8	17.0	21.5	16.6	21.6	21.6	19.6	19.0	15.5	13.5	14.0	15.0	13.1	13.6	12.6	14.8
19		11.8	17.0	13.5	12.3	12.6	14.6	14.0	13.6	11.8	8.6	17.0	16.8	18.1	15.0	14.1	16.6	16.6	16.5	14.1	13.1	10.4	10.3	10.4	11.9	13.8
20		12.3	12.5	12.5	20.3	18.5	13.6	15.3	13.5	12.1	13.5	13.1	17.0	17.3	17.5	16.3	17.0	15.5	12.6	10.8	10.3	10.8	11.6	11.1	11.8	14.0
21		13.5	11.6	13.3	14.0	13.6	13.5	11.3	11.9	12.6	12.1	10.8	15.6	16.8	16.6	15.6	16.6	17.1	17.0	13.6	13.1	12.1	11.6	11.8	12.3	13.7
22		12.6	13.0	13.8	13.6	13.5	12.3	12.3	12.3	11.9	12.1	13.6	14.1	15.1	15.0	15.3	17.0	18.3	17.0	15.5	13.6	11.8	11.6	11.6	11.9	13.7
23		11.9	12.1	12.5	12.6	13.5	13.5	13.5	11.9	13.0	13.6	14.6	14.1	15.1	17.0	18.3	18.0	15.0	13.0	13.6	13.3	11.9	11.6	11.6	11.8	13.6
24		12.3	13.3	13.6	13.6	13.3	13.0	12.8	13.3	13.3	13.5	13.5	13.3	15.1	10.1	10.4	6.4	12.8	10.4	10.4	13.1	13.3	6.6	5.4	8.6	11.7
25	D	10.1	13.5	14.1	14.8	14.8	19.1	15.3	9.8	25.0	24.6	36.7	25.1	31.7	17.0	11.4	13.6	12.1	4.1	5.4	9.6	9.8	10.3	11.9	12.5	15.5
26	D	14.1	20.8	13.6	18.6	18.5	16.3	14.0	12.1	12.3	13.6	15.1	17.1	2.9	14.8	18.0	17.5	20.3	18.5	13.5	13.6	11.9	11.6	11.4	11.4	14.6
27		13.8	13.8	13.8	15.3	19.1	23.6	15.8	18.6	22.1	21.5	16.6	14.0	14.6	8.4	16.5	16.3	14.0	10.8	13.5	9.4	11.4	11.9	10.8	13.0	14.9
28		12.1	13.3	18.5	15.0	15.1	15.0	14.3	13.6	13.1	13.8	12.8	13.6	13.8	15.0	15.8	17.0	19.3	18.6	16.8	14.6	13.6	13.1	13.5	13.1	14.8
29	Q	12.5	13.6	14.0	14.0	14.0	14.8	13.6	12.8	13.1	13.5	13.6	13.5	13.8	15.1	16.3	17.3	18.8	18.6	17.6	16.6	15.3	13.1	12.3	11.9	14.6
30		12.5	13.5	13.6	13.8	15.6	16.5	14.1	13.6	15.0	23.3	14.3	17.3	16.8	14.8	14.8	15.8	18.6	18.0	15.8	14.0	12.5	12.1	13.3	13.0	15.1
31		12.5	12.6	13.1	13.5	13.5	13.6	13.5	13.3	16.1	17.5	14.5	15.5	18.6	21.6	20.0	12.5	6.6	10.1	15.5	14.0	13.5	13.5	11.9	13.5	14.2
MEAN	A	12.5	13.3	13.7	13.9	14.3	14.1	13.3	12.6	14.3	14.3	15.6	16.4	16.6	16.0	16.5	16.8	16.9	15.4	14.3	12.9	12.1	11.7	11.8	12.1	14.2
MEAN	Q	12.8	13.1	13.7	13.8	13.7	13.6	13.2	13.0	13.3	13.5	14.1	15.0	14.3	15.4	16.2	17.1	18.2	17.9	16.4	14.9	13.7	12.6	12.3	12.2	14.3
MEAN	D	12.2	14.1	12.6	13.1	13.8	14.9	12.6	10.1	16.3	14.8	22.1	20.1	17.2	16.5	16.6	17.3	17.3	14.4	12.2	10.9	11.3	11.3	12.2	12.4	14.4

VERTICAL INTENSITY

TABLE 3 MEANOOK — Z = 58000 PLUS TABULAR VALUES IN GAMMAS — JANUARY 1969

HOUR UT / DAY		0 TO 1	1 TO 2	2 TO 3	3 TO 4	4 TO 5	5 TO 6	6 TO 7	7 TO 8	8 TO 9	9 TO 10	10 TO 11	11 TO 12	12 TO 13	13 TO 14	14 TO 15	15 TO 16	16 TO 17	17 TO 18	18 TO 19	19 TO 20	20 TO 21	21 TO 22	22 TO 23	23 TO 24	MEAN
1		688	687	683	676	671	670	666	654	649	617	578	637	655	650	629	643	647	652	653	658	664	667	670	667	655
2		666	666	666	667	671	670	666	665	665	664	659	649	653	658	655	666	669	670	673	669	663	666	667	667	665
3	Q	667	665	665	662	662	664	664	665	665	665	662	662	662	657	660	661	664	666	668	668	667	666	666	666	664
4		662	660	662	662	662	662	662	657	656	656	656	651	648	656	659	665	666	666	665	667	666	666	666	666	661
5		666	660	660	660	656	660	661	661	661	661	660	659	656	656	656	659	662	665	666	666	667	665	662	662	661
6	Q	661	661	660	660	660	660	660	660	660	660	660	659	659	659	659	660	660	664	665	665	665	661	660	660	661
7		661	660	658	658	658	658	657	657	657	649	649	607	489	624	662	663	661	663	661	657	662	665	665	667	649
8		674	671	674	680	693	681	673	637	636	649	677	673	668	661	665	668	669	669	669	669	673	672	672	672	669
9		678	680	678	672	669	674	672	669	668	666	666	666	663	662	661	667	668	669	669	669	669	667	669	668	669
10	Q	667	667	666	663	665	666	666	665	666	669	668	662	645	648	660	660	662	666	667	666	667	667	669	668	664
11		667	663	664	664	664	664	667	668	667	670	668	666	663	657	656	661	658	659	658	662	666	666	668	664	664
12		670	667	664	664	664	667	667	670	664	659	603	600	632	637	626	616	625	633	650	662	670	672	672	672	651
13	Q	670	667	667	667	663	663	663	663	661	656	643	637	658	658	659	661	663	663	662	667	667	667	668	667	662
14		668	676	679	679	674	670	655	621	615	662	623	633	669	662	662	661	661	661	661	663	664	668	672	686	660
15	D	692	693	697	697	704	681	685	682	671	652	639	653	647	651	669	663	663	662	660	669	669	664	670	674	671
16		674	676	671	679	691	704	716	675	674	647	627	647	601	568	608	648	663	669	668	669	664	665	669	670	660
17	D	674	680	719	712	752	741	719	683	644	550	574	639	612	634	659	647	659	657	683	679	683	688	686	698	670
18	D	711	691	687	682	693	687	647	591	669	640	647	506	589	627	632	664	660	668	674	681	687	683	681	682	657
19		692	699	681	683	677	680	683	681	647	555	559	623	641	644	663	668	663	662	669	685	682	673	671	673	661
20		671	674	679	683	688	693	695	676	668	659	658	658	634	647	650	651	664	662	663	669	670	670	670	673	668
21		680	681	676	674	673	664	635	646	662	654	628	658	659	658	662	664	668	668	669	669	669	670	668	665	663
22		664	664	664	664	659	659	659	662	642	623	662	668	660	660	662	664	664	667	668	670	669	665	664	663	661
23		668	665	665	664	668	668	671	670	665	663	660	658	650	654	658	665	665	657	656	658	659	658	658	662	662
24		664	659	659	659	659	659	659	658	658	658	657	651	644	589	534	527	552	599	641	663	676	711	687	699	643
25	D	718	778	715	682	691	694	657	612	539	536	710	536	509	563	561	634	623	657	681	691	711	705	693	686	649
26	D	740	754	687	704	699	675	663	659	658	660	662	577	515	585	599	682	675	670	670	668	673	674	673	680	663
27		682	680	675	676	675	671	669	597	576	555	567	601	591	586	644	645	658	665	671	676	680	682	686	682	645
28		688	687	694	682	671	671	668	665	665	662	651	663	663	662	660	669	665	663	663	662	668	673	674	673	669
29	Q	670	668	670	668	665	663	663	659	662	662	660	659	658	658	663	665	662	662	663	668	669	668	667	664	664
30		665	668	668	667	664	667	670	662	647	580	524	646	662	659	659	662	660	659	659	660	662	663	663	662	652
31		662	660	660	662	662	662	662	659	657	640	626	595	622	591	612	615	628	634	651	659	663	668	670	663	645
MEAN A		677	678	675	673	675	673	668	656	651	639	638	636	632	638	644	653	656	659	664	668	670	671	671	672	660
MEAN Q		667	665	665	664	663	663	663	662	663	662	659	656	657	656	660	661	662	664	665	667	667	666	666	665	663
MEAN D		707	719	701	695	708	696	674	646	636	608	646	582	575	612	624	658	656	663	674	677	685	683	680	684	662

HORIZONTAL INTENSITY

TABLE 4 MEANOOK H = 12500 PLUS TABULAR VALUES IN GAMMAS FEBRUARY 1969

HOUR UT / DAY		0 TO 1	1 TO 2	2 TO 3	3 TO 4	4 TO 5	5 TO 6	6 TO 7	7 TO 8	8 TO 9	9 TO 10	10 TO 11	11 TO 12	12 TO 13	13 TO 14	14 TO 15	15 TO 16	16 TO 17	17 TO 18	18 TO 19	19 TO 20	20 TO 21	21 TO 22	22 TO 23	23 TO 24	MEAN
1	Q	726	732	734	731	731	732	731	732	730	730	732	732	734	734	735	732	728	723	714	720	713	715	721	724	728
2	D	729	734	735	735	737	737	735	734	726	725	720	717	721	715	748	734	759	711	359	192	615	649	680	814	686
3	D	837	865	995	982	944	880	714	549	523	579	593	435	432	349	608	747	726	678	610	622	666	778	687	706	688
4		710	721	716	719	727	721	724	734	729	711	724	721	720	723	726	726	716	715	710	711	716	723	714	729	720
5		735	745	741	734	727	724	723	726	719	720	659	696	724	730	728	728	721	713	710	713	714	720	714	720	720
6		723	728	723	724	732	746	756	744	713	649	646	738	727	728	726	724	721	713	714	719	718	723	723	713	719
7		725	732	732	731	732	732	732	736	731	724	723	677	724	734	732	731	724	713	698	686	705	713	721	721	721
8		705	724	739	740	734	732	736	734	732	730	731	734	735	734	734	732	718	700	715	715	714	713	713	724	726
9	Q	734	735	732	734	736	736	735	735	734	734	732	732	732	732	725	731	732	721	711	711	714	714	721	730	729
10		734	738	735	736	735	734	735	735	726	732	724	734	735	728	744	735	713	715	729	713	711	690	711	708	726
11	D	961	1054	792	709	714	708	512	571	374	-1	-215	42	28	216	301	200	170	477	631	704	785	766	759	755	500
12		738	735	734	734	729	728	727	728	726	721	720	719	718	720	721	720	718	714	710	710	705	706	714	711	721
13		710	720	721	725	732	735	732	734	710	642	703	732	726	710	677	701	734	727	723	720	716	700	709	724	715
14		723	734	735	725	724	735	734	736	732	730	713	701	714	726	732	725	723	716	718	721	714	715	699	698	722
15	D	709	730	734	721	742	734	752	742	724	657	635	732	737	734	732	734	724	709	679	659	679	704	710	713	714
16		719	721	731	736	737	742	734	721	581	726	728	710	678	724	734	716	711	713	713	713	715	715	720	723	715
17	Q	724	732	729	731	732	731	731	736	732	726	730	731	735	735	734	727	724	721	715	711	704	709	713	713	725
18	Q	719	724	727	732	734	734	734	734	734	734	735	735	736	736	736	732	726	721	716	713	710	710	714	719	727
19		726	732	735	734	735	742	742	735	741	739	740	734	669	710	738	737	731	713	704	700	701	698	711	720	724
20		724	730	732	731	730	724	731	734	734	732	736	725	721	734	737	741	724	705	710	699	689	688	700	713	722
21		710	720	734	734	731	723	721	724	735	734	734	734	732	735	735	729	720	704	688	689	692	697	707	715	720
22	Q	723	729	734	734	735	734	734	734	738	741	738	737	734	736	744	745	732	721	708	700	697	699	703	719	727
23		731	732	737	734	734	731	742	734	735	731	705	700	700	705	748	748	741	720	697	692	692	700	711	725	722
24		734	731	734	736	734	727	734	736	710	735	744	741	742	742	744	736	725	719	711	708	700	700	707	714	727
25		727	723	726	735	737	735	734	732	742	738	735	723	735	745	745	741	727	711	703	699	696	699	700	711	725
26		721	725	734	730	748	734	736	725	689	726	745	742	735	736	745	742	732	708	694	692	699	704	711	721	724
27	D	723	734	727	745	745	745	741	731	734	741	741	741	744	731	657	566	575	661	719	711	711	689	678	705	708
28		715	715	725	724	746	758	770	599	699	725	734	732	711	714	713	710	688	708	715	699	693	711	715	723	714
MEAN	A	735	746	743	740	741	738	727	716	701	690	682	690	689	696	710	706	699	702	690	684	703	709	710	722	711
MEAN	Q	725	730	731	732	734	733	733	734	734	733	734	734	734	734	734	734	728	722	713	711	707	709	714	721	727
MEAN	D	792	823	796	778	776	761	691	665	616	540	495	533	533	549	609	596	591	647	600	578	691	717	703	738	659

DECLINATION

TABLE 5 MEANOOK — D = 23.5 DEGREES EAST PLUS TABULAR VALUES IN MINUTES — FEBRUARY 1969

DAY		0 TO 1	1 TO 2	2 TO 3	3 TO 4	4 TO 5	5 TO 6	6 TO 7	7 TO 8	8 TO 9	9 TO 10	10 TO 11	11 TO 12	12 TO 13	13 TO 14	14 TO 15	15 TO 16	16 TO 17	17 TO 18	18 TO 19	19 TO 20	20 TO 21	21 TO 22	22 TO 23	23 TO 24	MEAN
1	Q	13.5	13.3	13.6	13.8	13.6	13.5	13.5	13.1	13.8	14.0	13.6	14.0	13.6	13.6	14.6	16.3	17.3	16.8	15.6	13.3	13.6	11.9	13.5	13.5	14.0
2	D	12.5	12.5	12.8	13.1	12.8	12.8	12.8	12.3	13.6	15.3	15.3	15.8	15.6	15.3	18.1	15.3	20.5	28.1	63.6	29.0	15.1	13.6	10.9	8.6	17.3
3	D	14.3	14.0	10.4	5.1	.4	10.8	12.6	.3	6.8	33.3	26.3	51.2	32.2	29.2	39.0	26.8	23.5	22.0	16.6	8.6	6.8	8.3	7.4	8.9	17.3
4		11.8	14.1	14.3	15.1	14.8	14.8	14.1	16.8	13.1	11.3	17.3	16.6	18.6	16.8	17.5	18.8	22.0	18.5	15.0	13.6	11.4	8.4	9.3	7.9	14.7
5		7.6	4.8	13.3	15.0	14.3	15.3	15.1	12.1	15.5	15.1	13.5	13.8	16.5	18.5	18.8	20.8	19.6	16.5	13.3	11.8	11.4	11.1	13.6	14.0	14.2
6		14.0	13.5	13.6	27.1	21.5	14.0	18.8	11.8	13.8	13.1	13.5	15.6	14.5	15.6	17.1	19.0	19.3	19.1	15.8	13.8	12.5	10.1	11.4	12.8	15.5
7		13.6	13.3	13.5	13.6	13.5	13.5	12.1	15.3	12.1	14.3	17.1	20.1	20.6	21.6	18.5	22.1	21.8	19.8	18.3	11.9	8.8	8.8	8.4	8.3	15.0
8		8.4	10.1	13.5	13.8	14.0	16.6	16.5	13.5	13.6	15.0	15.3	16.3	15.5	16.8	18.5	20.0	21.5	15.6	11.4	10.6	9.9	10.1	11.1	11.4	14.1
9	Q	10.4	10.6	11.8	13.0	13.3	13.5	13.5	13.5	13.6	14.1	15.3	15.3	15.5	15.3	15.6	17.6	18.5	19.0	18.0	16.0	13.5	11.8	10.9	10.1	14.1
10		8.9	9.1	10.3	12.1	13.6	13.8	13.8	15.3	11.9	13.5	15.5	16.8	13.6	11.9	15.6	20.1	20.5	18.5	16.3	13.8	13.5	8.3	1.9	4.1	13.0
11	D	5.1	13.8	10.9	15.1	16.8	18.6	15.5	26.6	36.2	67.4	75.2	56.7	69.1	39.0	16.8	17.6	12.5	20.6	13.5	8.1	11.3	8.3	3.9	6.4	24.4
12		9.9	11.3	12.8	13.6	12.1	14.0	15.0	13.6	14.0	15.0	16.6	16.5	16.1	16.0	17.0	19.1	20.6	20.3	20.6	15.5	12.6	11.8	10.6	11.9	14.9
13		12.6	8.9	11.8	13.5	12.5	13.8	10.1	10.3	9.6	15.0	16.8	15.3	15.5	16.8	15.3	18.5	17.1	17.0	15.8	16.0	15.0	14.8	11.9	10.1	13.9
14		11.8	10.4	10.6	11.3	12.1	13.3	13.8	14.1	13.8	15.1	17.0	13.5	18.5	18.3	15.6	18.6	18.8	18.3	14.3	12.3	12.1	10.4	10.6	10.1	13.9
15	D	8.6	9.4	10.8	23.3	14.1	13.6	15.1	12.1	13.5	11.6	11.3	11.8	15.1	18.3	15.1	18.1	18.6	17.1	16.6	9.9	4.3	8.1	10.1	11.4	13.3
16		8.6	10.4	10.9	12.1	12.5	18.3	21.3	12.5	7.1	15.0	15.5	16.6	20.1	20.5	18.1	19.5	16.8	13.1	11.8	12.8	14.5	13.6	12.1	12.6	14.4
17	Q	11.9	11.9	12.1	12.5	12.1	12.1	12.3	10.3	11.8	14.3	16.1	17.5	16.5	15.3	16.6	17.5	17.6	17.3	16.0	14.3	14.0	13.3	11.8	12.8	14.1
18	Q	12.8	11.9	11.9	12.1	12.8	12.8	12.6	12.3	12.3	12.5	13.0	13.5	13.6	14.6	15.6	17.5	18.3	16.8	14.1	11.6	10.4	11.6	11.8	11.8	13.3
19		11.6	10.3	10.4	10.6	11.9	8.8	10.1	10.6	10.4	11.9	13.5	15.3	11.8	18.6	18.8	23.3	21.5	20.1	17.6	15.0	11.4	10.8	10.3	11.4	13.6
20		11.3	11.8	11.9	11.8	11.9	13.5	13.1	12.1	12.6	14.0	13.5	15.5	15.6	13.0	15.1	17.8	16.3	12.5	12.5	12.3	12.3	12.1	12.3	11.9	13.2
21		10.9	12.1	12.3	13.3	13.5	14.3	23.8	13.6	11.8	11.9	12.5	13.8	14.0	15.1	15.6	17.5	19.5	20.6	16.3	15.1	12.5	11.8	10.6	10.8	14.3
22	Q	10.8	10.6	11.6	11.9	12.1	11.9	11.9	13.1	12.5	12.3	12.1	13.5	11.8	12.5	15.5	18.1	18.3	17.0	16.8	15.3	12.3	10.1	9.9	9.9	13.0
23		9.9	10.7	10.4	11.9	11.7	14.1	24.2	16.6	12.2	12.0	7.4	13.2	14.1	12.6	18.6	19.2	21.9	22.7	19.2	15.4	13.7	10.5	10.7	10.5	14.3
24		11.2	12.0	12.7	12.2	12.0	13.4	13.6	12.6	12.0	12.4	13.9	15.1	13.7	14.4	15.7	19.9	22.4	20.4	18.7	17.1	14.2	11.9	11.0	10.4	14.3
25		9.2	10.5	12.2	12.0	12.0	11.7	13.6	13.7	13.1	13.6	13.6	11.9	12.4	15.7	16.9	18.7	20.4	20.7	17.6	17.6	15.7	13.7	12.0	10.4	14.1
26		10.4	10.5	10.7	15.4	10.4	12.4	12.7	14.6	21.9	18.6	16.9	16.9	15.2	14.2	17.7	18.2	19.4	21.4	13.4	10.5	11.9	11.7	12.0	12.0	14.5
27	D	12.0	11.9	15.4	12.4	10.2	12.9	10.0	17.6	15.9	12.7	13.7	13.9	12.4	15.2	18.9	-0.1	10.9	15.7	15.2	14.1	12.4	12.2	12.4	13.6	13.0
28		13.4	13.6	12.7	12.9	11.9	10.7	15.2	10.4	15.4	15.7	15.6	16.7	16.7	17.4	20.1	18.2	18.2	12.6	16.1	15.1	14.4	12.0	13.2	10.0	14.5
MEAN	A	11.0	11.3	12.1	13.6	12.7	13.5	14.5	13.2	13.7	16.4	17.0	17.9	17.8	17.2	17.7	18.4	19.1	18.5	17.5	13.9	12.2	11.1	10.6	10.6	14.7
MEAN	Q	11.9	11.7	12.2	12.7	12.8	12.8	12.8	12.5	12.8	13.4	14.0	14.7	14.2	14.3	15.6	17.4	18.0	17.4	16.1	14.1	12.8	11.7	11.6	11.6	13.7
MEAN	D	10.5	12.3	12.1	13.8	10.9	13.7	13.2	13.8	17.2	28.1	28.4	29.9	28.9	23.4	21.6	15.5	17.2	20.7	25.1	13.9	10.0	10.1	9.0	9.8	17.0

VERTICAL INTENSITY

TABLE 6 MEANOOK Z = 58000 PLUS TABULAR VALUES IN GAMMAS FEBRUARY 1969

HOUR UT / DAY		0 TO 1	1 TO 2	2 TO 3	3 TO 4	4 TO 5	5 TO 6	6 TO 7	7 TO 8	8 TO 9	9 TO 10	10 TO 11	11 TO 12	12 TO 13	13 TO 14	14 TO 15	15 TO 16	16 TO 17	17 TO 18	18 TO 19	19 TO 20	20 TO 21	21 TO 22	22 TO 23	23 TO 24	MEAN
1	Q	659	662	662	662	660	660	659	659	658	659	659	658	658	658	660	662	658	659	667	663	659	660	665	663	660
2	D	659	659	659	659	659	659	659	659	638	639	638	627	636	639	658	638	648	639	640	591	695	707	706	676	654
3	D	669	673	683	723	705	663	597	598	611	587	591	522	601	487	593	654	663	667	665	681	695	722	691	691	643
4		681	683	679	679	680	680	688	693	686	676	687	687	674	671	669	670	664	665	668	665	659	662	669	682	676
5		692	719	698	680	681	682	681	657	663	669	632	634	647	659	663	664	664	665	669	674	671	676	674	675	670
6		677	677	693	707	706	719	724	691	670	635	593	671	673	673	670	673	673	675	679	677	671	674	683	695	678
7		683	682	673	669	669	670	671	667	674	671	660	601	624	650	660	657	658	660	668	660	665	670	685	683	664
8		683	693	685	683	685	694	685	671	670	668	668	662	667	660	659	659	659	658	669	669	673	674	671	670	672
9	Q	671	671	670	670	669	668	664	663	669	669	667	665	660	660	659	659	662	668	671	669	668	664	665	669	666
10		670	670	671	671	669	662	663	658	638	611	609	624	651	648	664	658	659	669	670	670	669	671	706	712	661
11	D	768	760	794	697	683	687	535	486	467	310	374	772	811	640	561	642	647	676	705	734	733	688	704	693	649
12		686	687	687	688	696	695	694	689	690	692	686	683	677	676	676	678	677	674	675	674	675	675	680	702	684
13		702	699	695	687	686	687	675	696	651	636	651	672	672	659	634	641	661	669	674	672	680	678	672	681	672
14		671	680	678	686	683	682	677	674	671	670	647	623	635	641	661	671	672	670	672	674	674	672	674	687	669
15	D	683	684	689	710	686	694	699	687	674	623	598	649	660	658	663	661	658	660	665	672	674	684	687	683	671
16		696	684	683	682	681	677	671	666	590	659	661	636	586	625	659	660	672	669	670	671	676	674	672	669	662
17	Q	665	663	663	664	664	671	669	665	666	661	663	663	664	660	664	669	671	671	668	672	672	672	671	661	666
18	Q	660	660	660	660	660	660	660	660	660	660	660	660	660	659	660	663	665	663	663	665	664	661	661	660	661
19		660	661	661	668	676	686	683	671	661	660	659	647	582	574	619	635	648	659	665	661	670	671	669	663	655
20		660	660	660	668	689	684	671	661	658	645	645	635	628	645	649	653	653	646	643	645	652	660	668	671	656
21		671	672	668	660	660	664	653	657	658	659	658	659	658	658	660	660	660	658	660	660	661	663	663	661	661
22	Q	659	658	659	659	659	659	660	659	653	652	651	651	648	641	647	649	652	657	657	659	659	661	666	664	656
23		664	660	660	659	660	676	645	647	657	648	610	593	604	588	640	657	657	653	651	653	659	663	664	664	647
24		664	660	660	660	660	668	665	658	609	625	654	652	653	655	657	659	659	658	657	660	660	663	663	663	656
25		663	664	669	669	660	660	659	658	645	651	652	642	643	657	660	664	665	661	660	660	664	670	670	669	660
26		666	663	668	672	712	684	670	630	528	587	645	655	649	645	652	659	660	651	643	657	661	674	676	672	653
27	D	664	668	677	672	689	676	663	622	640	660	657	648	648	636	598	513	571	664	670	681	682	687	682	686	652
28		683	676	683	681	686	695	623	569	624	649	669	668	654	653	654	659	647	651	657	657	661	675	687	694	661
MEAN	A	676	677	678	677	678	677	663	653	642	637	637	649	651	642	649	653	657	662	665	666	672	674	677	677	662
MEAN	Q	663	663	663	663	663	664	663	661	661	660	660	659	658	656	658	660	662	663	665	666	664	664	666	663	662
MEAN	D	689	689	701	692	684	676	631	610	606	564	571	644	671	612	614	622	638	661	669	672	696	698	694	686	654

HORIZONTAL INTENSITY

TABLE 7 MEANOOK H = 12500 PLUS TABULAR VALUES IN GAMMAS MARCH 1969

DAY	HOUR UT	0 TO 1	1 TO 2	2 TO 3	3 TO 4	4 TO 5	5 TO 6	6 TO 7	7 TO 8	8 TO 9	9 TO 10	10 TO 11	11 TO 12	12 TO 13	13 TO 14	14 TO 15	15 TO 16	16 TO 17	17 TO 18	18 TO 19	19 TO 20	20 TO 21	21 TO 22	22 TO 23	23 TO 24	MEAN
1		688	707	716	721	721	724	723	724	726	724	727	726	725	724	726	723	700	654	700	700	703	708	719	711	713
2		707	732	768	777	726	721	723	723	723	723	721	679	636	704	731	732	727	715	706	704	708	711	713	715	718
3	Q	724	725	731	732	731	732	732	734	734	734	735	735	735	734	734	734	724	720	708	700	700	701	705	714	724
4	Q	723	726	734	734	734	734	734	734	734	735	736	736	736	735	739	736	727	716	711	705	713	717	706	710	727
5		713	726	734	732	734	735	740	737	744	740	736	668	714	746	746	741	736	725	709	700	708	713	723	732	726
6		721	728	742	735	744	745	747	737	735	730	670	690	746	745	737	721	709	678	699	699	698	694	708	725	720
7		724	734	727	740	758	770	757	749	746	721	723	734	730	678	645	710	726	698	665	689	703	715	709	727	720
8		721	739	756	758	755	739	732	732	726	677	732	700	703	738	735	726	723	709	699	701	709	710	715	703	722
9		723	734	737	736	741	736	741	734	732	713	744	736	708	697	688	723	736	718	697	701	714	721	715	725	723
10	Q	734	732	735	736	734	741	742	741	732	711	741	736	735	737	741	741	738	734	727	715	715	713	713	721	731
11		726	736	735	746	746	746	743	728	690	645	616	581	603	714	731	727	746	730	710	678	705	726	790	876	715
12	D	904	856	925	865	843	737	384	481	467	350	354	702	739	701	701	678	645	668	711	709	724	720	725	729	680
13		726	745	743	730	731	730	736	733	727	727	726	722	725	731	726	718	715	719	717	714	714	720	725	725	726
14		732	733	733	727	733	735	735	735	735	735	732	735	735	735	727	720	716	714	693	691	701	690	722	728	724
15		745	749	815	805	814	729	716	689	417	509	566	550	647	690	696	671	719	725	704	714	721	721	721	735	690
16		731	722	730	737	750	720	611	567	538	354	515	758	743	747	757	756	742	725	715	712	712	720	735	750	689
17	D	791	923	933	736	813	856	787	739	721	613	690	677	272	637	758	746	660	613	670	706	716	772	728	724	720
18		724	731	737	755	756	736	648	649	679	638	668	728	743	745	745	733	720	680	716	712	712	702	726	715	712
19		733	745	735	736	738	736	737	727	671	745	746	746	746	746	748	745	735	716	705	705	719	725	712	747	731
20		853	996	973	732	725	724	724	693	761	662	655	746	731	724	709	699	669	647	677	691	694	741	778	788	741
21		766	736	757	736	738	755	725	657	708	687	683	670	732	742	733	742	732	712	702	690	689	710	728	715	719
22		736	745	745	757	733	733	738	737	707	635	671	658	689	700	700	710	718	719	691	687	691	717	725	727	711
23	D	724	722	724	733	735	735	736	736	737	737	741	747	745	747	736	712	706	704	629	644	677	795	1092	1016	750
24	D	815	708	801	944	965	746	688	583	385	-204	54	244	534	738	748	735	730	719	710	717	720	720	716	711	634
25	D	709	701	706	707	707	710	712	489	368	484	701	735	667	663	626	699	701	690	673	690	717	722	749	776	671
26		742	733	712	716	720	717	721	721	725	728	690	688	724	725	691	701	717	697	690	704	708	722	724	733	715
27	Q	725	720	727	729	721	725	730	728	735	736	733	737	736	738	738	739	738	722	712	712	712	712	717	721	727
28	Q	727	731	735	735	732	747	746	736	738	738	742	743	742	738	735	738	720	717	722	711	712	712	718	727	731
29		731	733	737	735	735	738	740	735	706	670	726	743	711	712	707	705	722	710	721	715	707	727	745	784	725
30		779	721	727	735	733	730	732	735	716	712	735	735	735	733	733	732	712	677	669	679	700	725	711	732	722
31		726	746	733	738	746	746	745	738	706	714	722	735	737	729	733	746	728	700	660	681	695	698	710	726	722
MEAN	A	743	749	759	749	751	739	716	699	676	639	669	694	697	722	723	724	717	702	697	699	707	719	736	744	716
MEAN	Q	726	727	732	733	730	736	737	734	734	731	738	737	737	736	737	738	729	722	716	709	711	711	712	719	728
MEAN	D	789	782	818	797	813	757	661	606	536	396	508	621	591	697	714	714	689	679	679	693	711	746	802	791	691

DECLINATION

TABLE 8 MEANOOK D = 23.5 DEGREES EAST PLUS TABULAR VALUES IN MINUTES MARCH 1969

DAY	HOUR UT	0 TO 1	1 TO 2	2 TO 3	3 TO 4	4 TO 5	5 TO 6	6 TO 7	7 TO 8	8 TO 9	9 TO 10	10 TO 11	11 TO 12	12 TO 13	13 TO 14	14 TO 15	15 TO 16	16 TO 17	17 TO 18	18 TO 19	19 TO 20	20 TO 21	21 TO 22	22 TO 23	23 TO 24	MEAN
1		10.2	10.4	12.2	13.4	13.4	13.4	13.4	13.4	12.7	13.1	13.7	14.6	14.9	15.1	17.4	18.7	17.1	10.0	3.4	7.5	8.7	10.2	9.0	11.4	12.4
2		10.2	9.4	14.2	7.2	13.7	12.7	12.4	13.6	13.2	13.7	14.9	11.5	11.0	10.9	18.7	20.1	20.6	19.1	16.2	15.4	13.7	12.6	12.4	12.4	13.7
3	Q	12.2	12.2	12.2	12.4	12.9	12.9	12.6	12.2	12.4	13.6	13.7	13.9	13.6	14.2	15.6	18.2	19.4	19.2	17.2	15.4	13.6	11.9	10.9	11.5	13.9
4	Q	11.9	11.9	11.9	12.0	12.2	12.2	12.4	12.6	12.6	12.4	13.1	13.1	13.6	13.4	15.4	18.4	18.7	16.6	15.2	11.2	9.7	6.7	5.9	5.9	12.4
5		9.9	11.7	12.0	12.6	12.6	12.2	11.9	11.9	12.0	12.2	13.6	16.9	18.7	18.6	20.9	20.4	18.7	19.4	16.6	15.1	12.2	10.5	9.5	7.5	14.1
6		10.4	9.2	8.7	10.7	10.5	11.5	11.4	12.2	15.2	15.2	17.1	21.1	15.6	16.1	18.4	16.9	14.9	11.7	12.4	11.5	10.5	8.9	7.5	7.7	12.7
7		8.5	8.7	11.9	12.0	8.7	10.7	14.2	12.7	16.6	12.4	11.9	13.4	15.6	9.4	10.4	17.2	20.7	19.2	12.2	8.4	5.4	6.0	8.7	7.4	11.8
8		8.4	8.4	7.2	10.4	15.1	12.7	12.6	14.2	13.9	14.9	16.9	17.2	12.0	15.1	17.1	18.9	19.9	18.9	14.9	14.4	12.0	11.9	10.7	9.4	13.6
9		8.9	8.7	8.4	7.5	8.7	12.4	13.2	12.4	15.1	19.1	18.4	16.6	20.2	17.6	21.6	20.6	16.9	19.4	15.6	14.4	13.7	12.2	12.2	10.7	14.3
10	Q	8.7	9.9	9.9	8.5	10.7	10.0	12.4	11.9	14.2	18.9	14.4	13.7	13.9	14.1	15.7	17.2	18.7	19.4	19.1	15.2	12.7	12.6	12.0	11.4	13.6
11		10.0	8.5	9.9	10.9	10.2	8.7	17.2	12.0	25.4	26.6	29.9	28.1	42.9	24.4	20.2	18.6	18.4	18.9	17.1	18.7	12.6	10.5	7.5	7.9	17.3
12	D	7.2	6.9	1.2	3.0	-5.2	1.4	13.4	23.7	33.6	18.2	26.9	19.1	14.9	17.6	16.1	17.6	14.1	17.9	17.1	14.1	13.2	12.0	10.2	9.2	13.5
13		10.7	18.7	12.0	11.5	12.0	12.0	14.2	12.7	12.7	14.1	14.4	13.7	13.6	16.6	18.7	20.6	20.7	18.7	16.1	13.7	10.4	10.4	8.7	8.5	14.0
14		7.4	5.2	5.9	9.0	12.0	11.4	12.4	12.4	13.2	13.7	14.2	16.6	15.4	16.6	20.6	22.1	19.7	19.9	14.1	12.7	10.4	9.0	5.5	5.7	12.7
15		3.4	2.0	10.7	2.0	7.0	14.2	11.5	15.4	12.7	34.1	26.9	28.1	27.2	23.4	23.7	15.9	15.9	20.1	12.0	10.0	10.4	11.2	11.7	10.5	15.0
16		12.0	12.0	12.0	11.4	13.4	24.6	5.0	17.4	17.2	36.8	29.8	17.1	20.6	23.2	19.2	19.2	19.4	20.4	18.2	15.9	12.6	11.5	9.9	9.2	17.0
17	D	2.5	6.5	3.9	9.9	4.9	9.2	10.2	12.0	12.7	15.1	19.2	19.9	22.2	18.7	20.7	25.2	26.9	7.2	2.4	8.4	13.6	9.9	11.2	11.9	12.7
18		12.4	12.6	12.0	14.4	14.1	15.1	18.2	21.4	21.6	10.9	17.4	12.7	15.7	17.2	20.1	20.7	22.1	16.7	14.4	15.7	13.7	11.7	9.0	12.9	15.5
19		12.0	12.0	11.9	12.0	12.2	11.9	11.7	22.1	17.6	15.4	12.6	13.7	14.2	16.1	19.9	21.9	22.2	21.6	18.4	14.4	13.6	8.9	2.0	-4.1	13.9
20		3.5	-6.2	-6.0	11.9	12.4	12.4	10.4	20.2	8.7	10.5	16.6	15.1	15.6	18.2	18.7	24.4	23.9	16.6	8.2	8.4	8.2	7.0	3.2	3.4	11.1
21		7.4	7.5	4.0	9.2	11.7	12.0	18.7	10.5	18.2	14.1	11.9	12.0	12.2	14.7	18.7	21.9	24.1	23.9	20.4	17.2	9.0	6.7	5.4	5.5	13.2
22		5.0	5.4	5.9	12.0	11.5	13.2	12.6	12.7	26.9	24.9	25.7	20.7	15.2	14.9	18.7	19.9	21.9	22.1	20.7	13.2	10.4	7.2	5.4	4.7	14.6
23	D	5.9	8.9	11.0	11.0	11.9	12.0	12.7	12.6	13.7	13.6	13.4	14.4	15.2	16.7	19.1	23.6	20.4	22.1	36.8	33.6	34.1	32.1	8.7	-8.3	16.5
24	D	5.0	4.7	-34.5	-34.7	-8.2	-2.3	-9.7	12.7	33.4	40.8	75.8	37.6	20.6	15.2	20.4	25.1	25.4	24.4	22.7	20.2	18.7	16.9	15.4	13.6	15.0
25	D	12.6	12.0	11.9	13.6	13.6	14.1	13.6	19.9	24.4	30.4	22.2	18.2	23.7	24.4	23.7	21.9	21.7	18.4	13.6	10.4	10.4	11.5	12.7	16.2	17.3
26		11.9	14.2	12.4	12.6	12.9	12.7	14.1	16.2	20.9	14.4	14.6	11.2	14.4	14.7	14.2	17.1	21.2	16.4	16.9	13.4	11.5	9.4	8.7	8.7	13.9
27	Q	9.7	10.4	10.4	11.4	12.2	12.0	11.7	12.2	14.4	15.2	14.9	14.4	14.1	14.7	16.1	18.7	19.2	20.1	18.7	16.9	13.6	12.6	10.7	10.5	13.9
28	Q	10.2	10.4	10.7	11.7	11.7	14.6	11.9	12.6	13.1	13.6	13.7	13.4	13.7	13.6	14.9	17.2	19.9	19.2	17.1	16.6	14.1	12.2	11.2	10.0	13.6
29		8.7	8.5	8.7	10.4	11.0	11.5	12.2	18.2	20.9	21.2	20.4	15.9	13.7	14.9	14.1	16.7	18.2	16.1	15.4	16.1	15.7	11.9	9.5	10.2	14.2
30		3.9	9.0	10.7	12.0	15.4	13.4	13.4	12.6	10.5	13.4	14.1	14.1	13.9	15.6	18.7	21.9	24.1	25.7	14.2	9.4	8.5	9.2	8.5	7.4	13.3
31		9.4	8.9	13.7	13.9	10.2	10.2	9.9	10.7	10.9	10.9	11.4	12.0	12.6	12.4	18.9	22.6	23.6	23.7	18.6	9.0	7.5	9.4	10.0	10.2	12.9
MEAN	A	8.7	9.0	8.0	9.2	10.5	11.8	12.0	14.4	16.8	17.8	19.1	16.8	16.8	16.4	18.3	20.0	20.3	18.8	16.0	14.1	12.4	11.1	9.2	8.4	14.0
MEAN	Q	10.5	10.9	11.0	11.2	11.9	12.4	12.2	12.3	13.3	14.7	14.0	13.7	13.8	14.0	15.5	18.0	19.2	18.9	17.5	15.1	12.7	11.2	10.1	9.9	13.5
MEAN	D	6.6	7.8	-1.3	.6	3.4	6.9	8.0	16.2	23.6	23.6	31.5	21.8	19.3	18.5	20.0	22.7	21.7	18.0	18.5	17.3	18.0	16.5	11.6	8.5	15.0

TABLE 9 MEANOOK   Z = 58000 PLUS TABULAR VALUES IN GAMMAS   MARCH 1969

DAY		0 TO 1	1 TO 2	2 TO 3	3 TO 4	4 TO 5	5 TO 6	6 TO 7	7 TO 8	8 TO 9	9 TO 10	10 TO 11	11 TO 12	12 TO 13	13 TO 14	14 TO 15	15 TO 16	16 TO 17	17 TO 18	18 TO 19	19 TO 20	20 TO 21	21 TO 22	22 TO 23	23 TO 24	MEAN
1		676	664	665	665	661	661	660	660	660	660	659	660	660	658	660	660	660	651	648	648	659	664	681	683	662
2		705	712	711	741	701	672	661	660	661	659	648	622	590	636	658	670	669	664	666	669	672	672	671	670	669
3	Q	666	663	664	664	663	663	660	660	660	660	660	660	658	658	659	660	660	664	663	663	664	664	664	663	662
4	Q	661	660	660	660	660	660	660	659	659	659	659	658	658	657	660	660	659	657	651	660	664	690	689	681	663
5		670	660	660	660	659	659	659	657	658	660	655	593	577	631	640	645	643	649	651	658	659	660	660	665	650
6		663	663	671	671	675	672	668	637	649	647	552	564	642	654	658	648	648	648	661	661	661	666	666	671	651
7		672	694	696	700	701	727	707	695	680	646	634	652	648	588	540	583	629	636	651	659	683	689	669	681	661
8		680	692	704	696	694	700	677	675	652	599	647	634	629	663	669	664	664	664	664	668	672	671	678	686	668
9		693	684	684	684	696	696	670	660	629	610	660	653	616	587	578	634	672	668	660	672	674	672	663	659	657
10	Q	665	660	661	671	676	675	676	674	652	604	657	660	660	660	660	659	657	655	648	659	659	660	660	660	660
11		660	663	664	675	669	688	686	665	609	574	612	507	488	580	615	646	669	663	657	669	748	743	736	728	650
12	D	681	719	612	667	731	648	555	541	640	731	662	682	673	649	648	637	640	664	685	682	684	676	677	678	661
13		677	695	689	676	671	666	666	661	665	665	660	637	647	662	666	662	660	660	666	672	673	683	689	689	669
14		684	689	707	701	687	682	676	673	670	662	643	648	658	656	654	653	653	655	661	666	673	677	685	687	671
15		700	724	747	770	762	682	689	684	587	551	636	551	573	576	561	558	599	649	656	673	676	689	685	685	653
16		676	671	671	677	696	661	634	694	746	632	519	662	660	671	678	675	670	669	666	665	670	671	673	684	666
17	D	697	753	768	717	701	585	696	683	665	589	601	614	548	561	685	682	641	600	636	673	699	731	685	673	662
18		670	672	677	697	711	700	575	593	618	569	576	635	662	673	673	666	661	658	664	666	673	684	685	677	656
19		672	673	669	671	667	665	665	620	575	652	664	662	664	664	666	661	661	661	661	664	666	671	673	695	661
20		730	709	730	705	673	685	672	575	685	637	623	675	661	661	661	660	649	649	652	661	675	707	738	744	676
21		721	709	721	706	708	735	675	495	610	610	608	612	653	670	670	673	673	667	662	672	675	685	701	681	666
22		684	690	700	721	697	673	669	662	593	555	597	613	591	612	623	623	649	658	660	661	667	688	694	694	653
23	D	690	684	666	662	669	665	665	654	654	648	650	660	660	659	658	641	630	636	638	636	672	701	635	413	648
24	D	334	478	435	519	576	532	653	624	731	702	1106	1079	700	709	724	735	712	717	709	711	706	703	700	696	679
25	D	696	690	691	691	691	695	683	660	728	658	640	697	649	653	642	671	667	673	673	685	684	685	708	728	681
26		701	706	684	678	682	684	678	676	658	677	629	601	642	673	655	660	673	670	675	673	677	687	693	695	672
27	Q	696	684	677	682	678	685	682	671	650	658	660	661	669	673	675	677	677	676	676	676	676	676	676	673	674
28	Q	676	673	673	673	673	673	677	675	672	670	667	669	670	669	670	670	671	666	666	670	667	662	664	664	670
29		665	664	664	664	665	672	687	646	617	588	613	658	642	646	649	642	666	664	672	682	676	684	701	750	661
30		732	684	677	675	693	677	677	671	647	623	659	661	666	670	672	673	672	667	676	685	684	690	684	683	675
31		679	685	701	684	669	665	666	647	601	608	619	626	640	650	653	667	664	669	670	678	678	677	673	673	660
MEAN	A	673	680	677	681	682	671	665	649	651	634	648	651	637	646	651	655	659	660	663	669	676	683	683	678	663
MEAN	Q	673	668	667	670	670	671	671	668	659	650	661	662	663	663	665	665	665	664	661	665	666	671	671	668	666
MEAN	D	620	665	635	651	674	625	650	632	683	666	732	747	646	646	671	673	658	658	669	677	689	699	681	638	666

HORIZONTAL INTENSITY

TABLE 10 MEANOOK H = 12500 PLUS TABULAR VALUES IN GAMMAS APRIL 1969

HOUR UT DAY		0 TO 1	1 TO 2	2 TO 3	3 TO 4	4 TO 5	5 TO 6	6 TO 7	7 TO 8	8 TO 9	9 TO 10	10 TO 11	11 TO 12	12 TO 13	13 TO 14	14 TO 15	15 TO 16	16 TO 17	17 TO 18	18 TO 19	19 TO 20	20 TO 21	21 TO 22	22 TO 23	23 TO 24	MEAN
1	D	735	741	743	749	747	760	777	779	743	629	591	699	714	748	758	742	690	616	658	666	657	722	779	710	715
2		731	732	728	733	733	735	733	735	735	735	726	724	721	714	735	717	668	635	673	691	706	724	758	821	723
3		896	909	760	782	732	715	708	693	711	726	728	725	711	729	726	715	690	683	671	693	700	704	712	730	731
4		732	738	742	747	756	746	727	716	613	616	643	638	624	701	749	731	727	710	689	684	695	704	694	725	702
5		737	725	732	742	737	740	660	662	694	676	718	740	739	739	741	739	714	712	701	704	701	689	710	726	716
6		746	746	756	751	750	743	741	735	736	746	743	743	739	733	730	721	725	707	688	683	678	719	709	732	729
7		802	778	779	835	814	772	659	607	685	701	719	701	639	655	702	735	702	690	674	704	701	712	707	733	717
8		736	745	738	735	726	722	725	726	726	726	711	731	720	710	724	724	717	711	706	701	704	711	717	700	720
9		724	722	736	745	755	814	811	735	725	663	635	635	643	657	681	670	671	693	683	676	720	706	714	733	706
10	Q	716	725	729	735	737	753	757	646	727	721	698	706	737	732	724	724	704	676	690	706	706	712	717	727	717
11		715	736	737	742	756	746	770	779	617	650	678	690	669	750	757	740	716	697	692	701	711	723	723	723	717
12		725	727	728	732	733	737	734	736	737	739	742	738	744	743	748	743	731	716	712	715	726	759	727	795	736
13	D	856	888	813	734	765	827	798	779	772	739	678	663	653	598	593	644	667	628	634	672	719	793	861	881	736
14		868	1056	803	701	703	719	710	720	723	715	715	682	656	727	731	699	705	688	688	703	731	775	761	773	740
15		794	740	737	764	773	737	664	716	566	640	613	534	634	738	736	737	711	700	690	691	699	712	713	720	698
16		723	738	744	756	780	783	545	650	700	726	692	607	612	723	722	713	710	681	695	692	713	760	759	780	709
17	D	791	847	820	715	723	758	539	567	582	628	546	584	625	624	658	613	651	687	676	670	727	728	748	785	679
18		822	835	893	759	737	717	645	680	727	733	727	711	678	716	729	726	717	701	695	694	695	723	723	710	729
19	Q	736	738	739	726	728	732	734	734	736	736	738	739	737	713	736	734	716	694	690	702	706	716	727	716	725
20		747	728	733	726	736	737	739	738	737	737	740	743	736	736	738	736	720	702	701	701	710	702	716	719	727
21	Q	741	727	715	728	736	736	738	734	736	740	744	744	747	749	749	747	736	725	719	716	709	710	726	721	732
22		738	746	756	760	760	770	779	783	746	756	749	702	747	758	758	761	743	728	719	716	706	711	721	725	743
23	Q	728	742	736	739	744	743	740	747	749	749	747	748	734	718	746	747	726	720	715	716	712	712	715	733	734
24		736	756	742	742	759	747	756	752	750	752	752	752	754	759	762	759	736	733	716	710	716	721	725	730	742
25		782	737	736	744	739	739	754	752	752	749	750	743	730	736	734	726	733	723	710	711	713	723	747	743	738
26	Q	739	748	747	746	739	742	743	747	747	749	750	748	746	747	748	738	736	718	718	711	723	722	721	743	738
27		757	769	743	737	747	744	739	738	746	726	681	717	753	746	717	738	737	716	715	717	717	726	728	746	733
28	D	749	756	759	777	803	583	613	164	303	715	386	508	481	330	581	736	768	753	739	747	740	747	747	739	634
29		734	732	730	725	727	721	729	738	739	733	727	736	726	723	739	713	695	708	718	701	706	738	772	827	731
30	D	769	772	803	813	814	591	650	725	572	572	680	713	665	593	605	648	715	720	717	722	738	762	765	750	703
MEAN	A	760	769	755	747	750	737	714	700	694	707	692	695	694	701	718	720	712	699	696	701	710	726	735	747	720
MEAN	Q	732	736	733	735	737	741	742	722	739	739	735	737	740	732	740	738	723	706	706	710	711	715	721	728	729
MEAN	D	780	801	788	758	771	704	675	603	594	657	576	633	627	579	639	676	698	681	685	696	716	750	780	773	693

DECLINATION

TABLE 11 MEANOOK D = 23.5 DEGREES EAST PLUS TABULAR VALUES IN MINUTES APRIL 1969

HOUR UT / DAY		0 TO 1	1 TO 2	2 TO 3	3 TO 4	4 TO 5	5 TO 6	6 TO 7	7 TO 8	8 TO 9	9 TO 10	10 TO 11	11 TO 12	12 TO 13	13 TO 14	14 TO 15	15 TO 16	16 TO 17	17 TO 18	18 TO 19	19 TO 20	20 TO 21	21 TO 22	22 TO 23	23 TO 24	MEAN
1	D	10.0	9.0	9.5	8.9	11.9	6.5	8.2	11.4	11.4	14.4	17.6	21.9	25.2	18.7	20.1	21.9	27.1	17.1	20.6	10.9	3.2	4.9	11.7	7.7	13.7
2		6.5	9.0	10.4	9.0	10.5	10.7	11.4	12.0	12.9	13.6	13.7	18.2	15.2	15.1	22.1	25.4	23.4	14.2	8.0	13.7	14.9	7.0	3.2	1.7	12.6
3		2.5	-3.8	4.0	6.7	10.7	11.5	13.7	11.7	12.2	14.1	13.7	13.7	12.9	16.6	20.4	24.2	25.4	22.6	20.6	18.6	10.7	8.2	5.9	7.0	12.7
4		5.5	7.5	10.7	13.7	11.0	9.9	10.7	12.6	11.2	9.0	18.1	13.4	13.7	13.9	18.2	20.7	22.2	23.9	21.7	17.7	14.1	10.9	7.4	7.5	13.6
5		8.0	10.7	11.4	12.2	12.9	15.4	3.9	19.7	18.1	20.6	20.7	17.1	17.9	18.1	19.1	20.2	21.6	18.2	14.9	13.6	10.9	8.5	6.9	5.4	14.4
6		5.2	6.2	6.2	5.0	4.7	8.9	8.4	10.5	14.2	11.7	10.5	10.9	11.5	13.1	16.9	19.2	18.4	20.4	18.6	12.9	6.5	5.0	4.4	1.2	10.4
7		.5	3.0	-0.0	4.5	5.2	2.2	13.2	6.7	18.4	16.4	12.5	13.2	13.2	16.4	18.4	19.2	18.7	15.4	13.2	11.3	6.8	7.2	8.0	4.3	10.3
8		5.5	4.7	6.2	10.3	10.3	10.7	10.3	11.7	13.0	13.2	11.7	11.8	13.0	13.2	14.5	15.5	15.4	15.9	14.4	13.2	10.5	8.3	5.7	8.3	11.1
9		3.1	7.9	7.9	7.6	7.1	1.9	6.7	11.9	14.6	21.8	24.1	26.8	31.3	26.8	24.9	17.3	15.3	13.1	11.9	8.4	7.1	3.7	7.9	7.1	13.2
10	Q	9.7	8.2	8.7	9.4	8.6	8.2	8.2	7.7	16.4	17.8	14.8	18.1	17.8	16.9	17.9	18.8	19.6	11.9	7.7	7.4	8.2	4.4	2.9	1.7	11.3
11		4.2	8.2	7.9	8.7	6.2	7.4	4.4	3.1	19.6	22.6	21.4	17.1	22.6	20.1	19.8	18.9	19.6	17.3	11.7	9.6	9.1	8.6	9.4	8.6	12.8
12		8.6	8.7	9.6	9.9	9.9	9.2	9.9	10.1	10.2	14.4	11.6	10.7	13.6	16.1	17.8	18.3	19.6	20.1	12.6	11.1	11.1	14.8	6.4	7.9	12.2
13	D	-0.1	-1.6	3.4	6.4	6.1	-2.3	5.4	.4	5.1	8.2	14.9	18.4	19.9	24.6	36.5	33.3	31.1	31.0	13.3	10.4	13.6	13.1	7.1	4.4	12.6
14		1.1	-13.8	6.4	9.9	9.9	9.4	10.2	11.2	10.2	11.6	12.6	12.7	16.4	17.9	20.3	23.4	22.3	20.3	15.3	10.7	12.6	10.6	5.1	1.9	11.2
15		2.4	5.2	8.4	10.7	14.8	13.8	8.4	11.4	3.9	10.2	14.4	6.6	17.9	22.4	23.4	23.1	21.4	18.1	11.6	10.1	6.6	6.6	6.4	6.7	11.9
16		6.4	6.4	7.6	6.6	5.2	5.4	-0.1	13.4	14.4	13.3	14.9	19.8	16.9	20.6	23.8	24.4	22.3	21.6	10.4	9.7	10.6	5.4	2.7	-0.3	11.7
17	D	.4	-3.1	-2.3	11.7	11.2	6.7	-3.3	11.4	18.4	13.6	12.4	23.6	24.4	23.1	23.3	25.3	19.3	16.6	11.6	4.2	5.2	4.4	2.7	3.1	11.0
18		2.1	-0.7	-0.4	8.3	10.0	20.7	11.3	14.7	12.8	12.3	11.3	11.5	12.6	11.8	16.3	17.7	18.5	18.3	13.1	11.0	6.5	4.6	3.6	5.8	10.6
19	Q	4.6	9.5	9.5	9.8	12.0	12.6	11.3	11.0	11.5	11.5	11.5	11.8	12.0	14.7	18.7	21.5	21.5	18.7	14.8	10.1	7.1	5.8	4.5	5.1	11.7
20		3.6	8.0	8.1	10.1	11.1	10.8	15.2	13.5	12.8	12.0	12.6	13.0	13.3	16.2	18.5	21.3	23.2	22.3	16.5	15.5	11.5	7.5	5.6	6.3	12.9
21	Q	6.0	6.8	10.1	11.5	11.5	11.5	12.1	12.0	11.6	11.6	10.8	11.5	13.1	14.8	16.7	19.8	21.5	21.3	17.3	11.6	7.3	5.3	4.6	4.3	11.9
22		3.5	3.6	4.5	5.3	6.1	5.1	5.3	9.6	13.3	15.0	9.8	8.1	16.0	16.3	16.5	19.8	21.7	22.3	18.8	13.5	10.0	7.1	6.3	6.3	11.0
23	Q	7.5	9.8	11.1	9.8	11.1	11.8	14.3	11.5	13.1	11.3	11.5	11.6	9.8	13.1	17.8	20.2	22.2	21.5	16.0	14.8	10.3	6.8	5.1	4.3	12.4
24		4.5	6.5	9.3	11.8	8.1	5.5	17.3	11.3	11.3	11.3	11.8	13.0	14.8	18.0	19.3	20.8	22.0	20.8	16.7	13.8	8.6	7.3	7.0	7.5	12.4
25		4.3	11.3	9.5	9.8	9.8	11.5	15.3	14.5	11.3	11.0	11.0	11.3	11.5	15.5	17.7	18.7	18.7	17.8	14.3	10.0	8.0	6.8	6.8	8.1	11.8
26	Q	8.8	11.3	14.8	9.8	9.8	10.8	11.5	11.5	11.5	10.5	11.3	12.8	13.3	20.2	20.0	20.3	19.7	19.7	18.0	10.5	6.6	5.3	6.1	6.5	12.5
27		7.5	8.0	13.7	15.5	14.3	13.7	14.3	15.0	13.0	11.5	16.0	16.7	16.0	16.7	18.0	19.2	18.3	18.2	14.7	8.8	6.6	5.1	4.6	5.3	12.9
28	D	6.0	6.2	6.7	6.4	3.0	-25.4	-9.0	4.0	.5	21.4	48.6	48.3	44.8	55.5	26.2	20.2	22.2	19.6	8.5	7.9	6.7	8.2	9.7	8.9	14.8
29		9.5	8.2	9.5	9.7	9.5	10.4	12.9	11.4	11.7	13.4	13.6	16.2	18.2	21.6	23.2	25.7	23.1	18.1	14.2	11.4	5.9	4.2	2.9	4.2	12.9
30	D	3.4	2.9	3.5	1.5	6.9	2.7	13.0	14.1	11.4	10.0	11.9	12.0	16.4	9.5	13.2	12.5	12.9	12.7	12.9	6.2	3.4	5.4	6.7	5.9	8.8
MEAN	A	5.0	5.5	7.5	9.0	9.3	7.9	9.2	11.0	12.3	13.6	15.0	15.7	17.2	18.6	20.0	20.9	20.9	19.0	14.5	11.3	8.7	7.0	5.9	5.4	12.1
MEAN	Q	7.3	9.1	10.9	10.1	10.6	11.0	11.5	10.7	12.8	12.5	12.0	13.2	13.2	15.9	18.2	20.1	20.9	18.6	14.8	10.9	7.9	5.5	4.7	4.4	12.0
MEAN	D	3.9	2.7	4.2	7.0	7.8	-2.3	2.9	8.3	9.4	13.5	21.1	24.9	26.2	26.3	23.9	22.6	22.5	19.4	13.4	7.9	6.4	7.2	7.6	6.0	12.2

VERTICAL INTENSITY

TABLE 12 MEANOOK

Z = 58000 PLUS TABULAR VALUES IN GAMMAS

APRIL 1969

HOUR UT / DAY		0 TO 1	1 TO 2	2 TO 3	3 TO 4	4 TO 5	5 TO 6	6 TO 7	7 TO 8	8 TO 9	9 TO 10	10 TO 11	11 TO 12	12 TO 13	13 TO 14	14 TO 15	15 TO 16	16 TO 17	17 TO 18	18 TO 19	19 TO 20	20 TO 21	21 TO 22	22 TO 23	23 TO 24	MEAN
1	D	670	666	671	687	700	701	713	715	682	570	565	587	622	660	670	667	662	641	664	754	749	731	750	688	674
2		693	695	685	688	683	673	676	672	666	662	649	624	644	632	652	659	653	649	654	672	723	760	754	772	679
3		723	719	730	737	702	684	661	625	649	666	672	666	647	662	670	664	665	678	673	709	712	701	705	700	684
4		697	713	713	659	699	709	650	661	585	552	567	597	588	634	678	675	683	683	679	681	691	693	675	693	661
5		685	682	673	675	672	673	548	581	636	619	634	658	661	665	669	664	654	676	670	677	681	677	677	677	658
6		690	689	687	694	712	693	675	673	608	660	670	664	664	661	660	658	661	659	658	665	665	677	687	713	673
7		753	734	754	750	701	628	684	638	637	649	654	640	569	575	613	664	672	667	675	702	673	676	672	683	669
8		697	706	701	695	688	673	672	670	662	653	619	660	660	652	653	656	658	661	662	664	671	676	690	673	670
9		674	673	677	685	701	733	714	695	660	579	511	543	549	550	544	547	565	624	660	674	714	696	677	677	638
10	Q	673	673	673	673	674	683	695	594	650	638	623	601	649	661	657	666	672	660	659	672	685	685	690	696	663
11		694	677	678	686	695	696	702	617	598	623	606	592	554	638	674	685	688	685	682	678	676	677	674	674	660
12		674	673	671	671	671	674	676	676	672	666	670	665	666	667	674	674	673	676	673	673	671	674	674	703	673
13	D	787	855	806	712	713	706	654	629	691	678	639	618	598	554	519	539	592	638	666	713	738	790	807	807	685
14		792	775	749	688	678	679	674	674	674	666	654	635	618	662	673	667	674	676	668	680	704	753	751	756	693
15		774	741	704	722	700	672	691	643	464	543	607	619	542	655	671	679	678	676	686	678	676	676	674	674	660
16		674	680	686	708	729	708	582	661	627	647	637	607	606	648	654	659	672	674	676	673	690	748	735	726	671
17	D	753	771	815	721	692	672	688	574	594	636	576	591	539	506	570	611	650	674	673	685	695	694	703	719	658
18		741	759	708	716	721	626	527	570	650	665	665	655	644	667	676	684	686	685	677	674	670	676	690	694	672
19	Q	698	701	685	673	666	665	663	663	663	663	663	665	662	650	654	662	666	665	661	661	662	666	679	680	668
20		696	689	682	670	666	666	673	671	662	661	661	661	659	655	659	660	661	655	650	650	653	659	677	698	666
21	Q	715	690	677	674	672	671	671	668	661	660	654	665	665	663	661	659	659	661	654	650	650	655	672	677	667
22		684	668	661	660	660	660	673	663	650	655	653	613	631	662	662	663	654	660	659	659	653	661	666	667	658
23	Q	664	671	665	665	666	672	666	648	658	661	659	661	652	622	637	652	652	650	653	652	659	660	661	666	657
24		667	683	696	684	694	637	673	667	662	661	661	661	661	661	660	660	652	655	653	650	652	652	659	666	664
25		705	707	676	667	664	672	629	631	662	662	661	650	635	641	641	638	647	658	660	664	671	673	683	682	662
26	Q	673	676	673	661	660	661	660	660	660	660	654	647	650	652	656	660	661	660	660	662	670	675	676	684	663
27		685	701	700	676	672	677	669	661	664	634	553	549	643	638	616	625	648	659	664	661	665	664	660	660	652
28	D	661	660	661	669	684	369	572	660	873	811	782	782	654	750	613	675	723	677	671	664	671	671	672	672	679
29		673	672	673	672	673	673	673	673	673	672	670	673	670	661	667	661	653	649	654	660	670	694	708	760	674
30	D	721	724	718	753	744	572	576	652	601	447	579	616	597	578	581	623	665	679	685	695	696	702	718	690	651
MEAN	A	703	704	698	690	688	663	656	650	650	641	636	635	627	639	643	652	660	664	666	675	682	690	694	698	667
MEAN	Q	685	682	675	669	668	670	671	647	659	657	651	648	656	650	653	660	662	659	657	659	665	668	676	681	664
MEAN	D	719	735	734	708	707	604	640	646	688	628	628	639	602	610	590	623	659	662	672	702	710	718	730	715	670

TABLE 13 MEANOOK — H = 12500 PLUS TABULAR VALUES IN GAMMAS — MAY 1969

DAY	HOUR UT	0 TO 1	1 TO 2	2 TO 3	3 TO 4	4 TO 5	5 TO 6	6 TO 7	7 TO 8	8 TO 9	9 TO 10	10 TO 11	11 TO 12	12 TO 13	13 TO 14	14 TO 15	15 TO 16	16 TO 17	17 TO 18	18 TO 19	19 TO 20	20 TO 21	21 TO 22	22 TO 23	23 TO 24	MEAN
1		769	765	749	749	756	736	723	690	691	702	731	725	731	723	726	713	713	700	691	705	732	736	727	736	726
2	D	738	756	741	752	749	744	737	738	720	620	748	749	716	666	691	710	702	715	678	696	709	749	770	749	723
3		732	738	747	747	757	743	681	586	636	691	666	649	694	713	658	690	706	698	702	715	725	713	733	730	702
4		746	747	739	758	742	742	741	738	744	730	719	734	736	739	737	726	713	717	700	705	713	722	725	747	732
5		771	758	742	747	741	743	746	747	747	742	741	715	671	667	731	725	718	713	697	702	694	722	731	753	728
6		744	740	759	767	758	691	749	748	747	747	741	730	721	736	749	744	736	716	707	712	723	728	716	738	735
7	Q	769	769	764	753	752	747	751	747	620	691	747	744	748	751	748	744	740	733	730	731	725	720	719	727	736
8		736	752	752	752	749	754	760	749	749	748	751	756	758	764	747	762	760	747	749	742	741	738	758	736	750
9		743	750	760	758	749	760	747	746	653	709	746	751	736	763	763	747	737	725	718	713	713	758	757	740	739
10		767	741	762	759	773	779	785	622	634	732	748	721	757	747	751	742	740	721	722	731	727	731	730	748	736
11	Q	761	758	757	746	749	747	749	746	743	727	751	750	758	759	758	750	744	731	734	728	720	720	723	733	743
12		740	755	753	753	751	750	751	752	749	761	759	762	768	774	779	770	758	735	745	735	737	744	783	792	757
13	D	815	918	877	835	940	780	772	548	438	379	327	367	243	499	571	627	665	686	752	770	813	830	998	1034	687
14	D	1029	1019	875	804	766	631	687	616	642	571	630	706	747	728	680	659	677	711	706	706	737	844	1028	1358	773
15	D	1196	1007	1111	993	823	645	619	701	543	77	113	133	-78	-97	-223	34	150	468	655	785	813	888	982	1103	560
16	D	1063	1019	939	719	687	660	265	447	678	247	469	530	568	737	743	750	737	735	737	724	721	733	739	762	684
17		763	792	836	872	871	838	495	567	668	658	683	678	671	704	737	747	738	729	711	704	723	757	758	766	728
18		973	862	776	748	770	749	510	687	605	547	606	742	770	770	748	750	745	726	720	708	703	721	751	729	726
19		759	738	743	741	742	748	749	749	748	750	748	724	659	676	710	765	747	741	728	723	714	717	744	748	734
20		781	780	780	747	748	747	729	748	751	747	757	755	753	761	757	769	772	755	735	748	735	729	732	769	753
21		771	789	792	781	783	757	730	701	710	670	516	504	589	669	589	702	752	737	740	735	742	730	754	770	709
22		773	758	762	761	750	747	754	752	745	691	617	561	582	667	720	724	760	769	759	737	733	728	737	748	722
23		764	772	755	750	748	748	748	729	749	700	677	726	669	747	755	749	745	726	728	737	738	743	748	749	737
24		763	761	758	759	788	809	804	735	730	734	754	750	745	704	692	730	750	728	723	726	727	747	779	813	750
25		872	811	762	747	737	743	747	747	749	748	750	759	765	761	758	748	737	717	714	720	737	743	753	759	753
26	Q	759	760	752	752	743	747	750	753	757	759	748	742	765	769	766	751	735	716	702	703	723	737	751	754	746
27	Q	761	758	755	755	750	750	752	753	757	750	749	745	754	754	750	753	748	731	723	724	728	734	757	759	748
28		763	763	759	762	760	765	765	757	740	739	721	755	759	758	748	735	717	728	723	719	724	718	737	726	743
29	Q	751	755	751	752	748	751	755	750	757	751	749	742	745	740	747	731	726	713	712	714	726	720	762	781	743
30		761	770	758	755	766	769	755	750	688	723	757	720	682	750	754	727	690	737	739	735	737	739	755	751	740
31		783	780	763	783	758	690	750	748	722	730	748	737	685	716	738	753	738	742	734	739	745	737	755	779	744
MEAN	A	804	795	785	770	765	742	711	705	697	664	676	683	673	697	696	711	713	718	720	725	732	744	771	793	729
MEAN	Q	760	760	756	752	748	748	751	750	727	736	749	745	754	755	754	746	739	725	720	720	724	726	742	751	743
MEAN	D	968	944	909	821	793	692	616	610	604	379	457	497	439	506	492	556	586	663	705	736	759	809	903	1001	685

DECLINATION

TABLE 14 MEANOOK D = 23.5 DEGREES EAST PLUS TABULAR VALUES IN MINUTES MAY 1969

HOUR UT / DAY		0 TO 1	1 TO 2	2 TO 3	3 TO 4	4 TO 5	5 TO 6	6 TO 7	7 TO 8	8 TO 9	9 TO 10	10 TO 11	11 TO 12	12 TO 13	13 TO 14	14 TO 15	15 TO 16	16 TO 17	17 TO 18	18 TO 19	19 TO 20	20 TO 21	21 TO 22	22 TO 23	23 TO 24	MEAN
1		4.2	10.2	9.7	9.7	14.6	11.9	11.0	7.5	9.9	16.6	14.6	15.1	15.7	17.7	20.7	20.9	20.2	19.4	13.2	8.7	6.7	5.5	6.4	6.4	12.4
2	D	7.2	6.2	7.4	13.2	14.4	13.2	13.2	12.5	10.4	7.2	16.6	13.0	14.7	15.6	20.4	25.7	28.6	15.6	24.6	2.7	3.7	4.7	5.9	4.9	12.6
3		8.9	11.0	11.2	11.4	16.4	31.1	21.2	14.7	15.1	18.2	15.6	17.2	21.6	16.4	20.6	18.4	18.2	16.7	10.9	7.4	7.9	6.5	4.7	6.2	14.5
4		6.7	7.5	9.7	9.7	19.6	9.7	9.7	10.5	13.0	12.0	12.5	14.4	16.6	18.4	20.6	20.7	22.2	18.7	14.4	8.7	8.0	8.0	6.4	3.0	12.5
5		4.4	7.2	8.0	8.4	10.2	10.4	9.9	11.4	11.4	10.0	9.7	8.0	10.0	9.9	16.4	21.4	21.1	19.4	13.2	9.7	5.0	4.5	4.4	5.5	10.4
6		6.4	6.7	8.0	8.0	11.7	8.7	21.4	16.2	11.5	11.0	11.5	13.0	14.2	17.1	17.6	20.9	20.2	20.4	15.6	11.0	9.2	6.5	5.7	3.5	12.3
7	Q	3.6	4.6	5.4	6.3	10.3	10.4	10.6	10.9	9.3	16.3	13.1	12.8	14.8	16.6	17.8	19.5	19.5	18.6	15.8	12.6	9.6	8.3	7.6	6.3	11.7
8		6.3	6.3	8.3	8.3	9.3	8.3	10.6	11.4	11.3	12.3	12.9	12.9	16.0	16.3	16.5	21.3	18.3	18.8	11.3	9.9	8.3	8.6	7.9	9.8	11.7
9		8.4	6.6	7.9	10.8	13.1	11.3	13.8	14.6	29.1	20.3	15.5	13.6	17.3	18.1	20.1	20.8	19.6	19.8	14.8	12.4	7.9	7.3	6.9	4.6	14.0
10		5.6	7.4	8.1	10.3	12.9	12.9	9.9	15.8	14.6	11.8	10.9	11.1	14.5	17.3	19.5	19.8	20.1	20.0	10.9	8.3	7.3	7.8	8.3	7.9	12.2
11	Q	7.1	9.3	9.6	9.9	11.3	12.4	10.3	12.4	15.0	17.1	14.1	12.9	15.8	18.1	19.6	21.1	21.6	19.6	14.5	12.8	9.9	8.1	6.6	6.3	13.2
12		7.9	9.6	11.4	11.4	11.8	10.4	11.1	12.9	14.3	12.9	11.6	11.1	14.0	18.0	21.0	21.6	21.3	19.0	14.6	15.3	7.6	8.1	5.1	1.8	12.7
13	D	-0.1	-6.1	1.9	4.9	4.6	12.1	2.1	7.4	30.3	32.8	41.3	45.7	26.6	43.5	44.0	30.5	27.5	22.5	11.4	8.4	9.4	5.3	5.8	1.6	17.2
14	D	-1.7	-1.1	-1.2	8.3	14.3	13.6	8.6	12.9	18.8	18.6	12.4	14.0	17.3	20.3	26.3	24.6	21.8	16.0	11.6	25.6	17.0	10.3	-1.2	-7.6	12.5
15	D	-14.6	-13.9	-51.7	-48.8	-32.1	-6.8	1.6	1.6	4.3	78.2	52.7	47.9	49.0	33.8	46.7	50.4	32.5	32.3	17.0	19.6	24.5	19.6	13.6	13.8	15.5
16	D	9.8	3.3	-3.2	2.6	-1.4	-4.9	-1.2	-4.4	14.5	15.1	9.4	18.1	15.3	15.8	19.5	22.6	22.8	22.3	17.1	12.4	7.9	6.6	6.4	6.1	9.7
17		7.6	7.3	9.3	.8	4.4	5.1	14.6	13.3	14.0	18.3	12.1	13.8	17.3	21.1	24.5	23.3	21.8	20.0	16.3	10.4	5.9	3.6	2.3	.8	12.0
18		-4.1	-0.4	7.8	7.4	6.6	7.1	-7.1	9.9	11.8	18.0	21.6	16.0	15.5	19.8	26.1	29.0	26.3	26.1	14.6	6.1	7.9	6.8	5.1	5.4	11.8
19		6.3	9.4	9.1	10.4	11.6	11.1	11.6	11.8	12.4	12.1	10.3	11.6	12.8	20.1	22.1	19.6	19.6	16.0	12.8	10.4	6.1	4.3	4.2	4.1	11.7
20		6.3	9.4	11.1	10.3	9.6	12.8	16.6	14.6	12.9	11.6	10.1	10.9	16.0	19.5	21.8	23.8	21.3	18.1	14.1	8.9	8.8	6.3	6.3	6.8	12.8
21		7.9	7.6	11.1	13.8	15.0	17.8	26.1	19.6	17.6	15.1	30.0	39.3	33.8	24.5	22.6	22.3	21.3	19.8	16.8	13.3	12.8	7.8	6.3	5.6	17.8
22		4.4	6.3	7.3	15.0	10.1	9.6	10.1	12.9	12.8	14.1	14.0	31.8	35.0	30.0	29.0	19.6	20.3	17.3	15.8	10.3	8.8	6.9	6.4	6.3	14.8
23		7.4	7.6	9.9	11.6	11.3	11.1	12.1	18.3	21.3	14.1	21.0	15.1	25.0	27.0	22.1	22.8	21.1	18.1	14.1	14.1	9.6	8.6	6.8	5.6	14.8
24		6.3	8.1	8.1	8.4	6.3	2.1	9.6	11.1	12.4	14.8	13.3	14.6	14.8	17.8	17.8	17.8	20.8	17.8	11.4	6.8	1.9	3.6	1.4	3.3	10.4
25		5.3	9.6	11.1	12.1	8.8	8.3	9.3	9.4	9.3	7.9	8.8	12.3	15.5	18.6	21.1	21.1	20.6	19.3	10.3	7.6	4.9	6.3	6.8	7.6	11.3
26	Q	9.3	9.6	12.6	12.4	9.9	9.4	9.3	9.4	9.6	8.4	9.9	12.4	16.1	20.0	20.5	20.3	19.6	16.8	12.6	7.9	6.6	6.6	6.3	7.3	11.8
27	Q	8.1	8.1	7.9	8.1	9.1	9.4	9.8	9.8	11.1	12.9	14.1	15.1	17.8	19.6	18.0	19.6	21.0	18.6	15.5	13.5	9.9	8.3	6.3	6.4	12.4
28		6.3	6.6	8.1	8.3	9.4	8.9	4.4	6.8	14.8	12.1	20.1	19.3	19.5	20.3	24.6	23.0	16.6	11.3	7.8	6.8	7.9	6.3	4.4	6.4	11.7
29	Q	6.4	8.0	8.2	8.9	9.4	9.7	9.5	9.5	11.0	9.9	11.5	11.0	16.4	19.6	21.6	19.6	20.2	18.1	15.4	8.5	7.0	4.9	2.9	3.5	11.3
30		5.5	4.9	6.7	7.0	7.4	6.7	8.9	7.9	8.2	14.2	9.7	7.4	12.9	21.9	24.4	26.6	19.7	11.2	12.0	11.0	8.7	6.2	5.2	6.2	10.9
31		4.4	5.2	7.9	5.9	11.4	25.4	11.9	11.2	19.6	15.2	11.2	12.5	13.4	20.6	23.2	20.6	20.9	16.4	15.7	17.2	12.5	8.4	5.2	3.0	13.3
MEAN	A	5.1	5.9	6.0	7.3	9.1	10.3	10.3	11.1	13.9	16.4	15.9	16.9	18.5	20.4	22.8	22.9	21.5	18.8	14.1	10.9	8.7	7.1	5.7	5.1	12.7
MEAN	Q	6.9	7.9	8.8	9.1	10.0	10.3	9.9	10.4	11.2	12.9	12.6	12.9	16.2	18.8	19.5	20.0	20.4	18.3	14.7	11.1	8.6	7.2	5.9	6.0	12.1
MEAN	D	.1	-2.3	-9.4	-4.0	-0.1	5.5	4.9	6.0	15.6	30.4	26.5	27.7	24.6	25.8	31.4	30.8	26.6	21.7	16.3	13.8	12.5	9.3	6.1	3.8	13.5

VERTICAL INTENSITY

TABLE 15 MEANOOK   Z = 58000 PLUS TABULAR VALUES IN GAMMAS   MAY 1969

DAY		0 TO 1	1 TO 2	2 TO 3	3 TO 4	4 TO 5	5 TO 6	6 TO 7	7 TO 8	8 TO 9	9 TO 10	10 TO 11	11 TO 12	12 TO 13	13 TO 14	14 TO 15	15 TO 16	16 TO 17	17 TO 18	18 TO 19	19 TO 20	20 TO 21	21 TO 22	22 TO 23	23 TO 24	MEAN
1		696	699	689	689	641	667	649	557	576	602	648	655	661	660	661	662	670	673	666	662	676	681	673	673	658
2	D	673	683	683	695	676	688	675	673	643	553	637	673	649	611	623	635	644	644	681	672	699	730	728	685	665
3		682	679	677	673	683	590	579	517	517	594	577	561	591	635	595	626	656	671	677	679	685	687	693	693	634
4		688	673	671	682	687	673	673	667	652	656	624	640	659	661	662	662	666	661	659	661	667	676	679	687	666
5		717	697	673	673	673	662	661	662	660	659	661	638	591	576	628	652	661	662	662	667	672	679	685	709	662
6		697	684	687	696	690	561	599	640	667	667	661	652	642	649	664	669	672	669	666	670	673	673	676	685	663
7	Q	705	707	709	721	721	703	683	681	590	601	643	661	664	672	672	665	661	660	659	653	653	656	660	661	669
8		666	675	676	689	694	687	696	685	671	662	666	664	661	661	653	650	661	660	660	655	652	659	676	683	669
9		684	676	679	685	700	720	687	667	551	600	637	664	650	675	675	664	655	649	658	659	661	675	697	703	665
10		693	667	677	700	718	695	683	540	581	611	640	634	661	660	659	664	669	672	673	677	688	673	675	675	662
11	Q	673	675	677	671	672	673	669	650	636	566	628	644	659	658	653	649	652	653	653	655	661	671	675	676	656
12		673	678	678	676	671	670	669	667	660	655	649	660	669	672	672	665	659	649	647	649	655	667	691	721	668
13	D	754	768	697	703	706	707	618	721	655	711	653	658	636	517	512	524	613	696	707	709	735	747	771	712	676
14	D	685	634	707	735	658	481	648	640	596	445	520	607	656	661	647	628	649	655	667	685	748	753	701	613	642
15	D	661	729	321	289	551	666	703	697	576	640	452	682	806	435	666	516	547	650	709	793	815	780	780	669	631
16	D	646	697	625	526	593	718	735	790	705	532	578	525	573	675	685	697	691	689	693	693	691	702	719	728	663
17		734	748	778	778	770	694	626	636	635	620	646	636	626	624	655	683	691	693	691	693	694	707	712	732	688
18		791	741	734	723	724	672	547	660	664	596	536	641	678	688	675	675	673	673	672	681	684	694	709	694	676
19		709	693	684	679	685	682	678	673	666	671	666	647	593	576	606	661	664	661	662	673	678	676	683	685	665
20		705	712	707	685	682	644	599	650	656	661	676	672	672	673	664	656	671	671	664	670	672	682	685	708	672
21		723	734	731	736	730	672	635	613	623	576	470	476	546	564	555	617	659	676	685	681	693	705	715	723	647
22		700	684	685	689	683	682	685	676	646	555	461	449	449	514	587	635	654	673	677	683	673	667	673	675	632
23		683	687	689	697	687	683	670	614	647	612	557	618	563	636	665	673	672	662	658	660	671	675	681	673	655
24		673	669	666	667	687	619	687	664	644	624	659	664	660	635	614	632	659	660	652	656	661	672	688	708	659
25		753	701	697	693	673	672	671	667	661	649	658	667	664	665	661	660	661	660	662	660	672	683	695	699	675
26	Q	694	685	677	671	664	667	669	667	664	660	630	606	649	660	661	660	656	656	652	642	649	660	667	673	660
27	Q	673	673	669	662	662	661	661	661	661	661	661	652	659	652	655	656	655	648	650	652	654	659	661	672	660
28		672	665	664	664	664	671	685	671	648	649	631	648	661	666	649	646	646	649	658	658	661	667	676	673	660
29	Q	673	671	669	664	661	662	664	662	656	659	659	652	649	649	660	659	660	653	656	652	656	661	682	705	662
30		702	699	685	676	685	697	679	658	567	597	652	626	561	637	660	650	635	646	664	670	672	672	683	685	657
31		694	696	694	696	650	542	659	659	612	622	659	647	578	608	636	664	675	671	664	673	677	702	718	717	659
MEAN	A	696	693	676	674	679	661	659	654	632	618	616	630	634	630	643	647	657	663	668	672	681	687	694	690	661
MEAN	Q	684	682	680	678	676	674	669	664	642	629	644	643	656	658	660	658	657	654	654	651	655	662	669	677	662
MEAN	D	684	702	607	590	636	652	676	704	635	576	568	629	664	580	627	600	629	667	691	710	738	742	740	681	655

HORIZONTAL INTENSITY

TABLE 16 MEANOOK H = 12500 PLUS TABULAR VALUES IN GAMMAS JUNE 1969

HOUR UT / DAY		0 TO 1	1 TO 2	2 TO 3	3 TO 4	4 TO 5	5 TO 6	6 TO 7	7 TO 8	8 TO 9	9 TO 10	10 TO 11	11 TO 12	12 TO 13	13 TO 14	14 TO 15	15 TO 16	16 TO 17	17 TO 18	18 TO 19	19 TO 20	20 TO 21	21 TO 22	22 TO 23	23 TO 24	MEAN
1		759	781	788	780	759	757	747	744	744	744	747	747	737	737	744	748	739	727	701	704	723	726	734	747	744
2		753	764	764	780	760	757	732	654	740	751	753	745	735	749	749	739	723	708	695	717	724	726	738	751	738
3		774	754	758	745	750	753	757	749	744	753	753	754	760	758	759	747	737	726	718	714	726	742	762	751	748
4		754	751	766	769	750	750	758	737	748	753	749	735	712	733	758	762	745	718	695	700	707	711	734	750	739
5		760	775	793	759	748	757	750	744	750	751	748	750	763	754	749	741	742	734	733	735	739	728	732	747	749
6	Q	749	755	755	754	755	755	757	757	755	757	759	758	761	759	759	739	733	730	724	728	743	750	759	771	751
7		780	779	768	764	773	776	774	769	764	751	719	700	599	702	729	720	727	734	737	737	745	749	752	773	743
8		783	783	789	764	753	810	807	791	783	781	770	781	791	791	780	771	748	713	750	741	739	781	769	768	772
9		755	784	778	791	764	761	750	750	755	751	740	728	699	706	741	718	687	690	714	720	761	784	847	862	751
10		759	801	806	768	731	750	779	716	617	677	689	729	714	719	755	755	713	692	706	723	724	724	729	747	730
11		752	769	748	738	744	759	758	759	660	750	768	764	762	758	759	759	763	741	714	711	722	735	790	743	747
12	D	771	804	905	1054	934	758	655	740	554	627	700	672	729	754	734	732	718	719	701	714	723	751	751	757	748
13	D	758	781	811	876	750	744	790	771	756	749	746	745	673	660	682	712	701	692	694	704	727	770	774	808	745
14	D	761	761	770	758	772	777	760	662	665	771	774	775	603	494	714	756	741	727	731	740	743	748	774	751	730
15		758	760	780	769	756	750	746	754	760	764	758	653	616	673	724	771	771	740	709	715	738	746	738	749	737
16	D	754	802	783	793	796	796	766	752	555	607	762	750	752	743	687	704	723	729	735	736	731	748	765	766	739
17	D	801	899	916	813	749	746	744	742	752	746	688	763	779	775	771	745	735	691	673	704	727	725	731	738	756
18	Q	750	748	750	749	744	743	745	748	751	754	758	760	769	764	757	754	733	719	717	718	724	735	748	748	745
19		745	753	751	759	748	751	750	757	762	759	748	768	766	763	760	752	765	758	740	727	721	745	755	750	752
20		782	805	769	768	768	751	745	749	633	690	716	714	739	751	759	766	771	760	745	737	737	738	761	766	747
21		769	770	762	753	758	761	758	747	744	726	722	722	734	724	740	762	750	740	734	747	739	735	745	760	746
22	Q	759	763	760	758	751	749	750	750	750	751	752	753	768	774	770	762	739	724	724	724	728	737	743	757	750
23		764	770	760	762	759	758	750	751	750	749	750	769	759	757	769	739	737	750	754	748	750	759	765	781	757
24		783	774	799	796	761	763	737	759	738	742	741	718	699	731	717	745	726	723	733	734	747	768	761	757	748
25		760	771	763	748	740	762	770	750	748	739	750	738	723	696	714	728	692	679	717	720	737	742	763	773	738
26		783	769	748	751	758	760	759	753	755	747	742	714	709	692	686	703	721	723	721	724	723	726	733	744	735
27		742	754	775	769	749	749	757	750	748	749	742	723	720	749	755	742	751	745	737	737	742	748	741	737	746
28	Q	761	751	748	749	757	755	759	757	759	758	757	758	757	759	758	758	751	743	735	729	729	728	717	734	748
29	Q	750	768	758	771	758	757	758	759	758	751	750	745	753	770	772	770	747	712	699	703	713	727	740	759	748
30		759	754	759	759	750	753	759	757	753	761	761	765	773	778	769	759	728	714	723	726	729	751	764	769	753
MEAN	A	763	775	779	779	761	759	754	746	725	739	744	740	728	732	744	745	735	723	720	724	732	743	754	760	746
MEAN	Q	754	757	754	756	753	752	754	754	755	754	755	755	761	765	763	757	741	726	720	720	728	735	741	754	748
MEAN	D	769	809	837	859	800	764	743	733	656	700	734	741	707	685	718	730	724	711	707	720	730	748	759	764	744

DECLINATION

TABLE 17 MEANOOK — D = 23.5 DEGREES EAST PLUS TABULAR VALUES IN MINUTES — JUNE 1969

HOUR UT / DAY		0 TO 1	1 TO 2	2 TO 3	3 TO 4	4 TO 5	5 TO 6	6 TO 7	7 TO 8	8 TO 9	9 TO 10	10 TO 11	11 TO 12	12 TO 13	13 TO 14	14 TO 15	15 TO 16	16 TO 17	17 TO 18	18 TO 19	19 TO 20	20 TO 21	21 TO 22	22 TO 23	23 TO 24	MEAN
1		4.5	4.2	8.9	6.4	8.0	10.9	12.0	9.7	10.0	10.9	10.7	11.4	14.7	16.4	20.1	21.4	20.4	18.2	13.6	12.2	8.7	6.4	6.4	6.4	11.4
2		7.5	8.0	8.0	8.5	13.2	8.5	6.9	8.0	11.9	12.0	10.5	11.2	13.9	20.1	22.4	24.2	22.4	19.9	14.1	6.9	3.5	-0.1	1.7	4.9	11.2
3		3.4	6.7	7.9	9.5	8.0	8.5	8.0	7.7	7.0	8.2	8.0	10.2	13.2	16.6	20.9	22.1	22.7	18.7	9.7	8.4	6.4	1.9	1.2	3.0	9.9
4		4.2	7.5	8.9	7.9	6.7	7.2	6.4	13.2	14.6	8.5	8.5	12.2	17.9	24.2	23.9	23.1	18.6	19.7	14.2	11.4	8.5	5.0	4.9	6.2	11.8
5		5.0	6.0	8.2	11.0	9.2	9.5	9.5	9.2	7.9	9.7	8.5	11.9	16.2	19.7	23.6	26.9	23.2	18.6	14.9	10.2	7.9	4.7	4.5	4.9	11.7
6	Q	6.2	8.0	10.0	11.4	11.2	10.2	9.7	8.0	8.0	9.0	10.9	13.2	17.7	21.7	23.2	24.6	24.7	15.7	13.2	8.4	3.5	3.0	1.5	1.7	11.5
7		2.9	5.0	6.5	4.9	5.2	4.7	6.9	7.5	7.7	6.7	11.5	16.4	14.1	18.4	23.1	25.2	21.4	16.1	10.0	6.9	5.9	5.5	5.5	5.9	10.2
8		8.2	7.7	10.0	11.2	10.5	6.7	4.4	9.7	10.0	8.7	12.7	13.0	21.6	23.2	24.7	27.6	27.1	21.7	7.7	12.0	3.2	.0	1.9	2.2	11.9
9		1.9	1.7	5.9	8.0	6.7	6.9	6.4	7.5	7.9	6.9	8.5	13.9	17.7	22.6	30.1	30.6	27.7	24.1	12.2	6.4	5.2	1.5	1.0	1.4	10.9
10		7.9	4.9	6.9	7.0	7.5	4.4	9.9	6.7	10.5	12.9	13.0	13.4	13.2	21.2	24.7	23.7	24.6	19.4	15.2	11.0	6.0	2.4	3.2	4.4	11.4
11		6.0	8.4	11.7	9.7	8.5	11.9	10.9	7.4	4.9	16.6	11.5	13.0	15.6	17.9	19.7	20.2	21.4	20.7	16.7	8.9	4.9	1.5	.5	4.5	11.4
12	D	2.7	2.9	-8.5	-18.8	.4	14.1	14.1	7.4	14.1	22.9	15.1	12.7	15.6	19.9	23.4	22.4	21.4	19.1	16.2	4.9	2.5	3.0	5.2	6.2	9.9
13	D	5.5	5.5	4.4	-0.8	10.5	16.2	8.5	6.5	7.2	8.2	11.0	16.4	18.4	21.7	6.9	24.4	25.6	21.1	13.9	5.5	4.4	6.7	6.2	.4	10.6
14	D	.6	1.0	6.3	14.3	13.8	8.1	4.8	2.8	10.1	8.0	6.8	10.6	13.8	29.0	29.2	26.0	25.3	17.8	16.5	13.5	9.8	9.6	9.1	7.5	12.3
15		6.6	7.8	9.1	11.3	11.3	9.5	9.5	9.6	16.3	11.0	6.0	12.0	13.7	23.7	28.2	23.5	22.0	21.2	15.7	9.5	5.6	5.0	6.6	7.0	12.6
16	D	8.1	8.5	12.0	10.5	8.5	8.5	21.2	13.5	18.8	31.2	12.1	11.0	16.5	20.0	24.8	24.5	23.5	17.8	14.5	9.8	4.5	5.3	6.0	5.6	14.0
17	D	4.5	3.3	9.1	9.0	8.1	10.1	17.3	24.0	10.0	7.3	8.5	9.8	17.3	21.0	23.5	23.3	25.7	24.8	15.8	6.3	6.5	6.8	6.8	6.8	12.7
18	Q	8.1	9.6	10.0	9.8	10.0	9.3	10.1	11.5	10.6	10.5	11.0	13.0	14.7	15.7	18.2	21.2	20.7	16.8	7.6	6.0	5.0	4.5	4.6	6.6	11.0
19		8.5	8.6	9.5	10.1	8.5	9.0	9.3	7.8	13.0	14.7	16.0	13.7	16.2	16.7	17.2	18.0	16.5	14.8	13.0	8.1	6.0	2.6	5.3	6.5	11.2
20		5.0	9.8	11.0	11.6	18.2	12.1	14.7	9.8	18.2	12.3	14.7	14.5	18.2	18.2	21.8	22.7	20.3	16.5	10.0	8.3	6.0	4.3	3.1	5.0	12.8
21		7.3	9.5	9.8	10.0	10.3	13.1	16.8	11.8	10.0	6.6	11.8	16.7	20.3	21.8	20.7	23.3	21.5	18.2	16.3	11.1	9.8	7.6	6.8	7.8	13.3
22	Q	8.5	10.1	11.3	11.3	9.8	9.8	9.3	9.1	9.5	9.8	9.8	13.0	16.2	16.8	17.2	20.2	18.8	16.2	14.0	9.8	7.6	6.3	6.1	6.1	11.5
23		6.1	6.8	8.6	8.3	8.1	8.3	9.0	9.1	8.5	9.5	12.8	14.7	14.8	17.3	19.3	22.3	20.0	14.8	11.1	9.5	7.8	4.6	4.0	4.0	10.8
24		5.0	5.0	9.6	9.6	8.5	13.3	12.5	11.3	14.7	11.5	10.6	11.1	12.8	20.0	22.2	18.2	21.3	18.0	11.5	5.6	5.8	4.6	4.6	4.6	11.3
25		6.3	7.3	9.3	9.6	9.8	9.6	9.5	9.6	7.8	9.5	11.8	12.8	15.7	14.2	18.3	21.5	24.8	18.5	8.1	7.0	5.0	3.3	2.1	2.1	10.6
26		-0.0	5.5	9.5	8.1	8.6	8.6	8.1	8.3	8.6	8.1	9.5	6.8	11.5	14.8	16.2	13.5	13.3	16.5	14.5	11.6	6.3	5.6	5.1	4.5	9.3
27		5.5	6.6	8.6	11.8	10.8	9.0	10.6	10.1	9.1	8.8	9.1	11.5	15.0	17.7	20.3	21.5	18.7	18.0	13.7	11.3	9.3	7.1	6.6	6.8	11.6
28	Q	6.1	6.5	8.1	9.0	9.0	9.5	10.1	9.5	9.5	8.8	8.1	9.6	12.6	14.8	17.3	19.2	19.8	18.2	15.7	8.3	5.0	2.8	3.1	4.5	10.2
29	Q	6.3	7.8	9.8	9.6	9.8	9.0	8.5	9.6	10.3	11.3	11.8	13.3	18.3	20.0	21.5	23.5	22.8	20.3	14.3	9.5	6.3	4.1	4.6	5.0	12.0
30		7.5	9.8	10.8	9.3	8.3	8.6	10.5	10.8	10.6	9.0	10.0	13.1	15.5	16.0	19.8	20.7	20.8	18.5	10.1	5.8	.5	-2.0	-1.4	-0.2	10.1
MEAN	A	5.5	6.7	8.4	8.3	9.2	9.5	10.2	9.6	10.6	11.0	10.7	12.5	15.8	19.4	21.4	22.6	21.9	18.7	13.1	8.8	5.9	4.1	4.2	4.7	11.4
MEAN	Q	7.1	8.4	9.9	10.2	10.0	9.6	9.6	9.6	9.6	9.9	10.3	12.4	15.9	17.8	19.5	21.7	21.4	17.4	13.0	8.4	5.5	4.1	4.0	4.8	11.2
MEAN	D	4.3	4.2	4.7	2.8	8.3	11.4	13.2	10.8	12.0	15.5	10.7	12.1	16.3	22.3	21.6	24.1	24.3	20.1	15.4	8.0	5.5	6.3	6.7	5.3	11.9

VERTICAL INTENSITY

TABLE 18 MEANOOK

Z = 58000 PLUS TABULAR VALUES IN GAMMAS

JUNE 1969

DAY	HOUR UT	0 TO 1	1 TO 2	2 TO 3	3 TO 4	4 TO 5	5 TO 6	6 TO 7	7 TO 8	8 TO 9	9 TO 10	10 TO 11	11 TO 12	12 TO 13	13 TO 14	14 TO 15	15 TO 16	16 TO 17	17 TO 18	18 TO 19	19 TO 20	20 TO 21	21 TO 22	22 TO 23	23 TO 24	MEAN
1		697	705	709	695	697	697	689	673	670	660	653	660	662	664	662	667	669	664	660	671	683	676	673	672	676
2		671	671	671	684	697	703	666	519	624	656	666	649	635	650	667	666	661	658	654	656	659	660	666	681	658
3		706	709	707	684	676	672	669	667	659	659	662	665	671	669	659	653	649	650	649	648	659	662	673	697	670
4		708	693	688	693	699	690	678	600	611	662	661	646	606	626	650	656	650	646	638	649	660	662	671	677	659
5		681	694	711	684	670	671	672	667	661	653	650	647	671	661	652	641	649	649	648	649	658	660	658	662	663
6	Q	664	664	667	671	667	664	662	661	661	661	664	664	664	658	659	649	640	637	636	644	659	670	677	689	660
7		700	707	702	696	703	705	697	684	667	655	623	613	541	601	638	649	669	681	675	672	673	675	673	693	666
8		720	729	720	695	682	707	689	661	659	649	634	652	665	656	647	650	650	647	636	636	654	707	729	718	675
9		697	707	712	699	684	675	661	661	664	661	656	638	614	614	644	643	622	624	640	672	734	777	782	768	677
10		709	723	734	711	673	676	683	655	570	583	611	659	654	649	673	676	662	661	656	659	662	671	666	672	665
11		673	685	679	665	667	683	673	669	578	624	673	673	671	661	661	660	661	659	659	660	665	670	685	682	664
12	D	696	710	774	745	696	596	608	674	515	621	625	631	660	665	654	655	662	676	684	678	673	686	686	690	665
13	D	688	704	724	701	639	650	713	698	684	676	665	673	626	602	598	614	638	650	648	660	682	722	759	741	673
14	D	696	689	710	700	674	676	698	644	654	673	686	686	618	554	627	677	661	651	662	662	667	695	715	710	670
15		697	685	688	690	694	677	672	667	650	671	653	560	537	565	582	656	663	650	648	660	674	673	671	676	652
16	D	679	700	718	719	719	695	683	636	597	488	618	645	641	631	591	589	626	642	657	663	662	665	686	707	652
17	D	724	760	745	722	712	696	633	578	650	650	537	618	674	674	670	653	653	648	647	647	650	654	663	673	664
18	Q	679	673	670	666	661	661	661	662	665	667	671	669	669	662	659	658	656	650	647	648	649	658	660	661	662
19		661	661	660	664	661	661	661	652	647	623	649	670	666	661	654	640	640	649	649	650	659	667	673	678	657
20		687	700	693	690	696	616	661	672	479	526	565	588	608	635	635	648	660	660	658	659	664	669	673	673	642
21		673	676	672	662	669	675	656	652	652	625	590	597	613	611	637	660	660	659	653	658	664	670	661	670	651
22	Q	671	673	667	662	661	661	661	661	661	661	652	652	666	662	659	656	656	652	650	652	659	662	672	671	661
23		664	661	660	661	661	661	659	659	655	647	644	654	652	647	647	637	638	635	640	649	659	672	688	709	657
24		712	695	703	684	685	655	613	654	625	652	658	642	607	649	641	660	661	660	655	658	669	684	688	697	663
25		683	673	676	671	661	665	676	660	660	637	652	650	640	619	626	654	647	636	635	649	661	685	700	696	659
26		694	699	683	662	673	673	661	661	660	648	636	608	613	612	575	603	640	661	679	664	665	671	673	676	654
27		673	678	697	697	683	665	664	662	661	659	649	624	625	659	667	660	661	661	659	659	661	675	685	693	666
28	Q	691	676	671	661	661	661	661	660	650	647	643	652	661	664	662	660	654	649	641	638	649	655	652	659	658
29	Q	664	671	662	670	665	661	660	660	649	649	652	654	656	664	661	661	656	648	641	637	647	649	649	664	656
30		676	678	675	670	661	660	660	655	647	658	661	664	667	662	659	659	649	646	638	635	637	649	658	659	658
MEAN	A	688	692	695	686	678	670	667	653	636	640	642	643	638	640	644	650	652	652	651	655	664	675	682	687	662
MEAN	Q	674	671	668	666	663	662	661	661	657	657	656	658	663	662	660	657	653	647	643	644	653	659	662	669	659
MEAN	D	696	713	734	717	688	663	667	646	620	622	626	651	644	625	628	637	648	653	660	662	667	684	702	704	665

HORIZONTAL INTENSITY

TABLE 19 MEANOOK H = 12500 PLUS TABULAR VALUES IN GAMMAS JULY 1969

HOUR UT / DAY		0 TO 1	1 TO 2	2 TO 3	3 TO 4	4 TO 5	5 TO 6	6 TO 7	7 TO 8	8 TO 9	9 TO 10	10 TO 11	11 TO 12	12 TO 13	13 TO 14	14 TO 15	15 TO 16	16 TO 17	17 TO 18	18 TO 19	19 TO 20	20 TO 21	21 TO 22	22 TO 23	23 TO 24	MEAN
1	D	779	784	771	769	781	780	781	368	696	727	726	739	726	762	775	759	739	724	707	704	737	735	764	759	733
2		794	781	779	772	757	760	735	729	750	755	757	758	760	761	766	750	737	714	696	692	698	727	747	752	747
3		764	769	761	759	758	758	753	758	757	759	758	763	769	771	769	750	735	717	717	716	723	739	751	757	751
4	Q	754	755	753	753	759	761	759	759	759	759	762	766	764	770	770	766	758	741	728	714	717	727	738	759	752
5	Q	764	773	769	765	769	769	759	759	759	759	760	755	748	761	768	759	745	731	723	726	729	734	739	740	753
6		758	763	763	764	765	766	768	768	763	769	771	779	780	778	763	749	766	770	760	751	738	735	742	748	761
7		759	771	772	771	781	771	760	762	764	759	755	755	770	769	772	764	741	730	730	726	737	737	740	745	756
8		757	749	748	750	762	763	759	759	755	755	754	759	766	758	759	750	744	738	723	726	727	738	760	751	750
9		768	791	790	780	780	779	767	760	734	748	746	746	747	736	737	730	722	719	713	716	725	728	752	761	749
10		754	771	779	779	758	757	749	747	747	737	713	736	747	746	733	713	737	737	736	736	738	747	758	750	746
11		730	746	760	757	749	754	762	760	761	762	761	761	767	768	759	744	729	734	734	728	727	738	747	758	750
12		793	818	814	815	844	801	779	692	615	754	757	767	782	787	771	777	768	749	737	712	727	777	736	734	763
13	D	758	785	785	775	813	623	779	740	635	669	736	749	771	796	796	795	782	747	723	680	701	725	746	770	745
14	D	768	763	778	795	789	749	743	739	723	718	764	758	738	750	790	770	752	736	713	715	703	717	748	753	749
15		758	774	760	759	758	751	751	754	751	750	744	725	750	769	769	767	738	725	711	702	702	716	736	758	745
16		770	778	779	765	759	758	754	756	756	758	671	738	769	775	775	759	742	741	729	727	744	761	754	754	753
17		768	777	757	761	769	749	757	758	750	754	757	758	764	758	759	753	733	725	716	722	726	737	748	750	750
18		763	762	758	757	756	757	760	756	758	756	734	725	756	736	758	760	747	731	730	736	734	746	756	758	749
19	Q	757	758	757	757	758	760	765	752	754	758	760	767	769	769	768	758	741	725	723	733	736	736	744	756	752
20	Q	761	759	768	752	753	754	757	759	762	761	767	769	782	790	791	781	768	758	757	752	744	748	760	771	763
21		764	758	761	757	758	759	762	769	771	777	779	782	781	778	768	750	734	734	738	738	748	751	770	768	761
22		760	770	750	747	759	767	769	753	758	749	752	761	764	758	756	747	748	748	738	738	747	746	747	751	753
23		764	760	748	749	746	749	747	749	751	752	749	742	749	752	752	748	726	715	715	725	742	751	767	748	746
24		744	743	748	747	754	757	754	747	748	748	757	756	757	757	756	750	747	737	738	737	747	748	748	748	749
25		747	759	768	758	750	756	744	747	749	750	756	757	757	757	758	748	739	734	707	723	746	759	769	748	749
26	D	759	747	769	767	758	758	748	749	758	758	757	769	760	757	718	751	768	761	756	756	748	757	767	823	759
27	D	686	722	707	723	737	756	561	140	387	636	713	723	648	692	746	738	719	703	703	734	741	744	734	747	673
28		748	757	742	737	736	746	738	636	713	739	747	746	748	751	748	741	746	741	741	738	736	733	734	737	737
29	Q	747	746	743	747	744	746	754	756	747	747	747	746	756	757	752	747	738	731	723	723	719	723	736	747	742
30		759	738	743	742	749	758	757	758	768	759	760	767	760	775	769	779	748	710	681	721	725	719	762	781	749
31		764	748	746	758	743	748	751	755	752	758	762	764	756	751	755	746	733	719	704	707	714	731	743	748	744
MEAN	A	759	764	762	761	763	755	751	716	731	746	749	754	757	761	762	755	744	733	724	724	730	739	750	756	748
MEAN	Q	757	758	758	755	757	758	759	757	756	757	759	761	764	769	770	762	750	737	731	730	729	734	743	754	753
MEAN	D	750	760	762	766	775	733	722	547	640	701	739	748	728	752	765	763	752	734	721	718	726	736	752	770	732

DECLINATION

TABLE 20 MEANOOK D = 23.5 DEGREES EAST PLUS TABULAR VALUES IN MINUTES JULY 1969

HOUR UT / DAY		0 TO 1	1 TO 2	2 TO 3	3 TO 4	4 TO 5	5 TO 6	6 TO 7	7 TO 8	8 TO 9	9 TO 10	10 TO 11	11 TO 12	12 TO 13	13 TO 14	14 TO 15	15 TO 16	16 TO 17	17 TO 18	18 TO 19	19 TO 20	20 TO 21	21 TO 22	22 TO 23	23 TO 24	MEAN
1	D	2.5	4.6	7.8	5.5	4.3	2.0	2.6	-1.4	15.0	9.6	9.8	14.7	16.5	26.2	28.0	27.8	25.8	22.5	15.5	8.6	6.8	1.5	2.8	4.6	11.0
2		7.8	8.1	7.8	11.5	10.0	10.0	8.0	9.8	8.3	8.1	10.1	13.5	17.8	20.5	22.3	22.5	20.2	18.3	16.0	11.3	6.8	4.0	3.5	6.8	11.8
3		8.1	8.5	10.0	10.1	9.5	9.3	9.5	8.6	9.6	9.8	11.3	14.7	17.7	20.3	21.0	23.2	23.0	18.8	11.3	4.6	1.3	1.8	4.5	6.5	11.4
4	Q	7.8	8.5	9.0	8.3	8.0	8.1	8.5	9.0	9.3	10.0	11.3	13.0	15.8	19.2	20.0	21.3	21.8	20.2	15.2	8.1	4.1	.3	.6	3.3	10.9
5	Q	5.5	7.1	9.0	9.0	9.5	8.5	7.8	8.1	8.5	10.1	12.5	12.1	14.8	19.7	22.0	23.3	23.2	19.8	14.8	8.0	4.5	1.1	-1.4	2.0	10.8
6		3.0	5.0	7.3	8.0	8.1	8.1	7.5	7.1	8.1	9.6	12.0	14.7	15.2	18.3	21.5	21.7	21.3	20.0	16.5	11.3	7.6	5.0	3.0	2.3	10.9
7		1.5	3.1	6.3	7.8	8.1	8.1	8.6	8.8	9.3	11.3	13.1	16.2	20.8	22.5	23.2	20.0	23.8	19.0	13.7	10.0	6.0	1.3	-0.0	1.1	11.0
8		3.1	6.2	7.9	8.2	8.1	9.1	7.7	8.4	8.9	10.2	12.1	13.1	13.8	17.8	19.8	20.1	20.3	19.6	13.6	9.1	6.6	3.4	2.9	4.6	10.6
9		6.6	6.7	8.2	7.9	9.2	9.1	7.4	10.7	11.7	10.6	12.4	15.3	18.6	19.8	19.9	22.8	23.4	21.6	15.8	6.6	2.6	-0.3	1.2	4.7	11.4
10		8.1	6.7	9.7	9.1	7.7	7.6	6.4	7.6	6.4	8.4	9.1	11.9	14.9	16.4	19.8	19.4	21.1	18.6	12.9	8.7	4.2	2.1	3.7	5.2	10.2
11		7.1	8.9	10.2	10.1	9.2	9.1	9.1	10.1	11.9	9.9	10.6	12.1	14.8	16.9	17.3	20.6	22.1	17.1	11.2	6.4	4.4	1.9	3.6	5.6	10.8
12		6.9	6.6	5.4	5.6	5.2	11.6	7.2	10.1	10.2	14.1	11.4	13.3	17.1	21.4	20.3	23.4	24.9	22.4	16.4	11.7	6.6	6.2	6.4	5.1	12.1
13	D	7.1	8.2	9.9	9.1	6.1	7.2	11.1	10.1	16.8	21.3	14.9	13.3	13.8	17.1	21.6	21.8	19.3	17.4	19.4	13.9	.2	-1.9	1.2	4.7	11.8
14	D	8.1	11.6	12.4	10.2	21.4	13.4	11.4	19.9	16.1	12.4	10.7	8.7	13.3	18.3	21.8	22.9	21.4	18.3	10.9	6.7	3.6	5.2	5.7	7.2	13.0
15		10.1	12.9	13.4	11.2	9.9	9.6	9.7	9.9	13.8	11.4	7.1	7.4	10.9	16.9	22.3	24.6	22.9	20.4	17.1	12.1	7.7	6.4	6.4	7.4	12.6
16		8.7	10.4	12.1	13.4	15.4	11.6	11.4	10.1	8.7	8.4	9.1	17.8	17.4	22.8	23.1	22.4	21.6	14.8	15.1	8.2	7.4	9.6	8.1	9.2	13.2
17		9.1	10.4	12.4	11.4	11.2	13.3	11.4	9.4	8.7	8.9	8.9	11.9	14.6	16.1	19.9	19.9	18.6	15.3	12.9	8.2	6.4	4.4	4.9	5.1	11.4
18		5.9	7.7	8.6	9.4	9.6	9.9	10.2	10.6	13.1	12.9	10.1	15.3	16.6	16.8	17.8	18.8	19.9	18.1	13.6	9.9	6.6	6.1	7.4	8.1	11.8
19	Q	8.4	8.9	9.4	9.7	9.9	10.1	12.4	11.6	13.3	11.1	10.4	11.9	14.6	15.4	16.8	18.4	17.6	14.1	8.4	5.1	5.1	5.1	4.7	5.2	10.7
20	Q	6.9	8.2	8.6	9.9	9.6	11.2	10.1	9.6	9.7	10.7	11.2	11.1	13.4	16.9	19.9	22.8	22.6	18.1	14.3	8.9	4.6	3.4	3.2	5.1	11.3
21		8.1	9.9	9.9	9.7	8.7	8.4	9.6	8.7	8.7	8.6	10.1	11.6	13.1	16.3	21.3	20.6	18.4	16.9	7.4	3.1	1.7	2.2	3.4	7.4	10.2
22		7.9	6.6	8.6	8.6	7.2	6.1	6.9	7.9	11.1	11.2	11.2	13.3	16.4	19.9	21.1	19.9	21.6	19.9	14.6	10.6	9.7	8.2	6.7	5.2	11.7
23		6.7	6.2	5.7	6.7	8.4	8.9	9.7	9.7	9.9	10.1	8.6	11.4	13.4	15.3	16.9	16.8	16.9	17.3	8.4	7.1	7.9	7.7	6.7	8.9	10.2
24		8.7	8.4	8.4	8.2	8.6	9.9	9.7	11.9	10.7	10.4	11.6	13.3	15.6	17.4	19.8	21.9	19.9	17.9	15.6	12.9	11.7	9.9	9.4	9.1	12.5
25		8.6	8.1	8.9	8.2	8.4	11.2	10.2	10.7	9.6	9.9	11.7	13.3	14.8	15.1	16.6	16.4	16.4	16.3	13.1	8.6	6.1	5.9	5.2	7.7	10.9
26	D	7.9	8.4	6.7	6.7	10.7	7.4	6.6	8.2	9.9	10.2	11.7	12.9	15.8	19.9	18.8	29.6	26.6	23.4	20.1	13.9	10.1	6.6	6.2	10.9	12.9
27	D	49.8	47.5	13.4	2.7	3.6	16.3	12.2	10.9	35.3	22.9	15.1	16.4	18.6	22.9	22.3	22.6	21.8	21.8	18.4	9.9	5.9	6.2	7.2	7.9	18.0
28		10.2	11.2	11.9	11.4	10.1	11.6	13.1	3.1	9.7	11.4	11.6	11.7	16.6	18.1	19.6	19.8	20.4	18.6	18.6	14.3	11.6	10.1	8.9	9.1	13.0
29	Q	8.7	8.6	9.2	9.2	9.7	10.2	10.2	13.3	11.4	11.4	12.1	13.4	15.6	17.9	19.8	23.1	23.3	18.3	11.7	6.9	3.6	4.6	4.9	4.7	11.7
30		5.4	8.6	8.4	8.2	8.2	8.1	8.2	8.1	8.7	10.6	11.1	11.4	12.1	13.4	15.3	19.9	21.4	22.1	10.7	3.6	.4	-0.1	5.4	7.1	9.8
31		8.9	9.6	9.4	10.4	9.4	9.7	8.7	9.2	9.6	11.6	10.6	12.7	17.3	17.3	21.6	21.3	20.9	17.6	13.8	7.9	5.2	4.9	3.7	5.2	11.5
MEAN	A	8.5	9.4	9.2	8.9	9.1	9.5	9.1	9.4	11.4	11.2	11.1	13.0	15.5	18.5	20.4	21.6	21.4	18.9	14.1	8.9	5.7	4.3	4.5	6.0	11.6
MEAN	Q	7.5	8.3	9.0	9.2	9.3	9.6	9.8	10.3	10.4	10.7	11.5	12.3	14.8	17.8	19.7	21.8	21.7	18.1	12.9	7.4	4.4	2.9	2.4	4.1	11.1
MEAN	D	15.1	16.1	10.1	6.9	9.2	9.3	8.8	9.6	18.6	15.3	12.5	13.2	15.6	20.9	22.5	25.0	23.0	20.7	16.9	10.6	5.3	3.5	4.6	7.1	13.3

VERTICAL INTENSITY

TABLE 21 MEANOOK | Z = 58000 PLUS TABULAR VALUES IN GAMMAS | JULY 1969

DAY		0 TO 1	1 TO 2	2 TO 3	3 TO 4	4 TO 5	5 TO 6	6 TO 7	7 TO 8	8 TO 9	9 TO 10	10 TO 11	11 TO 12	12 TO 13	13 TO 14	14 TO 15	15 TO 16	16 TO 17	17 TO 18	18 TO 19	19 TO 20	20 TO 21	21 TO 22	22 TO 23	23 TO 24	MEAN
1	D	661	671	673	667	672	683	685	493	636	636	613	637	619	652	649	644	638	646	649	655	685	671	683	685	650
2		709	695	697	711	685	662	624	602	647	635	660	666	666	661	661	656	652	647	650	652	648	656	659	660	661
3		662	667	672	672	664	661	660	659	660	661	661	664	660	655	648	648	648	649	648	644	644	647	650	662	657
4	Q	672	672	663	659	657	657	657	659	657	658	660	661	660	660	659	655	648	648	651	651	651	652	658	660	658
5	Q	663	670	670	664	661	663	661	658	657	653	660	653	642	648	658	655	655	649	642	636	639	643	647	654	654
6		660	660	658	657	655	655	653	658	658	660	660	659	659	655	649	640	636	637	640	637	639	640	647	651	651
7		653	653	654	658	660	672	663	658	654	655	636	643	645	646	647	639	636	634	635	629	635	647	660	672	649
8		678	670	660	657	660	666	658	657	651	648	648	653	659	651	649	649	648	649	658	654	658	666	672	684	659
9		696	712	722	722	707	710	682	663	634	660	658	659	655	648	648	657	654	651	653	654	672	674	672	671	672
10		670	675	700	696	689	681	672	664	659	634	610	637	653	657	649	641	660	660	661	663	658	659	671	681	663
11		684	682	684	672	660	658	658	659	649	648	651	657	658	658	659	660	655	646	647	649	659	671	683	695	663
12		711	743	746	759	773	734	696	645	525	625	658	659	671	664	652	649	658	659	658	651	655	682	704	696	678
13	D	681	692	720	702	699	598	696	596	523	482	598	636	660	670	671	670	659	649	659	671	681	696	696	696	654
14	D	694	696	695	711	684	676	655	622	517	570	645	663	636	613	660	659	660	668	659	658	663	670	684	686	659
15		678	680	678	674	668	663	660	651	625	613	634	615	643	666	660	661	659	658	658	659	663	671	681	687	659
16		686	683	684	690	686	675	668	664	663	655	529	574	639	645	659	654	654	652	649	659	663	672	678	672	656
17		668	675	672	671	677	665	660	661	651	642	648	659	663	655	658	660	653	653	660	666	661	665	670	669	662
18		661	661	660	660	660	660	660	655	652	642	624	595	647	635	636	651	651	651	655	655	655	653	660	663	650
19	Q	660	660	659	659	659	659	652	637	641	639	637	653	660	658	654	654	655	655	655	665	664	659	664	665	655
20	Q	661	661	660	659	659	659	653	652	653	654	655	655	651	652	649	651	643	641	642	645	651	657	658	660	653
21		664	665	664	657	654	654	653	653	653	654	653	655	654	648	642	636	636	647	642	653	659	665	672	684	655
22		685	691	682	670	659	673	698	674	681	674	657	665	667	660	660	654	648	650	647	648	650	660	664	676	666
23		677	657	653	657	653	654	652	651	652	651	647	639	648	654	660	664	659	656	658	659	657	660	677	688	658
24		680	667	659	653	654	658	657	656	653	656	657	658	659	653	650	648	647	641	642	646	648	654	658	653	655
25		654	657	667	676	679	671	641	657	660	654	654	653	657	658	659	658	658	659	659	658	658	659	665	667	660
26	D	668	663	677	698	693	685	667	658	657	658	658	662	653	641	569	589	623	629	624	634	642	648	664	722	653
27	D	604	703	539	648	683	658	659	654	658	611	622	646	614	628	662	676	665	664	663	693	682	674	665	668	652
28		675	682	674	671	671	669	654	564	599	651	670	673	675	671	667	665	663	660	657	663	663	663	665	662	659
29	Q	658	659	658	658	659	659	659	659	659	658	652	657	658	657	662	662	659	656	652	650	653	648	653	656	657
30		667	670	668	662	659	659	659	659	658	659	660	659	658	659	654	647	640	646	657	651	668	669	675	691	661
31		701	685	664	671	662	659	659	660	653	647	646	646	657	659	652	650	650	645	645	652	656	664	670	671	659
MEAN	A	672	677	672	676	673	666	662	644	641	640	643	649	653	653	652	652	651	650	651	654	657	662	669	674	658
MEAN	Q	663	665	662	660	659	659	656	653	653	652	653	656	654	655	656	656	652	650	649	649	651	652	656	659	656
MEAN	D	662	685	661	685	686	660	673	605	610	591	627	649	636	641	642	648	649	651	651	662	671	672	679	691	654

HORIZONTAL INTENSITY

TABLE 22 MEANOOK H = 12500 PLUS TABULAR VALUES IN GAMMAS AUGUST 1969

HOUR UT / DAY		0 TO 1	1 TO 2	2 TO 3	3 TO 4	4 TO 5	5 TO 6	6 TO 7	7 TO 8	8 TO 9	9 TO 10	10 TO 11	11 TO 12	12 TO 13	13 TO 14	14 TO 15	15 TO 16	16 TO 17	17 TO 18	18 TO 19	19 TO 20	20 TO 21	21 TO 22	22 TO 23	23 TO 24	MEAN
1	Q	761	758	759	755	753	751	747	754	756	755	748	739	739	743	748	746	733	724	703	695	698	711	737	750	740
2		748	749	749	749	750	749	751	753	754	756	758	762	767	774	759	765	755	733	717	713	715	717	732	748	747
3	D	757	767	779	765	753	754	761	762	762	753	755	731	729	741	740	740	729	711	688	726	733	754	791	781	748
4		783	806	847	768	755	710	733	741	739	711	617	683	746	760	751	738	703	695	689	712	724	738	766	758	736
5		761	760	767	767	767	734	748	750	748	748	749	727	673	747	762	754	747	733	722	716	717	724	736	749	742
6		759	786	780	755	757	756	749	754	752	755	755	747	757	760	758	749	738	728	724	725	727	727	734	756	749
7		757	758	760	759	757	758	757	763	758	766	765	768	765	757	743	746	740	728	716	704	715	727	763	767	750
8		787	765	751	748	753	752	758	767	756	760	757	634	740	747	755	752	727	716	719	721	721	747	738	771	743
9		763	756	784	775	747	747	748	749	750	756	756	755	747	738	746	757	737	724	723	735	734	737	756	758	749
10		771	765	756	755	756	756	754	748	633	686	755	752	736	735	737	737	732	715	713	720	726	735	745	754	736
11	Q	755	755	754	751	755	754	755	756	758	763	757	761	756	767	766	763	746	737	728	732	739	743	754	763	753
12	D	769	791	767	783	821	767	768	757	623	766	723	490	686	732	745	747	716	665	733	748	755	763	755	753	734
13		748	757	746	755	764	745	745	747	673	714	755	748	748	750	753	744	726	708	704	727	747	747	767	763	741
14		764	747	754	760	757	756	738	692	755	734	655	699	701	686	706	734	744	724	715	723	734	737	744	747	729
15		755	757	756	756	759	756	756	748	757	755	755	757	766	765	765	757	745	735	735	735	735	747	746	746	752
16		749	754	757	759	758	757	757	757	763	756	754	758	765	773	775	766	734	732	726	728	735	738	738	750	752
17		766	785	788	796	806	777	761	746	745	747	756	756	756	759	755	737	722	704	706	711	724	736	745	748	751
18		755	764	755	746	754	756	757	758	759	757	764	767	760	744	714	737	747	727	716	724	733	742	755	756	748
19	D	775	765	763	749	756	765	754	751	736	702	722	748	745	755	764	753	714	713	696	703	745	755	756	805	745
20		735	736	755	753	754	759	709	652	721	724	755	756	746	717	737	739	719	708	703	709	725	733	755	764	732
21		764	756	739	754	755	756	755	755	757	757	757	754	745	734	733	735	714	718	719	719	724	744	747	763	744
22		736	755	751	755	760	758	757	761	764	766	766	760	755	756	757	748	735	733	722	724	746	724	746	767	750
23		780	757	755	777	838	788	757	766	767	724	633	674	715	736	745	749	726	715	723	725	731	735	756	781	744
24		773	759	755	755	753	756	756	757	757	756	751	745	746	749	765	757	744	724	717	721	726	733	745	763	748
25	Q	758	758	756	766	757	758	755	754	755	756	756	756	757	755	750	736	717	706	704	713	717	726	743	749	744
26	D	757	765	760	758	764	765	766	765	766	716	635	734	716	766	778	765	743	725	727	734	747	769	745	784	748
27	D	808	850	981	1066	716	799	770	744	683	628	609	656	727	747	743	736	725	715	700	716	748	753	763	768	756
28		756	765	765	767	766	746	755	753	748	744	747	755	754	744	736	732	720	706	693	702	716	725	735	743	740
29	Q	749	756	764	757	758	757	756	759	760	758	757	756	760	756	749	744	736	717	704	701	706	717	727	747	744
30	Q	755	756	757	757	760	766	768	755	756	763	761	765	765	750	758	756	744	728	721	713	716	717	738	757	749
31		766	767	765	764	764	765	766	746	748	755	759	757	754	754	751	745	716	703	704	714	726	743	750	758	747
MEAN	A	762	765	770	770	762	757	754	749	741	741	734	731	743	748	750	747	731	718	713	719	729	737	749	760	745
MEAN	Q	756	757	758	757	757	757	756	756	757	759	756	756	756	754	754	749	735	722	712	711	715	723	740	753	746
MEAN	D	773	788	810	824	762	770	764	756	714	713	689	672	721	748	754	748	725	706	709	725	745	759	762	778	746

DECLINATION

TABLE 23 MEANOOK D = 23.5 DEGREES EAST PLUS TABULAR VALUES IN MINUTES AUGUST 1969

DAY		0 TO 1	1 TO 2	2 TO 3	3 TO 4	4 TO 5	5 TO 6	6 TO 7	7 TO 8	8 TO 9	9 TO 10	10 TO 11	11 TO 12	12 TO 13	13 TO 14	14 TO 15	15 TO 16	16 TO 17	17 TO 18	18 TO 19	19 TO 20	20 TO 21	21 TO 22	22 TO 23	23 TO 24	MEAN
1	Q	8.4	9.5	10.1	10.0	10.3	10.5	10.6	11.1	11.4	11.1	11.1	12.1	13.8	15.9	20.1	22.5	22.5	20.3	14.6	9.5	5.2	3.1	3.2	5.0	11.8
2		6.9	8.9	10.5	10.1	10.0	10.1	10.5	10.5	10.6	10.5	12.1	14.0	17.9	20.8	22.1	25.8	24.8	23.2	16.4	9.3	1.1	-1.3	.8	3.4	12.0
3	D	6.8	7.7	7.9	6.1	8.7	8.7	9.5	10.0	9.5	16.1	15.6	14.0	18.2	23.8	25.8	24.3	22.7	19.3	10.5	6.4	2.4	1.4	2.3	2.1	11.7
4		3.1	3.2	8.5	15.8	10.1	11.1	8.0	8.0	7.6	4.7	8.0	15.0	15.1	20.1	22.7	24.1	22.1	14.8	13.4	8.7	5.2	7.2	7.6	8.4	11.4
5		9.2	10.5	9.8	18.2	11.1	16.3	10.9	9.7	10.5	11.6	11.8	11.3	11.9	18.7	20.9	22.1	22.1	16.1	10.0	6.1	4.5	3.5	5.8	8.4	12.1
6		8.9	8.2	11.8	9.2	12.2	15.1	11.3	8.9	9.7	10.0	10.1	11.6	16.3	17.9	18.5	21.4	19.6	16.4	9.7	3.9	-0.2	-1.0	1.9	4.0	10.6
7		6.6	7.7	7.9	8.4	8.9	11.6	17.5	14.6	13.0	11.4	13.0	13.5	18.0	20.0	21.3	19.6	16.7	13.2	11.3	6.6	4.7	3.4	5.5	8.5	11.8
8		11.1	13.4	11.4	9.2	8.4	8.5	8.9	12.9	20.8	16.6	11.6	11.9	19.8	23.7	25.6	20.9	18.2	13.5	10.5	6.4	5.0	7.1	5.8	6.9	12.8
9		10.1	10.5	11.6	15.0	11.3	8.4	9.3	13.2	18.4	12.6	11.8	10.0	14.8	19.5	19.3	18.5	16.7	12.4	9.8	6.1	6.9	7.2	9.2	11.6	12.3
10		11.4	11.4	11.9	11.6	13.2	11.6	10.0	9.2	6.4	8.2	13.0	13.2	17.5	21.3	20.9	21.1	18.2	17.5	12.6	10.1	8.0	6.9	6.8	7.1	12.5
11	Q	8.4	9.8	10.0	10.0	9.3	9.8	10.1	10.3	10.3	10.0	11.4	13.8	17.7	19.2	21.1	21.6	19.6	18.2	11.3	6.8	8.2	7.7	8.0	8.4	12.1
12	D	8.4	8.0	7.9	10.0	10.5	22.1	11.9	10.0	5.6	18.7	8.7	15.0	21.1	19.3	18.0	21.4	19.2	7.9	.2	3.9	3.5	6.6	8.4	9.5	11.5
13		10.3	8.9	9.7	11.4	11.3	8.5	7.4	8.5	-1.5	5.2	10.5	10.3	16.3	19.5	18.7	17.7	17.2	16.1	10.1	5.2	5.2	6.1	8.5	10.6	10.5
14		11.8	11.6	10.1	10.0	9.7	11.4	10.1	11.3	11.6	8.7	10.9	13.8	11.6	14.5	19.8	21.7	19.8	16.7	12.1	5.3	3.5	5.3	7.2	8.4	11.5
15		8.5	9.5	9.5	9.5	9.5	9.7	10.0	11.6	11.4	11.8	12.9	13.5	13.7	16.3	18.2	18.0	18.0	16.3	13.4	8.2	7.1	6.8	6.6	8.7	11.6
16		10.1	10.0	10.0	10.1	10.1	10.1	10.3	11.4	11.8	12.2	9.2	13.5	15.0	16.7	17.9	17.7	16.7	15.1	8.7	3.5	4.2	4.8	5.6	8.2	11.0
17		10.2	9.9	9.2	3.4	2.3	9.9	6.5	11.2	11.2	13.3	12.1	13.1	15.4	17.6	19.1	19.5	18.4	16.2	11.5	7.0	4.6	4.9	5.1	6.8	10.8
18		8.3	8.4	11.5	8.4	8.4	8.8	9.7	9.9	10.0	9.9	12.5	11.5	13.7	16.5	16.2	20.8	21.5	19.1	13.4	6.7	5.7	6.2	6.7	8.3	11.3
19	D	8.1	8.3	10.0	7.9	8.1	15.0	14.5	11.7	9.9	9.6	5.7	15.4	19.5	21.0	20.8	22.3	19.4	11.5	9.6	6.2	3.6	-1.1	5.1	5.2	11.1
20		6.5	8.4	9.9	13.1	10.4	11.3	8.1	10.0	18.6	13.9	13.7	14.1	16.3	16.2	19.2	18.3	17.8	13.4	9.7	7.3	6.3	6.5	6.3	8.4	11.8
21		9.4	9.4	9.1	9.9	18.6	9.9	8.8	9.6	9.9	11.2	11.7	13.1	14.5	16.0	17.4	20.5	17.4	10.8	14.4	11.7	7.9	8.1	8.3	8.1	11.9
22		8.6	7.5	7.8	8.1	9.1	9.2	9.9	10.5	11.2	11.7	12.1	13.3	16.2	18.3	19.7	19.5	19.7	16.2	8.3	4.1	2.3	2.6	3.8	4.7	10.6
23		3.3	4.1	6.3	4.9	3.8	6.5	7.0	12.9	12.3	10.5	6.3	11.7	16.5	23.6	22.8	19.2	16.5	13.9	11.3	8.4	7.0	7.1	8.1	8.3	10.5
24		8.6	8.4	9.6	11.7	9.9	9.7	9.6	9.9	10.7	13.1	13.4	19.9	21.3	23.1	24.4	24.0	21.3	19.7	13.1	8.6	5.5	5.2	5.4	6.8	13.0
25	Q	9.2	11.8	13.1	8.4	8.3	8.3	9.4	8.4	9.9	11.5	12.1	12.9	14.1	14.9	17.8	19.2	19.7	18.3	13.6	8.9	6.3	5.1	6.2	7.9	11.5
26	D	8.6	8.6	9.2	9.4	8.8	8.3	8.6	11.5	11.7	5.2	4.6	17.8	17.9	18.1	23.2	24.2	22.4	17.6	11.3	6.5	3.4	3.4	4.7	3.3	11.2
27	D	1.7	-4.6	6.8	10.0	3.3	13.3	8.1	7.1	12.8	21.0	20.7	17.8	14.7	19.5	20.3	18.4	15.2	14.9	8.4	4.2	5.4	8.4	9.7	10.5	11.2
28		11.7	11.0	8.4	7.3	13.1	11.8	11.7	11.3	11.3	11.5	12.0	14.4	16.3	18.1	20.2	21.3	20.8	17.4	10.2	1.8	3.4	4.7	6.8	8.6	11.9
29	Q	9.9	10.2	10.0	9.7	9.7	9.6	9.9	10.0	10.8	11.8	12.8	13.6	16.2	18.4	22.6	23.7	23.4	18.1	12.8	6.8	3.9	3.3	4.7	6.8	12.0
30	Q	8.6	9.9	9.6	9.6	9.9	9.7	12.0	11.5	9.6	11.7	12.8	12.9	14.5	14.1	19.4	21.2	22.9	20.7	15.0	9.9	6.0	3.8	4.7	6.5	11.9
31		8.3	8.9	9.1	9.2	9.9	10.2	11.2	14.9	17.9	13.7	12.9	13.1	12.9	17.8	20.8	23.7	23.1	16.0	11.0	5.1	3.3	3.1	2.5	3.6	11.8
MEAN	A	8.4	8.7	9.6	9.9	9.6	10.8	10.0	10.7	11.1	11.6	11.5	13.6	16.1	18.7	20.5	21.1	19.8	16.2	11.2	6.7	4.8	4.7	5.8	7.2	11.6
MEAN	Q	8.9	10.2	10.6	9.5	9.5	9.6	10.4	10.3	10.4	11.2	12.0	13.1	15.3	16.5	20.2	21.6	21.6	19.1	13.5	8.4	5.9	4.6	5.4	6.9	11.9
MEAN	D	6.7	5.6	8.4	8.7	7.9	13.5	10.5	10.0	9.9	14.1	11.0	16.0	18.3	20.4	21.6	22.1	19.8	14.2	8.0	5.4	3.7	3.8	6.0	6.1	11.3

VERTICAL INTENSITY

TABLE 24 MEANOOK | Z = 58000 PLUS TABULAR VALUES IN GAMMAS | AUGUST 1969

DAY	HOUR UT	0 TO 1	1 TO 2	2 TO 3	3 TO 4	4 TO 5	5 TO 6	6 TO 7	7 TO 8	8 TO 9	9 TO 10	10 TO 11	11 TO 12	12 TO 13	13 TO 14	14 TO 15	15 TO 16	16 TO 17	17 TO 18	18 TO 19	19 TO 20	20 TO 21	21 TO 22	22 TO 23	23 TO 24	MEAN
1	Q	666	659	657	653	653	653	653	653	652	646	637	634	634	634	642	644	644	646	650	650	650	651	655	658	649
2		659	664	663	661	662	662	651	652	651	651	651	653	654	654	650	646	648	648	643	641	643	645	651	654	652
3	D	653	655	661	663	659	652	651	650	648	634	644	634	618	623	625	623	628	630	633	646	651	668	701	718	649
4		737	751	747	711	679	607	644	653	644	610	515	588	644	670	670	656	653	654	667	673	671	674	673	663	661
5		662	669	677	695	689	619	652	660	657	653	654	628	574	626	645	660	659	659	651	653	658	658	659	667	653
6		669	683	697	683	661	659	657	659	659	659	659	651	660	660	659	652	652	654	656	655	652	641	642	653	660
7		654	653	653	655	659	661	643	632	652	659	658	659	654	651	650	649	648	649	643	647	658	670	688	708	656
8		715	696	678	660	658	656	658	650	611	624	640	525	586	623	634	659	660	659	659	646	643	659	668	677	648
9		680	689	707	725	678	665	659	642	633	641	652	634	631	618	617	640	646	649	650	658	654	668	676	686	658
10		682	678	677	678	681	689	681	654	552	517	624	644	632	612	605	630	657	659	668	676	672	670	668	662	649
11	Q	660	659	659	659	659	659	659	659	659	659	658	659	659	659	657	656	653	653	648	642	646	648	650	658	656
12	D	668	676	710	724	715	641	658	660	520	612	611	425	552	604	626	644	651	633	650	658	651	659	668	669	637
13		669	670	667	670	677	669	643	651	498	526	624	643	649	652	659	659	660	663	660	665	669	677	686	678	649
14		672	670	668	668	669	672	636	557	632	611	493	576	584	584	620	649	660	664	667	668	662	665	666	667	637
15		667	660	659	659	659	660	661	658	650	659	659	660	659	659	659	659	659	659	651	648	650	658	662	668	659
16		666	659	659	659	657	657	654	651	650	639	619	630	650	658	657	654	648	641	638	641	651	661	670	675	652
17		681	698	724	753	771	726	696	673	658	655	662	660	659	661	661	659	659	655	655	660	668	670	669	667	679
18		667	678	690	670	659	658	652	651	650	644	640	652	659	649	611	610	636	640	640	647	653	659	659	659	651
19	D	669	676	685	690	679	681	653	650	602	513	491	581	611	624	643	650	656	657	667	678	696	725	759	675	651
20		665	668	687	691	697	690	602	494	584	592	611	659	659	640	648	662	670	671	669	668	670	672	676	678	651
21		673	673	669	670	660	658	656	655	656	658	659	659	654	640	630	633	641	633	641	653	655	659	660	671	655
22		659	662	659	659	659	659	658	658	658	659	652	643	633	642	649	652	658	655	649	649	650	651	653	659	653
23		670	668	660	667	696	686	666	651	669	642	563	538	575	623	642	655	670	670	668	676	687	688	682	687	654
24		685	690	688	679	671	661	661	660	660	660	643	642	653	646	658	659	657	652	650	650	655	659	660	667	661
25	Q	670	676	671	670	669	670	660	643	649	652	654	659	660	660	660	660	660	660	654	656	660	662	663	661	661
26	D	661	661	660	660	660	660	661	653	662	617	427	550	553	584	635	653	660	664	660	660	660	661	662	677	636
27	D	717	735	737	605	498	687	690	663	637	475	545	594	624	644	645	659	660	660	660	680	687	689	681	691	648
28		690	694	698	721	678	600	670	667	660	649	668	675	672	664	660	660	664	661	660	660	662	673	680	678	669
29	Q	670	662	663	663	662	661	660	660	661	661	661	661	660	660	653	650	652	654	652	659	660	666	670	671	661
30	Q	669	661	660	660	661	662	669	670	654	661	660	661	662	652	660	661	666	662	660	660	662	665	666	664	662
31		660	660	660	660	660	659	659	614	622	643	660	662	668	668	667	666	660	650	651	660	668	672	679	681	659
MEAN	A	674	676	679	676	668	661	657	645	634	625	619	624	634	640	645	651	655	654	654	657	660	666	671	673	654
MEAN	Q	667	664	662	661	661	661	660	657	655	656	654	655	655	653	654	654	655	655	653	653	656	659	661	662	658
MEAN	D	674	681	691	668	642	664	662	655	614	570	544	557	592	616	635	646	651	649	654	665	669	680	694	686	644

HORIZONTAL INTENSITY

TABLE 25 MEANOOK — H = 12500 PLUS TABULAR VALUES IN GAMMAS — SEPTEMBER 1969

DAY	HOUR UT	0 TO 1	1 TO 2	2 TO 3	3 TO 4	4 TO 5	5 TO 6	6 TO 7	7 TO 8	8 TO 9	9 TO 10	10 TO 11	11 TO 12	12 TO 13	13 TO 14	14 TO 15	15 TO 16	16 TO 17	17 TO 18	18 TO 19	19 TO 20	20 TO 21	21 TO 22	22 TO 23	23 TO 24	MEAN
1	Q	736	756	762	763	754	755	757	755	756	764	760	759	761	761	757	746	729	709	694	706	719	733	744	746	745
2	Q	753	760	762	763	763	763	765	763	757	756	761	763	760	765	763	746	728	706	695	706	722	736	745	757	748
3		766	765	764	765	764	764	765	765	765	764	766	757	763	764	756	746	726	719	724	726	734	733	753	763	753
4		756	756	756	755	756	759	759	739	765	769	770	766	764	756	752	739	724	714	714	730	745	757	754	747	750
5		749	752	755	765	765	765	770	770	766	764	765	754	703	654	383	588	698	734	735	729	773	821	873	878	738
6	D	805	744	790	784	753	715	673	755	764	729	585	503	743	736	750	732	735	726	726	732	746	757	753	745	728
7		757	756	745	742	754	753	753	753	682	677	735	657	714	733	755	734	733	723	695	714	739	756	777	785	734
8		760	777	785	810	891	1016	746	848	818	736	725	784	774	744	727	743	745	732	723	725	741	745	754	757	775
9		751	753	741	750	746	755	695	732	763	754	752	726	671	631	692	721	722	733	733	732	735	748	752	746	731
10		754	757	754	748	750	755	753	754	754	754	754	754	746	733	717	725	735	716	716	725	737	734	738	756	742
11		781	760	784	762	753	747	744	713	653	715	756	739	746	728	741	746	726	725	724	722	745	755	756	765	741
12		765	739	747	756	751	768	760	756	763	736	756	746	756	747	744	736	722	714	721	724	733	744	753	754	745
13	Q	756	755	755	755	753	754	756	755	745	736	755	744	756	757	754	735	719	706	722	724	724	746	796	947	754
14		941	990	889	794	760	742	731	774	726	648	651	682	674	683	723	722	623	630	721	724	725	746	796	819	746
15		940	982	893	788	765	742	742	776	722	747	651	684	672	682	722	722	624	630	695	705	703	726	753	764	743
16		757	755	747	747	747	746	756	736	732	733	753	744	742	756	755	747	748	734	732	733	744	751	754	757	746
17		755	755	754	755	761	762	763	765	765	760	757	692	761	764	751	744	744	733	714	714	738	741	746	748	748
18	D	765	766	780	781	791	789	777	769	764	744	745	716	706	701	741	754	726	675	703	724	747	763	756	774	748
19		780	773	773	766	777	776	764	756	754	725	736	756	746	741	746	739	733	732	719	718	724	734	746	756	749
20		755	750	757	756	755	751	757	733	662	706	757	749	734	724	734	726	761	710	733	734	734	746	745	755	739
21		765	757	757	762	766	761	763	755	737	761	764	765	761	755	746	735	733	732	735	741	750	755	759	756	753
22	Q	746	755	756	757	756	762	756	761	766	769	755	756	763	764	756	747	737	743	733	735	749	755	756	755	754
23		753	756	757	758	760	762	765	764	763	767	772	775	773	745	734	745	746	727	723	730	743	744	753	756	753
24		754	763	758	756	769	764	765	755	756	746	736	757	756	756	754	742	727	712	715	723	742	753	756	752	749
25		754	746	757	758	745	763	752	749	754	758	758	754	755	750	740	714	713	723	714	729	727	731	755	756	744
26	Q	747	757	756	755	755	758	763	765	752	704	764	766	763	762	756	745	733	722	713	719	725	735	752	754	747
27		760	759	759	759	764	763	764	764	764	764	764	764	772	765	763	763	737	727	724	723	728	748	764	763	755
28	D	783	776	773	768	765	768	778	776	775	766	755	251	556	640	660	722	740	712	652	702	740	752	783	765	715
29	D	773	780	773	769	776	807	779	473	186	148	333	544	652	628	463	543	725	711	729	707	740	787	847	978	652
30	D	899	853	736	825	814	784	834	441	204	186	258	33	255	529	705	647	669	679	714	745	784	746	755	756	619
MEAN	A	777	777	769	766	766	769	757	739	711	703	712	688	717	722	718	723	722	713	716	723	738	749	764	777	738
MEAN	Q	748	757	758	759	756	758	759	760	755	746	759	758	761	762	757	744	729	717	712	718	728	741	759	792	750
MEAN	D	805	784	771	785	780	773	768	643	539	515	535	409	582	647	664	680	719	700	705	722	751	761	779	804	692

DECLINATION

TABLE 26 MEANOOK D = 23.5 DEGREES EAST PLUS TABULAR VALUES IN MINUTES SEPTEMBER 1969

DAY	HOUR UT	0 TO 1	1 TO 2	2 TO 3	3 TO 4	4 TO 5	5 TO 6	6 TO 7	7 TO 8	8 TO 9	9 TO 10	10 TO 11	11 TO 12	12 TO 13	13 TO 14	14 TO 15	15 TO 16	16 TO 17	17 TO 18	18 TO 19	19 TO 20	20 TO 21	21 TO 22	22 TO 23	23 TO 24	MEAN
1	Q	8.4	9.6	9.6	9.7	9.1	8.9	8.4	9.6	10.0	10.0	10.7	11.5	13.1	16.5	19.9	21.8	21.5	20.2	13.4	8.4	3.6	3.3	5.1	8.1	11.3
2	Q	8.3	8.4	8.4	8.6	9.9	8.9	9.4	8.3	9.9	11.5	12.5	13.1	15.4	16.8	19.2	21.3	22.9	19.5	11.8	7.5	3.6	3.6	5.1	7.0	11.3
3		8.3	8.4	8.4	8.4	9.2	9.9	10.0	10.0	10.2	11.2	11.5	13.3	17.1	19.4	20.8	19.7	21.0	17.1	11.5	7.6	6.7	8.3	7.3	6.8	11.8
4		6.8	6.7	4.9	6.5	6.5	9.7	9.6	10.0	9.9	10.7	11.7	13.1	14.4	16.0	18.1	19.2	17.9	11.7	6.5	3.4	1.8	4.7	7.6	10.2	9.9
5		10.8	9.7	8.3	8.3	8.4	9.4	9.7	11.5	12.8	14.4	13.9	12.1	8.6	11.5	14.5	19.1	11.5	8.3	6.8	3.1	2.2	5.4	9.9	11.3	10.1
6	D	8.6	7.6	6.8	19.5	10.2	19.4	19.2	17.3	13.1	13.4	18.3	16.3	13.9	16.5	18.1	19.4	14.9	14.4	7.3	4.2	4.9	8.3	7.9	8.4	12.8
7		8.4	9.6	9.9	8.6	9.1	9.7	10.5	12.9	22.9	22.9	11.5	5.1	13.4	18.1	18.4	17.6	17.6	11.8	4.4	4.4	1.5	3.8	8.4	5.9	11.1
8		9.1	10.0	13.1	14.4	6.0	7.1	-10.7	-27.0	21.5	26.6	22.8	14.4	14.9	19.1	17.9	14.7	15.2	12.1	8.4	5.2	5.1	5.5	8.3	11.3	10.2
9		12.8	12.8	11.3	11.0	9.9	11.2	.1	11.7	11.3	12.8	13.1	9.6	11.2	12.8	16.2	17.8	16.0	13.1	7.5	5.4	5.9	7.3	9.2	10.7	10.8
10		14.7	15.5	10.7	13.4	13.1	8.3	8.1	8.4	10.2	11.5	11.8	12.0	14.1	15.0	14.7	13.7	14.5	12.8	3.3	3.1	4.2	5.2	8.1	10.0	10.7
11		9.2	11.2	11.0	12.8	8.4	8.1	8.6	9.9	15.8	16.2	14.7	14.9	16.0	14.9	16.5	17.6	16.3	11.2	10.2	3.6	.7	3.6	8.3	9.9	11.2
12		11.0	11.5	10.4	9.9	11.5	14.7	9.9	8.3	10.5	7.0	12.9	13.1	.1	15.2	17.9	18.1	16.2	15.5	9.9	9.9	5.9	7.0	9.7	10.7	11.1
13	Q	11.7	11.3	9.9	9.9	11.3	9.4	9.1	9.7	8.8	.5	13.1	13.1	16.6	17.9	17.9	19.7	19.5	14.9	9.9	6.7	4.1	6.2	8.1	8.4	11.2
14		9.9	10.2	11.0	13.3	11.3	10.7	9.9	9.9	10.0	12.3	7.9	14.5	16.3	18.9	20.5	21.6	20.8	13.6	9.1	10.2	4.2	3.0	2.2	6.7	11.6
15		3.3	9.3	11.4	14.4	12.8	8.2	19.3	1.6	14.8	16.5	17.0	18.2	26.7	27.8	25.7	15.7	3.2	-0.5	4.1	7.2	7.8	6.7	7.4	10.6	12.1
16		10.1	8.5	11.4	23.9	11.1	16.1	12.8	10.4	15.1	12.8	12.4	13.3	16.4	17.2	19.1	19.1	18.6	16.1	13.0	11.2	9.8	10.1	9.8	9.8	13.7
17		9.5	8.5	9.1	8.8	9.8	9.8	9.9	9.9	10.7	12.4	13.3	23.0	28.8	23.9	24.3	21.7	17.8	18.6	3.5	3.5	4.5	4.0	4.9	6.7	12.4
18	D	5.4	5.9	9.9	7.5	5.4	9.9	6.9	10.9	8.7	12.4	11.1	9.8	9.6	13.2	18.3	15.9	16.5	9.9	2.2	1.9	6.4	6.7	5.9	5.6	9.0
19		7.0	5.8	9.6	11.6	16.2	15.3	10.6	9.8	11.1	9.9	11.4	12.8	12.2	14.0	16.4	16.1	16.5	14.8	14.0	12.2	9.8	9.1	8.2	8.3	11.8
20		8.3	8.2	9.9	12.7	11.1	13.8	13.6	11.4	15.3	18.6	13.8	14.9	13.0	14.4	17.5	16.2	11.6	13.3	8.5	9.5	8.8	7.0	7.7	8.2	12.0
21		8.5	8.2	8.2	8.8	9.6	11.2	10.4	7.8	6.9	11.1	11.6	14.0	13.8	14.9	16.2	15.6	13.6	13.5	9.8	9.3	9.1	9.0	8.3	8.5	10.7
22	Q	8.8	8.8	9.1	8.8	9.8	9.1	2.9	10.4	12.2	13.5	14.8	16.2	16.4	16.1	16.2	16.9	16.4	14.6	12.0	9.8	8.2	7.7	8.3	9.8	11.5
23		9.6	9.5	9.3	9.0	9.6	10.1	9.8	9.1	11.1	11.9	13.0	13.8	14.4	12.7	13.0	17.5	15.3	12.2	8.0	6.9	8.2	5.3	6.6	8.2	10.6
24		9.8	8.5	8.2	9.1	9.5	11.4	8.5	9.5	12.4	13.2	16.5	17.7	17.0	16.2	18.0	18.2	18.2	17.3	13.0	11.1	7.0	7.2	7.8	8.8	12.2
25		9.3	9.8	8.3	9.8	17.3	11.4	7.4	9.8	9.8	11.4	12.7	13.8	14.6	16.1	17.8	14.6	11.6	12.7	12.8	9.5	6.1	4.6	4.9	6.4	10.9
26	Q	9.5	9.6	9.9	9.9	10.1	10.4	11.2	19.4	11.6	7.8	14.8	14.6	14.4	16.1	17.8	19.6	20.9	18.0	14.3	11.4	9.8	8.3	8.0	8.0	12.7
27		8.5	8.7	9.3	9.8	9.8	10.1	11.1	11.1	11.1	11.4	11.9	12.5	13.0	14.9	16.5	20.1	20.7	16.4	12.2	10.7	7.5	3.7	1.1	1.4	11.0
28	D	.8	3.2	9.1	9.3	9.5	8.3	8.0	9.8	10.1	15.9	14.9	14.8	35.9	37.3	29.1	24.6	22.5	20.1	8.7	3.2	4.0	4.9	4.8	7.7	13.2
29	D	9.6	11.1	9.6	18.2	12.7	7.8	6.6	4.8	-12.8	3.2	11.2	32.8	24.1	34.1	38.4	20.6	9.6	12.5	7.2	4.9	6.7	6.7	9.8	26.7	13.2
30	D	12.2	6.6	-7.9	6.7	6.6	5.3	5.6	-3.6	-45.1	40.9	47.0	39.4	36.0	9.6	12.4	14.6	14.8	11.2	18.3	12.7	13.2	9.6	10.6	12.2	12.0
MEAN	A	8.9	9.1	8.9	11.1	10.2	10.5	8.9	8.4	9.3	13.5	14.5	15.3	16.4	17.6	18.9	18.3	16.5	13.9	9.4	7.3	6.0	6.2	7.3	9.1	11.5
MEAN	Q	9.3	9.6	9.4	9.4	10.0	9.4	8.2	11.5	10.5	8.7	13.2	13.7	15.2	16.7	18.2	19.9	20.2	17.4	12.3	8.7	5.8	5.8	6.9	8.3	11.6
MEAN	D	7.3	6.9	5.5	12.2	8.9	10.2	9.3	7.8	-5.2	17.1	20.5	22.6	23.9	22.1	23.3	19.0	15.7	13.6	8.7	5.4	7.0	7.3	7.8	12.1	12.0

VERTICAL INTENSITY

TABLE 27 MEANOOK — Z = 58000 PLUS TABULAR VALUES IN GAMMAS — SEPTEMBER 1969

HOUR UT / DAY		0 TO 1	1 TO 2	2 TO 3	3 TO 4	4 TO 5	5 TO 6	6 TO 7	7 TO 8	8 TO 9	9 TO 10	10 TO 11	11 TO 12	12 TO 13	13 TO 14	14 TO 15	15 TO 16	16 TO 17	17 TO 18	18 TO 19	19 TO 20	20 TO 21	21 TO 22	22 TO 22	23 TO 24	MEAN
1	Q	670	652	664	665	671	670	661	660	644	655	657	660	662	664	665	665	661	660	646	647	646	651	659	660	659
2	Q	659	660	660	661	660	660	661	661	665	666	666	664	660	660	660	660	656	655	647	647	646	651	660	660	659
3		656	656	657	656	656	656	655	655	654	653	651	636	638	650	655	657	655	647	646	646	646	651	655	662	652
4		666	667	671	679	689	670	660	660	660	660	660	659	660	656	656	656	653	646	646	655	651	656	660	660	661
5		656	653	652	653	654	655	660	668	668	658	644	632	546	472	505	426	596	683	693	709	716	733	759	773	644
6	D	723	679	721	717	696	568	468	642	670	644	521	586	641	649	664	660	661	669	668	674	676	692	695	675	652
7		678	684	675	670	665	665	666	651	564	560	642	578	617	630	660	669	683	671	672	686	703	712	726	736	661
8		711	711	717	727	709	546	530	471	661	661	644	689	699	676	662	678	684	685	689	687	681	676	671	674	664
9		675	680	675	673	671	666	507	613	672	664	660	642	613	595	598	614	659	673	674	676	679	687	690	691	652
10		695	696	688	688	685	676	668	669	665	665	667	667	669	660	652	645	651	660	663	662	671	674	671	669	670
11		690	715	754	736	711	688	662	613	559	624	661	661	664	656	669	671	670	670	671	669	672	672	672	671	671
12		679	671	670	672	678	627	656	661	662	635	653	655	659	662	662	666	666	664	669	672	670	671	670	669	663
13	Q	665	665	665	665	669	669	662	664	647	624	652	631	650	661	661	661	661	665	660	659	661	666	666	668	659
14		665	666	671	671	667	666	664	660	653	624	604	631	645	644	647	660	657	651	650	664	658	700	728	753	662
15		755	709	602	721	697	690	689	627	646	630	621	622	630	601	601	552	572	587	653	684	681	684	692	709	652
16		708	691	698	690	684	681	670	650	648	674	664	651	670	679	677	676	675	675	679	675	675	675	675	671	675
17		670	668	667	664	666	665	668	668	668	660	649	552	627	636	632	641	650	651	660	646	651	660	666	666	652
18	D	676	682	708	693	707	706	657	679	666	648	644	641	622	653	612	654	660	660	678	668	687	703	685	715	671
19		715	717	726	694	644	645	656	672	670	633	632	657	662	664	667	675	676	674	670	670	670	670	676	676	671
20		672	669	670	671	674	676	665	636	545	582	651	653	646	635	631	642	655	666	672	677	673	672	670	675	653
21		672	671	672	677	677	669	672	654	625	652	656	656	661	662	661	662	663	666	666	664	669	671	671	676	664
22	Q	676	675	674	673	676	669	710	628	641	663	654	653	661	662	665	666	670	671	671	671	670	668	663	661	666
23		665	665	665	665	665	665	663	665	666	665	664	660	661	634	606	622	637	649	656	669	680	699	708	684	662
24		673	671	677	667	690	693	685	685	680	662	633	651	656	665	665	666	669	666	672	661	671	666	664	665	669
25		670	672	671	679	683	689	612	636	673	671	662	661	663	661	656	641	647	652	663	670	680	681	680	678	665
26	Q	665	669	667	670	668	669	670	669	661	596	641	664	663	663	664	666	663	661	689	693	694	698	700	699	669
27		699	699	699	699	699	699	699	699	699	699	699	699	698	698	698	698	698	697	694	697	701	694	697	693	698
28	D	707	740	722	699	693	694	697	703	692	688	690	458	440	571	614	674	669	688	683	693	705	735	767	730	673
29	D	733	729	724	734	722	743	739	545	739	549	573	730	729	667	606	553	648	666	704	716	723	732	758	537	679
30	D	434	504	453	535	723	742	693	722	936	823	694	798	718	609	666	710	699	697	751	750	758	722	723	728	691
MEAN	A	676	676	674	679	682	669	654	650	663	650	647	647	648	643	645	646	659	664	672	675	679	684	689	683	665
MEAN	Q	667	664	666	667	669	667	673	657	651	641	654	655	660	662	663	664	662	662	663	663	664	667	670	670	663
MEAN	D	654	667	665	676	708	691	651	658	740	670	625	643	630	630	633	650	667	676	697	700	710	717	725	677	673

HORIZONTAL INTENSITY

TABLE 28 MEANOOK — H = 12500 PLUS TABULAR VALUES IN GAMMAS — OCTOBER 1969

HOUR UT / DAY		0 TO 1	1 TO 2	2 TO 3	3 TO 4	4 TO 5	5 TO 6	6 TO 7	7 TO 8	8 TO 9	9 TO 10	10 TO 11	11 TO 12	12 TO 13	13 TO 14	14 TO 15	15 TO 16	16 TO 17	17 TO 18	18 TO 19	19 TO 20	20 TO 21	21 TO 22	22 TO 23	23 TO 24	MEAN
1	D	776	752	757	757	760	764	583	625	672	638	527	529	581	744	744	733	740	732	729	729	727	726	743	737	700
2	D	758	767	755	752	755	721	672	454	124	56	292	432	506	722	593	654	631	766	743	747	735	752	751	746	620
3	D	744	750	736	744	745	702	712	731	684	687	709	648	579	621	602	637	701	742	725	734	744	744	756	752	705
4		752	745	753	753	752	740	755	752	746	704	733	725	736	751	747	755	742	712	714	736	731	741	747	752	740
5		745	746	752	759	753	756	765	758	755	740	719	741	762	754	756	750	754	731	721	721	730	734	733	747	745
6	D	756	755	752	756	765	773	765	748	746	735	671	714	721	724	717	735	711	683	682	701	724	732	733	745	731
7		752	765	765	776	775	756	724	715	734	733	744	751	745	745	749	744	733	728	717	719	725	733	733	744	742
8	Q	749	751	755	758	756	760	760	760	767	768	768	766	762	756	756	753	752	742	729	728	734	742	745	748	753
9		745	755	761	761	756	766	753	755	756	761	761	762	762	761	756	754	755	742	735	740	732	725	743	764	753
10	D	765	777	775	796	832	830	797	758	680	590	341	560	639	684	746	752	736	732	721	705	725	733	745	748	715
11		754	746	757	758	763	737	743	742	755	722	661	752	717	701	753	752	750	724	722	731	737	743	752	755	739
12		766	755	756	762	761	754	746	604	701	744	744	731	699	722	713	711	734	734	735	741	748	757	765	767	735
13		747	747	748	747	750	754	754	745	751	750	726	725	752	738	746	752	739	733	716	725	736	733	743	753	742
14	Q	752	754	755	754	754	754	753	754	755	756	755	757	756	753	745	743	732	722	714	716	722	733	742	745	745
15	Q	749	752	753	752	752	752	749	747	746	748	744	738	753	762	759	752	743	727	719	722	733	742	745	746	745
16		751	752	753	753	754	754	736	756	765	763	763	762	762	754	750	742	726	723	732	731	722	734	736	742	747
17		742	743	748	753	748	751	746	746	753	755	755	762	762	762	756	753	744	735	733	732	735	741	732	736	747
18		738	743	744	745	752	754	763	754	750	723	681	743	766	754	753	752	745	734	722	733	745	754	753	754	744
19		763	763	758	762	766	763	761	761	754	773	763	734	641	716	751	745	734	722	722	725	739	752	744	741	744
20		744	745	754	755	755	757	758	756	755	759	756	762	763	762	759	755	751	743	724	725	733	735	736	743	750
21		753	754	755	758	759	762	761	759	723	714	773	765	762	760	753	732	723	733	735	732	740	749	742	745	748
22		753	754	753	754	753	765	765	761	755	737	762	755	754	749	753	745	734	718	715	721	732	739	742	743	746
23		749	753	753	753	756	758	756	754	757	760	762	761	760	761	755	754	745	736	726	733	737	727	740	743	750
24		755	751	745	747	764	766	775	744	743	716	755	721	683	742	757	745	745	741	733	735	739	753	744	753	744
25		757	766	757	750	752	752	758	753	752	753	752	753	757	759	759	757	751	742	724	722	732	723	734	742	748
26	Q	748	752	755	754	753	753	754	753	751	756	755	755	754	757	759	754	750	738	731	722	732	741	744	751	749
27		754	761	765	762	761	761	764	764	754	751	760	762	753	745	764	764	753	742	732	724	711	703	734	735	749
28		753	752	753	755	764	761	760	755	753	757	756	761	762	755	754	745	733	732	722	720	719	722	733	741	747
29		743	752	753	752	757	762	764	759	753	754	761	762	762	764	762	753	743	731	719	712	721	731	738	744	748
30	Q	752	753	755	759	758	757	761	762	755	754	754	755	760	759	756	751	743	731	722	725	735	744	750	753	750
31		760	762	761	752	753	751	742	739	719	732	713	682	703	732	762	754	751	740	724	720	722	732	734	744	737
MEAN A		752	754	755	757	759	757	747	733	722	713	707	720	722	741	742	741	736	732	724	726	732	737	742	747	737
MEAN Q		750	753	755	756	755	755	756	755	755	757	755	754	757	758	755	751	744	732	723	723	731	740	745	749	748
MEAN D		760	760	755	761	771	758	706	663	581	541	508	577	605	699	680	702	704	731	720	723	731	737	745	745	694

TABLE 29 MEANOOK D = 23.5 DEGREES EAST PLUS TABULAR VALUES IN MINUTES OCTOBER 1969

HOUR UT DAY		0 TO 1	1 TO 2	2 TO 3	3 TO 4	4 TO 5	5 TO 6	6 TO 7	7 TO 8	8 TO 9	9 TO 10	10 TO 11	11 TO 12	12 TO 13	13 TO 14	14 TO 15	15 TO 16	16 TO 17	17 TO 18	18 TO 19	19 TO 20	20 TO 21	21 TO 22	22 TO 23	23 TO 24	MEAN
1	D	12.4	13.3	17.3	12.2	14.4	13.0	7.5	17.0	19.1	10.9	19.3	20.6	13.0	14.4	16.7	17.8	19.6	10.3	10.4	11.7	12.8	12.7	11.4	9.8	14.1
2	D	10.6	24.9	11.1	9.6	11.7	15.9	2.1	25.2	50.5	42.5	38.4	35.9	5.6	9.6	7.8	10.9	10.6	11.2	13.5	11.9	10.1	11.4	11.2	11.4	16.8
3	D	11.4	12.0	26.5	20.9	11.6	13.0	9.9	11.9	5.8	6.2	11.4	18.0	6.2	-0.7	-6.5	-4.5	5.3	14.6	8.8	11.6	10.1	11.2	10.7	11.2	9.9
4		11.4	12.8	11.7	11.6	12.5	10.3	13.3	12.8	13.0	7.5	14.0	14.8	12.7	14.1	13.3	15.9	17.5	15.6	12.0	11.7	11.2	11.1	9.6	9.8	12.5
5		12.2	10.9	10.3	11.2	11.1	16.2	14.4	11.2	12.0	16.1	15.9	16.5	13.2	13.0	14.4	16.7	16.9	18.0	16.4	9.6	8.5	6.7	8.2	8.5	12.8
6	D	9.5	9.6	11.6	19.9	10.6	11.6	13.8	8.8	11.2	12.0	5.3	11.6	11.6	14.1	9.8	10.6	13.3	6.7	-0.5	.3	3.2	4.1	6.7	9.5	9.4
7		10.6	9.6	8.7	20.1	11.1	11.6	16.2	9.3	10.4	10.9	11.6	13.0	12.0	12.8	15.6	16.5	15.9	14.8	12.4	9.5	7.4	6.2	6.6	7.5	11.7
8	Q	9.1	10.6	10.4	10.6	11.2	11.2	11.4	11.4	13.0	12.0	12.0	12.2	12.5	13.8	13.0	14.3	14.9	14.0	11.6	8.2	6.7	7.0	7.4	8.2	11.1
9		9.3	9.9	10.1	10.3	10.9	11.6	8.8	9.6	11.6	11.4	11.6	12.8	12.0	13.2	14.3	15.4	18.2	14.9	14.8	9.9	9.6	4.3	7.8	9.3	11.3
10	D	8.7	8.2	9.5	13.3	10.1	9.6	13.6	11.9	14.0	27.3	46.5	24.1	21.2	12.0	16.2	14.3	9.6	8.2	12.4	8.3	6.7	6.6	8.0	9.9	13.8
11		9.8	9.9	11.6	11.1	10.1	14.8	14.3	13.3	13.5	11.6	9.5	12.8	22.8	14.6	19.3	17.7	17.5	14.9	9.9	8.0	6.4	6.6	9.3	9.8	12.5
12		9.6	10.4	14.4	10.1	10.1	9.8	9.9	-3.7	13.3	13.6	19.1	20.9	20.4	24.3	16.5	9.9	9.8	12.7	12.8	8.5	8.2	8.2	9.5	9.9	12.0
13		9.3	9.5	10.1	9.8	10.0	11.3	7.2	7.1	8.7	10.1	7.4	15.6	14.8	13.7	15.1	16.4	15.1	12.2	8.8	6.1	4.2	5.3	7.1	8.4	10.1
14	Q	8.7	9.0	10.0	10.1	10.0	10.0	10.0	9.8	10.0	10.1	10.5	11.3	11.6	12.2	13.8	15.3	15.6	13.2	8.0	4.3	3.8	4.3	7.1	8.7	9.9
15	Q	8.8	10.0	10.5	10.3	10.5	10.3	4.0	8.7	10.1	11.9	10.8	10.3	16.9	16.9	15.6	16.6	16.7	15.3	12.1	9.3	8.7	8.7	9.0	10.0	11.3
16		9.0	8.8	9.0	9.2	8.7	7.2	2.4	8.4	10.5	10.5	11.6	11.9	12.1	12.9	14.6	16.7	15.6	7.1	4.0	4.0	1.0	1.6	3.8	5.3	8.6
17		7.1	8.4	8.8	8.7	8.7	9.0	8.8	10.3	10.5	10.8	11.1	11.9	11.9	12.1	13.5	15.3	16.9	15.1	12.1	8.7	6.6	4.2	3.5	3.8	9.9
18		5.0	7.0	8.6	8.7	9.7	8.6	19.8	8.7	11.6	12.4	13.6	12.0	12.1	12.0	12.3	14.5	14.9	13.6	10.5	7.1	6.8	6.3	8.4	7.1	10.5
19		6.5	6.6	6.8	6.6	6.3	6.8	8.6	6.3	6.6	11.5	13.6	17.1	13.6	16.5	13.1	13.4	14.9	13.1	7.3	6.3	5.5	5.4	7.0	8.4	9.5
20		8.1	8.7	8.4	8.4	8.6	8.9	8.7	10.2	10.4	10.8	11.5	11.3	11.8	12.0	13.7	15.0	15.2	15.0	13.1	9.7	7.1	7.0	7.0	8.7	10.4
21		7.6	8.4	8.6	8.9	9.2	10.0	10.2	10.0	11.8	18.4	16.6	13.6	13.2	13.6	15.2	16.5	11.2	10.2	8.1	4.6	5.0	5.5	8.3	10.0	10.6
22		8.6	8.6	8.5	8.8	9.9	13.3	7.0	8.6	10.1	9.8	12.0	13.8	16.4	13.6	11.9	14.8	14.8	14.1	10.3	7.5	7.2	9.0	9.1	8.8	10.7
23		8.6	7.2	9.1	8.5	9.3	10.4	12.8	7.8	11.7	10.1	10.7	11.1	11.4	11.5	12.5	13.3	14.0	13.6	8.8	6.5	5.9	7.8	7.2	8.5	9.9
24		7.2	9.3	10.4	11.4	10.7	5.3	13.0	16.5	16.4	15.1	11.9	15.1	13.5	11.7	14.9	16.0	13.5	12.2	8.6	8.0	8.6	8.8	8.6	8.3	11.5
25		8.3	8.5	8.6	8.8	9.8	14.9	8.3	9.8	10.3	10.1	11.4	12.0	11.5	11.9	13.1	14.8	14.9	14.6	12.0	9.3	8.3	8.3	7.2	8.6	10.6
26	Q	8.5	8.7	8.9	9.3	9.3	8.7	14.7	14.0	13.0	10.2	10.3	11.6	11.6	11.9	13.4	15.0	16.3	16.3	13.0	10.0	7.9	6.6	6.8	7.6	11.0
27		8.1	8.5	8.5	8.9	8.7	8.9	9.7	9.8	10.6	13.0	12.9	11.9	11.9	10.5	13.2	16.4	16.6	16.6	14.7	11.8	9.8	5.0	3.2	5.2	10.6
28		4.2	5.2	6.6	7.1	8.7	9.5	11.4	11.6	13.2	13.4	11.0	11.1	11.4	12.7	13.4	15.1	15.0	13.0	11.9	8.1	5.2	3.2	5.2	6.8	9.7
29		8.4	8.6	8.8	11.2	11.8	9.9	9.9	8.6	9.9	9.9	10.2	11.2	11.3	11.5	12.6	13.4	14.2	13.6	12.8	8.3	5.2	5.1	6.0	8.0	10.0
30	Q	8.6	9.4	9.7	9.7	9.9	9.9	11.7	9.7	8.4	9.6	10.2	11.0	11.3	12.5	12.9	14.6	14.9	14.7	11.7	9.7	8.0	7.8	8.1	8.3	10.5
31		8.3	9.1	9.9	11.2	13.1	9.9	10.9	13.1	17.1	14.9	12.9	9.7	16.3	14.6	13.3	13.3	13.6	14.9	11.7	9.9	8.1	8.0	7.6	8.1	11.6
MEAN	A	8.8	9.7	10.4	10.9	10.3	10.7	10.5	10.6	12.8	13.1	14.0	14.4	13.2	12.9	13.2	14.3	14.6	13.4	10.8	8.3	7.2	6.9	7.6	8.5	11.1
MEAN	Q	8.8	9.5	9.9	10.0	10.2	10.0	10.3	10.7	10.9	10.8	10.8	11.3	12.8	13.5	13.8	15.1	15.7	14.7	11.3	8.3	7.0	6.9	7.7	8.5	10.8
MEAN	D	10.5	13.6	15.2	15.2	11.7	12.6	9.4	15.0	20.1	19.8	24.2	22.0	11.5	9.9	8.8	9.8	11.7	10.2	8.9	8.7	8.6	9.2	9.6	10.4	12.8

VERTICAL INTENSITY

TABLE 30 MEANOOK   Z = 58000 PLUS TABULAR VALUES IN GAMMAS   OCTOBER 1969

HOUR UT / DAY		0 TO 1	1 TO 2	2 TO 3	3 TO 4	4 TO 5	5 TO 6	6 TO 7	7 TO 8	8 TO 9	9 TO 10	10 TO 11	11 TO 12	12 TO 13	13 TO 14	14 TO 15	15 TO 16	16 TO 17	17 TO 18	18 TO 19	19 TO 20	20 TO 21	21 TO 22	22 TO 23	23 TO 24	MEAN
1	D	739	753	750	738	736	727	613	610	665	644	662	562	645	680	698	699	722	723	723	722	724	732	742	741	698
2	D	736	748	747	727	724	624	619	575	571	761	618	557	604	610	544	687	702	747	743	732	733	737	740	748	681
3	D	742	740	728	717	731	694	676	682	693	642	658	614	581	565	541	560	635	702	720	719	712	712	720	717	675
4		721	723	721	719	708	686	709	709	707	645	679	685	684	694	707	712	713	712	710	712	713	716	722	724	705
5		727	726	716	721	721	722	717	716	686	656	653	681	701	702	712	712	716	717	718	715	719	718	710	716	708
6	D	717	718	728	726	751	750	726	710	706	690	716	663	664	676	680	693	704	719	726	724	726	717	709	716	711
7		714	728	742	769	742	728	702	645	685	693	697	704	709	710	713	712	711	710	709	704	710	713	713	713	712
8	Q	713	709	709	709	709	709	709	709	690	706	707	706	705	705	705	705	703	704	703	704	706	713	720	716	707
9		710	714	710	710	709	707	695	704	709	704	705	700	703	704	710	711	708	705	701	693	691	700	707	706	705
10	D	707	717	740	782	710	692	712	710	662	624	582	633	609	683	688	679	673	687	710	727	755	748	735	725	695
11		728	741	745	726	717	709	681	690	700	676	618	671	644	596	652	686	717	712	708	708	717	722	719	710	696
12		719	727	746	721	727	727	718	521	634	662	662	643	591	551	568	616	654	700	718	717	717	718	717	711	674
13		711	710	710	709	710	718	709	673	710	701	617	597	662	688	700	701	701	700	697	699	700	704	707	709	693
14	Q	664	663	663	663	663	663	662	662	661	662	663	663	661	662	661	664	665	666	660	660	664	665	666	666	663
15	Q	666	665	664	665	669	666	629	649	637	645	633	631	636	645	654	660	656	668	666	665	666	666	666	665	655
16		664	665	664	664	665	653	609	633	662	664	663	662	657	656	654	655	656	653	651	655	657	664	666	676	657
17		675	670	663	663	664	665	665	664	662	656	648	663	657	656	656	661	659	657	656	659	665	666	674	698	663
18		696	681	673	665	663	671	647	662	673	632	626	641	664	663	663	665	671	671	665	662	662	660	657	662	662
19		662	663	665	666	665	663	672	599	584	664	672	647	559	590	646	665	664	665	665	669	672	675	673	671	651
20		671	665	665	672	673	673	671	665	664	664	663	662	661	662	664	665	664	664	665	663	665	672	669	665	666
21		667	665	663	664	663	663	664	654	605	578	645	672	665	663	662	656	653	656	671	672	671	668	665	663	657
22		663	664	663	668	662	680	690	671	670	626	644	644	644	655	664	663	664	668	672	672	667	664	664	664	663
23		666	667	666	666	664	667	678	662	668	669	664	664	662	663	664	666	667	664	660	662	666	672	672	670	666
24		662	670	672	696	700	665	693	652	672	631	652	647	579	628	653	653	663	665	664	666	670	671	667	669	661
25		667	663	663	664	670	657	672	669	663	659	649	661	660	661	661	663	663	662	661	659	661	662	668	667	663
26	Q	664	663	663	662	663	664	662	657	662	670	670	668	663	662	663	669	670	669	661	662	663	663	664	663	664
27		663	663	663	663	665	666	669	670	669	652	641	662	653	643	653	663	669	670	671	672	678	681	691	680	665
28		683	684	687	695	690	679	670	668	671	671	672	670	663	662	666	667	663	663	663	665	671	675	670	669	672
29		668	667	669	671	671	669	662	661	661	661	664	665	663	663	665	669	671	670	672	670	669	669	670	669	667
30	Q	669	667	664	663	662	662	661	660	662	662	661	661	660	661	662	664	669	669	669	664	662	661	662	662	663
31		661	661	661	669	669	670	669	632	603	611	593	622	574	604	630	648	668	671	669	669	671	677	677	672	648
MEAN A		691	692	693	694	691	684	675	659	663	661	655	652	648	654	660	671	678	684	685	685	688	690	690	690	676
MEAN Q		675	673	672	672	673	673	664	667	662	669	666	666	665	667	669	672	673	675	672	671	672	673	675	675	670
MEAN D		728	735	739	738	730	697	669	657	660	672	647	606	621	643	630	664	687	716	724	725	730	729	729	729	692

HORIZONTAL INTENSITY

TABLE 31 MEANOOK   H = 12500 PLUS TABULAR VALUES IN GAMMAS   NOVEMBER 1969

DAY \ HOUR UT		0 TO 1	1 TO 2	2 TO 3	3 TO 4	4 TO 5	5 TO 6	6 TO 7	7 TO 8	8 TO 9	9 TO 10	10 TO 11	11 TO 12	12 TO 13	13 TO 14	14 TO 15	15 TO 16	16 TO 17	17 TO 18	18 TO 19	19 TO 20	20 TO 21	21 TO 22	22 TO 23	23 TO 24	MEAN
1	Q	751	750	752	753	753	754	754	755	756	757	760	761	762	762	764	757	745	735	731	722	723	732	741	744	749
2		747	751	752	753	753	754	753	753	750	745	754	762	764	762	744	702	700	731	729	721	731	733	751	754	744
3	D	762	764	746	754	765	766	753	707	623	685	752	754	752	742	732	713	745	753	735	732	724	730	743	747	737
4		742	751	754	743	751	753	752	752	742	701	692	734	760	757	757	759	753	742	730	721	719	722	731	742	740
5		743	742	752	761	764	764	760	753	754	764	763	765	763	763	752	741	751	751	742	740	741	742	750	754	753
6	Q	761	761	761	759	760	760	759	764	763	764	764	765	765	763	761	753	745	741	739	739	748	749	753	764	757
7		768	769	753	757	751	742	733	731	679	731	730	741	722	764	770	767	761	750	741	742	739	733	734	742	744
8		753	753	754	749	741	744	722	739	751	744	751	751	761	763	753	730	744	711	700	710	740	742	754	760	743
9	D	749	763	760	765	772	554	575	710	630	239	359	584	639	700	494	737	744	749	689	721	741	751	755	761	664
10	D	760	754	753	764	803	808	918	769	751	814	802	745	558	621	725	753	750	720	703	669	694	752	743	749	745
11		760	751	752	751	744	750	751	731	732	725	723	733	754	752	733	722	744	741	732	724	733	740	752	758	741
12		751	740	763	761	765	770	761	754	750	740	751	760	756	757	760	752	734	720	724	730	733	741	744	743	748
13		753	763	760	762	760	759	757	750	745	749	759	756	751	760	758	753	749	740	732	731	733	742	748	751	751
14	Q	762	760	760	762	760	760	760	759	758	754	759	759	757	754	752	750	742	737	730	731	733	740	746	748	752
15	Q	751	752	753	754	754	754	754	754	754	754	755	757	757	756	756	751	746	743	740	741	743	748	750	753	751
16		750	764	764	764	764	764	763	763	760	760	763	764	763	763	763	762	760	741	740	741	746	749	751	760	757
17		763	769	767	767	770	770	764	763	762	762	763	762	760	760	760	759	753	744	743	745	749	750	749	758	759
18		759	763	771	764	763	769	762	760	760	759	763	762	762	767	765	764	753	741	740	743	740	739	742	752	757
19		759	762	763	763	764	763	760	754	760	763	762	762	751	746	760	762	759	748	733	737	728	719	737	739	752
20		750	760	763	762	762	760	759	759	760	759	760	762	760	760	760	759	756	751	746	742	741	745	749	752	756
21	Q	759	759	759	760	760	759	758	759	760	762	762	760	760	762	757	755	758	751	743	740	741	743	750	752	756
22		760	762	768	765	779	786	790	770	765	764	763	764	763	762	760	762	757	748	742	732	740	753	759	754	761
23		759	762	763	763	762	764	762	762	762	764	765	766	764	766	764	758	745	742	727	725	732	741	742	751	754
24		759	761	758	757	758	758	753	757	758	718	739	765	769	768	758	762	759	746	739	739	737	740	745	750	752
25		759	765	766	765	763	765	761	761	750	759	759	731	751	766	762	750	741	748	732	731	734	738	739	749	752
26		758	773	773	782	773	779	771	759	752	752	753	759	759	758	756	762	750	718	720	731	739	730	745	758	755
27	D	759	762	759	761	772	771	729	559	513	289	627	616	615	630	719	670	750	731	716	717	741	750	749	739	685
28		751	763	769	766	757	756	751	756	699	721	762	759	751	748	759	761	758	749	736	730	718	736	730	739	747
29		761	758	752	757	759	752	741	738	729	751	738	749	731	750	739	756	728	710	721	750	722	740	745	740	742
30	D	740	759	762	759	754	728	639	627	610	691	758	761	752	751	752	729	696	698	728	730	737	732	738	746	724
MEAN	A	755	759	759	760	762	755	751	741	728	715	737	746	741	748	745	747	746	738	730	730	734	740	746	750	744
MEAN	Q	757	757	757	758	758	758	757	758	758	758	760	761	760	759	758	753	747	741	736	735	738	742	748	752	753
MEAN	D	754	760	756	760	773	725	723	674	625	544	660	692	663	689	685	720	737	730	714	714	727	743	746	749	711

DECLINATION

TABLE 32 MEANOOK   D = 23.5 DEGREES EAST PLUS TABULAR VALUES IN MINUTES   NOVEMBER 1969

HOUR UT / DAY		0 TO 1	1 TO 2	2 TO 3	3 TO 4	4 TO 5	5 TO 6	6 TO 7	7 TO 8	8 TO 9	9 TO 10	10 TO 11	11 TO 12	12 TO 13	13 TO 14	14 TO 15	15 TO 16	16 TO 17	17 TO 18	18 TO 19	19 TO 20	20 TO 21	21 TO 22	22 TO 23	23 TO 24	MEAN
1	Q	8.0	8.3	10.1	9.6	9.9	9.7	9.7	9.7	9.9	9.9	10.1	10.4	11.2	11.3	12.9	15.0	18.3	18.1	15.0	11.5	8.4	8.1	8.0	7.8	10.9
2		8.0	4.8	8.5	9.5	10.0	10.0	10.1	10.9	14.6	14.9	8.3	10.6	11.1	10.1	8.5	6.7	4.8	7.4	12.8	13.0	8.5	8.0	7.9	8.3	9.5
3	D	8.3	6.4	9.5	9.0	9.6	8.3	14.5	16.2	12.8	14.5	10.8	11.2	11.1	8.7	11.4	9.8	10.3	15.3	14.6	11.6	11.9	9.6	8.2	8.0	10.9
4		8.2	8.7	8.5	10.8	10.0	9.8	10.9	13.2	13.0	9.8	7.9	11.6	9.1	8.5	10.8	13.3	14.6	15.9	11.7	9.6	8.2	6.7	6.2	6.9	10.2
5		6.4	8.0	9.6	9.5	10.9	10.0	9.6	10.0	11.2	10.1	9.8	10.0	11.4	11.4	10.8	8.3	11.6	13.3	11.4	9.8	8.5	8.0	8.0	8.2	9.8
6	Q	8.4	9.0	9.4	9.7	9.5	9.9	9.9	8.2	8.1	9.2	9.5	10.0	10.3	11.0	11.6	13.2	14.4	12.6	10.0	9.5	7.6	7.4	7.8	6.5	9.7
7		6.6	6.5	10.0	8.2	6.1	9.4	11.3	14.4	12.7	19.7	10.7	10.8	14.4	14.2	16.1	16.5	12.9	13.2	7.8	7.8	6.0	5.8	6.3	8.2	10.6
8		9.5	9.7	9.9	9.7	11.8	8.1	12.6	11.1	8.7	8.1	7.6	8.2	10.8	11.3	10.7	4.7	14.4	13.1	3.6	6.5	4.7	1.6	4.5	5.2	8.6
9	D	8.4	10.0	11.1	10.0	8.1	1.8	28.2	14.8	13.4	9.5	8.1	11.3	23.9	17.7	19.5	9.5	8.1	14.7	1.6	-1.4	3.1	5.0	7.8	8.2	10.5
10	D	9.4	9.6	10.9	10.7	13.5	6.7	28.7	11.4	7.2	-6.7	2.5	5.9	19.3	15.4	17.8	19.6	18.9	12.8	9.9	3.6	1.7	8.0	8.1	9.4	10.6
11		8.0	9.6	9.8	11.0	12.5	11.5	9.6	6.4	11.0	7.8	11.5	8.1	9.6	11.7	12.3	11.5	15.9	14.4	11.4	10.4	9.6	8.0	7.7	8.1	10.3
12		6.4	10.9	10.6	10.3	13.5	12.5	9.8	9.7	9.3	6.1	9.5	11.1	10.9	10.0	12.4	15.4	17.9	14.6	9.7	8.8	7.9	6.4	7.6	7.7	10.4
13		7.9	8.2	9.5	9.8	10.0	10.0	9.8	8.5	9.2	10.9	10.1	11.3	13.4	12.7	12.5	16.1	14.0	11.4	7.9	7.9	7.6	6.3	6.8	7.7	10.0
14	Q	7.6	8.0	9.0	9.5	9.7	9.8	9.8	10.0	10.0	9.7	10.8	10.9	11.1	11.3	12.5	14.0	14.5	14.0	11.1	9.0	7.7	6.4	7.6	7.7	10.1
15	Q	7.9	8.7	9.2	9.3	9.5	9.5	9.5	9.5	9.5	9.7	9.7	10.0	10.8	10.9	11.9	13.5	15.4	14.0	11.1	9.3	7.9	7.9	7.7	8.2	10.0
16		7.9	9.3	9.7	9.5	9.5	9.8	10.3	9.7	10.1	9.8	10.6	10.8	10.8	11.1	12.2	14.2	16.6	15.9	10.9	9.3	7.6	6.4	7.4	7.6	10.3
17		8.0	8.2	9.3	9.5	9.7	9.7	9.7	9.7	9.8	9.8	11.1	10.9	11.1	11.3	12.2	13.7	15.9	14.5	9.5	9.5	8.4	6.4	6.6	7.7	10.1
18		8.4	8.0	8.2	9.5	9.8	9.7	9.7	10.5	11.3	10.9	12.4	12.5	12.7	12.1	12.2	14.2	15.6	15.9	9.5	7.9	8.0	8.2	7.7	7.6	10.5
19		7.9	8.8	9.2	9.3	9.5	9.5	11.7	9.7	11.1	9.8	10.9	12.5	9.8	7.4	10.9	13.7	13.8	12.4	7.9	6.3	6.6	4.7	8.2	9.2	9.6
20		8.3	9.8	11.8	9.6	9.8	9.9	9.8	10.7	9.4	11.2	11.4	11.2	10.9	11.0	11.8	12.8	12.6	12.6	11.2	10.4	10.1	9.4	8.1	9.1	10.5
21	Q	9.1	8.9	9.4	9.8	9.6	9.4	9.6	9.6	9.6	9.9	11.0	11.2	11.0	11.4	11.2	11.5	13.1	14.1	12.3	11.0	9.4	7.7	7.5	8.0	10.2
22		9.4	9.8	9.4	9.8	8.1	6.4	7.2	7.5	6.7	7.8	8.3	9.8	11.2	12.5	11.4	13.0	14.6	15.1	10.9	8.6	5.9	4.1	6.5	7.8	9.2
23		9.4	9.4	9.8	9.9	9.8	9.4	9.4	9.1	9.4	9.4	9.8	10.2	11.0	11.4	12.5	14.4	15.7	14.6	7.7	4.9	4.4	5.9	7.0	8.1	9.7
24		9.6	9.8	10.1	9.9	9.9	9.8	9.9	9.1	9.4	3.5	6.4	9.8	11.5	12.5	9.9	14.3	14.4	12.5	9.9	8.0	7.8	6.4	6.5	8.1	9.5
25		9.3	9.6	9.8	9.9	9.8	9.4	13.0	13.1	11.7	9.8	9.9	8.1	11.2	15.4	14.4	14.7	13.0	15.5	9.6	8.1	7.5	6.2	3.5	3.0	10.2
26		4.7	6.5	5.8	6.1	10.0	12.7	10.0	9.9	9.5	9.5	9.7	11.0	11.1	11.1	11.5	15.8	12.9	2.0	-1.1	1.0	5.0	7.6	8.1	9.0	8.3
27	D	10.0	11.1	11.8	11.3	16.3	29.0	16.0	11.5	8.2	6.5	20.6	18.9	5.0	11.1	11.3	12.9	12.3	11.0	6.6	-1.4	4.7	7.1	6.6	7.6	11.1
28		9.7	9.9	11.1	12.9	14.8	11.3	16.0	22.1	7.9	5.0	9.9	11.0	11.0	8.2	11.3	13.4	15.2	14.7	12.6	8.1	4.7	4.5	6.3	5.7	10.7
29		7.9	8.9	9.4	11.5	11.5	11.3	14.4	22.9	13.1	11.1	5.3	5.7	11.5	1.8	8.2	13.1	12.1	13.2	14.2	11.0	8.2	6.5	7.8	6.5	10.3
30	D	7.9	13.7	11.0	15.0	13.1	12.9	8.1	7.4	13.2	11.3	7.9	9.4	10.7	10.3	10.5	8.1	-1.3	1.8	5.7	8.4	8.1	7.9	9.5	9.7	9.2
MEAN	A	8.2	8.9	9.7	10.0	10.5	10.2	12.0	11.2	10.4	9.3	9.7	10.5	11.6	11.2	12.1	12.9	13.4	13.0	9.6	7.9	7.2	6.7	7.2	7.7	10.1
MEAN	Q	8.2	8.6	9.4	9.6	9.6	9.7	9.7	9.4	9.4	9.7	10.2	10.5	10.9	11.2	12.0	13.5	15.1	14.6	11.9	10.1	8.2	7.5	7.7	7.6	10.2
MEAN	D	8.8	10.2	10.8	11.2	12.1	11.8	19.1	12.3	11.0	7.0	10.0	11.3	14.0	12.7	14.1	12.0	9.7	11.1	7.7	4.2	5.9	7.5	8.0	8.6	10.5

VERTICAL INTENSITY

TABLE 33 MEANOOK — Z = 58000 PLUS TABULAR VALUES IN GAMMAS — NOVEMBER 1969

DAY		0 TO 1	1 TO 2	2 TO 3	3 TO 4	4 TO 5	5 TO 6	6 TO 7	7 TO 8	8 TO 9	9 TO 10	10 TO 11	11 TO 12	12 TO 13	13 TO 14	14 TO 15	15 TO 16	16 TO 17	17 TO 18	18 TO 19	19 TO 20	20 TO 21	21 TO 22	22 TO 23	23 TO 24	MEAN
1	Q	673	672	670	669	667	663	661	661	661	660	660	661	660	661	663	664	666	664	667	668	668	667	667	668	665
2		668	677	671	672	667	668	667	655	631	615	633	647	659	658	651	634	642	658	666	674	671	669	680	706	660
3	D	724	717	687	680	693	668	693	649	594	602	658	668	660	659	648	655	669	677	678	679	690	696	689	681	671
4		670	669	677	690	697	678	668	651	638	595	547	615	658	667	670	672	673	672	670	677	679	679	680	679	661
5		677	675	670	676	677	681	670	667	666	648	660	660	659	660	658	649	659	657	653	657	659	660	660	660	663
6	Q	659	659	659	659	660	660	660	649	654	657	658	658	659	659	660	660	660	659	658	657	657	659	657	658	658
7		658	659	666	669	673	673	651	628	535	557	574	601	547	640	664	663	658	660	666	670	678	681	686	686	643
8		688	675	673	668	667	674	599	628	637	621	629	641	658	660	648	619	641	649	665	671	688	715	712	718	660
9	D	700	683	669	676	675	628	537	584	592	603	468	403	586	656	661	704	673	696	651	658	667	673	670	668	633
10	D	667	666	667	688	724	731	675	649	675	646	633	692	525	545	626	666	695	678	683	685	704	706	694	685	667
11		687	678	677	675	673	669	658	629	627	634	628	656	657	659	651	657	676	669	668	676	682	675	675	674	663
12		677	685	682	674	674	667	671	667	658	633	638	664	666	668	674	674	674	675	674	674	674	676	675	674	670
13		674	675	669	667	667	666	666	660	634	637	667	674	665	668	666	662	660	658	657	665	671	674	674	674	665
14	Q	675	674	674	674	673	667	666	665	665	664	665	665	665	664	666	669	673	671	670	670	666	665	664	664	668
15	Q	665	665	665	665	665	664	663	663	663	663	663	663	664	664	664	664	665	666	666	665	665	665	665	665	664
16		666	666	666	666	666	665	665	665	659	656	661	661	661	661	661	665	666	666	664	666	666	665	665	665	664
17		665	664	663	662	662	661	661	661	661	659	660	664	664	664	665	666	670	666	665	666	664	663	664	667	664
18		665	665	666	664	664	665	666	665	665	662	657	658	657	661	665	667	668	669	664	665	666	667	667	667	664
19		666	665	665	665	665	667	675	665	668	666	665	658	649	636	647	655	657	658	658	664	665	674	677	674	663
20		675	685	693	680	674	667	666	665	665	658	658	664	664	663	664	666	666	663	661	658	658	659	661	664	667
21	Q	664	661	661	661	661	663	664	664	658	657	660	658	656	657	657	658	659	658	663	665	666	666	666	666	661
22		665	664	665	668	684	711	712	687	674	666	665	664	658	656	656	657	658	657	658	658	666	667	664	666	668
23		666	665	664	663	663	661	659	659	659	659	658	658	658	658	658	661	665	664	663	666	668	668	667	669	663
24		669	668	668	667	666	665	659	656	649	606	610	648	656	657	650	657	653	659	661	665	667	669	675	671	657
25		668	667	666	663	664	666	659	657	654	659	658	628	627	647	658	657	656	658	655	659	667	667	672	678	659
26		686	707	706	737	707	694	676	673	668	667	667	665	661	662	665	666	665	638	640	650	675	666	667	666	674
27	D	668	670	669	675	694	641	643	518	489	412	401	595	526	533	563	598	667	649	684	687	681	685	688	699	614
28		714	711	705	694	691	687	667	639	627	628	667	667	658	657	666	671	669	667	667	675	675	685	694	679	673
29		676	684	682	675	672	672	658	614	629	646	634	658	639	602	634	657	652	657	696	724	715	734	708	703	667
30	D	718	687	708	716	694	657	611	607	572	602	666	675	666	667	666	655	649	647	659	685	687	684	678	685	664
MEAN	A	676	675	674	675	676	670	658	647	638	631	632	646	643	649	655	659	663	663	665	670	673	676	675	676	661
MEAN	Q	667	666	666	666	665	663	663	660	660	660	661	661	661	661	662	663	665	664	665	665	664	664	664	664	663
MEAN	D	695	685	680	687	696	665	632	601	584	573	565	607	592	612	633	656	671	670	671	679	686	689	684	684	650

HORIZONTAL INTENSITY

TABLE 34 MEANOOK H = 12500 PLUS TABULAR VALUES IN GAMMAS DECEMBER 1969

HOUR UT / DAY		0 TO 1	1 TO 2	2 TO 3	3 TO 4	4 TO 5	5 TO 6	6 TO 7	7 TO 8	8 TO 9	9 TO 10	10 TO 11	11 TO 12	12 TO 13	13 TO 14	14 TO 15	15 TO 16	16 TO 17	17 TO 18	18 TO 19	19 TO 20	20 TO 21	21 TO 22	22 TO 23	23 TO 24	MEAN
1		750	750	758	758	759	757	751	752	749	748	741	713	718	751	751	750	746	748	739	732	731	738	740	749	745
2		752	759	759	758	752	750	752	749	748	756	757	751	750	755	759	761	759	752	742	739	738	740	743	752	752
3		762	764	769	763	767	765	763	764	763	767	766	767	767	768	769	763	761	751	749	748	745	748	758	773	761
4		768	767	770	773	781	780	772	769	769	764	751	748	761	731	744	769	760	748	747	741	748	750	758	761	760
5	D	760	761	761	761	760	758	769	767	764	748	709	656	665	689	750	769	758	698	726	732	718	739	756	772	739
6	D	760	779	772	770	758	740	787	758	741	670	717	730	749	719	678	708	761	758	745	741	736	748	749	750	743
7		758	761	758	758	760	757	751	757	758	739	738	758	760	762	761	761	760	753	747	748	746	739	740	749	753
8		760	760	758	760	763	762	762	760	758	760	762	763	762	762	761	760	756	754	749	748	748	749	751	749	757
9	D	751	758	761	779	767	770	769	767	762	766	768	766	750	760	755	760	761	760	757	750	751	743	742	756	759
10		761	768	766	764	763	762	760	761	763	761	762	761	768	768	769	770	768	762	760	751	736	728	729	751	759
11		743	761	767	762	768	768	760	740	762	758	766	768	767	762	769	771	768	747	738	739	738	747	755	764	758
12		764	768	760	770	761	750	757	757	757	758	760	757	750	760	762	761	757	748	743	740	742	747	758	770	757
13	Q	772	772	767	769	770	769	766	761	767	766	767	768	768	768	769	769	767	750	740	739	743	757	760	766	763
14		770	773	777	774	775	772	771	770	770	769	768	767	768	769	766	760	763	750	741	739	747	752	760	763	764
15		769	771	771	770	772	771	769	767	768	754	751	777	776	771	769	769	767	747	738	735	745	750	757	760	762
16	D	759	750	770	778	769	768	762	761	759	757	764	749	759	759	767	738	739	753	739	737	730	739	747	759	755
17		767	759	760	765	769	769	769	768	767	759	756	751	769	766	767	766	762	752	740	737	740	746	749	757	759
18		759	761	762	767	768	769	768	768	767	768	766	767	767	767	767	766	760	757	749	746	746	749	755	765	762
19		768	769	769	768	767	766	767	767	767	766	762	769	768	769	768	767	760	754	751	759	763	765	767	769	765
20	Q	771	777	778	777	775	773	770	770	771	771	772	771	769	770	769	770	769	760	756	759	760	759	759	767	768
21	Q	775	777	769	772	771	771	770	769	769	768	768	769	769	768	768	767	763	759	757	756	757	757	759	762	766
22		771	775	775	777	777	776	752	750	767	762	762	761	757	767	779	777	777	760	759	757	757	756	755	759	765
23	D	764	769	768	768	757	759	761	747	745	697	709	727	765	728	705	761	763	740	727	754	747	748	756	756	747
24		762	767	773	770	768	766	760	759	761	756	749	718	707	749	765	760	759	740	748	743	738	733	732	756	752
25		760	760	763	762	761	763	762	754	717	744	763	757	749	737	740	750	749	747	746	739	751	754	757	756	752
26		758	760	759	760	762	758	755	756	754	752	738	747	768	768	768	766	735	747	745	737	729	735	755	759	753
27		758	763	756	759	756	768	763	756	746	716	665	707	760	768	762	762	751	744	743	741	738	739	746	755	747
28		760	764	766	766	764	762	762	764	763	763	753	758	766	762	759	759	760	748	748	749	747	748	749	758	758
29		759	765	768	769	767	767	766	765	763	748	756	765	767	768	770	769	761	756	755	748	747	747	750	759	761
30	Q	767	768	769	767	768	766	768	768	767	766	764	766	767	768	772	775	770	763	758	756	755	755	758	761	765
31	Q	767	769	770	768	768	769	768	767	766	766	760	767	767	768	769	770	768	767	765	758	748	746	751	764	764
MEAN	A	762	765	766	767	766	764	764	761	759	753	751	751	756	757	759	762	760	751	747	745	744	747	752	759	757
MEAN	Q	770	773	770	770	770	769	768	767	768	767	766	768	768	768	769	770	767	760	755	754	753	755	757	764	765
MEAN	D	758	763	766	771	762	759	769	760	754	728	733	725	738	731	731	747	756	742	739	743	736	743	750	759	749

DECLINATION

TABLE 35 MEANOOK D = 23.5 DEGREES EAST PLUS TABULAR VALUES IN MINUTES DECEMBER 1969

DAY	HOUR UT	0 TO 1	1 TO 2	2 TO 3	3 TO 4	4 TO 5	5 TO 6	6 TO 7	7 TO 8	8 TO 9	9 TO 10	10 TO 11	11 TO 12	12 TO 13	13 TO 14	14 TO 15	15 TO 16	16 TO 17	17 TO 18	18 TO 19	19 TO 20	20 TO 21	21 TO 22	22 TO 23	23 TO 24	MEAN
1		9.8	10.0	10.1	10.4	11.1	10.8	9.8	10.8	9.5	10.0	11.2	8.5	8.2	10.0	11.4	11.2	11.1	11.6	11.7	11.1	9.6	8.5	8.3	8.5	10.1
2		9.6	9.6	9.8	9.8	11.6	11.2	11.1	9.5	6.6	8.5	9.6	10.0	10.1	11.6	11.4	11.9	14.5	14.5	11.6	9.6	6.7	6.2	6.7	8.0	10.0
3		8.5	9.8	9.8	10.0	10.1	10.3	10.0	9.8	9.3	9.6	9.8	10.0	10.1	11.1	11.9	13.7	15.9	14.8	13.0	11.2	9.3	6.4	6.2	5.0	10.2
4		6.9	8.7	9.6	10.1	9.6	7.9	9.5	9.6	9.6	10.0	8.5	8.0	10.4	11.4	12.0	16.2	13.2	13.0	11.1	9.3	8.2	8.0	6.9	8.5	9.8
5	D	9.6	9.8	10.1	10.4	10.0	11.4	13.3	9.8	7.4	9.5	6.9	3.2	11.7	14.6	8.2	13.0	13.3	-4.5	-3.1	3.3	4.8	5.4	8.2	6.1	8.0
6	D	8.1	8.4	16.0	10.1	7.0	24.7	15.0	14.4	8.1	3.4	6.8	9.6	12.8	11.7	6.5	6.8	13.1	14.4	11.5	10.9	6.8	8.4	8.3	9.7	10.6
7		11.2	11.3	11.2	10.4	11.5	12.9	12.9	10.1	10.1	8.0	3.9	10.2	11.7	12.8	12.1	12.9	12.8	13.1	12.1	9.9	9.6	8.4	9.7	9.9	10.8
8		9.9	10.1	11.8	12.0	11.2	13.3	11.2	9.7	9.9	9.7	10.2	11.2	10.9	11.3	11.3	11.7	11.8	13.4	11.5	11.0	9.9	9.6	8.4	8.9	10.8
9	D	9.9	9.7	12.8	14.9	10.2	10.9	11.2	10.1	9.9	10.1	10.4	11.7	11.5	11.2	12.9	14.9	14.7	11.8	10.7	10.2	9.7	8.3	7.6	8.1	11.0
10		8.4	10.1	11.0	11.2	11.0	10.5	10.2	11.0	10.1	9.7	10.1	9.9	10.4	11.3	12.3	13.1	14.1	11.0	9.7	10.1	8.6	6.8	5.5	3.8	10.0
11		6.5	8.3	10.1	12.8	11.8	12.9	11.8	11.7	12.6	9.7	13.1	12.9	12.9	14.9	19.2	17.8	18.4	16.8	13.3	11.2	8.3	6.7	6.7	6.7	12.0
12		6.9	8.4	8.2	10.5	11.4	11.6	11.6	11.9	10.2	8.2	10.0	11.4	8.2	9.8	11.6	13.4	14.8	15.0	13.9	10.2	8.2	6.9	7.1	8.4	10.3
13	Q	7.9	8.5	10.0	10.2	11.0	11.6	10.0	8.9	9.7	9.7	9.8	10.3	11.3	11.6	11.9	13.0	14.7	14.8	13.4	11.1	8.5	8.1	6.9	7.1	10.4
14		8.2	8.5	9.7	10.0	10.0	10.2	10.0	9.8	9.8	10.2	10.3	10.3	11.4	11.9	13.4	11.8	15.1	15.0	12.7	11.3	8.4	6.8	6.6	6.8	10.3
15		8.4	9.7	10.2	11.3	11.3	11.3	10.2	10.2	10.0	8.5	6.8	12.1	12.9	11.6	12.9	13.5	16.3	16.6	11.6	9.7	7.9	6.8	6.8	6.3	10.5
16	D	6.8	8.1	8.4	11.3	11.8	11.3	11.4	18.2	8.2	10.3	10.2	11.6	11.1	10.5	12.1	12.7	12.1	14.7	13.4	11.3	8.4	6.3	6.8	7.7	10.6
17		7.9	8.2	9.8	10.3	11.6	11.6	11.4	11.1	11.0	11.4	12.4	11.4	11.8	11.9	12.1	13.9	14.5	14.2	12.2	10.2	10.0	9.0	8.7	8.7	11.1
18		8.9	9.8	10.3	11.0	10.8	10.5	10.3	10.2	10.2	10.3	10.2	11.0	10.8	11.1	11.3	11.9	13.2	13.5	12.9	11.6	9.5	8.1	7.9	8.1	10.5
19		8.5	9.7	10.0	10.2	10.2	11.3	10.0	10.2	10.3	11.0	11.4	11.8	13.0	11.6	12.1	13.2	13.5	13.2	11.6	10.3	9.8	8.9	8.4	7.6	10.7
20	Q	8.4	8.7	9.8	10.2	10.2	10.0	10.3	10.2	10.2	10.3	11.3	11.6	11.6	11.4	11.6	11.9	13.2	13.4	10.3	10.2	9.5	8.2	8.2	7.6	10.3
21	Q	7.9	7.6	8.9	10.2	10.2	10.0	9.3	10.0	9.8	10.0	10.3	11.0	11.0	11.3	11.4	12.7	13.0	13.2	12.6	11.4	10.2	9.7	8.4	8.7	10.4
22		8.1	9.1	9.9	10.1	10.1	9.9	7.0	12.9	11.8	9.7	10.2	12.9	10.7	11.3	14.9	16.2	14.7	12.8	10.1	9.6	8.8	8.1	8.6	9.7	10.7
23	D	9.9	10.1	11.2	10.2	12.8	9.7	11.5	10.1	9.7	9.9	18.1	16.3	15.0	13.1	6.5	11.2	12.8	8.3	.7	4.9	5.1	6.5	8.3	9.6	10.1
24		8.4	13.1	13.3	12.8	10.1	9.7	9.7	10.5	10.1	11.2	11.0	8.9	12.3	11.3	13.3	14.1	13.4	12.5	10.4	8.3	5.7	5.5	6.5	8.4	10.4
25		9.9	11.2	10.5	11.5	19.2	18.1	11.3	9.7	3.8	13.1	10.5	13.4	12.9	11.5	9.9	12.0	9.9	8.4	5.7	5.2	4.7	6.7	7.3	8.9	10.2
26		10.4	10.7	10.2	10.1	10.2	11.2	12.1	9.7	11.3	10.5	9.9	8.4	11.8	12.9	13.8	13.3	9.6	6.2	11.2	8.3	4.9	6.2	8.1	8.6	10.0
27		10.7	11.5	9.9	14.1	8.3	12.9	11.5	10.9	8.0	9.1	-1.1	11.2	12.0	12.9	12.8	13.8	14.7	13.1	13.1	12.3	11.5	11.5	10.7	10.7	11.1
28		10.1	9.7	9.9	10.7	11.3	10.9	9.9	9.9	9.7	10.5	9.6	9.9	11.3	11.0	11.3	12.9	13.3	12.3	11.0	10.1	8.4	9.2	9.7	9.7	10.5
29		10.1	10.5	11.5	11.8	11.2	11.2	10.9	10.2	8.1	9.6	11.5	11.5	11.7	11.8	12.8	12.6	12.6	13.1	12.9	11.7	11.0	10.2	9.9	9.7	11.2
30	Q	9.9	10.1	10.1	9.9	11.7	9.9	10.5	10.9	10.9	10.7	9.7	11.3	11.2	11.5	11.3	12.6	14.2	14.9	14.6	13.4	11.2	9.9	9.6	9.7	11.2
31	Q	9.7	9.9	10.2	10.9	11.0	10.4	9.9	10.2	10.4	10.2	9.7	11.2	9.9	11.2	11.3	12.6	14.6	14.6	14.4	12.8	11.0	9.7	8.3	8.6	10.9
MEAN	A	8.9	9.6	10.5	10.9	10.9	11.6	10.8	10.7	9.5	9.8	9.8	10.7	11.4	11.7	11.9	13.0	13.7	12.6	11.0	10.0	8.6	7.9	7.9	8.2	10.5
MEAN	Q	8.8	9.0	9.8	10.2	10.8	10.4	10.0	10.0	10.2	10.2	10.2	11.1	11.0	11.4	11.5	12.6	13.9	14.2	13.0	11.8	10.1	9.1	8.3	8.3	10.7
MEAN	D	8.9	9.2	11.7	11.4	10.3	13.6	12.5	12.5	8.7	8.6	10.5	10.5	12.4	12.2	9.2	11.7	13.2	8.9	6.6	8.1	7.3	7.0	7.8	8.2	10.1

VERTICAL INTENSITY

TABLE 36 MEANOOK Z = 58000 PLUS TABULAR VALUES IN GAMMAS DECEMBER 1969

HOUR UT / DAY		0 TO 1	1 TO 2	2 TO 3	3 TO 4	4 TO 5	5 TO 6	6 TO 7	7 TO 8	8 TO 9	9 TO 10	10 TO 11	11 TO 12	12 TO 13	13 TO 14	14 TO 15	15 TO 16	16 TO 17	17 TO 18	18 TO 19	19 TO 20	20 TO 21	21 TO 22	22 TO 23	23 TO 24	MEAN
1		688	678	675	670	667	666	666	665	656	650	649	631	620	646	657	649	646	645	647	659	675	675	675	675	660
2		672	669	669	670	671	674	669	657	622	651	659	659	651	649	659	668	672	667	668	671	674	674	675	675	664
3		676	675	676	673	671	672	671	670	669	669	669	669	668	669	670	676	674	670	669	670	670	669	674	676	671
4		669	669	670	672	674	676	670	667	666	660	650	629	646	629	611	643	648	659	660	659	659	660	662	664	657
5	D	666	666	665	665	667	676	657	643	660	639	641	498	518	560	587	620	641	611	631	658	669	696	690	689	638
6	D	705	716	745	725	648	651	707	672	660	592	647	660	658	640	601	641	659	667	672	676	673	679	684	678	669
7		677	676	668	667	670	673	674	660	662	648	631	650	658	660	666	667	667	667	668	669	669	670	672	669	665
8		668	668	669	672	671	670	668	667	666	660	666	664	663	664	664	665	666	666	660	666	667	667	668	669	666
9	D	669	673	679	688	669	668	668	667	667	665	663	658	641	647	647	658	660	660	665	668	669	668	667	668	665
10		669	669	668	668	667	667	668	666	661	661	667	662	665	667	668	669	668	666	664	668	668	669	678	709	669
11		697	687	686	680	680	681	616	579	660	668	672	677	671	652	648	663	670	671	660	664	664	665	665	673	665
12		674	674	676	687	695	687	677	668	668	666	665	662	660	660	665	669	669	669	668	669	668	667	668	669	671
13	Q	670	669	669	670	670	670	666	653	666	667	667	668	667	661	661	662	664	662	665	668	668	669	668	669	666
14		669	667	667	668	667	667	666	665	662	661	661	661	660	661	661	660	661	661	665	668	668	667	670	671	665
15		668	669	669	669	668	667	666	665	661	641	611	652	660	661	660	665	662	663	663	668	675	676	669	671	662
16	D	680	689	690	688	677	674	678	613	650	654	671	660	659	661	659	632	642	652	667	674	672	674	673	672	665
17		678	679	680	673	670	670	669	669	668	661	653	650	669	668	669	669	668	662	662	669	672	671	671	672	668
18		671	671	670	669	668	668	667	667	667	665	663	664	663	663	663	664	665	666	666	669	664	662	662	669	666
19		669	668	669	670	670	670	669	668	667	664	663	662	661	663	663	668	668	669	651	651	649	645	645	645	662
20	Q	645	646	645	645	646	646	648	647	646	644	645	643	643	644	643	644	645	644	649	651	648	644	645	648	645
21	Q	651	652	656	656	654	652	649	647	646	646	645	645	644	644	645	646	646	645	648	646	645	646	646	646	648
22		650	645	645	644	645	646	643	636	663	657	653	645	634	616	627	626	633	636	645	646	644	646	651	651	643
23	D	652	649	649	653	656	654	648	643	620	530	528	561	616	599	581	635	643	644	645	655	660	659	665	667	630
24		699	679	663	654	653	653	652	652	652	645	626	606	523	605	637	646	648	648	652	649	649	654	655	660	644
25		657	656	659	658	661	641	659	649	617	629	658	647	632	617	625	659	647	647	651	655	654	658	668	662	649
26		660	657	657	657	656	655	642	628	621	634	622	626	637	646	647	647	635	636	641	646	649	653	679	682	646
27		684	675	684	675	642	663	658	645	628	586	553	557	623	648	651	651	651	658	669	666	661	661	661	660	646
28		654	652	652	654	654	654	651	651	650	647	637	635	649	649	649	648	647	650	655	655	656	657	657	658	651
29		659	660	662	658	656	655	654	651	635	617	612	638	651	651	650	651	651	652	658	656	656	657	657	657	650
30	Q	656	655	655	655	656	657	656	655	655	654	647	646	648	650	651	655	656	657	657	657	655	656	656	655	654
31	Q	652	652	653	653	654	654	652	651	650	648	629	629	641	648	650	650	651	656	657	650	654	657	657	656	650
MEAN	A	670	668	669	668	664	664	661	653	653	644	643	639	642	645	646	654	656	656	658	661	662	664	666	667	657
MEAN	Q	655	655	656	656	656	656	654	651	652	652	646	646	648	649	650	651	652	653	655	654	654	654	654	655	653
MEAN	D	674	679	686	684	663	664	672	648	651	616	630	607	618	621	615	637	649	647	656	666	668	675	676	675	653

MEAN VALUES OF MAGNETIC ELEMENTS

HORIZONTAL INTENSITY-ALL DAYS

TABLE 37 MEANOOK   H = 12500 PLUS TABULAR VALUES IN GAMMAS   1969

U.T.	JAN	FEB	MAR	APR	MAY	JUN	JUL	AUG	SEP	OCT	NOV	DEC	YEAR	SUMMER	EQUINOX	WINTER
0-1	729	735	743	760	804	763	759	762	777	752	755	762	758	772	758	746
1-2	734	746	749	769	795	775	764	765	777	754	759	765	763	775	762	751
2-3	735	743	759	755	785	779	762	770	769	755	759	766	762	774	760	751
3-4	736	740	749	747	770	779	761	770	766	757	760	767	758	770	755	751
4-5	737	741	751	750	765	761	763	762	766	759	762	766	757	763	757	752
5-6	737	738	739	737	742	759	755	757	769	757	755	764	751	753	750	748
6-7	732	727	716	714	711	754	751	754	757	747	751	764	740	743	733	743
7-8	724	716	699	700	705	746	716	749	739	733	741	761	727	729	718	735
8-9	716	701	676	694	697	725	731	741	711	722	728	759	717	723	701	726
9-10	704	690	639	707	664	739	746	741	703	713	715	753	709	722	691	715
10-11	702	682	669	692	676	744	749	734	712	707	737	751	713	726	695	718
11-12	700	690	694	695	683	740	754	731	688	720	746	751	716	727	699	722
12-13	701	689	697	694	673	728	757	743	717	722	741	756	718	725	707	722
13-14	712	696	722	701	697	732	761	748	722	741	748	757	728	735	721	728
14-15	726	710	723	718	696	744	762	750	718	742	745	759	733	738	725	735
15-16	732	706	724	720	711	745	755	747	723	741	747	762	734	739	727	737
16-17	725	699	717	712	713	735	744	731	722	736	746	760	728	731	722	732
17-18	717	702	702	699	718	723	733	718	713	732	738	751	720	723	712	727
18-19	709	690	697	696	720	720	724	713	716	724	730	747	716	719	709	719
19-20	706	684	699	701	725	724	724	719	723	726	730	745	717	723	712	716
20-21	711	703	707	710	732	732	730	729	738	732	734	744	725	730	721	723
21-22	716	709	719	726	744	743	739	737	749	737	740	747	734	741	733	728
22-23	718	710	736	735	771	754	750	749	764	742	746	752	744	756	744	731
23-24	724	722	744	747	793	760	756	760	777	747	750	759	753	767	754	739
MEAN	720	711	716	720	729	746	748	745	738	737	744	757	734	742	728	733

MEAN VALUES OF MAGNETIC ELEMENTS

DECLINATION-ALL DAYS

TABLE 38 MEANOOK   D = 23.5 DEGREES EAST PLUS TABULAR VALUES IN MINUTES   1969

U.T.	JAN	FEB	MAR	APR	MAY	JUN	JUL	AUG	SEP	OCT	NCV	DEC	YEAR	SUMMER	EQUINOX	WINTER
0-1	12.5	11.0	8.7	5.0	5.1	5.5	8.5	8.4	8.9	8.8	8.2	8.9	8.3	6.9	7.9	10.1
1-2	13.3	11.3	9.0	5.5	5.9	6.7	9.4	8.7	9.1	9.7	8.9	9.6	8.9	7.7	8.3	10.8
2-3	13.7	12.1	8.0	7.5	6.0	8.4	9.2	9.6	8.9	10.4	9.7	10.5	9.5	8.3	8.7	11.5
3-4	13.9	13.6	9.2	9.0	7.3	8.3	8.9	9.9	11.1	10.9	10.0	10.9	10.2	8.6	10.0	12.1
4-5	14.3	12.7	10.5	9.3	9.1	9.2	9.1	9.6	10.2	10.3	10.5	10.9	10.5	9.3	10.1	12.1
5-6	14.1	13.5	11.8	7.9	10.3	9.5	9.5	10.8	10.5	10.7	10.2	11.6	10.9	10.0	10.2	12.4
6-7	13.3	14.5	12.0	9.2	10.3	10.2	9.1	10.0	8.9	10.5	12.0	10.8	10.9	9.9	10.1	12.7
7-8	12.6	13.2	14.4	11.0	11.1	9.6	9.4	10.7	8.4	10.6	11.2	10.7	11.1	10.2	11.1	11.9
8-9	14.3	13.7	16.8	12.3	13.9	10.6	11.4	11.1	9.3	12.8	10.4	9.5	12.2	11.7	12.8	12.0
9-10	14.3	16.4	17.8	13.6	16.4	11.0	11.2	11.6	13.5	13.1	9.3	9.8	13.2	12.5	14.5	12.4
10-11	15.6	17.0	19.1	15.0	15.9	10.7	11.1	11.5	14.5	14.0	9.7	9.8	13.7	12.3	15.7	13.0
11-12	16.4	17.9	16.8	15.7	16.9	12.5	13.0	13.6	15.3	14.4	10.5	10.7	14.5	14.0	15.5	13.9
12-13	16.6	17.8	16.8	17.2	18.5	15.8	15.5	16.1	16.4	13.2	11.6	11.4	15.6	16.5	15.9	14.3
13-14	16.0	17.2	16.4	18.6	20.4	19.4	18.5	18.7	17.6	12.9	11.2	11.7	16.5	19.2	16.4	14.0
14-15	16.5	17.7	18.3	20.0	22.8	21.4	20.4	20.5	18.9	13.2	12.1	11.9	17.8	21.3	17.6	14.5
15-16	16.8	18.4	20.0	20.9	22.9	22.6	21.6	21.1	18.3	14.3	12.9	13.0	18.6	22.1	18.4	15.3
16-17	16.9	19.1	20.3	20.9	21.5	21.9	21.4	19.8	16.5	14.6	13.4	13.7	18.3	21.1	18.1	15.8
17-18	15.4	18.5	18.8	19.0	18.8	18.7	18.9	16.2	13.9	13.4	13.0	12.6	16.4	18.1	16.3	14.9
18-19	14.3	17.5	16.0	14.5	14.1	13.1	14.1	11.2	9.4	10.8	9.6	11.0	13.0	13.1	12.7	13.1
19-20	12.9	13.9	14.1	11.3	10.9	8.8	8.9	6.7	7.3	8.3	7.9	10.0	10.1	8.8	10.2	11.2
20-21	12.1	12.2	12.4	8.7	8.7	5.9	5.7	4.8	6.0	7.2	7.2	8.6	8.3	6.3	8.6	10.0
21-22	11.7	11.1	11.1	7.0	7.1	4.1	4.3	4.7	6.2	6.9	6.7	7.9	7.4	5.1	7.8	9.4
22-23	11.8	10.6	9.2	5.9	5.7	4.2	4.5	5.8	7.3	7.6	7.2	7.9	7.3	5.1	7.5	9.4
23-24	12.1	10.6	8.4	5.4	5.1	4.7	6.0	7.2	9.1	8.5	7.7	8.2	7.8	5.8	7.8	9.7
MEAN	14.2	14.7	14.0	12.1	12.7	11.4	11.6	11.6	11.5	11.1	10.1	10.5	12.1	11.8	12.2	12.4

MEAN VALUES OF MAGNETIC ELEMENTS

VERTICAL INTENSITY-ALL DAYS

TABLE 39 MEANOOK Z = 58000 PLUS TABULAR VALUES IN GAMMAS 1969

U.T.	JAN	FEB	MAR	APR	MAY	JUN	JUL	AUG	SEP	OCT	NOV	DEC	YEAR	SUMMER	EQUINOX	WINTER
0-1	677	676	673	703	696	688	672	674	676	691	676	670	681	682	686	675
1-2	678	677	680	704	693	692	677	676	676	692	675	668	682	684	688	675
2-3	675	678	677	698	676	695	672	679	674	693	674	669	680	681	686	674
3-4	673	677	681	690	674	686	676	676	679	694	675	668	679	678	686	673
4-5	675	678	682	688	679	678	673	668	682	691	676	664	678	674	686	673
5-6	673	677	671	663	661	670	666	661	669	684	670	664	669	665	672	671
6-7	668	663	665	656	659	667	662	657	654	675	658	661	662	661	663	663
7-8	656	653	649	650	654	653	644	645	650	659	647	653	651	649	652	652
8-9	651	642	651	650	632	636	641	634	663	663	638	653	646	636	657	646
9-10	639	637	634	641	618	640	640	625	650	661	631	644	638	631	646	638
10-11	638	637	648	636	616	642	643	619	647	655	632	643	638	630	646	638
11-12	636	649	651	635	630	643	649	624	647	652	646	639	642	636	646	642
12-13	632	651	637	627	634	638	653	634	648	648	643	642	640	640	640	642
13-14	638	642	646	639	630	640	653	640	643	654	649	645	643	641	646	643
14-15	644	649	651	643	643	644	652	645	645	660	655	646	648	646	650	648
15-16	653	653	655	652	647	650	652	651	646	671	659	654	654	650	656	655
16-17	656	657	659	660	657	652	651	655	659	678	663	656	658	654	664	658
17-18	659	662	660	664	663	652	650	654	664	684	663	656	661	655	668	660
18-19	664	665	663	666	668	651	651	654	672	685	665	658	664	656	671	663
19-20	668	666	669	675	672	655	654	657	675	685	670	661	667	660	676	666
20-21	670	672	676	682	681	664	657	660	679	688	673	662	672	666	681	669
21-22	671	674	683	690	687	675	662	666	684	690	676	664	677	672	687	671
22-23	671	677	683	694	694	682	669	671	689	690	675	666	680	679	689	672
23-24	672	677	678	698	690	687	674	673	683	690	676	667	680	681	687	673
MEAN	660	662	663	667	661	662	658	654	665	676	661	657	662	659	668	660

MEAN VALUES OF MAGNETIC ELEMENTS

HORIZONTAL INTENSITY-QUIET DAYS

TABLE 40 MEANOOK H = 12500 PLUS TABULAR VALUES IN GAMMAS 1969

U.T.	JAN	FEB	MAR	APR	MAY	JUN	JUL	AUG	SEP	OCT	NOV	DEC	YEAR	SUMMER	EQUINOX	WINTER
0-1	728	725	726	732	760	754	757	756	748	750	757	770	747	756	739	745
1-2	733	730	727	736	760	757	758	757	757	753	757	773	750	758	743	748
2-3	734	731	732	733	756	754	758	758	758	755	757	770	750	756	745	748
3-4	734	732	733	735	752	756	755	757	759	756	758	770	750	755	745	749
4-5	733	734	730	737	748	753	757	757	756	755	758	770	749	754	745	749
5-6	733	733	736	741	748	752	758	757	758	755	758	769	750	754	748	748
6-7	733	733	737	742	751	754	759	756	759	756	757	768	750	755	749	748
7-8	732	734	734	722	750	754	757	756	760	755	758	767	748	754	743	748
8-9	732	734	734	739	727	755	756	757	755	755	758	768	747	749	746	748
9-10	730	733	731	739	736	754	757	759	746	757	758	767	747	751	743	747
10-11	730	734	738	735	749	755	759	756	759	755	760	766	750	755	747	747
11-12	730	734	737	737	745	755	761	756	758	754	761	768	749	754	747	748
12-13	730	734	737	740	754	761	764	756	761	757	760	768	752	759	749	748
13-14	734	734	736	732	755	765	769	754	762	758	759	768	752	761	747	749
14-15	735	734	737	740	754	763	770	754	757	755	758	769	752	760	747	749
15-16	734	734	738	738	746	757	762	749	744	751	753	770	748	753	742	748
16-17	728	728	729	723	739	741	750	735	729	744	747	767	738	741	731	743
17-18	719	722	722	706	725	726	737	722	717	732	741	760	727	728	719	735
18-19	712	713	716	706	720	720	731	712	712	723	736	755	721	721	714	729
19-20	711	711	709	710	720	720	730	711	718	723	735	754	721	720	715	728
20-21	712	707	711	711	724	728	729	715	728	731	738	753	724	724	720	728
21-22	718	709	711	715	726	735	734	723	741	740	742	755	729	729	727	731
22-23	723	714	712	721	742	741	743	740	759	745	748	757	737	742	734	736
23-24	729	721	719	728	751	754	754	753	792	749	752	764	747	753	747	741
MEAN	728	727	728	729	743	748	753	746	750	748	753	765	743	748	739	743

DECLINATION-QUIET DAYS

TABLE 41 MEANOOK D = 23.5 DEGREES EAST PLUS TABULAR VALUES IN MINUTES 1969

U.T.	JAN	FEB	MAR	APR	MAY	JUN	JUL	AUG	SEP	OCT	NOV	DEC	YEAR	SUMMER	EQUINOX	WINTER
0-1	12.8	11.9	10.5	7.3	6.9	7.1	7.5	8.9	9.3	8.8	8.2	8.8	9.0	7.6	9.0	10.4
1-2	13.1	11.7	10.9	9.1	7.9	8.4	8.3	10.2	9.6	9.5	8.6	9.0	9.7	8.7	9.8	10.6
2-3	13.7	12.2	11.0	10.9	8.8	9.9	9.0	10.6	9.4	9.9	9.4	9.8	10.4	9.6	10.3	11.3
3-4	13.8	12.7	11.2	10.1	9.1	10.2	9.2	9.5	9.4	10.0	9.6	10.2	10.4	9.5	10.2	11.6
4-5	13.7	12.8	11.9	10.6	10.0	10.0	9.3	9.5	10.0	10.2	9.6	10.8	10.7	9.7	10.7	11.7
5-6	13.6	12.8	12.4	11.0	10.3	9.6	9.6	9.6	9.4	10.0	9.7	10.4	10.7	9.8	10.7	11.6
6-7	13.2	12.8	12.2	11.5	9.9	9.6	9.8	10.4	8.2	10.3	9.7	10.0	10.6	9.9	10.6	11.4
7-8	13.0	12.5	12.3	10.7	10.4	9.6	10.3	10.3	11.5	10.7	9.4	10.0	10.9	10.1	11.3	11.2
8-9	13.3	12.8	13.3	12.8	11.2	9.6	10.4	10.4	10.5	10.9	9.4	10.2	11.2	10.4	11.9	11.4
9-10	13.5	13.4	14.7	12.5	12.9	9.9	10.7	11.2	8.7	10.8	9.7	10.2	11.5	11.2	11.7	11.7
10-11	14.1	14.0	14.0	12.0	12.6	10.3	11.5	12.0	13.2	10.8	10.2	10.2	12.1	11.6	12.5	12.1
11-12	15.0	14.7	13.7	13.2	12.9	12.4	12.3	13.1	13.7	11.3	10.5	11.1	12.8	12.7	13.0	12.8
12-13	14.3	14.2	13.8	13.2	16.2	15.9	14.8	15.3	15.2	12.8	10.9	11.0	14.0	15.5	13.7	12.6
13-14	15.4	14.3	14.0	15.9	18.8	17.8	17.8	16.5	16.7	13.5	11.2	11.4	15.3	17.7	15.0	13.0
14-15	16.2	15.6	15.5	18.2	19.5	19.5	19.7	20.2	18.2	13.8	12.0	11.5	16.7	19.7	16.4	13.8
15-16	17.1	17.4	18.0	20.1	20.0	21.7	21.8	21.6	19.9	15.1	13.5	12.6	18.2	21.3	18.3	15.1
16-17	18.2	18.0	19.2	20.9	20.4	21.4	21.7	21.6	20.2	15.7	15.1	13.9	18.9	21.3	19.0	16.3
17-18	17.9	17.4	18.9	18.6	18.3	17.4	18.1	19.1	17.4	14.7	14.6	14.2	17.2	18.2	17.4	16.0
18-19	16.4	16.1	17.5	14.8	14.7	13.0	12.9	13.5	12.3	11.3	11.9	13.0	13.9	13.5	13.9	14.4
19-20	14.9	14.1	15.1	10.9	11.1	8.4	7.4	8.4	8.7	8.3	10.1	11.8	10.8	8.8	10.8	12.7
20-21	13.7	12.8	12.7	7.9	8.6	5.5	4.4	5.9	5.8	7.0	8.2	10.1	8.6	6.1	8.4	11.2
21-22	12.6	11.7	11.2	5.5	7.2	4.1	2.9	4.6	5.8	6.9	7.5	9.1	7.4	4.7	7.4	10.3
22-23	12.3	11.6	10.1	4.7	5.9	4.0	2.4	5.4	6.9	7.7	7.7	8.3	7.3	4.4	7.3	10.0
23-24	12.2	11.6	9.9	4.4	6.0	4.8	4.1	6.9	8.3	8.5	7.6	8.3	7.7	5.4	7.8	10.0
MEAN	14.3	13.7	13.5	12.0	12.1	11.2	11.1	11.9	11.6	10.8	10.2	10.7	11.9	11.6	12.0	12.2

MEAN VALUES OF MAGNETIC ELEMENTS

VERTICAL INTENSITY-QUIET DAYS

TABLE 42 MEANOOK Z = 58000 PLUS TABULAR VALUES IN GAMMAS 1969

U.T.	JAN	FEB	MAR	APR	MAY	JUN	JUL	AUG	SEP	OCT	NOV	DEC	YEAR	SUMMER	EQUINOX	WINTER
0-1	667	663	673	685	684	674	663	667	667	675	667	655	670	672	675	663
1-2	665	663	668	682	682	671	665	664	664	673	666	655	668	671	672	662
2-3	665	663	667	675	680	668	662	662	666	672	666	656	667	668	670	662
3-4	664	663	670	669	678	666	660	661	667	672	666	656	666	666	670	662
4-5	663	663	670	668	676	663	659	661	669	673	665	656	665	665	670	662
5-6	663	664	671	670	674	662	659	661	667	673	663	656	665	664	670	662
6-7	663	663	671	671	669	661	656	660	673	664	663	654	664	662	670	661
7-8	662	661	668	647	664	661	653	657	657	667	660	651	659	659	659	659
8-9	663	661	659	659	642	657	653	655	651	662	660	652	656	652	658	659
9-10	662	660	650	657	629	657	652	656	641	669	660	652	654	649	654	659
10-11	659	660	661	651	644	656	653	654	654	666	661	646	655	652	658	657
11-12	656	659	662	648	643	658	656	655	655	666	661	646	655	653	657	655
12-13	657	658	663	656	656	663	654	655	660	665	661	648	658	657	661	656
13-14	656	656	663	650	658	662	655	653	662	667	661	649	658	657	660	655
14-15	660	658	665	653	660	660	656	654	663	669	662	650	659	658	663	658
15-16	661	660	665	660	658	657	656	654	664	672	663	651	660	656	665	659
16-17	662	662	665	662	657	653	652	655	662	673	665	652	660	654	665	660
17-18	664	663	664	659	654	647	650	655	662	675	664	653	659	652	665	661
18-19	665	665	661	657	654	643	649	653	663	672	665	655	658	650	663	663
19-20	667	666	665	659	651	644	649	653	663	671	665	654	659	649	665	663
20-21	667	664	666	665	655	653	651	656	664	672	664	654	661	654	667	662
21-22	666	664	671	668	662	659	652	659	667	673	664	654	663	658	670	662
22-23	666	666	671	676	669	662	656	661	670	675	664	654	666	662	673	662
23-24	665	663	668	681	677	669	659	662	670	675	664	655	667	667	673	662
MEAN	663	662	666	664	662	659	656	658	663	670	663	653	661	659	666	660

MEAN VALUES OF MAGNETIC ELEMENTS

HORIZONTAL INTENSITY-DISTURBED DAYS

TABLE 43 MEANOOK H = 12500 PLUS TABULAR VALUES IN GAMMAS 1969

U.T.	JAN	FEB	MAR	APR	MAY	JUN	JUL	AUG	SEP	OCT	NOV	DEC	YEAR	SUMMER	EQUINOX	WINTER
0-1	729	792	789	780	968	769	750	773	805	760	754	758	786	815	783	758
1-2	745	823	782	801	944	809	760	788	784	760	760	763	793	825	782	773
2-3	745	796	818	788	909	837	762	810	771	755	756	766	793	829	783	766
3-4	746	778	797	758	821	859	766	824	785	761	760	771	786	817	775	764
4-5	749	776	813	771	793	800	775	762	780	771	773	762	777	783	784	765
5-6	747	761	757	704	692	764	733	770	773	758	725	759	745	740	748	748
6-7	724	691	661	675	616	743	722	764	768	706	723	769	714	711	703	727
7-8	696	665	606	603	610	733	547	756	643	663	674	760	663	662	629	699
8-9	669	616	536	594	604	656	640	714	539	581	625	754	627	654	562	666
9-10	639	540	396	657	379	700	701	713	515	541	544	728	588	623	527	613
10-11	638	495	508	576	457	734	739	689	535	508	660	733	606	655	532	632
11-12	579	533	621	633	497	741	748	672	409	577	692	725	619	664	560	633
12-13	606	533	591	627	439	707	728	721	582	605	663	738	628	649	602	635
13-14	687	549	697	579	506	685	752	748	647	699	689	731	664	673	655	664
14-15	724	609	714	639	492	718	765	754	664	680	685	731	681	682	674	687
15-16	739	596	714	676	556	730	763	748	680	702	720	747	698	699	693	701
16-17	713	591	689	698	586	724	752	725	719	704	737	756	699	697	702	699
17-18	700	647	679	681	663	711	734	706	700	731	730	742	702	704	698	705
18-19	698	600	679	685	705	707	721	709	705	720	714	739	698	710	697	688
19-20	689	578	693	696	736	720	718	725	722	723	714	743	705	725	709	681
20-21	707	691	711	716	759	730	726	745	751	731	727	736	728	740	727	716
21-22	715	717	746	750	809	748	736	759	761	737	743	743	747	763	749	730
22-23	716	703	802	780	903	759	752	762	779	745	746	750	766	794	776	729
23-24	722	738	791	773	1001	764	770	778	804	745	749	759	783	828	778	742
MEAN	701	659	691	693	685	744	732	746	692	694	711	749	708	727	693	705

MEAN VALUES OF MAGNETIC ELEMENTS

DECLINATION-DISTURBED DAYS

TABLE 44 MEANOOK D = 23.5 DEGREES EAST PLUS TABULAR VALUES IN MINUTES 1969

U.T.	JAN	FEB	MAR	APR	MAY	JUN	JUL	AUG	SEP	OCT	NOV	DEC	YEAR	SUMMER	EQUINOX	WINTER
0-1	12.2	10.5	6.6	3.9	.1	4.3	15.1	6.7	7.3	10.5	8.8	8.9	7.9	6.5	7.1	10.1
1-2	14.1	12.3	7.8	2.7	-2.3	4.2	16.1	5.6	6.9	13.6	10.2	9.2	8.4	5.9	7.7	11.4
2-3	12.6	12.1	-1.3	4.2	-9.4	4.7	10.1	8.4	5.5	15.2	10.8	11.7	7.0	3.4	5.9	11.8
3-4	13.1	13.8	.6	7.0	-4.0	2.8	6.9	8.7	12.2	15.2	11.2	11.4	8.2	3.6	8.7	12.4
4-5	13.8	10.9	3.4	7.8	-0.1	8.3	9.2	7.9	8.9	11.7	12.1	10.3	8.7	6.3	7.9	11.8
5-6	14.9	13.7	6.9	-2.3	5.5	11.4	9.3	13.5	10.2	12.6	11.8	13.6	10.1	9.9	6.8	13.5
6-7	12.6	13.2	8.0	2.9	4.9	13.2	8.8	10.5	9.3	9.4	19.1	12.5	10.4	9.3	7.4	14.3
7-8	10.1	13.8	16.2	8.3	6.0	10.8	9.6	10.0	7.8	15.0	12.3	12.5	11.0	9.1	11.8	12.2
8-9	16.3	17.2	23.6	9.4	15.6	12.0	18.6	9.9	-5.2	20.1	11.0	8.7	13.1	14.0	12.0	13.3
9-10	14.8	28.1	23.6	13.5	30.4	15.5	15.3	14.1	17.1	19.8	7.0	8.6	17.3	18.8	18.5	14.6
10-11	22.1	28.4	31.5	21.1	26.5	10.7	12.5	11.0	20.5	24.2	10.0	10.5	19.1	15.2	24.3	17.7
11-12	20.1	29.9	21.8	24.9	27.7	12.1	13.2	16.0	22.6	22.0	11.3	10.5	19.3	17.3	22.8	17.9
12-13	17.2	28.9	19.3	26.2	24.6	16.3	15.6	18.3	23.9	11.5	14.0	12.4	19.0	18.7	20.2	18.1
13-14	16.5	23.4	18.5	26.3	25.8	22.3	20.9	20.4	22.1	9.9	12.7	12.2	19.2	22.3	19.2	16.2
14-15	16.6	21.6	20.0	23.9	31.4	21.6	22.5	21.6	23.3	8.8	14.1	9.2	19.5	24.3	19.0	15.4
15-16	17.3	15.5	22.7	22.6	30.8	24.1	25.0	22.1	19.0	9.8	12.0	11.7	19.4	25.5	18.5	14.1
16-17	17.3	17.2	21.7	22.5	26.6	24.3	23.0	19.8	15.7	11.7	9.7	13.2	18.6	23.4	17.9	14.3
17-18	14.4	20.7	18.0	19.4	21.7	20.1	20.7	14.2	13.6	10.2	11.1	8.9	16.1	19.2	15.3	13.8
18-19	12.2	25.1	18.5	13.4	16.3	15.4	16.9	8.0	8.7	8.9	7.7	6.6	13.1	14.1	12.4	12.9
19-20	10.9	13.9	17.3	7.9	13.8	8.0	10.6	5.4	5.4	8.7	4.2	8.1	9.5	9.5	9.8	9.3
20-21	11.3	10.0	18.0	6.4	12.5	5.5	5.3	3.7	7.0	8.6	5.9	7.3	8.5	6.8	10.0	8.6
21-22	11.3	10.1	16.5	7.2	9.3	6.3	3.5	3.8	7.3	9.2	7.5	7.0	8.2	5.7	10.0	9.0
22-23	12.2	9.0	11.6	7.6	6.1	6.7	4.6	6.0	7.8	9.6	8.0	7.8	8.1	5.9	9.2	9.3
23-24	12.4	9.8	8.5	6.0	3.8	5.3	7.1	6.1	12.1	10.4	8.6	8.2	8.2	5.6	9.2	9.8
MEAN	14.4	17.0	15.0	12.2	13.5	11.9	13.3	11.3	12.0	12.8	10.5	10.1	12.8	12.5	13.0	13.0

MEAN VALUES OF MAGNETIC ELEMENTS

VERTICAL INTENSITY-DISTURBED DAYS

TABLE 45 MEANOOK Z = 58C00 PLUS TABULAR VALUES IN GAMMAS 1969

U.T.	JAN	FEB	MAR	APR	MAY	JUN	JUL	AUG	SEP	OCT	NCV	DEC	YEAR	SUMMER	EQUINOX	WINTER
0-1	707	689	620	719	684	696	662	674	654	728	695	674	683	679	680	691
1-2	719	689	665	735	702	713	685	681	667	735	685	679	696	695	7C1	693
2-3	701	701	635	734	607	734	661	691	665	739	680	686	686	673	693	692
3-4	695	692	651	708	590	717	685	668	676	738	687	684	683	665	693	690
4-5	708	684	674	707	636	688	686	642	708	730	696	663	685	663	705	688
5-6	696	676	625	604	652	663	660	664	691	697	665	664	663	660	654	675
6-7	674	631	650	640	676	667	673	662	651	669	632	672	658	669	653	652
7-8	646	610	632	646	704	646	605	655	658	657	601	648	642	653	648	626
8-9	636	606	683	688	635	620	610	614	740	660	584	651	644	620	693	619
9-10	608	564	666	628	576	622	591	570	670	672	573	616	613	590	659	590
10-11	646	571	732	628	568	626	627	544	625	647	565	630	617	591	658	603
11-12	582	644	747	639	629	651	649	557	643	606	607	607	630	621	658	610
12-13	575	671	646	602	664	644	636	592	630	621	592	618	624	634	625	614
13-14	612	612	646	610	580	625	641	616	630	643	612	621	621	615	632	614
14-15	624	614	671	590	627	628	642	635	633	630	633	615	629	633	631	622
15-16	658	622	673	623	600	637	648	646	650	664	656	637	643	633	653	643
16-17	656	638	658	659	629	648	649	651	667	687	671	649	655	644	668	653
17-18	663	661	658	662	667	653	651	649	676	716	670	647	664	655	678	660
18-19	674	669	669	672	691	660	651	654	697	724	671	656	674	664	690	667
19-20	677	672	677	702	710	662	662	665	700	725	679	666	683	675	701	673
20-21	685	696	689	710	738	667	671	669	710	730	686	668	693	686	710	684
21-22	683	698	699	718	742	684	672	680	717	729	689	675	699	695	716	686
22-23	680	694	681	730	740	702	679	694	725	729	684	676	701	704	716	683
23-24	684	686	638	715	681	704	691	686	677	729	684	675	688	691	690	682
MEAN	662	654	666	670	655	665	654	644	673	692	650	653	661	655	675	655

THREE-HOUR RANGE INDICES, MEANOOK, 1969

Table 46

	January				February			
	D	H	Z	K	D	H	Z	K
1	1023 1210	2113 2211	2013 2110	2123 2211	0000 0110	0000 0111	0000 0000	0000 0111
2	0200 1100	0100 1200	0001 0110	0201 1210	0021 2463	0012 2475	0022 2353	0022 2475
3	0000 0100	0000 1100	0000 0000	0000 1100	4375 5432	5577 7544	4475 6433	5577 7544
4	0001 1000	0001 1111	0000 1000	0001 1111	2033 2322	3232 3312	2122 1102	3233 3322
5	0200 1000	0100 0000	0000 0000	0200 1000	2021 1111	2123 1111	2133 1000	2133 1111
6	0000 0110	0000 0101	0000 0000	0000 0101	1422 1111	2335 0122	2334 0001	2435 1122
7	0012 3132	0114 5222	0004 5001	0114 5232	1022 1121	1023 2122	1013 2111	1023 2122
8	1131 0110	1141 0111	0232 0000	1242 0111	2120 1211	2111 1211	1121 0000	2121 1211
9	1000 0010	2110 0110	0000 0000	2110 0110	0010 0110	0110 1111	0000 0000	0110 1111
10	0001 2110	0010 2100	0010 1000	0011 2110	1022 2113	1122 2223	0033 2103	1133 2223
11	0010 1110	0020 1111	0010 0100	0020 1111	3259 7633	7377 7754	5268 7733	7379 7754
12	1022 2210	0023 3201	0013 2220	1023 3211	2111 0121	3110 0112	1100 0002	3111 0122
13	0001 0100	0001 0101	0002 0000	0002 0101	1122 1112	2134 3312	1233 2212	2234 3312
14	1221 1122	1233 1112	1143 1012	1243 1122	0101 1011	2112 2112	1113 3001	2113 3112
15	2213 1122	2223 2232	0212 2121	2223 2232	1322 2232	2234 2323	1223 1112	2334 2333
16	0223 3211	1223 5302	0333 4200	1333 5312	1231 1211	2253 3211	1243 3200	2253 3211
17	2324 2221	3334 3333	3344 3222	3344 3333	0111 0000	0011 0111	0000 0000	0111 0111
18	1443 2211	2356 4222	2455 4211	2456 4222	0000 0110	0000 0101	0000 0000	0000 0111
19	2123 2111	2234 3212	2034 2011	2234 3212	0101 3220	0111 3211	0121 4200	0121 4221
20	1321 1221	2221 3231	1121 2221	2321 3231	0101 1221	0101 2322	0211 2111	0211 2322
21	1122 0100	2123 0111	1222 0000	2223 0111	1031 1110	2120 1211	1020 0000	2131 1211
22	0111 0010	0033 0101	0023 0000	0133 0111	0011 1111	0010 1212	0011 1000	0011 1212
23	0000 1110	0001 2111	0000 1000	0001 2111	1232 2221	1122 3212	0233 3110	1233 3222
24	0000 3221	1000 3323	0000 4332	1000 4333	0111 1110	1132 1111	0033 0000	1133 1111
25	2244 5322	3266 7533	3256 4332	3266 7533	1011 1101	1012 1201	1011 1000	1012 1201
26	3213 3221	4316 7312	4315 5311	4316 7322	1232 2220	2233 2221	0353 1010	2353 2221
27	0223 3211	2244 5312	2144 4211	2244 5312	2230 3531	1141 5543	1231 4521	2241 5543
28	2001 0110	1111 0111	1102 0000	2112 0111	0241 1212	2352 1323	0342 1112	2352 1323
29	0000 0110	1001 0102	0000 0000	1001 0112				
30	0113 1110	1114 1110	0024 0000	1124 1110				
31	0012 2211	0012 3211	0013 3211	0013 3211				

	March				April			
	D	H	Z	K	D	H	Z	K
1	1000 2322	3111 2322	1010 0212	3111 2322	0223 2343	2235 4445	1234 4244	2235 4445
2	3302 2100	4303 4201	3303 3000	4303 4201	2102 2332	3113 3424	2102 2132	3113 3434
3	0000 0110	1000 0111	0000 0000	1000 0111	5220 2222	6322 2333	5331 2122	6332 2333
4	0000 1122	0000 0123	0000 0012	0000 1123	3333 3221	2353 4222	2343 3101	3353 4222
5	1003 2111	2114 4112	1004 3000	2114 4112	1152 1211	3143 1213	0031 0011	3153 1213
6	1123 1210	2124 1322	0034 2111	2134 2322	1230 2132	1130 2223	1231 1012	1231 2233
7	2221 2232	2322 4332	2323 4322	2323 4332	3452 2221	4563 4333	3542 3121	4563 4333
8	1322 2111	3324 3212	2323 3001	3324 3212	2101 1111	2202 1112	2213 1001	2213 1112
9	1223 2201	2123 3221	0133 3311	2233 3321	0233 3122	2344 3233	1244 2332	2344 3333
10	1122 0020	2123 0111	1123 0000	2123 0121	0132 1211	1243 2322	0143 2121	1243 2322
11	1133 4223	1134 5335	0234 4233	1134 5335	1142 2110	2253 4321	1143 4100	2253 4321
12	5665 1321	6877 3322	6665 3210	6877 3322	0012 2133	1100 1234	0011 0013	1112 2234
13	2021 1121	2121 1111	1102 1100	2122 1121	3343 3323	5444 4345	4343 4433	5444 4445
14	1101 2121	2101 1213	1102 0011	2102 2223	4111 2222	7223 4333	4113 3111	7223 4333
15	3464 2211	4474 3323	3455 2321	4475 3323	2354 3221	3355 5322	2243 3110	3355 5322
16	0356 2110	1567 2222	0556 2101	1567 2222	1253 3222	2375 5333	1363 3222	2375 5333
17	4433 5421	6545 7434	4534 5333	6545 7434	3264 3321	4365 3434	4364 4322	4365 4434
18	0233 2211	2345 1312	1244 1111	2345 1312	4441 2121	5452 3212	5552 2112	5552 3222
19	0032 2133	2042 1234	0032 0013	2042 2234	2000 2121	2100 2222	2000 1002	2100 2222
20	5143 1312	6345 2333	4354 0123	6355 2333	1020 2121	2211 1222	1010 0002	2221 2222
21	3252 2121	3253 2222	2253 2012	3253 2222	2000 1120	2010 0212	2010 0002	2010 1222
22	1332 2221	2333 3222	2333 3210	2333 3222	0023 1220	2233 3222	1033 3101	2233 3222
23	1001 2255	1011 2146	1001 1137	1011 2257	1120 2121	2111 2212	0020 2000	2121 2222
24	6577 5321	7677 6323	6667 4211	7677 6323	2320 1221	3311 1222	2410 0102	3421 1222
25	1154 3222	3266 5233	1155 4313	3266 5333	2121 2121	3232 1212	2131 1111	3232 2222
26	2032 2221	3123 3332	2023 2112	3133 3332	2010 2131	2110 1222	1001 0011	2110 2232
27	1120 1011	2211 0211	1021 1000	2221 1211	2223 1120	2214 2222	2124 2201	2224 2222
28	0110 1211	1110 1222	0000 0100	1110 1222	1675 5421	4796 7434	2785 6412	4796 7434
29	0032 2222	1034 3323	0033 2313	1034 3323	1111 2322	4231 3234	2110 1123	4231 3334
30	2212 2222	3123 1334	3223 0012	3223 2334	3544 3231	3765 5433	3745 3322	3765 5433
31	2211 2230	3232 2432	2132 2110	3232 2432				

THREE-HOUR RANGE INDICES, MEANOOK, 1969

May	D	H	Z	K	June D	H	Z	K
1	2421 0110	3333 1212	2443 0010	3443 1212	2211 1110	3202 2222	2222 1010	3222 2222
2	1213 3352	2235 5343	1234 4233	2235 5353	0231 2111	1241 2222	0251 2002	1251 2222
3	0332 2111	2354 3223	0453 3211	2454 3223	1011 1211	2110 1112	1111 1012	2111 1212
4	0321 0120	2222 2212	1212 0111	2322 2222	1131 2100	2222 3212	1142 3111	2242 3212
5	1001 1211	3203 3222	3002 3112	3203 3222	1102 1210	2212 1111	2112 1110	2212 1211
6	1320 1100	2421 1112	2531 2001	2531 2112	0001 1210	1100 1122	0000 0111	1101 1222
7	1121 0000	2155 0001	1243 0000	2255 0001	1112 3210	2113 4212	1123 4202	2123 4212
8	0110 0101	1110 2212	1120 0102	1120 2212	1232 1321	1332 1333	1333 1123	1333 1333
9	0132 1122	1244 2123	0254 2102	1254 2123	2112 2142	3212 3344	2201 2242	3212 3344
10	1231 2110	3353 2212	2353 1100	3353 2212	1133 2210	4353 3322	2343 2100	4353 3322
11	1122 1110	1112 1121	0023 0010	1123 1121	1232 1131	2243 2223	1243 1002	2243 2233
12	0010 1122	1001 0133	0001 0113	1011 1133	3543 2231	5755 3222	4553 2211	5755 3232
13	3455 5423	5676 7436	3366 6524	5676 7536	1512 2232	3632 3323	2521 3323	3632 3333
14	5533 2245	6555 3357	5645 2345	6655 3357	2352 5322	4374 6324	2362 4213	4374 6324
15	8556 8644	5768 8766	8757 8645	8768 8766	1123 3221	3224 4232	2224 4221	3224 4232
16	5576 4010	6787 6223	5676 5002	6787 6223	1345 2222	3376 4323	2345 3313	3376 4323
17	1353 2111	3473 3124	3453 2103	3473 3124	4332 2220	5444 1332	4344 1211	5444 2332
18	3254 2331	5366 2333	4455 2112	5466 2333	1000 1101	2210 1211	1000 0110	2210 1211
19	2012 2220	3123 4323	2012 3111	3123 4323	0021 1111	1222 2223	0133 1111	1233 2223
20	2222 1110	3231 1222	1331 1112	3332 1222	3332 1111	3355 3222	2355 3111	3355 3222
21	1235 3111	2335 4423	2335 3312	2335 4423	0223 2120	2122 2212	1123 2010	2223 2222
22	1224 4120	2225 5322	1135 5210	2235 5322	0001 0110	0100 1211	0001 0000	0101 1211
23	0032 3221	3233 4221	1134 4110	3234 4221	0002 1210	1222 1212	0001 1122	1222 1222
24	0431 1221	2742 3323	1533 2212	2743 3323	3312 3221	3333 3212	2333 3112	3333 3222
25	2111 1110	5101 0222	4111 0011	5111 1222	0022 2221	2222 2333	1122 2122	2222 2333
26	0001 1110	1112 1111	1003 1001	1113 1111	2002 2210	3113 2212	2103 3301	3113 3312
27	0000 1110	1010 1112	0000 0001	1010 1112	1111 1000	2212 2112	2202 2002	2212 2112
28	0232 2201	2233 2212	0122 1100	2233 2212	0000 0010	2101 0012	1011 0010	2111 0012
29	0011 1121	1011 2123	0000 1012	1011 2123	0011 0110	2211 2322	0010 1111	2211 2322
30	0123 3311	2244 4313	1254 4201	2254 4313	0111 1210	1110 1222	0010 0111	1111 1222
31	1432 2121	3433 3123	1533 3111	3533 3123				

July	D	H	Z	K	August D	H	Z	K
1	1152 3221	2273 3333	1163 3222	2273 3333	0011 0000	2112 1122	1001 1000	2112 1122
2	2221 0001	2231 1112	2332 0100	2332 1112	0012 1111	1001 2222	0000 0001	1012 2222
3	0001 0121	1101 1111	0100 1001	1101 1121	0322 3232	3213 2333	1102 1113	3323 3333
4	0000 1011	0100 0112	0000 0000	0100 1112	2323 1111	4424 2323	2424 2111	4424 2323
5	0001 1101	2101 2111	0001 1001	2101 2111	0312 2211	2434 4111	2433 4000	2434 4211
6	0001 1010	1101 1212	0000 0000	1101 1212	1211 0101	2101 0012	2210 0001	2211 0112
7	1001 1310	2201 2212	0112 1002	2212 2312	0321 1120	2221 2123	0120 0012	2321 2123
8	1001 1121	2200 1122	1100 0002	2201 1122	1033 2111	3125 2213	2034 4012	3135 4213
9	1121 1221	2231 1122	2231 1020	2231 1222	1231 2120	3321 2222	3331 2112	3331 2222
10	1112 1110	2213 2213	2213 1201	2213 2213	1234 2100	2155 1100	1254 2210	2255 2210
11	0021 1110	2110 1122	0111 0112	2121 1122	0001 1120	0111 2122	0000 0001	0111 2122
12	2231 1111	3353 1234	2353 1112	3353 1234	2443 3320	3456 5433	3456 4221	3456 5433
13	1433 2231	3654 2233	2655 1121	3655 2233	1133 1011	3343 0122	1155 1001	3355 1122
14	1322 2221	2433 4222	1434 3111	2434 4222	0133 2120	2154 3110	0144 3100	2154 3120
15	0022 2110	2122 3212	0132 2001	2132 3212	0021 2111	0020 1112	0020 0001	0021 2112
16	1213 2221	2115 1222	0215 2111	2215 2222	0002 1121	1012 1212	0002 1101	1012 1222
17	1211 1110	2211 1211	1111 0010	2211 1211	1331 1111	2231 0121	1210 0000	2331 1121
18	0012 0010	1012 2211	0003 1000	1013 2211	1001 1221	2112 3212	1101 2111	2112 3222
19	0111 0110	1121 0211	0022 0000	1122 0211	1333 2322	2334 2334	1233 2012	2334 2334
20	0100 1100	2111 1211	0000 0110	2111 1211	2231 1211	3462 3322	1142 1101	3462 3322
21	0000 1211	2010 2212	0000 1111	2010 2212	0311 2220	1200 2212	0100 0001	1311 2222
22	1121 1211	2221 1112	0121 0102	2221 1212	0101 2221	2100 1133	1001 0101	2101 2233
23	0001 0111	2112 0222	2001 1012	2112 0222	1223 3211	3324 2223	1212 2111	3324 3223
24	0010 0100	1120 1111	2010 0110	2120 1111	1212 2221	2202 2123	1001 1001	2212 2223
25	1220 0101	2220 1222	1220 0000	2220 1222	2110 1121	2100 1112	0011 0000	2110 1122
26	1213 3212	2203 4225	1211 4313	2213 4325	0024 3221	1116 3224	0014 2001	1126 3224
27	5563 2111	7584 4232	7573 3121	7584 4232	4534 2221	5745 3122	2533 1110	5745 3222
28	0031 0100	2252 1111	0042 0000	2252 1111	1311 1131	2311 2021	1311 1001	2311 2131
29	0010 0100	1110 0111	0000 0000	1110 0111	0001 2221	2000 1122	0000 0000	2001 2222
30	1000 1342	2111 2444	0000 1122	2111 2444	0031 2121	1121 1112	0110 0000	1131 2122
31	0001 1111	2211 1222	2111 1010	2211 1222	1131 2221	1031 1211	0021 0000	1131 2221

THREE-HOUR RANGE INDICES, MEANOOK, 1969

	September				October			
	D	H	Z	K	D	H	Z	K
1	1011 2121	1110 1211	1011 0000	1111 2221	3244 3311	2256 6322	1234 2111	3256 6322
2	0111 1111	1011 1200	0000 0000	1111 1211	3356 4421	3478 5622	2545 5411	3578 5622
3	0001 0221	1100 0112	0000 0000	1101 0222	3323 4320	3334 4422	2334 3411	3334 4422
4	1100 1110	0100 0112	0000 0000	1100 1112	1213 1110	2223 2322	0223 2110	2223 2322
5	0000 1122	2000 1124	0000 0102	2000 1124	1222 1120	1122 2211	1032 1011	1232 2211
6	2433 2221	4557 2322	2444 0011	4557 2322	2333 2221	1234 3331	0233 3211	2334 3331
7	1033 2222	2144 3223	0033 1011	2144 3223	1331 1010	1342 1011	0341 0000	1342 1011
8	2565 2220	3576 2211	1453 1000	3576 2221	0010 0010	0120 1121	0020 0000	0120 1121
9	0142 2210	1242 3212	0031 1100	1242 3212	0010 0222	0110 0122	0110 0000	0110 0222
10	2200 1121	2210 2121	1000 0000	2210 2121	2525 4322	3456 4323	3446 4132	3556 4333
11	3232 1222	2233 2121	1122 1000	3233 2222	1232 3101	2334 4212	1233 4201	2334 4212
12	1313 1111	2212 1110	0211 0000	2313 1111	2042 2210	2152 4310	1152 3300	2152 4310
13	0012 1110	0012 0001	0001 1000	0012 1111	0023 1110	0023 2010	0034 1000	0034 2110
14	1112 1223	1112 0224	0001 0011	1112 1224	0000 0111	0000 1111	0000 0000	0000 1111
15	5353 3331	5353 4332	4231 2220	5353 4332	0122 1100	1122 1010	0032 1000	1132 1110
16	1321 1110	2231 2012	1121 0000	2331 2112	0220 0211	0120 0211	0230 0011	0230 0211
17	0003 3231	1004 3232	0003 2110	1004 3232	0001 0111	1111 0211	1011 0012	1111 0212
18	2232 3321	2323 3333	1121 2111	2333 3333	1043 0010	2024 1221	2132 0000	2134 1221
19	2412 1111	2313 2112	1212 0000	2413 2112	0032 2221	1133 4222	0042 4001	1143 4222
20	1112 2210	2154 2212	0032 1110	2154 2212	0000 0021	1010 0221	0000 0001	1010 0221
21	0121 0111	1121 1111	1231 1000	1121 1111	1132 2211	1134 1222	1044 1110	1144 1222
22	1131 0211	1021 0011	0020 0000	1131 0211	1212 2210	2213 2221	1123 2100	2223 2221
23	0010 1211	1001 2212	0000 1101	1011 2212	0120 0110	1010 0212	0010 0010	1120 0212
24	0222 1111	2212 0122	0111 0000	2222 1122	2322 2211	2334 4112	1334 3010	2334 4212
25	0231 1221	1231 1212	0120 0101	1231 1222	0311 0011	1211 0212	1211 0000	1311 0212
26	0032 1110	2013 0012	0012 0000	2033 1112	0020 1010	1020 1211	0010 0000	1020 1211
27	0000 1113	0000 1113	0000 0001	0000 1113	0012 1211	1012 2222	0003 1001	1013 2222
28	3226 5332	3237 7434	1115 4212	3237 7434	1121 1121	2120 1211	1110 0011	2121 1221
29	1355 4444	2377 6635	1255 3414	2377 6645	0201 0010	0101 0212	0101 0000	0201 0212
30	6577 5332	7678 7343	5555 5111	7678 7343	0010 0010	0010 0111	0000 0000	0010 0111
31					0233 2110	1133 3211	0134 3100	1234 3211

	November				December			
	D	H	Z	K	D	H		
1	1022 1221	1112 2311	0022 1200	1122 2311	0012 2110	0023 3111	1122 2110	1123 3111
2	1122 1111	1112 2322	1133 1102	1133 2322	0120 0110	1131 1111	0031 0100	1131 1111
3	1432 2211	2355 2322	2344 1211	2455 2322	0000 0112	1111 1213	0000 0001	1111 1213
4	0122 1110	1223 1212	1224 1000	1224 1212	1101 2210	2112 3211	0002 3100	2112 3211
5	1100 1200	1111 2201	0102 1100	1112 2201	0123 2432	1224 5433	0124 4232	1224 5433
6	0110 0011	1020 0112	0010 0000	1120 0112	3533 3311	3544 5422	3534 4311	3544 5422
7	2233 2211	2232 4222	0144 1111	2244 4222	1122 0110	2122 1101	1012 1000	2122 1101
8	0231 2332	1231 1333	1141 1222	1241 2333	1100 1100	1111 1111	0000 0000	1111 1111
9	1545 4532	2667 6632	2657 5621	2667 6632	2300 2210	2211 2312	1211 1101	2311 2312
10	1545 4530	2465 7442	0455 5432	2565 7542	0010 0111	1111 1122	0001 0003	1111 1123
11	1122 1210	2123 2322	1122 1211	2123 2322	1142 2120	2142 2222	2142 2111	2142 2222
12	2212 1200	2222 0211	1012 0000	2222 1211	1210 1010	1221 1211	1111 1000	1221 1211
13	0022 1200	1122 2211	1022 1101	1122 2211	0010 0110	1110 1111	0010 0000	1110 1111
14	0000 0000	1100 0001	1000 0000	1100 0001	0000 1210	1111 1211	0000 0000	1111 1211
15	0000 0010	0000 0111	0000 0000	0000 0111	0002 1210	1113 1211	0013 1111	1113 1211
16	0001 0121	0011 0111	0001 0000	0011 0111	1031 2120	2132 3312	1142 2211	2142 3323
17	0000 0111	1000 0211	0000 0000	1000 0211	1001 0000	1112 1211	0001 1100	1112 1211
18	0000 0110	1111 1211	0001 0111	1111 1211	0000 0010	1111 1111	0000 0000	1111 1111
19	0021 2111	0021 2222	0021 1001	0021 2222	0000 1110	1111 1211	0000 1100	1111 1211
20	1011 0000	2101 0001	1001 0000	2111 0001	0000 0111	1111 1111	0000 0010	1111 1111
21	0000 0100	0000 1100	0000 0000	0000 1100	0223 3200	1334 4311	0124 4400	1334 4411
22	0321 1121	3321 1121	0220 0001	3321 1121	0031 2200	1131 2311	0031 2210	1131 2311
23	0000 0110	1001 0312	0000 0001	1001 0312	1000 0021	1111 1123	0000 0011	1111 1123
24	0002 1210	1013 1211	0012 1001	1013 1211	3103 2211	3213 3112	2103 4001	3213 4112
25	0021 2211	1022 3211	0012 2111	1022 3211	0331 2211	1332 2222	1232 2211	1332 2222
26	3320 0320	2231 1332	1220 0220	3331 1332	0131 1222	1132 1323	0032 1112	1132 1323
27	0445 4331	1458 5422	0356 3312	1458 5422	2323 1100	2334 2211	2334 2000	2334 2211
28	1232 1121	2143 1212	1133 1001	2143 1222	0001 0110	1113 1211	0001 0000	1113 1211
29	1032 3221	2032 4333	1122 3233	2132 4333	0011 0000	1112 1111	0022 0000	1122 1111
30	4333 2321	3444 2321	4544 1221	4544 2321	0101 0010	1111 1111	0001 0000	1111 1111
31					0001 0100	0111 1111	0002 0010	0112 1111